

NYSTAGMUS GENERATION, OCULOMOTOR TRACKING  
AND VISUAL MOTION PERCEPTION

by

SYOZO YASUI

Kogakushi, UNIVERSITY OF TOKYO

(1963)

M.S., MASSACHUSETTS INSTITUTE OF TECHNOLOGY

(1968)

SUBMITTED IN PARTIAL FULFILLMENT OF THE  
REQUIREMENTS FOR THE DEGREE OF  
DOCTOR OF PHILOSOPHY

at the

MASSACHUSETTS INSTITUTE OF TECHNOLOGY

September 1973

Signature of Author . . . . .  
Department of Aeronautics and Astronautics  
September 24, 1973

Certified by . . . . . Thesis Supervisor

. . . . . Thesis Supervisor

. . . . . Thesis Supervisor

. . . . . Thesis Supervisor

Accepted by . . . . .  
Chairman, Departmental Graduate Committee

Nystagmus Generation, Oculomotor  
Tracking and Visual Motion Perception

by  
Syozo Yasui

Submitted to the Department of Aeronautics and Astronautics, Massachusetts Institute of Technology, on September 24, 1973, in partial fulfillment of the requirements for the degree of Doctor of Philosophy.

Abstract

Principal classes of human horizontal eye movements are studied herein from biocybernetic points of view emphasizing functional relationships.

The classical psychological notion known as corollary discharge theory for the visual motion perception is introduced in the study of the oculomotor tracking system. The underlying hypothesis is that of perceptual feedback oculomotor control, in which the observer produces tracking eye movements on the basis of his subjective visual perception of target motion. This is recognized as a closed-loop version of the corollary discharge theory, describing both perceptual and oculomotor mechanisms within the same conceptual framework. A model is elaborated with respect to the smooth pursuit tracking system to the point of establishing an experimental basis for testing the hypothesis. Aiming at selectively activating the internal regenerative feedback that emerges from connecting the corollary discharge outflow with the postulated perceptual-feedback path, the experiment incorporates the forced visual tracking of a small foveal after-image undergoing vestibularly-induced apparent motion. Some pertinent subjective visual effects including the oculogyral illusion are discussed along with a possible further servomechanical refinement of this visual oculomotor control model.

The question of predictive oculomotor behavior is investigated in terms of periodic and nonperiodic-input frequency responses with regard to pursuit movements in the visual tracking and also the slow phase component of optokinetic nystagmus (OKN) and of vestibular nystagmus. Pursuit frequency response results are characterized by a conspicuous tendency toward large low-frequency phase lead with increasing stimulus bandwidth. A special type of predictive phase control scheme is suggested in interpreting this input-adaptive pursuit tracking phenomenon. Results for OKN slow phase also show evidence for the oculomotor prediction but with no such phase lead as found in the above pursuit case. This difference indicates the existence of separate central mechanisms controlling these two classes of visually evoked oculomotor reactions, in spite of their similar phenomenological features as apparent in the time

domain observation. In contrast, vestibular nystagmus slow phase representing a typical nonvisual oculomotor reflex failed to show a predictive behavior in the frequency range examined.

Nonperiodic-input frequency response characteristics of the saccadic subsystem for visual tracking are evaluated indirectly by the use of nonperiodic-input data for composite (saccade and pursuit) and pursuit movements determined experimentally above. The notion of effective saccadic input is introduced in this computation in order to assess the intrinsic saccadic frequency response, considering the dependence of saccadic response upon the tracking performance by the pursuit system. Resultant nonperiodic-input saccadic phase data are compared with the periodic-input counterpart in the literature, confirming the predictive nature of saccadic tracking. Further, both gain and phase results are discussed in the light of an existing mathematical model for the saccadic system.

Behavior of the fast phase in vestibular and optokinetic nystagmus is investigated regarding its characteristic relation to the slow phase movement. To account for the relevant phenomena observed similarly in both types of nystagmus, an efferent-feedforward type model is constructed based on a simple principle envisioned from experimental results, and tested by a series of hybrid computer simulations. This model is intended to predict the fast phase behavior for given slow phase motor information irrespective of its stimulus modality. This view is reinforced by clinical nystagmographic data from an acoustic neuroma patient. Another pathological case cited is central scotomata, in which reversal of the fast phase direction occurs with OKN. Dependence of OKN mechanism upon central versus peripheral vision as suggested by this example is examined in a normal subject by selective OKN stimulation to the peripheral retina, based on a computer graphic method for stimulus presentation coupled with feedback blanking signal from the eye movement monitor.

Doctoral Program Committee:

Laurence R. Young, Chairman  
Professor of Aeronautics and Astronautics

Renwick E. Curry  
Assistant Professor of Aeronautics and Astronautics

Charles M. Oman  
Assistant Professor of Aeronautics and Astronautics

Alfred D. Weiss  
Research Associate in Aeronautics and Astronautics  
Assistant Professor of Neurology, Department of Otolaryngology, Massachusetts Eye and Ear Infirmary

### Acknowledgement

The author gratefully acknowledges the guidance and support from his thesis supervisors; Professor Laurence R. Young, one of the pioneers in the field, was closely associated with the research in all phases. It was the author's immeasurable benefits to receive his inspiring advice and stimulation. Professor Renwick E. Curry was of particular help in discussing frequency response data especially for the saccadic system. Professor Charles M. Oman helped greatly in materials related to the vestibular system as well as editorial assistance. Doctor Alfred D. Weiss provided invaluable clinical data along with his illuminating comments that helped to discuss the nystagmus results.

Sincere thanks go to Mr. John R. Tole and Dr. John H. J. Allum, who developed the special computerized method vital to key sets of data analysis. The author also appreciates intriguing comments from Prof. Whitman Richards of the Department of Psychology. Not forgotten are the former staff members of the Man-Vehicle Laboratory, Dr. Jacob L. Meiry, Mr. John Hatfield and Dr. Noel Van Houtte, all of whom were helpful during the earlier stage of the research. Mrs. Sherry Modestino typed the final manuscript with excellent skill, for which the author is indebted. Appreciation is also expressed to the subjects for their voluntary participation in long hours of experimentation.

The author is particularly grateful to his wife, Tomoko, for her moral understanding and unfailing patience, besides assistance for preparing figures and typing draft.

This research was supported in part by NASA Grant NGR-22-009-025.

To My Late Father

Kenzo Yasui

## Table of Contents

<u>Chapter No.</u>	<u>Page No.</u>
I <u>Introduction</u>	24
1.1 Rationales and Objectives	27
1.1.1 On Perceptual Feedback to Oculomotor Centers	27
1.1.2 Comparison between Optokinetic Nystagmus Slow Phase and Pursuit Movement	29
1.1.3 Input-Adaptive Characteristics of Some Classes of Smooth Type Eye Movement: Quest of Predictive Behavior	29
1.1.4 Frequency Response of the Saccadic System with Nonperiodic Input: An Indirect Method	31
1.1.5 Nystagmus Fast Phase Behavior in Relation to Slow Phase Movement in Optokinetic and Vestibular Nystagmus	33
1.2 Applications: Biology, Psychology, Technology and Clinical Medicine	36
1.3 Organization of the Thesis	42
II <u>The Oculomotor Control System: A Review</u>	44
2.1 Dual-mode Visual Tracking Eye Movement	46
2.1.1 Saccadic System	48
2.1.2 Pursuit System	51
2.2 Optokinetic Nystagmus	60
2.3 Vestibular Nystagmus	63
2.4 Input-Adaptive Predictive Oculomotor Behavior	71
2.4.1 Dual-mode Tracking: Composite Response (Saccade and Pursuit)	71
2.4.2 Saccadic Response to Periodic Square-wave Inputs	83

2.4.3	Nature of Learning in Eye Movement Control	86
2.5	Summary	91
III	<u>After-image Tracking under Induced Vestibular Nystagmus: A Perceptual Feedback Model for the Pursuit Oculomotor System</u>	93
3.1	Introduction	95
3.2	Visual Judgement Mechanisms: A Review	98
3.3	Perceptual Feedback Hypothesis with Corollary Discharge Theory	104
3.4	Method	108
3.4.1	Rationale	108
3.4.2	Apparatus	112
3.4.3	Procedure	116
3.4.4	Data Processing and Analysis	119
3.5	Results and Discussions	127
3.5.1	Sinusoidal Vestibular Stimulation	127
3.5.2	Pseudo-random Vestibular Stimulation	138
3.6	Supplementary Discussions on Perceptual Feedback Model	147
3.6.1	Problem of Open-loop Structure	147
3.6.2	Block Diagram Nomenclature	148
3.6.3	Visual Velocity Sensations based on Afferent versus Efferent Monitoring	152
3.6.4	Partial Cancellation Hypothesis and Oculogyral Illusion	154
3.7	Summary and Conclusions	162
IV	<u>Frequency Response of the Pursuit System: Input-adaptive Characteristics and Possible Predictive Behavior</u>	167

4.1	Introduction	169
4.2	Method	172
4.2.1	Objectives	172
4.2.2	Apparatus and Procedure	172
4.2.3	Data Processing and Analysis	177
4.3	Results and Discussion	186
4.3.1	Periodic-input: Composite and Pursuit	186
4.3.2	Nonperiodic-input: Composite	192
4.3.3	Nonperiodic-input: Pursuit	204
4.4	Pursuit Phase Behavior: Discussion and Theory	213
4.4.1	Reliability of the Phase Result	213
4.4.2	A Phase Control Model for Pursuit Tracking	216
4.5	Summary and Conclusions	230
V	<u>Nonperiodic-input Frequency Response of the Saccadic Tracking System: An Indirect Evaluation</u>	234
5.1	Introduction	236
5.1.1	Background	236
5.1.2	Objectives	237
5.2	Inference from Experimental Results of Chapter IV	239
5.2.1	Apparent Saccadic Frequency Response	239
5.2.2	Intrinsic Saccadic Frequency Response	240
5.2.3	Periodic versus Nonperiodic-input Saccadic Phase Behavior	246
5.3	Comparison with Young's Sampled-data Model	248
5.3.1	Model Prediction based on 200 msec Sampling Period	248



	5.3.2	Model Prediction based on Estimated Inter-saccadic Period	253
	5.3.3	Reduced Latency: A Possible Model Improvement and its Implication	258
	5.4	Consistency of Experimental Results in Chapter IV	270
	5.5	Summary and Conclusions	275
VI		<u>Dynamical Study of Optokinetic Nystagmus Slow Phase</u>	278
	6.1	Introduction	279
	6.1.1	Background	279
	6.1.2	Objectives	280
	6.2	Experimental Protocol	282
	6.2.1	Apparatus	282
	6.2.2	Procedure	284
	6.2.3	Data Analysis	287
	6.3	Results and Discussions	289
	6.3.1	Transient Behavior, Latency and Linearity	289
	6.3.2	Slow Phase Frequency Response: Periodic-inputs	294
	6.3.3	Slow Phase Frequency Response: Nonperiodic-inputs	298
	6.4	Summary and Conclusions	313
VII		<u>Mechanism of Fast Phase Generation in Vestibular and Optokinetic Nystagmus</u>	315
	7.1	Introduction	317
	7.1.1	Preliminary Observations	317
	7.1.2	Evidence for Common Central Control of Nystagmus Fast Phase	320

7.2	Experimental Results and Discussions	325
7.2.1	Response to Constant Velocity Stimuli: Linear Relations	325
7.2.2	Sinusoidal Response	337
7.3	A System Engineering Model	343
7.3.1	Functional Implication of Average Deviation	343
7.3.2	Conceptual Description of Models	343
7.3.3	Model Analysis	349
7.4	Simulation of Model	369
7.4.1	Simulation 1	369
7.4.2	Simulation 2	373
7.5	OKN Pattern Change by Selective Stimulation to Peripheral Retina	379
7.6	Summary and Conclusions	386
VIII	<u>Principal Results, Conclusions and Recommendations</u>	390
8.1	On a Perceptual Feedback Model for the Pursuit Oculomotor System	391
8.2	On Optokinetic Nystagmus Slow Phase versus Pursuit Movement	402
8.3	Quest of Predictive Behavior in the Oculomotor System	405
8.4	On Saccadic Frequency Response with Nonperiodic Inputs	415
8.5	Fast Phase Behavior in Relation to Slow Phase Movement in Vestibular and Optokinetic Nystagmus	419
<u>Appendices</u>		
A	<u>Eye Movement Monitor: Sample Calibration Records</u>	425
B	<u>MITNYS-FFT, Two-step Data Reduction Procedure</u>	427

C	<u>FFT, Program Outline</u>	429
D	<u>Individual Subjects' Frequency Response Data</u>	474
E	<u>OKN Stimulus Display by Computer Graphics</u>	499
F	<u>Bode's Phase-attenuation Theorems and an Approximated Formula for the First Theorem</u>	507
	<u>References</u>	511
	<u>Biographical Sketch</u>	525

## List of Figures

<u>Figure No.</u>		<u>Page No.</u>
2.1	Typical record showing dual-mode visual tracking eye movement	46
2.2	Schematic illustration of Westheimer's observation for the characteristic saccadic response	49
2.3	Three typical eye movement patterns in response to a 10 deg/sec ramp input (from Robinson, 1965)	54
2.4	Basic structure of a linear velocity servo-mechanism	57
2.5	OKN eye movement responding to a constant velocity of stripe pattern	60
2.6	Typical record of vestibular nystagmus with sinusoidal skull rotation	63
2.7	Frequency response of vestibular nystagmus slow phase (published data)	67
2.8	Periodic (sine wave)-input composite frequency response data from publications	72
2.9	Nonperiodic-input (pseudo-random) composite frequency response data from previous publications	79
2.10	Average saccadic latencies in tracking square-wave inputs (from Dallos and Jones, 1963)	84
3.1	Two possible alternatives for visual motion perception:	
-a	Inflow theory (Sherrington, 1918)	100
-b	Outflow theory (Helmholtz, 1866)	100
3.2	Skeleton model for the pursuit tracking system based on corollary discharge theory and perceptual feedback hypothesis	106
3.3	Perceptual feedback model in three conditions:	

-a	Apparent after-image motion due to corollary discharge	110
-b	Forced visual tracking of after-image	110
-c	Vestibular nystagmus in complete darkness without after-image	110
3.4	View of the Bárány type rotating chair cab	113
3.5	Schematic drawing showing arrangement inside the rotating chair cab	114
3.6	Amplitude spectra of pseudo-random chair motion	118
3.7	Typical traces for a complete run with chair oscillation frequency at 0.5 Hz (After-image tracking experiment)	128
3.8	Transient features during after-image tracking experiment	130
3.9	Increase of eye velocity amplitude during after-image tracking	132
3.10	Typical traces for a complete run with chair oscillation frequency at 0.25 Hz (after-image tracking experiment)	133
3.11	Vestibular nystagmus slow phase frequency response (based on sinusoidal stimulation) in the dark	134
3.12	Frequency response comparison (based on sinusoidal stimulation) between after-image tracking eye movement and vestibular nystagmus slow phase in complete darkness without after-image	135
3.13	Sample traces during pseudo-random vestibular stimulation with no vision	139
3.14	Vestibular nystagmus slow phase frequency response in the dark; Periodic versus nonperiodic stimulation for head angular motion	140
3.15	Frequency response data; Smooth eye movement during visual tracking of vestibularly-induced after-image apparent motion versus normal vestibular nystagmus in the dark	143
3.16-a	Control theory representation for perceptual feedback pursuit tracking model including vestibular afferent	149

3.16-b	Schematic drawing of the globe-lens-retina system	149
3.17	Vestibularly induced eye movement patterns with and without visual fixation target	156
4.1	Pertinent views of experimental site:	
-a	Subject wearing eye movement monitor spectacle frame	173
-b	Wide white screen confronting subject	173
4.2	Stimulus amplitude spectra for single sine wave tracking	175
4.3	Pseudo-random input frequency spectra	176
4.4	Definition of amplitude and phase for periodic-input composite eye movement	179
4.5	Typical periodic-input records representing low, intermediate and high frequency responses	181
4.6	MITNYS-FFT data processing flow chart	184
4.7	Periodic-input composite frequency response data	187
4.8	Periodic-input pursuit frequency response data	188
4.9	Composite and pursuit Bode plots	189
4.10	Periodic-input composite frequency response as compared with published results	190
4.11	Typical sets of traces with pseudo-random inputs:	
-a	Input A	193
-b	Input B	194
-c	Input C	195
-d	Input D	196
4.12	Enlarged record showing satisfactory performance of MITNYS	197
4.13	Nonperiodic-input composite frequency response with various pseudo-random inputs	

-a	Input A	199
-b	Input B	200
-c	Input C	201
-d	Input D	202
4.14	Composite frequency response (pseudo-random input A) as compared with published nonperiodic-input results	203
4.15	Nonperiodic-input pursuit frequency response with various pseudo-random inputs:	
-a	Input A	205
-b	Input B	206
-c	Input C	207
-d	Input D	208
4.16-a	Nonperiodic-input pursuit result (pseudo-random input B) as contrasted with periodic-input counterpart	211
4.16-b	Nonperiodic-input pursuit result (pseudo-random input B) as contrasted with composite counterpart	212
4.17	Pursuit movement relative to over-all composite movement	215
4.18	Nonperiodic-input pursuit phase behavior	219
4.19	Asymptotic behavior of periodic-input pursuit phase	220
4.20	Schematic drawing illustrating the suggested interpretation for observed pursuit phase behavior	224
4.21	Schematic illustration for Eq. (4-5)	225
4.22	Nonperiodic-input pursuit phase behavior: experiment and model prediction	227
5.1	Frequency response results for composite, saccadic and pursuit movements for pseudo-random input B	241

5.2-a	General organization of visual tracking system	243
5.2-b	Decoupled diagram functionally equivalent to Fig. 5.2-a	243
5.3	Intrinsic and apparent nonperiodic-input saccadic frequency response results for pseudo-random input	245
5.4	Phase error of saccadic visual tracking	246
5.5	Versions of sampled-data saccadic visual tracking model:	
-a	Young's original configuration	249
-b	Dead zone removed	249
-c	$T_0$ replaced by mean inter-saccadic interval	249
5.6	Intrinsic saccadic frequency response result as compared with prediction by Young's original model	252
5.7	Histogram of inter-saccadic intervals	254
5.8	Intrinsic saccadic frequency response result and prediction by Young's model with sampling period of 0.51 sec	257
5.9	Sampled-data saccadic visual tracking model with parameters modified from Young's original values	262
5.10	Intrinsic saccadic frequency response result and theoretical prediction by Young's model with modified parameter values (input B)	263
5.11	Intrinsic saccadic frequency response result and theoretical prediction by Young's model with modified values (input C)	265
5.12	Reaction time delay of saccadic tracking eye movement	269
5.13	Evaluation of pursuit response characteristics	271
5.14	Complex vector diagrams for evaluating pursuit phase	
-a	0.11 Hz	273
-b	0.41 Hz	273



6.1	Computer-graphic OKN stimulus pattern displayed on CRT scope	282
6.2	Two distinct OKN patterns, "Look type" and "Stare type"	285
6.3	OKN response to a sudden initiation of constant-velocity stimulus motion	290
6.4	Slow phase latency and fast phase latency for OKN	292
6.5	Slow phase latency and fast phase latency versus stimulus speed	292
6.6	Maximum steady-state OKN slow phase velocity versus stimulus velocity	293
6.7	Typical OKN records with sine wave stimuli of different frequencies	295
6.8	OKN slow phase frequency response with periodic input as compared with periodic pursuit result	296
6.9	Typical set of traces for OKN with pseudo-random stimulation	299
6.10	OKN slow phase frequency response as compared with pursuit result, both under nonperiodic stimulation:	
-a	Input A	300
-b	Input B	301
-c	Input C	302
-d	Input D	303
6.11	OKN slow phase frequency response under nonperiodic stimulation as compared with periodic-input OKN slow phase result:	
-a	Input A	306
-b	Input B	307
-c	Input c	308
-d	Input D	309

7.1	Various nystagmus eye movement patterns:	
-a	Vestibular nystagmus in human	318
-b	Optokinetic nystagmus in human	318
-c	Vestibular nystagmus in rhesus monkey (from Young, 1973)	318
-d	OKN in rabbit (from Collewijn <u>et al</u> , 1971)	318
7.2	Post-rotatory vestibular nystagmus:	
-a	in human	318
-b	in pike (from ten Kate, 1969)	318
7.3	An acoustic neuroma case; a unilateral disturbance selective to fast phase behavior (Weiss, 1973)	322
7.4	OKN responding to various constant stimulus speeds	327
7.5	Schematic illustration for nystagmus parameters	328
7.6	OKN average reset position versus average slow phase velocity	331
7.7	OKN average fast phase size versus average slow phase velocity	332
7.8	OKN average fast phase interval versus average slow phase velocity	334
7.9	OKN average mean position versus average slow phase velocity	335
7.10	Representative OKN patterns with various frequencies	338
7.11	Typical vestibular nystagmus	338
7.12	Typical behavior of nystagmus parameters with respect to slow phase velocity's phase angle under sinusoidal stimulation	
-a	OKN, 0.1 Hz, TY	340
-b	Vestibular nystagmus, 0.1 Hz, SY	341
-c	OKN, 0.5 Hz, SY	342

7.13	Recent versions of Schmid's model for vestibular nystagmus generation (from Schmid, 1971)	345
7.14	Model proposed to account for the observed nystagmus pattern, and illustration for its operation	
-a	Alternative 1	347
-b	Alternative 2	347
-c	Operation of model	347
7.15	Frequency dependent behavior of nystagmus parameters as predicted by model	357
7.16	Behavior of nystagmus parameters with respect to slow phase velocity's phase angle under sinusoidal stimulation:	
-a	OKN, 0.1 Hz, TY	359
-b	OKN, 0.1 Hz, SY	360
-c	OKN, 0.1 Hz, JT	361
-d	OKN, 0.3 Hz, TY	362
-e	OKN, 0.3 Hz, JT	363
-f	OKN, 0.5 Hz, SY	364
-g	OKN, 0.7 Hz, JT	365
-h	Vestibular nystagmus, 0.1 Hz, SY	366
-i	Vestibular nystagmus, 0.25 Hz, SY	367
7.17	Simulation of model for OKN;	
-a	Arrangement	370
-b	Results	370
7.18	Simulation of model for vestibular nystagmus	
-a	Arrangement	372
-b	Results	372
7.19-a	Arrangement for testing the model (alternative procedure)	374

7.19-b	Actual OKN as compared with model prediction obtained by the arrangement given in Fig. 7.19-a	375
7.20-a	Actual vestibular nystagmus in the dark as compared with model prediction obtained by the arrangement given in Fig. 7.19-a	377
7.20-b	Trace showing vestibular nystagmus in presence of a visual fixation target. Diagram showing a simple eye movement model for this condition.	377
7.21	Schematic presentation of two distinct OKN patterns (from Hood, 1967)	380
7.22	Computer-generated stripe-pattern for OKN stimulation to selective retinal area based on feedback-blanding	382
7.23	OKN patters by selective stimulation to peripheral retina in contrast with normal cases	384
A.1	Sample calibration records of eye movement monitor	426
B.1	Generalized operational diagram for MITNYS-FFT data reduction procedure	428
D.1	Vestibular nystagmus slow phase in complete darkness, sinusoidal vestibular stimulation	479
D.2	Smooth eye movement resulting from after-image tracking under induced vestibular nystagmus; sinusoidal vestibular stimulation	480
D.3	Vestibular nystagmus in complete darkness, pseudo-random vestibular stimulation	481
D.4	Smooth eye movement resulting from after-image tracking under induced vestibular nystagmus, pseudo-random vestibular stimulation	482
D.5	Periodic-input composite frequency response	483
D.6	Periodic-input pursuit frequency response	484
D.7	Nonperiodic-input composite frequency response with various pseudo-random inputs:	
-a	Input A	485

-b	Input B	486
-c	Input C	487
-d	Input D	488
D.8	Nonperiodic-input pursuit frequency response with various pseudo-random inputs:	
-a	Input A	489
-b	Input B	490
-c	Input C	491
-d	Input D	492
D.9	Nonperiodic-input pursuit frequency response, test run data	493
D.10	Periodic-input OKN slow phase frequency response	494
D.11	Nonperiodic-input OKN slow phase frequency response with various pseudo-random inputs:	
-a	Input A	495
-b	Input B	496
-c	Input C	497
-d	Input D	498
E.1	OKN stimulus display system and schematic illustration for optional visual patterns	505
E.2	OKN stimulus velocity calibration record	506
F.1	Illustrative sketch showing piece-wise linear approximation for gain data used to compute corresponding phase shift characteristics based on Bode's first theorem	509

## List of Tables

<u>Table No.</u>		<u>Page No.</u>
3.1	Peak-to-peak position, velocity and acceleration amplitude for the applied chair oscillation	117
3.2	Events in one experimental run (After-image tracking experiment)	120
3.3	Summary of data reduction procedure	125
3.4	Summary of student's t-test results:	
(a)	Smooth eye movement during visual tracking of vestibularly-induced after-image apparent motion versus normal vestibular nystagmus in the dark: Sinusoidal vestibular stimulation	145
(b)	Vestibular nystagmus slow phase in the dark: Pseudo-random versus sinusoidal vestibular stimulation	145
(c)	Smooth eye movement during visual tracking of vestibularly-induced after-image apparent motion versus normal vestibular in the dark: Pseudo-random vestibular stimulation	145
4.1	Compensatory phase lead as computed based on the suggested scheme for pursuit phase control	226
5.1	Two alternative predictions based on Young's sampled-data model	259
6.1	Summary of student's t-test results:	
(a)	OKN slow phase versus pursuit movement, periodic stimulation	311
(b)	Periodic versus nonperiodic-input OKN slow phase	311
(c)	OKN slow phase versus pursuit movement, nonperiodic stimulation	312
7.1	Numerical summary: Fast phase interval and various proportionality constants in relation to average OKN slow phase velocity	337
8.1	Summary of oculomotor predictive results	406

C.1	FFT program listing	431
D.1	Illustrative sample of FFT printout	475
D.2	Input-output matching of Fourier amplitude peaks:	
	(a) Vestibular nystagmus slow phase with no vision	477
	(b) Smooth eye movement during after-image tracking under vestibular stimulation	477
D.3	Input-output matching of Fourier amplitude peaks:	477
	(a) Dual-mode visual tracking eye movement; Composite (pursuit and saccade)	477
	(b) Dual-mode visual eye movement, pursuit only	477
D.4	Input-output matching of Fourier amplitude peaks; OKN slow phase	478
E.1	OKN program listing	501

## Chapter I

### Introduction

Man interacts with his surroundings in a wide variety of behavioral ways that all depend upon sensory-motor coordination. Prerequisite to this achievement is the detection of relative motion between man and external objects or references through utilization of various sensory modalities.

Of prime importance to this end is the visual source of information. Under certain criterion depending on a particular situation, the quality of the relevant visual information is optimized and maintained by means of controlled movements of the receptor organ, the eye. Different types of eye movements that occur under different environmental conditions are functionally interpretable from this fundamental point of view. This is true for even some classes of the eye movement that can be elicited nonvisually in the laboratory. In the natural environment, it is likely that such nonvisual stimuli indirectly result in a visual motion in a certain expected kinematic relationship to the observer.

One recognizes the oculomotor system itself as a sensory-motor system within the hierarchical structure of the over-all sensory motor system that ultimately governs body orientation or posture as well as such dynamic behavior as walking. In contrast with the human auditory system for example, the special feature of the motor augmentation to this particular sensing



device indicates the high priority placed upon information from this sensory modality in coordinating various daily activities.

The oculomotor system, being a relatively self-contained sensory motor organization, has always attracted considerable interest from physiologists. In addition to its functional importance, the eye movements are externally observable, and various instruments have been devised to enable quantitative measurement and recording. Further, the relevant stimulus to the oculomotor system can be prepared usually with comparatively little technical difficulty. It is chiefly for these reasons that eye movements have also been widely used in clinical tests for diagnosing neurological disorders.

The system engineering approach to living systems has been a conspicuous trend in recent years, where measurement and analysis of stimulus and response form the basis of deducing the functional structure embodying a biological system in question. The application of engineering principles appears to have been most successful in the field of oculomotor research. Besides the relatively easy external accessibility, the principal reason for this may be that the ultimate goal of the system is in most cases apparent a priori or at least hypothesized on a more plausible basis as compared with many other biological systems. Further, the obvious presence of the natural visual feedback has particularly facilitated servomechanical description of the eye movement in visual tracking.

The general pattern of the present research basically

follows such a control engineering methodology. This chapter first states the objectives of the thesis rather specifically, along with the underlying motivations and rationales. This is followed by a discussion of the significance of the research in some broader perspectives, including its potential application, to areas other than the field of oculomotor control. Finally, a brief editorial note is made regarding the organization of the thesis.

## 1.1 Rationales and Objectives

This thesis attempts to further advance knowledge of the oculomotor system in several research areas, mostly from functional points of view. The investigation deals with three major types of eye movement: dual-mode tracking movement, (pursuit and saccade), optokinetic nystagmus (OKN), and vestibular nystagmus. These eye movement types are regrouped or further divided into subcategories in accordance with phenomenological and functional factors pertinent to the present research objectives. In each of the specific subjects focussed on in this thesis, a series of experiments are devised, performed and evaluated in order to either investigate problems involved or examine a hypothesis posed. All experiments are restricted to the aforementioned categories of the horizontal eye movement in human subjects, and thereby no surgical intervention is involved. The use of humans however, advantageously allows us to introduce a psychophysical approach as developed in the following subsection.

### 1.1.1 On Perceptual Feedback to Oculomotor Centers

Measurement and analysis between physical target motion and eye movement response have formed the basis of most system engineering models proposed in the past for the oculomotor system. The approach introduced herein directs attention to the visually perceived target motion as a potentially useful infor-

mation in addition to the external input/output system variables.

Various behavioral evidence indicates that the oculomotor command signal is intimately involved in giving rise to the visual perception of motion. Conceptually accounting for this visual judgement mechanism is a generally accepted model known as "the outflow cancellation theory" or "the corollary discharge theory" stemming from the classical work of Helmholtz (1866).

The present theme is to examine the converse possibility: the perceived motion might in turn influence the system that controls the eye movement. The subject might produce eye movements based on what he subjectively perceives as a target motion, not necessarily based on physical motion of the actual target nor on the retinal image motion per se. Through this perceptual feedback, the classical model of the visual motion perception in psychophysics would now yield a new closed-loop structure, which would in turn form a skeleton model of the eye movement control system.

While an essentially similar concept has been suggested briefly in the literature (Robinson, 1969, Rashbass, 1969) in interpreting an engineering model proposed by Young et al (1968) for the smooth pursuit system, it is the present objective to further pursue consequences and implications of this hypothesis

to the point of establishing an experimental basis for the perceptual-oculomotor system with respect to the perceived target velocity and smooth pursuit movement. The experiment, to this end, incorporates analysis of eye movements during after-image tracking task under induced vestibular nystagmus.

### 1.1.2 Comparison between Optokinetic Nystagmus Slow Phase and Pursuit Movement

Optokinetic nystagmus (OKN) is maintained by an observer viewing a relative motion of a large visual field, rather than a small spot of target as in the case of the smooth pursuit movement. Despite this difference in the type of visual stimulus, when compared in the time domain, OKN slow phase and the pursuit movement appear to show many common features. Functionally, both eye movements respond substantially to stimulus velocity. These observations might suggest that the two systems share common central neural mechanisms. The object here is to more closely examine this commonly held notion, in terms of time domain transient responses and also frequency responses.

In order to realize pure velocity-step stimuli for an accurate assessment of OKN transient characteristics emphasizing OKN latency measurement, the stripes for the stimulus pattern were generated with computer graphics instead of using the traditional motor-driven rotating drum.

Frequency domain comparison between OKN slow phase and pursuit movement were explored in conjunction with the question of the input-adaptive capacity of the oculomotor system, which is a part of the subject in the following subsection.

### 1.1.3 Input-Adaptive Characteristics of Some Classes of Smooth Type Eye Movement: Quest of Predictive Behavior

The eyes execute both saccadic and smooth pursuit move-

ments in following a continuous motion of a spot of visual target. The visual fixation performance achieved by such composite eye movements is improved with stimulus periodicity, as best demonstrated in terms of frequency response. In particular, the phase lag during the periodic-input tracking is considerably smaller than is observed for the nonperiodic mode, and appears incompatible with the innate oculomotor reaction time, a nonlinear phenomenon that most authors agree to hypothetically attribute to a predictive or learning capacity of the oculomotor system. A similar contradictory phase behavior is known to occur in the situation, where periodic square-wave stimuli are applied and only the saccadic system can be activated.

Given that the predictive behavior is observed in the composite movement, i.e., pursuit plus saccade, as well as for the saccadic system acting alone, the first inquiry here, is as to whether the pursuit component might show such a predictive behavior of its own. Since various evidence indicates that the pursuit system and saccadic system are under separate control by the central nervous system, it should be, in fact, more rational to examine each of the two constituent components separately, rather than in terms of the original composite movement. This approach is made feasible by means of a special hybrid computer processor built by Allum et al (1973) which can extract a continuous trace of the pure pursuit movement by removing all saccades from the original eye movement record. Also emphasized in the present series of visual tracking experiments is the avoidance of the possible nonlinear effect that could result from the pursuit velocity saturation at high stimulus velocities.

The stimulus speed is carefully adjusted during each of the pertinent frequency response measurements. Ignorance of this precaution appears to be a weakness in most previous works dealing with the composite movement causing a certain confusion in assessing the intrinsic nature of the predictive behavior.

Recent results in the literature show the predictive response also in the vergence oculomotor system as well as in the accommodative (ocular lens focussing) system. An analogous input-adaptive behavior is well known in the area of manual control. When this positive evidence is contrasted with the negative evidence reported in the animal's visual tracking system (rhesus monkey) and also in the human pupillary regulating mechanism, it might appear that the prediction belongs to those human sensory-motor activities that are more or less under voluntary control, perhaps, in addition, requiring a visual stimulus. With this motivation, a similar line of study will be advanced as to the search for the predictive behavior in optokinetic and vestibular nystagmus, which are functionally related involuntary eye movements, mediated by different stimulus modalities.

#### 1.1.4 Frequency Response of the Saccadic System with Non-Periodic Input: An Indirect Method

The evidence for the predictive capacity of the saccadic system rests on the observation that its innate reaction time becomes much reduced when responding to periodic square-wave

inputs as compared with the average latency following a sudden initiation of target motion.

The main object here is to obtain nonperiodic-input saccadic frequency response, which has not been done experimentally before. Real assessment of the saccadic system's predictive characteristics could be made only when periodic and nonperiodic-input results are both available.

The latter version could be obtained, in principle, by a random sequence of discrete jumps in target position. However, instead of adopting such a direct method, an indirect approach shall be undertaken basing the evaluation upon the nonperiodic-input frequency response data established for the composite and pursuit system in the series of experiments described in the preceding subsection. The inherent interference effect of the pursuit system upon the saccadic system will be carefully taken into account in order to evaluate the intrinsic saccadic frequency response that would be obtained if the saccadic system were acting alone in response to a random discrete input.

Another objective is to compare the above final result with analytical predictions by Young's sampled data saccadic model (1962), which is intended to describe the saccadic response to unpredictable inputs. This model adequately predicts many basic features of the saccadic response, but has not been tested previously in the frequency domain in terms of intrinsic saccadic characteristics as implied here.



### 1.1.5 Nystagmus Fast Phase Behavior in Relation to Slow Phase Movement in Optokinetic and Vestibular Nystagmus

Regarding either optokinetic or vestibular nystagmus, the following nystagmus features have been described in the literature: fast phase resets the eye ball away from the center in the direction of fast phase, suggesting that fast phase is not a simple centering reflex. As a result, mean over-all eye position normally tends to deviate from center in the above described direction.

These phenomena appear to hold, in fact, in both optokinetic and vestibular nystagmus, according to this author's own preliminary observation showing an almost indistinguishable over-all response pattern in both types of nystagmus in response to sinusoidal stimulation at an equal frequency. This might suggest that there is some common fast phase generating mechanism which utilizes slow phase information irrespective of stimulus modality.

A primary objective is to investigate the function of such a hypothetical fast phase generator by a series of controlled experiments involving constant-velocity as well as sinusoidal stimuli. To this end, various nystagmus parameters will be evaluated in relation to slow phase velocity considering a number of successive nystagmus beats. Behavior of "reset position" (eye position immediately after fast phase) shall be particularly emphasized, for it appears to contain the most pertinent information reflecting the intrinsic functional characteristic of the fast phase generator in question.

The next objective will be to construct a simple mathematical model for this fast phase generating mechanism on the basis of the above experimental results and analysis. While some quantitative models have been recently proposed by others (Schmid, 1971; Barnes, 1973) for vestibular nystagmus accounting for the observed fast phase behavior, the emphasis in the present model making shall lie in the treatment of both optokinetic and vestibular nystagmus within the same functional framework in regard to their fast phase. Such an attempt can be rationalized not only by the similar phenomenological observation between the two types of nystagmus, but also by a functional consideration on the observed direction of fast phase leading to an advantageous quick acquisition of new visual information in both types.

In order to further reinforce the aforementioned emphasis of the model, a search will be made for a pathological case which, in both vestibular and optokinetic nystagmus (in the same patient), breaks the normal trend of fast phase behavior without affecting the normal slow phase response.

Finally, of interest is the OKN pattern change reported by Hood (1967) in a central scotomata patient (one suffering from no foveal vision), where the OKN fast phase direction is toward center as opposed to the normal case described. A selective OKN stimulation to the peripheral retina is possible, by a computer graphic approach to generating the OKN stimulus pattern employing a feedback signal from a photo-electric eye movement monitor.

This feedback-blanking method is expected to mimic the condition of central scotomata in the normal subject. The aim is then to examine whether this arrangement would result in a similar change of OKN pattern in the normal subject as was observed by Hood in the real central scotomata case. That is, to investigate whether or not the response anomaly is simply due to a secondary effect of the absence of central vision.

## 1.2 Applications: Biology, Psychology, Technology and Clinical Medicine

The system engineering approach, when applied to a biological system, as is the case in this dissertation, often finds it necessary to legitimize itself against the methodological skepticism still held by many. Arguments for this defense appear to be already classical. Typical rationalization emphasizes the following two major points as objectives:

- (1) To provide a conceptual framework within which further understanding could be made in terms of physiology and anatomy: guided by a functional relationship described by an engineering model, the physiologist could interpret a result, postulate a hypothesis and design a new experiment in search of the living counterpart of the engineering analog;
- (2) To provide a mathematical description which could quantitatively predict behavior of the underlying process in a new situation: Of particular importance is the application to human engineering, where man and machine interact with each other, each as a separate unit, but only when taken together, create a functioning system. A thorough knowledge of a human's functional capacity as well as his limitations are therefore of great value;

this is especially true when one is confronted by today's ever-increasing technological sophistication observed in the nonhuman part of the system.

First, it should be emphasized here that, in a particular application, failure in one of the above two possibilities does not necessarily jeopardize the other.

As system engineering is concerned with information processing, the degree of achievement toward these goals depends fundamentally upon measurement of relevant signals that reflect the biological system under investigation. The system engineering approach is often referred to as a "black box" method, by which the underlying internal organization is deduced using engineering principles, on the basis of the observed functional relation between the external input/output variables. As such, the physiological and anatomical correspondance may not be determined uniquely. However, this should be due to inavailability of relevant data, and should not be regarded as an inherent limitation of the approach itself. The idea is potentially more than a behaviorism-type assessment of stimulus response relation. Neurophysiological data, for instance, can also be amenable to the system engineering analysis. Once "system engineering" is applied to living systems, it becomes a branch of biological science by itself, referred to as biocybernetics. Like any other discipline of science, achievement of this "system science" depends on information from measurement.

The idea of considering the psychophysical correlate, such as the perceived visual velocity as dealt with here, in addition to physical system variables, represents one step toward the increase of available information sources in the research. Even more important than this is the notion of the perceptual feedback to motor centers. These concepts suggested in this thesis appear to find many potential applications to human sensory-motor behaviors not restricted to the visual-oculomotor system as discussed subsequently. Unlike most cases in experimental psychology, a subjective response is viewed not necessarily as the final output of a system, but as an intermediate signal that could influence the motor output which might in turn affect the subjective response. The impossibility of performing single unit recordings with the human subject could be compensated for by man's privileged ability to express the perceptual impressions that originate in mechanisms internal to this whole perceptual-motor process.

In the thesis, the perceptual-feedback motor concept has led to an organization that contains the two systems, perceptual and oculomotor, at the same time. The psychologist can now take a fresh look at the century-old cancellation theory that has been heretofore essentially an open-loop concept.

A particularly interesting application would be the consideration of various perceptual illusions in close association with the present theme. There is no question that the study of illusions is of significant practical importance, considering its potentially hazardous effect upon manual control. For ex-

ample, a number of aviation accidents have been traced to mis-operations stemming from illusory judgements by pilots. Realizing that an illusion only represents one form of subjective perception, this fact is good evidence for the theory of perceptual feedback in motor response. For instance, one could imagine a situation where a pilot, disoriented by some initial cause, makes a wrong turn resulting in, say, the Coriolis illusion, which in turn might intensify the original illusion and further deteriorate his sensory-motor reconciliation leading to another still worse move. The process could be a hopelessly disastrous loop. The principle behind this instability is quite analogous to that underlying the mutual interaction between visual perception and oculomotor response as conceptualized in this thesis.

Referring back to the oculomotor behavior, if the observer can produce eye movements based on what he perceives as target motion, his eye must respond even to an illusory target motion, as is the case, for instance, in the oculogyral illusion. This illusion has been much discussed in the literature in its relation to vestibular nystagmus, but its exact mechanism is still in dispute. Although the perceptual-oculomotor feedback consideration might well introduce a further complication in substantiating the nature of the oculogyral illusion, such an analysis has a practical value, for example, in design of an instrumentation panel for a vehicle with high acceleration performance capability.

The present after-image tracking experiment, corresponding

to a special case of the oculogyral illusion, could be evaluated also in terms of understanding visual-vestibular interaction.

Study of the input-adaptive nature of the oculomotor system should provide a valuable insight into both basic and applied areas. For example, the dependence on stimulus periodicity in various sensory-motor behaviors might have some relation to the notion of biological rhythm or clocks.

Views suggested to interpret relevant results in this part of the research might be extended to apply in the analogous predictive input-adaptive behavior that has been observed in the realm of manual control. Exploration of this aspect of the human operator's behavior, especially as to the manner in which the neuromuscular delay is compensated, would give valuable insights which could be used as design information for better man-machine systems. Also, once these biological predictive mechanisms are understood, the result in turn could be applied to man-machine systems.

As to the nystagmus fast phase behavior dealt with here, the relevant knowledge could extract further pieces of useful clinical information from nystagmographic data, which have already been of important diagnostic value in otology and ophthalmology. Such a prospect needs to be preceded by close examination of nystagmus records in pertinent pathological cases. The present attention to the clinical report on the OKN pattern change in a central scotomata patient as well as the disturbance of optokinetic and vestibular nystammus in an



acoustic neuroma patient represents an example of such case studies. While the feedback-blanking technique for the special OKN stimulation is developed in this thesis in the above connection, its basic principle appears to offer a new methodology in tackling those controversial problems that are related to the dependence of OKN response upon selective areas of the healthy retina.

### 1.3 Organization of the Thesis

While the thesis consists of eight chapters plus appendices, the scope of the research may be divided essentially into three principal issues: (1) perceptual feedback in the oculomotor control system, (2) input-adaptive or predictive oculomotor characteristics, (3) fast phase behavior in vestibular and optokinetic nystagmus.

Chapter II reviews known properties of the pertinent classes of eye movements, emphasizing functional concepts and control engineering models. Some subjects are discussed critically from standpoints presented in the thesis.

The theory of perceptual feedback eye movement control is explored in Chapter III with particular regard to the smooth pursuit movement.

Investigation of predictive oculomotor behavior is presented in different places in the thesis depending on the particular type of eye movement dealt with: the latter part of Chapter III for vestibular nystagmus slow phase, Chapter IV for the composite and smooth pursuit response in the dual-mode visual tracking, Chapter V for the saccadic component, and finally Chapter VI for optokinetic nystagmus slow phase. (Results from these scattered parts are unified in Chapter VIII, however.)

A study on nystagmus fast phase generation is contained in Chapter VII.

The final chapter, Chapter VIII, summarizes major findings and conclusions of this dissertation, whereas the initial objectives of the research are defined in the current chapter. Chapter VIII also includes recommendations for further research, which are somewhat more specific than the applications of the research already presented.

## CHAPTER II

### The Oculomotor Control System: A Review

This chapter reviews the essence of previous studies on each of the classes of eye movement dealt with in this thesis: dual-mode visual tracking movements (saccade and pursuit), optokinetic nystagmus and vestibular nystagmus. Also reviewed is the literature regarding the predictive oculomotor behavior, a subject pertinent to many of the subsequent chapters. Some specific information, however, is left to relevant chapters, either being omitted or described only very briefly here.

Throughout the present chapter, functional aspects are emphasized in the framework of system engineering concepts with a particular reference to control theory descriptions of the oculomotor system, whereas neurophysiological and anatomical correlates are less weighted. Some background materials are discussed critically from standpoints of the present research. For more general information regarding the biocybernetically oriented oculomotor research field, consult Robinson (1968) or Bowen (1971) for example.

#### 2.1 Dual-mode Visual Tracking Eye Movement

##### 2.1.1 Saccadic System

##### 2.1.2 Pursuit System

#### 2.2 Optokinetic Nystagmus (OKN)

#### 2.3 Vestibular Nystagmus

## 2.4 Input-adaptive Predictive Oculomotor Behavior

2.4.1 Dual-mode Tracking: Composite Response (Saccade and Pursuit)

2.4.2 Saccadic Response to Periodic Square-wave Inputs

2.4.3 Nature of Learning in Eye Movement Control

## 2.5 Summary

## 2.1 Dual-mode Visual Tracking Eye Movement

In tracking a continuous motion of a visual object, the eyes normally execute two distinct types of eye movement: continuous portions, called smooth pursuit, and discrete jumps interspersed among them, called saccade. A typical trace is given in Figure 2.1.

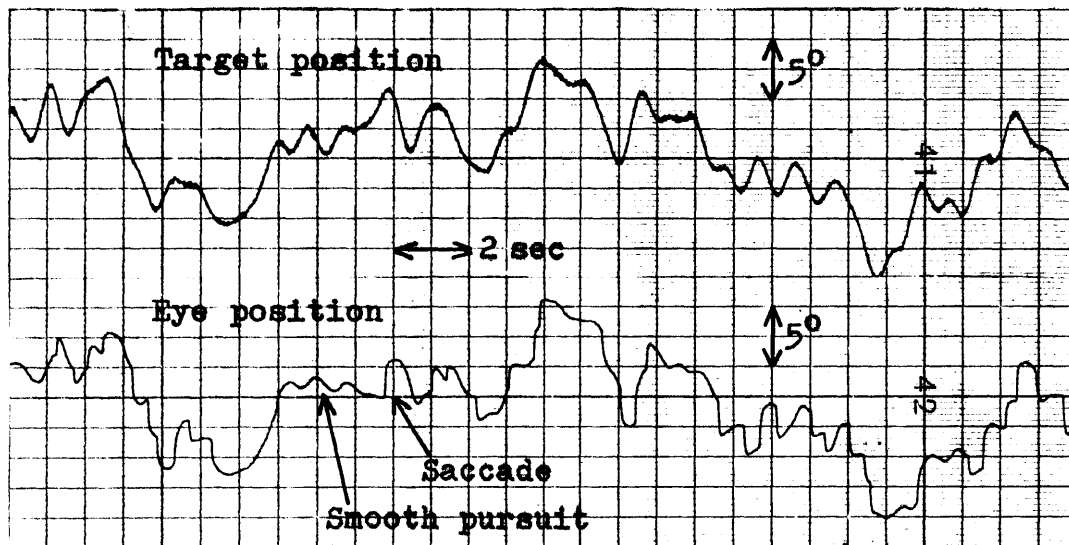


Fig. 2.1 A typical record showing dual-mode visual tracking eye movement.

While a great deal of evidence shows that these two components are under separate control of the central nervous system, they are both used to maintain the image of a moving object on the central field of the retina, the fovea, which provides the best visual acuity. The dual mode of this operation is basically as follows.

The pursuit system controls the eye velocity so as to

match the target velocity. This is done on a continuous basis. The saccadic system has no control upon the velocity response, its task being to correct the position error, which may be caused not only by its own failure, but also may be due to any inadequacy in the pursuit tracking performance. This position error correction by the saccadic system is done, not continuously, but discretely at intermittent instances. If the position error has developed since the previous check so as to find the retinal image outside the foveal region, the image will be brought back to the central area upon execution of a rapid eye movement by the saccadic system.

Many biological systems act as servomechanisms that operate on the principle of negative feedback. The oculomotor tracking system appears to be a typical example, for the innate visual feedback provides the obvious source of negative feedback in the first place.\*

Fender and Nye (1961) were probably the first to attempt to characterize the eye tracking system from a control engineering point of view. Their model is notable especially with regard to the introduction of the frequency response method and the variable feedback technique.\*\* However it does not differ-

---

\* Ocular rotation in a given direction produces an angular shift of the retinal image that is opposite in direction.

\*\* Developed originally by Riggs and Turlumey (1959). Artificial feedback is externally introduced in parallel with the innate visual feedback by adding a signal proportional to the measured eye position to the original signal that drives a target motion. By manipulating value of this proportionality constant, the experimenter can meet any feedback specification of the modified system, including, for example, open-loop and positive feedback conditions.

entiate the saccadic and pursuit modes and cannot account for the functional and behavioral differences between the two. Young (1962) and Young and Stark (1963) published an oculomotor control model which does describe parallel control branches for saccadic and pursuit systems. Also, in contrast with work by Fender and Nye, Young's model is intended to account for those frequency responses obtained with random target motions rather than with periodic ones. The response difference on the stimulus periodicity is one of the most intriguing features of the oculomotor system that will be described later in Section 2.4. However, subsequent materials for the oculomotor system model making in this section assume only the random-input tracking mode.

#### 2.1.1 Saccadic System

The discrete nature of the position control constitutes the most important characteristic of the saccadic system: it stems from the observation made by Westheimer (1954b) that when a step displacement is applied to the target position, the eye responds after about 200 msec with a jumping shift in the same direction. But, if the target steps back to the original position less than 200 msec later, say 100 msec later, after the initial displacement, the returning saccadic jump occurs not 100 msec, but at least 200 msec after the first saccadic response. Figure 2.2 schematically shows these events.



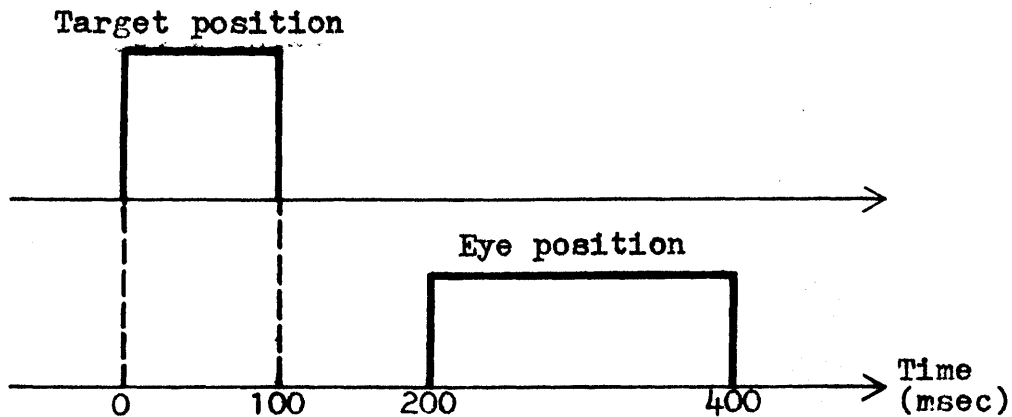


Fig. 2.2 Schematic illustration of Westheimer's observation (1954b) for the characteristic saccadic response.

The implication of this result is that the system is not under a continuous control with a pure delay of 200 msec, which would predict the first and second saccadic to be separated by 100 msec. It is not the simple pure delay of 200 msec alone, but in addition a refractory period of at least 200 msec which can account for this observation.

This is one of the principal bases on which Young (1962) constructed a mathematical model of the saccadic system with application of the sampled-data control theory.\* His sampled-

---

\* Young's original sampled-data model contained both saccadic and pursuit systems, based on the assumption that both of the two systems are discrete and sampled. His pursuit model was a sampled-data velocity servo. However, as will be described in the next subsection, the pursuit system later proved to be continuous rather than discrete, and was so treated in his revised model (Young et al, 1968) for the dual-mode tracking.

data model adequately predicts many aspects of the saccadic response including those observed in the open-loop condition (Young, 1962; Young and Stark, 1963). Since Young's model was intended to be deterministic and mathematically analyzable, it was destined to introduce various simplifications in describing the nondeterministic biological servomechanism. Since the exposition of the original version of Young's model, new observations have been made to disclose many other characteristic behaviours of the saccadic system. Among them are the two most important examples given below.

First, Wheelless et al (1966) modified the classical experiment by Westheimer in that the second step-displacement of the target position was made to go beyond the original baseline onto the side opposite to the first one. In this case, as the duration of the first target pulse decreased from 200 msec, the system tended to respond only to the second displacement ignoring the first one in some probabilistic manner. This may suggest two alternative possibilities or their combination:

- (1) the sampling pulse has a finite but nondeterministic width in which later information is more weighted,
- (2) synchronization of sampling instances relative to the first appearance of target motion is determined only stochastically.

The latter scheme of sampling was considered in the revised sampled-data model of Young et al, and its feasibility was demonstrated by a computer simulation (Young et al, 1968).

Second, Rashbass (1961) demonstrated that, in response to a step-ramp target motion,\* the subject sometimes followed the target with a single pursuit movement and failed to produce a saccade despite the large position error in the early time course. This behavior most often occurred when the magnitude of the initial step and the subsequent ramp velocity were adjusted such that the target recrossed its original position within 150 - 200 msec, approximately corresponding to one saccadic latency period. Taking the relatively large saccadic dead zone (about  $\pm 0.5^\circ$ ) into consideration, a considerable extent of this observation could be accounted for by the finite sampling time and/or by the nonsynchronous stochastic sampler.

Yet, there is still another possibility that the saccadic system might use the velocity information as well to some degree. For example, Robinson (1968) suggests that Young's model could be improved by having some linear combination of the saccadic error and the sampled error rate information for determination of the saccadic amplitude.

### 2.1.2 Pursuit System

Given that the saccadic system and the smooth pursuit system are distinct behaviorally as well as in terms of central mechanisms, separate observation of the two eye movement com-

---

\* Constant velocity target movements preceded by a step movement in the opposite direction.

ponents would be desirable in order to define their functional characteristics more clearly. While a square-wave type discrete target motion can stimulate the saccadic system alone, it is difficult, if not impossible, to design an experiment which produces the smooth eye movement only\*. Another difficulty in making a quantitative description of the pursuit system lies in the fact that this biological system is subject to considerable variability and plasticity. What is known about the smooth pursuit system is more qualitative than quantitative.

It has been shown that the smooth pursuit system fundamentally differs from the saccadic system in two basic aspects: in contrast to the saccadic system, the smooth pursuit system responds substantially to input target velocity rather than target position; and it is continuous rather than discrete.

For example, the aforementioned step-ramp experiment by Rashbass (1961) can be assessed also from the viewpoint of the pursuit system: when a pure pursuit movement is obtained with an appropriately prepared step-ramp input, there is a period of time at the beginning of the movement when the eye is actually moving away from the target although its velocity is approaching the target velocity. Fender (1962), also used a step-ramp, but under open-loop conditions, and reinforced the conclusion that the smooth pursuit system responds to target velocity regardless of target position. However, as will be discussed later, recent studies indicate that the above conclusion is not strictly accurate.

---

\*Some pharmacological agents such as ether are known to suppress saccades without apparent interference with smooth pursuit movement. This type of differentiation can also be found in pathological cases.

Continuous nature of the smooth pursuit system was shown by Robinson (1965). His principal supporting evidence for this is the demonstration that the smooth pursuit system is capable of individual responses to two target motions spaced as little as 75 msec apart. Hence, the system is either sampled at a rate greater than 13 per second or is a continuous system and is not sampled at all.

Robinson (1965) reported three major eye movement patterns in response to a 10 deg/sec ramp input, and the percent of observation for each. His results are redrawn in Figure 2.3. First there is a latency time in response of smooth pursuit movements. Robinson obtained the latency of 125 msec on the average, whereas Westheimer (1954b), Rashbass (1961) and Yarbus (1967) all reported a somewhat higher figure of about 150 msec, for conditions in which the target motion consisted of a series of unpredictable random changes in velocity and direction. In any case, these numbers may be compared to a somewhat higher estimate of 200 msec, which is generally accepted as a working value for the saccadic latency. And it may be of some interest that, as far as latency is concerned, the smooth pursuit system is less variable than the saccadic system (Wheless et al, 1967; Stark et al, 1962; and Fender, 1964).

In Figure 2.3, response 1 is Robinson's most frequent observation (59% occurrence), in which a saccade occurs 237 msec after the onset of stimulus movement. This response type is characterized by overshoot in the smooth pursuit velocity. Young (1969) suggested that this overshoot could be interpreted

Eye position (deg.)

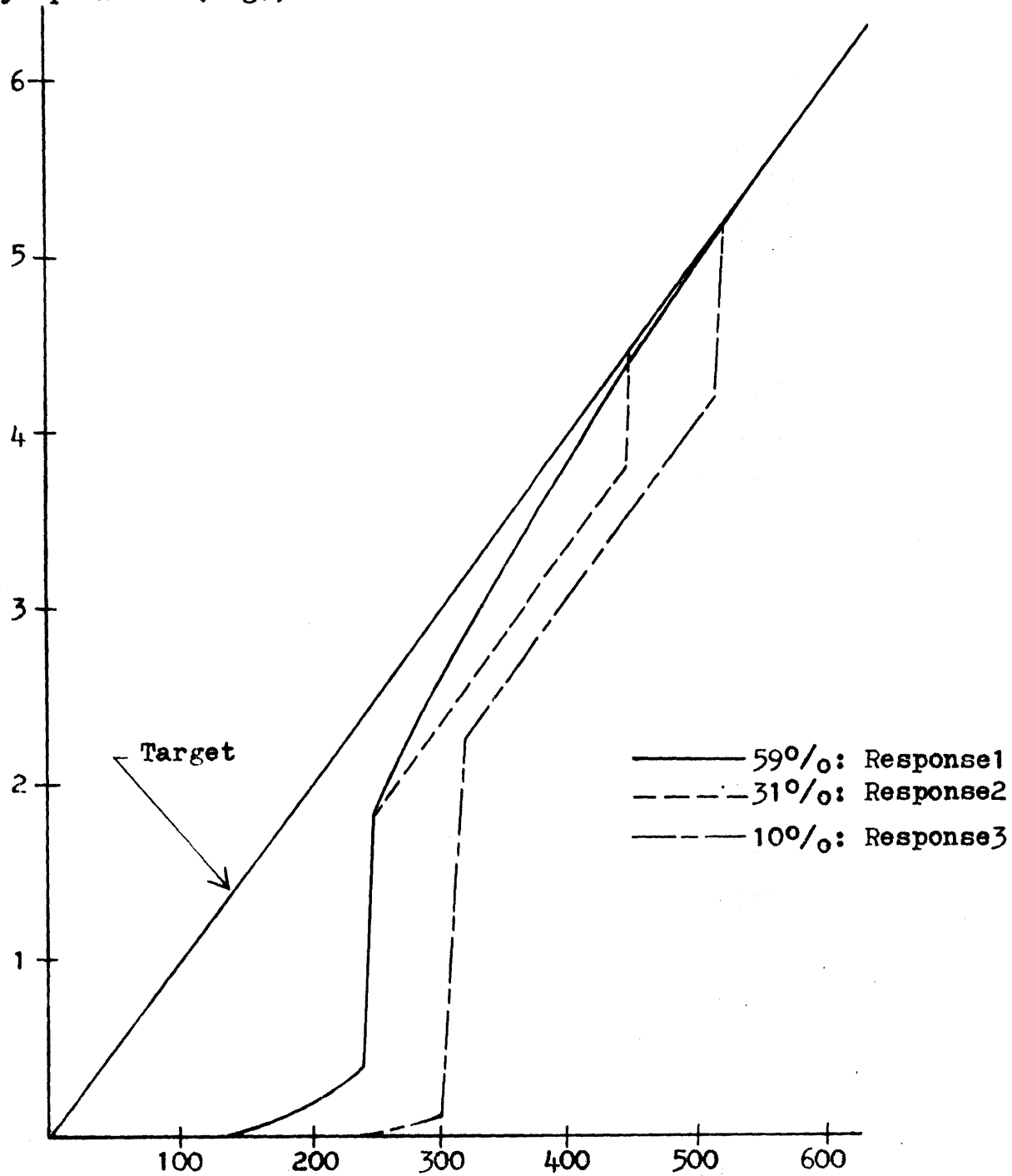


Fig. 2.3 Three typical eye movement patterns in response to a 10 deg/sec ramp input (From Robinson; 1965).

as evidence for the smooth pursuit system retaining some capability of position error correction. Earlier, Johnson (1963) made a similar observation in favor of this view. Such a possibility has, in fact, been indicated by Kommerall and Täumer (1971) who deliberately formed visual after-images slightly off the fovea. The subjects were asked to track such after-images. Their eye movement records clearly show smooth pursuit movements in the same direction as after-image displacement. Hence, the notion that the smooth pursuit system utilizes only velocity information does not seem to be absolute. Probably, the smooth pursuit system responds principally to velocity stimuli, but it is also responsive to position error to some extent.

Robinson's response 2 (31% occurrence), on the other hand, shows no such velocity overshoot, a situation which necessitates a secondary correcting saccade 200 msec after the first. In response 3 (10% occurrence), a saccade occurs quite late and is accompanied by an abrupt increase in the pursuit velocity. This seems to contradict the notion of independence between the saccadic and smooth pursuit systems; as Robinson noted, there is some degree of nonlinear interaction between the two systems in the form of saccadic augmentation which produces discrete appearing changes in pursuit velocity.

The smooth pursuit system has nonlinear characteristics of its own; saturation and threshold. Pursuit movements can be elicited by visual targets moving with angular velocity of up to 30 - 40 deg/sec. Within this saturation limit, eye velocity frequently matches target velocity (Dodge et al, 1930). As to threshold, Rashbass (1961) estimated that a target velocity of at least about 0.8 deg/sec is required to produce any significant

smooth pursuit movement.

Attempts to model the pursuit visual tracking in terms of control systems theory have been confronted by difficulties that arise chiefly from the pursuit system's inherent high degree of variability as well as from the limitation in selectively stimulating this oculomotor system. Even so, the notion that the pursuit system is a velocity servo independent of the saccadic system appears to be a useful concept, at least as a first-order approximation. A difference between the target velocity and the eye velocity would be the performance error of this velocity servo system which, owing to the visual feedback, is available as velocity of the retinal image relative to the retina. Detection of a relevant error signal is a crucial prerequisite to any servo operation, and velocity of retinal image in fact has been electrophysiologically identified at various levels in the visual pathway, depending on the evolutionary stage of the animal's visual system (Barlow et al, 1964; Hubel and Wiesel, 1962; Sterling and Wickelgren, 1969). The error information is in turn to be used for providing new eye movement appropriately so as to reduce the error and thus to achieve the goal of eye tracking. A linear velocity servo in general can be cast into a block diagram as shown in Figure 2.4.

In terms of the oculomotor servo elements to be identified in this block diagram, transfer function,  $G_c(s)$ , characterizing the controller, determines how the velocity error signal should be transformed neurologically before being used as smooth pursuit oculomotor command, and the transfer function,  $G_p(s)$ , char-



acterizing the plant or controlled element, describes how the eyeball would respond mechanically to that oculomotor command.

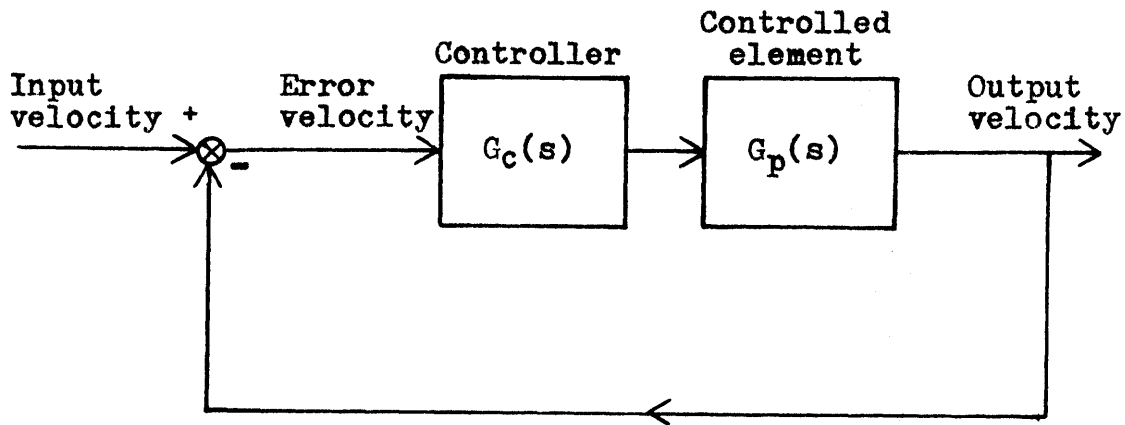


Fig. 2.4 Basic structure of a linear velocity servomechanism.

A transfer function is operationally equivalent to a linear differential equation, in that one can be derived from the other by the method of Laplace which involves a transformation between corresponding variables (Laplace variable,  $s$ , and time,  $t$ ). Both mathematical expressions can predict the behavior of a system or of a component within a whole system, in terms of how the output signal will act in relation to a given input. In theory, a transfer function can be written only for systems which are linear and deterministic. However, no physical systems, especially biological ones, meet such a requirement perfectly. As noted previously, the smooth pursuit system manifests a considerable degree of variability along with its inherent nonlinear properties.

Yet, to give up the transfer function method because of its theoretical limitations in the face of the above facts, would mean the loss of many of the benefits expected from the control engineering approach. The application of transfer functions in analyzing the pursuit system then could be justified only as a qualitative means to conceptualize underlying principles, rather than as a quantitative means to make deterministic predictions upon system responses.

An analysis based on input-output (target movement - eye movement) measurements could enable one to make engineering inference only upon the combined transfer characteristics of the neurological controller,  $G_c(s)$ , and the globe mechanical plant,  $G_p(s)$ . In general, elements that constitute the internal structure of a system cannot be differentiated by such a stimulus-response type approach alone. This inherent limitation calls for the measurement of some other relevant information carried along signal flows that embody the oculomotor control system. For example, force measurements and electromyographic recordings have begun to identify  $G_p(s)$  describing the mechanical characteristics of the eye (Robinson, 1964 and 1965; Thomas, 1967 and 1969; Cook and Stark, 1967; Childress and Jones, 1967). These works have arrived at mechanical descriptions that differ considerably from Westheimer's earlier model (1954a, b). It has been revealed that the eye ball dynamics have corner frequencies much lower than Westheimer's prediction.\*

---

\*Westheimer's model was derived from the oversimplified assumption that a saccade was a step response of the ocular mechanical apparatus. Though too simple a description now, the model was the first mathematical analysis of the globe mechanics considering passive mechanical elements, such as inertia, elasticity, and friction involved in the building tissues.

As to the transfer function for the neurological transformation,  $G_c(s)$ , Young's earlier pursuit model (1962) for example, making a correction to yield its continuous version, gives the form of  $(Ke^{-st})/s$ , i.e., gain  $K$ , integration  $1/s$  and latency  $e^{-st}$  in series. The involvement of one integration renders this pursuit model a type one servo. As Young later (1969) argued, in the presence of the relatively large latency, the notion of a type zero servo, in which there is no integration, would be precluded for reasons of loop stability.

In the course of making revisions on his previous model, as an alternative to resolve the stability problem, Young et al (1968) proposed a continuous nonfeedback model in which smooth pursuit movements respond not to the retinal error velocity per se but to the velocity of the target itself. In support of this view, Childress (1967) demonstrated that retinal slip of a target is, in itself, not a sufficient stimulus for pursuit tracking: A sudden mechanical release of the eye ball from a deviated position failed to induce corrective pursuit movement, despite the fact that the image of a stationary fixation point slowly moved across the retina. Implication of the above pursuit model of Young et al, has been suggested by Robinson (1969) and Rashbass (1969), and it will be discussed in Chapter III, as it essentially leads to the central concept explored in that chapter.

## 2.2 Optokinetic Nystagmus (OKN)

Optokinetic nystagmus (OKN) is maintained by an observer viewing the relative motion of a large visual field rather than that of a small and specific visual target. Eye movement of a train passenger looking through a window is a good example. The traditional laboratory device for OKN study is a rotating hollow cylinder with its inside wall featuring black and white vertical stripes. As shown in Figure 2.5, OKN typically manifests a saw-tooth-wave pattern formed by rhythmically alternating fast and slow phase components. The response is very reflexive and involuntary in nature.

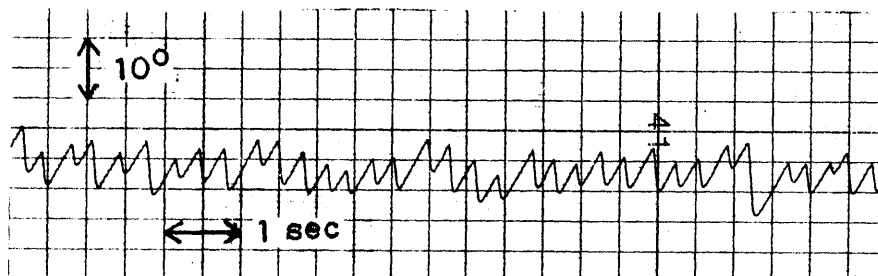


Fig. 2.5 OKN eye movement responding to a constant velocity of stripe pattern

Like the smooth pursuit movement, OKN slow phase is responsive substantially to the stimulus velocity. Its function

is to minimize slip motion of the retinal image so as to maintain a clear vision of the moving visual surroundings. There are some other response features shared with the pursuit movement, as will be described in Chapter VI. There appears to have been a trend to presuppose that OKN slow phase component is simply a smooth pursuit tracking movement, an idea that will be closely examined in Chapter VI.

Due to obvious mechanical restraints, the eye ball can travel along its orbit only a finite distance in either direction. This calls for a means to reset the eye ball in a new position from which the slow phase movement can start again. This requirement is sufficed by fast phase, but this resetting behavior is not a simple centering reflex as explored in Chapter VII.

Finally two distinct OKN patterns have long been known to occur in humans, depending on the subject's mental attitude while performing OKN (Ter Braak, 1936; Rademaker and Ter Braak, 1948; Nelson and Stark, 1962; Honrubia et al, 1968): One pattern can be produced following the instruction, "stare straight ahead". This category is characterized by a tendency toward small amplitude and high frequency nystagmus beats. The other pattern requires the instruction, "follow the stripes". This type shows a lower frequency and greater average amplitude. The former version of OKN is called subcortical or "stare" OKN, whereas the latter is called cortical or "look" OKN. This classification rests on some circumstantial evidence as to whether the cortex participates or is not involved in the nystagmus production.

For instance, the "look" OKN may need some degree of conscious or voluntary effort, while animals supposedly can perform only the "stare" type OKN. In any event, it is the "stare" type of OKN which will be meant by the term OKN henceforth in this thesis.

### 2.3 Vestibular Nystagmus

The potential stimulus to the oculomotor system is not restricted to be visual. An example of this is the oculomotor reflex maintained during more than minimal head rotation in space. Its pure form can be observed in the dark with no visual cues; otherwise it would be interfered with by possible additions of OKN. Figure 2.6 presents a typical nystagmus record of human vestibular nystagmus responding to a sinusoidal angular head motion about the earth-vertical axis.

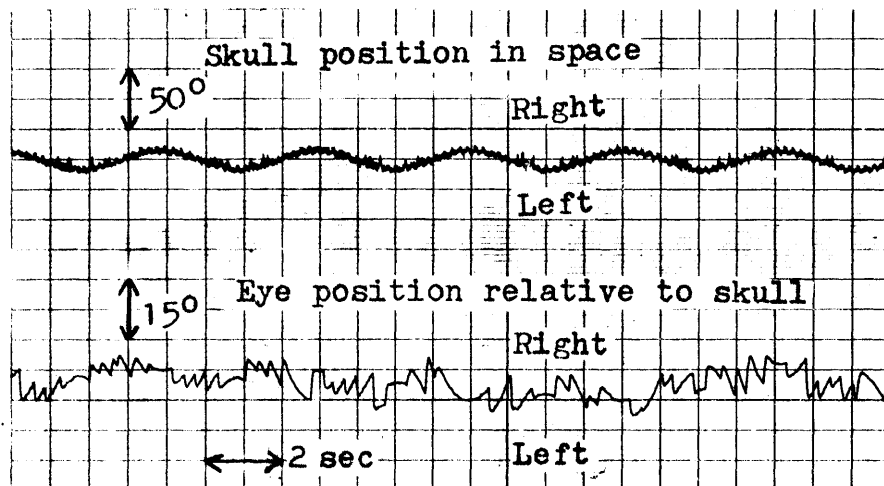


Fig. 2.6 Typical record of vestibular nystagmus with sinusoidal skull rotation

As in the case of OKN, the normal response pattern is characterized by a slow and a fast phase component. The role of the fast phase is presumably similar to that described for OKN. The direction of slow phase movements with respect to the

skull tends to be opposite to that of the head motion in space, as is apparent in Figure 2.6. The interpretation of this feature is that the slow phase movements help to compensate for head movements arising from various daily activities, which would otherwise blur the visual images on the retina. Thus, it appears that, although vestibular and optokinetic nystagmus are mediated by different stimulus modalities, both have evolved for the same behavioral end, the maintenance of clear visual information against a changing visual environment resulting not only from motion of the optical surroundings themselves but also from the observer's own head movements.

The sense organs responsible for the oculomotor reflex to head rotation are the three semicircular canals arranged approximately orthogonally in the inner ear.

Each canal is filled with a fluid, endolymph, which flows within the canal duct whenever an angular acceleration in the plane of the canal is experienced by the head. Motion of the endolymph moves the cupula, a gelatinous structure occluding an enlarged portion of the canal, the ampulla. The cupula deflection is detected by underlying sensory haircells and coded into neural discharge rates in the nerve endings synapsing on them.

The mechanics of the semicircular canal have been described by a torsion pendulum model stemming from the work of Steinhausen (1931). This model is characterized by second-order dynamics: the inertia, spring restoring torque and damping of a torsion pendulum are analogous, respectively, to the inertia of the



endolymph ring, the elastic restoring force of the cupula, and viscous damping of the endolymph in the canal. Upon normalization, the pendulum model leaves three constant parameters to be determined numerically. Experimental evidence in animals indicates that the dynamics are overdamped, and characterized by two widely separated time constants.

Since the first exposition of the torsion pendulum model, evaluation of two time constants in humans has relied on behavioral experiments. There are two major methods: one based on the measurement of subjective sensation of rotation velocity and the other based on the measurement of vestibular nystagmus slow phase velocity. The key assumption on which these methods rest is that the cupula displacement signal is proportional to the subjective velocity for the former method, and to the nystagmus slow phase velocity for the latter.

For the rotation about the earth-vertical axis with the head erect, these procedures have yielded the value of the long time constant ranging from 7 to 10 seconds as evaluated from subjective sensation (Van Egmond et al, 1949; Groen, 1960; Jones et al, 1964), and the value ranging from 8 to 16 seconds as evaluated from nystagmus (Groen, 1960; Jones et al, 1964; Benson and Bodin, 1965). The short time constant, on the other hand, has too small a value to be directly assessed experimentally. Based on a resonance method employing a torsion swing, Van Egmond et al (1949) obtained an estimated value of 0.1 second for the short time constant\*.

---

\* Theoretical estimates suggest, however, that the actual value must be considerably shorter, on the order of 0.005 second (Steer, 1967; Money et al, 1971).

The wide separation of the two time constants, as evidenced above, has led to a prediction that there is an extensive frequency range in which the cupula displacement becomes approximately in phase with the angular velocity of the head. Jones and Milsum (1965), Mayne (1965), Meiry (1965) and others have stressed that, within such a frequency bandwidth, the semicircular canals act as integrating accelerometers or velocity transducers and that the nystagmus slow phase becomes compensatory. Making the reasonable assumption that the two time constants of the torsion pendulum model are 10 seconds and 0.1 second, this frequency range would become from 0.017 Hz to 1.7 Hz. A considerable amount of data are available for subjective and nystagmus frequency responses (Niven and Hixon, 1961; Meiry, 1965; Hixon and Niven, 1970; Benson, 1969). Nystagmus Bode plots as reproduced from these authors are shown in Figure 2.7. These experimental results are in fair agreement with the foregoing frequency domain predictions, except for some discrepancies notable in the lower end of the bandwidth particularly for subjective data, and in the higher end for nystagmus data.

These discrepancies, combined with some departure from the torsion pendulum model evident in the time domain data, lead to the conclusion that both the subjective velocity and slow phase velocity are not precisely proportional to the cupula displacement as assumed before.

Young and Oman (1968) proposed a mathematical "adaptation model", which modifies the cupula signal in giving rise to the subjective velocity in a manner to decrease its response with

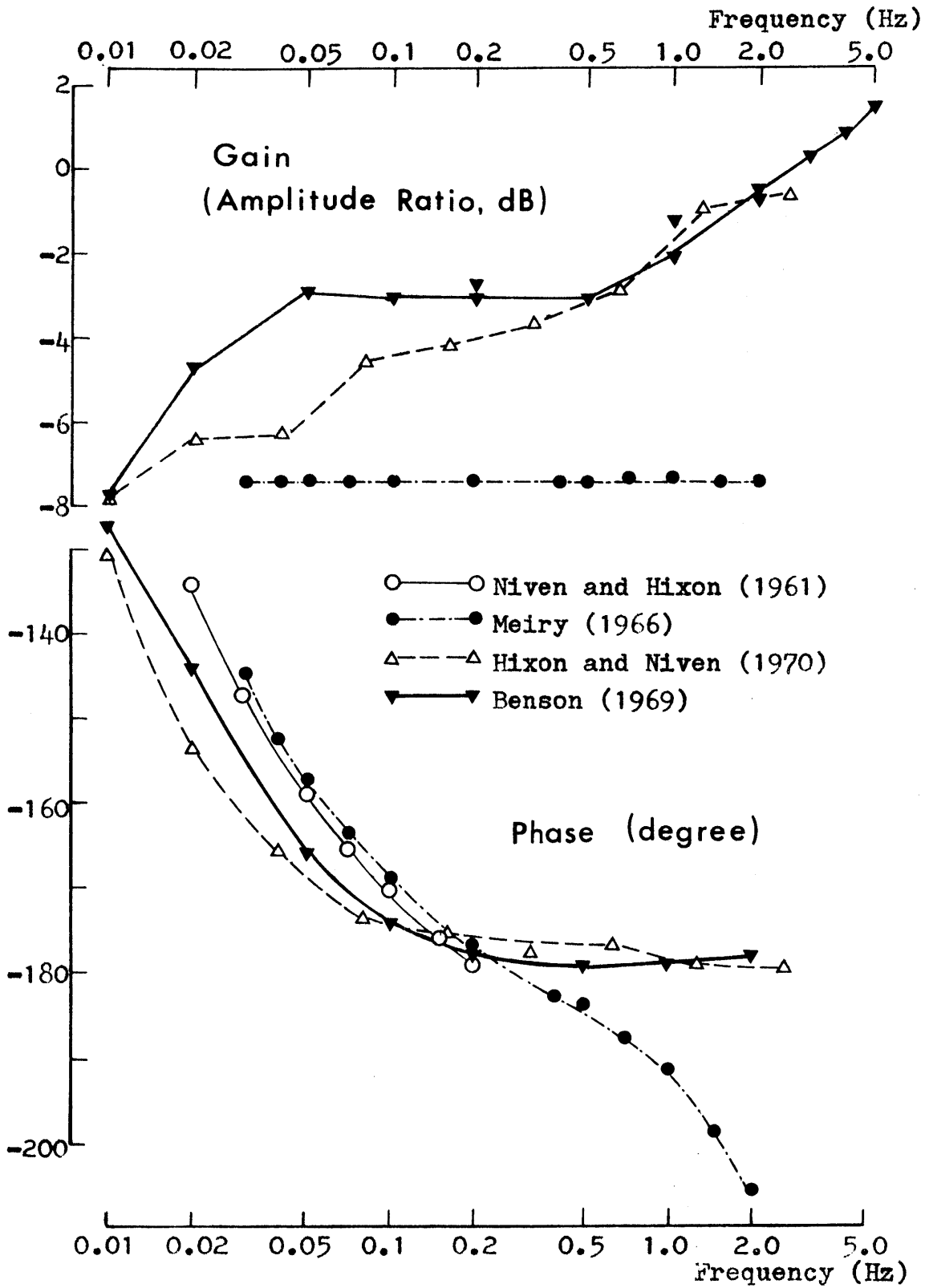


Fig. 2.7 Frequency response of vestibular nystagmus slow phase (input = head velocity; output = eye velocity).

a time constant of 30 seconds in the subjective pathway and 120 seconds in the nystagmus pathway.\* Their adaptation model accounts for some overshoot in the subjective velocity observed following a velocity step input, and it accounts for the apparent difference in the long time constant estimated from the subjective and nystagmus data. In terms of frequency domain, these adaptation models improve the torsion pendulum model in the low frequency region.

As shown in Figure 2.7, a marked departure of the high frequency nystagmus data from the torsion pendulum model (starting at about 0.5 Hz) has been reported by Niven and Hixon (1970) as well as by Benson (1969).\*\* It seems as though a lead network were cascaded to the torsion pendulum model.

Recently, similar high frequency lead and low frequency adaptation behavior was revealed from single unit recordings of first order afferents innervating the semicircular canal of the squirrel monkey (Goldberg and Fernández, 1971). This finding indicates that rate sensitive and adaptive dynamics are manifest in the periphery. These effects could either be due to peripheral, inherently afferent mechanisms and/or be the result of more central activity mediated in the periphery via efferent pathways.

Apart from the above phenomena, it may be said that the slow phase movement is compensatory in nature with its velocity

---

\* According to Oman's latest evaluation (1972), the nystagmus adaptation time constant ranges from 60 to 120 seconds.

\*\* It is suspected that the eye movement measuring device used by Meiry happened to involve a first-order lag filter with a cut-off frequency of about 0.5 Hz. If this had been the case, this filter would be cancelled by the above lead network, and his result would essentially describe the torsion pendulum model itself, as appears to be the case.

being approximately proportional to the head angular velocity in magnitude.\*

Since the input to the vestibulo-ocular system is an angular acceleration of the head and the final output is an angular deviation of the eye, a double integration must exist between the transduction of acceleration and subsequent instantaneous eye position. As described already, the first integration is mechanically performed by the semicircular canal in the frequency range of present concern. The question is as to where the second integration takes place. Robinson (1968 and 1969) noted that the globe and extraocular muscles would be very inaccurate as another possible mechanical integrator due to the presence of other poles and zeros in its transfer function (Robinson, 1965), and that this "pseudo-integrator" would not become effective until about 0.6 Hz. Based on circumstantial evidence, Robinson then went on to speculate about the brainstem reticular formation as a probable site of the second integration, and he also suggested that this integration can be reset by a train of impulsive bursts of discharge rate, which has been found to co-

---

\* The angular velocity of the skull is not completely matched by the relative velocity of the eye with respect to the skull. the latter is only 40% - 60% of the former as is evident from the amplitude plots of Bode diagram given in Figure 2.7. The compensation is not perfectly achieved by the vestibulo-ocular reflex alone, a fact stressed by Meiry (1965) and others. In natural environments, visual surroundings provide additional stimuli for producing smooth pursuit movement or optokinetic nystagmus to cooperate with the vestibular system in stabilizing visual images during head movements. Meiry also stressed the role of the neck proprioceptors in contributing to this stabilization.

relate with the nystagmus fast phase occurrence (Schaefer, 1965; Yamanaka and Bach-y-Rita, 1968; Horcholle and Tyč-Dumont, 1968).

Sugie and Jones (1965 and 1966), on the other hand, stressed the functional significance of the fast phase in regard to the integration in question. According to them, the nystagmus fast phase is viewed not merely as a resetting means but also as an operation crucial for accomplishing the integration over the neural signal coming from the cupula. They maintain that each fast phase saccade is not a simple step change in position but has an exponentially decaying tail following the initial saccadic jump. This tail is usually hidden in the slow phase trace, but actually each fast phase, whenever it occurs, contributes to the slow phase by means of the tail which produces an additional slow phase component. Individually such contributions may be small, dying out quickly with a time constant of 1 second or so. However, there are so frequent successive fast phases that the above effect becomes cumulative so as to eventually develop a key functional role in integrating the incoming cupula signal. These authors have formulated this process mathematically, and later Outerbridge (1969) has made further theoretical refinement including a series of computer simulations. This notion of Sugie and Jones could affect discussions for interpreting experimental results in Chapter III. However, some counterevidence is cited against the theory in that chapter.\*

---

\* The principal experimental evidence for Sugie-Jones theory stems from their comparative close examination of slow phase movements in cats during different degrees of fast phase suppression using varying levels of ether anaesthesia.

## 2.4 Input-adaptive Predictive Oculomotor Behavior

The performance attained by visual oculomotor tracking depends upon the complexity of the stimulus wave form: Fixation on the moving visual object is maintained more accurately if the object is driven by a regular periodic signal than if it is driven by an apparently nonperiodic and random signal. This input-adaptive phenomenon has been explored by many investigators in certain classes of the visual tracking task, and their major results are reviewed here.

### 2.4.1 Dual-mode Tracking: Composite Response (Saccade and Pursuit)

The predictive behavior has been studied extensively in the past, particularly for eyes that execute both saccadic and smooth pursuit movements in following a continuous motion of a visual object. It is best demonstrated in terms of frequency response data (Bode plots) obtained with periodic versus non-periodic inputs.

The frequency response was obtained first for regular sine wave inputs by Sünderhauf (1960) and subsequently by many others (Fender and Nye, 1961; Stark et al, 1962; Dallos and Jones, 1963; Werner et al, 1972). Their Bode plots are redrawn in Figure 2.8.\* These results agree on the following general point:

---

\* If the tracking were perfect, amplitude ratio (gain) would be unity (0 dB) and there would be no phase shift.

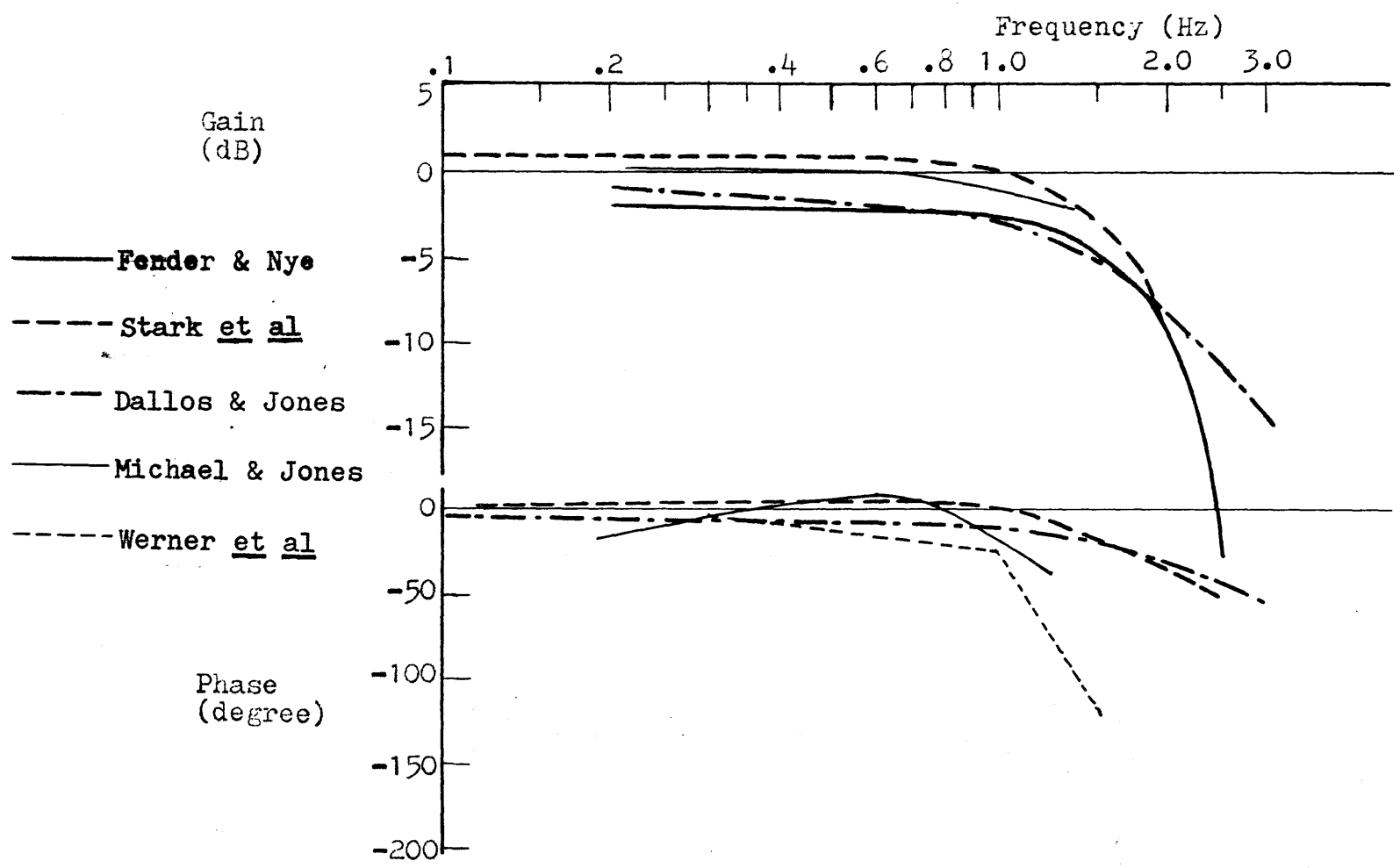


Fig. 2.8 Periodic (sine wave)-input composite frequency response data from previous publications



the phase lag in the low and intermediate frequency range is surprisingly small if one considers the system's inherent reaction time. As noted earlier in this chapter, the saccadic and pursuit systems have their average latency time of about 200 msec and 150 msec respectively. To assume even the shorter value of 150 msec for representing the over-all reaction time would lead one to predict a phase lag of about 1 radian ( $57^\circ$ ) at 1 Hz, resulting from this pure delay only. The actual phase lag, however, was at most  $30^\circ$  at that frequency, as indicated in Figure 2.8. Even some phase lead was observed at intermediate frequencies by some of these authors. It is, in part, this phase discrepancy which has led many investigators to postulate the existence of some neurological predictive mechanism for overcoming the innate neuromuscular transmission delays in the oculomotor system.

There have been repeated arguments in the literature as to the less-than-minimum phase characteristics observed in the predictive tracking. For example, results by Stark et al and by Dallos and Jones, as presented in Figure 2.8, indicate that the gain starts to decline quite rapidly between 1.5 Hz and 2.0 Hz. But phase lag in that frequency region is still small. It is, in fact, too small to be expected from the phase-attenuation theorems of Bode. Consequently, the system has been said to be of the less-than-minimum phase type.\*

---

\* See Appendix F for Bode's theorems and the less-than-minimum phase characteristics. The predictive nature of the periodic eye tracking refers to the phase lag being considerably smaller than that expected from the average oculomotor reaction time. The phase-gain relation is not necessarily essential to the predictive behavior per se.

However, there appears to be some question as to the relevancy of discussing these composite (saccade and pursuit) frequency response results in terms of Bode's theorems: There are reasons to suspect that the maximum target velocity might have exceeded the saturation limit of pursuit velocity in many of the published experiments dealing with composite response, particularly in the high frequency range which is most crucial to the present issue on the phase-gain relation. In the first place, one must be very careful about minimizing any a priori known nonlinear effect in the course of a measurement, if one is to work with the frequency response which is a linear concept. Otherwise, the frequency response would lose its meaning, and consequently so would Bode's theorems. As noted previously, pursuit tracking suffers from velocity saturation at target velocities higher than about 30° per second. This implies that the position amplitude of an input sinusoid at 1 Hz, for example, should be kept under 4.8° in order to avoid the saturation effect in pursuit response.\* This limiting value for allowable position amplitude becomes smaller with increasing frequency.

The experiment by Werner et al quite possibly violated this restriction, for they used stimuli with constant position amplitudes as large as 50°, 38.6° and 26.4° for all the frequencies

---

\* Stimulus velocity = stimulus position amp. x  $2\pi f \cos 2\pi ft$ .  
Max. stimulus velocity = stimulus position amp. x  $2\pi f$   
Max. allowable stimulus position amp. at  $f$  = pursuit saturation velocity /  $(2\pi f)$  = 4.8 /  $f$   
Max. allowable freq. for a given position amplitude  $A$  = pursuit saturation velocity /  $(2\pi A)$  = 4.8 /  $A$ . where pursuit saturation velocity is assumed to be 30°/sec, and  $f$  and  $A$  are given in Hz and degrees respectively.

they examined. Michael and Jones used a constant amplitude of  $15^\circ$ , which gives the maximum allowable frequency of only 0.32 Hz. Though others apparently had much smaller position amplitudes, they were not very specific about this matter in their publications. Even so, assuming that they used the same amplitudes for all frequencies as indicated in their sample traces at particular frequencies, the amplitude was  $5^\circ$  for Stark et al, and  $2^\circ$  for Dallos and Jones. Accordingly, the latter authors probably met the amplitude requirement up to about 2.4 Hz. Yet, this is still not quite high enough to ascertain their less-than-minimum phase relationship as apparent in the frequency range from 2.0 to 3.0 Hz. The amplitude of  $5^\circ$  adopted by the former investigators appears worse from the standpoint that the pursuit linearity was perhaps good only up to about 0.95 Hz.

Fender and Nye (1961) performed the variable feedback experiment with regular sine wave stimuli. By using a constant input amplitude of  $3.4^\circ$  for each test frequencies (as stated clearly in their report), they found the less-than-minimum phase characteristics in the open-loop condition. By definition of the open-loop condition, this amplitude was not that of the actual stimulus exposed to the eye, but that of the input signal for driving the whole open-loop system: the stimulus motion actually seen by the subject was provided by the sum of the above input signal and the signal representing his eye movement. Therefore the stimulus amplitude could not have been smaller than  $3.4^\circ$

at any frequency, and hence their stimulus velocity was probably not under the presumed pursuit saturation velocity at least for frequencies greater than 1.4 Hz. Moreover, the eye movement in the low to intermediate frequency range for the open-loop condition tends to become much greater than the original driving signal, as found by Fender and Nye themselves and by later investigators. Taking this into account, the frequency of the allowable limit might have been even lower. Checking with one of their data points, for instance, at 0.6 Hz, the open-loop gain is 10 dB which corresponds to 3.2. Hence, the amplitude of the stimulus becomes:  $3.4 \times (3.2 + 1) = 14.2^\circ$ . The maximum stimulus velocity at this frequency is therefore:  $2\pi \times 0.6 \times 14.2 = 57.5^\circ$  per second, which is about twice as large as the pursuit saturation velocity assumed in this calculation. In view of this, the less-than-minimum phase behavior found by Fender and Nye in the open-loop condition could have been, at least in part, due to the nonlinearity of saturation type in the pursuit system.\*

In concluding the present argument, the pursuit saturation would reduce pursuit gain by definition, which would in turn, imply a certain decrease in composite gain. But, the saturation type nonlinearity is only amplitude sensitive, so that the phase part of the Bode plot would exhibit little dependence on input magnitude level. The result would be an apparent less-than-minimum phase characteristic. Work by Watanabe and Yoshida (1968)

---

\* In this work, Fender and Nye used another amplitude of much smaller value ( $1.1^\circ$ ) for the driving signal. However, the corresponding Bode plot for the open-loop condition was not presented in the publication.

supports this point. They tested different amplitudes ranging from  $0.5^\circ$  to  $7^\circ$  for the predictive tracking. Their data show that composite gain decreases progressively with increasing stimulus amplitude at a given frequency in the intermediate-high frequency range, but phase lag is affected by input amplitude variation to a much lesser extent. At 1.5 Hz, for instance, gain was as much as 10 dB less with  $7^\circ$ -amplitude input than with  $0.5^\circ$ -amplitude input, whereas phase lag was  $35^\circ$  and  $25^\circ$ , respectively, for the former and latter input. This result thus indicates the possibility of observing an apparent less-than-minimum phase characteristic with large stimulus amplitudes.

While the precaution to avoid the pursuit saturation by keeping a small enough input amplitude appears to have been somewhat overlooked previously in the frequency response measurement (not only in the foregoing predictive case, but also in the subsequent nonpredictive case), smaller input amplitudes would increase another nonlinear effect due to the saccadic dead zone. This implies an inherent limitation in maintaining over-all linearity of the composite system. Work in this thesis on the present aspect of the visual tracking system (Chapters IV,V) emphasizes the above consideration in addition to the central idea that the pursuit and saccadic response, being known to originate from separate systems, should be assessed separately.

In any event, previous studies on the nonperiodic-input case are reviewed next.

If the previous small phase lag in contradiction to the neuromuscular delay were due to a predictive mechanism, prediction of future target information should be much less easy

for nonperiodic inputs so that such a predictor would no longer be very powerful. Appropriate stimuli and a Fourier analysis on stimulus-response data are required in order for the nonperiodic-input frequency response to emerge. This was done by Young and Stark (1963)\*, and by Dallos and Jones (1963). Their results and those by later investigators (Michael and Jones, 1966; Werner et al, 1972) are presented in Figure 2.9.

Before comparing those results with the previous predictive ones, one should note that some quantitative discrepancies evident within these nonperiodic-input results must not be taken very seriously, for detailed experimental protocol differed from one author to another in many ways. Among them were the method for generating the nonpredictable target motion, its magnitude at various frequencies, and of course, the particular subjects used: First in order to prevent the subject from anticipating future target motion, Dallos and Jones as well as Michael and Jones employed Gaussian random signals supplied by the low-frequency random noise generator with appropriate filtering, where others used a sum of at least four sine waves of incommensurate frequencies to drive the target. Thus the degree of randomness somewhat depended on the particular authors. Second, no specific information was found in any of these reports as to the stimulus position amplitude or maximum instantaneous velocity.

---

\* Instead of the nonpredictive Bode plot given by Stark, Vossius and Young (1962), which did not show the characteristic peak in gain plot, one of their later publications (Young and Stark, 1963) is referenced here.

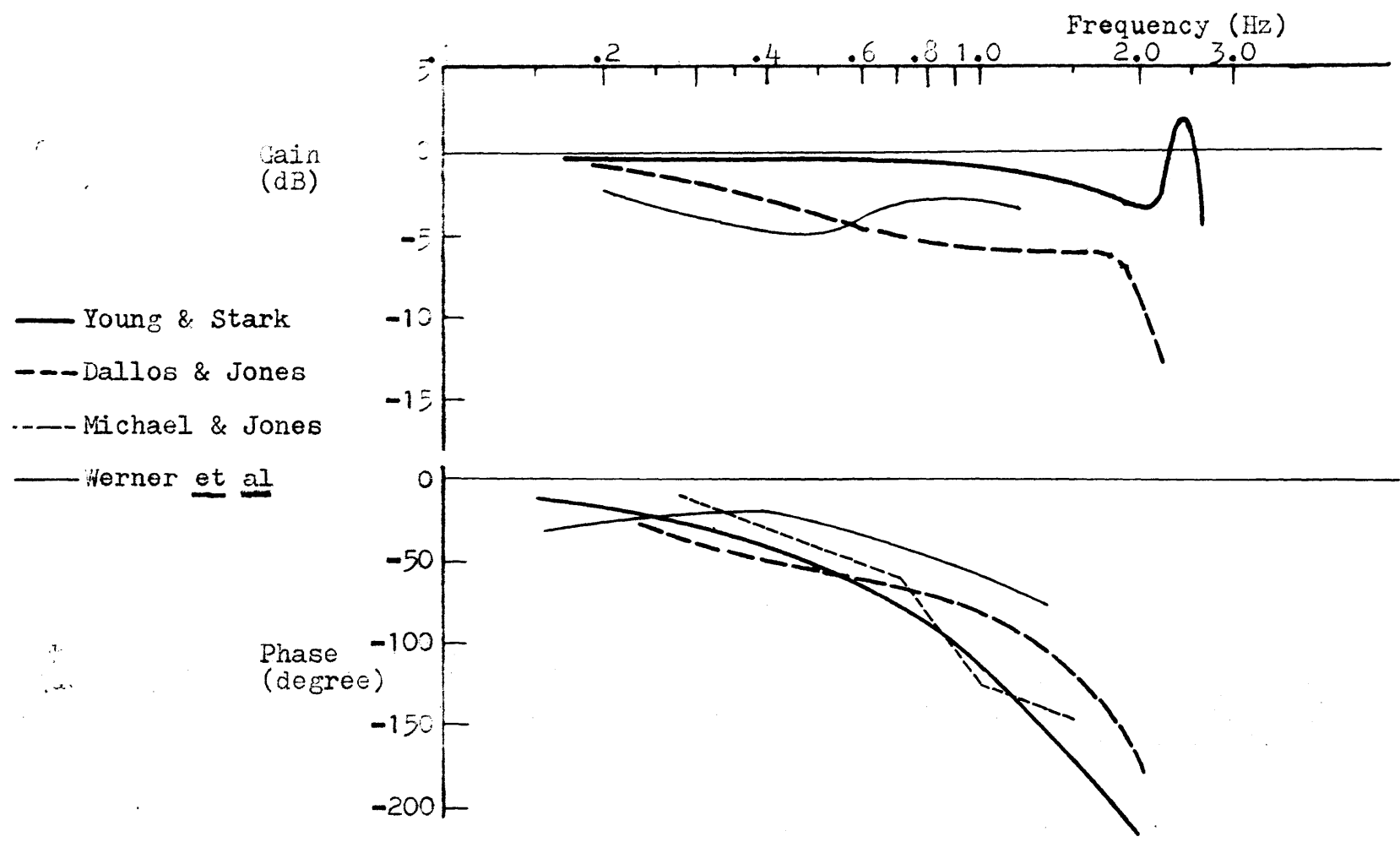


Fig. 2.9 Nonperiodic-input (pseudo-random) composite frequency response data from previous publications

(At best, Michael and Jones indicated a RMS value of  $6.29^\circ$  for their random signal.) As emphasized in the previous subsection, the stimulus motion should be controlled carefully for minimizing potential system nonlinearities. Otherwise, the Bode plot would become different from one measurement to another, depending on how nonlinear the system is during each measurement. Finally, Wheelless et al (1967) report the effect of target luminance as well as the effect of its contrast against the ambient light upon the Bode gain plot.

Nevertheless, the Bode plots given in Figure 2.9 show certain common features and indicate some clear difference from the predictive tracking case: the gain starts to decline at a much lower frequency (when compared within the same authors), though it increases again and subsequently exhibits a conspicuous peak in the high frequency region due to saccades. The phase lag is much greater, as much as  $60^\circ$  at 1 Hz; in contrast, it was at most only  $30^\circ$  at 1 Hz in the predictive case.

Unlike the predictive case, an essentially minimum-phase transfer function plus a pure delay can approximate at least some of these nonperiodic-input Bode plot results: A formal curve fitting by Dallos and Jones (1963) using a second-order lag, a lag-lead and a pure delay in series was successful for their own gain and phase data. A prediction based on the revised sampled-data model of Young et al (1968) is also in fair agreement with these nonperiodic-input frequency response results in general.



Dallos and Jones (1963) computed the open-loop transfer function both for periodic and nonperiodic inputs, on the basis of their corresponding closed-loop experimental results presented here. Their object was to deduce what transfer function should be cascaded with the nonperiodic-input open-loop transfer function in order to realize the periodic-input open-loop transfer function. The resultant transfer function would have to represent the predictor. According to this result, the predictor contains a series combination of a low-pass filter with a cut-off frequency of about 0.5 Hz and an element whose gain is independent of frequency and whose phase is an increasing function of frequency as described by a third order polynomial in the Laplace Variable. In the mid frequency range, this predictor approximates some signal amplification plus a negative delay of about 280 msec, which slightly overcompensates\* for the average reaction time of the visual tracking system.

All the foregoing points may suggest that something special and unconventional from standard control engineering viewpoints occurs during the periodic mode rather than during the nonperiodic mode, i.e. the phenomenon of prediction which arises in the periodic-input tracking. However, the following concept of Michael and Jones and their experimental evidence suggests that the mechanism of such a prediction always works in principle per se regardless of the degree of complexity of the input signal.

---

\* An alternative opinion is that 280 msec is very close to the composite (pursuit plus saccadic) reaction time.

Michael and Jones (1966) treated predictability as a continuous stimulus parameter affecting the system response: at one extreme is a regular sine wave which can be maximally predictable, while at the other extreme is a wide band random noise signal which is by definition unpredictable. By controlling the bandwidth of a narrow-band Gaussian noise generator to provide signals of graded stimulus predictability, they found a statistically significant increase in phase lag with increasing randomness (i.e. increasing bandwidth) of the stimulus. This result indicates that a continuous change in stimulus predictability produces a continuous change in the phase response characteristics.

#### 2.4.2 Saccadic Response to Periodic Square-wave Inputs

Square wave signals have been used to selectively stimulate the saccadic system. The visual tracking with square-wave inputs has been explored in connection with the learning and predictive behavior by Stark et al (1962) and by Dallos and Jones (1963). Their results agree on the following conclusions:

The latency between step changes in target position and corresponding saccadic shifts for fixation was, in the steady state, strongly dependent on the repetition rate of the square-wave input. Specifically, as indicated in Figure 2.10 (redrawn from Dallos and Jones, and essentially the same diagram was obtained by Stark et al), the average latency at very low rates was about the same as the average value of 200 msec obtained with a sudden displacement of target position. As the repetition rate increased, the time delay began to decrease and reached its minimum at some intermediate rate, where the response occasionally even preceded the stimulus step change resulting in a negative latency. As the repetition rate was raised further, the latency increased again and approached its presumed innate value of 200 msec.

The above evidence indicates that the saccadic system utilizes a predictive mechanism to overcome its inherent neuromuscular time delay. Such a compensation proved to be most effective and sometimes over-effective at intermediate rates. As Dallos and Jones note, square-wave inputs produce a strong "resonance" in the mid-frequency range giving a sharp decrease in

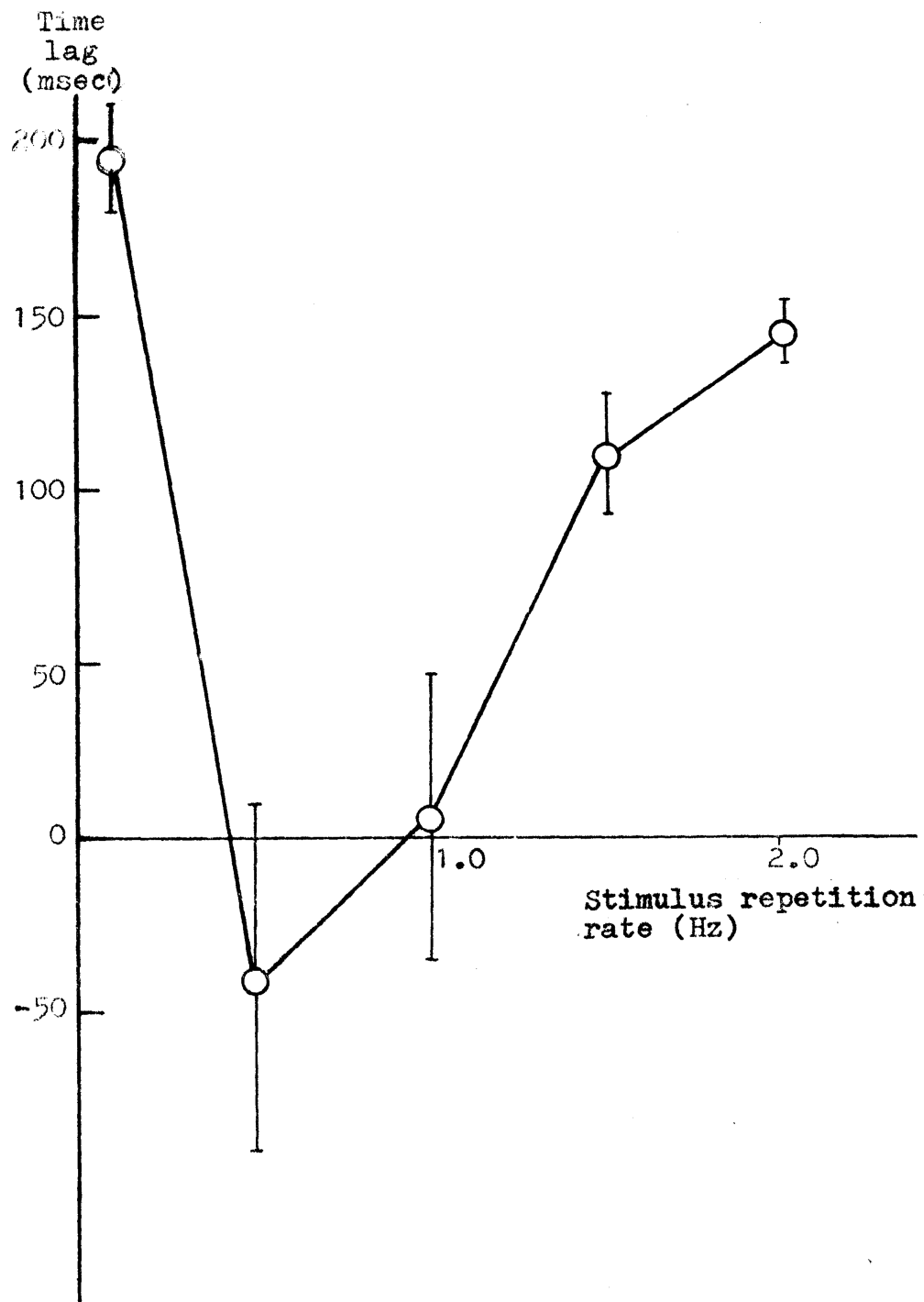


Fig. 2.10 Average saccadic latencies in tracking square-wave inputs (from Dallos and Jones, 1963)

phase lag, whereas no such favored frequency band emerges from the sinusoidal tests. In this connection, Sugie (1968) attributed the "resonance" phenomenon to the interaction between the characteristics of the square-wave input and the sampled nature of the saccadic system as follows:

In the case of the square-wave stimuli, it must be only the repetition period which provides useful information for the oculomotor prediction. Due to the imperfect human memory, longer repetition periods must be more difficult to remember accurately. On the other hand, if the repetition period becomes so short that the repetition rate becomes greater than the Nyquist frequency of the underlying sampling process, the input may change its position twice during a single sampling period. In that event, incorrect estimation of the repetition period would occur. (Execution of saccades is based on the sampled information. In addition, Sugie implicitly assumes here that evaluation and memorization of the repetition period also depends on the sampled information of the target motion.) Consequently, either at lower or higher stimulus rates, remembered periods would suffer from greater statistical variances. It follows that there must exist some intermediate rate at which the statistical error can be minimized. Hence, prediction must stem from the best memory at such a rate, and thereby it should be most effective there.

### 2.4.3 Nature of Learning in Eye Movement Control

Any predictive behavior is presumably a result of learning from past experiences. If the reduction of phase lag in the periodic tracking were due to prediction, the oculomotor system would have to spend some time initially in analyzing a new incoming periodic input wave form before establishing the relevant knowledge in order to become ready for sending the proper predictive signal to the oculomotor centers. Works by Stark et al (1962) and more extensively by Dallos and Jones (1963) were directed to this question of the acquisition of learning.

Dallos and Jones examined average latencies in each of the first several cycles of the tracking responses to both sinusoidal and regular square-wave inputs. First, they found that, in general, learning developed faster\* for signals with higher frequencies. Second, they showed that the rate of improvement was considerably greater for a continuous stimulus than for a discontinuous one at the same frequency. While the stimulus periodicity has proved to be a crucial factor for prediction, Dallos and Jones suggest that the information content per unit time within periodic signals may be the parameter that determines the speed of learning.

Occurrence of the predictive phenomena is not restricted to the visual oculomotor tracking of the foregoing classes. Zuber

---

\* in terms of the absolute time scale, not in terms of the number of cycles.

(1965) performed the frequency response measurement of the vergence oculomotor system\* by applying periodic and nonperiodic stimuli. His result indicates that the vergence system also utilizes a predictor, though it appears less effective than in the version system. Stark et al (1965a) report predictive behavior in the accommodating (ocular lens focussing) system.\*\* Robinson (1968) and Sugie (1968) point out singing and dancing as other examples of predictive behavior in man. Robinson comments that it would be strange if man could not utilize his ability of anticipation in the predictive tracking which is a similar rhythmic behavior. Stark et al (1962) cite results in the manual tracking control area that are analogous to those in the visual oculomotor tracking (Elkind and Forgie, 1959; McRuer and Krendel, 1959; Stark et al, 1961), and they stress the importance of controlling the predictability of stimulus in studying complex biological control systems in general. It is, in part, this suggestion which motivates the examination of the possible presence of predictive behavior in the slow phase component of vestibular (Chapter III) and optokinetic (Chapter VI) nystagmus.

The question as to whether the ability of prediction in

---

\* The vergence movements refer to motion of the two eyes in opposite direction in order to maintain binocular fixation, whereas the types of eye movements discussed thus far belong to the version system in which the two eyes move in the same direction.

\*\* In contrast, evidence is negative for such an anticipatory behavior in the pupillary system (Stark, 1968).

these sensory-motor activities belongs solely to the highly developed human brain is of great interest. In this regard, Fuchs (1967) failed to observe any predictive visual tracking behavior in the rhesus monkey. Furthermore, Fuchs placed the animal under the variable feedback condition. When the total feedback was raised to a certain value, the monkey's eye movements broke into a sustained oscillation. This finding is consistent with the phenomenon of limit cycles, which is expected to occur in a class of control systems with an excess negative feedback gain and with some nonlinear property. In contrast, Robinson (1965) found that this was not the case with human subjects: Robinson adjusted the total negative feedback gain such that it would lead to instability for the transfer function of the nonpredictive tracking mode but to stability for the periodic mode. The eye movement result was that the oscillation started and stopped in a somewhat erratic way. As Robinson explains, this was because the subject predicted the periodic oscillations caused by instability of his own system. By this predictive action, the subject would be about to suppress these oscillations. However, as the oscillation stopped, prediction would also cease and the oscillation would start again.\* Absence of such intermittent self-generated oscillations in the monkey thus reinforced the conclusion that the animal's oculomotor tracking system did not incorporate the predictive mechanism.

---

\* A similar phenomenon is known in manual control (Smith, 1963).



Finally, one should note the approach by St-Cyr and Fender (1969) to the input-adaptive nature of visual tracking. They maintain that the oculomotor behavior might be accounted for by the single factor of simple time delay, which is composed of two parts: A constant absolute delay of about 70 msec due to the neuromuscular transmission and an average delay that is variable and determined by a particular stimulus. Based on their experimental data and on a subsequent computation, St-Cyr and Fender showed that the above variable part was inversely proportional to the average rate of information transfer between stimulus and response. Following this finding, they went on to show that the variable portion of the delay time was proportional to the average time required by the retinal image to sweep across enough receptors so that the integrated neural messages could generate the minimum afferent signal to overcome a threshold for the initiation of a new corrective eye movement. By attributing the "predictive behavior" solely to change in the time delay (which obviously would lead to a nonlinear model), St-Cyr and Fender meant to challenge the prevailing notion of predictor and less-than-minimum phase phenomenon\*: They hold that these concepts are consequences of the "forced linearization" imposed by the very making of servo models for the oculomotor system, and that

---

\* Similarly, Lässing (1965) suggested that differences in eye tracking behavior with predictable and nonpredictable inputs do not necessarily indicate a mechanism of learning or prediction, but may reflect the influence of nonlinearities.

there exists no such thing as a predictor.

But terms such as "prediction" or "learning" are designated to those behavioral events that are phenomenologically observed in various biological activities. The underlying processes are to be understood in most cases including oculomotor tracking. But in the end they must be explainable in terms of physical laws. And, in some cases possibly including the visual tracking, prediction or learning might well turn out to be ultimate manifestations of simple and known physical relations such as, for example, those proposed by St-Cyr and Fender themselves.

## 2.5 Summary

The visual oculomotor tracking is characterized by the dual-mode operation incorporating the pursuit and saccadic movements. The pursuit system is continuous and responds chiefly to velocity signals, whereas the saccadic system corrects substantially for position error at discrete instances. A great deal of evidence indicates that the two systems are under separate neurological control. Certain control theory descriptions for the visual tracking exist in the literature.

Optokinetic nystagmus is an oculomotor reflex induced by relative motion of a large visual field. A typical response consists of periodically alternating fast and slow phase component. Slow phase movement minimizes slip motion of retinal images by following the field motion, while fast phase resets the deviated eye at a new position. Various similarities exist between OKN slow phase and the pursuit component during the dual-mode tracking, suggesting that the two eye movement systems might share common central mechanisms.

Vestibular nystagmus is an involuntary eye movement of nonvisual origin. It is elicited by a head rotation in space. As in OKN, the response pattern is characterized by the slow and fast phase component. The former component has a compensatory function to help stabilization of the eyes in space against head motion. Dynamics relating this compensatory slow phase movement to the input head rotation can be quantitatively accounted for, to a substantial extent, by mechanical properties

of the sense organ, the semicircular canals.

Vestibular and optokinetic nystagmus, though mediated by different stimulus modalities, have evolved apparently for the same behavioral goal, maintenance of a clear visual reference.

One of the most important characteristics of the human oculomotor system is its input-adaptive capacity. This is recognized as a predictive or learning behavior, in which the stimulus periodicity is detected and utilized to improve the accuracy of visual tracking. Relevant evidence for the composite movement in the dual-mode tracking are a considerable reduction of the innate oculomotor reaction time with periodic inputs, and a trend of decreasing phase lag with increasing stimulus periodicity. The saccadic system selectively stimulated by periodic square-waves shows a similar predictive compensation for overcoming the system's reaction time delay due to the inherent neuromuscular transmission. Predictive results have been obtained also in the vergence system as well as in the accommodative system. Analogous phenomena involving prediction are well known in the area of manual control. Negative evidence has been reported, however, regarding the pupillary system and the visual tracking oculomotor system in the rhesus monkey.

## Chapter III

### After-image Tracking under Induced Vestibular Nystagmus: A Perceptual Feedback Model for the Pursuit Oculomotor System

The classical psychophysical concept known as outflow cancellation theory for visual motion perception is reconsidered and extended to form a new closed-loop version that describes both the perceptual and oculomotor systems in the same conceptual framework. This is recognized as a perceptual feedback oculomotor control model, in which the visual tracking oculomotor efferent is produced based on what the observer perceives as target motion.

This hypothesis is examined herein with respect to pursuit oculomotor tracking by a series of controlled experiments involving vestibular stimulation and a foveal after-image. After-image tracking eye movements are analyzed along with the subject's report as to apparent motion of the after-image target. On the basis of comparisons with the normal vestibular nystagmus in complete darkness without after-image, the result is interpreted as evidence to support the perceptual feedback hypothesis. Finally, coupled with servo-mechanical discussions, a further refinement of the model is suggested to account for some pertinent subjective phenomena including the oculo-ogyral illusion.

Certain parts of the present investigation have some relevancy to the problem of predictive oculomotor behavior as well.

- 3.1 Introduction
- 3.2 Visual Judgement Mechanisms: A Review
- 3.3 Perceptual Feedback Hypothesis with Corollary Discharge Theory
- 3.4 Method
  - 3.4.1 Rationale
  - 3.4.2 Apparatus
  - 3.4.3 Procedure
  - 3.4.4 Data Processing and Analysis
- 3.5 Results and Discussions
  - 3.5.1 Sinusoidal Vestibular Stimulation
  - 3.5.2 Pseudo-random Vestibular Stimulation
- 3.6 Supplementary Discussions on Perceptual Feedback Model
  - 3.6.1 Problem of Open-loop Structure
  - 3.6.2 Block Diagram Nomenclature
  - 3.6.3 Visual Velocity Sensations based on Afferent versus Efferent Monitoring
  - 3.6.4 Partial Cancellation Hypothesis and Oculogyral Illusion
- 3.7 Summary and Conclusions

### 3.1 Introduction

As described in Subsection 2.1.2, Young et al (1968) have proposed that the information essential to the smooth pursuit system is the velocity of the stimulus itself, not the retinal error velocity which would be the crucial signal for a servo operation. Young et al cite "the quick release experiment" by Childress (1967; Subsection 2.1.2) in support of their non-feedback pursuit model. As Robinson (1969) argues, since the target velocity is not directly available to the central nervous system from retinal slip velocity alone, the implication of this nonfeedback model must be that eye movement velocity information is added to the retinal error so as to recreate a signal proportional to target velocity in space.

In the realm of visual psychology, on the other hand, the mechanism by which one perceives motion of visual objects has been a classical subject since the era of Helmholtz, and a perceived visual motion is reconstructed with a scheme implied in the above interpretation. This psychophysical mechanism can be modelled by a widely accepted theory described subsequently. Led by this line of consideration, Rashbass (1969) poses the question: "... Could vision and smooth tracking be using the same signal? In other words, does the eye track what it sees?"

This raises the possibility of studying the oculomotor tracking system in the psychophysical framework or of using psychophysical methods to deduce the internal organization that

governs eye movements. Note that the approach would be feasible only in humans where surgical procedures for neurophysiological probe are not possible.

On the basis of a reconsideration of the classical theory for visual motion perception, this chapter further pursues and refines the suggestion by Rashbass to the point of proposing and experimentally supporting a basic perceptual-oculomotor model for the pursuit tracking system.

This chapter also includes investigations of the input-adaptive predictive behavior in vestibular nystagmus slow phase, which in turn has some relation to the present chapter's major issue just discussed.

The following is a quote from Jung's remarks addressed to the Symposium on Cerebral Control of Eye movements and Motor Perception held in Freiburg i. Br., Germany, July 1971:

"... 'How do we see with moving eyes?' The perceptual integration of space, time and motion in the visual world obviously needs a precise correlation of visual messages with ocular movements. The cerebral correlation of eye movements and vision has remained a neglected field of research until the last two decades, in spite of many papers on oculomotor functions and nystagmus. Only during recent years have we begun to understand what questions should be asked about the central coordination of eye movements and on what theoretical framework experiments should be planned."

And Jung comes to the point parallel to the theme of this chapter,



"The extensive older literature on ocular movements which has accumulated since Helmholtz' (1866) and Hering's (1879), respectively, contains relatively little information on the brain mechanism which coordinates vision and eye movements, and treats mainly their relation to perception. We need more cooperation between subjective and objective visual physiology in order to relate experiment and theory in this field. Models of eye movements do not suffice for basic theories if they are not well correlated with neurophysiological and psychophysical results....."

### 3.2 Visual Judgement Mechanisms: A Review

As the starting point for the subsequent development of this chapter, attention is directed herein to the process responsible for giving rise to subjective visual sensation of target motion. That perceived motion does not directly reflect the retinal image motion is indicated by the following example:

If an observer exercises eye movements voluntarily when viewing a stationary object, he will normally report that the object remains stationary despite the fact that the visual image moves across the retina. Conversely, if the observer visually follows a target moving with a certain speed, he perceives that the target is indeed moving, even though the visual image may be virtually stationary at the center of the retina. These achievements imply that the observer takes account of his eye movements as well as the image on his retina in making judgements about movements in the visual environment.

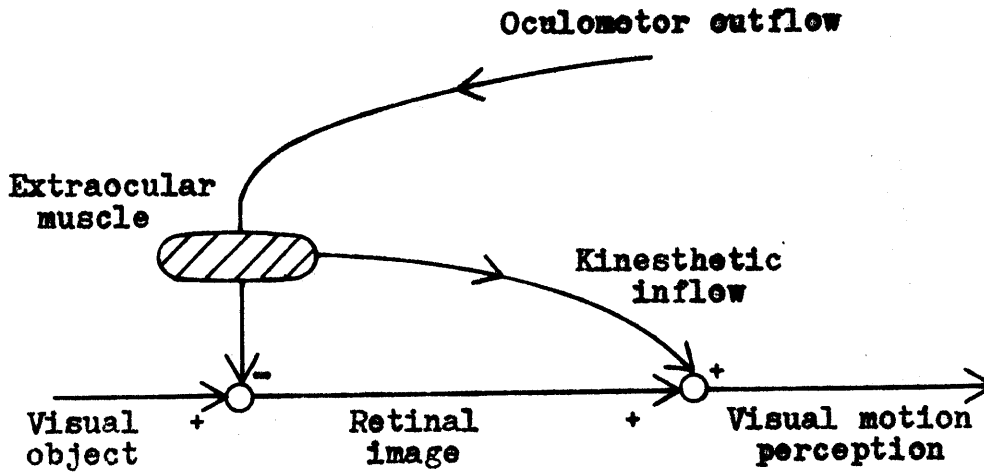
Normally, in these two cases, only saccades will be executed in the first case and smooth pursuit movements will dominate in the second case. There is some evidence to indicate that information as to smooth eye movements engaged in visual tracking is not fully but only partially taken into account by the mechanisms associated with velocity perception. However, this particular aspect will not jeopardize the basic concept of the visual-judgement mechanism that will be outlined in the following paragraphs. For the time being, this point will be put aside in order not to complicate the illustration.

The observer must combine the two sources of information, oculomotor and visual, in such a way as to result in impressions that are normally consistent with the external physical world. Signals regarding eye movements to be used in visual judgement could be the kinesthetic inflow from the extraocular muscles as first suggested by Sherrington (1918), or could be a copy of the central outflow to the oculomotor muscle as originally proposed by Helmholtz (1866) and later elaborated on by von Holst (1950, 1954, 1957) and others. The motor outflow information in the latter alternative is the eye movement command signal, which was referred to by Helmholtz as "effort of will" and subsequently has often been called "corollary discharge". These two possibilities, inflow theory and outflow theory, are shown schematically in Figure 3.1-a and 3.1-b respectively. The following behavioral evidence tends to support the outflow theory, despite the anatomical evidence as to muscle spindles found in the extraocular muscles of higher animals including man (Cooper and Daniel, 1949; Cooper et al, 1953 and 1955; Green and Jampel, 1966)\*.

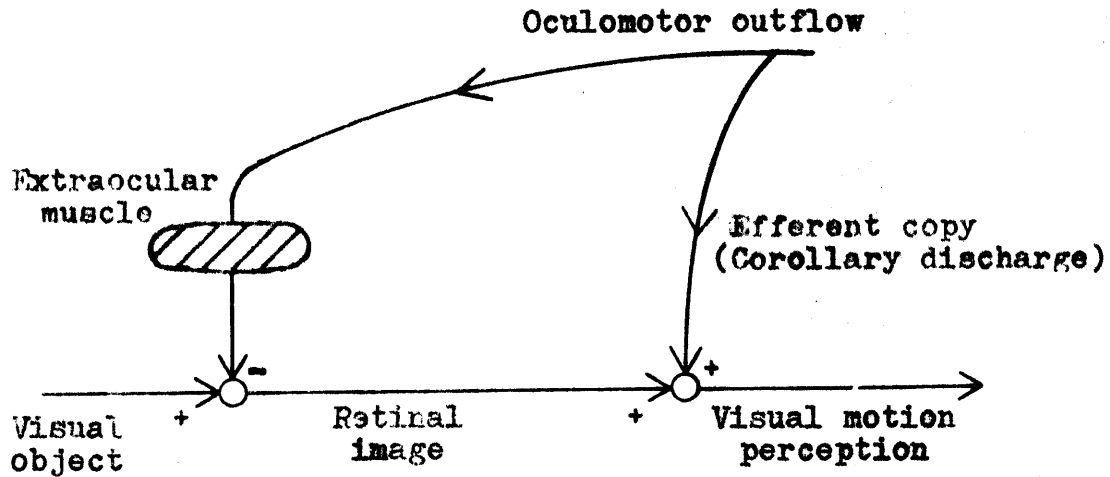
---

\* Of course, this does not mean to preclude possible functional importance of the extraocular muscle stretch receptor at the subconscious level for, say, a fine tuning of the oculomotor coordination functions in a similar way as in skeletal muscle systems. For example, Fuchs and Kornhuber (1969) have shown projection of afferent fibers from the extraocular muscle spindles to the cerebellum in the cat. Intracellular recording of Ito et al (1969) in cat lateral rectus muscle fibers shows activities in response to vestibular stimulation. Although possible physiological roles of the extraocular stretch afferent have been discussed by Bach-y-Rita (1969, 1971) and by others, its exact role still remains one of the most controversial mysteries in oculomotor physiology.

(a) Inflow theory (Sherrington, 1918)



(b) Outflow theory (Helmholtz, 1866)



Figs. 3.1 Two possible alternatives for visual motion perception. Note effective cancellation of eye movement interference with retinal image motion.

[1] When the eye ball is moved passively by a finger, a stationary visual object appears to move.\* The muscle spindles in the extraocular muscle are doubtless stimulated no matter whether the eye movement is executed actively or passively. Consequently, if the afferent nerve impulses from the muscle spindles were the crucial information for the visual judgement process, the visual object would have to be judged stationary as it would be in the case of active eye movements. Clearly the motor outflow from eye movement centers is absent with passive eye movements, and the moving retinal image is left uncompensated.

[2] If the eye muscles are paralyzed, any attempt to move the eyes results in an apparent movement of the stationary surroundings in the same direction as the attempted movement (Helmholtz, 1866; Kornmuller, 1930; Mach, 1866, Hering, 1879). In this case, the motor outflow reaches the visual judgement center, but is not accompanied by any movement of the retinal image.

[3] The inflow theory assumes conscious position sense of the eye ball for which evidence seems to be negative: For example, Brindley and Merton (1969) reported that in the absence of visual cues subjects fail to detect passive movements of one or both eyes, and when the eyes are occasionally

---

\* This fact was known to Helmholtz, Mach and Hering.

mechanically restrained by the experimenter, the subject cannot tell whether he has succeeded in an attempted eye movement or not.

[4]        When an after-image is formed and eye movements are executed voluntarily, the after-image is reported to move with the eye. Since the after-image is absolutely stationary relative to the retina regardless of eye movements, the eye movement information is not accompanied by the motion signal from the retina. But the above test alone does not differentiate between the inflow theory and the outflow theory. However, if the eye is moved passively with a finger, the after-image is judged to be stationary. In this case, there is neither outflow information nor is there retinal image motion. This may be the most convincing evidence of all for the outflow theory, for in all the preceding experiments disturbing forces were introduced in addition to the natural force of the extra-ocular muscles on the eyeball, either to passively move the eye or to prevent active movements.

One may generally conclude that the ability to judge seen movements depends on the interplay of information from the centers which are responsible for the control of eye movements, and information from visual centers indicating image movements on the retina. The effect of actual eye movements on the retinal image is compensated and cancelled by the motor outflow information.

In passing, we should note what Mackey (1958) claims to be an alternative theory. He wrote:

"... Briefly, the argument is that if perception is the adaptive 'keeping up to date' of an organism's state of organization for activity in its world, what requires informational justification is not the maintenance of stability but the perception of change. The internal state of organization, which implicitly represents the perceived world, should remain unaltered unless sufficient information (in the technical sense) arrives to justify a change, by indicating that the current state of organization is significantly mismatched to the state of affairs sampled by the receptor system. Thus the retinal changes resulting from voluntary movement evoke no perception of world-motion, because they are not an awkward consequence to be compensated, but part of the goal to be achieved....."

The "cancellation theory" and what may be called the "evaluation theory" of Mackey, both account for the facts which have been outlined, and on the face of it, the two theories seem to be operationally equivalent and they can be represented by the same feedforward type scheme shown in Figure 3.1-b.

### 3.3 Perceptual Feedback Hypothesis with Corollary Discharge Theory

On the face of the foregoing psychophysical evidence indicating intimate participation of oculomotor information, one should consider the converse possibility, that the perceived motion of a visual target might in turn influence the system that controls eye movements. Henceforth considering only the smooth pursuit movement, this reduces to the hypothesis that the pursuit movement might be produced based on what the observer perceives as target velocity. This hypothesis is exactly equivalent to the suggestion previously quoted from Rashbass.

According to this concept, as long as the observer subjectively sees a visual object moving continuously, he might be able to maintain pursuit eye movements in an attempt to follow that target motion. Existence of a moving visual target in the physical reality may not be an absolutely necessary condition for performing the pursuit tracking. That is, pursuit tracking movements might well be induced by an apparent motion or by an illusory movement of a visual object. One can speculate further that this might be the case even for "imagined visual movements", referring to smooth pursuit movements found in REM sleep (rapid eye movement sleep) and presumably associated with dreams (Dement, 1964), and to pursuit movements obtained by Steinbach and Held (1968) during experiments in which they asked subjects to follow their hands visually while they moved them behind



a screen. As a correlate of these thoughts, one might add the following consideration:

The apparent motion of a real target during passive eye movements has been explained by saying that passive movements accompany no outflow command and thus the moving retinal image is left uncompensated. However, according to the present view, there is a possibility that a subjectively perceived motion during passive eye movement may well in turn initiate an oculomotor outflow if the observer is to attempt to track that perceived motion (and such an attitude will normally be the case if the subject is told to pay attention to what he sees).

In any event, it appears that the eye movement control system could be studied in connection with the perceived motion of visual objects, and that such a subjective impression, once measured by an appropriate psychophysical technique, could provide, in addition to the eye movement itself, another form of output information.

In summary, one may postulate that perceived velocity information obtained through the previously described visual judgement mechanism is sent back to motor centers where it is used, at least in part, for constructing the smooth pursuit oculomotor efferent command. The visual judgement mechanism, operating according to the illustration given in Figure 3.1-b, would then become a new closed-loop system, that would in turn form, at least partially, a skeleton model of the smooth pursuit oculomotor control. The whole structure describes both

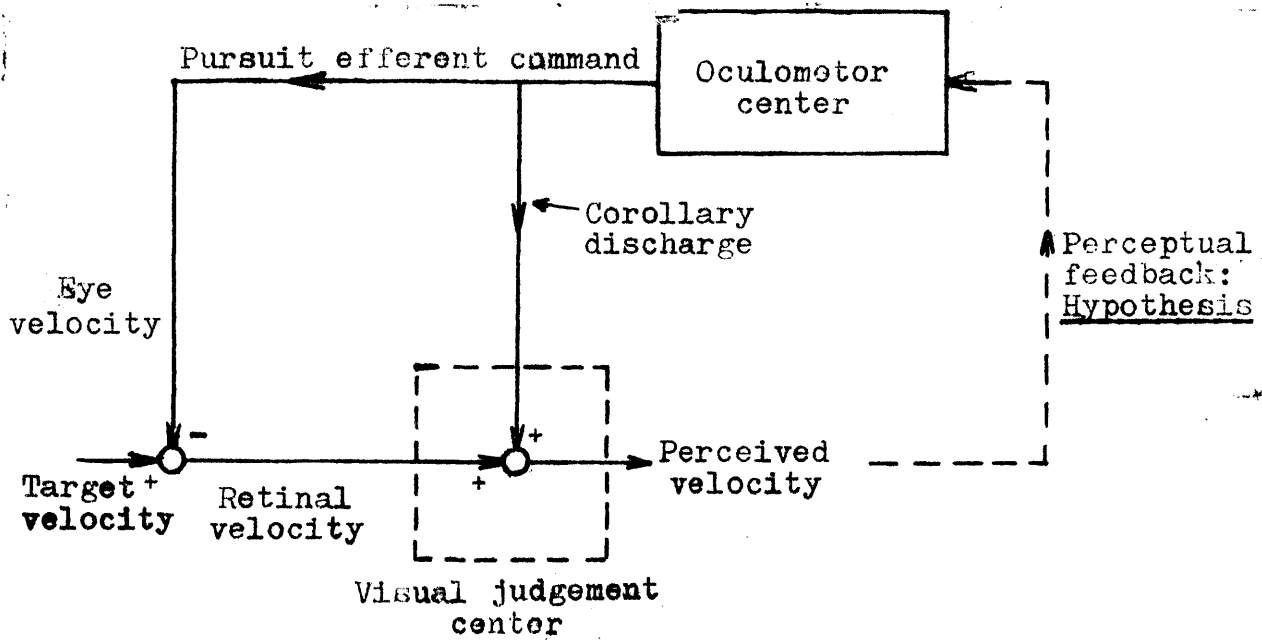


Fig. 3.2 Skeleton model for the pursuit tracking system based on corollary discharge theory and perceptual feedback hypothesis.

of the processes, perceptual and oculomotor, at the same time. Such an organization is schematically shown in Figure 3.2, in which the source for creating the smooth pursuit command is a signal proportional to the perceived velocity. Characteristic to the model is the internal regenerative feedback as emerged from looping the corollary discharge and the perceptual feedback.\*

The first step in an investigation should be to determine whether or not the postulated scheme is actually feasible, and the above diagram is intended only to indicate possible information flow pathways, and details such as gain, dynamics and conduction delay potentially present in each segment of relevant pathways are not shown at this stage.

---

\* Gregory (1958) describes the perceived motion of a visual after-image in the condition similar to the aforementioned experiment by Steinbach and Held (1968): If the velocity of the observer's hand is changed, the after-image may seem to lead or lag, and then lock on to the locus of the hand being tracked in total darkness. The after-image motion appears smooth indicating that the ocular movement belongs to the smooth pursuit movement as reconciled with the result by Steinbach and Held. The observation is also an example to show the feasibility of the corollary discharge theory with respect to the pursuit tracking.

### 3.4 Method

The following experiment was designed primarily to examine the view posed in the preceding section on the smooth pursuit eye movement control. As described in Figure 3.2, the model assumes the subjectively perceived velocity as a source of information for generating the pursuit tracking movement. The experimental arrangement aims at selectively activating the internal regenerative feedback loop that characterizes the perceptual feedback oculomotor model under consideration.

#### 3.4.1 Rationale

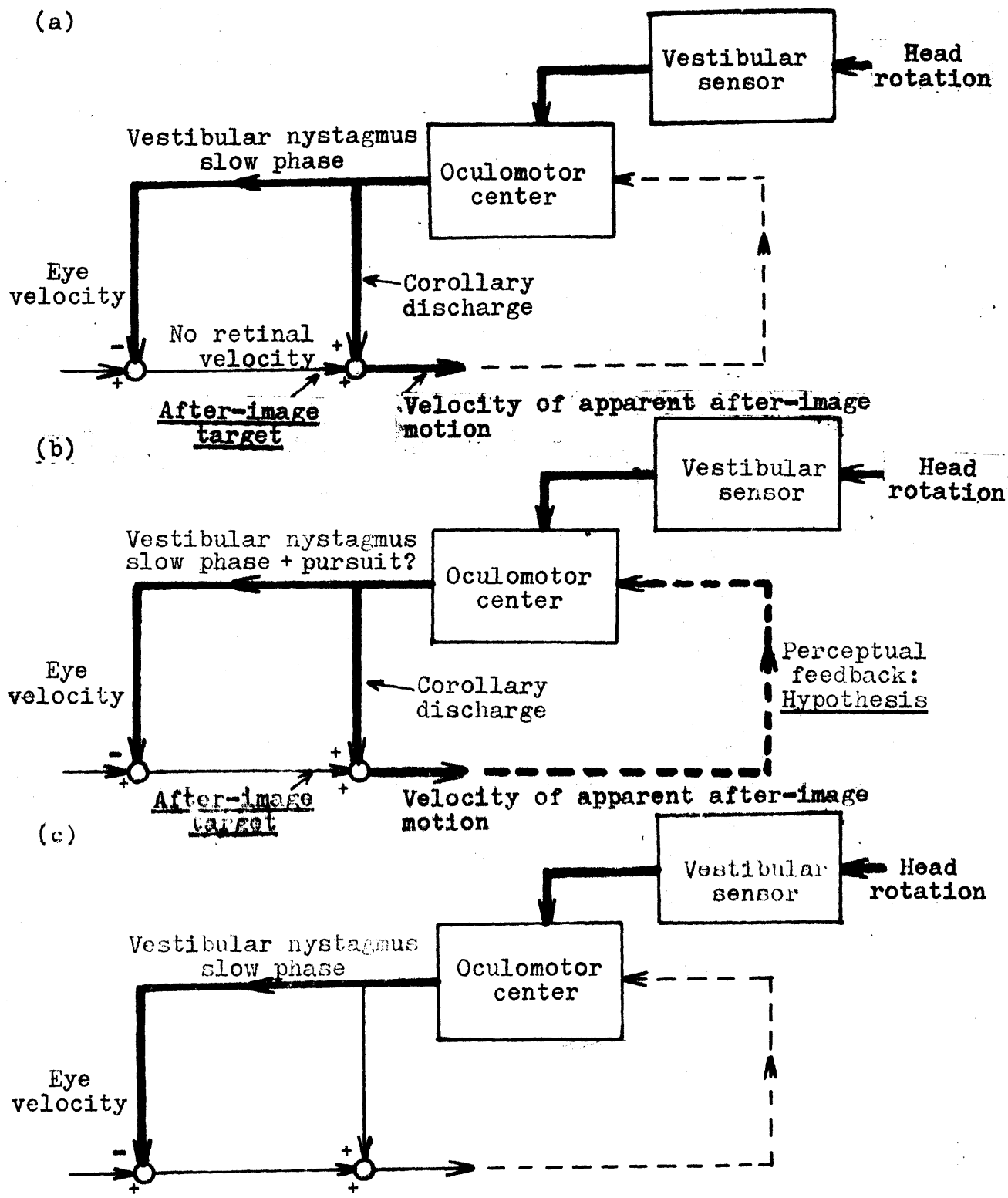
The subjects were placed inside a Bárány type rotating chair with their head upright. A visual after-image was impressed at the fovea and used as a target for the visual tracking task in otherwise total darkness. Since the after-image is absolutely stationary with respect to the retina, there can be no retinal velocity information regardless of eye movements. Nor could there be any visual input from the outside. In terms of the signal flow diagram depicted in Figure 3.2, this would imply that the visual negative feedback loop becomes open, and that only the inner positive feedback loop, which stems from the visual judgement mechanism and the perceptual feedback hypothesis, can be potentially operational. Assuming the after-image is established exactly at the fovea, no input is present to

stimulate the pursuit system in the situation up to this point.\*

In order to force the eye to move, the vestibulo-ocular reflex was induced by rotating the subject about the earth-vertical axis in the Bárány chair. The after-image began to move with respect to the subject in a manner related to the applied chair motion, confirming similar observations in the literature (Graybiel and Hupp, 1946; Whiteside et al, 1963; Wurtz and Goldberg, 1971; Grüsser and Grüsser, 1972). Since motion information is purely absent in the visual afferent from the retina with the after-image target, the observed apparent motion of the after-image must be mediated only through the corollary discharge reflecting the vestibular nystagmus slow phase efferent. This implies, contrary to some authors (Howard and Templeton, 1966), that the motor outflow responsible for the vestibulo-ocular reflex can reach the visual-judgement center. Figure 3.3-a illustrates these points.

While similar types of experiments incorporating visual after-image and vestibular stimulation by the above authors are directed primarily to the study of the problem of visual-vestibular interaction\*\*, the crucial points in the present investigation were the instructions to the subject, and the controlled

- 
- \* Off-fovea after-images can elicit smooth pursuit movements as noted in Subsection 2.1.2 (Kommerell and Täumer, 1971).
  - \*\* The vestibularly induced after-image apparent motion can be recognized as a special case of the oculogyral illusion. The oculogyral illusion is a typical manifestation of visual-vestibular interaction, and will be discussed later.



Figs. 3.3 (a) Apparent after-image motion due to corollary discharge, (b) Forced visual tracking of after-image, (c) Vestibular nystagmus in complete darkness without after-image.

eye movement measurement and analysis along with the subsequent special interpretation given to the results.

The subjects were asked to visually track the apparent motion of the after-image. This instruction was very important with regard to the main purpose of the experiment, for it was intended to force the postulated perceptual feedback to become active. The expected situation is indicated by thicker lines in Figure 3.3-b, which is characterized by the conspicuous emergence of the internal regenerative feedback loop vital to the perceptual-oculomotor model under examination.

If the smooth portion of the eye movements during such an after-image tracking task under induced vestibulo-ocular reflex should become different from the slow phase of the normal vestibular nystagmus in complete darkness without after-image (corresponding to Figure 3.3-c), the difference could be interpreted as the smooth pursuit component which would be created and introduced to the oculomotor system, additively, through the inner regenerative feedback loop activated in accordance with the subject's effort to track the motion he perceives. In other words, comparing Figure 3.3-b and Figure 3.3-c, the eye movement difference could be attributed to the extra regenerative loop in the former figure, and the difference might be recognized as a secondary product of the original vestibular nystagmus slow phase efferent.

For this purpose of eye movement comparison, the vestibular nystagmus was measured in the total darkness as well, with the

same vestibular stimuli as applied in the after-image tracking case. For reasons that will become clear subsequently, a pseudo-random chair motion was also tested in addition to pure sinusoidal oscillations.

#### 3.4.2 Apparatus

The rotating chair of the M.I.T. Man-Vehicle Laboratory, constructed by Katz (1967) which appears in Figure 3.4 was used to provide angular motion stimulation about the earth-vertical axis. The subject sat in a cab on a chair with head upright. The chair drive unit consists of two 15 ft-lb torque motors and a pulse-width-modulated power amplifier. The rotation angle of the chair was measured through a 20-turn helical potentiometer geared to the motor shaft. Some servomechanical improvements were made on the original chair system in order to raise the cut-off frequency and thereby to increase the highest testable stimulus frequency. The final version of the over-all chair system was a type one position servo with a lead-lag analog compensation network inserted into the forward path, and its cut-off frequency was about 0.21 Hz.

Figure 3.5 sketches the inside view of the rotating chair. Located one foot away, ahead of the subject's right eye was a commercial photographic electronic flash (Canon Speedlite 100, using capacitance discharge and Xenon bulb), which was employed to produce an after-image at the fovea. The estimated retinal size of the after-image was about 1 mm x 1 mm. There were three



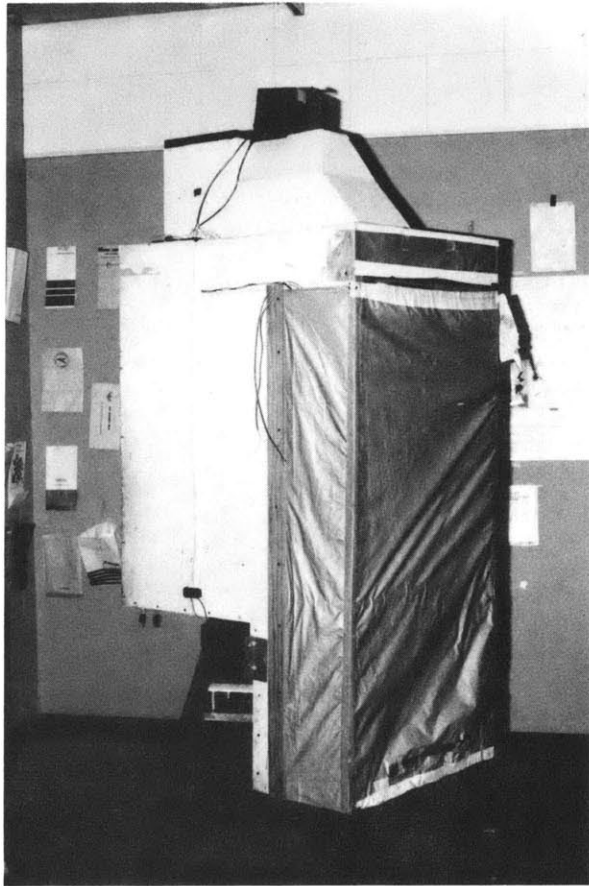
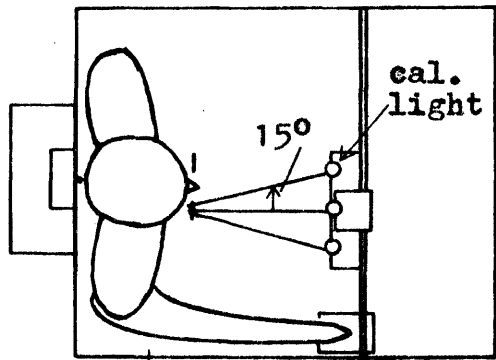


Fig. 3.4 View of the B ar any type rotating chair cab.



Flash unit and calibration lights seen by subject.

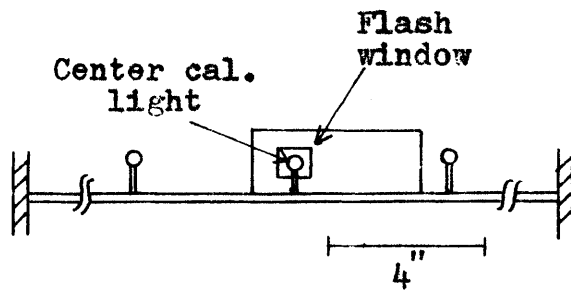
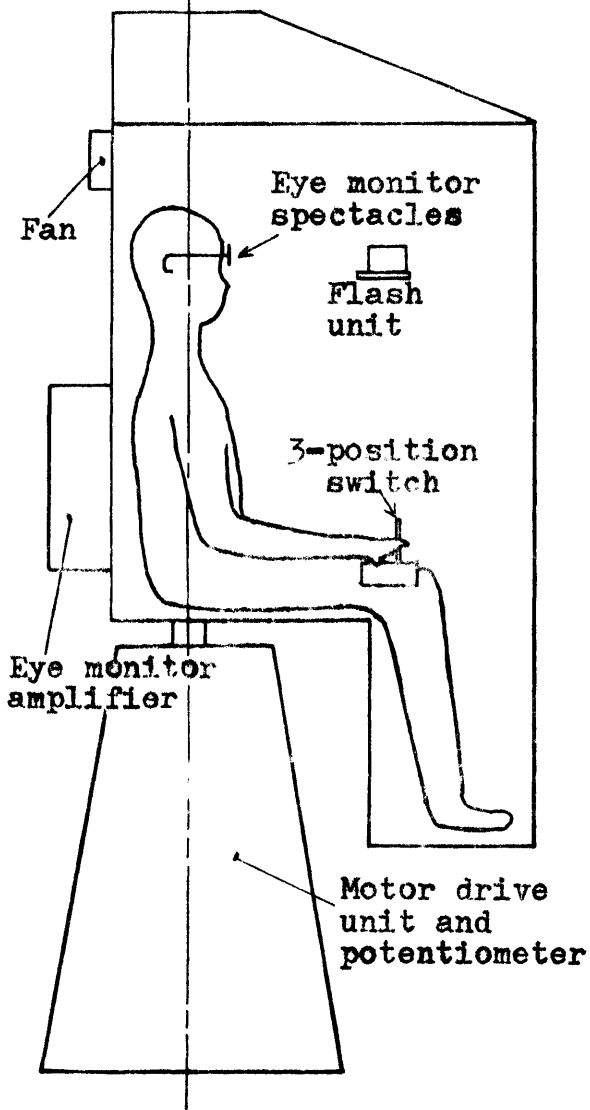


Fig. 3.5 Schematic drawing showing arrangement inside the rotating chair cab.

lights (15° right, center, 15° left) that could be turned on for calibrating the eye movement monitor. The left eye was occluded. The location of the center calibration light was adjusted in such a way that, when the subject fixated on it with his right eye, this eye would rest about at its center position with respect to the skull (at the primary gaze position). Prior to each flash, the center light was lit and the subject was asked to make his best effort to maintain visual fixation upon this light. The center of the flash bulb was placed behind the center light. In addition to ensuring establishment of the after-image at the right eye's fovea, this arrangement presumably minimized any "initial condition" in the eye movement at the moment of after-image formation.

The subject wore a spectacle frame on which a pulsed infrared photoelectronic eye movement monitor (Model SGHV-2, manufactured by Biometrics, Inc.) was mounted. According to the specifications, its maximum linearity range is  $\pm 15^\circ$  and maximum resolution is  $\pm 1/4^\circ$ .\* Only the horizontal movement of the right eye was measured. A head band was used to prevent the head from moving within the rotating chair. A dental bite board was not used, because it was judged sufficiently uncomfortable as to hinder subject concentration. A 3-position switch was provided inside the chair for the subject to report the direction of

---

\* The same instrument is used for measuring eye movements throughout the thesis. Sample calibration records are given in Appendix A.

after-image's apparent motion (right to left, left to right and either no motion or loss of after-image). Minor features included a motor driven fan for air conditioning as well as for masking unwanted external noise, a motion sickness bag and an attention/emergency alarm bell.

### 3.4.3 Procedure

Four male subjects were used for the experiment. They all appeared to show no apparent disorder in either vestibular functions or in oculomotor tracking performance.

First, the rotating chair was driven sinusoidally at different frequencies. Table 3.1 summarizes the frequencies tested for different subjects along with the corresponding chair oscillation amplitudes in terms of angular position, velocity and acceleration. Besides these purely sinusoidal stimulations, the chair was moved in a pseudo-random fashion by applying a prepared driving command signal. This signal, stored on a magnetic tape, had been made by mixing 10 sinusoids of harmonically unrelated frequencies. The Fourier analysis of the actual record of pseudo-random chair motion carrying a typical subject resulted in the frequency spectra shown in Figure 3.6. And this result is essentially the same for other subjects except for small changes in peak power levels.

An experimental run, defined as a course of experiments for one subject under one particular sinusoidal or pseudo-random stimulation, began with the eye movement monitor calibration.

Position (deg/sec)

Freq. (Hz)	SY	JT	BC	CO
0.025	84.4	71.6	86.0	87.1
0.060	--	60.0	77.4	70.0
0.100	51.6	40.3	55.7	64.0
0.250	22.9	11.5	20.6	13.7
0.500	5.0	4.3	4.9	4.5
0.700	--	1.8	2.6	2.0

Velocity (deg/sec)

Freq. (Hz)	SY	JT	BC	CO
0.025	13.3	11.3	13.6	13.8
0.060	--	22.6	29.2	26.4
0.100	32.4	25.4	35.0	40.6
0.250	35.8	17.9	32.2	21.4
0.500	15.7	13.5	15.4	14.1
0.700	--	8.0	11.4	8.8

Acceleration (deg/sec<sup>2</sup>)

Freq. (Hz)	SY	JT	BC	CO
0.025	1.90	1.61	1.93	1.96
0.060	--	8.65	11.10	10.10
0.100	20.60	16.10	22.30	25.60
0.250	57.20	28.80	51.50	34.20
0.500	50.00	43.00	49.00	45.00
0.700	--	35.30	51.00	39.40

Table 3.1 Peak-to-peak position, velocity and acceleration amplitude for the applied chair oscillation\*

\* Amplitude of the chair driving command signal was occasionally adjusted at each frequency to compensate for the body inertia difference among the subjects.

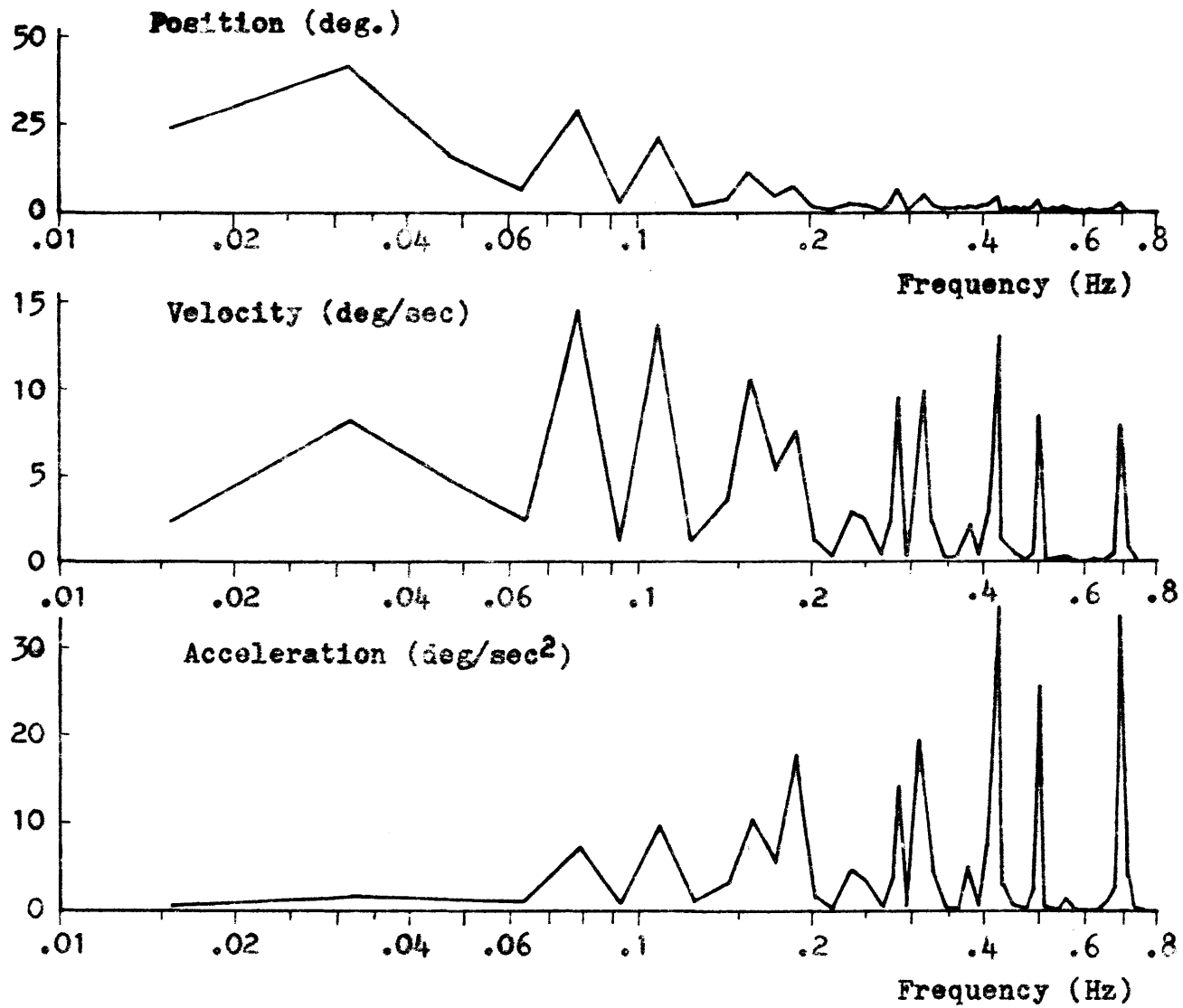


Fig. 3.6 Amplitude spectra of pseudo-random chair motion with a typical subject (based on discrete Fourier analysis)

Then the vestibular nystagmus in total darkness was recorded. The subject was asked to count numbers from 100 backward in his mind in an effort to maintain a high enough arousal level during this measurement (Collins et al, 1960; Howard and Templeton, 1966). This stage lasted for 2 to 4 minutes. Without stopping the ongoing chair motion, the after-image was then impressed at the fovea of the right eye by a flash. The eye movement was measured while the subject was concentrating on tracking the visual after-image in motion. The subject's loss of after-image was apparent for the experimenter either from a prolonged neutral output from the 3-position switch, or from a characteristic change in the eye movement described subsequently. After the final loss of after-image, the measurement was continued for approximately another minute before concluding the run. Table 3.2 presents a full description of all events in chronological order for one complete run, and this table clearly indicates the specific instructions that were given to the subjects.

#### 3.4.4 Data Processing and Analysis

Data for each experimental run were recorded on a four-channel Brush chart recorder model 240 for on-line monitoring and inspection. At the same time, data were stored on a magnetic tape by means of an eight channel Precision Instrument type recorder model P.S. 200A for later data analysis.

(E): Experimenter

(S): Subject

- 3 min. (S) Rest  
(E) Calibration lights on.
- 3 min. (S) Cover left eye with occluder  
(E) Calibrate eye monitor and record the result.
- (E) Start chair motion
- 15 sec.
- (E) Calibration lights off.
- 2 min. (S) Count numbers from 100 backward in mind.  
(4 min. for (E) Record vestibular nystagmus, chair position,  
0.025 Hz) etc.
- (E) Calibration lights on.
- 3 min. (E) Recalibrate eye monitor and record the result.
- (S) Maintain visual fixation on center light.
- 10 sec.
- (E) Ring attention bell.
- 5 sec.
- (E) Deliver flash and turn lights off simultaneously.
- 2.5 min. (S) Track after-image visually, and report apparent  
direction of its motion by 3-position switch.  
(E) Record vestibular nystagmus, chair position,  
etc.  
(S) Report every loss of after-image by holding  
3-position switch in neutral. Whenever it  
reappears, resume tracking task.  
(E) Continue recording for another minute after  
final loss of after-image. (Recovery of  
after-image can be known from 3-position  
switch report).
- (E) Repeat entire run if necessary.
- 3 min. (S) Rest  
(E) Prepare for another run.

Table 3.2 Events in One Experimental Run



Data pertinent here are: (1) chair position, (2) eye movement, (3) direction of subjective after-image motion. During each run, the eye movement signal was observed to note:

- (1) Change of eye movement pattern from condition of no vision to after-image tracking situation.
- (2) Temporal relation between direction of after-image motion (indicated by 3-position switch) and eye movement direction.

The frequency response characterizing the transfer function from chair velocity to smooth eye movement was obtained next in the form of a Bode diagram. The data reduction in this process involved the hybrid computer facilities of the Man-Vehicle Laboratory, featuring a DEC-PDP-8 digital computer and a GPS-200T analog computer. Data were processed through the hybrid programs "MITNYS" and "FFT". Briefly, MITNYS is a routine for extracting only the slow phase movement of the eye from nystagmus data. It was designed and written originally by Tole and Young (1971), and later improved by Allum et al (1973). Basically the program consists of two parts: the first part removes the fast phase saccades from the eye movement record and leaves a continuous trace of pure smooth movement only. The result is the so-called "cumulative eye position"; the imaginary eye position which would have been obtained if there had been no saccades. The second part of the program is essentially a digital differentiator that operates on the cumulative eye position and outputs the slow phase

velocity. MITNYS can be run on-line in real time, and its outputs, cumulative eye position and slow phase velocity, are analog voltage signals.

FFT is a Fourier analysis routine, based on the fast Fourier transform algorithm of Cooley and Tukey (1965), and it was written to fit the PDP-8 computer by this author. It was used here in obtaining the frequency response for runs with pseudo-random chair motion\*. The amplitude ratio in dB and phase shift (in degrees) at a given frequency were read directly from the computer printout, only if both the input power of chair motion and the output power of eye movement exhibit their peaks at that frequency. Since the system under investigation was, of course, not perfectly linear, input peaks and output peaks did not always occur at the same frequency. Based on each Fourier analysis result, relevant tables in Appendix D give a general idea as to the linearity of the system. On this basis, the system linearity was judged satisfactory if not as good as in later chapters dealing with other types of eye movement under pseudo-random stimulation.

Four cases were investigated:

- (1) Sinusoidal chair oscillation with no vision.
- (2) Sinusoidal chair oscillation with after-image

---

\* As summarized in Appendix B, the two-step procedure MITNYS-FFT is employed similarly in later chapters that involve eye movements with pseudo-random stimulus. Appendix C presents the program listing for FFT.

tracking.

(3) Pseudo-random chair motion with no vision.

(4) Pseudo-random chair motion with after-image tracking.

The input is the chair velocity or the subject's head angular velocity, and the output is the velocity of the smooth portion of the eye movements. It is equivalent to considering the chair position as input and the cumulative eye position as output. Somewhat different procedures were employed, depending upon the above different cases, in computing the amplitude ratio and the phase shift, for reasons that may be understood from Table 3.3 given at the end of the current section.

Some additional technical remarks associated with the relevant data acquisition and reduction are noted in the remainder of the section. Since the frequency response is meaningful only in the steady state, the eye movement data taken at least within about 30 seconds after the start of chair movement were not analyzed. This 30 second interval is practically sufficient in avoiding the transient period resulting from the long time constant (8 - 16 seconds) associated with the nystagmus slow phase response.\*

The measurement of horizontal eye movement with the present method is susceptible to interference from vertical eye movements. Complete elimination of such a vertical-horizontal

---

\* 120 seconds time constant (0.0013 Hz corner frequency) of the nystagmus adaptation dynamics as established by Young and Oman (1968) should have little effect in the frequencies pertinent to this experiment.

interaction turned out to be quite difficult. Although the vertical eye movement was not measured, there were occasions where the eyes apparently moved vertically. This was indicated by vertical motion of the after-image as perceived by subjects\*. Whenever this vertical motion became conspicuous and comparable to the horizontal motion as judged from the subject's opinion, the data were rejected and the entire run repeated.

Some traces of the cumulative eye position obtained from MITNYS showed pronounced drifts to one direction, approximately with constant rates. Even a tiny imbalance of the eye movement monitor could lead to a sizable drift in the cumulative eye position, due to the nature of cumulative eye position itself. In fact many records were found to correlate with slight asymmetric adjustment of the eye movement monitor during the calibration stage. But not all records were of this type, and some might be real, suggesting possible directional preponderance of vestibular and/or oculomotor system (Young, 1971).\*\* Whatever the cause, a large drift can introduce in-negligible errors in FFT result especially at lower frequencies.\*\*\* For this reason, any large drift had to be removed from the original cumulative eye position trace by adding a

---

\* This was probably because the after-image was formed not exactly at the fovea but formed slightly up or down from there, and such a possibility may relate itself to the observations by Kommerell and Täumer (1971), as noted previously.

\*\* Alternatively, the after-image might have been slightly off-fovea, as in the case footnoted above.

\*\*\* This is due to the inherent nature of Fourier transform with a finite observation time (see Appendix C).

suitable counter drift signal, and the cumulative eye position after this possible correction was fed to FFT.

Table 3.3 Summary of data reduction procedures

(1) Sinusoidal chair oscillation with no vision:

To obtain the slow phase velocity, the eye movement data were differentiated directly by the velocity routine of MITNYS (not through differentiating cumulative position), bypassing the routine for obtaining the cumulative eye position. Spikes resulting from differentiation of the fast phase saccades were ignored. The sinusoidal eye movement velocity trace thus obtained by hand was compared with the sinusoidal input chair velocity in terms of velocity amplitude and phase difference. FFT was not used.

(2) Sinusoidal chair oscillation with after-image:

As it turned out, the eye movement in this case was a smooth sinusoid, lacking the fast phase saccades. Thus a direct comparison between eye position and chair position was made except for the two lowest frequencies tested (0.025 and 0.060 Hz). At such low frequencies of oscillation, the eye movement amplitude became very large due to the loss of the fast phase saccades.\* For this

---

\* In the normal vestibular nystagmus in complete darkness, successive fast phase saccades would continuously reset the deviated eye position to limit the overall range of eye movement.

reason, the eye movement monitor tended to saturate, making accurate reading of the position amplitude difficult. Thus, instead of working with eye position, the maximum eye movement velocity (which was assumed to occur when the eye ball was at its center position) was read and compared with the peak chair velocity. Neither MITNYS nor FFT was used.

(3) Pseudo-random chair motion with no vision:

MITNYS was used to obtain the cumulative eye position, which was then fed to FFT together with the recorded chair position in order to obtain the desired frequency response. Both MITNYS and FFT were used.

(4) Pseudo-random chair motion with after-image:

The fast phase saccades\* were virtually absent and the eye movement became smooth. The frequency response was obtained directly between the chair position and the original eye position record through FFT. MITNYS was not used.\*\*

---

\* "Saccade" is often used to mean nystagmus fast phase as well, although this is a loose usage of the term (see Chapter II).

\*\* Except for a few runs where several fast phase movements were observed and had to be removed by MITNYS before FFT.

### 3.5 Results and Discussion

The smooth portion of the vestibulo-ocular reflex eye movement was analyzed in terms of frequency response relating eye velocity to chair velocity in four different cases: (1) sinusoidal head rotation in the total darkness, (2) sinusoidal head rotation and after-image tracking, (3) pseudo-random head rotation in the total darkness, (4) pseudo-random head rotation and after-image tracking. The corresponding results, statistically deduced over subjects\*, are summarized in Bode plot representation, and comparative discussions are given to them to examine the hypothesized perceptual feedback pursuit model as well as some supplementary issues related to the predictive oculomotor behavior.

#### 3.5.1 Sinusoidal Vestibular Stimulation

Figure 3.7 shows a typical recording obtained with a harmonic chair oscillation. The frequency of oscillation for this particular run was 0.5 Hz. Traces from the top correspond to chair position, eye position, cumulative eye position (obtained from MITNYS) and 3-position switch output indicating direction of the perceived after-image motion.

In the first portion of measurement, during which the

---

\* The original frequency response data points for all these cases can be found in Appendix D (Figures D.1 through D.4).

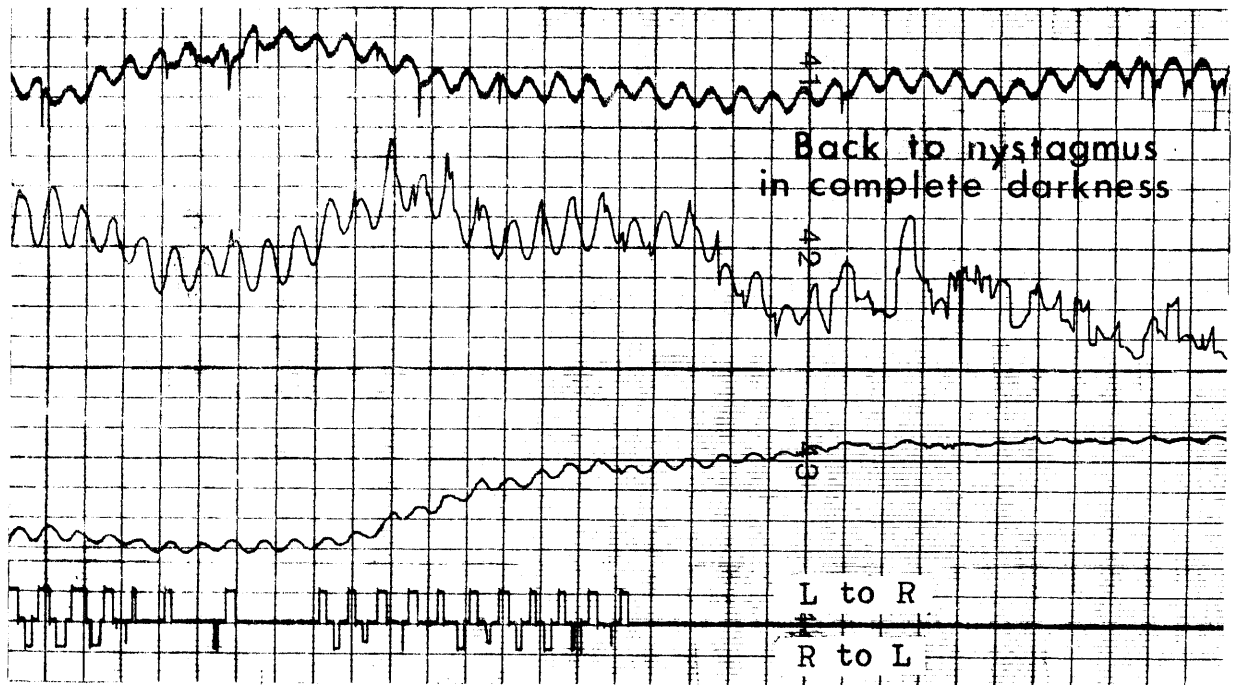
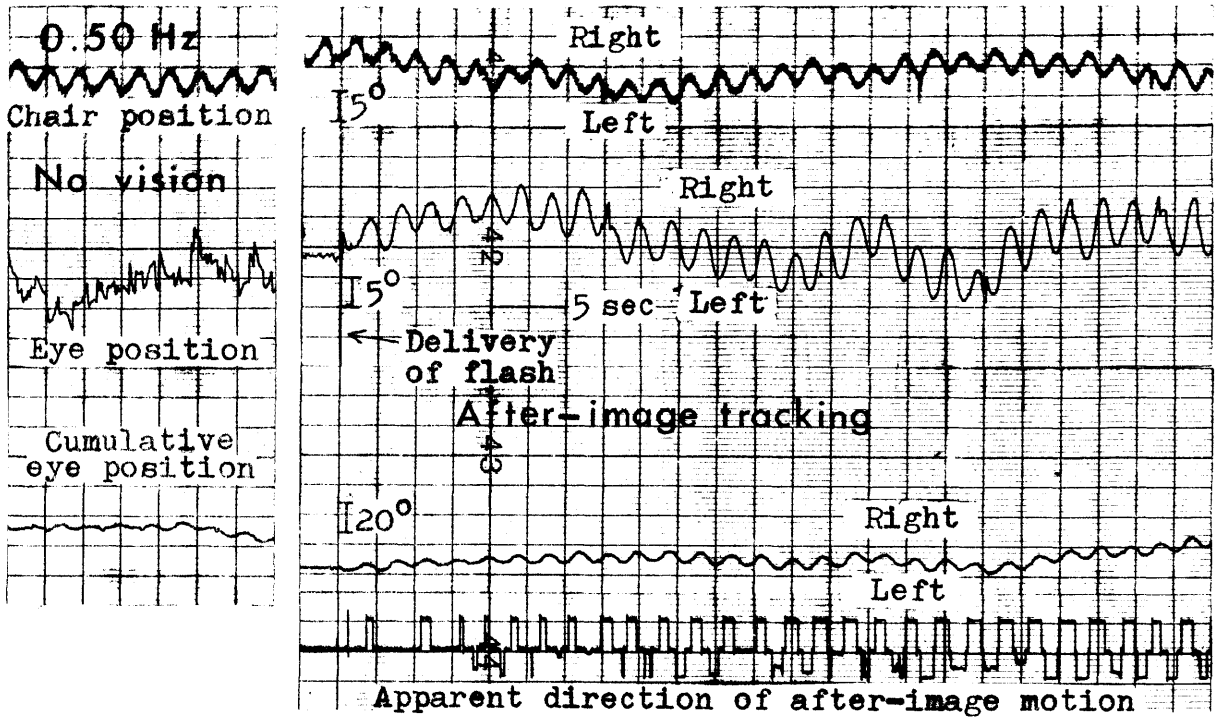


Fig. 3.7 Typical traces for a complete run with chair oscillation frequency at 0.50 Hz.



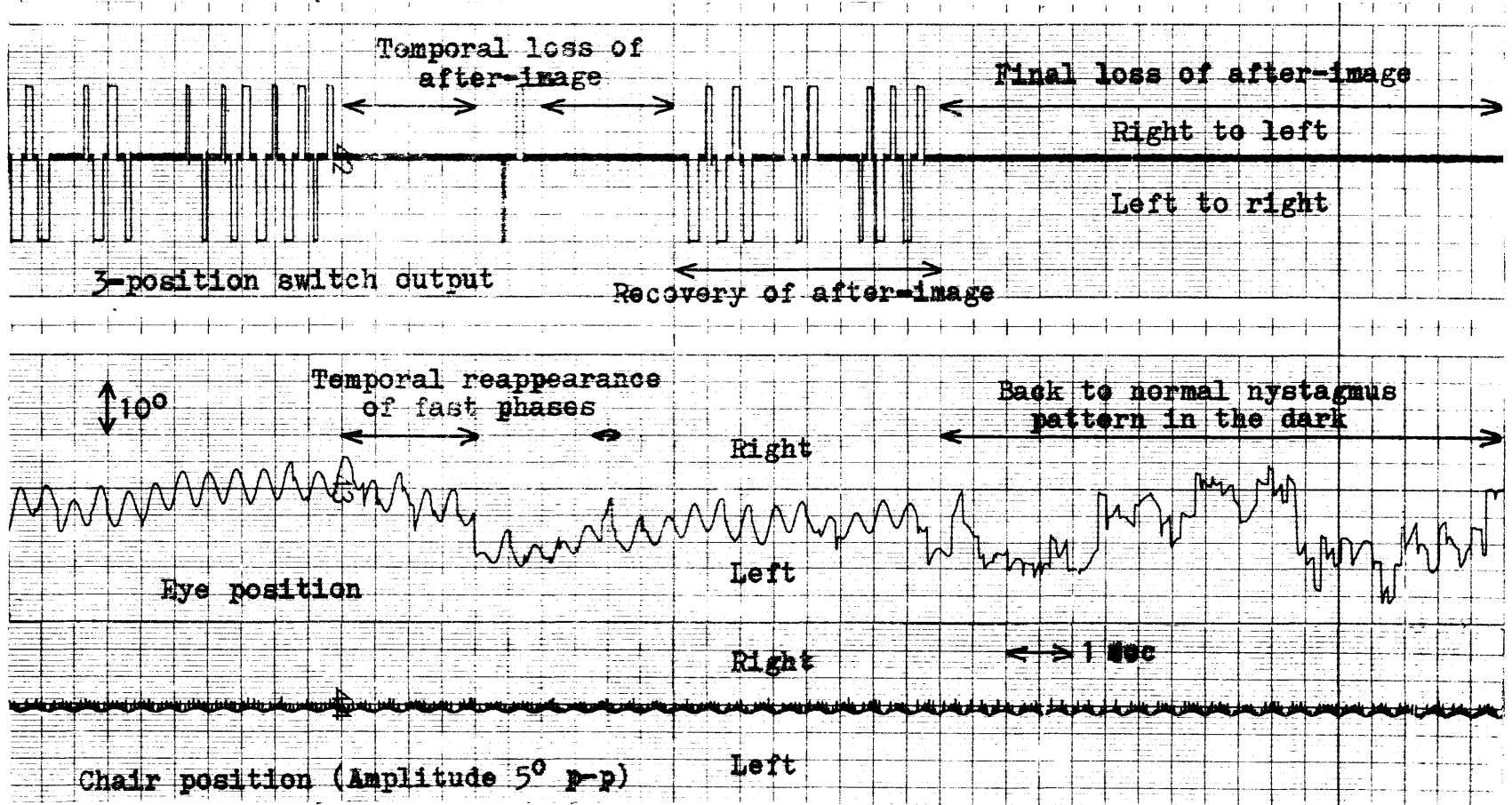
the inside of the chair was completely darkened and the subject had no vision, the familiar vestibular nystagmus can be seen. After this, the visual fixation light was turned on temporarily. (This fixation interval is obvious from the eye movement trace.) The light flash came from this fixation direction so that the after-image was established at the fovea. The instant of flash delivery is indicated by the eye movement monitor's special response in the form of a spike.

Then the after-image tracking began. Notice that the fast phase movement almost disappeared and the eye movement tended to become smooth. And the apparent motion of the visual after-image seems to be in phase with the ongoing smooth eye movement, as indicated by the 3-position switch output. This is consistent with the visual judgement mechanism as described by the corollary discharge theory or equally by its closed-loop version proposed in this chapter: as apparent from Figure 3.3-b the perceived after-image motion must describe the eye movement itself\*.

As time went on, the subject occasionally lost the fading after-image for a moment. This is apparent from no report

---

\* In fact, an after-image has been used as a subjective means to measure the eye movement. However, aside from its lack of objectivity, this method might give some incorrect information, according to the perceptual feedback hypothesis under present investigation: if the subject were to concentrate strongly in order to report as accurately as possible the trajectory of his perceived after-image motion, it would naturally lead him to keep tracking the after-image and thereby might alter the original eye movement of the experimenter's real interest which would be obtained without the after-image.



- 130 -

Fig. 3.8 Transient features indicating that disappearance or reappearance of nystagmus fast phases is correlated respectively with maintenance or loss of subjective perception of visual after-image target.

(sustained neutral level) from the 3-position switch.

Temporal reappearance of fast phases was often observed during such a transient period, as typically shown in Figure 3.8. This tendency suggests that the subjective perceptual loss of the after-image is more essential than the physical loss, for recovery of the nystagmus fast phase component.

Referring back to Figure 3.7, the transient stage lasted about 30 seconds as seen in the eye movement trace before the normal vestibular nystagmus with fast phase jumps eventually resumed in the total darkness after the final complete loss of the after-image.

Next, notice the cumulative eye position trace which indicates a somewhat greater amplitude attained during the after-image tracking, as compared with the cumulative position amplitude obtained in the total darkness. This difference can be shown also in terms of the velocity of smooth eye movement portions as revealed in Fig. 3.9. Other runs yielded more or less the same general trends as described above, and another sample result with a different subject and different oscillation frequency (0.25 Hz) is presented in Figure 3.10.

The eye movement difference as observed in the above inspection is what is expected from the perceptual feedback hypothesis for the pursuit tracking, and will be assessed more closely in the following frequency domain comparison.

The first case was for regular sinusoidal chair oscillation without vision, a situation which has been explored extensively by previous workers. Figure 3.11 shows that, within the limited frequency range tested here, the present

result is in fair agreement with those obtained by others that have confirmed the compensatory nature of the slow phase in the mid frequency range.

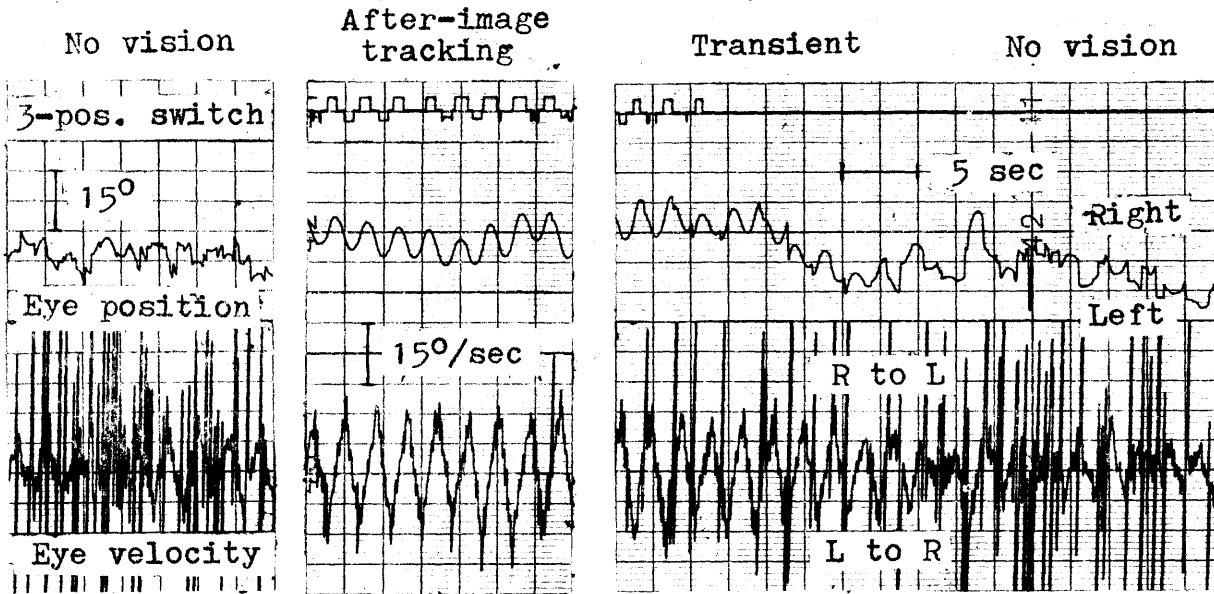


Fig. 3.9 Increase of eye velocity amplitude (smooth movements) during after-image tracking under the same vestibular stimulus condition ( sinusoidal chair oscillation at 0.5 Hz).

The second case was for regular sinusoidal chair motions with visual after-image whose apparent motion was being tracked visually by subjects. The corresponding frequency response result is presented in Figure 3.12 along with the result of the first case (Figure 3.11) for comparison. Also, the student's t-test was performed on these two cases under consideration, on the basis of the 5% significance level ( $p \leq 0.05$ )\*. This statistical result is summarized in Table 3.4-a appearing at the end of the current section. The following features have

\* For the student's t-test, consult, for example, "Statistical Method", Snedecov, G.W. and Cochran, W.G., The Iowa State University Press, Ames, Iowa, 1937 (First Edition).

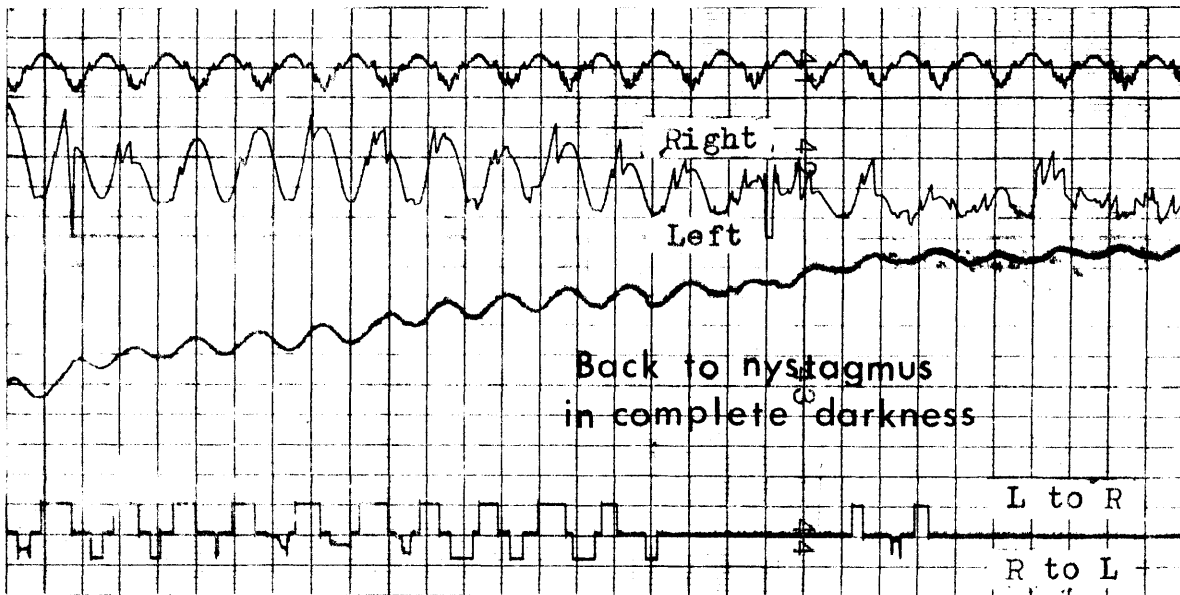
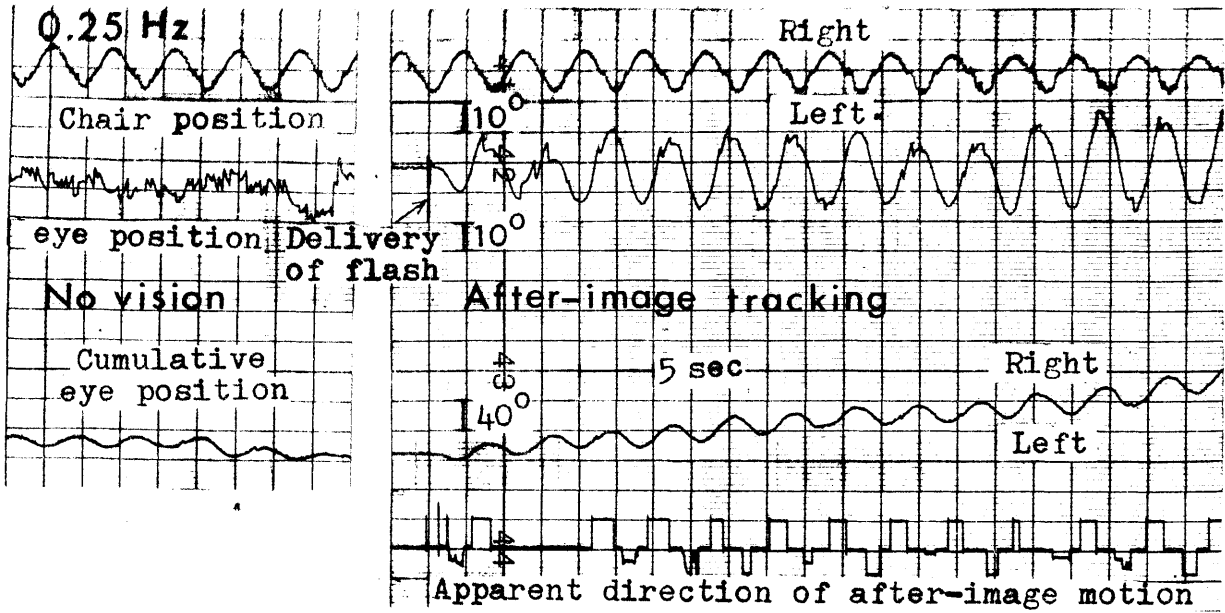


Fig. 3.10 Typical traces for a complete run with chair oscillation frequency at 0.25 Hz.

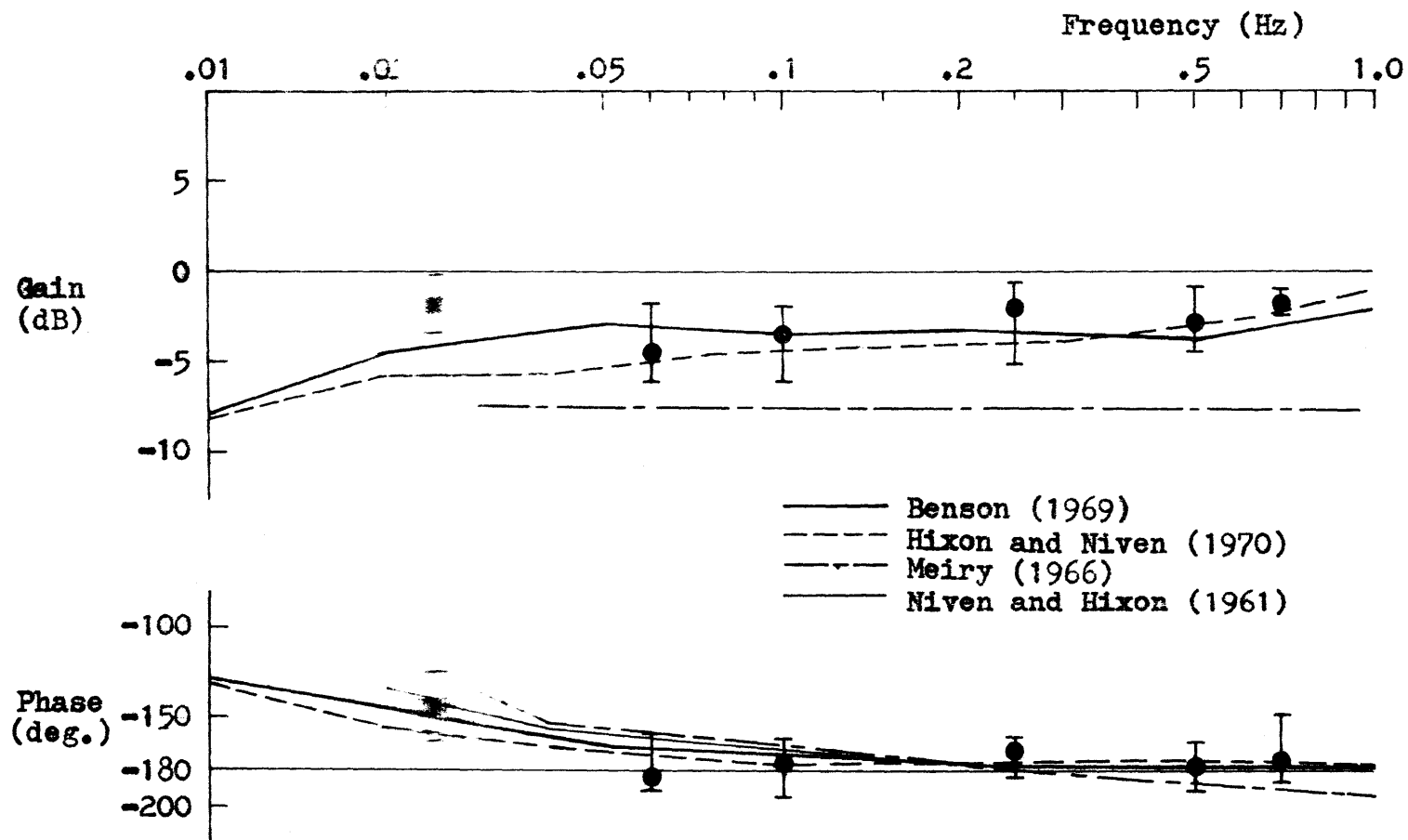


Fig. 3.11 Vestibular labyrinth slow phase frequency response (based on sinusoidal stimulation) in the dark. Median data points and one standard deviation are shown along with published data.

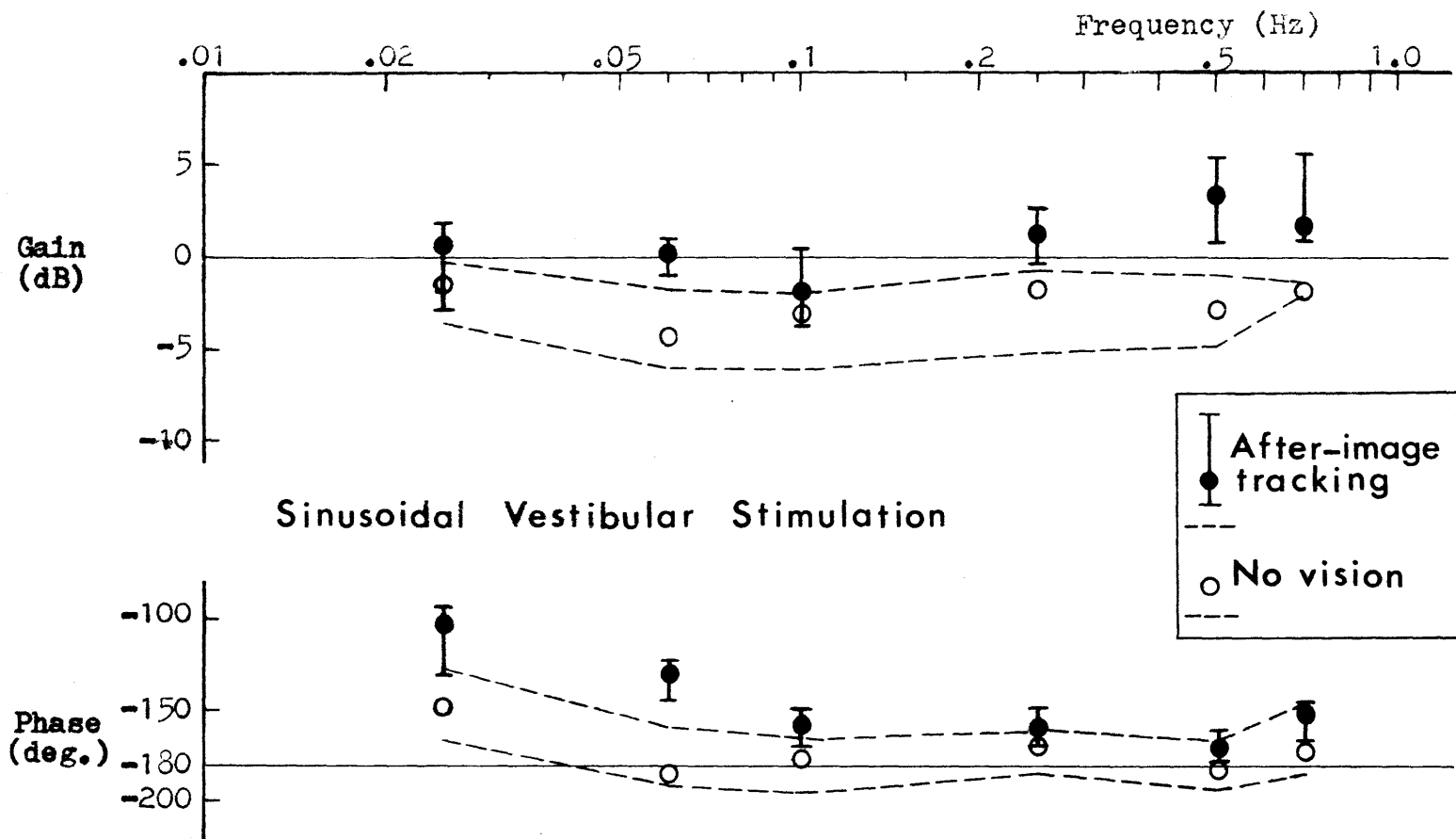


Fig. 3.12 Frequency response comparison (based on sinusoidal head rotation) between after-image tracking eye movement and vestibular nystagmus slow phase in complete darkness without after-image. Median data points and  $\pm$  one standard deviations are shown (4 subjects).

emerged from these data averaged over the subjects:

- (1) For the same harmonic chair oscillations, the amplitude of the slow phase velocity became somewhat greater in the second case (under after-image tracking) than in the first case (no vision), for almost all frequencies tested. (Direct appreciation of this feature has already been made with the sample raw data previously given.) The above trend appears to have become more significant as the input frequency became higher, although data points at 0.06 Hz would contradict such an opinion. At 0.70 Hz, the amplitude difference between the two cases was as much as about 6 dB; the slow phase velocity amplitude under the condition of after-image tracking was approximately twice as great as that with no visual input.
- (2) The phase was advanced up to about 40 degrees with after-image as compared to the case in the total darkness. This phase advancement held for all frequencies, and it was most prominent for the lowest two frequencies, 0.025 and 0.06 Hz as contrasted with less phase difference at higher frequencies.

Aside from detailed frequency-sensitive features at the present stage of investigation,\* it may be generally concluded

---

\* Quantitatively, the assessment is probably less accurate at the lowest two frequencies due to the somewhat crude means enforced in reducing the eye movement data inherently suffering from saturation during after-image tracking at these frequencies (see Table 3.3).



as supported from the statistical test, that smooth eye movement, obtained under the condition of visual after-image tracking with sinusoidal angular accelerations applied concurrently to the head, significantly differed in both amplitude and phase from the vestibular nystagmus slow phase in the dark.

This appears to be a positive result in the context of the rationale behind the present experiment: The above difference was due to the pursuit oculomotor command signal, which was introduced to the oculomotor system, in addition to the vestibulo-ocular reflex, in an effort to follow the after-image motion; an evidence to support the notion that the smooth pursuit movement can be produced according to a subjective motion that the observer visually perceives.

On the other hand, however, in the face of the finding that the nystagmus fast phase component disappeared during after-image tracking, this interpretation of the result might become interfered with or further complicated, if not wholly jeopardized, by the notion of Sugie and Jones (1965, 1966 and outlined in Section 2.3), which stresses the importance of fast phase movements in regard to their functional role crucial in integrating the vestibular afferent for achieving subsequent compensatory movements.

Nevertheless, some counter evidence can be given against this theory: contrary to the ether-controlled fast phase suppression experiment by Sugie and Jones, the compensatory phase relation between head rotation and slow phase response

seems to be preserved even in the absence of the vestibular nystagmus fast phase component as is apparent in the following data:

- (1) Vestibular nystagmus records by ten Kate (1969) in the pike with small stimulus magnitudes below the fast threshold.
- (2) Smooth portions of the eye movement trace typically obtained under vestibular stimulation plus a visual fixation target, as will be shown and discussed in Subsection 3.6.4.

On this ground, it is concluded here that the observed eye movement difference resulted not from the loss of the fast phase component, but from the perceptual feedback in favor of the proposed pursuit visual tracking model.

### 3.5.2 Pseudo-random Vestibular Stimulation

The third case of the present series of experiments was for a pseudo-random chair excitation in complete darkness. Figure 3.13 shows a typical record. Traces from the top correspond to chair position, vestibular nystagmus eye position and cumulative eye position. The frequency response result for the nystagmus slow phase component, obtained through methods which were described previously, is plotted with

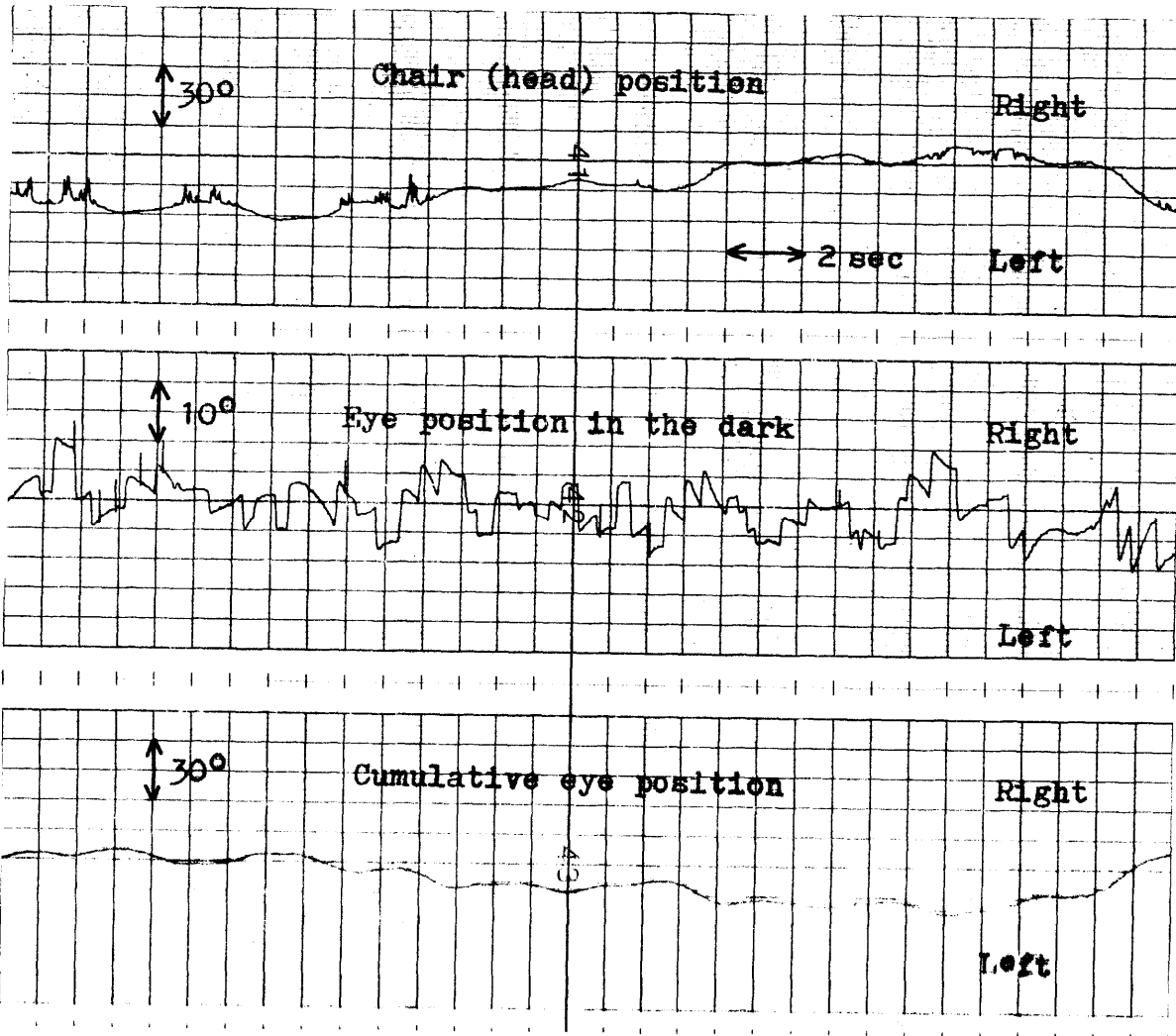


Fig. 3.13 Sample traces during pseudo-random vestibular stimulation with no vision.

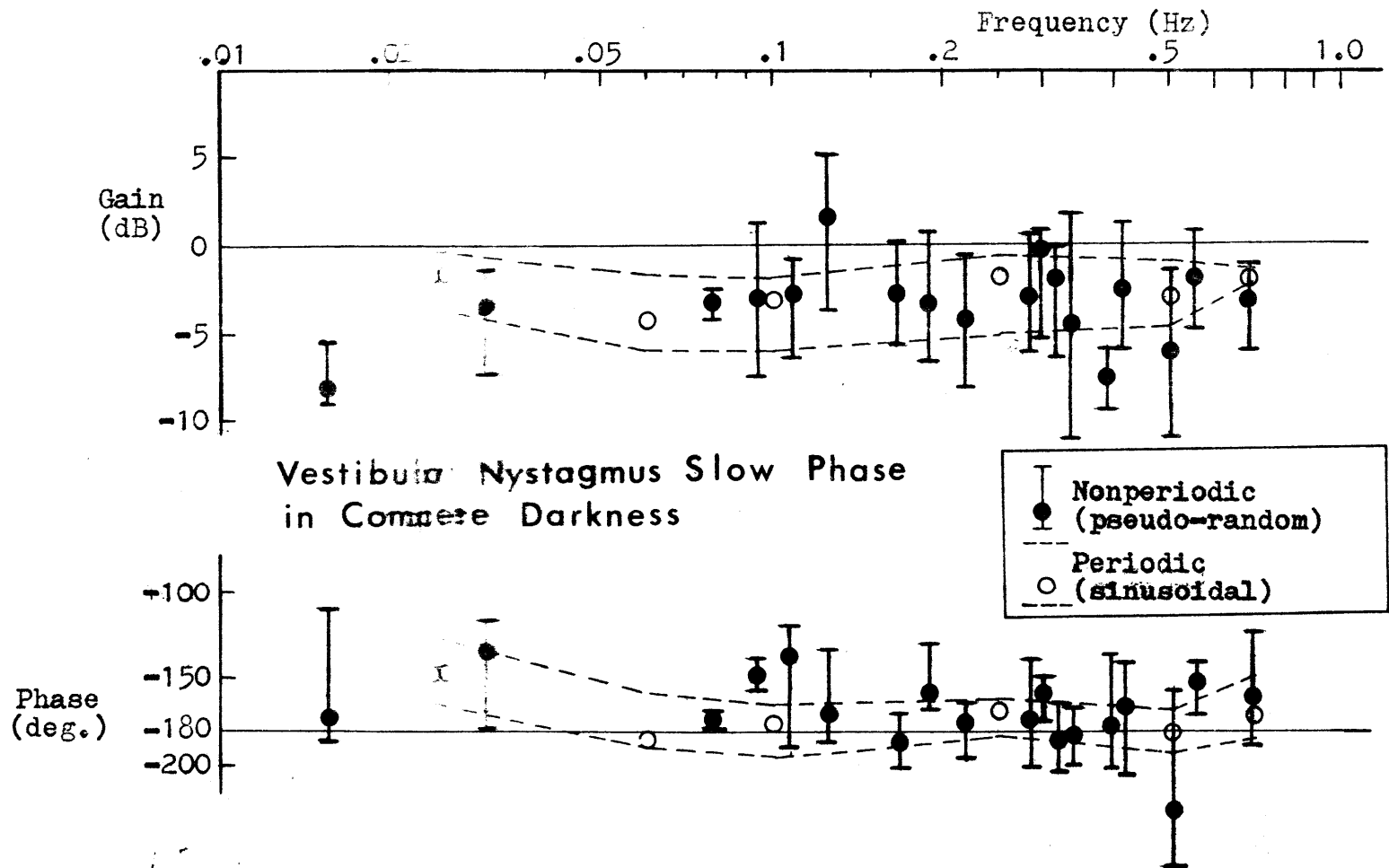


Fig. 3.14 Vestibular nystagmus slow phase frequency response results (4 subjects) in the dark. Periodic versus nonperiodic stimulation to head angular motion. Median data points and  $\pm$ one standard deviations are shown.

closed circles in Figure 3.14\*.

This part of the experiment was intended to examine the possible predictive behavior of the slow phase component in the vestibulo-ocular reflex arc. Such a study has been already suggested by Outerbridge (1969) and Young (1971). To this end, the present result was compared with the frequency response obtained in the first case (i.e., Figure 3.10; sinusoidal chair motion in complete darkness) as indicated by open circles in Figure 3.14. The corresponding student's t-test result ( $p \leq 0.05$ ) is given in Table 3.4-b.

There appears to be no substantial difference between the two cases, indicating that prediction is not involved in this non-visual oculomotor response at least in the relatively low frequency region tested here. On the other hand, Young (1971) has suggested that, if a predictive mechanism were

---

\* Despite the fact that the chair driving signal was a sum of 10 sinusoids, there are 18 frequencies giving rise to data points in Figure 3.14. However, this discrepancy is only an apparent one for the following two-fold reason:

First, due to some nonlinear aspect of the chair dynamics (chiefly attributed to friction in the drive unit), some new harmonics could be created while certain original high-frequency components were lost. Second, the frequency resolution in the computer printout was 0.0156 Hz in accordance with the sampling epoch chosen here (64 sec) with the current discrete Fourier transform algorithm. Thus, the computed value of a particular stimulus frequency was subject to fluctuations with a range of  $\pm 0.0156$  Hz.

When, all individual subjects' Bode plot results are combined, the above two effects make it appear as if there were 18 input frequency components. It is reemphasized that features of the stimulus frequency spectra given in Figure 3.6 remained basically the same for each individual subject.

present, it might contribute, at least to some extent, to the lead network-like behavior reported by Benson (1969) and Niven and Hixon (1970) in connection with their high frequency nystagmus data (see Section 2.3). Unfortunately however, due to the power limitation in driving the rotating chair, it was not possible to examine the above possibility of a high-frequency prediction mechanism whose effect would start around the upper end of the present bandwidth.

The fourth case was again for the condition of after-image tracking but with the same pseudo-random chair motion as in the preceding case. Figure 3.15 gives the corresponding frequency response results (closed circles)\*. Data for subject CO were discarded because of a technical failure in the eye movement measurement. In this case, the after-image target appeared to move randomly rather than periodically while being tracked visually. In Figure 3.15 this after-image tracking frequency response is compared with the preceding result (open circles) for the vestibular nystagmus under the same random chair motion but with no visual input.

It appears that the eye movement amplitude became somewhat greater during after-image tracking over the frequency range

---

\* The preceding footnote applies here as well. Due to the limited time interval of the after-image's persistence, the sampling epoch had to be cut in half (i.e., 32 seconds instead of the previous value of 64 seconds). This doubled the frequency resolution, resulting in  $\pm 0.0312$  Hz for the fluctuation range in the printout results.

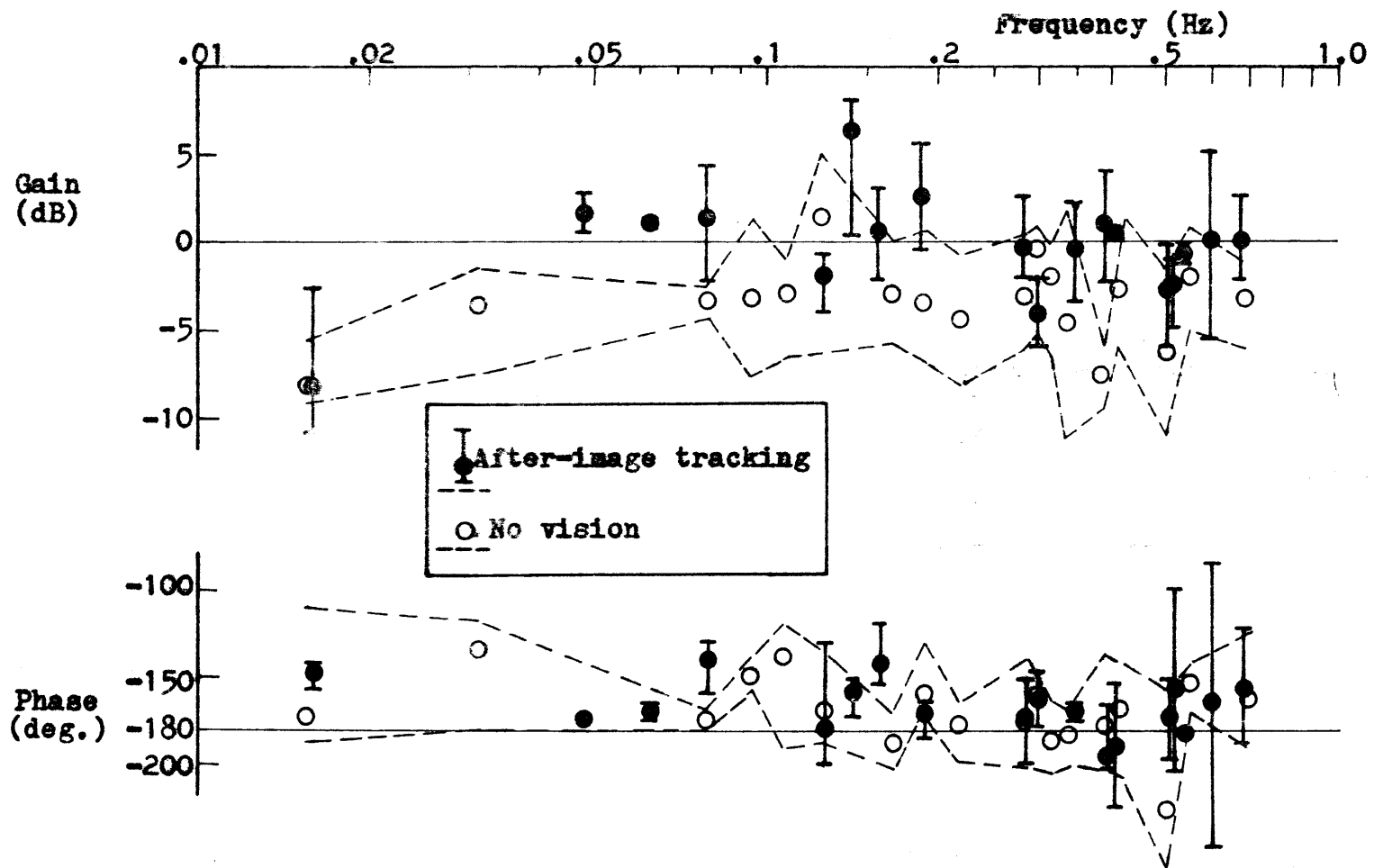


Fig. 3.15 Frequency response data for two types of smooth eye movement under pseudo-random vestibular stimulation: Smooth eye movement during visual tracking of vestibularly-induced after-image apparent motion versus normal vestibular nystagmus slow phase in the dark.

investigated. Statistical significance of the difference, however, is not as conspicuous as in the previous sinusoidal stimulus comparison, nor is it quite consistent throughout the frequency range as indicated in Table 3.4-c. Even so, similar to the previous interpretation, some positive trend of the eye movement difference probably resulted from the perceptual feedback to the pursuit oculomotor center in tracking the pseudo-random after-image's apparent motion. This would mean that it is the perceived visual motion itself not its predictability which is essential to the perceptual feedback.



Frequency (Hz)		.01	.02	.03	.04	.06	.08	.1	.2	.3	.4	.6	.8
Fig. 3.12	Gain	After-image	0			+		0		+		+	+
		No vision	0				-		0		-		-
	Phase	After-image	+				+		+		+	0	0
		No vision	-				-		-		-	0	0

(a) Smooth eye movement during visual tracking of vestibularly-induced after-image apparent motion versus normal vestibular nystagmus slow phase in the dark: Sinusoidal vestibular stimulation

Frequency (Hz)		.01	.02	.03	.04	.06	.08	.1	.2	.3	.4	.6	.8
Fig. 3.14	Gain	Pseudo-random		-		0		0		0		0	0
		Sinusoidal		+			0		0		0		0
	Phase	Pseudo-random		0			0		+		0		0
		Sinusoidal		0			0		-		0		0

(b) Vestibular nystagmus slow phase in the dark: Pseudo-random versus sinusoidal vestibular stimulation. (Original pseudo-random input data are linearly interpolated to provide data at frequencies chosen for sinusoidal stimulation.)

Tables 3.4 Summary of student's t-test results based on 5 % level of significance. In the illustrative example on right, mean value of a quantity at frequency of  $f_1$  is greater under condition X than Y with probability of at least 0.95. The converse statement is held at  $f_2$ . At  $f_3$ , no positive conclusion can be drawn with more than 95 % confidence as to dependence of the quantity upon the two different conditions X and Y. (Illustrative example)

	$f_1$	$f_2$	$f_3$
X	+	-	0
Y	-	+	0

		Frequency (Hz)											
		.01	.02	.03	.04	.06	.08	.1	.2	.3	.4	.6	.8
FIG. 3.15	Gain	After-image	0	-----	-----	-----	0	0	0 +	-----	+0	+0	00 +
		No vision	0	-----	-----	-----	0	0	0 -	-----	-0	-0	00 -
	Phase	After-image	0	-----	-----	-----	+	0	+ -	-----	00	00	0- 0
		No vision	0	-----	-----	-----	-	0	- +	-----	00	00	0+ 0

(c) Smooth eye movement during visual tracking of vestibularly-induced after-image apparent motion versus normal vestibular nystagmus slow phase in the dark: Pseudo-random vestibular stimulation

Tables 3.4 (Continued)

### 3.6 Supplementary Discussion on Perceptual Feedback Model

#### 3.6.1 Problem of Open-loop Structures

Having obtained an affirmative evidence for the perceptual feedback hypothesis for the pursuit tracking, the corresponding model may deserve a further refinement from the present skeleton type structure (Figure 3.2) particularly in the framework of control systems theory. While some recommendations to this end are summarized in Section 8.1, this section, based on some psychophysical evidence in the literature, develops servomechanical arguments to try to answer the following question that appears to arise from the perceptual feedback oculomotor control model:

The model reduces to yield the appearance of an open-loop feedback arrangement, due to the cancellation between the actual eye movement and the corollary discharge, or in other words between the innate negative visual feedback loop and the internal positive feedback loop emerged from the perceptual feedback hypothesis. It is, in fact, for this reason that the open-loop pursuit model by Young et al (1968) has been interpreted by Robinson (1969) and Rashbass (1969) to imply essentially the same perceptual feedback concept as that considered here. However, an open-loop (nonfeedback) organization sounds quite unlikely as a biological system which is apt to confront various uncertain factors such as external noise disturbances

as well as variations in functional characteristics of the constituent elements. It would be particularly strange, if the oculomotor tracking system were to avoid exploiting the apparently beneficial feature of the built-in visual negative feedback loop. A solution to this problem might be that the cancellation is accomplished not fully but only partially in association with the pursuit eye movement and the subjective impression of a moving visual object. The system as a whole would then remain under negative feedback control, without destroying the essential aspect of the visual judgement mechanism. This point is analyzed on a preliminary basis in the following section along with some supporting psychophysical evidence.

### 3.6.2 Block Diagram Nomenclature

The basic model for the perceptual feedback pursuit oculomotor control system presented in Figure 3.2 can be redrawn to yield the block diagram shown in Figure 3.16-a. This diagram includes the oculomotor signal originating in the semicircular canal. Within the pertinent frequency range, head angular acceleration is essentially integrated twice to give rise to the compensatory eye movement (compensatory slow phase position). While the first integration takes place mechanically at the semicircular canal, the second integration is performed neurologically (see Section 2.3). As evident from the vestibularly induced apparent motion of the visual after-image, the vestibulo-

Fig. 3.16-a Control theory representation for the perceptual feedback pursuit tracking model including vestibular afferent signal.

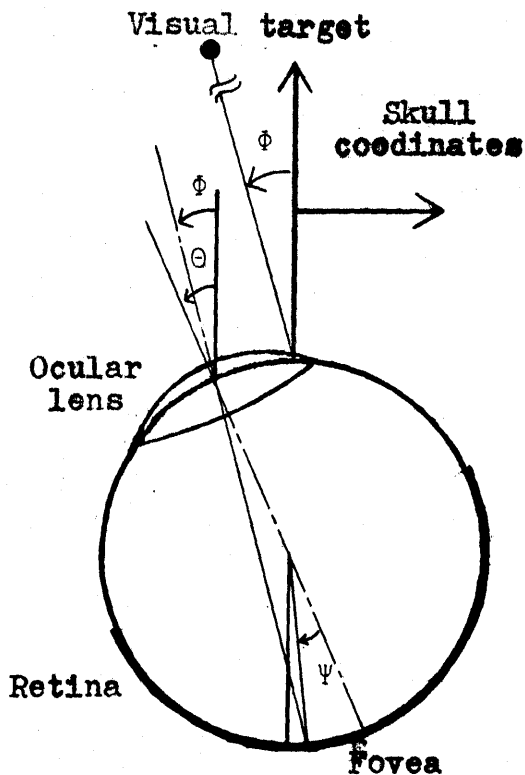
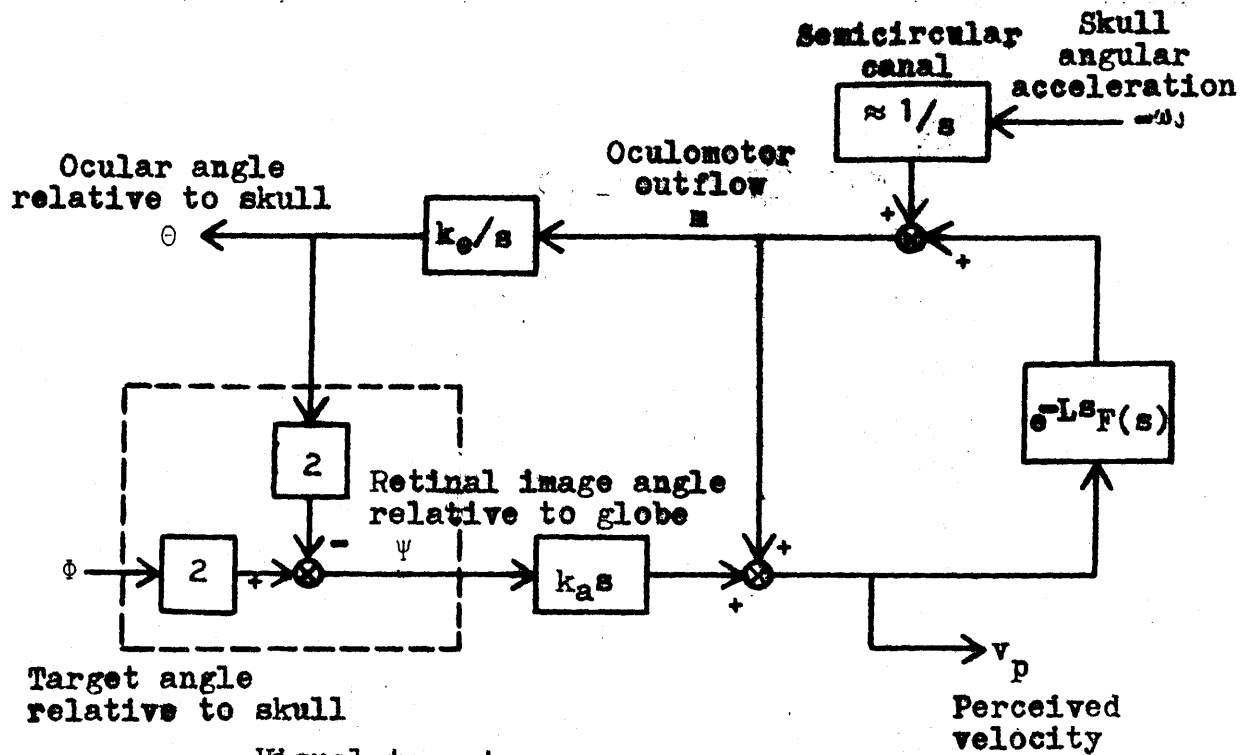


Fig. 3.16-b Schematic drawing of the globe-lens-retina system showing  $\psi = 2(\phi - \theta)$ .

lar nystagmus slow phase pathway must join the pursuit system before the branching of the motor outflow on its way to the visual judgement center.

Since the latency of the vestibulo-ocular reflex is much smaller than that of the pursuit system, the former is ignored and the latter, as represented by  $e^{-Ls}$  ( $L \approx 150$  msec), should be located before the aforementioned vestibular-pursuit junction. A considerable portion of the pursuit delay time might be attributed to conduction time of the visual afferent from the retina to the visual perception center. The corollary discharge pathway also might introduce some transport lag. However, the last two possible contributions are not taken into account in the present consideration.

Future research might assess how the visually perceived information could be converted to the pursuit oculomotor efferent. Probably, this transformation would be highly nonlinear as suggested by the result obtained in the next chapter on another aspect of the pursuit tracking.\*

The transduction of the retinal image velocity into the visual afferent firing rate is assumed to incorporate a constant gain,  $k_a$ , which has a dimension of (discharge rate)/

---

\* Even so, suppose for the illustrative purpose that transfer function,  $F(s)$ , were given to describe this perceptual-oculomotor relation. Then, the eye movement difference previously discussed in the after-image tracking experiment would correspond to the closed-loop transfer function of the internal regenerative loop as given from Figure 3.16-a by the expression:  $1/[1 - e^{-Ls} sF(s)]$ . If  $F(s) = 1/s$  for instance, the regenerative loop would behave as a pseudo-integrator (with a gain of  $1/L$ ) at low frequencies.

(degree/sec). The constant,  $k_e$ , scales the eye position in proportion to the oculomotor efferent discharge frequency,  $m$ , and its dimension is the inverse of that of  $k_a$ . This corresponds to a pure gain approximation of the oculomotor mechanical plant. The discharge rate, to which the visual velocity of the perceived target motion is assumed to be proportional, is designated by  $v_p$ .

Finally, two gain factors of 2 are associated with the retinal summing point as it appears in the diagram in Figure 3.16-a. This is due to the physical fact that the optical nodal point of the ocular lens is located not at the globe center, which is approximately the center of globe rotation, but located about the anterior surface of the eye ball. Figure 3.16-b shows an idealized geometry\*, where the distance of the visual target is assumed very large compared with the dimension of the eye ball. Immediately one obtains the relation

$$\Psi = 2(\Phi - \Theta) \quad (3-1)$$

from this figure, where:

- $\Phi$ : Angle of visual target relative to the skull
- $\Theta$ : Angle of ocular rotation relative to the skull.
- $\Psi$ : Angle of retinal image relative to the center of the ocular globe

---

\* The actual arrangement is, of course, much more complex than assumed here. For instance, the ocular globe is not a perfect sphere, and the center of rotation does not remain at a fixed point (Alpern, 1962).

In terms of velocity, Eq. 3-1 is rewritten as:

$$\dot{\Psi} = 2(\dot{\Phi} - \dot{\Theta}) \quad (3-2)$$

### 3.6.3 Visual Velocity Sensation based on Afferent versus Efferent Monitoring

The subjective velocity of a moving visual target is greater when judged by the stationary eyes than when judged by the eyes following the target motion. In the former case, there is no motor activity, and the velocity estimation must depend entirely on the information from the retina. In the latter situation, on the other hand, (if the target velocity is not too high), the visual tracking is performed mostly by smooth pursuit movements, and the retinal image remains virtually stationary. In this case, little velocity information is provided visually from the retina, and consequently the velocity must be estimated essentially from the efferent motor information responsible for pursuit movements. Dichgans et al (1969) showed by psychophysical experiments that, for a wide range of physical target velocities, the afferent visual information evokes about 1.7 times greater visual velocity sensation than the efferent motor information does.\* Jung (1971) poses the question why such a difference exists. This psychophysical

---

\* As Dichgans et al further noted, when the ocular following movements lag behind the higher target velocities, the afferent and efferent information can be combined for the velocity information.



consequence might be understood, as discussed in the the following section, in terms of the partial cancellation associated with the perceptual feedback model proposed for the pursuit tracking.

A signal proportional to the perceived velocity,  $v_p$ , in general can be expressed from Figure 3.16-a as:

$$v_p = 2K_a(\dot{\phi} - \dot{\theta}) + \dot{\theta}/k_e \quad (3-3)$$

When the eyes are stationary,  $\dot{\theta}$  is zero. Thereby the perceived velocity,  $v_{aff}$ , is given as:

$$v_{aff} = 2k_a\dot{\phi} \quad (3-4)$$

On the other hand, when the eyes follow the visual motion,

$$\dot{\theta} \approx \dot{\phi} \quad (3-5)$$

assuming that the target velocity is not too great and the oculomotor tracking is performed adequately. The corresponding subjective velocity,  $v_{eff}$ , becomes:

$$v_{eff} \approx \dot{\theta}/k_e \approx \dot{\phi}/k_e \quad (3-6)$$

Thus the ratio of the two subjective velocities can be expressed as:

$$\frac{v_{aff}}{v_{eff}} = 2k_a k_e \quad (3-7)$$

If  $v_{aff}$  were equal to  $v_{eff}$  ( $k_a k_e = 1/2$ ), it would mean that the visual negative feedback and the inner positive feedback just cancel each other. As a result, no effective feedback would operate upon the pursuit system. If  $v_{aff}$  were less

than  $v_{\text{eff}}$  ( $k_a k_e < 1/2$ ), the net feedback would be positive and the system feasibility would become worse than the open-loop case. Thus,  $v_{\text{aff}}$  must be greater than  $v_{\text{eff}}$  ( $k_a k_e > 1/2$ ) in order to provide the pursuit system with a net negative feedback effect for proper servomechanical operation. This requirement is, in fact, consistent with the evaluation by Dichgans et al, which gives:

$$\frac{v_{\text{aff}}}{v_{\text{eff}}} = 1.7 \quad (3-8)$$

Hence,

$$k_a k_e = 1.7/2 \quad (> 1/2) \quad (3-9)$$

Thus, it may be said that the outflow cancellation is done only slightly above 50% ( $100 \times 1/1.7$ ). It appears as though the corollary discharge took little into account the factor of 2 arising from the ocular kinematic relation so as to maintain the effective negative feedback.

#### 3.6.4 Partial Cancellation Hypothesis and Oculogyral Illusion

The foregoing concept of partial cancellation, or partial compensation appears to be consistent with the phenomenon of the oculogyral illusion as discussed in the following. The oculogyral illusion refers to the apparent movement of a visual target following stimulation of the semicircular canal by angular acceleration. Usually the oculogyral illusion is studied in a darkened environment, and the visual field is restricted to a

point of light. This precludes the optokinetic stimulation which would otherwise be produced. Extensive descriptions of this illusion can be found in the literature (Graybiel and Hupp, 1946; Whiteside et al, 1963; Clark, 1949, 1963; Peters, 1969).

When the subject is asked to fixate on a real target which is physically stationary relative to him, the visual target appears to move with respect to him. The direction of this perceived visual motion tends to be opposite to that of the vestibular nystagmus slow phase movement which would be induced by the same angular stimulation in complete darkness without the visual target.

Eye movements under the above conditions were measured previously by Meiry (1965). He found that the vestibular nystagmus is not completely inhibited despite the subject's visual fixation effort. As compared with the normal vestibular nystagmus in the dark, the eye movement still contains slow phase like smooth movements, interrupted by a number of successive corrective saccades due to the visual fixation attempt which overrides the fast phase component of nystagmus. The over-all eye movement is confined within  $\pm 0.5^\circ$  of its mean position. The author repeated Meiry's experiment and confirmed these observations. (The oculogyral illusion undoubtedly occurred, as evident from the subjects' verbal reports.) Figure 3.17 presents a typical record obtained under a sinusoidal chair oscillation (0.1 Hz) along with the normal vestibular nystagmus measured in the dark by applying the same motion stimulus. The following trend was observed for various oscillation frequencies tested (up to 0.7 Hz).

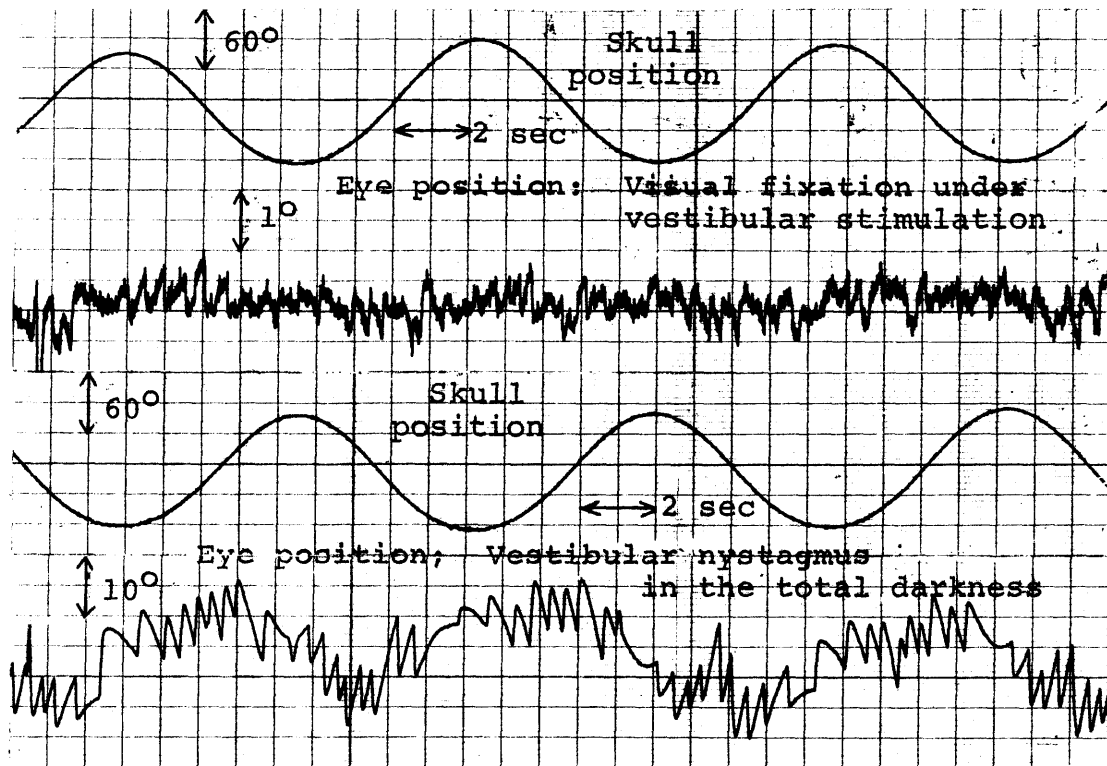


Figure 3.17 Vestibularly induced eye movement patterns with and without visual fixation target.

The smooth eye movement portions observed under the condition of oculogyral illusion essentially remained periodic as is apparent from the above record. In comparison with the normal nystagmus slow phase, the velocity amplitude became much reduced but the phase relation with respect to the chair motion did not undergo a substantial change; the eye motion was still in the compensatory direction, making it appear as a remnant of the slow phase response.

A straightforward explanation would be that the strength of the nystagmus slow phase motor signal was simply reduced without affecting the phase relation, due to the presence of

the visual fixation target.\* However, the situation might well be more complex, for the smooth pursuit system also could be involved via the visual feedback in counteracting the eye's tendency to drift away from the fixation point due to the nystagmus slow phase efferent.

In any case, the miniature slow phase-like smooth movements can cause the target image to slip on the retina. This could account for the oculogyral illusion with correct prediction in regard to the direction of the illusory motion. Thus, one might assert that oculomotor signals for involuntary eye movements such as the one considered here are not conveyed to the visual judgement center through the corollary discharge (Bruell and Albee, 1955; Howard and Templeton, 1966). However, the use of an after-image target in place of a real target also leads to the illusory perception of visual velocity, as confirmed in this thesis in agreement with many others (Graybiel and Hupp, 1946; Whiteside et al, 1963; Wurtz and Goldberg, 1971; Grüsser and Grüsser, 1972). An after-image produces no retinal velocity signal, and the after-images apparent motion must imply that the involuntary eye movement signal does reach the visual-judgement center.\*\* (Recall, in contrast, that the

---

\* According to this view, the present eye movement behavior may be good evidence against the aforementioned theory of Sugie and Jones for vestibular nystagmus generation, for the compensatory phase relation appears preserved even without the fast phase component of nystagmus (observed saccades are due to the visual fixation not the nystagmus fast phase).

\*\* Peters (1969) and Wurtz and Goldberg (1971) also emphasize this point.

after-image remains motionless during passive eye movements by a finger). Another evidence supporting this point is that the oculogyral illusion is observed by patients suffering paralysis of the eye muscles (Byford, 1961).

Hence, it appears to be the partial cancellation which could account for the oculogyral illusion for both real and after-image targets. The following analysis examines this suggestion with regard to the directional relationship between the apparent motion and the eye movement.\*

The subscripts, 1, 2, 3, used in the following notations refer to case 1, case 2 and case 3, respectively. Case 1 involves no vision, corresponding to the usual vestibular nystagmus measurement in the dark. In case 2, a real fixation target is provided, whereas the target is replaced by a visual after-image in case 3. Eye movement measurements were done thus far for all of the above three cases. On the basis of these results, it may be said that the smooth eye movement velocity is roughly  $180^\circ$  out of phase with the head angular velocity,  $\omega$ , in all

---

\* In the literature, Peters (1969) proposes a somewhat different possibility leading to the illusory motion for both types of target. According to him, an involuntary oculomotor outflow can be taken into account by the corollary discharge cancellation mechanism, provided that the eyes are to move in response to that command (explaining the after-image case). However, whenever both voluntary and involuntary innervation occur simultaneously in antagonistic eye muscles, the voluntary component of motor outflow takes precedence over the involuntary portion in the visual judgement mechanism so that apparent visual motion results in the direction of voluntary innervation (accounting for the real-target oculogyral illusion).

cases. And one can write:

$$\dot{\theta}_1 \approx -k_1\omega \quad (\text{case 1: no vision}) \quad (3-10)$$

$$\dot{\theta}_2 \approx -k_2\omega \quad (\text{case 2: real target}) \quad (3-11)$$

$$\dot{\theta}_3 \approx -k_3\omega \quad (\text{case 3: after-image target}) \quad (3-12)$$

where the  $k_i$ 's are positive proportionality constants. The perceived velocity is generally expressed as given in Eq. 3-3.

In case 2, the fixation target is stationary, i.e.,  $\dot{\phi}_2 = 0$ . The retinal slip velocity caused by the eye velocity,  $\dot{\theta}_2$ , is actually  $-2\dot{\theta}_2$ . The corresponding visual afferent signal is given by  $-2k_a\dot{\theta}_2$ . This retinal velocity undergoes the subsequent compensation through the efferent copy,  $\dot{\theta}_2/k_e$ . From Eq. 3-3, the perceived velocity,  $v_2$ , becomes:

$$v_2 = \frac{1}{k_e} (-2k_a k_e + 1) \dot{\theta}_2 \quad (3-13)$$

But,  $K_a k_e = 1.7/2$  stemming from Dichgans et al, so that the outflow cancellation is only partially done to result in the apparent velocity:

$$v_2 \approx -0.7 \frac{1}{k_e} \dot{\theta}_2 \quad (3-14)$$

or from Eq. 3-11,

$$v_2 = 0.7 \frac{k_2}{k_e} \omega \quad (3-15)$$

In terms of the slow phase velocity in the dark, this can be further rewritten using Eq. 3-10:

$$v_2 = -0.7 \frac{k_e}{k_1 k_a} \dot{\theta}_1 \quad (3-16)$$

$v_2$  and  $\dot{\theta}_1$  have the opposite sign. Thus the equation describes

the illusion with correct prediction as to its direction of movement with respect to the nystagmus slow phase in the dark.

In case 3, the after-image target produces no retinal velocity, i.e.,  $\dot{\phi}_3 - \dot{\theta}_3 = 0$ . The velocity perception occurs due to the efferent copy alone, so that the subjective velocity,  $v_3$ , is given by:

$$v_3 = \dot{\theta}_3 / k_e \quad (3-17)$$

This predicts that the after-image will appear to move with the eyes, as actually observed in the time correlation between the 3-position switch report and the eye movement measured during the after-image tracking. Using Eqs. 3-10 and 3-12, the above equation can be approximately rewritten in terms of the nystagmus slow phase velocity in the dark:

$$v_3 \approx \frac{k_3}{k_1 k_e} \dot{\theta}_1 \quad (3-18)$$

This result is reconciled with the present as well as published observation that the after-image apparent motion was basically in the same direction as the vestibular nystagmus slow phase movement in the dark or in the direction opposite to the perceived motion described for a real target (Graybiel and Hupp, 1946; Whiteside et al, 1963).\*

Hence, it appears that the oculogyral illusion for both

---

\* These authors apparently did not measure eye movements in the case of after-image target, however.



real and after-image target can be accounted for by the partial cancellation concept that preserves the negative feedback control mode for the perceptual feedback pursuit oculomotor model.

### 3.7 Summary and Conclusions

Various behavioral evidence indicates that eye movement information intimately and vitally participates in the mechanism responsible for visual motion perception. The outflow cancellation theory is a widely accepted concept that accounts for this process. Central to this concept is a copy signal of the motor outflow (corollary discharge) which compensates for the effect of actual eye movements upon the retinal image motion so as to evoke visual impressions normally consistent with the external physical world.

The present oculomotor control model is a closed-loop feedback extension of this classical psychophysical theory: the perceived motion of a visual target might in turn influence the system that controls eye movements. That is, the oculomotor command signal might be generated on the basis of what the observer subjectively perceives as target motion.

An experiment was devised and conducted to examine the above perceptual feedback hypothesis. Vestibular nystagmus was induced in a darkened environment inside a rotating chair. A small visual after-image was impressed at the foveal region by means of a flashgun. Preliminary observation confirmed the following points noted by previous authors in similar type experiments: the visual after-image appeared to move in a manner related to the imposed chair motion. This apparent after-image motion must be due to the corollary discharge,

for retinal motion is impossible with an after-image. Contrasted with no after-image motion perceived with passive eye movements by a finger, this is evidence to show that the vestibular slow phase afferent does reach the visual judgement center envisioned by the cancellation theory.

Crucial points in the present experiment were the instruction to the subject and the subsequent eye movement measurement and analysis. The subject was asked to maintain visual tracking of the after-image. This was intended to force the postulated perceptual feedback to become active. Considering the nature of the after-image, the following rationale may be established: if the smooth portion of the subject's eye movement should become different from the slow phase of the vestibular nystagmus in complete darkness without after-image, the eye movement difference would be very likely attributable to the regenerative loop, emerged from the corollary discharge theory and the perceptual feedback hypothesis, which would create the pursuit oculomotor efferent as a secondary product of the original vestibular nystagmus slow phase efferent.

The eye movement traces were characterized by (1) normal vestibular nystagmus in complete darkness, (2) tendency toward disappearance of fast phase during after-image tracking, (3) transient period due to occasional losses and/or gradual fading of the after-image, and (4) return to the initial pattern after the final loss of after-image. After having confirmed that

the after-image apparent motion (whose direction was reported on-line by the subject using a 3-position switch) was in phase with eye movements as consistent with the corollary discharge theory, a comparative frequency-domain analysis on the above eye movement data yielded a statistically significant difference between after-image tracking movement and vestibular nystagmus slow phase without after-image.

In relation to the sinusoidal head rotation with the Bárány type chair, the eye movement amplitude tended to be greater for the former case than the latter (for example, the amplitude difference was about two-fold at 0.7 Hz), whereas the opposite trend was observed for the relative phase lag. This difference is pronounced, especially for higher-frequency amplitude and for lower-frequency phase shift, although the lower-frequency data are probably less accurate quantitatively due to a technical problem inherent in that frequency region.

In any event, the above conspicuous eye movement difference, aside from its frequency-dependent details at present, supports the hypothesis that the subject tracks the visual motion he perceives.

The experiment was repeated with and without after-image by driving the rotating chair pseudo-randomly rather than sinusoidally. The perceived after-image motion became presumably unpredictable in contrast with the preceding sinusoidal case. Though not as statistically significant as before, some eye movement difference was obtained also, in the present

case, between the condition of after-image tracking and that without after-image, suggesting that the periodicity or predictability of the perceived visual information is not an essential factor for operation of the perceptual feedback.

The suggested perceptual-oculomotor model reduces to yield the appearance of an open-loop (nonfeedback) configuration, due to the cancellation between the actual eye movement and the corollary discharge, that is, between the innate negative visual feedback and the internal positive feedback loop resulting from the corollary discharge theory and the perceptual feedback hypothesis. It is for this reason that Robinson (1969) and Rashbass (1969) have interpreted the open-loop pursuit model by Young et al (1968) as a similar type of model as is considered in this chapter. However, an open-loop control is somewhat difficult to imagine for a biological system. It would be even more strange for the oculomotor case, if the system were to avoid to take advantage of the built-in negative feedback loop. An answer to this question could be that the outflow cancellation is achieved not fully, but only partially for the pursuit movement. The system as a whole would then remain under negative feedback control. This possibility appears to be consistent with the phenomenon of the oculogyral illusion (for both a real and after-image target) as well as the psychophysical evidence by Dichgans et al (1969) showing that the afferent visual information evokes about 1.7 times

greater visual velocity sensation than the efferent motor information.

The visual eye tracking system has been extensively studied in the past in the framework of automatic control theory. The internal structure of the system has been deduced on the basis of servomechanical principles, in accordance with the "black box" approach stemming from measurement and analysis of external input (visual stimulus) and output (eye movement) variables. Also, a considerable amount of oculomotor research has been in progress in recent years based on relevant single-unit recordings in animals for direct assessment of physiology and anatomy of the oculomotor system. The psychophysical approach introduced in this chapter, on the other hand, assumes the use of human subjects with whom no surgical method is possible. In addition to objective information as to external physical input/output variables, perceptual information may be recognized as another useful system variable that reflects to some degree, the mechanisms internal to the biological control system in question.

Finally, foregoing nystagmus data with sinusoidal and random-input in the dark allowed examination of the question of predictive capacity in the vestibular nystagmus slow phase component. The result in this nonvisual oculomotor reflex was found to be statistically negative at least in the frequency range tested (up to 0.7 Hz).

## Chapter IV

### Frequency Response of the Pursuit System:

#### Input-adaptive Characteristics and Possible Predictive Behavior

Following a reevaluation of the predictive oculomotor behavior explored by many previous investigators in the dual-mode tracking eye movement, this chapter focusses on the question of whether the smooth pursuit component has its own predictive capacity. Regular sine wave stimuli and several pseudo-random stimuli are tested. Proper adjustment of the stimulus magnitude is emphasized in order to minimize the possible pursuit velocity saturation, whereas such a precaution appears to have been somewhat overlooked in the past. Pursuit eye movements are properly isolated from original eye movement data by eliminating saccades.

Results are assessed in detail in the frequency domain. A special interpretation is suggested in the context of the oculomotor predictive capacity to account for some characteristic input-adaptive features found in the phase behavior of the pursuit tracking system.

- 4.1 Introduction
- 4.2 Method
  - 4.2.1 Objectives
  - 4.2.2 Apparatus and Procedure
  - 4.2.3 Data Processing and Analysis
- 4.3 Results and Discussion
  - 4.3.1 Periodic-input: Composite and Pursuit
  - 4.3.2 Nonperiodic-input: Composite
  - 4.3.3 Nonperiodic-input: Pursuit
- 4.4 Pursuit Phase Behavior: Discussion and Theory
  - 4.4.1 Reliability of the Phase Result
  - 4.4.2 A Phase Control Model for Pursuit Tracking
- 4.5 Summary and Conclusions



#### 4.1 Introduction

Accuracy of the visual fixation on a moving object is improved by exploiting the stimulus periodicity, as best demonstrated in terms of frequency response. The dependence of the input-output phase relation upon complexity of the stimulus wave form is particularly conspicuous and intriguing: the phase lag during the periodic-input tracking is considerably smaller than is observed for the nonperiodic mode, and appears incompatible with the underlying innate oculomotor reaction time, a nonlinear phenomenon that most authors hypothetically attribute to a predictive or learning capacity of the oculomotor tracking system. This special oculomotor characteristic is known to exist in the human eye movement of some different categories induced by certain types of visual stimuli, and the relevant literature has been reviewed in Section 2.4. Further exploration of this important oculomotor property is one of the major research subjects in this thesis, and this chapter focusses on the smooth pursuit tracking movement from such a viewpoint.

A continuous motion of a small visual target is tracked by a composite of pursuit and saccadic movements. This dual-mode oculomotor system is reviewed in Section 2.1 along with the two subsystems, pursuit and saccade. Achievement of better visual tracking performance with periodic stimuli is generally true for the composite dual-mode system as well as the saccadic system acting alone.

The question then is whether the pursuit movement incorporates a predictive behavior of its own. In this regard, Vossius (1965) showed that the subject was able to continue making corrective pursuit tracking movements for a while after the visual target (sine wave at 1 Hz) was suddenly blanked. While the demonstration must imply the pursuit system's predictive capability, this chapter aims at characterizing the pursuit tracking system in the frequency domain in an attempt to provide a further insight into the underlying predictive process in question.

The two types of eye movement, pursuit and saccade, are functionally distinct and evidently under separate control by the central nervous system. Accordingly, it would be more rational to study each of the two constituent components separately rather than in terms of the original composite data. However, while the saccadic system can be activated selectively by a square-wave stimulus motion, a stimulation exclusive to the pursuit system cannot be sustained sufficiently long enough for a frequency response study under normal circumstances. Thus, one would be bound to base such a study on composite eye movement data that incorporates both saccade and pursuit movements. Acquisition of the relevant information must be negotiated with such composite data, and the hybrid computer routine MITNYS employed in the previous chapter becomes useful also for that purpose.

As the frequency response is a linear concept, possible nonlinear effects (other than the predictive behavior in question) must be minimized a priori by proper stimulus adjustment in order not to confuse the result. The most likely nonlinearity in this regard is the pursuit velocity saturation at high input velocities. As discussed in Section 2.4, ignorance of this particular nonlinearity in experimental preparation might well lead to an apparent less-than-minimum phase behavior, a result that may have nothing to do with the system's predictive function. For this reason, the stimulus velocity magnitude is carefully maintained small enough to prevent pursuit velocity saturation throughout the present series of experiments, whereas this precaution appears to have been somewhat overlooked in the past, having caused the probably misleading emphasis on the special gain-phase relation (less-than-minimum phase) obtained in the literature with the periodic-input composite frequency response.

## 4.2 Method

### 4.2.1 Objectives

The primary aim of the subsequent series of experiments is to investigate the question of predictive oculomotor behavior in the smooth pursuit tracking system; specifically, to obtain the frequency response considering only pursuit movements in terms of Bode plots under periodic versus nonperiodic stimulus conditions.

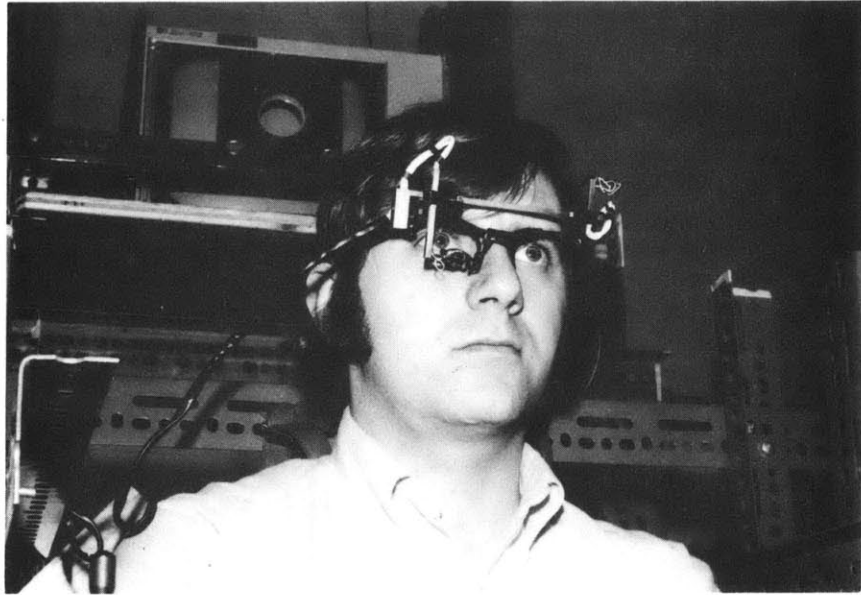
For the purpose of comparative assessment, the frequency response of the original composite eye movement also needs to be obtained for both periodic and nonperiodic-input tracking.

For the reason given in the previous subsection, it is also of importance to compare the composite result with those obtained by other investigators.

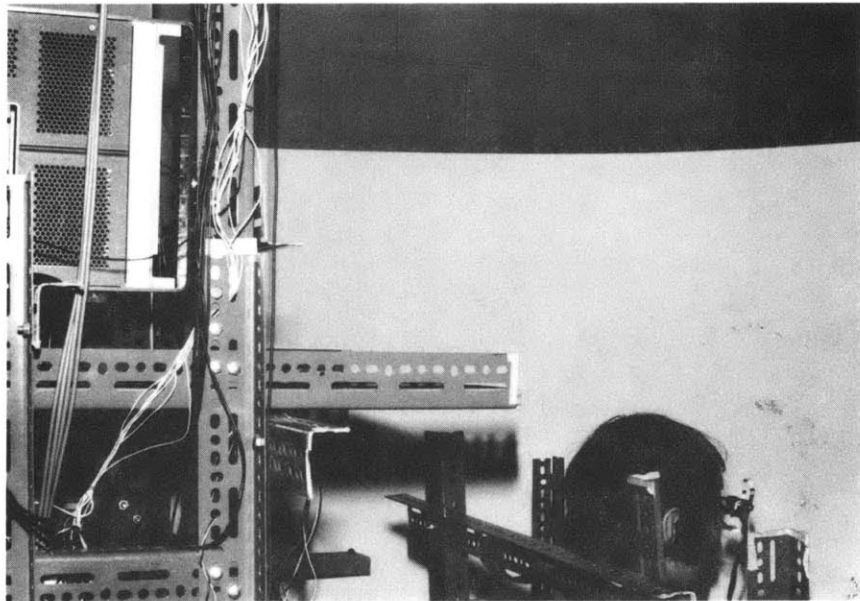
### 4.2.2 Apparatus and Procedure

Figures 4.1 show pertinent portions of the experimental site: a spot of visual target was presented on a white screen confronting the subject, through a projection lens which magnified the source target motion generated on a CRT console (CRT: 1300A X-Y Display, manufactured by Hewlett Packard, Inc.). The center of the screen was approximately 3 feet 4 inches away from the subject's eyes. The curvature of the screen was ad-

- (a) Subject wearing eye movement monitor spectacle frame with CRT and projection lens behind him.



- (b) Wide white screen confronting the subject for stimulus presentation.

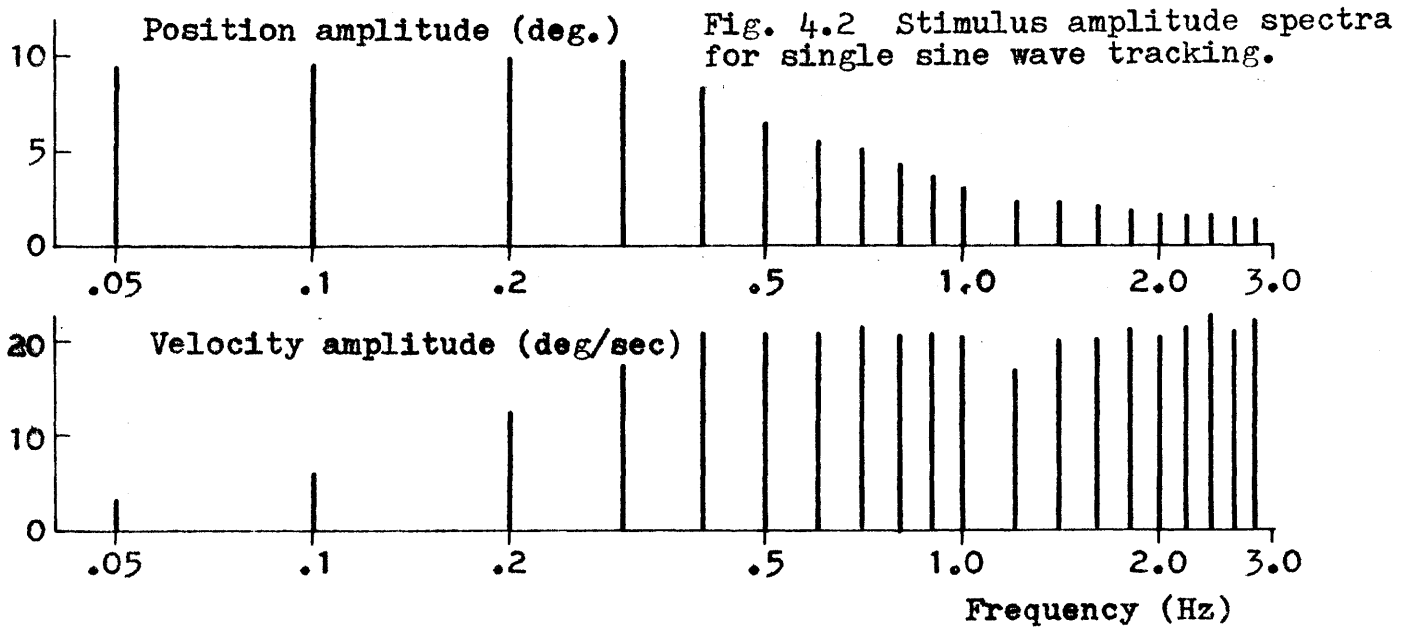


**Figs. 4.1** Pertinent views of the experimental site. (The same setup was used for OKN experiments described in later chapters.)

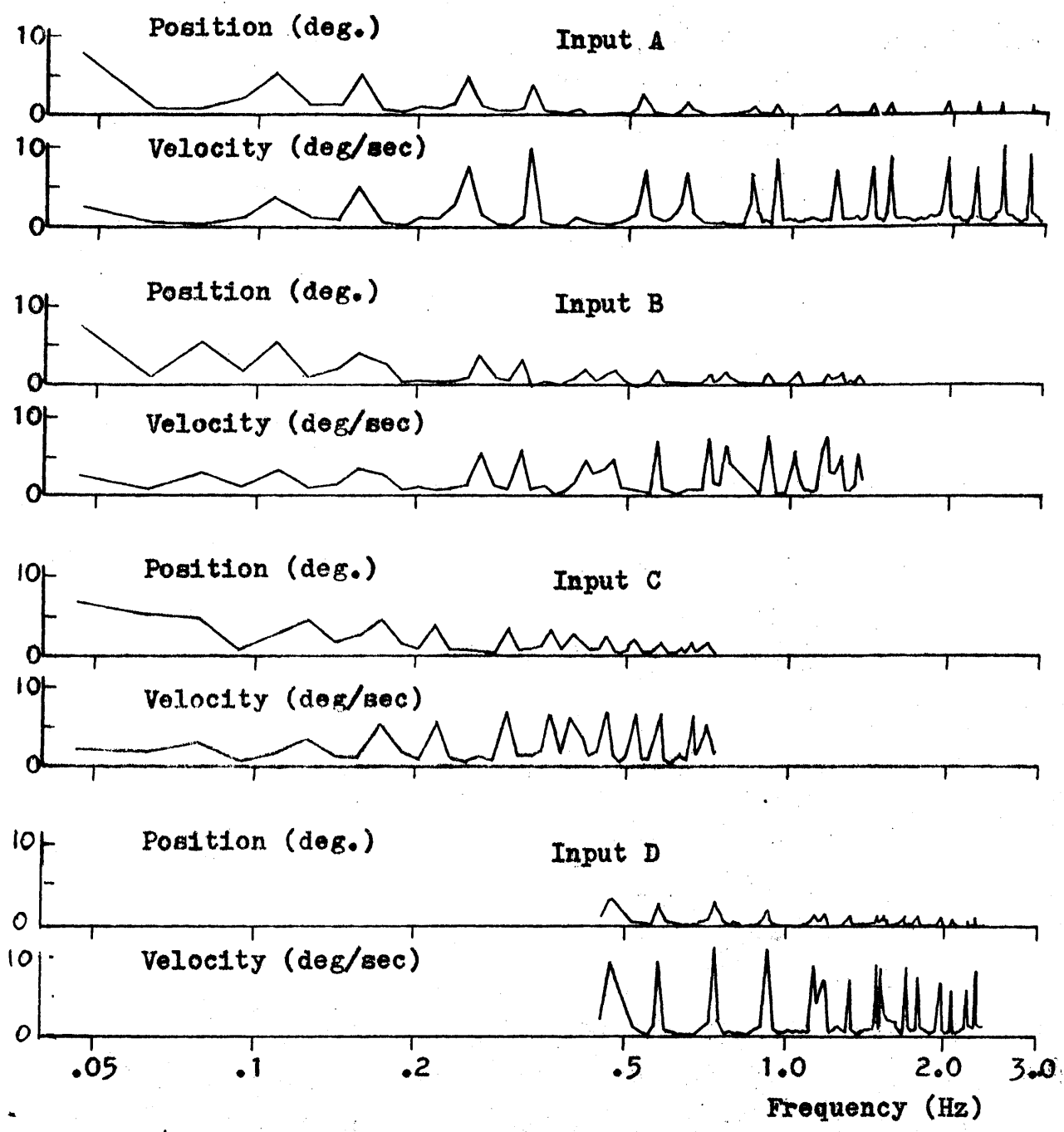
justed such that a linear displacement on the CRT console (which was proportional to the stimulus driving voltage) was proportional to the corresponding angular displacement of the target viewed by the subject. The experiment was carried out in a darkened room, which was very quiet. The exposed portion of the CRT console was covered during measurement in order to cut the ambient light. The subject was dark adapted. He wore a spectacle frame, on which was mounted a pulsed infrared photo-electronic eye movement monitor (Model SGHV-2 manufactured by Biometrics, Inc.). The subject sat upright in a chair. While binocular vision was allowed in each run, only the horizontal movement of the right eye was measured. A head band was used to prevent head movement. Three small lamps were placed on the screen presenting the calibration reference ( $10^\circ$  right, center, and  $10^\circ$  left). They were turned on only during the calibration period, which occurred prior to each experimental run. Three male and one female subject were used.

The experiment consisted of two sessions for each subject. In the first session, single sine wave inputs supplied by a low-frequency oscillator were presented. A single run, corresponding to one particular frequency, lasted for 30 seconds (or longer for low frequencies) to accumulate enough cycles. A total of twenty sinusoids of different frequencies were tracked to cover the relevant frequency range. Figure 4.2 shows position amplitude and velocity amplitude (maximum speed) of the stimulus motion for each frequency. Note that, for every frequency, the velocity amplitude was maintained under the pursuit

saturation velocity which is known to occur at a target rate between 30°/sec and 40°/sec. (Dodge *et al*, 1930).



The second session measured eye movements when following the stimuli driven by the pseudo-random signals supplied from a prepared analog tape. Four pseudo-random signals (A, B, C, and D) with different frequency band characteristics were tested. They were adequately nonpredictable, being made from summing sixteen sine waves of harmonically unrelated frequencies. The input frequency spectra corresponding to these pseudo-random signals were evaluated by Fourier analysis and are shown in terms of position and velocity amplitude in Figure 4.3. This result indicates that stimulus velocity amplitude



3. 4.3 Pseudo-random input frequency spectra obtained by FFT.



for each individual component hidden in the signal was within the allowable range assumed here. However, because of the nature of the trigonometric summation, this fact alone does not necessarily assure that the maximum instantaneous velocity of the over-all signal was actually held below the pursuit saturation level. Nonetheless, velocity estimation based on direct time differentiation of each pseudo-random position signal confirmed fulfillment of the linearity requirement assumed for the pursuit system. A single run in the second session, corresponding to one of these four pseudo-random inputs, lasted for two minutes, the time span necessary for the subsequent Fourier analysis.

#### 4.2.3 Data Processing and Analysis

For each run in both sessions, i.e. periodic and non-periodic\*, the target position signal and the eye movement monitor output (including each renewed calibration mark) were recorded and stored on a magnetic tape by an eight-channel Precision Instrument type recorder model P.S. 200 A for the subsequent data reduction. For on-line inspection, these stimulus and response signals were also monitored on a Brush chart recorder, model 240.

There are four different cases to be analyzed: periodic-composite; periodic-pursuit only; nonperiodic-composite; and

---

\* Adjectives "periodic" and "nonperiodic" are used interchangeably with "sinusoidal" and "pseudo-random" in this thesis.

nonperiodic-pursuit only. The procedure of data analysis depends on the particular case.

Eye movement data for the periodic-input cases were analyzed by hand directly on the relevant traces reproduced with a recording paper speed appropriate to the particular test frequency. Due to the hybrid aspect (continuous and discrete) of the composite eye movement, amplitude and phase should be clearly defined here: Amplitude of the periodic-input composite eye movement was defined as half of the difference between the extreme right and the extreme left eye position in one cycle period; the phase reference time was defined as the time when the pursuit velocity became zero. In order to evaluate phase shift, this reference time was to be compared with time when the stimulus velocity became zero. Usually the over-all composite eye movement reached its positional peak at the phase reference time just defined, but it did not always do so, as illustrated in Figure 4.4.

In accordance with these definitions, the phase value is the same for composite and pursuit movements at a given stimulus frequency. They differ only in amplitude: the latter response yields a smaller amplitude than the former due to the loss of the saccadic contribution.

In order to evaluate amplitude of predictive pursuit movements efficiently, all saccades were removed and continuous traces of the pure smooth movements (cumulative eye position) were obtained from the original data by means of the hybrid computer processor, MITNYS, described in Subsection 3.4.4 and Appendix B.

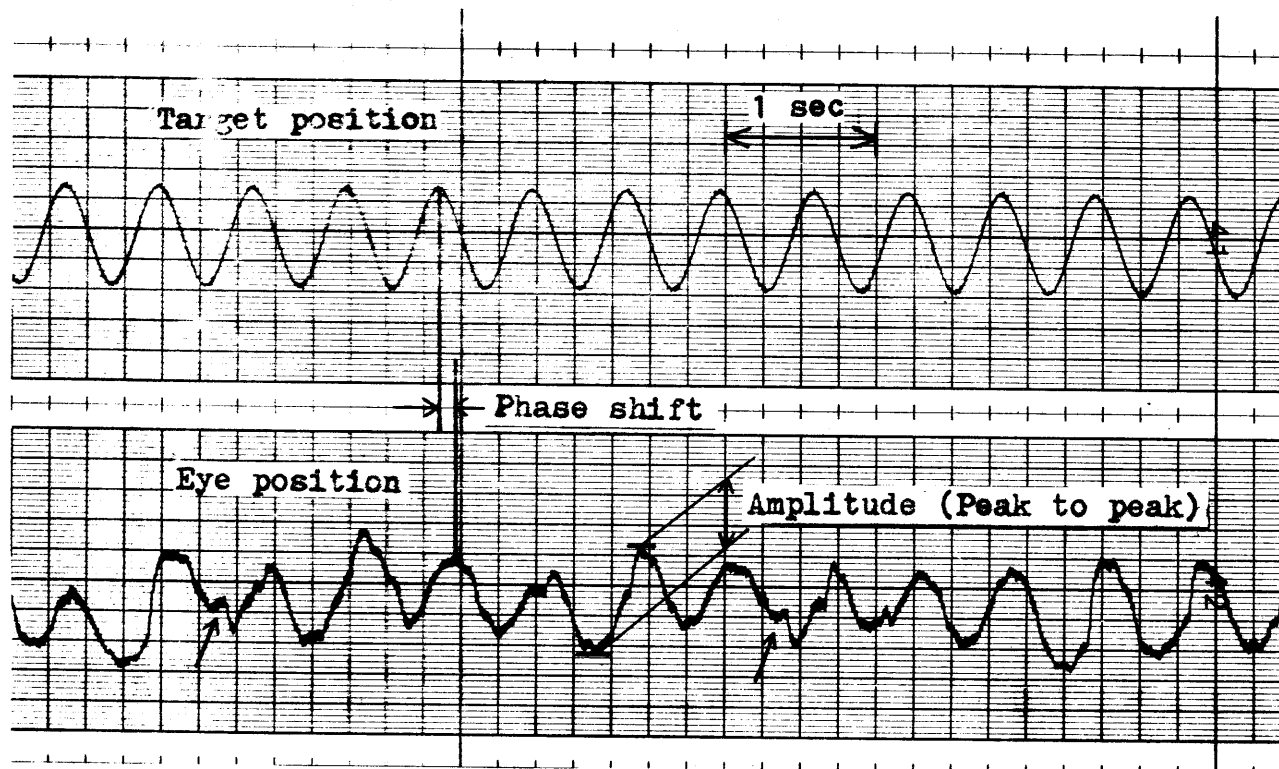


Fig. 4.4 Definition of amplitude and phase for periodic-input composite eye movement. Usually composite eye movement has its position peak at zero slow phase velocity. But this is not always true as indicated by arrows.

Figure 4.5 presents three typical periodic input composite records, representing low, intermediate, and high frequency responses. As reported by other workers, saccadic movements became dominant for frequencies increasing from intermediate to high. Further, particularly at these frequencies, amplitude and phase of the oculomotor response were not the same from one cycle to another even in the steady state, but were subject to certain fluctuations. (The amplitude variation in the composite movement can be accounted for by some randomness in number as well as in total size of saccades executed in one cycle.) For this reason, median values for the amplitude and the phase were obtained from many successive cycles (excluding the first several cycles).

As frequency was increased above 2.4 Hz, the over-all eye movement tended to become somewhat irregular. This was chiefly due to the tendency of the occurrence of saccades to become incoherent with the sinusoidal periodicity. (But the sinusoidal pattern with the right stimulus frequency was still detectable in regard to the smooth pursuit movements.) Many cycles contained no saccade, while others contained a few, most contained just one. In such a situation, the composite eye movement loses its meaning in terms of sinusoidal component, and hence no frequency response can be obtained at these high frequencies. On the other hand, pursuit movements measured in this high frequency range became so small in comparison to the background

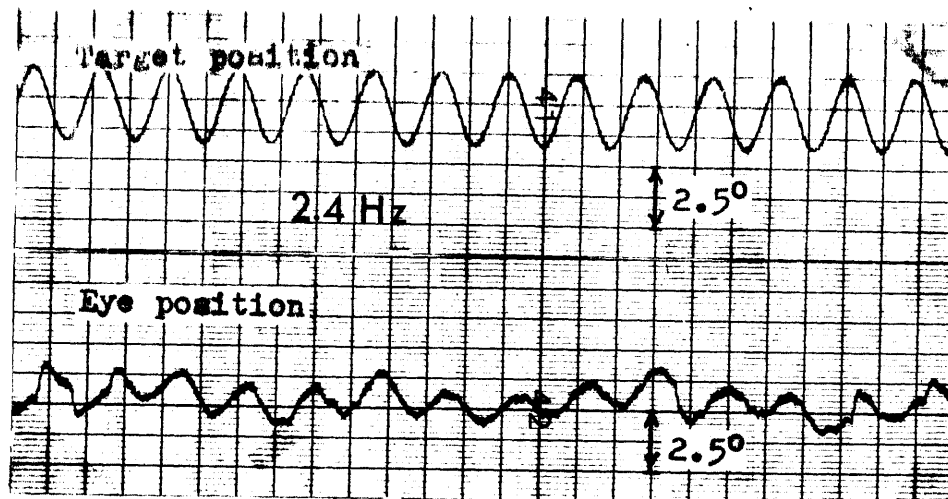
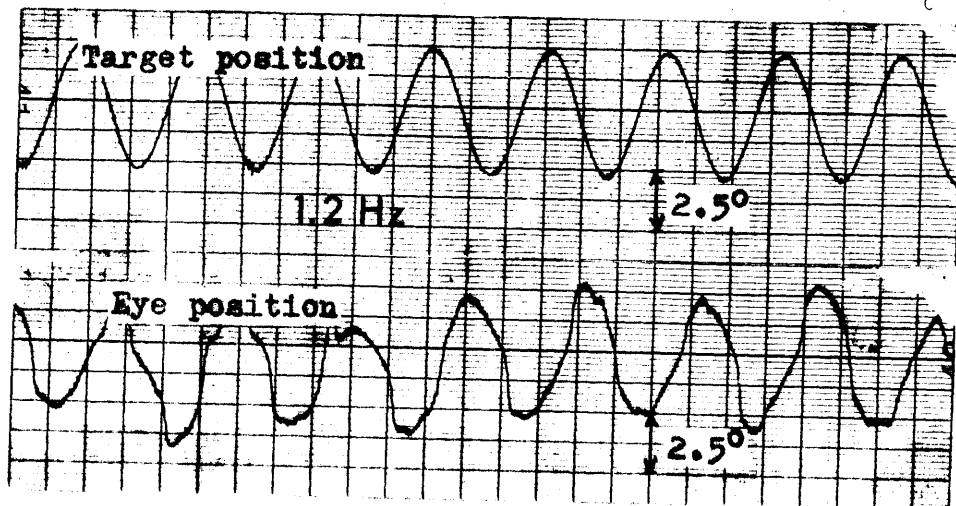
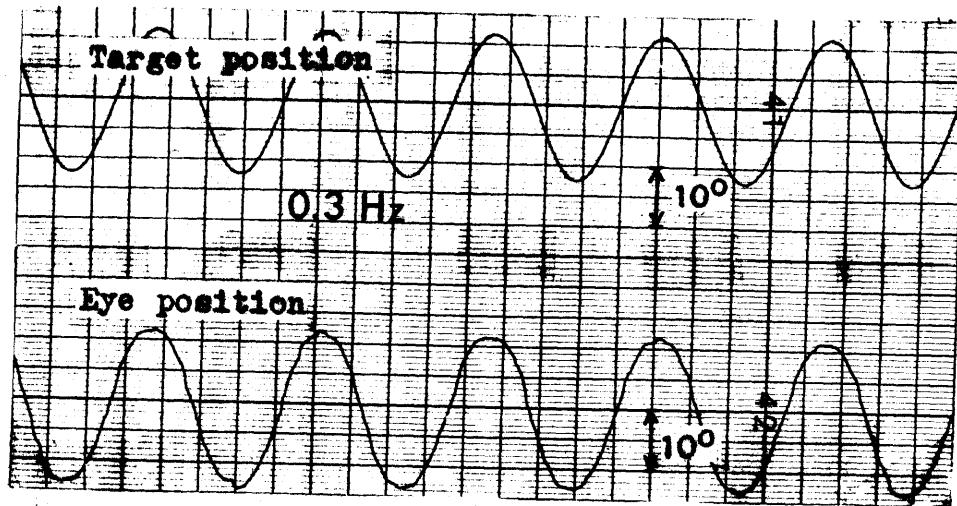


Fig. 4.5 Typical periodic-input records representing low, intermediate and high frequency responses

noise of the eye movement monitor that the original eye movement records needed suitable low-pass filtering before reading the relevant information as accurately as possible.

Data for the nonperiodic-input cases underwent Fourier analysis using the hybrid computer routine, FFT, described in Subsections 3.4.4 and Appendix C. For the composite eye movement, this was done directly with the reproduced data incorporating stimulus position and over-all eye position. In order to obtain the frequency response of the pursuit system, an additional intermediate step was necessary to remove all saccades and to acquire the continuous cumulative position. This was done again by the hybrid processor, MITNYS\*, developed by Allum et al, (1973).

While the tape recorder reproduced the original eye movement to feed into MITNYS, the resultant cumulative eye position (being outputted from MITNYS in real time\*\*) was recorded and stored onto a new channel of the magnetic tape. In order to cancel the time delay involved in this reproducing and recording operation (about 1 second with the present equipment), the target position signal had to be reproduced as well, at the same time, and then restored back onto another new channel. This restored target position and the recorded cumulative eye position for the

---

\* The present procedure is analogous to the one in the previous chapter, where the fast phase was removed by MITNYS before performing Fourier analysis on the slow phase of the vestibular nystagmus induced by the pseudo-random head rotation. (See also, Appendix B for the two-step procedure, MITNYS-FFT).

\*\* Actually there was a 25 msec processing delay inherent to MITNYS.

final signals to be reproduced as actual input data for the subsequent FFT operations. These steps are illustrated in Figure 4.6.

The sampling rate of FFT was 8 samples per second, permitting the highest testable frequency of 4 Hz. The input buffer size (516 per channel) of the current FFT program with the above sampling rate led to the sampling epoch (total sampling interval of 64 seconds and the frequency resolution of 0.0156 Hz. Three different sampling epochs with some portions overlapping were used, chosen somewhat arbitrarily from a continuous record representing a single run.

As encountered in Chapter III, some of the cumulative eye position traces exhibited considerable drift with more or less constant rates in one direction. Due to the nature of the cumulative eye position, they could be caused by even a relatively small imbalance of the eye movement monitor. Otherwise they might be real. In any event, according to the FFT algorithm employed, these drifts could cause non-negligible errors in the Fourier results, and therefore, as in Chapter III, they were compensated artificially by adding appropriate counter-drifts before being inputted to FFT (see Appendix C).

All individual subjects' frequency response data in this chapter can be found in Appendix D (Figures D-5 through D-9). Tables D-3 included in this appendix summarize the frequency correspondence in Fourier coefficient peaks between input and output for each experiment involving pseudo-random stimulation.

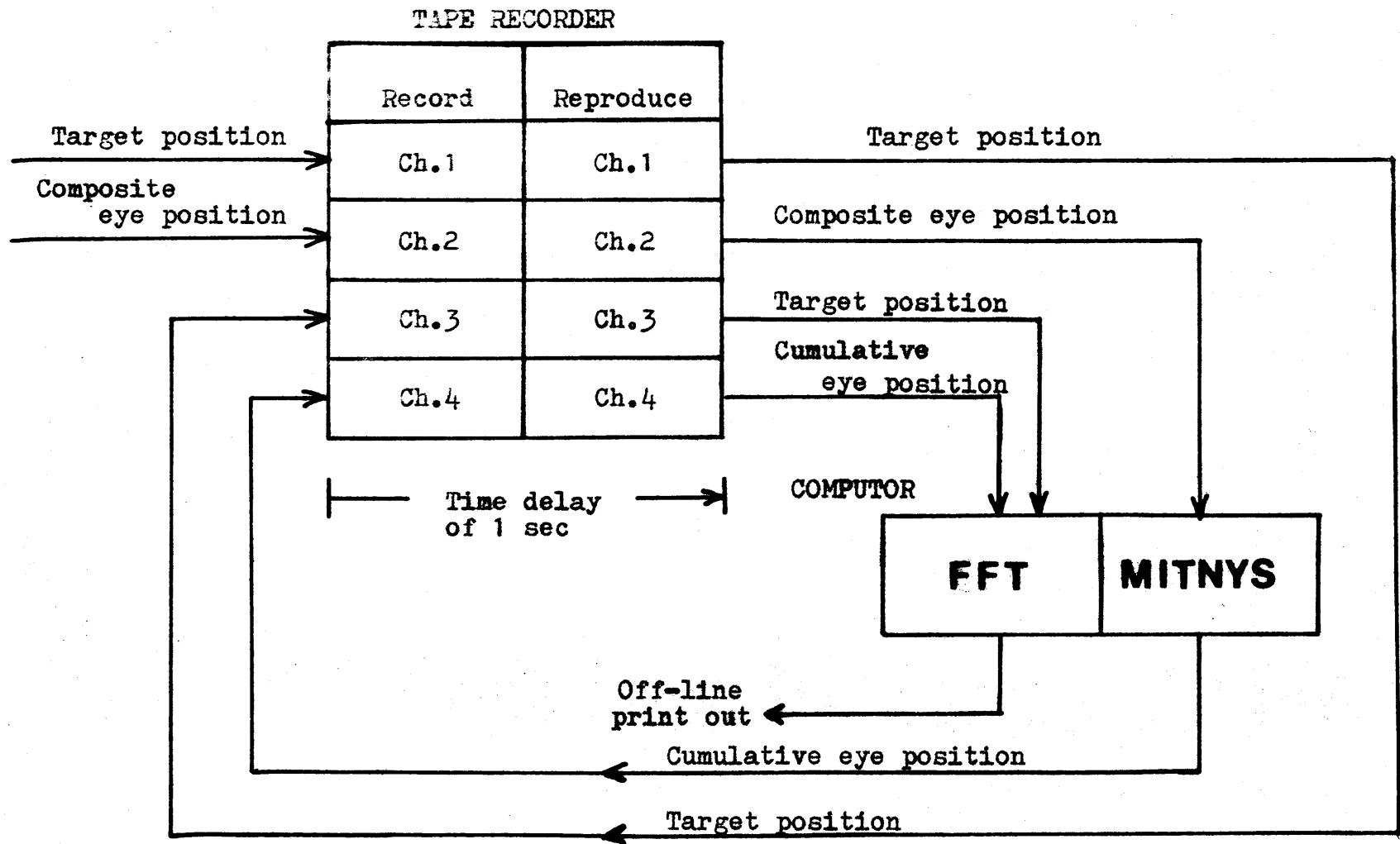


Fig. 4.6 MITNYS-FFT data processing flow chart



Except for a few cases, this information shows a substantial degree of matching between input and output peak frequencies, indicating that the system linearity is adequate enough to justify the present frequency response approach.

## 4.3 Results and Discussion

### 4.3.1 Periodic-input: Composite and Pursuit

Typical time-domain traces of the periodic-input response were presented in the previous section. The frequency response result corresponding to the periodic-input composite movement is shown in Figure 4.7, whereas the result considering only the predictive pursuit movement is shown in Figure 4.8. These Bode plots were statistically reduced from Figures D-5 and D-6 given in Appendix D, which presents individual subjects data points and indicates some degree of inter-subject variance.

First, the composite movement and pursuit movement yielded exactly the same phase plot. This was due to the present definition of phase as given in the preceding section. Also by definition, the gain was greater at each frequency for the composite response than when only the pursuit movement was taken into account. Comparison between the two gain plots in Figure 4.9 (where the median data points in Figure 4.7 and Figure 4.8 are reproduced) indicates that this difference became enhanced with increasing frequency, which in turn suggests the greater relative importance of saccades in correcting tracking errors at high frequencies. Note that no attempt was made to obtain the composite gain for the highest three frequencies tested for the reason given in the previous section.

Figure 4.10 compares the predictive composite result obtained here with those of other authors as previously given in

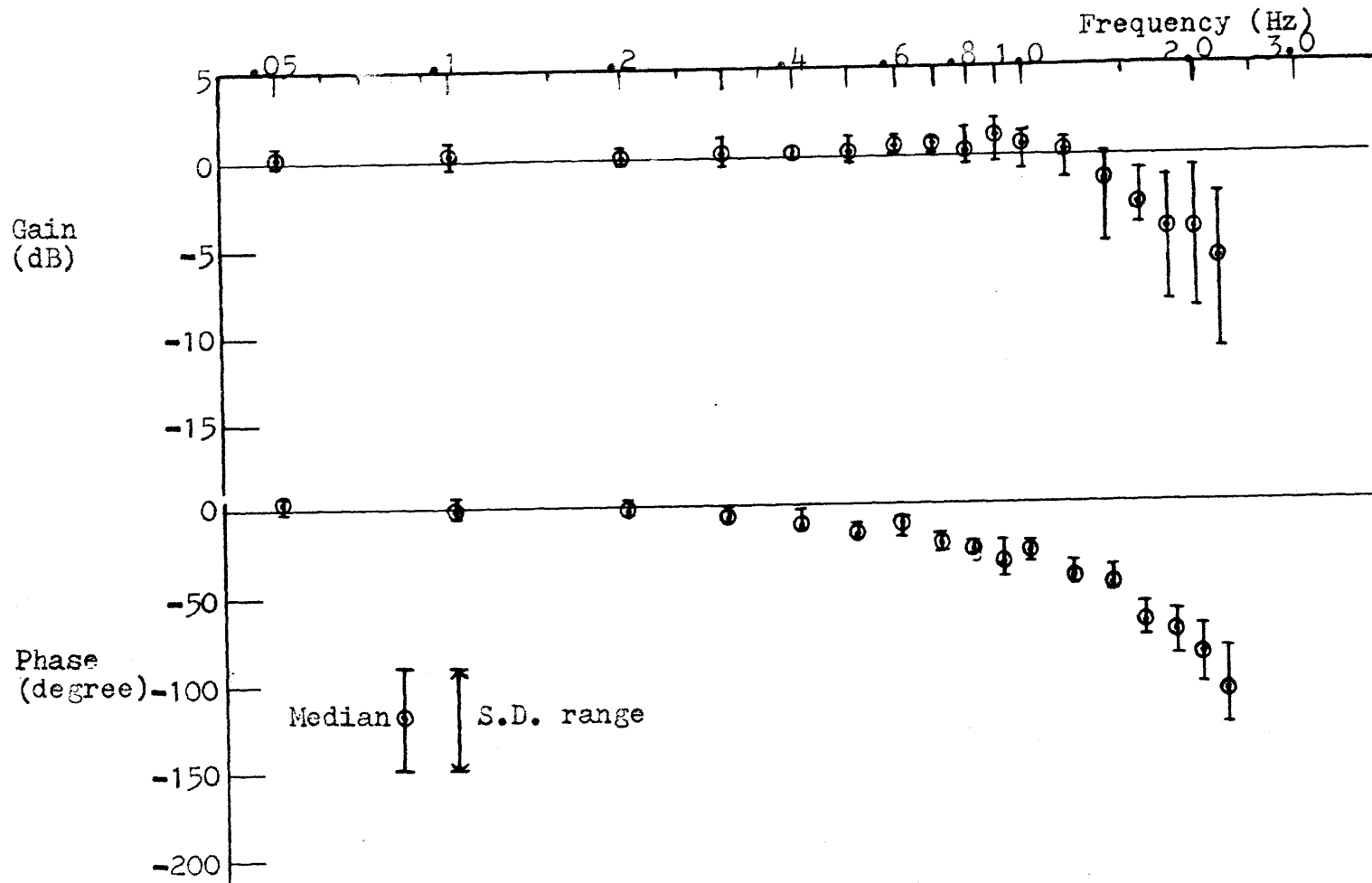


Fig. 4.7 Periodic-input composite frequency response (average for four subjects)

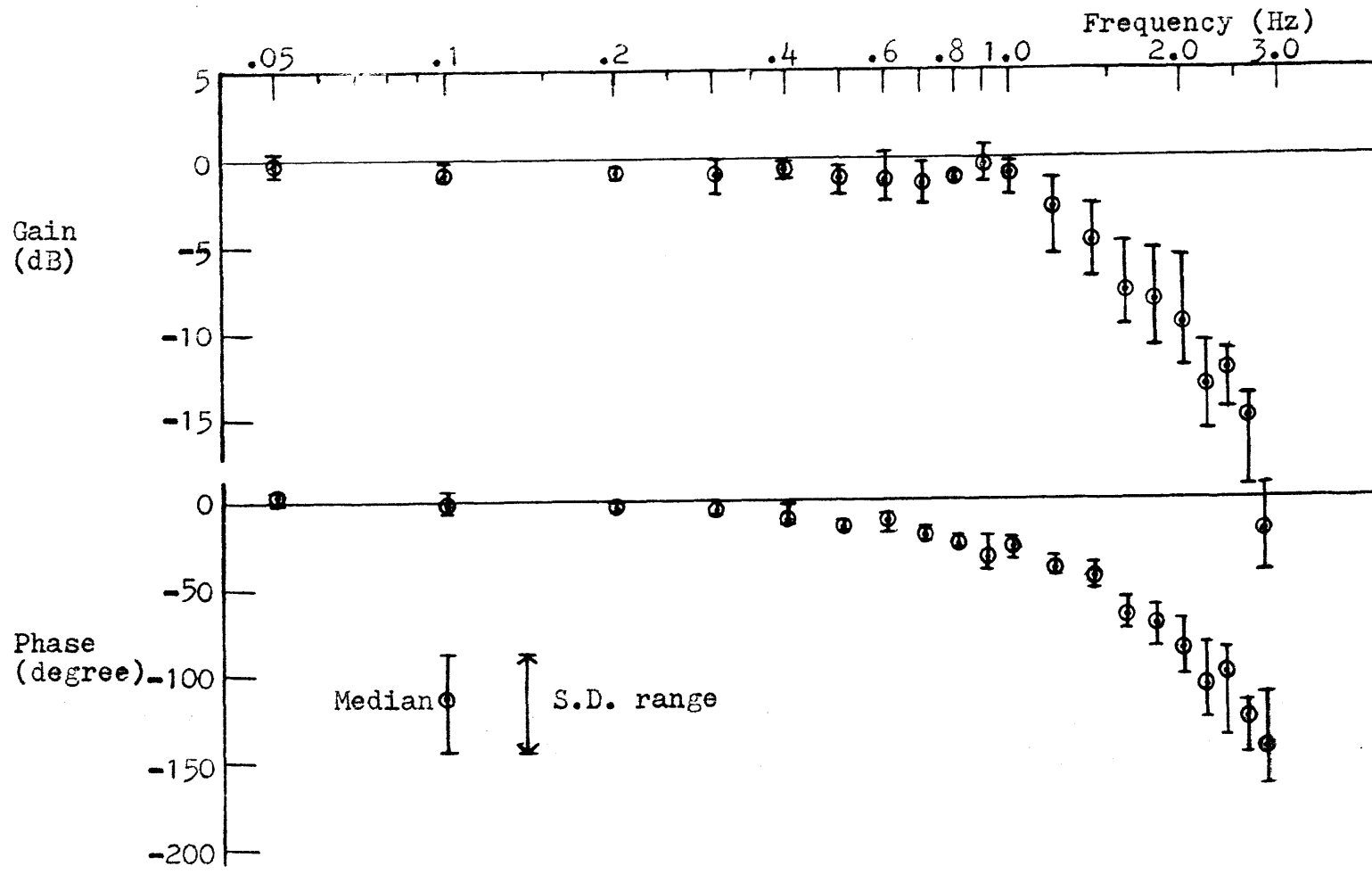


Fig. 4.8 Periodic-input pursuit frequency response (average for four subjects)

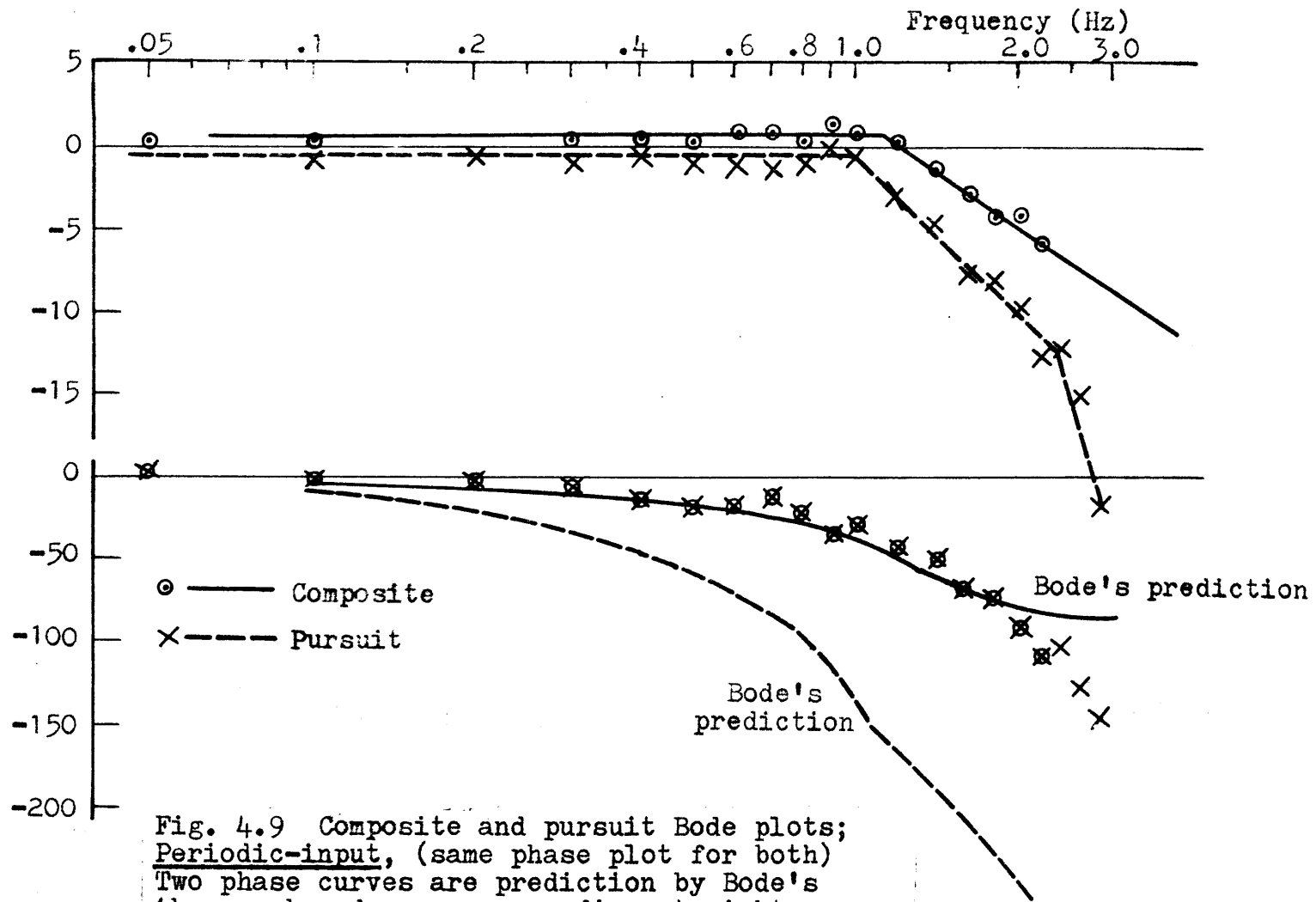


Fig. 4.9 Composite and pursuit Bode plots; Periodic-input, (same phase plot for both) Two phase curves are prediction by Bode's theorem based on corresponding straight-line gain approximations

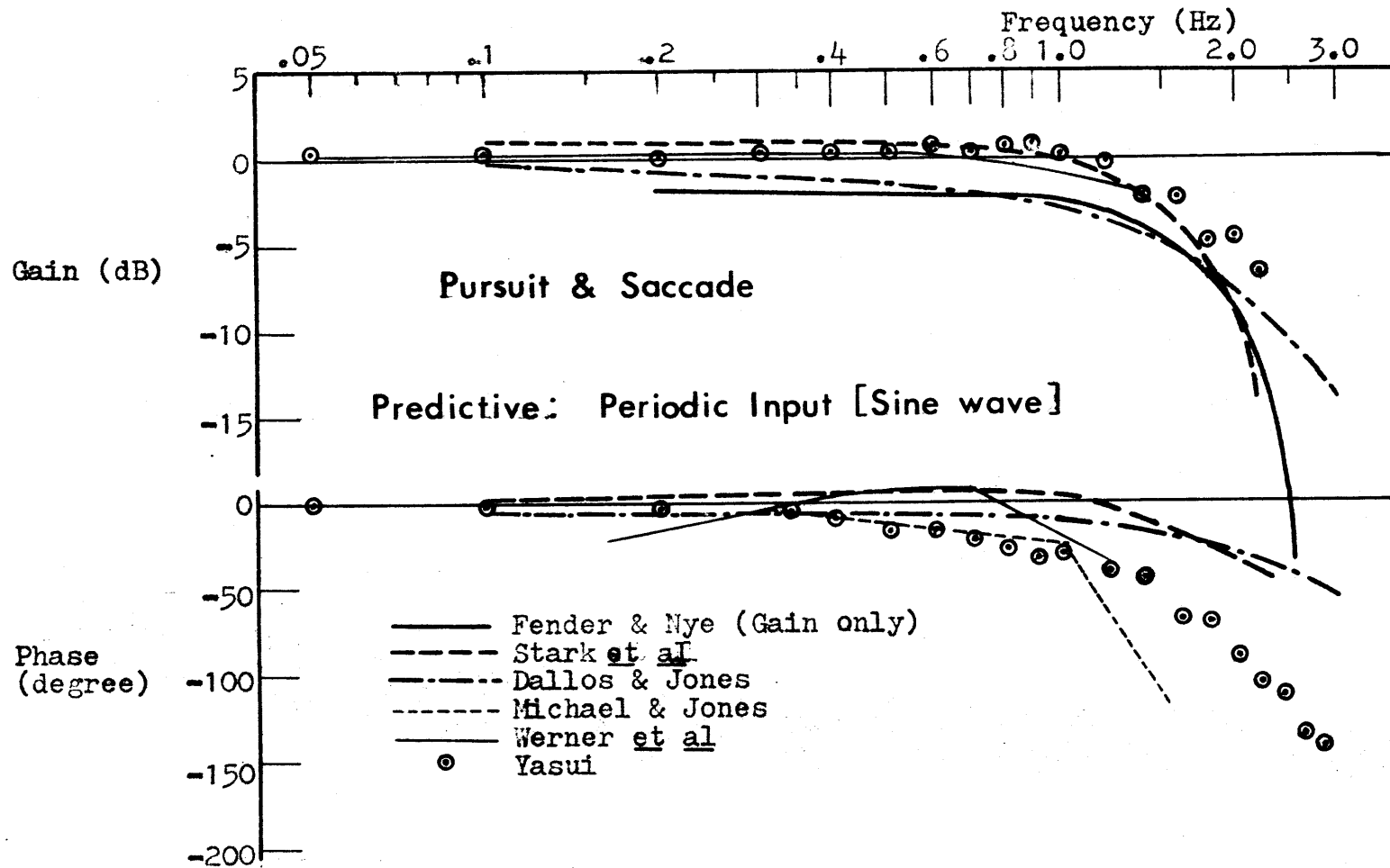


Fig. 4.10 Periodic-input composite frequency response as compared with published results

Figure 2.8. The present result appears to be at some variance with others; somewhat greater gain at high frequencies and considerably larger phase lag at intermediate and high frequencies.\*

On the basis of the relevant discussion in Section 2.4, this discrepancy might be attributed to avoidance of the pursuit velocity saturation, which was probably better accomplished here, than by other authors referenced previously. Although this possibility is not fully conclusive\*\*, the present gain-phase relation seems to have a tendency against the less-than-minimum phase behavior that has been frequently described in the literature for the periodic-input tracking. This point was further examined as follows.

The first theorem of Bode was applied to the present periodic-input result. Composite gain data points were fitted by the solid straight lines as shown in the gain portion of Figure 4.9.\*\*\* Given a set of approximate straight segments such as the above, an equation to calculate the corresponding phase was derived from the first theorem of Bode, as given in Appendix F.

---

\* But the present phase lag was still substantially smaller than what would be predicted by the inherent oculomotor latency, i.e., assuming 150 msec for the latency,  $28^\circ$  as compared to  $53.5^\circ$  at 1 Hz, and  $88^\circ$  as compared to  $107^\circ$  at 2 Hz. Also, as shown later, it was still much smaller than the phase lag obtained with any of the present pseudo-random inputs.

\*\* For instance, phase lag obtained here is still considerably greater than even the result of a small amplitude study ( $0.5^\circ$ ) by Watanabe and Yoshida (1968).

\*\*\* Note that these straight lines are not the same in kind as the familiar asymptotes useful in drawing the approximate gain characteristics of a transfer function.

Application of this equation to the present case has yielded the phase shift as shown by the solid curve in the phase portion of Figure 4.9. Comparison between this prediction and the actual phase data points do not clearly indicate the less-than-minimum phase characteristics, contrary to the commonly held opinion on this matter, but rather it appears to support the minimum phase behavior that implies an effective elimination of the underlying oculomotor reaction time presumably by a predictive mechanism.\*

The periodic-input pursuit frequency response, on the other hand, has indisputably revealed the less-than-minimum phase behavior, as shown in Figure 4.9 by the greater phase lag (the broken curve) calculated on the basis of the straight line approximation (the broken lines) for the pursuit gain plots.

#### 4.3.2 Nonperiodic-input: Composite

Figures 4.11 show typical traces of the nonperiodic stimulus position, corresponding to composite eye position and cumulative position for each of the four different pseudo-random inputs. Figure 4.12 enlarges one of these records to emphasize adequate performance of MITNYS in producing cumulative eye position. First,

---

\* In contrast, the less-than-minimum phase behavior would imply an overcompensation. And the greater-than-minimum phase behavior, which actually tends to occur in the high frequency region according to the present observation, would indicate an inadequate compensation for the neuromuscular reaction delay.



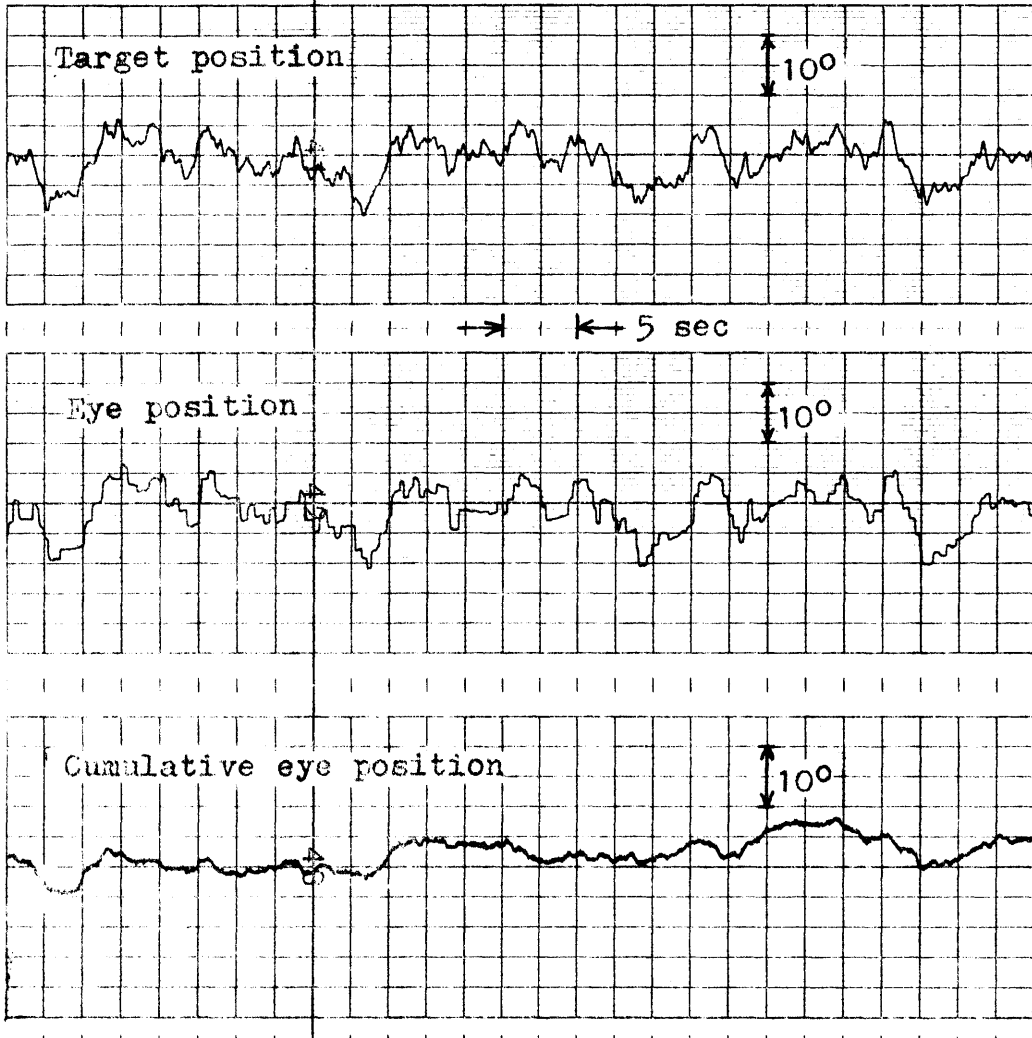


Fig. 4.11-a Typical set of traces with pseudo-random input A

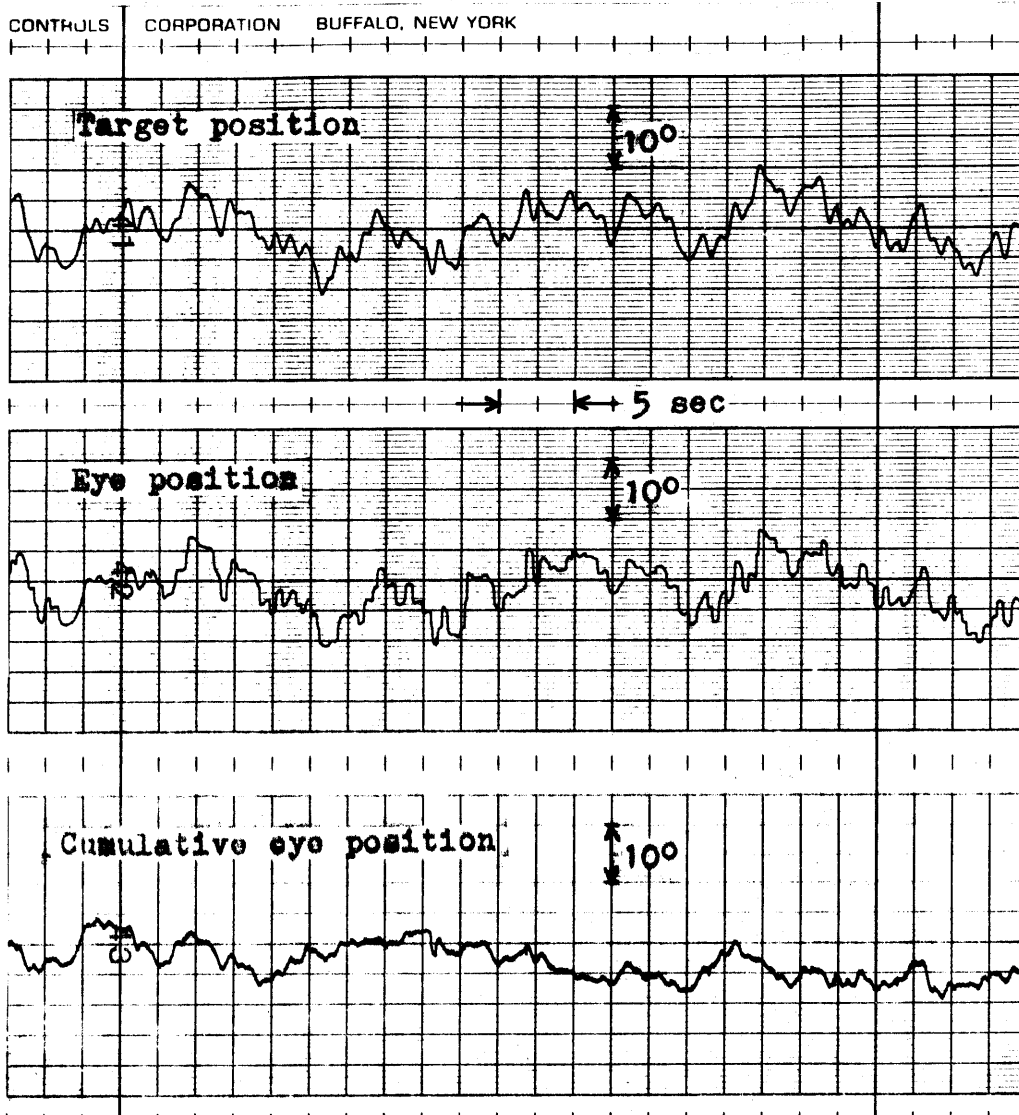


Fig. 4.11-b Typical set of traces with pseudo-random input B

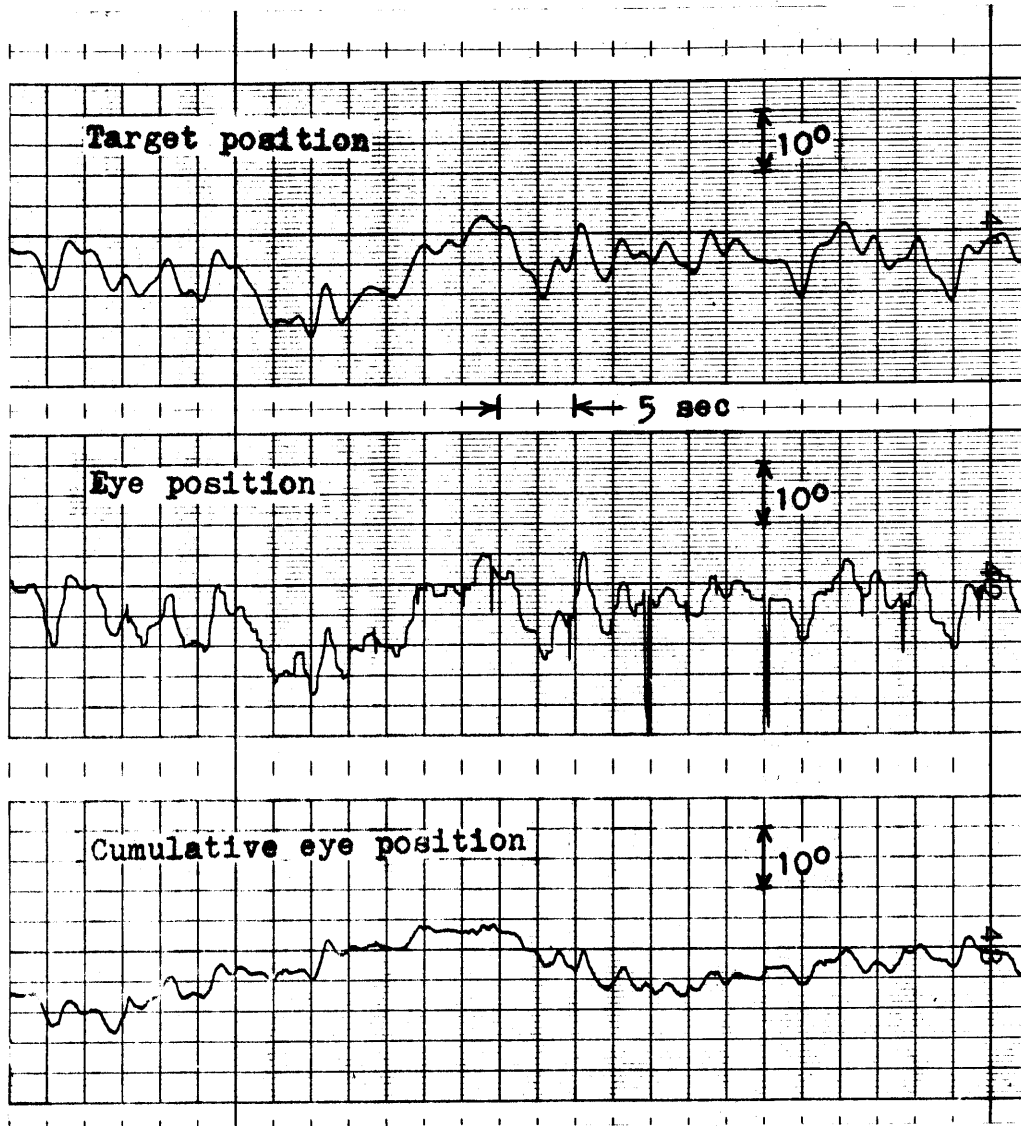


FIG. 4.11-c Typical set of traces with pseudo-random input C

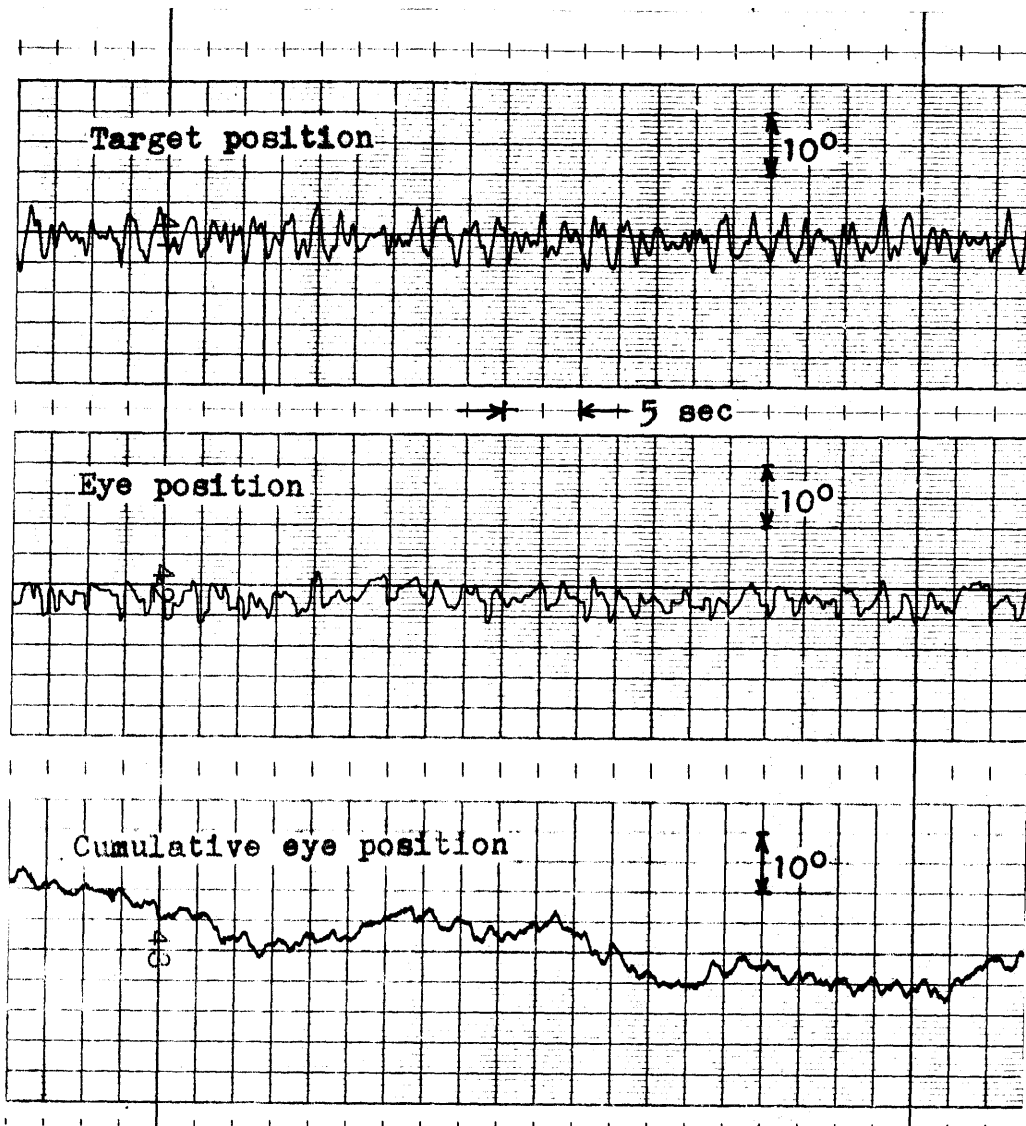


Fig. 4.11-d Typical set of traces with pseudo-random input D

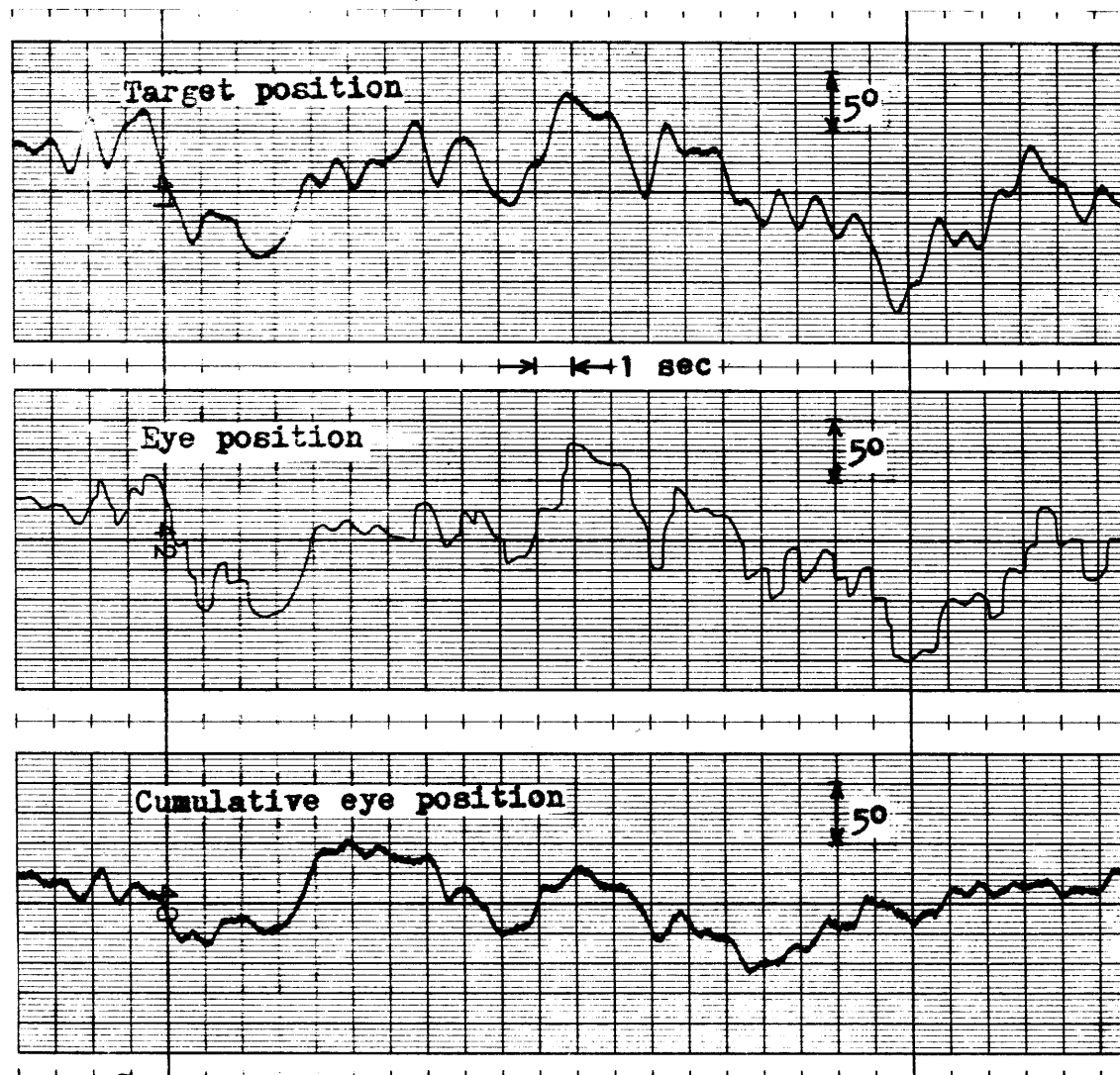


Fig. 4.12 Enlarged record showing satisfactory performance of MITNYS in obtaining cumulative eye position from original position by eliminating saccades (with input B)

the Bode plots of the composite response are shown in Figures 4.13a, b, c and d, respectively for pseudo-random inputs A, B, C, and D. (The original individual subject's data points can be found in Figures D.7a, b, c, and d in Appendix D.)

It is difficult to make a quantitative comparison among different investigators in the frequency response for the reasons mentioned previously. Nevertheless, one of the present results (corresponding to input A) is presented in Figure 4.14 along with others that were previously shown in Figure 2.9.

The general observation can be made as follows for the non-periodic-input composite frequency response data obtained here. Their qualitative features are basically consistent with those reported by others. For inputs A, B and C, gain was maintained close to unity at low and intermediate frequencies. (For input D, however, which was devoid of low frequency components, gain was somewhat less than unity in the lower half of its frequency band.)

The gain plot tended to exhibit its peak near the higher end of each stimulus band. Such a peak is a characteristic phenomenon known in the nonperiodic-input composite Bode plot, and it is interpreted as a manifestation of high energy concentration associated with corrective saccades. Accordingly, the frequency at which the peak tends to occur must be an increasing function of the average frequency of saccades. Inspecting the eye movement records shown in Figures 4.11, the average saccadic

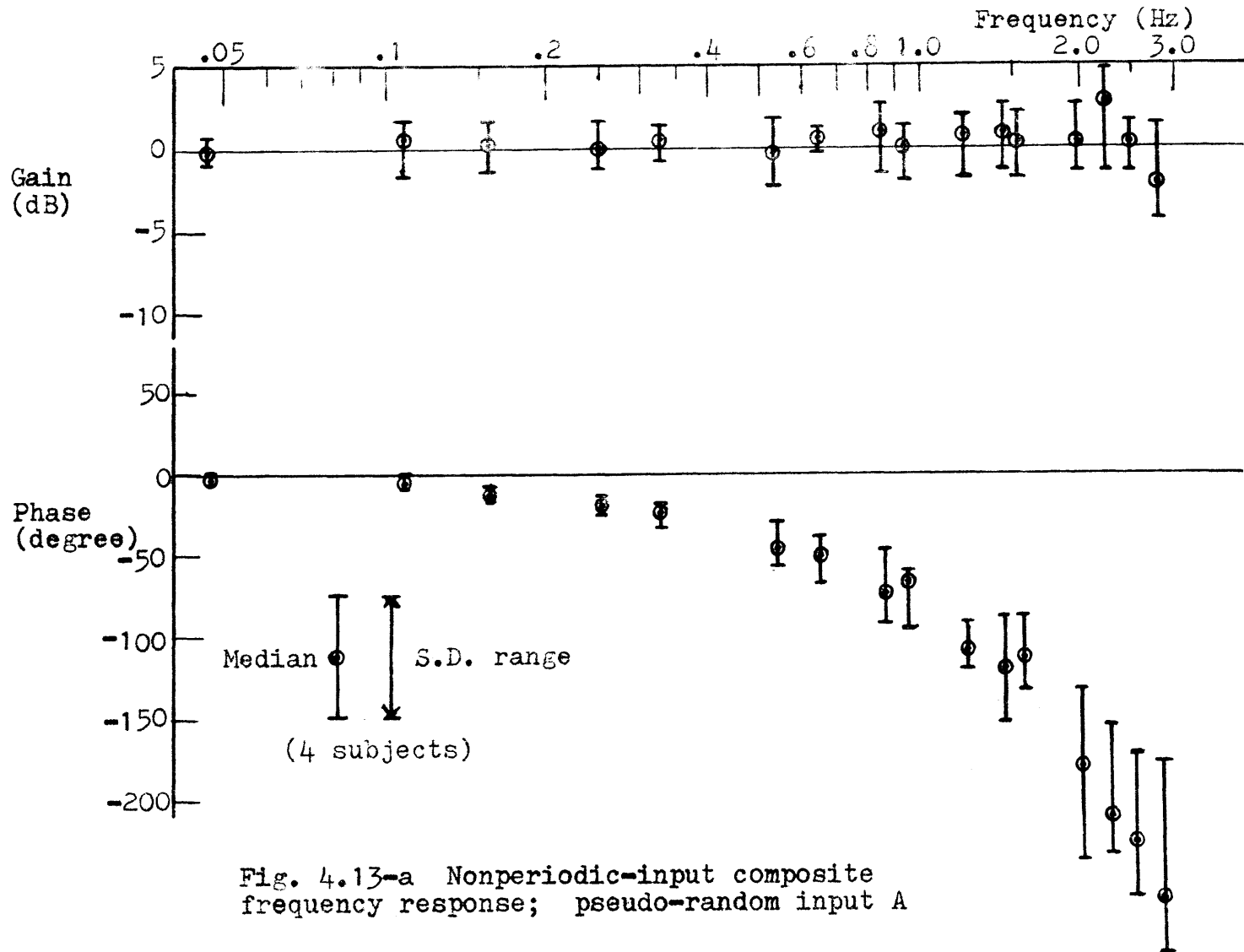


Fig. 4.13-a Nonperiodic-input composite frequency response; pseudo-random input A

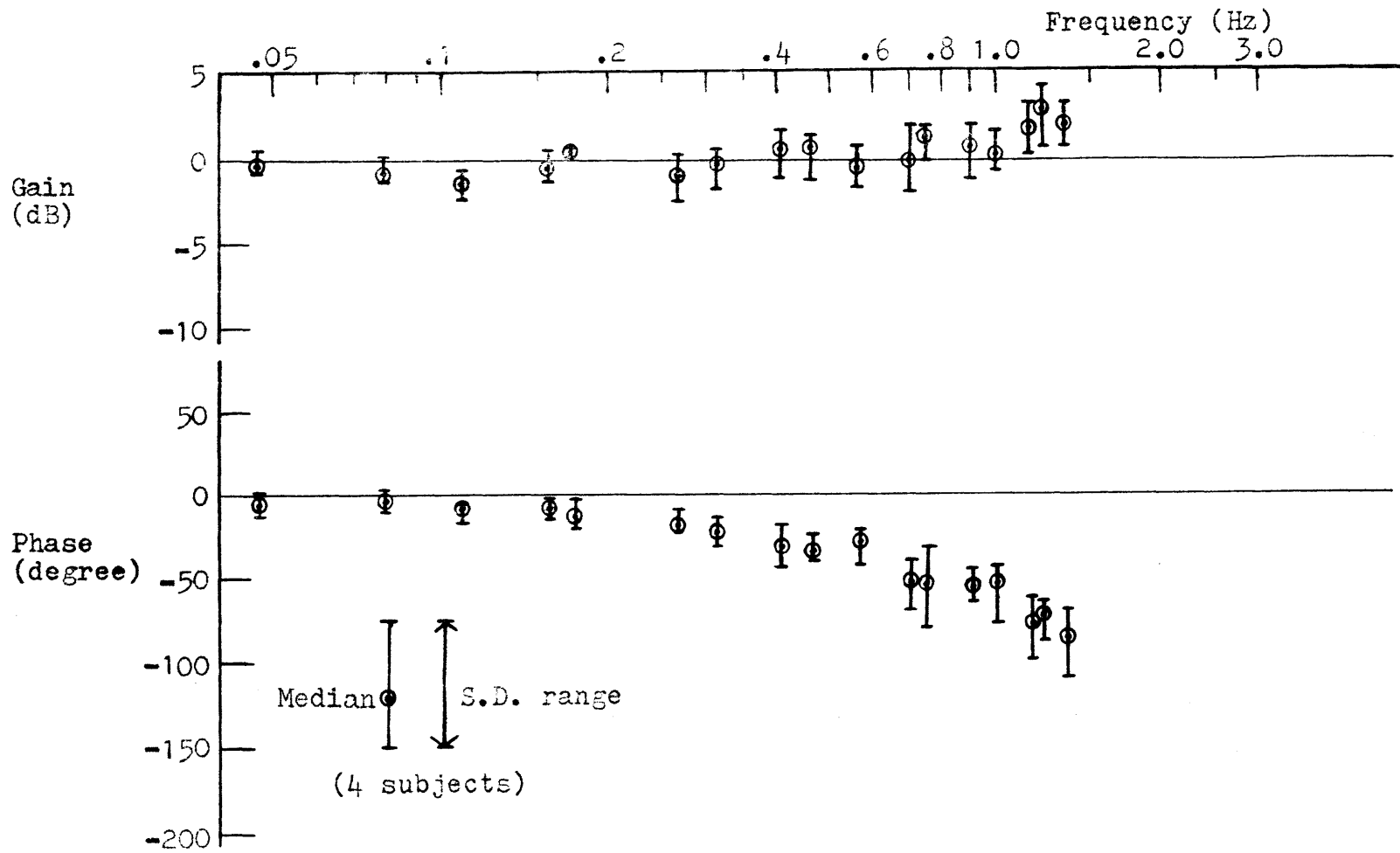


Fig. 4.13-b Nonperiodic-input composite frequency response; pseudo-random input B



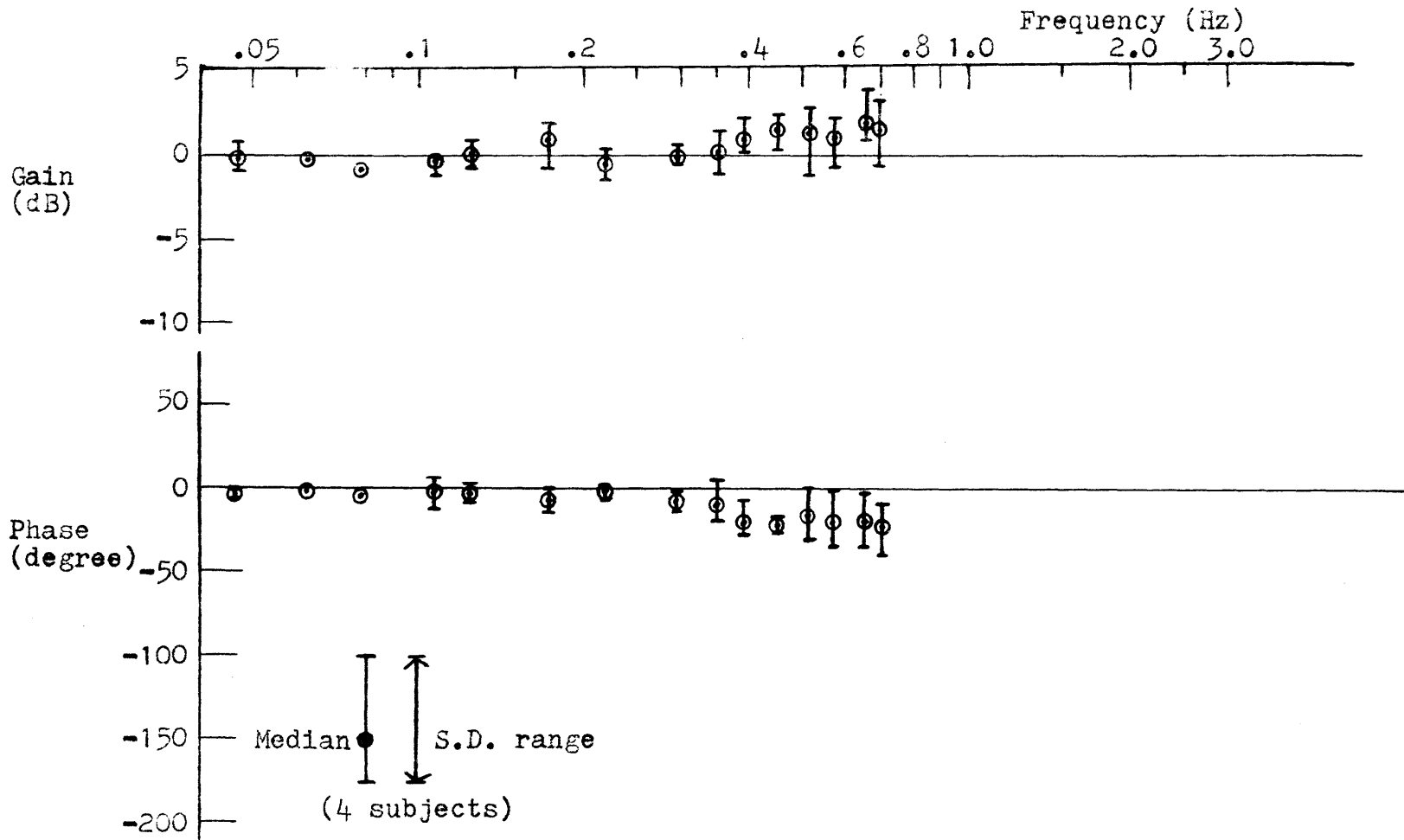


Fig. 4.13-c Nonperiodic-input composite frequency response; pseudo-random input C

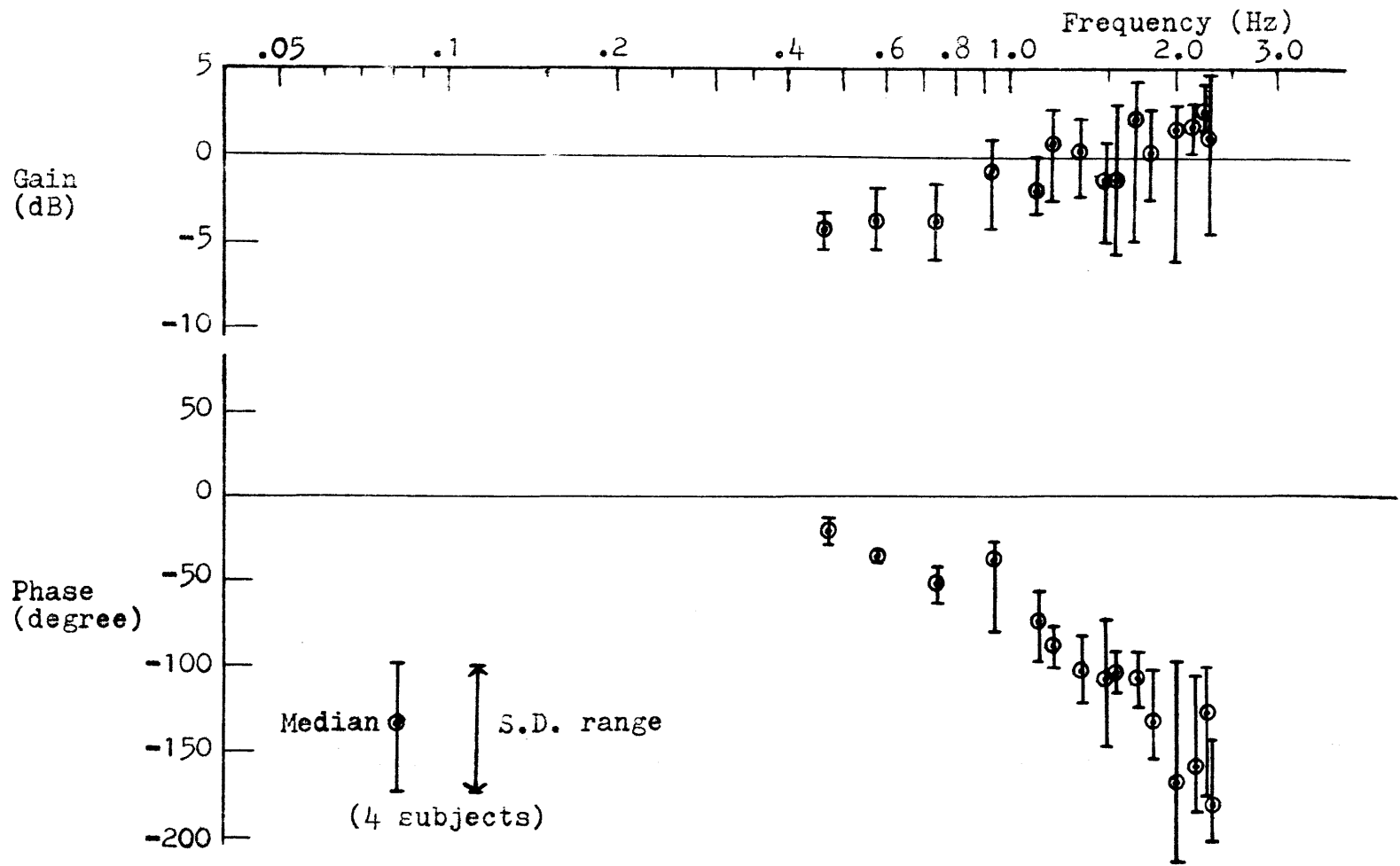


Fig. 4.13-d Nonperiodic-input composite frequency response; pseudo-random input D

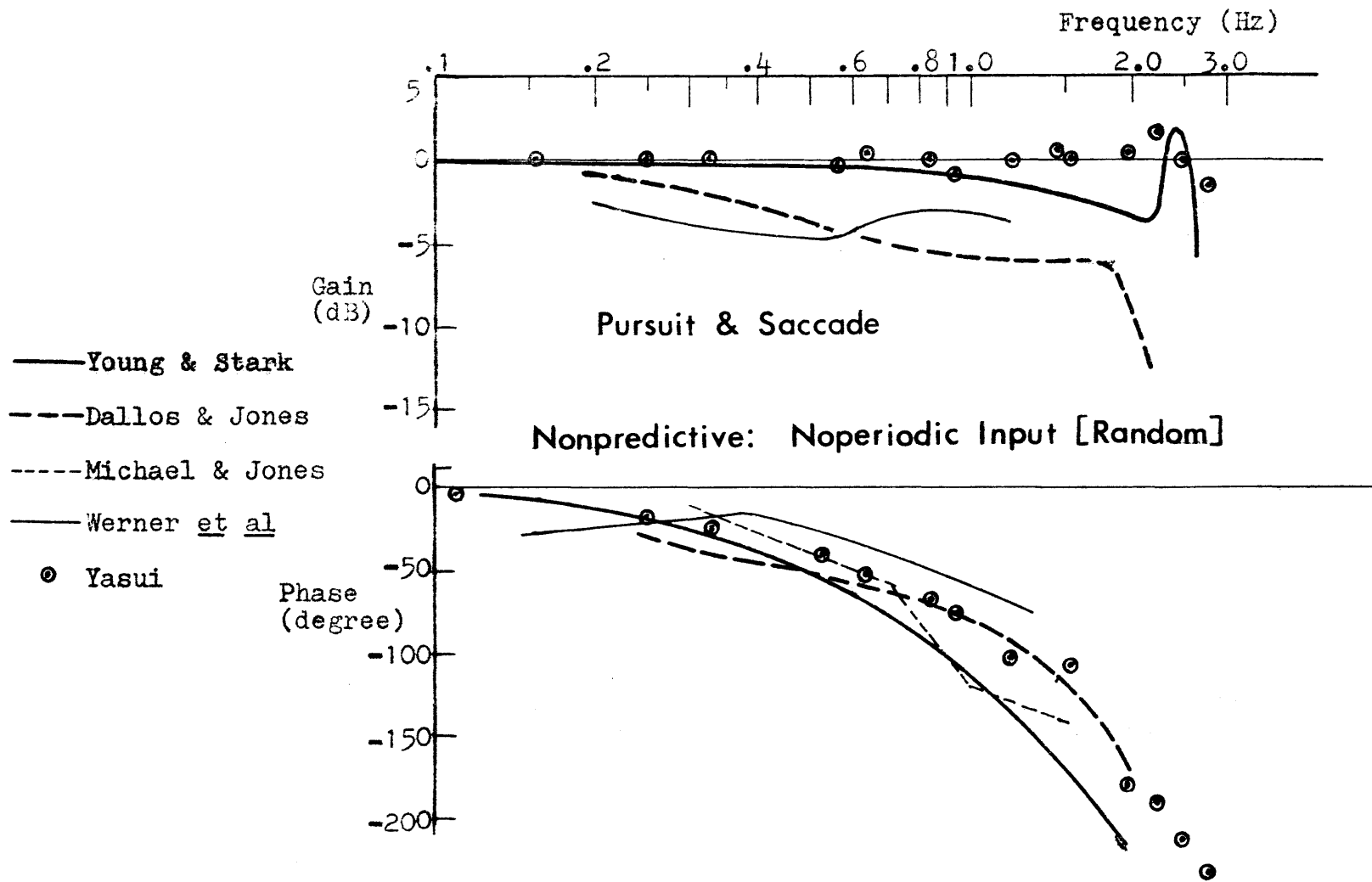


Fig. 4.14 Composite frequency response (for pseudo-random input A) as compared with published nonperiodic-input results

frequency increased clearly from input C to B, and further increased from B to A or D. That is, it increased with increasing input bandwidth. And apparently the peak in the frequency response increased in that order.

While the feature of phase behavior might seem more or less the same for all the pseudo-random inputs examined here, there appeared to be some trend that is consistent with the findings by Michael and Jones (1966): As the stimulus bandwidth becomes greater, the phase lag at a given frequency increased. As to the present result, this may be demonstrated best by comparing inputs A, B, and C in terms of their phase lags about a frequency of 0.6 Hz or 0.7 Hz: at 0.6 Hz, the phase lag was approximately 50°, 35°, and 25° respectively with the bandwidth of 2.80 Hz (input A), 1.34 Hz (input B) and 0.70 Hz (input C).

#### 4.3.3 Nonperiodic-input: Pursuit

Nonperiodic-input frequency response results considering only smooth pursuit portions of the response are presented in Figures 4.15-a, b, c, and d, respectively for pseudo-random target position A, B, C, and D. (These results are averages of the individual subjects' results as given in Figures D.8-a, b, c, and d in Appendix D.

For each pseudo-random input, the pursuit gain dropped over the entire frequency range in comparison with the composite gain. But this is expected in accordance with the definition of

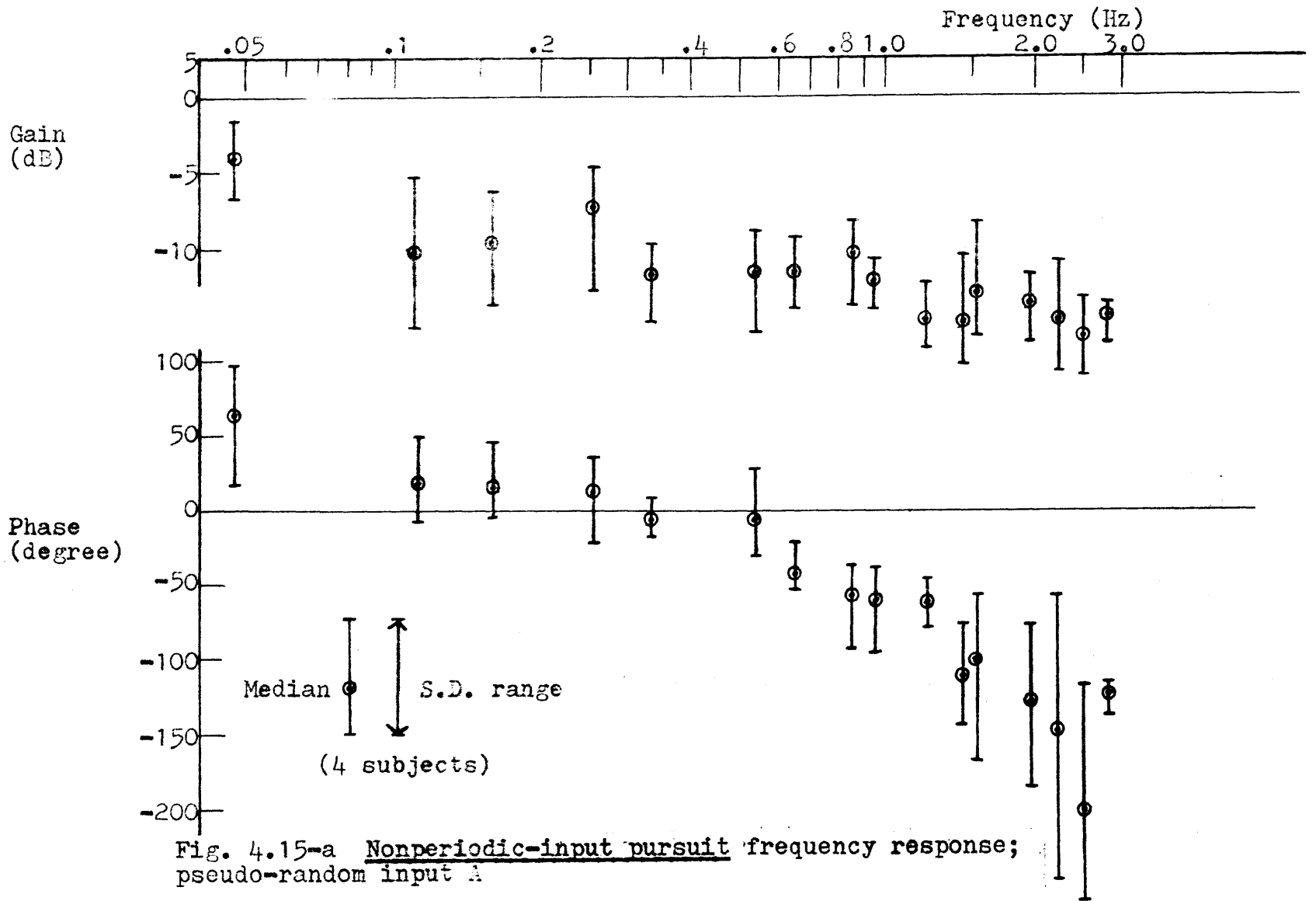


Fig. 4.15-a Nonperiodic-input pursuit frequency response; pseudo-random input A

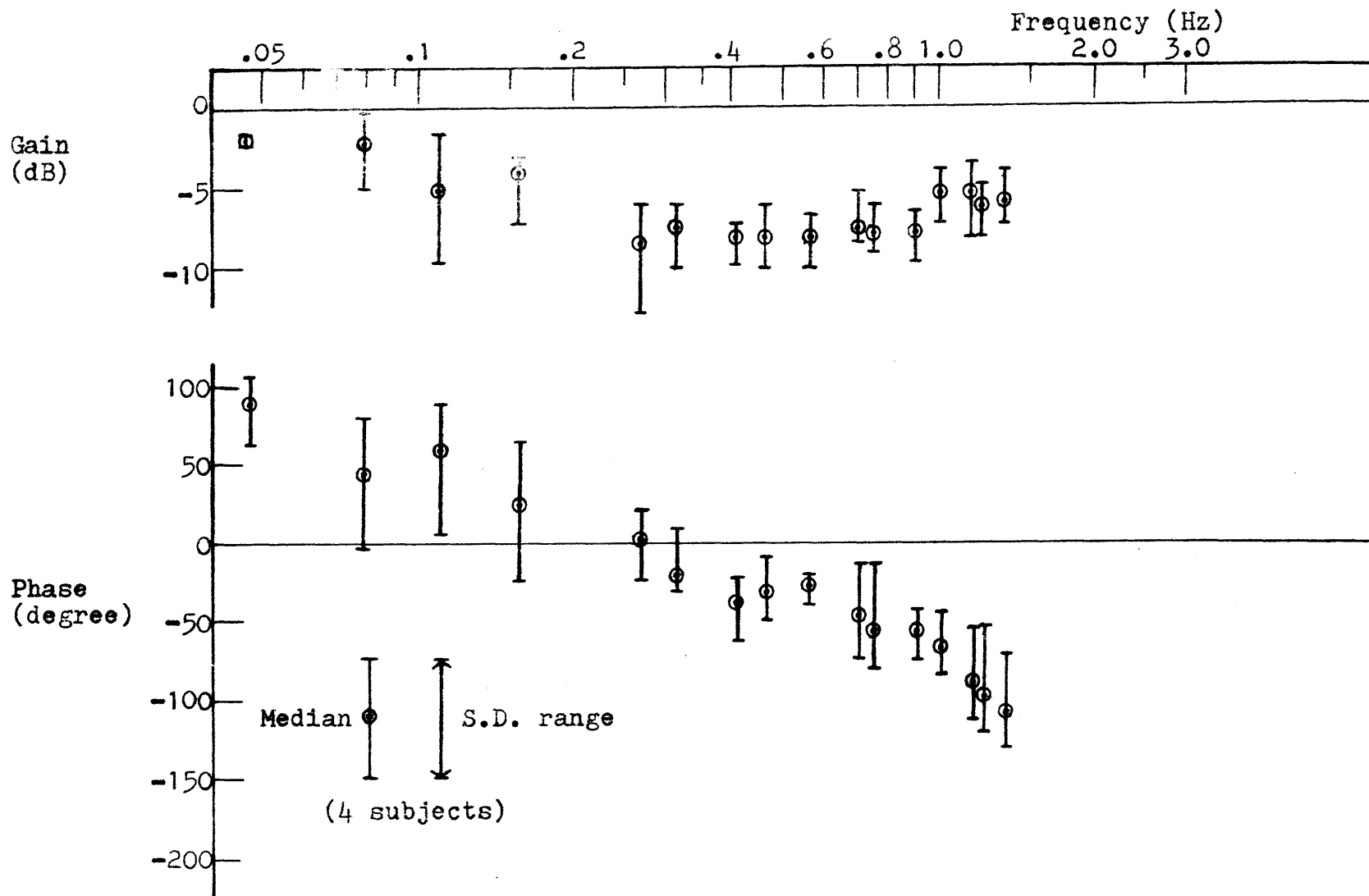


Fig. 4.15-b Nonperiodic-input pursuit frequency response; pseudo-random input B

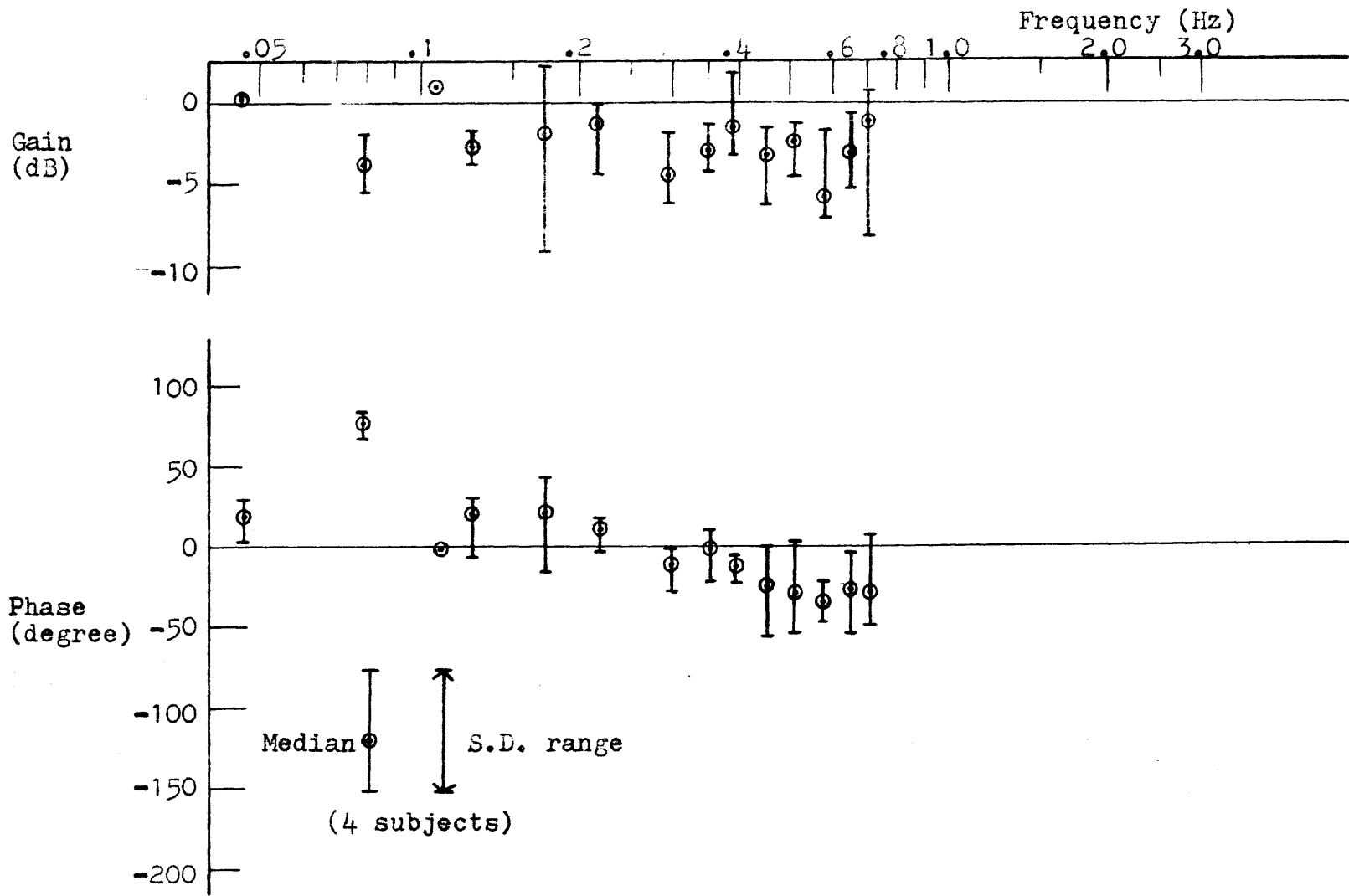


Fig. 4.15-c Nonperiodic-input pursuit frequency response; pseudo-random input C

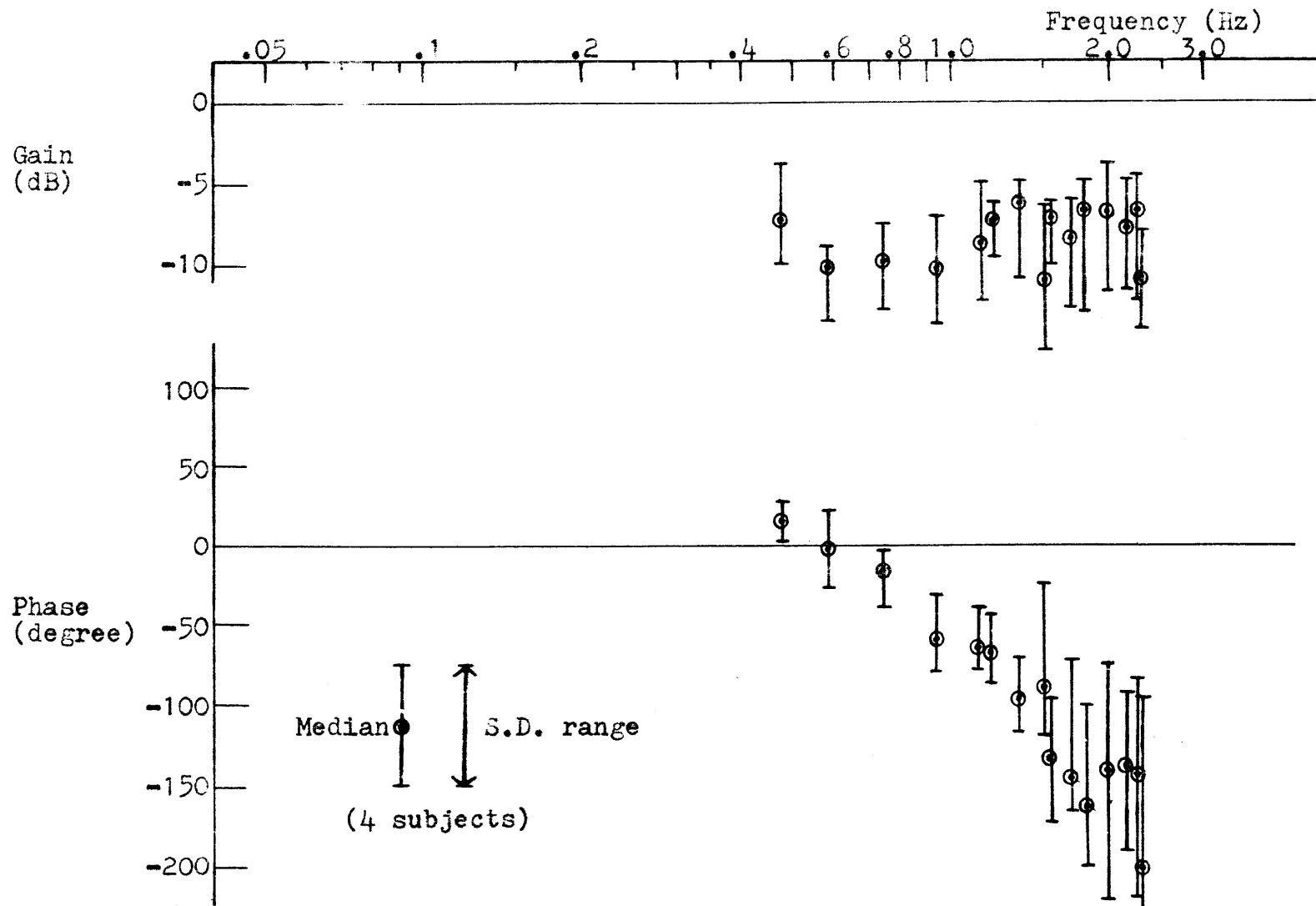


Fig. 4.15-d Nonperiodic-input pursuit frequency response; pseudo-random input D



the composite response. The gain attenuation was somewhat less prominent in the low-frequency range for the inputs A, B, and C, indicating the less significant role of saccadic movements in correcting for the tracking error in that range. Furthermore, the over-all pursuit gain appears to decline more as the input bandwidth becomes wider, suggesting the increasing importance of saccades with increasing bandwidth. This is consistent with the previous observation that the frequency at which the characteristic peak in the composite gain occurs tended to increase (i.e., more frequent saccades) with increasing bandwidth.

As evident in Figures 4.15, it is the phase behavior with which the pursuit system has revealed the most conspicuous feature in the nonperiodic-input tracking mode. This is the tendency of large phase lead in the low frequency region of each input band. The zero-phase shift tended to occur at some mid-frequency between 0.2 Hz and 0.6 Hz depending on the particular stimulus examined (approximately 0.40 Hz, 0.25 Hz, 0.22 Hz, and 0.55 Hz, respectively for input A, B, C and D). Phase lag increased monotonically with frequency about this point. While the statistical variance of these phase data was quite large over the whole frequency range of each input, there was some tendency for this to increase as the frequency was varied from the zero phase value, not only in its increasing direction, but also in its decreasing direction. Intra-subject variances were also apparent from Figures D.8 in Appendix D, in that the same subject who showed a very large low-frequency phase lead did not always do so for

another input at the same frequency.\* Despite these large intra- and inter-subject data scatterings, the greatest median values of the phase lead were as much as  $58^\circ$ ,  $84^\circ$ , and  $75^\circ$  found in the low frequency range of input A, B, and C respectively, and  $16^\circ$  for the input D in which low frequency components were absent. In order to reemphasize the above features of the nonperiodic-input pursuit response, the pursuit Bode plot (corresponding to pseudo-random input B, for example) is contrasted with the periodic-input pursuit result and also with the nonperiodic-input composite result for the same input B, as shown in Figure 4.16-a and Figure 4.16-b, respectively.

Further comments and discussions on the current phase result will continue in the following section.

---

\* Intra-subject variance should not refer to a relatively small scattering of data points obtained in Figures D.8 for the same subject, at the same frequency and with the same input: These data points were obtained essentially from a single experimental run.

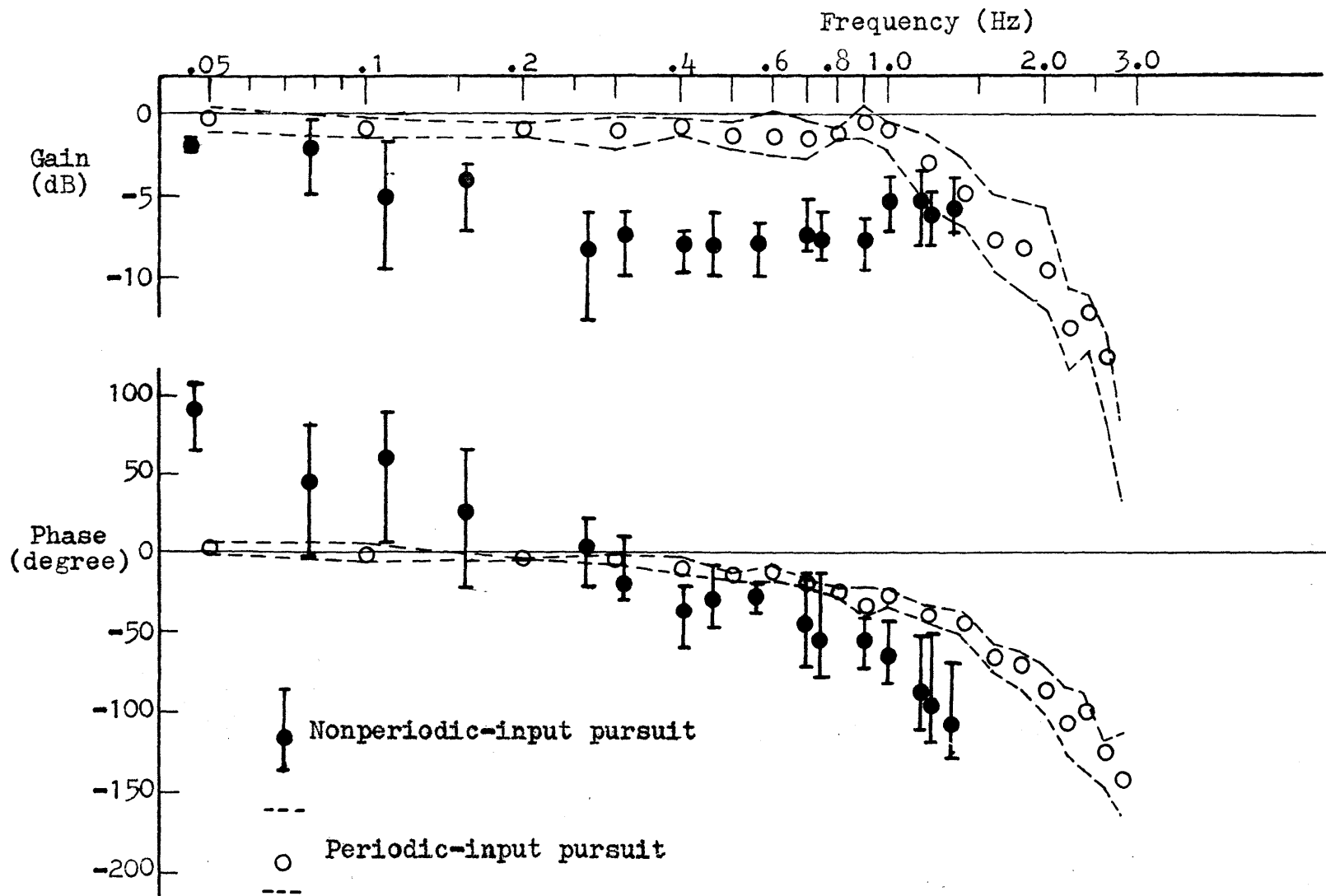


Fig. 4.16-a Nonperiodic-input pursuit result (pseudo-random input B) as contrasted with periodic-input counterpart, i.e., Fig. 4.8 and Fig. 4.15-b are combined.

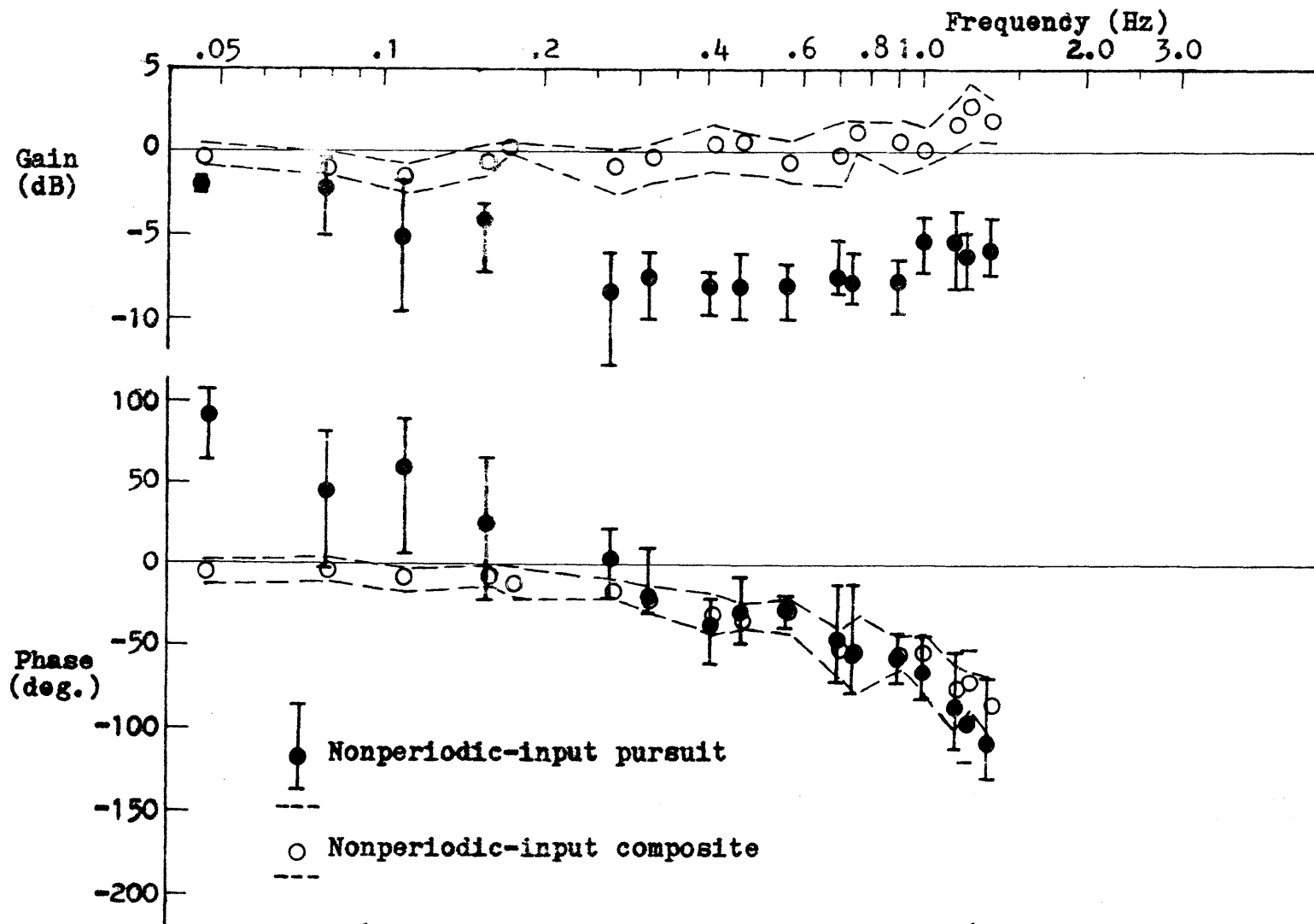


Fig. 4.16-b Nonperiodic-input pursuit result (pseudo-random input B) as contrasted with composite counterpart, i.e.,; Fig. 4.13-b and Fig. 4.15-b are combined.

#### 4.4 Pursuit Phase Behavior: Discussion and Theory

This section is devoted to discussion on the major experimental result in this chapter: the tendency of large low-frequency phase lead which emerged in the nonperiodic-input frequency response of the smooth pursuit system only. Reliability of this result should be checked first from the methodological point of view.

##### 4.4.1 Reliability of the Phase Result

There are several reasons to support the fact that the observed pursuit phase behavior is a real characteristic of the system, rather than an experimental artifact.

First, consider the nonpredictive composite frequency response results, where no such phase lead was found, but phase was rather slightly lagged and maintained close to zero at low frequencies as expected. Hence, this observation must preclude any possible defect in the FFT data processing stage as being responsible for the observed phase advancement in question.

Secondly, one might well suspect that it might have been an artifact in some way created by the hybrid computer routine, MITNYS, another necessary step involved in the data reduction\* for obtaining the pursuit frequency response. This possibility

---

\* The 25 msec processing delay of MITNYS should be negligible. At best, it could contribute only to phase lag, not to phase lead.

was unlikely too: Chapter VI will show Bode plots of the slow phase of the optokinetic nystagmus responding to essentially the same pseudo-random stimuli as used in this chapter. The data reduction procedure for that purpose followed exactly the same steps as here, incorporating MITNYS in addition to FFT. As will be shown in Chapter VI, phase remained close to zero in this nystagmus case as well, again as expected. And it turned out to be far from the phase behavior at low frequencies obtained in this chapter with the pursuit tracking system.\*

Third, visual inspection of the original nonperiodic-input records such as those shown in Figure 4.17 reveals that pursuit movement was often not in the same direction as the over-all composite movement. Thus, at least, the pursuit phase should not be expected to be similar to the composite phase that produces little phase shift at low frequencies.

Fourth, Chapter V will show that the large low-frequency phase lead in the pursuit result is internally consistent with the composite frequency response result, provided that a sampled data model of Young's (1962) type is assumed for the saccadic system.

Finally, due to the optical arrangement employed in the

---

\* For the input D, however, a similar phase lead was obtained in the lower end of its frequency band. But as will be discussed later, the input motion of the OKN stripe-pattern became so small for this particular input signal (because of its high-frequency band characteristics) that the smooth movement was probably the same in class as the pursuit movement rather than the slow phase of nystagmus.

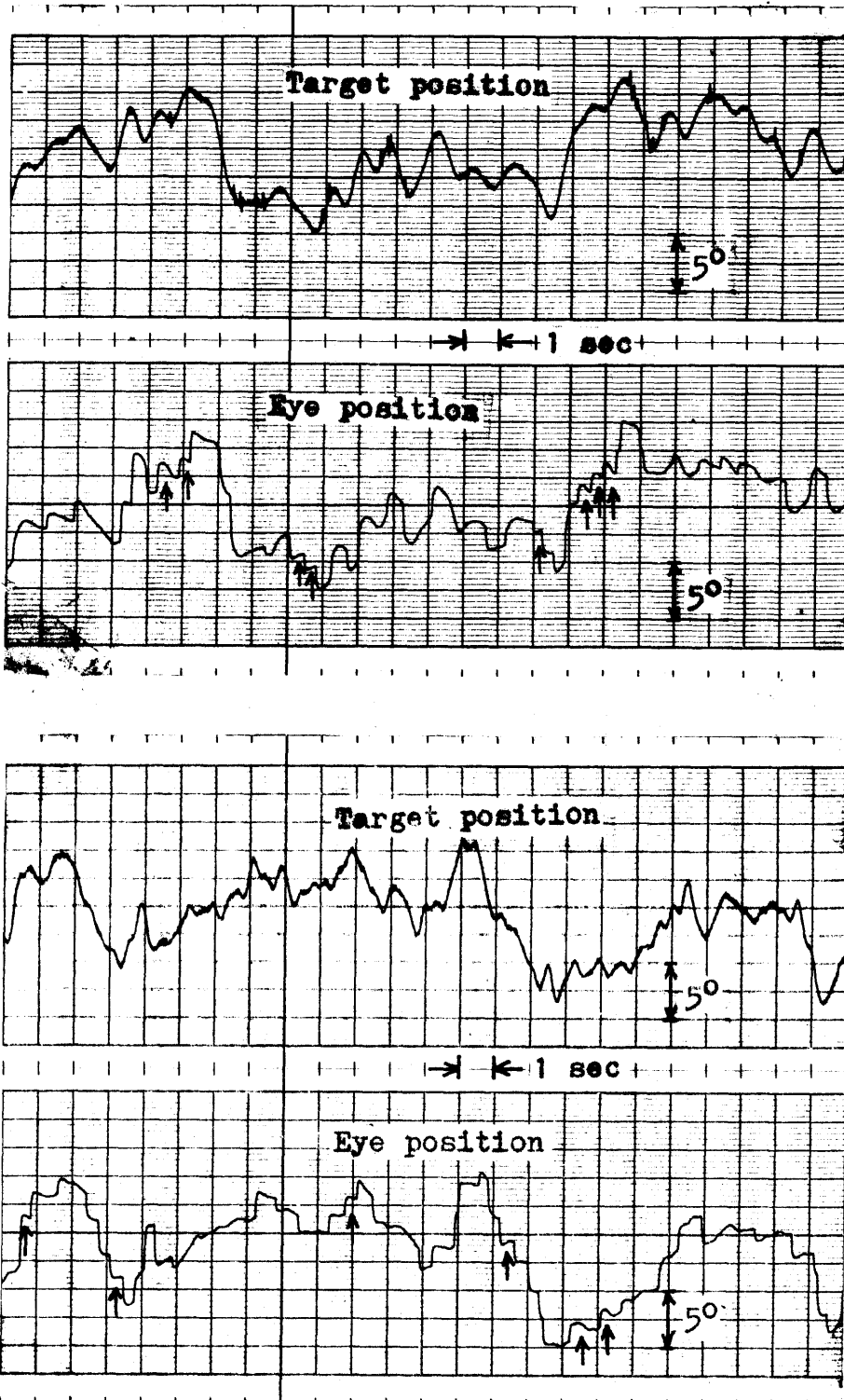


Fig. 4.17 Pursuit movement relative to over-all composite movement. They are not always in phase ; pursuit movement is often in direction opposite to over-all trend as indicated by arrows

experiment, the size of the visual target was not small enough to approximate a point target, but the target was a circular spot with a diameter of  $0.6^\circ$ , a relatively large figure in comparison with the range of target motion. The instruction asking the subject to try to fixate on the center of the spot was given, but actually it was not intended to be very meaningful for the reflexive nature of the oculomotor tracking. The visual fixation might have been drifting and wandering around within the spot of the circle. If this had been the case, such eye movements might have given rise to the observed phase behavior through some unknown mechanism. To check this possibility, a few relevant runs were repeated with a virtual point target presented directly on the CRT console. Figure D-9 in Appendix D shows the results of this test, which still indicates the presence of the phase lead at low frequencies, although not as large as some of those obtained previously.

#### 4.4.2 A Phase Control Model for Pursuit Tracking

In view of the foregoing consideration, it is assumed that the large low-frequency phase lead is a real characteristic of the smooth pursuit system exposed to a non-periodic stimulus. Noting that the pursuit system is now shown to be at least input-adaptive, we proceed to a preliminary attempt for interpreting the above specific finding. The following discussion refers only to the phase behavior of the pursuit system and no account



will be made for its relation to the gain result. In defense of such an approach, gain and phase could be controlled separately. All physical control systems do not necessarily have to obey, for instance, the phase-attenuation theorems of Bode. This is in fact quite likely the case with the visual tracking, as stressed by St-Cyr and Fender (1969) and others.

That the smooth pursuit system also has its own predictive mechanism is neatly demonstrated in the time domain by Vossius (1965, reviewed in section 4.1). The evidence is further supplemented by the frequency domain observation that phase lag of the pursuit system is too small in the periodic-input tracking mode to be accounted for by its innate reaction time as confirmed in this chapter.

Given these evidences, the assumption is introduced here that the pursuit system's predictive mechanism operates even when the input is random and "nonpredictable". This assumption is analogous to the concept explored for the composite eye movement tracking of Michael and Jones (1966, Section 2.4).

However, it might be still difficult to see any teleological advantage in having such a large phase lead as found at low frequencies. For instance, the median value of  $84^\circ$  phase lead was obtained at 0.046 Hz with the input B. This would imply that the prediction was as much as 5.1 seconds ahead in anticipating this frequency component hidden in the pseudo-random input. It seems highly improbable that the system does this "purposefully". Instead, the large phase lead is interpreted here as a cost to pay

for some special predictive scheme. It is assumed that the actual object of the predictive mechanism is to try to nullify some average phase lag which would otherwise be present, for it is presumably not possible due to some inherent physical limitations to make all frequency components equally yield zero phase shift.

Such an average phase lag should correspond to the phase lag that would appear at a certain intermediate frequency within the given input bandwidth. Hence, no phase shift must occur at that intermediate frequency. For all the pseudo-random input, even including the input D which contained no low frequency components, the zero-phase frequency was in fact found at some intermediate within the corresponding input bandwidth. Some trend that the phase data appears to yield the least variance around the zero-phase frequency may be consistent with the idea that the predictive mechanism exerts its primary effect at that frequency.

The foregoing view will be advanced further and made more specific on the basis of the following additional observations:  
(1) As shown in Figures 4.18, the trend of the nonperiodic-input pursuit data points could be matched approximately by a parallel upward-shift of the entire phase plot of the transfer function,

$$G(s) = \exp(-0.15s)/(1 + 0.1s)(1 + 0.5s)$$

that is,

$$\angle G(j\omega) = -0.15j\omega - \tan^{-1}0.1j\omega - \tan^{-1}0.5j\omega \quad (4-1)$$

( $\omega$ : angular frequency in radians)

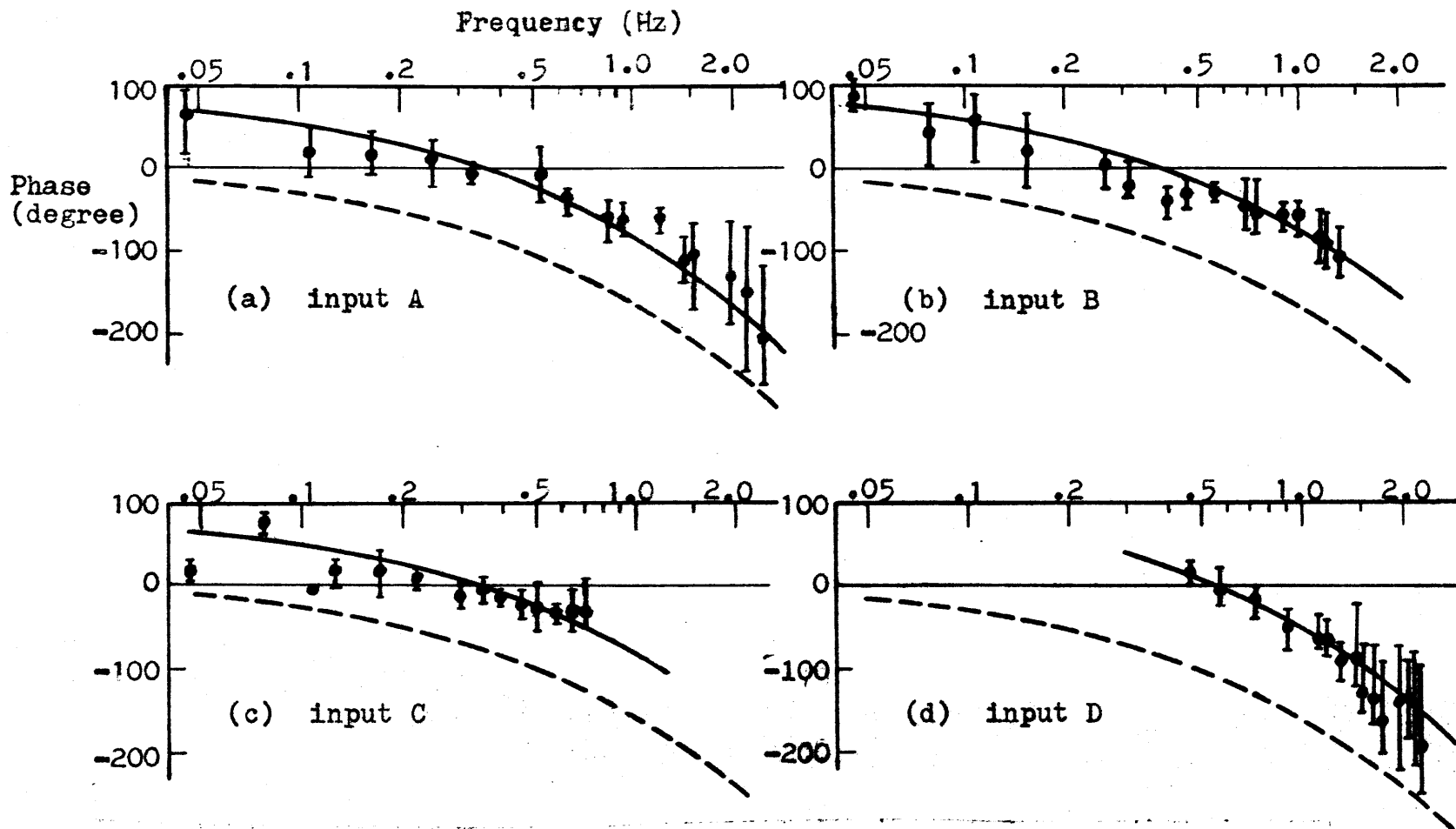


Fig. 4.18 Nonperiodic-input pursuit phase behavior as approximated by some upward shift of phase curve corresponding to transfer function,  $G(j\omega) = e^{-0.15j\omega}(1 + 0.1j\omega)(1 + 0.5j\omega)$ .  $G(j\omega)$  is indicated by broken curve.

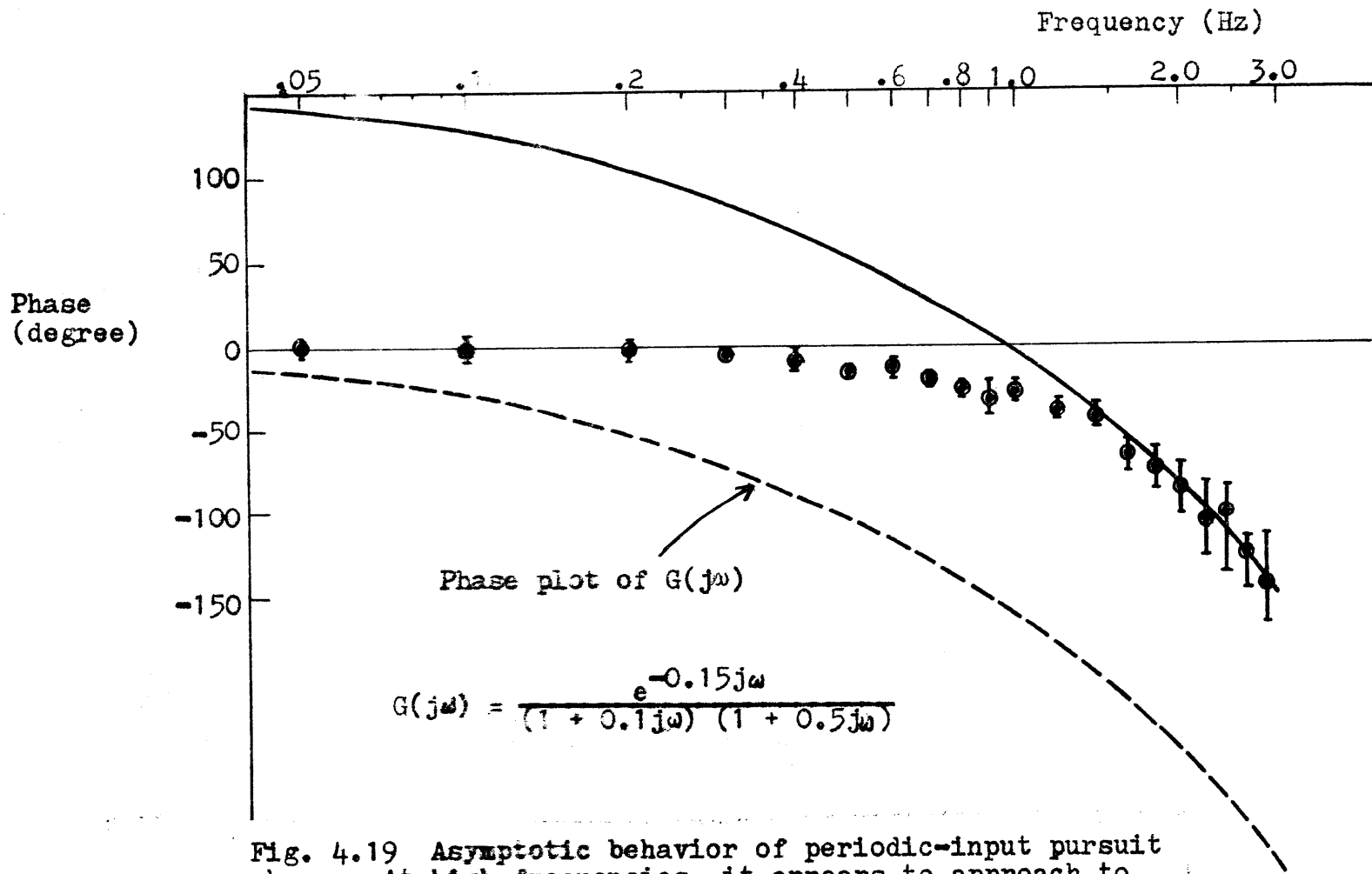


Fig. 4.19 Asymptotic behavior of periodic-input pursuit phase: At high frequencies, it appears to approach to the curve obtained by advancing phase plot of  $G(j\omega)$  by  $155^\circ$ . Zero-phase line gives another asymptote at the other extreme of frequency range.

by some constant angle depending upon a particular pseudo-random input.

(2) As shown in Figures 4.19, the upward shift of the same phase curve  $\angle G(j\omega)$  by a factor of  $155^\circ$  appears to give an asymptote for high frequency data points in the periodic-input tracking case.

Considering the pursuit system's inherent response variability, the quality of these curve fitting results may be satisfactory enough to indicate that a transfer function close to the above particular form is in some way inherently associated with the pursuit tracking system to affect its phase behavior.

Specifically it is postulated that the nonperiodic-input pursuit phase,  $\theta_n$ , is given by:

$$\theta_n(\omega) = \angle G(j\omega) + \frac{1}{W} \int_{\omega_1}^{\omega_h} \alpha(\omega) d\omega \quad (4-2)$$

where  $\omega_h$  = the highest frequency,  $\omega_1$  equals the lowest frequency,  $W$  is the stimulus bandwidth (i.e.,  $\omega_h - \omega_1$ ), and  $\angle G(j\omega)$  is given by Eq. 4-1.

While the implication of  $\alpha(\omega)$  will be given subsequently, the general form of expression is consistent with the aforementioned matching observation for the nonperiodic-input pursuit phase behavior; the second term on the right hand side, being the average of  $\alpha(\omega)$  over a given stimulus frequency bandwidth, corresponds to a positive constant phase angle to be added to  $\angle G(j\omega)$ .

For the periodic-input tracking case, in which  $\omega_h \rightarrow \omega_1$  and  $W \rightarrow 0$ , Eq. 4-2 reduces to the following equation to give the periodic-input pursuit phase,  $\theta_p$ :

$$\theta_p(\omega) = \angle G(j\omega) + \alpha(\omega) \quad (4-3)$$

That is, the average of  $\alpha(\omega)$  is  $\alpha(\omega)$  itself, when there is only a single frequency component in the input.

Therefore, it is now possible to determine the phase function,  $\alpha(\omega)$ , from the periodic-input experimental data according to:

$$\alpha(\omega) = \theta_p(\omega) - \angle G(j\omega) \quad (4-4)$$

Values of  $\theta_p(\omega)$  are available from the data points given in Figures 4.19, and  $\angle G(j\omega)$  can be computed as a function of frequency according to Eq. 4-1. The resultant  $\alpha(\omega)$  plot is shown in Figure 4.20. Note that the high-frequency asymptotic tendency, i.e.,  $\alpha(\omega) = 155^\circ$ , has come from the asymptotic behavior previously described in the periodic-input pursuit phase result.

Once  $\alpha(\omega)$  is thus established from the periodic-input phase data, the pursuit phase for any given nonperiodic-input can be predicted by Eq. 4-2. The system operation is illustrated graphically as depicted in Figure 4.20.

The inherent phase lag,  $\angle G(j\omega)$ , is a hidden property of the pursuit system in that it never appears on the surface by itself under any condition of the stimulus periodicity:  $\angle G(j\omega)$  is always accompanied by a constant phase lead depending upon a particular stimulus.  $\alpha(\omega)$  may be viewed as a potential generating source of such a phase lead in compensating for the innate phase lag.

For the periodic-input case, the pursuit phase is advanced from  $\angle G(j\omega)$  by an amount exactly equal to  $\alpha(\omega)$  at a given frequency, and the resultant phase must agree with the corresponding experimental data point. This is, however, a trivial consequence because  $\alpha(\omega)$  has been so defined.

For the nonperiodic-input case, on the other hand, the original phase,  $\angle G(\omega)$ , is shifted upward as a whole by a factor corresponding to the mean value of  $\alpha(\omega)$  averaged over a given input bandwidth. This process is in accordance with the phase equation, Eq. 4-2. As schematically shown in Figure 4.20, the result is consistent with the experimental nonperiodic-input pursuit phase result, accounting for the two conspicuous features: (1) large low-frequency phase lead, (2) occurrence of the zero phase shift at some mid frequency within the given input frequency band.

Next, this basic agreement between experiment and theory is examined with respect to each of the pseudo-random inputs (A, B, C, and D) actually used in this chapter. As a pseudo-

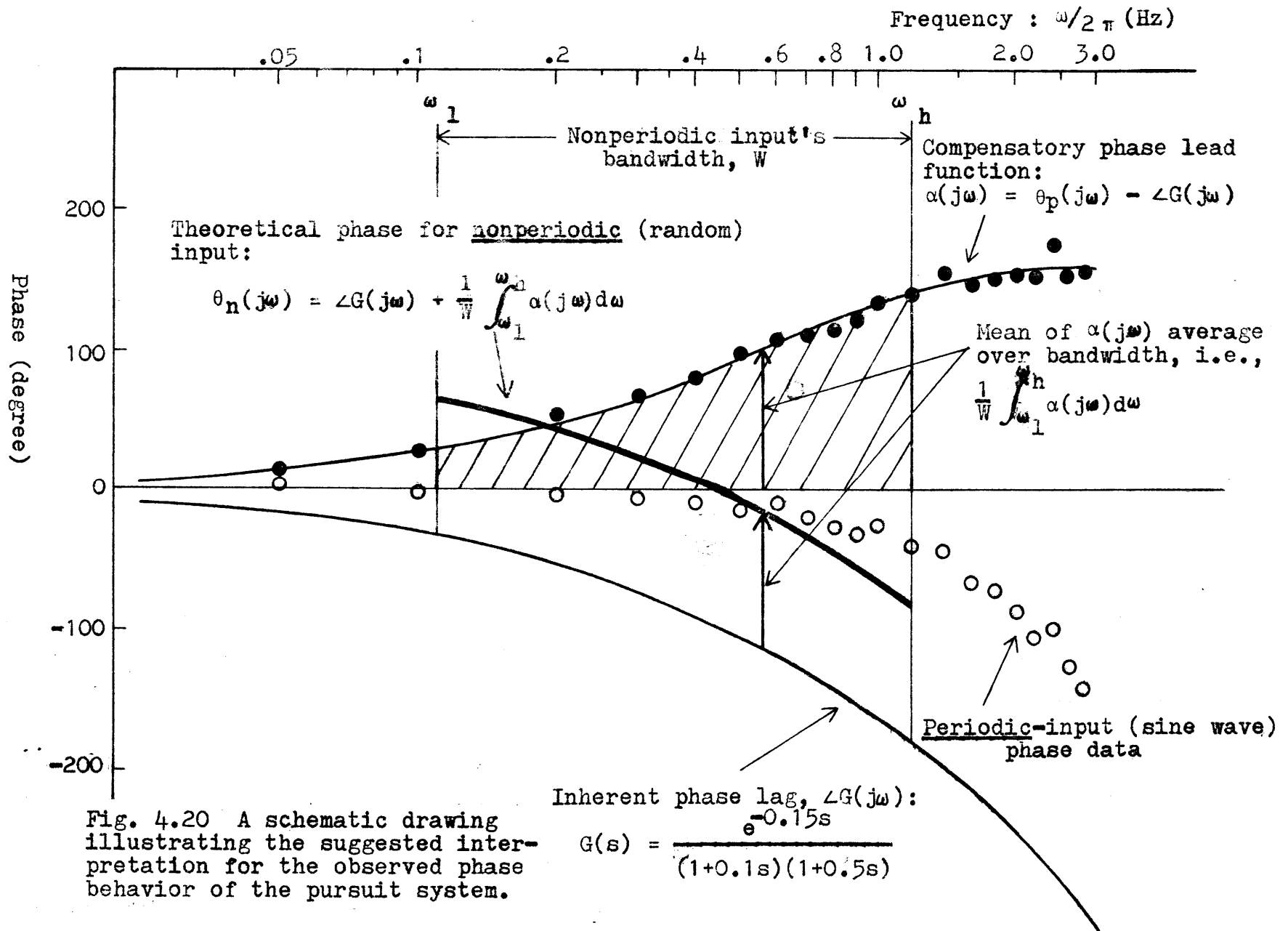


Fig. 4.20 A schematic drawing illustrating the suggested interpretation for the observed phase behavior of the pursuit system.



random input contains a finite number of sinusoids at discrete frequencies,  $\omega_1, \omega_2, \dots, \omega_n$ , the integral term in Eq. 4-2 needs to be rewritten in the following summation form as visualized from the diagram given in Figure 4.21

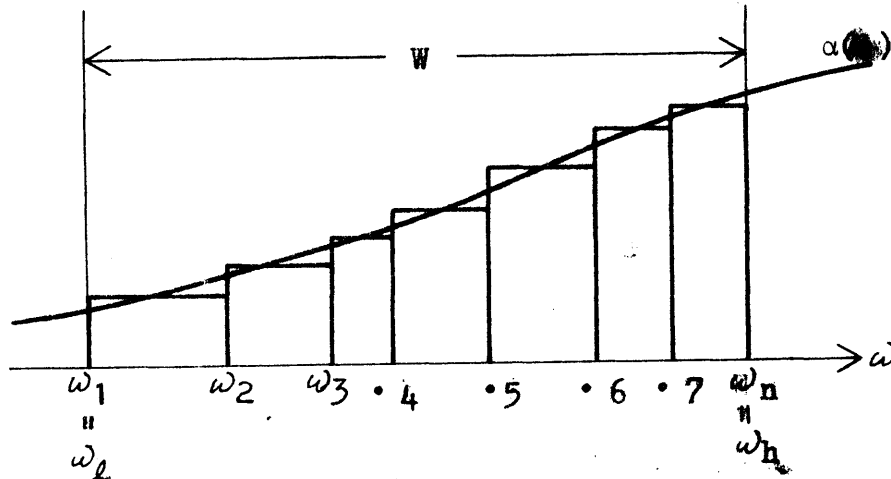


Fig 4.21 Schematic illustration for Eq. (4-5).

$$\frac{1}{W} \int_{\omega_l}^{\omega_h} \alpha(\omega) d\omega \approx \frac{1}{W} \sum_{i=1}^n \frac{\alpha(\omega_i) + \alpha(\omega_{i+1})}{2} \times \Delta\omega_i \quad (4-5)$$

where,  $\Delta\omega_i = \omega_{i+1} - \omega_i$

$$\omega_1 = \omega_l, \omega_n = \omega_h \text{ and } W = \omega_h - \omega_l$$

Table 4.1 lists the result of this numerical computation for each input. The nonperiodic-input pursuit phase plots as obtained by adding these compensatory phase values to  $\angle G(j\omega)$  are presented in Figures 4.22 along with the experimental counter-

parts obtained in this chapter.

Pseudo-random input	Compensatory phase lead
A	128°
B	93°
C	67°
D	133°

Table 4.1 Compensatory phase lead as computed based on the suggested scheme for pursuit phase control

This theoretical development has been intended to provide a qualitative explanation for the characteristic pursuit phase behavior, rather than to offer a quantitatively accurate phase prediction. In that context, Figure 4.22 demonstrates a reasonable agreement between experiment and theory.

The phase compensation process does not try to take care of each frequency component individually during the nonperiodic-input tracking. Instead the system treats the input frequency spectrum as a whole in compensating for the innate lag  $\angle G(j\omega)$ , giving each constituent frequency component an equal amount of phase lead which would be generated if the average frequency alone were present. This might result from a compromise with some inherent physical limitations that cannot allow it to make all frequency components equally yield the ideal zero-phase shift. Hence in an attempt to reduce the inherent phase lag  $\angle G(j\omega)$ , only the mid frequency region receives a real

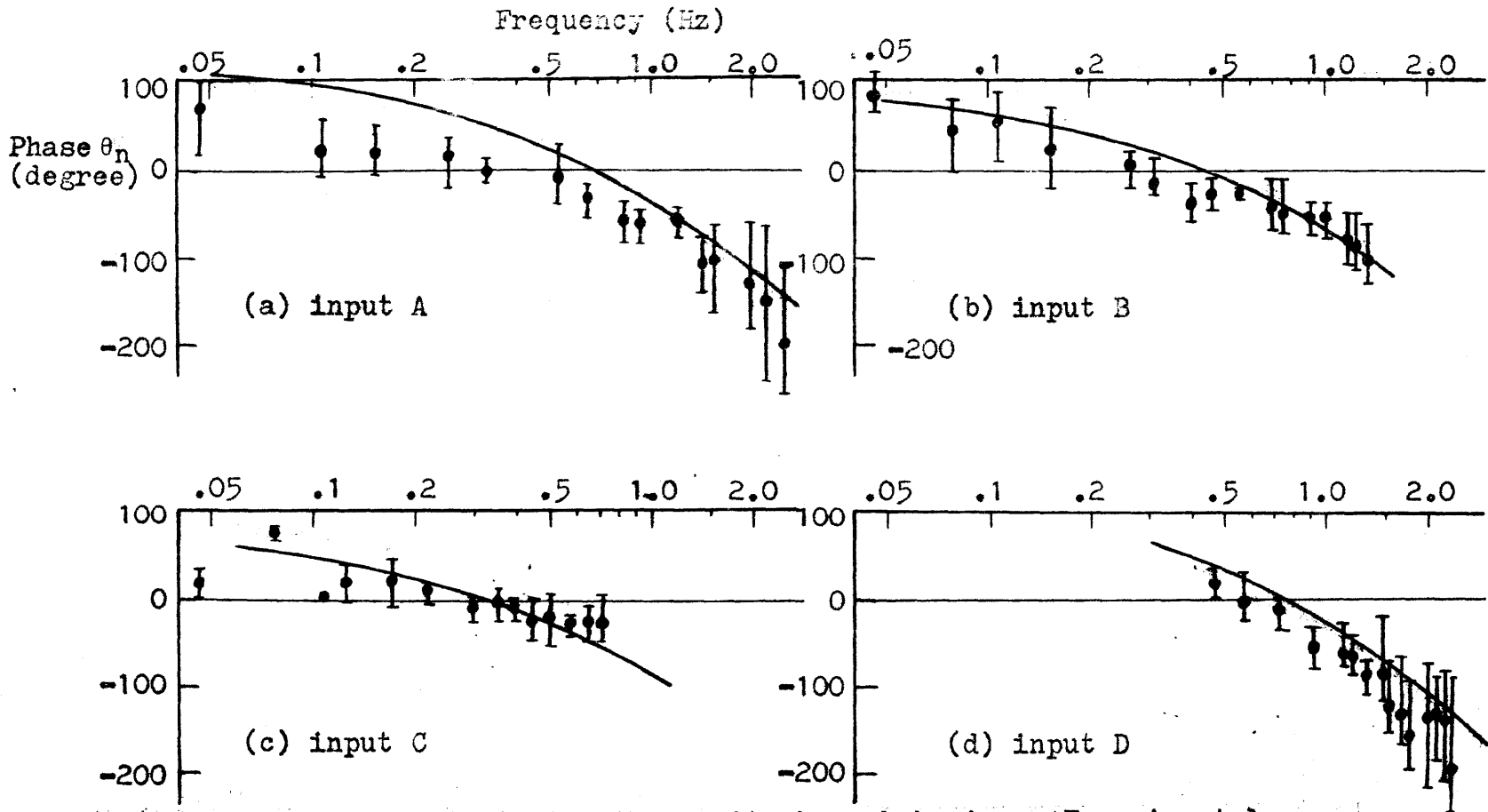


Fig. 4.22 Nonperiodic-input pursuit phase behavior: Experimental data and prediction by

$$\theta_n(\omega) = G(j\omega) + \frac{1}{W} \int_{\omega_1}^{\omega_h} \alpha(\omega) d\omega$$

where  $\alpha(\omega) = \theta_p(\omega) - G(j\omega)$   
 W: stimulus bandwidth,  $\omega_h$ : highest input frequency,  $\omega_1$ : lowest input frequency,  $\theta_p(\omega)$ : periodic-input phase data.

benefit for minimizing the over-all phase error, at the expense of excess phase lead at lower frequencies and insufficient compensation at high frequencies.

In essence, the whole theory discussed thus far is described by a single equation, Eq. (4-2), which considers the input bandwidth as a continuous parameter grading the stimulus periodicity. This concept of continuity is consistent with the notion by Michael and Jones (1966). The periodic-input pursuit tracking mode can be recognized as a special case as given by Eq. (4-3), which is a reduced version of the general phase equation, Eq. (4-2). Both  $\alpha(\omega)$  and  $\angle G(j\omega)$  involved in these equations are not stimulus-dependent. Once the input specification is given (i.e.,  $\omega_h$ ,  $\omega_l$  and  $W$ ), the pursuit phase behavior can be predicted, if not quantitatively very accurate, to yield the observed characteristic tendencies in the frequency domain.

The above phase control model should be regarded as a preliminary one. As will be suggested briefly in Section 8.3, only further investigation could solve some remaining problems; for example a proper block diagram description of the model along with a possible inclusion of the pursuit gain behavior. Nevertheless, on the basis of the present research, it appears that the pursuit system incorporates a predictive mechanism, which operates even with nonperiodic stimuli. Finally, a similar phase behavior (large low-frequency phase lead and zero-phase shift at some intermediate frequency) has been reported in a preview manual control task with pseudo-random inputs (Drewell, 1972). This might reinforce the view that the special aspect

of the observed pursuit phase behavior is a manifestation of a predictive mechanism.

#### 4.5 Summary and Conclusions

There is a substantial difference in the visual tracking performance by the dual-mode oculomotor system, depending on whether the stimulus motion is periodic or a apparently non-periodic and random. The periodic-input case yields a better maintenance of visual fixation, and moreover the corresponding oculomotor behavior appears incompatible with the underlying innate reaction time unless one postulates a predictive or learning mechanism. These phenomena characterizing the composite tracking eye movement (saccade and pursuit) have been demonstrated by many previous authors in terms of the frequency response, and they were reexamined in the course of the present series of experiments.

Given that a similar predictive behavior is known to occur also in the saccadic system acting alone, the central object was to investigate whether a predictive mechanism might be incorporated in the pursuit system that constitutes the other subsystem for the dual-mode oculomotor tracking. While Vossius (1965) obtained a positive evidence with a specially arranged time-domain observation, this chapter undertook the frequency-domain approach for the quest of the predictive behavior of the pursuit tracking system. To this end, saccades were removed and pure pursuit movements were properly extracted from the original composite eye movement traces by a hybrid computer routine developed by Allum et al (1973). Subsequent Fourier analysis has yielded the following results corresponding to the four cases investigated; (1) composite, periodic-input, (2)

composite, nonperiodic-input, (3) pursuit only, periodic-input,  
(4) pursuit only, nonperiodic-input:

While the nonperiodic-input composite frequency response results were generally in good agreement with relevant features explored by previous workers, the present periodic-input Bode plot failed to indicate a clear manifestation of the less-than-minimum phase behavior contrary to others. Instead, the result appears to support the minimum phase behavior, which suggests an effective compensation of the oculomotor reaction time rather than an overcompensation as implied by the less-than-minimum phase behavior. This disagreement with the literature, on the surface, comes from the fact that the present periodic-input phase lag is considerably greater than pertinent published data especially at high frequencies, though it is still much less than what would be expected from the innate reaction delay. Although not fully conclusive, the real reason for the above discrepancy might be that the stimulus amplitude level was carefully adjusted here, which would otherwise likely cause the pursuit velocity saturation especially at high frequencies as appears to have been the case in most of the published experiments.

The less-than-minimum phase behavior was evident, however, for the periodic-input pursuit Bode plot, which yielded the same phase (by definition of pursuit phase employed here) but produced greater high-frequency gain attenuation as compared with the periodic-input composite results. Increasing relative importance of saccadic movements with increasing

frequency was thus confirmed.

Nonperiodic-input pursuit results indicate that gain plot as a whole declines as input bandwidth increases. But these results are more markedly characterized by a tendency of large phase lead in the lower frequency region within a given input frequency spectrum. In one case, for example, inter-subject average value of the phase lead reached as much as about  $90^{\circ}$ . Zero-phase shift occurs at some mid frequency (0.3 - 0.5 Hz depending on a particular input band), only above which phase lag develops. Supported by various tests, this phase result was not likely an artifact somehow created in a certain step during the relevant data reduction procedure. It is thus concluded that the observed nonperiodic-input pursuit phase behavior is a real characteristic and that the pursuit system is at least input-adaptive.

This finding is interpreted, in part, on the basis of the notion of Michael and Jones (1966), which regards stimulus predictability (as represented by bandwidth) as a continuous parameter affecting the system response. An inherent phase lag associated with the pursuit system, as hypothesized from a comparative close examination on pursuit phase data with various bandwidths (including zero bandwidth, i.e., periodic-input case), is compensated by an additive phase lead determined through a simple averaging process over the given bandwidth. The object of the system is try to null some average phase lag, which would otherwise appear at a certain intermediate frequency within the given input bandwidth. Hence no



phase shift must occur in the vicinity of that intermediate frequency. By adding the compensatory phase lag (which increases with increasing frequency), only a region around the mid frequency would receive a real benefit for reducing the phase error, at cost of excess phase at lower frequencies and insufficient compensatory phase lead at higher frequencies. Thus, the rather unexpected pursuit phase behavior may be still regarded as a manifestation of a predictive mechanism, which operates, in principle per se, even under random stimulation. Finally notice that the periodic-input phase can be recognized as result of a special case of this operation.

## Chapter V

### Nonperiodic-input Frequency Response of the Saccadic Tracking System: An Indirect Evaluation

The saccadic system's intrinsic frequency response is evaluated on the basis of the nonperiodic-input composite and pursuit frequency response data experimentally obtained in the previous chapter.

First, the phase result is compared with the periodic-input counterpart found in the literature. Second, the Bode plot result including both gain and phase is discussed in detail in the framework of Young's sampled-data model for the saccadic oculomotor tracking system.

#### 5.1 Introduction

##### 5.1.1 Background

##### 5.1.2 Objectives

#### 5.2 Inference from Experimental Results of Chapter IV

##### 5.2.1 Apparent Saccadic Frequency Response

##### 5.2.2 Intrinsic Saccadic Frequency Response

##### 5.2.3 Periodic versus Nonperiodic-input Saccadic Phase Behavior

#### 5.3 Comparison with Young's Sampled-data Model

##### 5.3.1 Model Prediction based on 200 msec Sampling Period

##### 5.3.2 Model Prediction based on Estimated Inter-saccadic Period

- 5.3.3 Reduced Latency: A Possible Model Improvement and its Implication
- 5.4 Consistency of Experimental Results in Chapter IV
- 5.5 Summary and Conclusions

## 5.1 Introduction

### 5.1.1 Background

The eye movement pattern resulting from tracking a continuously moving visual object is characterized by the dual-mode operation as outlined in Section 2.1.

In connection with a study on the predictive oculomotor characteristics, the frequency response of the dual-mode oculomotor system has been obtained with the over-all composite eye movement by many investigators (reviewed in Subsection 2.4.1), and by this author in the previous chapter. But, since the composite eye movement incorporates saccades and pursuit movements which are known to be functionally distinct, it is desirable to study these two constituent movements separately rather than in terms of the original composite movement. For this reason, as a main objective of Chapter IV, the pursuit frequency response was isolated from the composite data in both periodic and nonperiodic stimulus conditions. The result has shown certain special input-adaptive features, which are interpreted as a manifestation of a predictive mechanism of the pursuit tracking system as conceptualized in Chapter IV.

Investigation selective to the saccadic system, on the other hand, has been done by using periodic square-wave inputs, as reviewed in Subsection 2.4.2 (Stark et al, 1962; Dallos and

Jones, 1963). While these prior works have provided evidence for the predictive capacity of the saccadic system by showing substantial reduction in the saccadic latency in comparison with the average latency in the transient response to a sudden stimulus displacement, the saccadic system's predictive characteristics might be further confirmed if periodic and non-periodic (random) input data become both available.

### 5.1.2 Objectives

The primary purpose of this chapter is then to obtain the nonperiodic-input frequency response accounting for the saccadic system only.

In principle, the nonperiodic-input saccadic frequency response could be evaluated by a Fourier analysis on the saccadic data which would be obtained with a random pattern of square-wave input (discrete random target motion). However, no further experiment is necessary in this chapter, for the desired information is already available indirectly from the nonperiodic-input results established in Chapter IV: vectorial subtraction of the pursuit frequency response from the composite counterpart would yield the saccadic frequency response.

However, because of an inherent interference from the pursuit system, the saccadic frequency response of this type is actually not the frequency response of the saccadic system

itself that would be obtained under a random discrete stimulation. Nevertheless, it is possible to evaluate the intrinsic nonperiodic-input saccadic frequency response by removing the interference effect with further use of the available data of the pursuit frequency response. These points will become more clear subsequently.

Once such a saccadic frequency response is inferred, it is the second objective of this chapter to compare it with that predicted by Young's sampled-data saccadic eye tracking model (1962; reviewed in Subsection 2.1.1), which is intended to describe nonperiodic-input responses. If these were in good agreement, not only would it confirm Young's model but also it would support the empirical validity of the rather unexpected phase result obtained in the previous chapter for the nonperiodic-input pursuit frequency response. This viewpoint is explored in the following third phase of this chapter.

The whole matter can be looked at from a different point of view by interchanging means and object in the previous approach: one can deduce the pursuit frequency response by presupposing Young's model first, that is, by subtracting its predicted saccadic response from the available experimental result for the composite frequency response. The object here is particularly to examine whether or not the large low-frequency phase lead would emerge also from the pursuit response evaluated in this way. This is to examine internal consistency of composite and pursuit frequency response results obtained in Chapter IV.

## 5.2 Inference from Experimental Results of Chapter IV

### 5.2.1 Apparent Saccadic Frequency Response

By definition, the following relation is always true:

$$\theta_s(t) = \theta_c(t) - \theta_p(t) \quad (5-1)$$

where  $\theta_c$ ,  $\theta_s$  and  $\theta_p$  represent the composite eye position, saccadic eye position and pursuit eye position respectively, all measured at time  $t$ . (By pursuit eye position is meant the cumulative eye position used in the previous chapter.)

Under the limited assumption that the oculomotor tracking system is linear and deterministic, the above time-domain equation can be rewritten in terms of the transfer function relating to the stimulus position  $\theta_i$ , which in turn leads to the following frequency response relation:

$$G_s(j\omega) = G_c(j\omega) - G_p(j\omega) \quad (5-2)$$

where  $\omega$  : angular frequency in radians and  $j = \sqrt{-1}$ , and

$G_c(j\omega) = \theta_c(j\omega)/\theta_i(j\omega)$  : Composite frequency response

$G_s(j\omega) = \theta_s(j\omega)/\theta_i(j\omega)$  : Saccadic frequency response

$G_p(j\omega) = \theta_p(j\omega)/\theta_i(j\omega)$  : Pursuit frequency response

$G_c(j\omega)$  and  $G_p(j\omega)$  for the nonperiodic-input case have been

determined experimentally in the preceding chapter. By using these data,  $G_s(j\omega)$  can be computed according to Equation 5-2. The result with the pseudo-random input B has turned out to be most appropriate to work with throughout this chapter, for it permits investigation for a wide frequency range with minimum interference of the side band effect arising in the subsequent theoretical consideration on the saccadic system.

Figure 5.1 shows the resultant  $G_s(j\omega)$ , indicated by the open circles, computed based on the median data points of  $G_c(j\omega)$  and  $G_p(j\omega)$  obtained with input B, which are indicated by closed circles and crosses respectively. Regardless of the fact that  $G_s(j\omega)$  only represents an apparent saccadic frequency response for the reason fully given in the next subsection, the following observations can be made from these frequency-domain data: In order to compensate for the relatively large pursuit gain deterioration apparent over almost the entire frequency range, the fixation had to rely more heavily on corrective saccadic movements in proportion. As to phase, the large pursuit phase lead in the low frequency region was counterbalanced by the large phase lag associated with saccadic movements.

### 5.2.2 Intrinsic Saccadic Frequency Response

The frequency response  $G_s(j\omega)$ , as evaluated above, does not purely reflect the saccadic system itself, however. This is



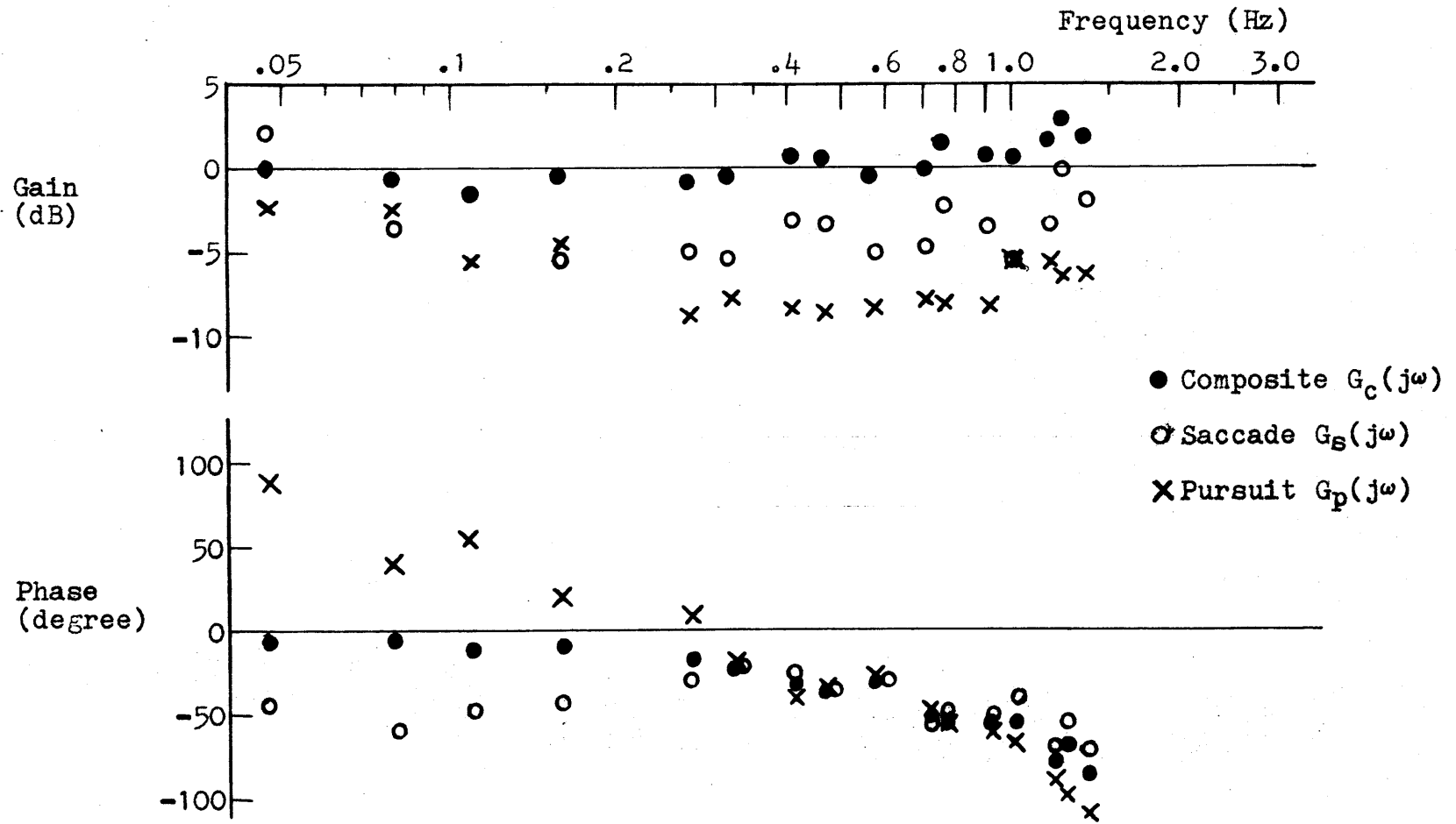


Fig. 5.1 Frequency response results for composite, saccadic and pursuit movements for pseudo-random input B. Note this saccadic result does not truly reflect the saccadic system itself due to the pursuit interference (average of four subjects).

because a part of the tracking is performed by the pursuit system. The saccadic system only needs to take care of the rest of it. The pursuit system is substantially a velocity servo. But, through the velocity control the pursuit system physically controls the eye position as well, while position information is basically the only stimulus to the saccadic system. For instance, if the velocity tracking were perfect and there were no position errors initially, the saccadic system would have nothing to do. It will be shown in the following that in the steady state the effective input to the saccadic system is the position error not corrected by the pursuit system.

Figure 5.2-a depicts a highly generalized diagram of the dual-mode tracking system\*, which employs only one assumption: the saccadic system does not interfere with the pursuit system. (The converse of this statement is clearly not true as discussed in the previous paragraph and also as is evident from this diagram.) Robinson (1965) reports that a saccadic movement appeared to produce some discrete change in pursuit velocity. But, as he noted, such a saccadic interference was relatively infrequent in occurrence,\*\* and on this basis the foregoing assumption may be accepted for the present discussion. Also note that possible utilization of position information by the pursuit

---

\* The pursuit system is not shown in feedback form, since there is no intension to discuss its internal structure in this chapter.

\*\* 10% occurrence; see Subsection 2.1.2.

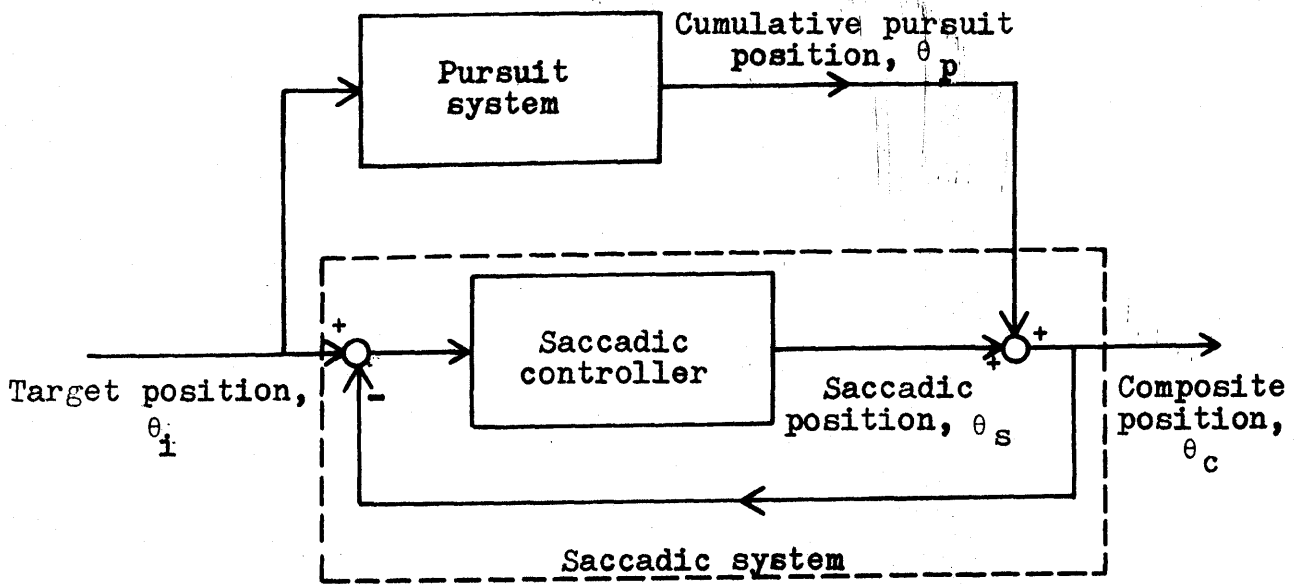


Fig. 5.2-a General organization of visual tracking system.

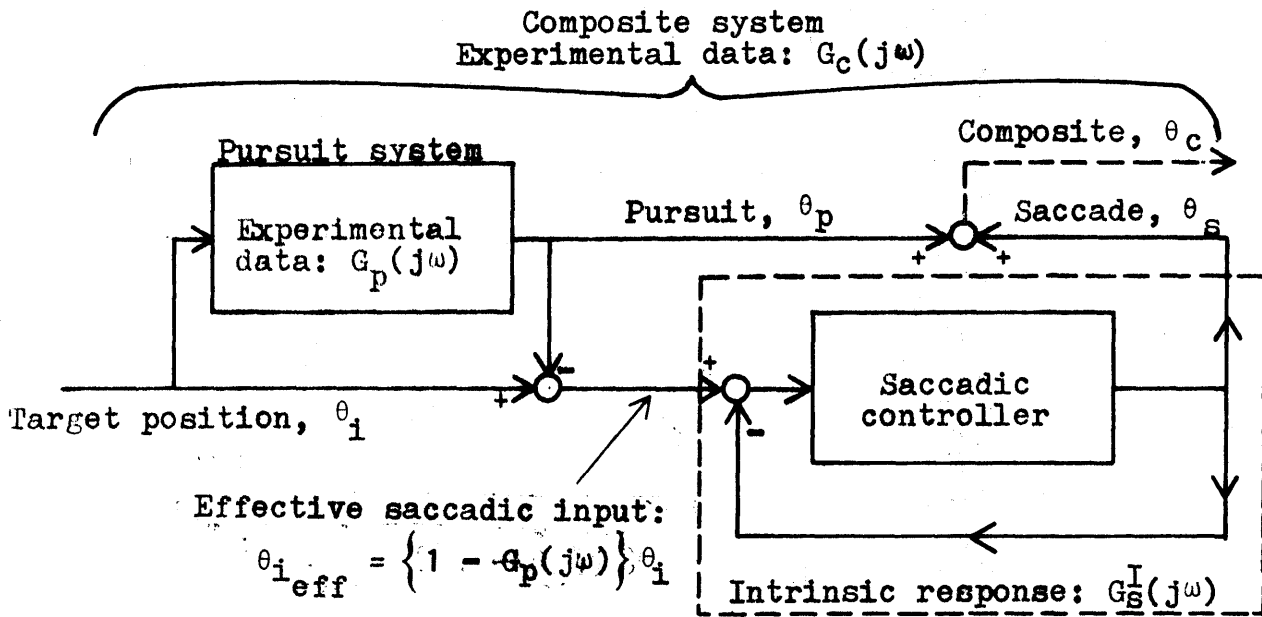


Fig. 5.2-b Decoupled diagram functionally equivalent to Fig. 5.2-a.

Saccadic Frequency response:

- $G_c(j\omega) - G_p(j\omega)$  - - - - - Apparent
- $\{G_c(j\omega) - G_p(j\omega)\} / \{1 - G_p(j\omega)\}$  - - - - - Intrinsic

system, as supported by the finding of Kommerell and Täumer (1971),\* disturbs neither the validity of the above assumption nor the signal flow diagram given in Figure 5.2-a.

The signal flow diagram shown in Figure 5.2-a becomes exactly equivalent to the one shown in Figure 5.2-b. The saccadic system has been decoupled here from the pursuit system. Herewith, the following important point emerges: the input to the saccadic system itself is, in fact, not the original position input,  $\theta_i(j\omega)$ , but is given by:

$$\theta_{i_{\text{eff}}}(j\omega) = \left\{ 1 - G_p(j\omega) \right\} \theta_i(j\omega) \quad (5-3)$$

Clearly, this effective input to the saccadic system,  $\theta_{i_{\text{eff}}}(j\omega)$ , is equal to the position error that should be charged to the pursuit system. Accordingly, the saccadic frequency response, which really characterizes the saccadic system, should be given by:

$$\frac{\theta_s(j\omega)}{\theta_{i_{\text{eff}}}(j\omega)} = \frac{G_s(j\omega)}{1 - G_p(j\omega)} = \frac{G_c(j\omega) - G_p(j\omega)}{1 - G_p(j\omega)} \quad (5-4)$$

The inverse of  $1 - G_p(j\omega)$  in the above equation represents the correction factor accounting for the pursuit interference effect and it is readily computed here. Making this correction upon

---

\* See Subsection 2.1.2

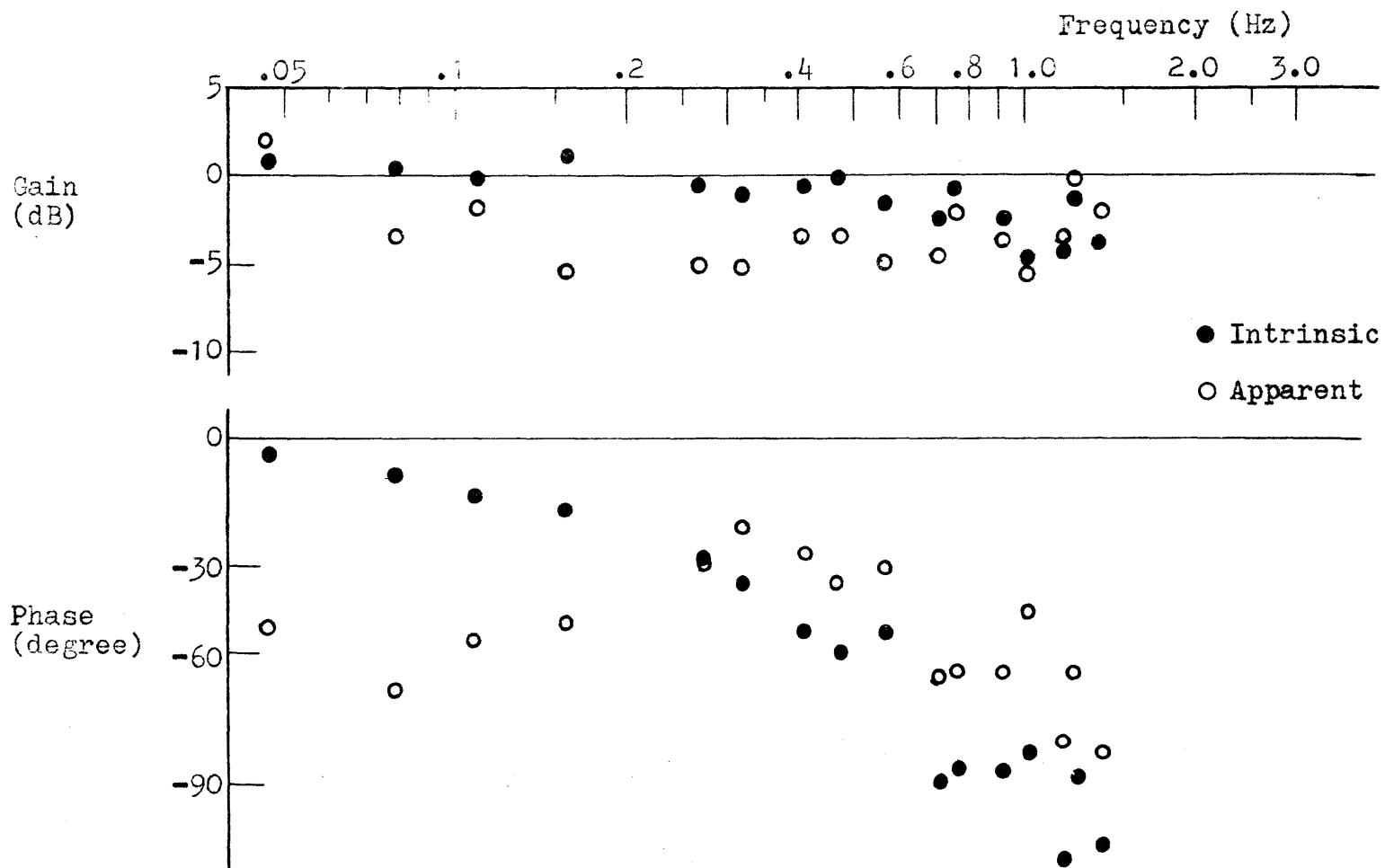


Fig. 5.3 Intrinsic and apparent nonperiodic-input saccadic frequency response results for pseudo-random input B (average of four subjects)

the apparent saccadic frequency response data ( $G_s(j\omega)$ , given in Figure 5.1), the intrinsic saccadic frequency response becomes as indicated by the closed circles in Figure 5.3.

### 5.2.3 Periodic versus Nonperiodic-input Saccadic Phase Behavior

A frequency response which would be obtained directly from the saccadic system acting alone (responding to a target with discontinuous random motion) would correspond to the intrinsic version of the foregoing result, not to the apparent one obtained before.

On the other hand, it may be of interest to compare this intrinsic nonperiodic-input result with a frequency response obtained with periodic square-wave inputs: the difference

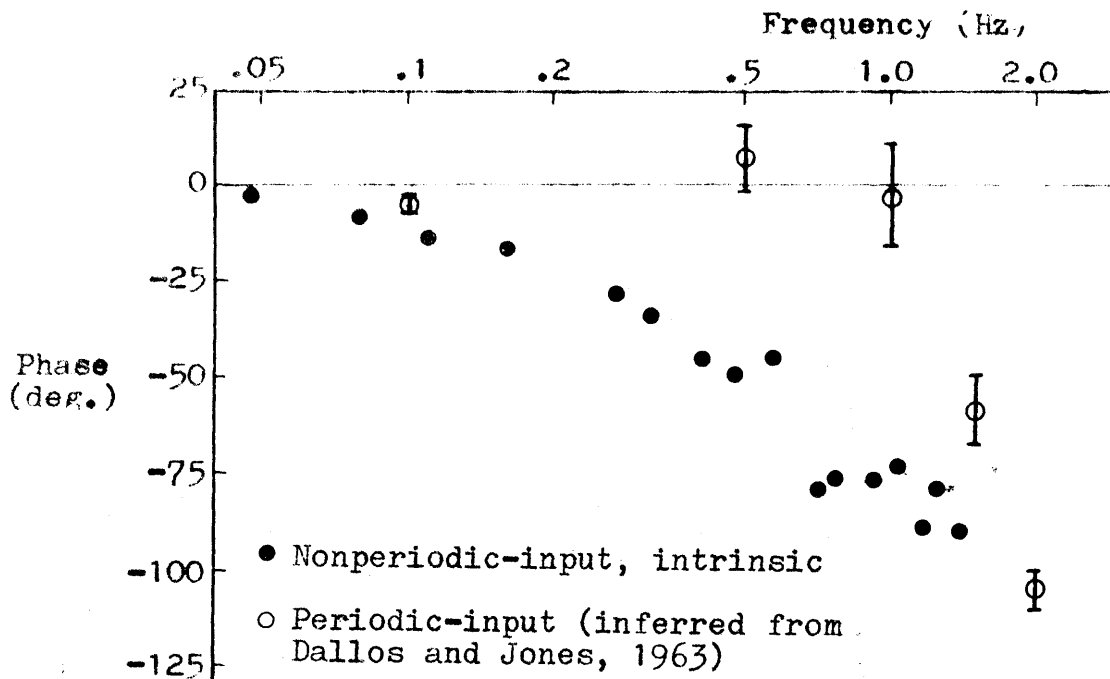


Fig. 5.4 Phase error of saccadic visual tracking

between the two would be a manifestation of the predictive property of the saccadic oculomotor system. Such a comparison was made with respect to phase, as shown in Figure 5.4. The phase versus frequency for the periodic-input case was calculated from the saccadic latency measurement (Figure 2.10) by Dallos and Jones (1963). Figure 5.4 clearly shows a substantial reduction of the saccadic phase error with periodic inputs especially in the mid frequency range, confirming the predictive behavior of the saccadic tracking system in the frequency domain.

### 5.3 Comparison with Young's Sampled-data Model

#### 5.3.1 Model Prediction based on 200 msec Sampling Period

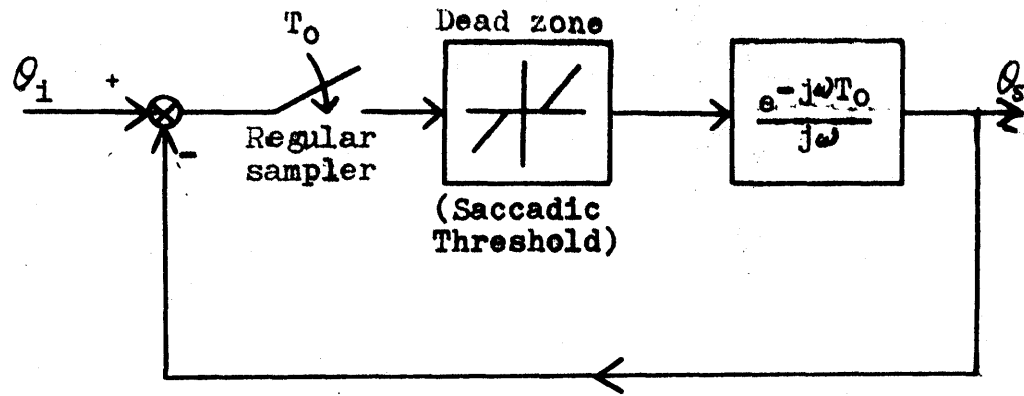
Figure 5.5-a shows the internal organization of the saccadic system when Young's sampled-data model is assumed. It is based on his original version (Young, 1962), which incorporates an input-synchronized deterministic sampler.

In describing the mechanical plant of the oculomotor system, Young assumed Westheimer's second-order model (Westheimer, 1954), but he reasonably neglected it in analyzing his model by considering its transfer characteristics. The diagram shown in Figure 5.5-a could already account for this simplification. However, as described in Subsection 2.1.2, Westheimer's model (which assumed saccades to be the step response of the mechanical plant) has proved to be oversimplified, and new descriptions have been proposed for the mechanical property by several later investigators. Even so, saccades may still be interpreted as the step response of some structure that includes certain neurological units in addition to the mechanical dynamics. In this context, Figure 5.5-a is not meant to ignore the oculomotor plant but implied to omit a specific internal identification of it.

Young assumed 0.2 second for one sampling interval,  $T_0$ , based on the average refractory period for saccadic movements.

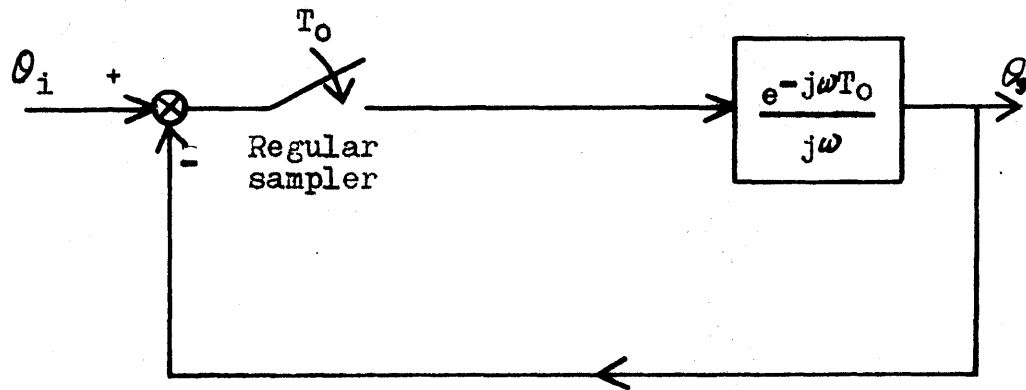


(a)

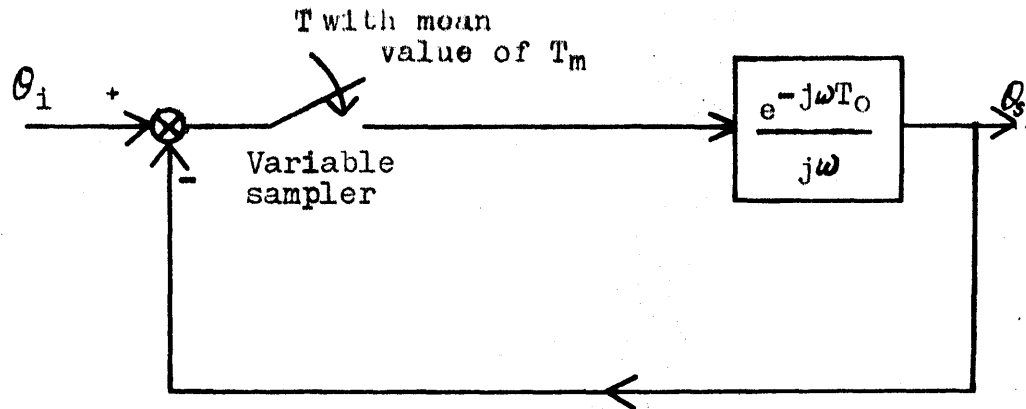


( $T_0 = 0.2$  sec)

(b)



(c)



Figs. 5.5 Versions of sampled-data saccadic visual tracking model ; (a) Young's original configuration, (b) dead zone removed for linear analysis, (c)  $T_0$  replaced by mean intersaccadic interval,  $T_m$ , which turned out much greater than 0.2 sec ( $T_m = 0.51$  sec) for the particular case being studied.

Each error sample impulse is delayed by one reaction time and then integrated to give a step in eye position in order to bring the eye to what had been the desired position one reaction time earlier. This reaction time is assumed to be 0.2 seconds, being equal to  $T_0$ .

Ignoring the saccadic dead zone meanwhile, the linearized system (Figure 5.5-b) was analyzed by Young as follows: first, the model equation can be derived as:\*

$$\theta_s(j\omega) = \frac{e^{-j\omega T_0}(1 - e^{-j\omega T_0})}{j\omega} \theta_i^*(j\omega) \quad (5-5)$$

where  $\theta_i^*(j\omega)$  is obtained first by passing the input signal  $\theta_i$  through an impulse modulator with sampling frequency,  $\omega_0 = 2\pi/T_0$ , and then by performing the Fourier transform upon the modulator output. And it is expressed as:\*\*

$$\theta_i^*(j\omega) = \frac{1}{T_0} \sum_{n=-\infty}^{\infty} \theta_i(j\omega + nj\omega_0) \quad (5-6)$$

$\theta_i^*(j\omega)$  is comprised of an infinite number of side bands ( $n \neq 0$ ), in addition to the fundamental band ( $n = 0$ ) corresponding to the original input spectrum. When the input frequency range exceeds the Nyquist frequency,  $\omega_0/2$ , the

---

\* Actually,  $\theta_i$  is meant to represent the effective input to the saccadic system,  $\theta_{i_{eff}}$ , defined by Equation 5-3. This

abbreviation will be used from now on until distinction between the two becomes necessary again in the next section.

\*\* See, for instance, E.I. Jury "Sampled Data Control Systems", John Wiley and Sons, Inc., New York, N.Y., 1958.

fundamental band becomes overlapped with the neighboring side bands. The result is that the input information is irretrievably lost in the higher overlapped portion ( $\omega_0/2$ ) and contaminated in the lower overlapped portion ( $\omega_0/2$ ) in the sampling process. Presupposing Young's value of 0.2 seconds for the sampling interval,  $T_0$ , without examining the actual eye movement record obtained here, the Nyquist frequency would become 2.5 Hz, which is sufficiently greater than 1.34 Hz, the highest frequency in the input spectrum used (pseudo-random input B). Thus no side band interference would occur and the following reduced version of Equation 5-6 would be valid for the input frequency range:

$$\theta_i(j\omega) = \frac{1}{T_0} \theta_i(j\omega) \quad (5-7)$$

Substitution of this result into Equation 5-5, the theoretical saccadic transfer function,  $G_s^T(j\omega)$ , would be expressed as:

$$\begin{aligned} G_s^T(j\omega) &= \frac{\theta_s(j\omega)}{\theta_i(j\omega)} = \frac{e^{-j\omega T_0} (1 - e^{-j\omega T_0})}{j\omega T_0} \\ &= \frac{\sin \frac{\omega T_0}{2}}{\frac{\omega T_0}{2}} \exp(-j \frac{3\omega T_0}{2}) \end{aligned} \quad (5-8)$$

As shown in Figure 5.6, the Bode plot of this form has led to

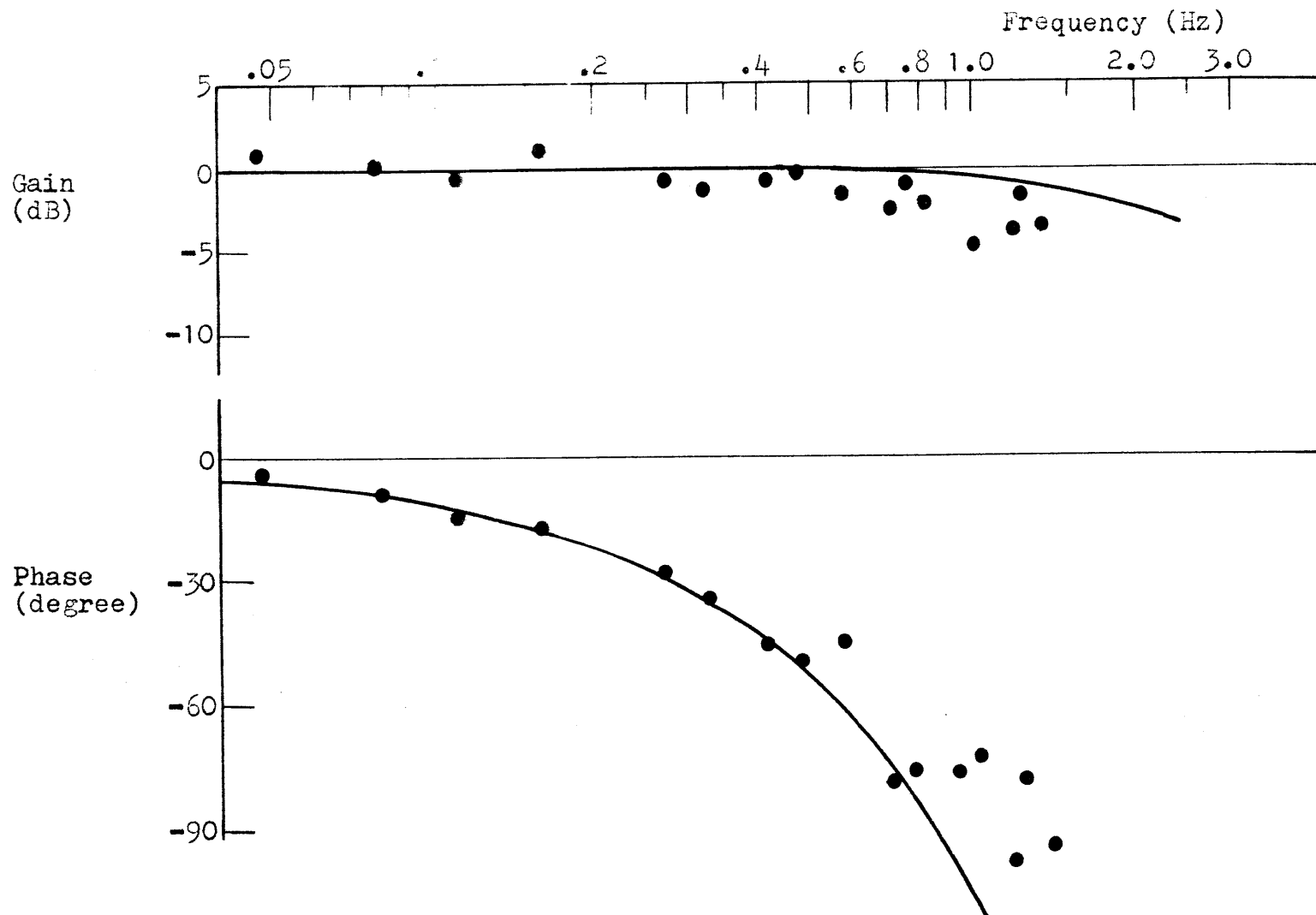


Fig. 5.6 Intrinsic saccadic response result (with input B) as compared with prediction by Young's sampled-data model (saccadic dead zone ignored), where 0.2 sec is presupposed for saccadic interval (see Fig. 5.5-b).

good agreement particularly for phase with the previous experimental result (intrinsic saccadic frequency response), except with some high-frequency data points.

### 5.3.2 Model Prediction based on Estimated Inter-saccadic Period

Next, instead of just assuming 0.2 seconds for the sampling interval, the original eye movement data for the pseudo-random input B were examined for each subject as to the actual time interval,  $T$ , between two successive saccades. Misestimation of the actual saccadic interval was highly improbable: a large gain scale and a fast speed were used for running the recording paper in spotting each saccade to obtain the statistic of saccadic intervals. It was impossible to overlook even the smallest saccades and the shortest inter-saccadic periods in the record.

Figure 5.7 shows the corresponding histograms accumulated for individual subjects (with the eye movement trace lasting for approximately 100 seconds for each) as well as for a composite of all subjects. The composite histogram yields a Poisson-type distribution, indicating that saccadic intervals ranging from 0.2 seconds to 0.3 seconds are most probable to occur. The mean value,  $T_m^*$ , was 0.51 second for the composite subject with

---

\*  $T_m$  is equal to the total running time for four subjects (about  $100 \text{ sec} \times 4$ ) divided by the corresponding total number of saccades. Hence,  $T_m$  is given not simply at the geometric center of the histogram, but at the center of gravity obtained by weighting saccadic intervals according to their length.

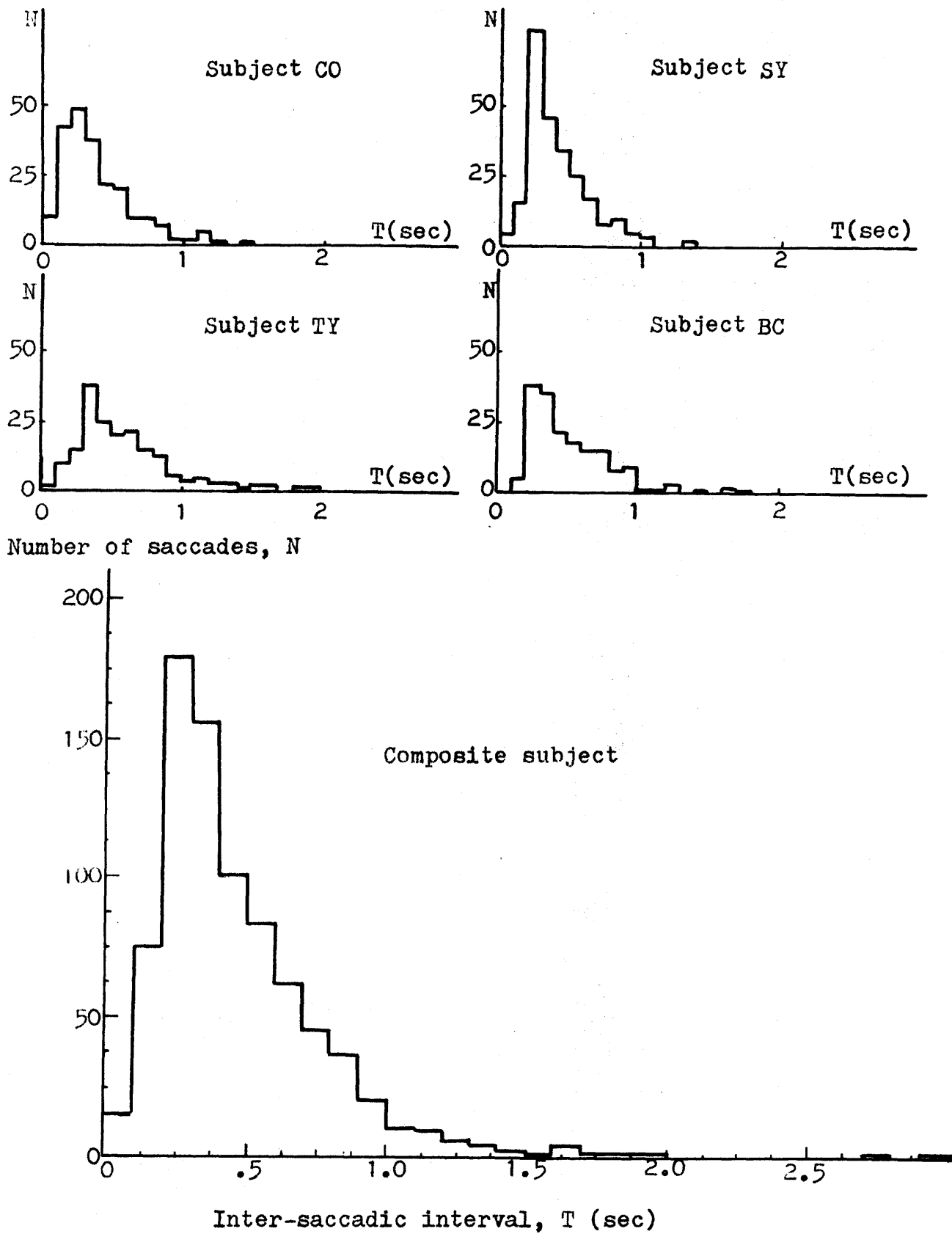


Fig. 5.7 Histograms of inter-saccadic intervals with pseudo-random input B

standard deviation of 0.10 second. This may be adequately consistent with the observation that the characteristic gain peak appeared around 1.2 Hz in the composite response with the present input (Figure 4.13-b). (A square-wave changing state every 0.51 second has the fundamental sinusoid at 0.98 Hz.)

The average inter-saccadic interval,  $T_m$ , obtained here is somewhat large in comparison to Young's estimate of 0.2 second. Possible reasons for this are: [1] Lack of high frequency sinusoids in the pseudo-random input examined, [2] relatively low maximum stimulus velocity for attempted maintenance of the pursuit linearity, [3] relatively large target size ( $0.6^\circ$  in diameter). Presumably any of these tends to reduce the need for corrective saccadic movements. Considering the functional object of the saccadic system, the dead zone presumably corresponds to the foveal region of the retina, whose diameter is approximately  $1^\circ$  in the visual angle. The dead zone of  $\pm 0.5^\circ$  based on this anatomical assessment may be regarded as a comparatively large one, since it operates on the error signal which is normally small.\*

Accordingly, one may argue that the histogram of inter-saccadic interval statistics cannot reflect samples which were below the saccadic threshold and hence resulted in no saccade,

---

\* Based on a simple statistical model combined with experimental data obtained with small step changes in input position, Young (1965) deduced a somewhat smaller value of  $0.25-0.3^\circ$  for the dead-zone amplitude, i.e., saccadic threshold level.

and that the inter-saccadic interval only represents an apparent sampling period. These are all true, and the intrinsic sampling period may well be indeed 200 msec. And, given the observed mean inter-saccadic interval of as large as 0.51 sec, the saccadic threshold effect was probably quite significant in the present oculomotor tracking experiment. However, all of these points are taken into account by the model diagram presented in Figure 5.5-c: A series combination of 0.2 sec-regular sampler and saccadic dead zone (threshold element), which appears in the original model configuration in Figure 5.5-a, can functionally reduce to a single sampler with sampling period of 200 msec plus a certain extra time interval depending on the threshold effect, as shown in Figure 5.5-c. Thus, the inter-saccadic interval should be the systems effective sampling period that is ultimately important in the context of the sampled-data model.

In accordance with the above rationale, the sampled-data model is reevaluated based on the mean saccadic frequency established here. The sampling interval is changed from  $T_0 = 0.2$  sec to  $T_m = 0.51$  sec, but  $T_0 = 0.2$  sec is retained for the reaction delay in this subsection. Figure 5.5-c shows the resultant system\* to be analyzed in the following. The average steady-state

---

\* If the intrinsic sampling is performed regularly, say at every 0.2 sec, the inter-saccadic interval must give some integral multiples of 200 msec, which does not seem to be true. For this reason, Young (1973) now prefers a gate, which opens 200 msec after the last saccade and passes on relevant information as soon as the position error exceeds the threshold. While this gate theory appears more likely the case, distinction between sampler and gate is not essential to the present analysis based on the mean inter-saccadic interval.



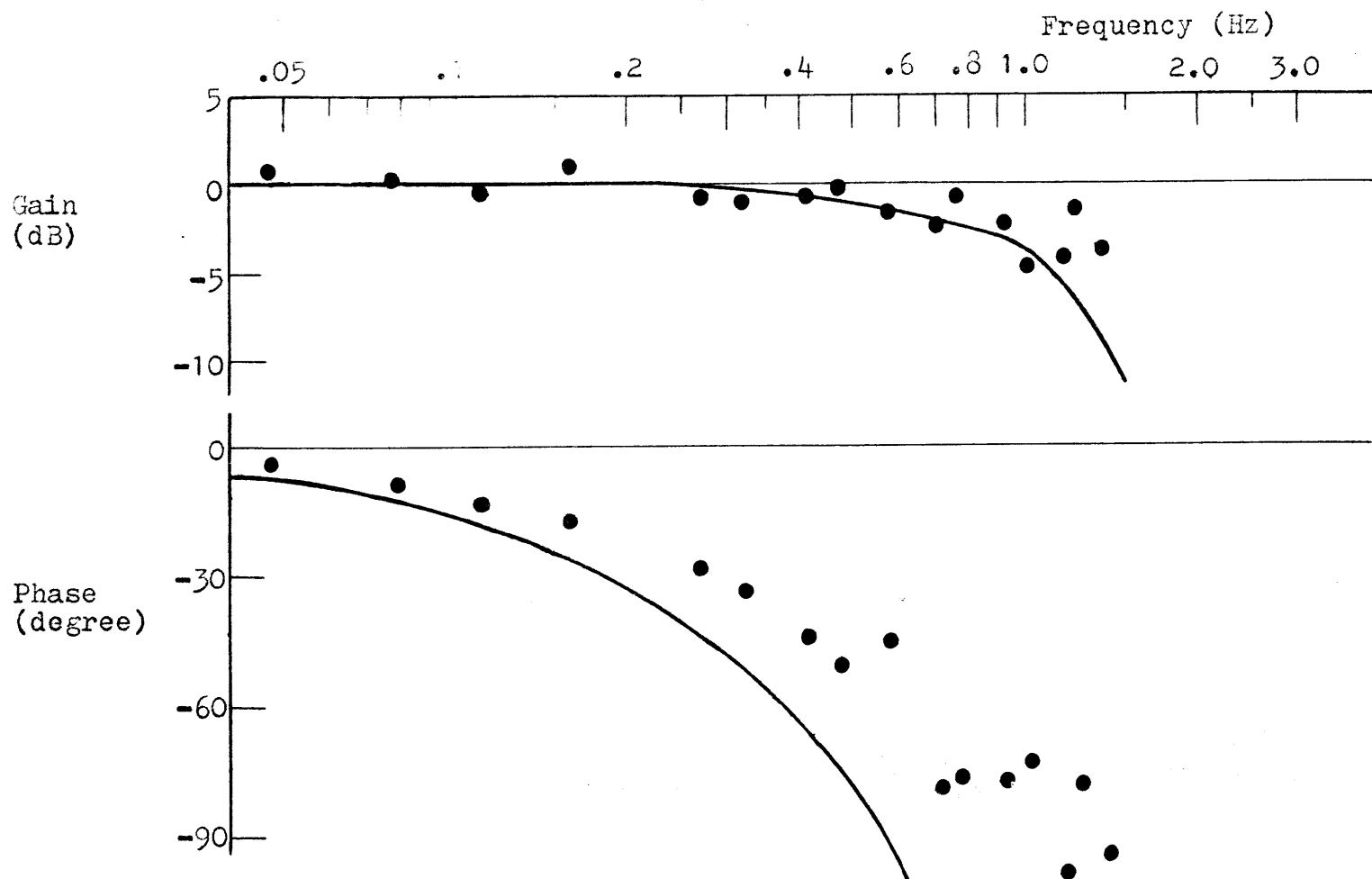


Fig. 5.8 Intrinsic saccadic frequency response result (with input B) and prediction by Young's sampled-data model where the present mean inter-saccadic value of 0.51 sec is used for the effective sampling period (see Fig. 5.5-c).

input-output relation is now given by:

$$\frac{\theta_s(j\omega)}{\theta_i(j\omega)} = \frac{e^{-j\omega T_0} (1 - e^{-j\omega T_m})}{j\omega T_m}$$

$$= \frac{\sin \frac{\omega T_m}{2}}{\frac{\omega T_m}{2}} \exp \left[ -j\omega \left( T_0 + \frac{T_m}{2} \right) \right] \quad (5-9)$$

(Note that this expression reduces to Equation 5-8 by setting  $T_m = T_0$ .)

Figure 5.8 shows the saccadic frequency response evaluated according to this equation with  $T_m = 0.51$  sec and  $T_0 = 0.2$  sec. In comparison with the matching result in the preceding subsection (Figure 5.6), the Bode plot has improved its gain match somewhat at intermediate frequencies, but has lost the previous good phase fit over the entire frequency range.\* This contrast between the two alternative matching attempts leads to a possible suggestion discussed in Subsection 5.3.3.

### 5.3.3 Reduced Latency: A Possible Model Improvement and its Implication

---

\* The sampling frequency now is  $1/5.1 = 1.96$  Hz, so that the Nyquist frequency is  $1.96/2 = 0.98$  Hz. But the highest frequency component in the input B is at 1.34 Hz. Thus, the model prediction applies to frequencies only up to  $0.98 - (1.34 - 0.98) = 0.62$  Hz due to the side-band interference effect discussed previously in Subsection 5.3.1.

Table 5.1 summarizes the foregoing two alternative matching studies attempted between the experimental response result and the prediction based on Young's sampled-data saccadic model.

Equation 5-12 in this table indicates that the gain-frequency relation is independent of the saccadic delay, and determined only by the (effective) sampling period. The improved gain fit by this equation supports the earlier point that the effective sampling period,  $T_m = 0.51$  sec, should be used instead of the presumed intrinsic one,  $T_0 = 0.20$  sec.

Direct use of original model parameters		Value of sampling period revised according to the present data		
Model Diagram: Figure 5.5-b		Model Diagram: Figure 5.5-c		
From Eq. 5-8: $T_0 = 0.20$		From Eq. 5-9: $T_m = 0.51, T_0 = 0.20$		
Result: Fig.5.6		Result: Fig.5.8		
gain	$= \frac{\sin \omega T_0/2}{\omega T_0/2}$ Equation 5-10	Fair	$= \frac{\sin \omega T_m/2}{\omega T_0/2}$ Equation 5-12	Good
Phase (in radian)	$= -\frac{3}{2} T_0 \omega$ Equation 5-11	Good	$= -(T_0 + \frac{T_m}{2}) \omega$ Equation 5-13	Bad

Table 5.1 Two alternative predictions based on Young's sampled-data model and their matching result with the experimental data

As revealed in Eq. 5-13, on the other hand, the phase lag depends on both saccadic delay and sampling period at a given

frequency. And it increases linearly with frequency, and accordingly the proportionality constant,  $T_0 + T_m/2$ , may be considered as the system's effective delay time. The phase equation, Eq. 5-11, is only a reduced form of Eq. 5-13 resulting from the assumption,  $T_m = T_0$  (= 200 msec). Despite the recognition that this assumption is inappropriate for the eye movement data obtained in this research, it has led to the good model prediction for phase, i.e., Eq. 5-11, which is given numerically by:

$$- \frac{1}{2} \times 3 \times 0.2 \times \omega = - 0.3\omega \quad (5-14)$$

By contrast, the phase equation, Eq. 5-13, reflects the observation,  $T_m = 0.51 \text{ sec} \neq 0.20 \text{ sec}$  and yields:

$$- (0.20 + \frac{1}{2} \times 0.51)\omega = -0.46 \omega \quad (5-15)$$

This is too large a lag to fit the phase data, as shown in Figure 5.8.

Given that  $T_m = 0.51 \text{ sec}$  and Eq. 5-13 have both been established, the above seemingly paradoxical conflict of the phase matching could be resolved by introducing the hypothesis that the saccadic reaction delay can be made smaller than 200 msec even during the nonperiodic-input tracking mode.

200 msec is a widely accepted value for the saccadic delay as assumed in Young's original model. This value is

obtained for the average saccadic latency observed in response to a sudden target displacement for which no prediction is possible.\* Prediction of the future target motion depends on information of the past changes of the stimulus status. And it is maximally effective with periodic inputs, where significant latency reduction in the saccadic response has been shown in the literature (Stark et al, 1962; Dallos and Jones, 1963). Therefore, if this latency decrease is due to prediction, its value even with a random input might well become smaller than, at least, the worst-case value of 200 msec, by a factor presumably dependent on the frequency spectrum of the given input.

This possibility would reduce the phase lag contributed by the saccadic delay, and thus could cut the excess over-all phase lag (computed by Eq. 5-15). Redesignating the saccadic delay by  $T_d$  which is no longer necessarily equal to  $T_0 = 200$  msec (see Figure 5.9), Eq. 5-13 becomes:

$$-(T_d + T_m/2)\omega = -(T_d + 0.51/2)\omega \quad (5-16)$$

If one chooses  $T_d = 45$  msec here, the phase lag becomes:

---

\* Some authors prefer a value somewhat less than 200 msec for the innate saccadic delay, however. Actually, Young et al assumed 150 msec in their revised sampled-data saccadic model. Also, Becker (1971), for instance, notes that the first corrective saccade usually occurs with latency of about 130 msec for  $3^\circ - 8^\circ$  step inputs though the average value approaches close to 200 msec for smaller steps.

$$-(0.45 + \frac{1}{2} \times 0.51)\omega = -0.3\omega \quad (5-17)$$

This expression is exactly the same as Eq. 5-14 which excellently matches the phase data as demonstrated in Figure 5.6.

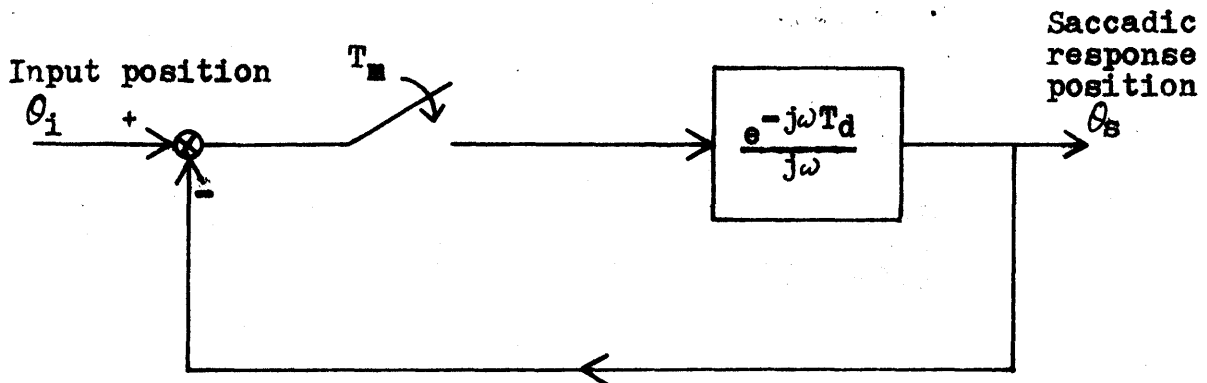


Fig. 5.9 Sampled-data saccadic visual tracking model with parameters modified from Young's original values:  $T_m$ ; mean inter-saccadic interval as effective sampling period, and  $T_d$ ; saccadic reaction delay. ( $T_m=510\text{msec}$  and  $T_d=45\text{msec}$  for pseudo-random input B).

Hence, as shown in Figure 5.10, the new model prediction gives a good agreement with the experimental data in both gain and phase, for it takes over good selective portions of the previous model predictions, i.e., gain from Figure 5.8 and phase from Figure 5.6.\*

The preceding result is based on the hypothesis that the saccadic reaction time was only 45 msec with the present pseudo-random stimulation to the saccadic system. Such a large decrease from 200 msec is known to occur but with

---

\* As footnoted previously, the model prediction is expected to be valid up to 0.62 Hz.

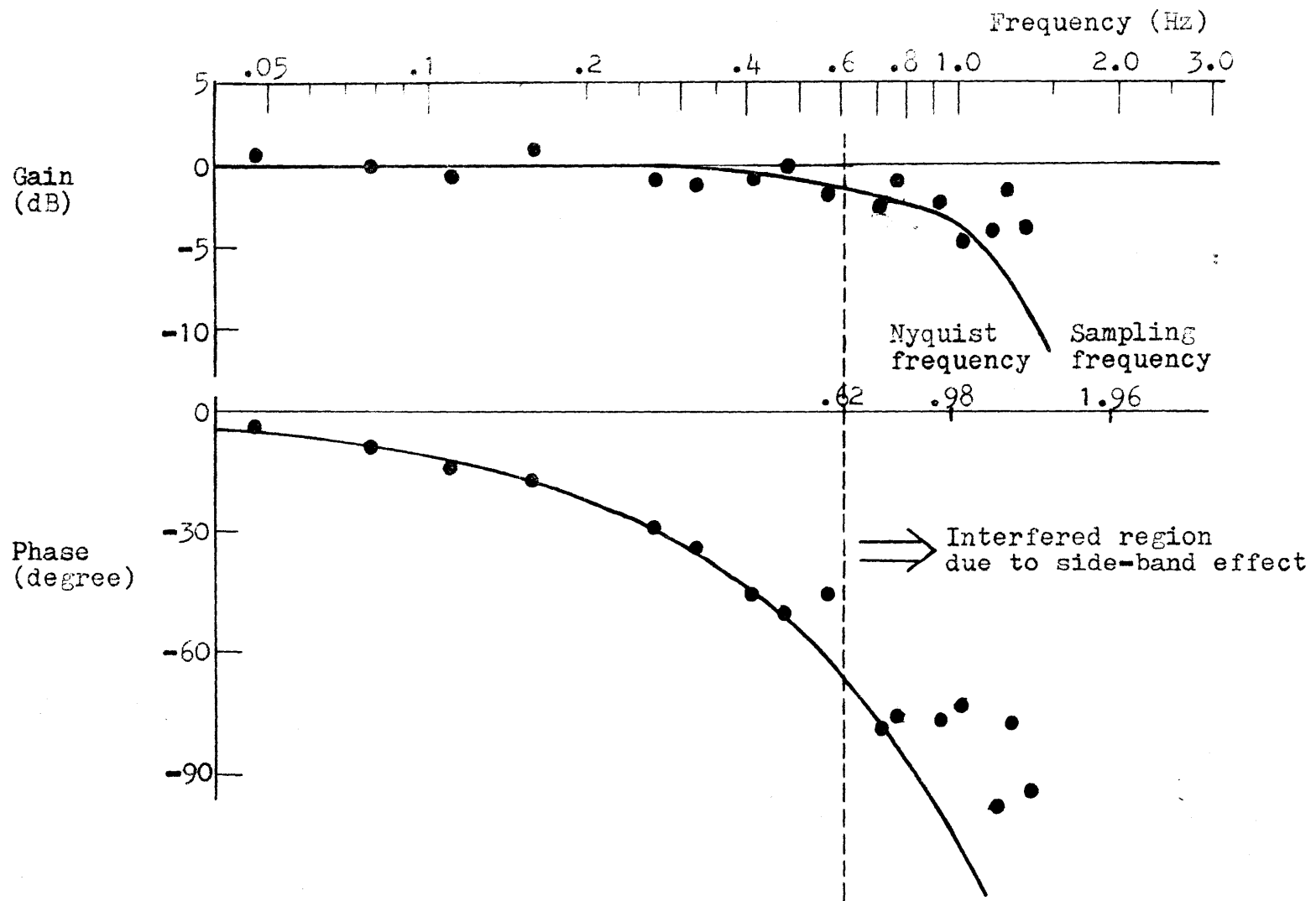


Fig. 5.10 Intrinsic saccadic frequency response result (with input B) and corresponding theoretical prediction by Young's sampled-data model with modified parameter vales,  $T_m=510\text{msec}$  and  $T_d=45\text{msec}$  (see Fig. 5.9 and text).

periodic square-wave inputs at some moderate repetition rates, presumably through predictive capability of the saccadic oculomotor system as discussed in Subsection 2.4.2 (Stark et al, 1962; Dallos and Jones, 1963). According to the result by Dallos and Jones (Figure 2.8), the saccadic latency likely becomes 45 msec somewhere near repetition rate of 1 Hz. In the case of periodic square-wave stimulation, saccades must be spaced virtually evenly. And, if the repetition rate is 1 Hz, the inter-saccadic interval must be 500 msec. This value for the inter-saccadic interval turns out to be almost the same as 510 msec, the mean intersaccadic interval obtained in this chapter by presenting the pseudo-random input B.

Before trying to interpret this consequence, one should insure that this is not a simple coincidence. To this end, the relevant steps up to this point have been repeated analogously with respect to the eye movement data obtained with another pattern of pseudo-random target motion corresponding to input C.

The resultant data points for the intrinsic saccadic frequency response are presented in Figure 5.11. The mean inter-saccadic interval averaged over four subjects with input C was 0.80 sec\* with one standard deviation of 0.22 sec. Aside from the rather poor gain fit resulting from Equation 5-12 with  $T_m$

---

\* Thus, the Nyquist frequency becomes 0.63 Hz, whereas input C contains frequency components up to 0.70 Hz. Hence, the model plot applies to the frequency range below  $0.63 - (0.70 - 0.63) = 0.56$  Hz.



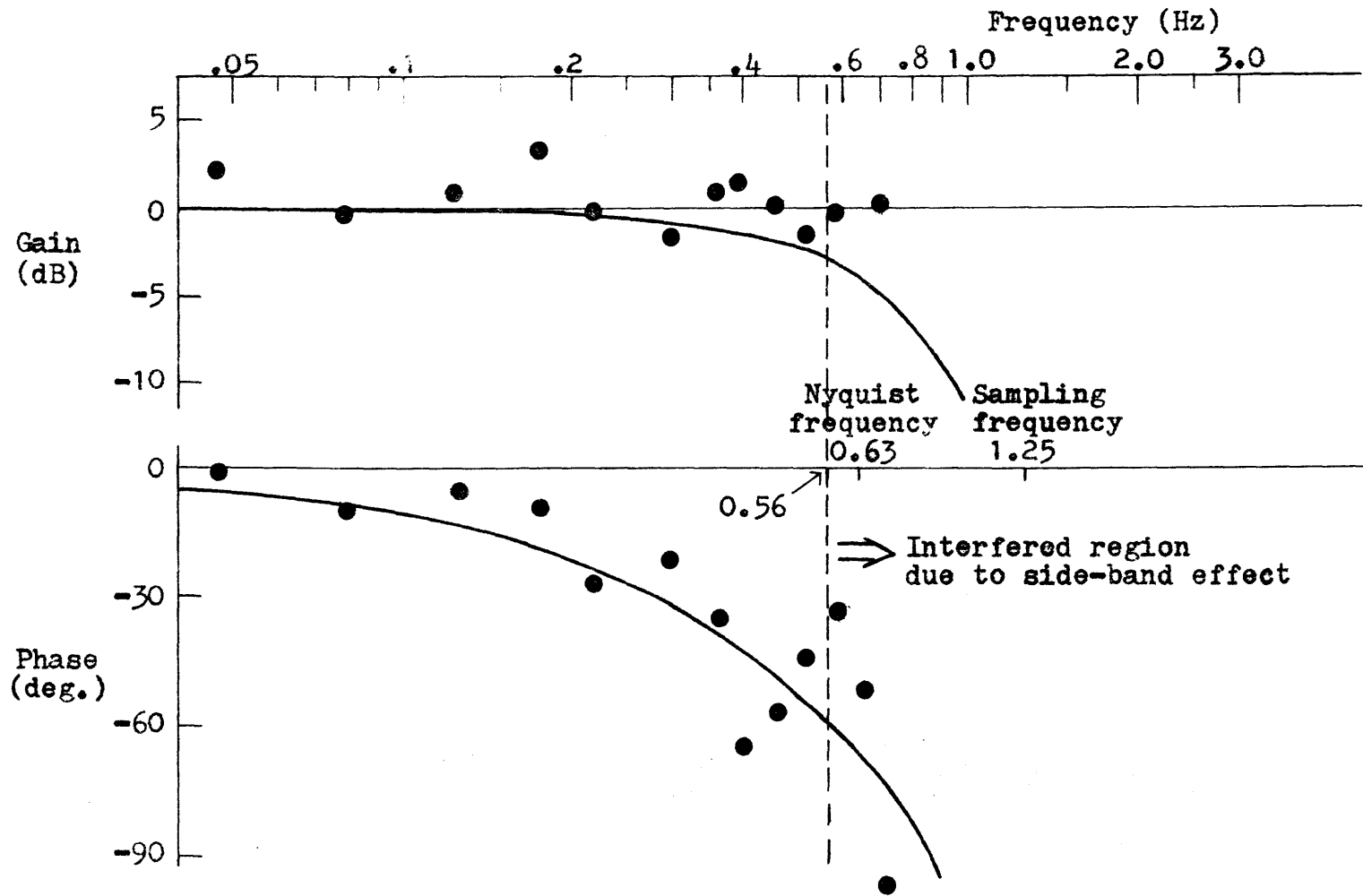


Fig. 5.11 Intrinsic saccadic frequency response result (with input C) and corresponding theoretical prediction by Young's sampled-data model with modified parameter values,  $T_m=800\text{msec}$  and  $T_d=-100\text{msec}$  (see Fig. 5.9 and text).

= 0.80 sec, the same phase prediction,  $-0.3\omega$ , as in the previous case for input B appears to describe the general trend of the present phase data points that suffer from a somewhat greater scattering than before. Given  $T_m = 0.80$  sec, this may imply the relation analogous to Equation 5-17:

$$-(T_d + \frac{1}{2} \times 0.80)\omega = -0.30\omega \quad (5-18)$$

Hence, one obtains  $T_d = -0.10$  sec, which means a negative latency. As shown in Figure 2.10, a negative saccadic latency was actually found by Dallos and Jones for a periodic square-wave input with repetition rate of 0.5 Hz. Their value tends to be somewhat greater than  $-0.10$  sec ( $-0.04$  mean  $\pm 0.50$  S.D.). But, the essential point is that repetition rate at 0.5 Hz corresponds to  $1/(2 \times 0.5) = 1.0$  sec for the inter-saccadic interval and that this value is not very far from  $T_m = 0.80$  sec for the mean inter-saccadic interval obtained under pseudo-random stimulation with input C. Thus, this situation is basically similar to the previous case with input B, and the following view is suggested.

In the case of periodic square wave inputs, on the one hand, the previous authors have shown that the saccadic latency decreases from 200 msec, depending upon stimulus repetition rate whose value equals one-half value of the corresponding regular sampling frequency of the saccadic response. On the

other hand, the foregoing results appear to indicate that a similar reduction phenomenon applies for the saccadic delay in the pseudo-random as a function of mean sampling frequency, i.e.,  $1/T_m$ .

Accordingly, if one considers the mean sampling frequency (or its half value), the reduction of saccadic delay could be described by a diagram such as the one shown in Figure 2.10, for not only periodic but also nonperiodic inputs. Thus, it might be said that the presumed predictive mechanism underlying the saccadic oculomotor system operates even with nonperiodic inputs in helping to compensate for the innate delay of 200 msec.

From the nonperiodic-input case, it may appear, on the surface, that the saccadic prediction is based upon the mean saccadic sampling frequency which is actually a parameter characterizing the system response rather than the input stimulus per se. This might suggest that the phenomenon of saccadic latency reduction is due to some "resonance effect"\* within the motor part of the oculomotor system.

However, the mean sampling frequency is apparently a function of over-all frequency spectrum feature of the given effective input to the saccadic system. This recognition leads to a second thought that the reduced saccadic delay is a

---

\* Dallos and Jones themselves suggest "resonance" for describing their characteristic v-shaped plot obtained for latency versus repetition rate. Note that a similar result has been reported by Stark et al (1962).

manifestation of the underlying predictive mechanism operating on some average basis of a given input frequency spectrum, as similar to the predictive scheme suggested for the pursuit tracking in the previous chapter.

Finally, it may be of some interest to add the following note. Thus far, the saccadic phase lag has been predicted by the effective delay,  $-(T_d + T_m/2)\omega$ , according to Equation 5-13. The previous two sets of phase data (corresponding to pseudo-random input B and C) have been both fitted approximately by the curve,  $-0.3\omega$ . It seems as though  $T_d$  adjusts itself in accordance with a given value of  $T_m$ , in order that the effective delay,  $T_d + T_m/2$  preserves its value of 300 msec as obtained by  $T_m = T_d = T_0 = 200$  msec assumed in Young's original model.

Although such a relation is extrapolated from the limited observation allowing only two check points, i.e. (45 msec and 510 msec) and (-100 msec, 800 msec) for ( $T_d$  and  $T_m$ ), this is graphically shown in Figure 5.12, predicting a monotonic increase of the saccadic reaction time with decreasing intersaccadic interval (or with increasing sampling rate) as qualitatively consistent with the higher-frequency segment of the V-shaped saccadic latency plot obtained by Dallos and Jones with periodic square-wave inputs.\*

---

\* The lower-frequency segment of the V-shaped plot represents data for the "forced saccadic tracking" of low-frequency periodic square-wave inputs. In tracking a reasonably random input, however, the corresponding mean sampling frequency is presumably unlikely to fall in that low frequency region.

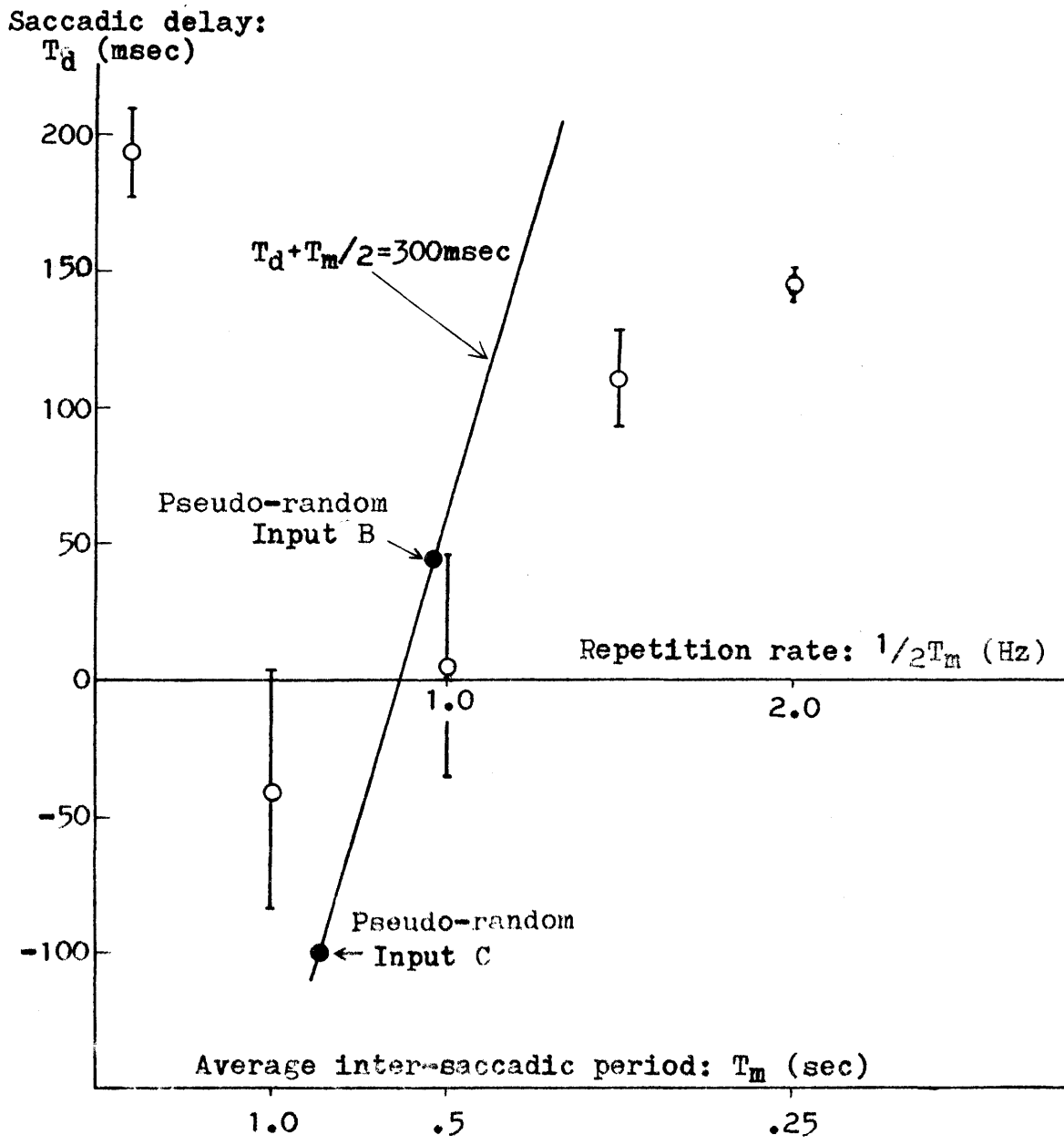


Fig. 5.12 Reaction time delay of saccadic tracking eye movement: Results deduced in this chapter based on pseudo-random stimulation (closed circles) and data by Dallos and Jones (1963) for periodic square-wave inputs (open circles).

#### 5.4 Consistency of Experimental Results in Chapter IV

Upon introduction of some numerical changes in Young's original model parameters, a relatively good reconciliation has been attained between experiment and theory as to the nonperiodic-input saccadic frequency response. But the experimental part here has been inferred from the composite and pursuit results established in Chapter IV. Hence, the above agreement appears to suggest validity of these original experimental data including the unexpected phase behavior of the pursuit system. The present section examines this point further, particularly in regard to the large low-frequency phase lead found in the preceding chapter with pseudo-random inputs.

The sampled-data model is presupposed here for the saccadic system, rather than as an object of investigation. Given its theoretical result in addition to the available data for the composite response, prediction on the pursuit frequency response must be possible. The transfer function,  $G_s^T(j\omega)$ , given by Equation 5-9, describes the sampled-data model that is shown in Figure 5.5-c. The over-all configuration of the system becomes as shown in Figure 5.13, stemming from the signal-flow diagram in Figure 5.2-b. Immediately, from this, the following equation can be derived for an input with spectrum lying below the

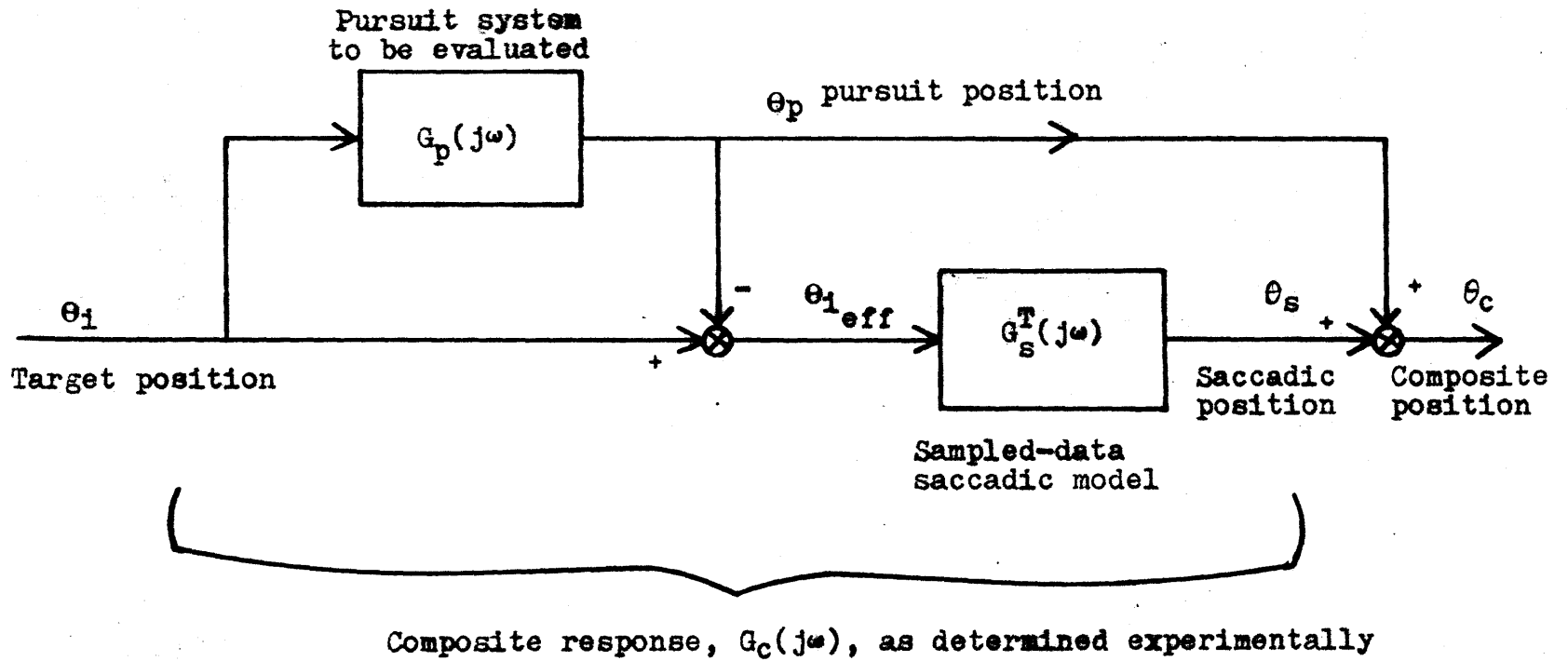


Fig. 5.13 Evaluation of pursuit response characteristics from combination of experimental data,  $G_c(j\omega)$  and theoretical prediction,  $G_s^T(j\omega)$ , i.e.,

$$G_p(j\omega) = G_c(j\omega) - G_s(j\omega) / 1 - G_s(j\omega)$$

Nyquist frequency:

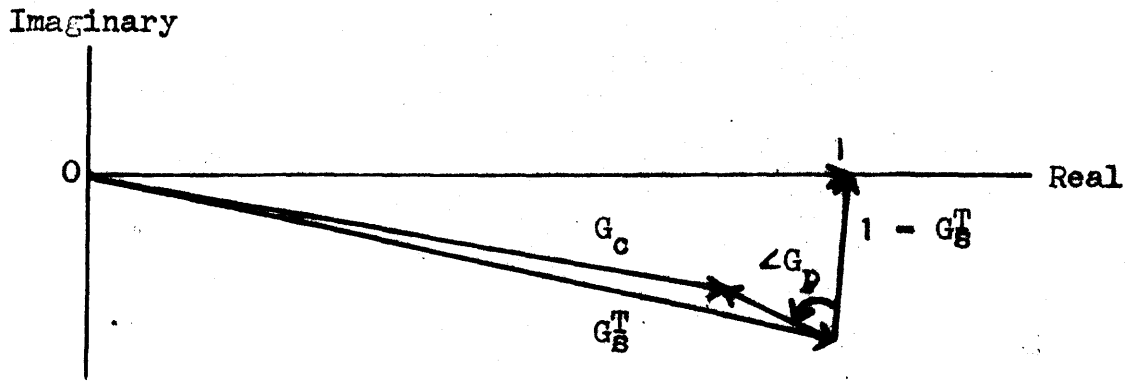
$$\begin{aligned}\theta_c(j\omega) &= \theta_p(j\omega) + \theta_s(j\omega) \\ &= G_p(j\omega)\theta_i(j\omega) + G_s^T(j\omega)\{1 - G_p(j\omega)\}\theta_i(j\omega)\end{aligned}\quad (5-19)$$

Hence, the pursuit response,  $G_p(j\omega)$ , can be expressed in terms of  $G_s^T(j\omega)$  and the composite response data,  $G_c(j\omega)$ :

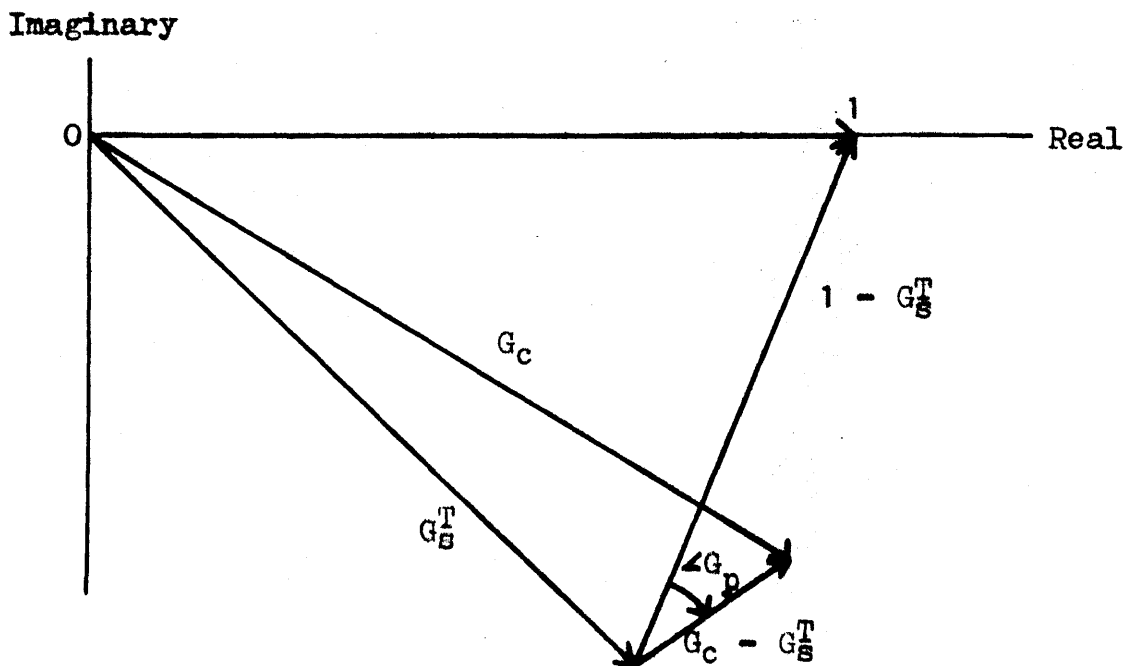
$$G_p(j\omega) = \frac{G_c(j\omega) - G_s^T(j\omega)}{1 - G_s^T(j\omega)} \quad (5-20)$$

By drawing complex vectors,  $G_c(j\omega) - G_s^T(j\omega)$  and  $1 - G_s^T(j\omega)$ , phase behavior of the pursuit system can be examined for the case with pseudo-random input B as an example. Theoretical plot for  $G_s^T(j\omega)$  and data points for  $G_c(j\omega)$  with input B are available in Figure 5.10 and Figure 4.13-b respectively. Figures 5.14 present two typical complex vector diagrams (data for  $G_c(j\omega)$  are based on median values). As illustrated in Figure 5.14-a (corresponding to 0.11 Hz), at a low frequency  $G_s^T(j\omega)$  and  $G_c(j\omega)$  both produce about the same small phase lag, while  $G_s^T(j\omega)$  maintains virtually a unit gain. In this case, even a slight gain attenuation in  $G_c(j\omega)$  can cause as large as nearly 90° phase advancement in  $G_p(j\omega)$ . As frequency increases, phase lag becomes somewhat greater for  $G_s^T(j\omega)$  than for  $G_c(j\omega)$ , while gain remains about at unity for both. The result is phase





(a) 0.11 Hz



(b) 0.41 Hz

Figs. 5.14 Complex vector diagrams for evaluating pursuit phase,  $G_p(j\omega)$ , with pseudo-random input B, on the basis of relevant composite data,  $G_C(j\omega)$  and sampled-data model's prediction,  $G_S^T(j\omega)$ , for the saccadic system : Relation,  $G_p(j\omega) = G_C(j\omega) - G_S^T(j\omega) / 1 - G_S^T(j\omega)$  holds. Upper diagram supports validity of large pursuit phase obtained by MITNYS-FFT in Chapter IV.

lag instead of phase lead (see Figure 5.14-b).

Under the premise of the sampled-data saccadic model with appropriate parameter values, these observations give another confirmation on the pursuit phase characteristics obtained experimentally in the previous chapter. In this evaluation,  $G_p(j\omega)$  has been deduced by using information concerning  $G_c(j\omega)$  as well as  $G_s^T(j\omega)$ . In the real system, however,  $G_c(j\omega)$  results subordinately from a combined consequence of  $G_p(j\omega)$  and  $G_s^T(j\omega)$ . In this context, the work in this section is meant to indicate the internal consistency of the experimental results rather than to offer an explanation for the pursuit phase behavior observed in Chapter IV. The special aspect of the pursuit phase result presumably originates in the pursuit system's own independent mechanism, which might be described, for instance, by the theory developed in that chapter.

## 5.5 Summary and Conclusions

Composite and pursuit results obtained experimentally in Chapter IV have permitted an indirect evaluation of saccadic frequency response characteristics for the nonperiodic-input tracking mode.

Straightforward vectorial difference between these two previous results gives an "apparent" saccadic frequency response, which describes saccadic movements in response to the stimulus given to the over-all dual-mode tracking system. The effective input to the saccadic system, however, is not this original stimulus, but position errors not corrected by the pursuit tracking. With further use of the pursuit data, the apparent saccadic frequency response was then corrected by taking the above point into account. The result represents the frequency response of the saccadic system itself.

The "Intrinsic" saccadic response presumably corresponds to what would be obtained if the saccadic system were acting alone in response to a random pattern of discontinuous input. The saccadic system's predictive capacity was confirmed by phase comparison between this nonperiodic-input result and the periodic-input phase plot inferred from the saccadic latency measurement performed by Dallos and Jones (1963) with periodic square-wave inputs.

Next, the intrinsic frequency response data were examined closely in the framework of Young's sampled-data model for the saccadic oculomotor tracking system (Young, 1962; Young and Stark, 1963). A good agreement was obtained between the present experimental data and the sampled-data model but under the following numerical changes of original model parameters: Young assumed 200 msec for both sampling period and saccadic delay in his original model. However, for the two sets of particular eye movement data obtained in this thesis with different input band characteristics, the estimated mean effective sampling period (averaged over four subjects) was 510 msec and 800 msec, both considerably large as compared with 200 msec. Given these values, the saccadic delay must assume substantially reduced values of 45 msec and -100 msec respectively in order for the model to match the Bode plot data. With periodic square-wave inputs, on the other hand, Dallos and Jones obtained the reduced saccadic latency of similar respective values for the stimulus repetition interval of  $2 \times 510$  msec and  $2 \times 800$  msec. This coincidence might suggest that the saccadic system's predictive mechanism can reduce the innate system delay even under random stimulation based on a certain average sampling behavior, which in turn reflects some average frequency band characteristics of the given input. Hence, this averaging behavior hypothesized for the saccadic oculomotor prediction is similar to a part of the interpretation given in the previous

chapter for the pursuit phase result.

Finally, the reconcilliation between experiment and model for the intrinsic saccadic frequency response, in turn, supports the internal consistency of the nonperiodic-input composite and pursuit frequency response (including the large low-frequency pursuit phase lead) that have been established experimentally in Chapter IV: Assuming Young's sampled-data saccadic model with the aforementioned parameter values, the special low-frequency behavior of the pursuit phase result was reconfirmed deductively, from close examination of the composite response data as well as, at the same time, from theoretical prediction by the model.

## Chapter VI

### Dynamical Study of Optokinetic Nystagmus Slow Phase

The slow phase component of optokinetic nystagmus ("stare type") is investigated in both the time and frequency domain.

Generation and display of the OKN stimulus pattern were accomplished by a computer graphical method, which allowed fast and accurate control of the stimulus motion. The desired frequency response data were obtained through the "MITNYS-FFT" procedure employed as in the earlier chapters.

Comparison with the other two types of smooth eye movement, smooth pursuit and vestibular nystagmus slow phase, was stressed, particularly in terms of the frequency response in assessing possible oculomotor predictive behavior.

#### 6.1 Introduction

##### 6.1.1 Background

##### 6.1.2 Objectives

#### 6.2 Experimental Protocol

##### 6.2.1 Apparatus

##### 6.2.2 Procedure

##### 6.2.3 Data Analysis

#### 6.3 Results and Discussions

##### 6.3.1 Transient Behavior, Latency and Linearity

##### 6.3.2 Slow Phase Frequency Response: Periodic-inputs

##### 6.3.3 Slow Phase Frequency Response: Nonperiodic-inputs

#### 6.4 Summary and Conclusions

## 6.1 Introduction

### 6.1.1 Background\*

The natural environment is rich in moving objects such as running animals and flying birds. While these relatively small and specific objects are the potential stimulus sources of the visual tracking behavior (as characterized by saccadic and pursuit movements), a motion of large visual surroundings, as required to elicit optokinetic nystagmus (OKN) in the laboratory, is unlikely to occur naturally unless it is caused by the animal's own head movement. A head movement, on the other hand, induces vestibular nystagmus, independently from vision, through stimulation of the mechanical receptor, the vestibular organ.

Accordingly, on one hand, there is a kinship between these optokinetic and vestibular oculomotor phenomena in terms of the presumed common behavioral end, that is, stabilization of the external visual world on the retina, compensating for head movements arising from the animal's daily activities. On the other hand, one can cite various similarities between OKN slow phase and pursuit response features (Grüttner, 1939; Merrill and Stark, 1963b; Collewijn, in rabbit, 1969, 1972) ; such as

- (1) Selective sensitivity to velocity stimuli
- (2) Range of latency (100 - 200 msec)
- (3) Rapid build-up of response velocity in matching a velocity-step input.

---

\* Basic aspects of OKN have been outlined in Section 2.2. This chapter deals with the "stare" type OKN rather than the "look" type.

This behavioral evidence might suggest that OKN slow phase and pursuit movements are controlled by some common central mechanisms.

### 6.1.2 Objectives

The foregoing viewpoints have motivated further study on the dynamical characteristics of OKN slow phase not only in the time domain but also in the frequency domain.

Time domain approach deals with the velocity-step response, incorporating measurement and examination upon the steady-state linearity between eye and stimulus velocities, system latency and the general features of transient behavior. In order to allow accurate evaluation of the relevant transient phenomena, it is desirable to achieve fast control of the stimulus motion.

Frequency response measurement aims at the question of predictive behavior in the OKN slow phase response. To this end, emphasis lies in the assessment of OKN slow phase characteristics in the frequency domain for both periodic and nonperiodic motions of the OKN stimulus pattern.

Instantaneous speed of the stimulus motion during each periodic or nonperiodic run ought to be always within the linearity range as will be ascertained by the preceding constant-velocity steady-state measurement. The same group of pseudo-random signals as employed in Chapter IV are to be used, in order to permit the subsequent frequency response comparison with the previous pursuit result characterized by the large low-frequency phase lead.

In addition, considering the functional intimacy between OKN and vestibular nystagmus, it would also be interesting to



compare, in the present context, these two oculomotor behaviors which are both reflexive in nature but mediated by different stimulus modalities, visual and vestibular. (Vestibular nystagmus slow phase was already investigated in Chapter III with regard to the possibility of predictive behavior, and the result appeared to be negative.)

Finally, much of the data in this chapter is useful also in the next chapter.

## 6.2 Experimental Protocol

### 6.2.1 Apparatus

The experimental arrangement in this chapter was analogous in many ways to that designed in Chapter IV for study on the smooth pursuit system. In particular, the present hardware features were exactly the same as described previously in Subsection 4.2.2.

The major difference was due to the special aspect of the stimulus required for OKN : The stripe-pattern was presented in place of the previous single spot of target. Generation of this visual pattern was accomplished on the basis of a computer graphic display technique described in Appendix E.

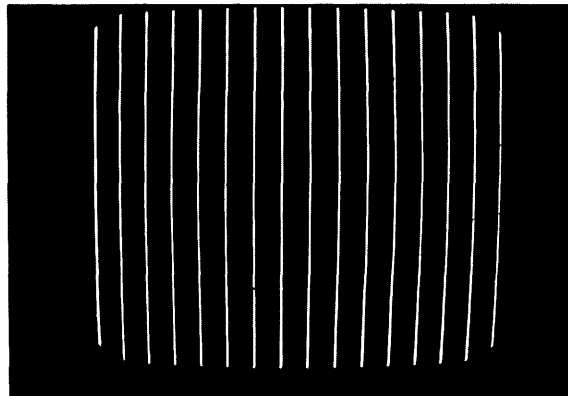


Fig. 6.1 Computer-graphic OKN stimulus pattern displayed on CRT scope.

Fig. 6.1 shows the stimulus pattern thus prepared on the CRT console which was then projected onto a white screen through an optical system for presentation to the subject. This magnified version of the stimulus pattern covered a substantial portion of subject's visual field, extending horizontally to  $+45^\circ$ , and vertically to  $34^\circ$  upward and  $15^\circ$  downward. (The experimental setup is the same as viewed in Figs. 4.1) As a result, separation of two adjacent stripes became  $6^\circ$ . Optical aberration associated with the projection lens caused each vertical stripe to appear about  $0.6^\circ$  wide.

The present computer-generated OKN stimulus pattern is characterized by its extremely rapid response to a motion command, which might be contrasted with the mechanically-controlled stimulus motion by a conventional rotating drum arrangement.\* For instance, there was virtually no delay time nor was there any rise time in the stimulus motion in response to a velocity-step command\*\*. Realization of such a true velocity-step stimulus is obviously advantageous for a reliable evaluation of OKN transient behavior.

---

\* Another aspect of the present method lies in its flexibility in modifying the stimulus pattern in many desired ways. For instance, Chapter VII will attempt to study OKN by selective stimulation to the peripheral retina, by blanking the portion of the stimulus field (corresponding to the central vision) as determined by up-dated eye position signal from the eye movement monitor.

\*\* Actual time delay was only  $20 \mu$  sec, due to the computer processing.

### 6.2.2 Procedure

Throughout the experiment, binocular vision was allowed, but only horizontal movement of the right eye was monitored.

Special care was taken to make sure that the "stare type" OKN was being executed during each run. It was found that most subjects used here needed some period of training to learn "how" to produce the desired pattern of nystagmus. Initially, they were able only to make the "look" type OKN despite the instruction to the contrary\*. There appeared to exist no verbal instruction that was immediately effective in successfully producing the "stare" type. At this stage, the instruction, "stare straight ahead", tended only to abolish the eye movement activity. As it turned out, the best recommendable way appeared to be a combination of the subject's voluntary random trial of different attitudes and the experimenter's simultaneous monitoring and judgement upon the performance reported back to the subject. Usually, improvement was not gradual but sudden ; once the subject was informed of his success, he became able to reproduce the desired pattern consistently even days later. Fig. 6.2 presents the corresponding before-and-after type of eye movement record taken from the same subject.

The experiment consisted of three sessions. The first

---

\* One could argue that it must be possible by a human subject to select a particular stripe at a time and then to follow its subsequent motion until it disappears from sight. A voluntary saccade resetting toward the opposite boundary of the stimulus field will pick a new stripe, and the result of repeating this process might be an OKN pattern of the "look" type.

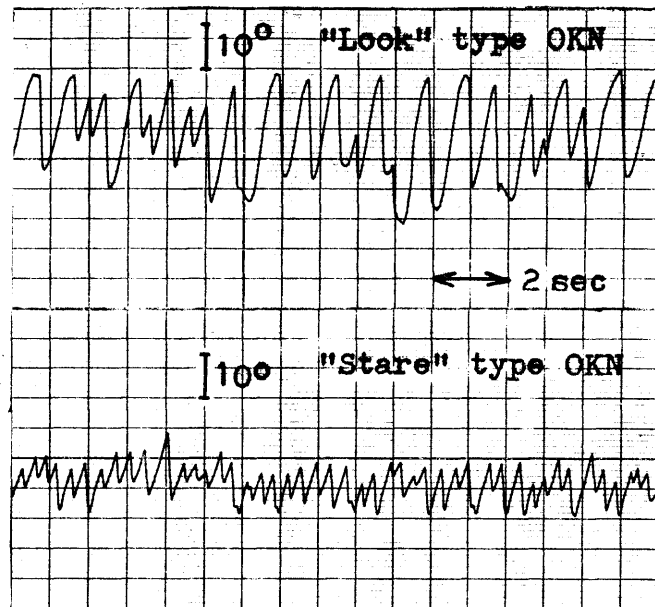


Fig. 6.2 Two distinct OKN patterns responding to the same constant stimulus speed ( $30^{\circ}/\text{sec}$ ): "Look" type (upper trace) and "Stare" type (lower trace). Only the latter is dealt with throughout the thesis.

session was designed to investigate the time course of slow phase response following step changes of the stripe velocity. Two male and one female adult subjects participated in this session\*. Various magnitudes of the stimulus field velocity were tested to examine transient characteristics as well as steady-state velocity-tracking performance by OKN slow phase movement. Direction of the group motion of stripes was abruptly reversed at some random occasions during each run in this session. Besides a reason related to the purpose of the next chapter, the above special stimulus feature was intended to yield latency estimation more reliable than one that would be obtained by the use of a simple velocity-step input, for eye movement prior to a velocity-step input would likely be contaminated by random spontaneous drift that may obscure the true initiation of slow phase response.

In the second session, frequency response measurement was undertaken for OKN slow phase under periodic stimulation. Regular sine wave signals were applied for commanding the field motion of the visual pattern. Amplitude of the sinusoidal field velocity was held constant for the entire frequency range at value of  $36^\circ/\text{sec}$ , about where slow phase velocity tended to start saturation as obtained subsequently. Three male and one female subjects were tested in this session.

The third session dealt with slow phase frequency response with pseudo-random stimuli. Two male and one female subjects

---

\* Subjects used in experiments in this chapter had no apparent abnormality in the eye movement. A preliminary test rejected one subject from the formal sessions, who showed a considerable directional preponderance in both pursuit and OKN slow phase movements.

participated in this session. Inputs for driving the stripe motion were pseudo-random signals A, B, C and D, the same as those used in Chapter IV for the nonperiodic-input dual-mode visual tracking except for the following difference. The originally prepared pseudo-random signals were applied directly as command for the field velocity of OKN stimulus pattern, whereas in Chapter IV they were passed through an analog low-pass filter,  $1/(1+s)$ , and then used to determine position of the target spot. For this reason, each spectrum here has a somewhat greater amplitude envelope in the low frequency region (below 1 rad/sec) as compared with its counterpart specified in Fig. 4.3. The instantaneous velocity of the OKN stimulus motion with each of the above pseudo-random inputs was maintained always under the estimated saturation velocity of OKN slow phase, as confirmed by a direct examination on the stimulus trace.

### 6.2.3 Data Analysis

Data reduction steps toward the final periodic-input and nonperiodic-input slow phase Bode plots were identical to those described in Chapter III for vestibular nystagmus, and also quite analogous to the procedure mentioned in Chapter IV for obtaining pursuit frequency responses.

Every fast phase jump was removed from the original OKN record by the special hybrid routine, MITNYS, to obtain the cumulative eye position that reflects the slow phase movement only. In addition, nonperiodic-input data underwent a Fourier analysis

by means of another hybrid routine, FFT.

However, due to the particular aspect of the OKN stimulus, velocity signal of the stimulus field motion (instead of a stripe's position signal, which may contain discontinuous jumps for resetting) was inputted to FFT along with the cumulative eye position. FFT result was then properly corrected to retrieve the right input-output relation, i.e., input=stimulus velocity, output=slow phase velocity.

Further technical details noted previously in Subsections 3.4.4 and 4.2.3 equally apply here ; these include the special recording-reproducing procedure, choice of FFT sampling rate and epoch, and artificial counterbalance for a likely large drift in the cumulative eye position.

Original Bode plot data for each individual subject can be found in Fig. D.10 and Figs. D.11 in Appendix D. Also included in Appendix D is Table D.4 which shows a substantial degree of matching between input and output peak frequencies in the FFT result for most cases. This in turn indicates adequacy of the system linearity and justifies the present frequency response approach.

Finally, the student's t-test was performed on the basis of the 5% level of confidence ( $p < 0.05$ ) for examining the question of difference in the OKN slow phase frequency response between the periodic and nonperiodic mode, as well as for comparing, under each mode of stimulus condition, the current OKN slow phase result with the pursuit result obtained in Chapter IV.



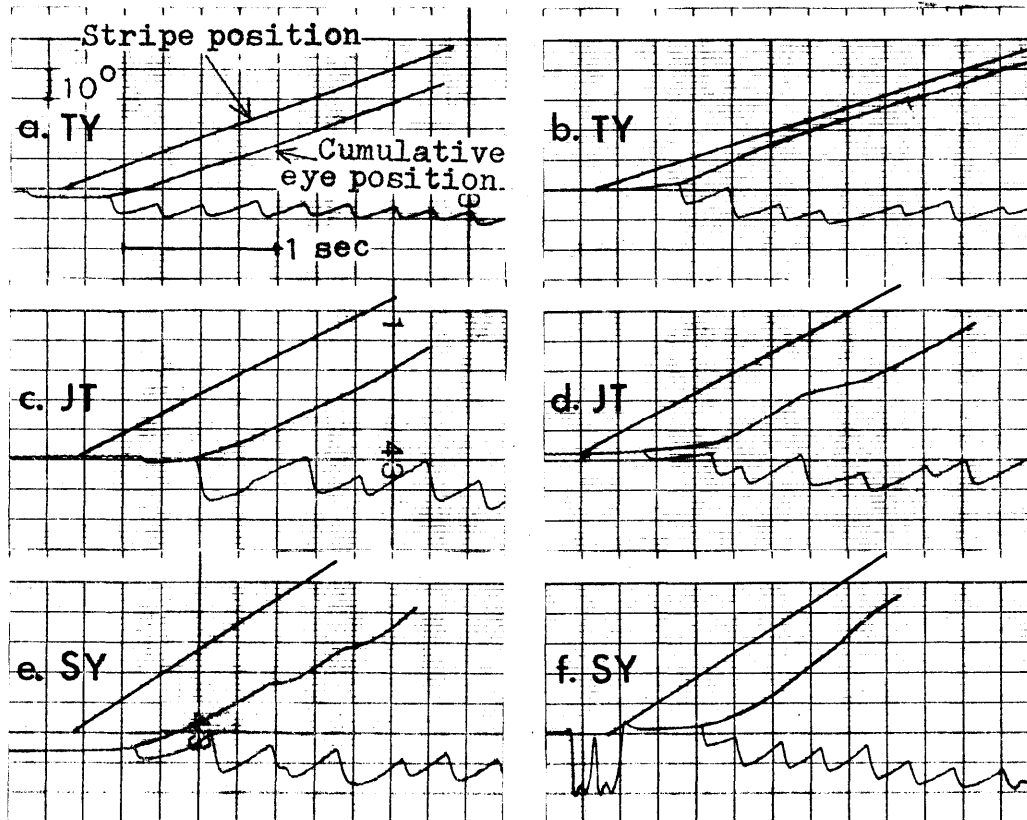
## 6.3 Results and Discussions

### 6.3.1 Transient Behavior, Latency and Linearity

Figs. 6.3 show traces for OKN transient response to a sudden initiation of constant-velocity stimulus motion. The transient behavior of slow phase appears similar to that of a pursuit velocity-step response, for example, as characterized by Robinson(1965 : See Subsection 2.1.2) :

- (1) Inter- and intra-subject variability in detailed response features
- (2) Quick development of the eye velocity (approximately 0.5~1.0 sec from the stimulus onset to the final matching with input velocity)
- (3) Possibility of the eye velocity overshoot (Fig. 6.3-b)
- (4) Latency value (as estimated closely in the following)

As pointed out earlier by Grüttner (1939), it appears also true here that OKN may begin either with a slow phase (Figs.6.3-b, d,e and f) or with a fast phase (Figs. 6.3-a and c). This would imply that latency range for slow phase and that for fast phase are overlapped each other. However, such a statement can be affected by accuracy of estimating the actual initiation of slow phase movement, which is generally not very clear because of the exponential-type gradual rise. Furthermore, unlike in an analogous latency measurement for the pursuit system (which deals with a fixation target), the initial slow phase response might well be obscured by a likely preexisting drift of the eye which may be



Figs. 6.3 OKN response to a sudden initiation of constant-velocity stimulus motion

free to move while waiting for the start of OKN stimulus motion\*.

In order to investigate the above latency question more closely, direction of the ongoing stripe motion was reversed occasionally in an unpredictable fashion during each experimental run, and corresponding changes in the eye movement were examined: Latencies for both slow and fast phase were measured, as illustrated for a typical case in Fig. 6.4\*\*. Fig. 6.5 plots such latency data against stimulus speed, accumulated over a composite of three subjects. Neither slow nor fast phase latency indicates a strong correlation with stimulus speed.\*\*\* While the fast phase latency time ranges from 300 msec up to 600 msec, majority of the slow phase latency data points fall between 100 msec and 200 msec as similar to the pursuit latency estimated by Westheimer (1954b), Rashbass (1961), Robinson(1965) and Yarbus (1967). Also note in this plot that in no case the slow phase latency exceeds the fast phase latency as defined in Fig. 6.4. This supports Stark's suggestion (1971) that OKN slow phase has a somewhat shorter delay time compared to fast phase, a situation analogous to the latency relation between the pursuit and saccadic component in the dual-mode tracking movement.

---

\* A fixation target could be presented, and turned off as soon as the OKN stimulus starts to move. But in that event, the oculomotor system might undergo switch of its functional mode from fixation to OKN, which may interfere with intrinsic aspect of OKN transient behavior.

\*\* Shift in the mean eye position following each stimulus reversal, as conspicuous in Fig. 6.3, is a subject of Chapter VII.

\*\*\* Interestingly, Collewijn (1972), working with much lower stimulus speeds in the rabbit, found a gradual increase of the OKN slow phase latency with diminishing input speed (less than  $1^\circ/\text{sec}$ ), a phenomenon Collewijn attributes to the discrete nature of the retinal receptors affecting the underlying data processing time of the visual information.

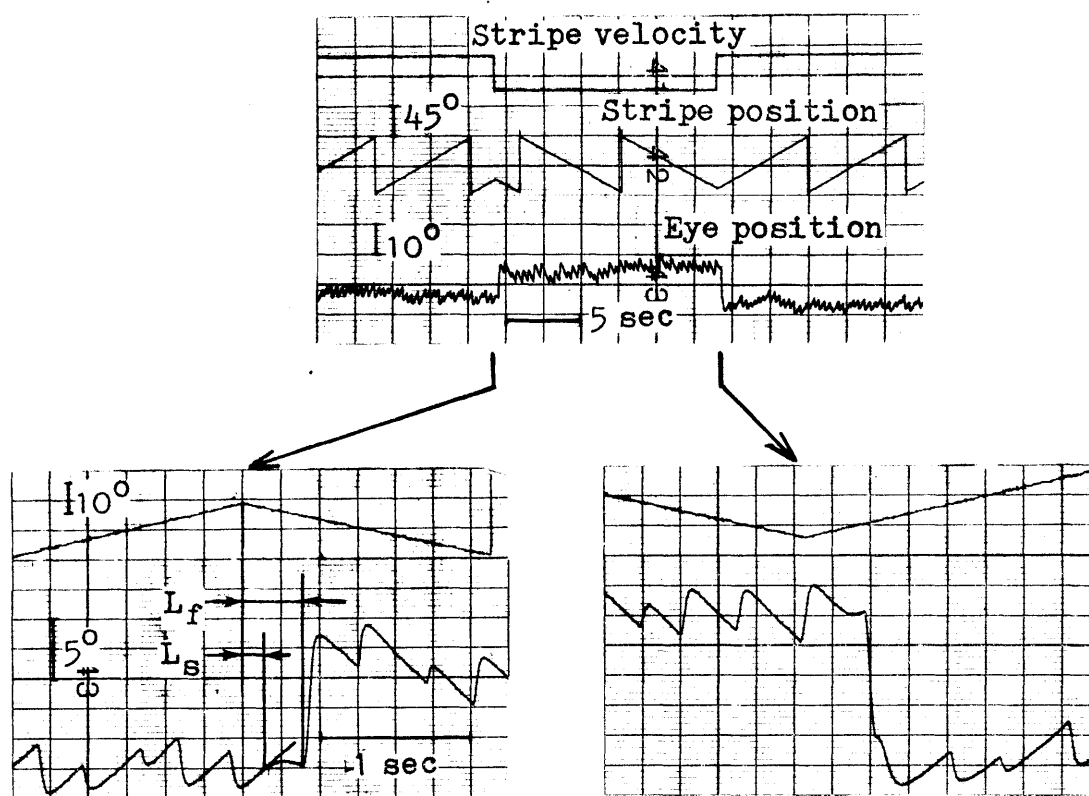


Fig. 6.4 Slow phase latency  $L_s$  and fast phase latency  $L_f$  for OKN

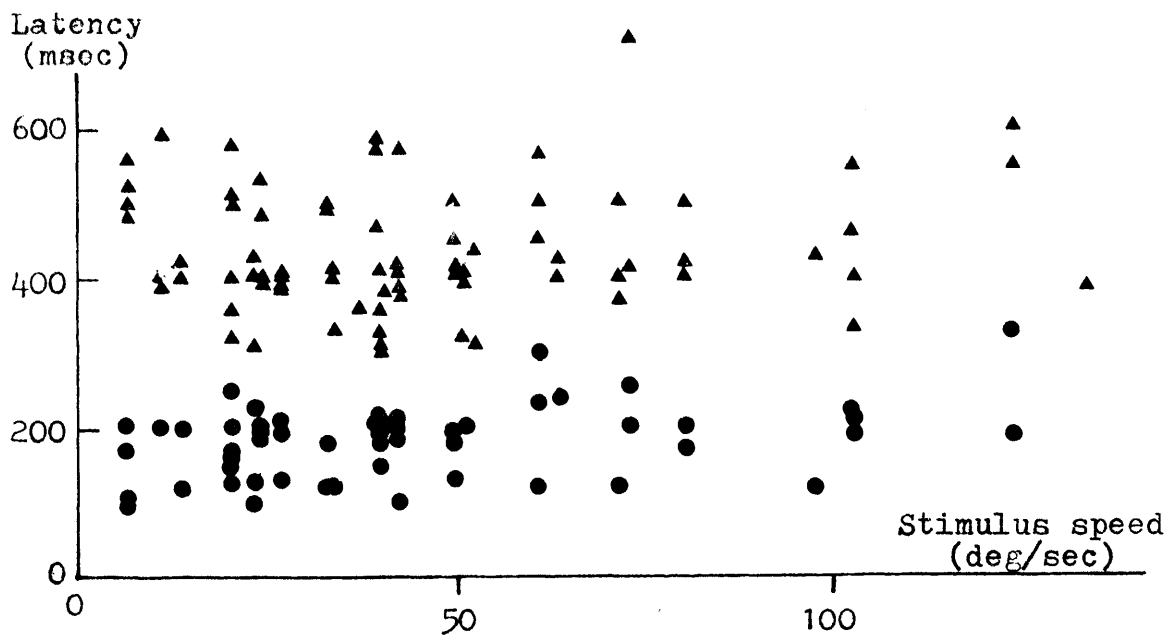


Fig. 6.5 Slow phase latency (●) and fast phase latency (▲) versus stimulus speed

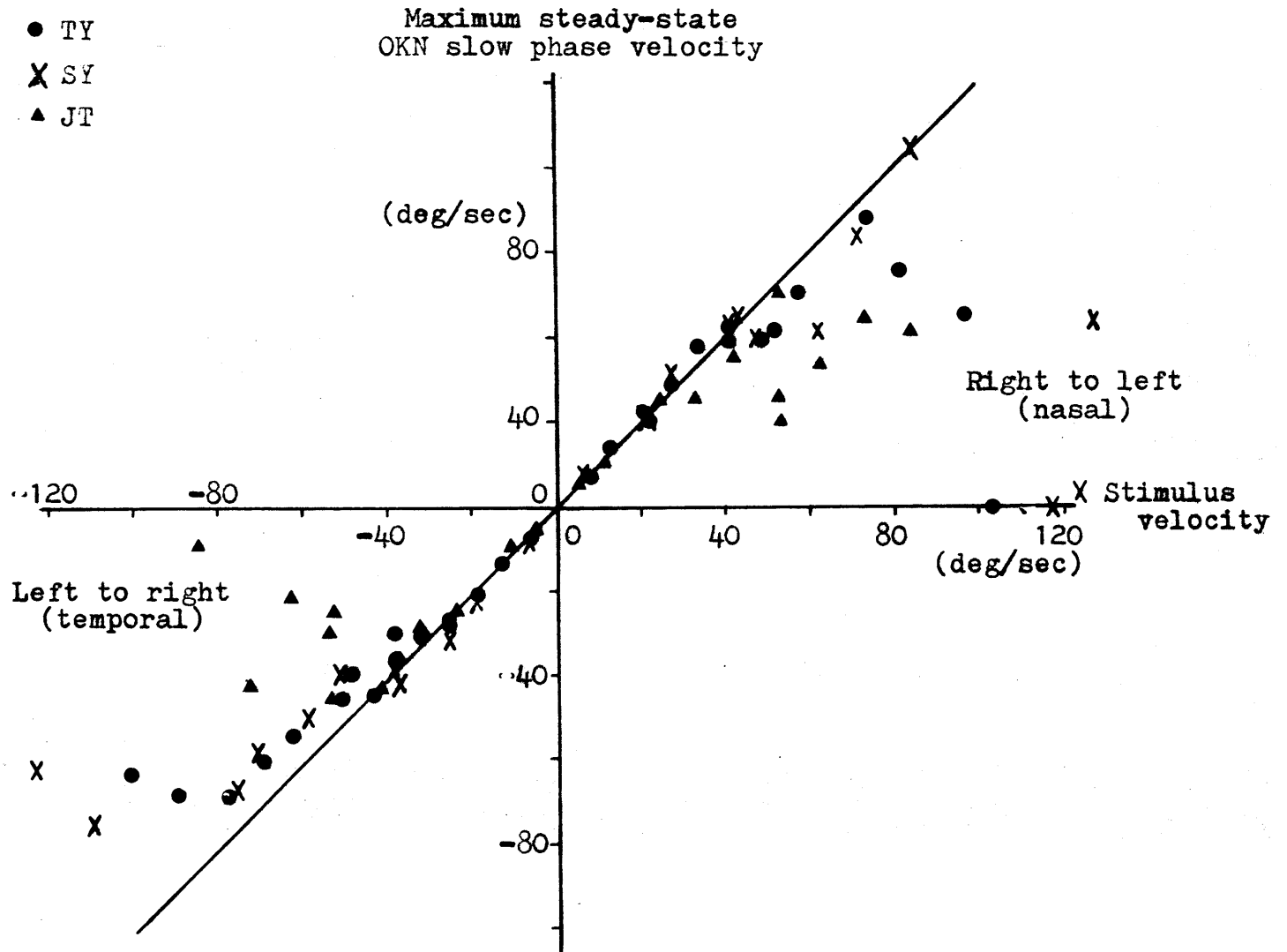


Fig. 6.6 Maximum steady-state OKN slow phase velocity versus stimulus velocity.

The maximum steady-state eye velocity is plotted versus stimulus velocity, as shown in Fig. 6.6. Particularly at higher stimulus speeds above 40°/sec or so, the regular OKN response was occasionally interrupted by periods of erratic response pattern. Slow phase speed during such intervals was variable and usually much smaller, and it is not included in the above plot. Fig. 6.6 shows that the maximum slow phase velocity matches the stripe velocity up to about +40°/sec, where the eye velocity starts to decline. This numerical result lies between the two previous reports (with controlled experiment for the "stare" type OKN), 60°/sec by Grüttner (1939) and 30°/sec by Honrubia et al (1968). The slow phase saturation limit as obtained here appears to be also in the same range as the pursuit movement (Dodge,et al, 1930).

### 6.3.2 Slow Phase Frequency Response : Periodic-inputs

Fig. 6.7 presents representative records for OKN with sine wave inputs. Fig. 6.8 shows the corresponding frequency response result for OKN ("stare" type) slow phase velocity with stripe velocity as input signal. The periodic-input pursuit result obtained in Chapter IV (Fig. 4.8) is also included in Fig. 6.8 for the purpose of comparison. At almost all the stimulus frequencies tested, no statistically significant difference ( $p < 0.05$ ) can be found between the above two Bode plots in either gain or phase, as indicated by the t-test result given in Table

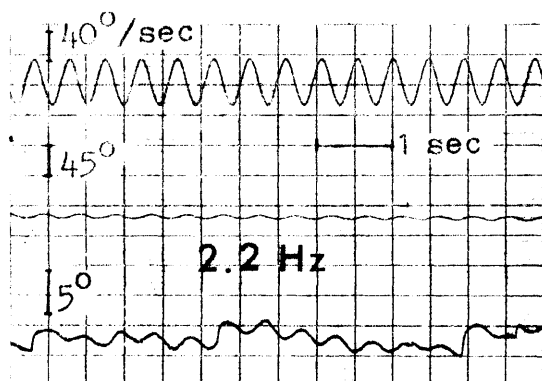
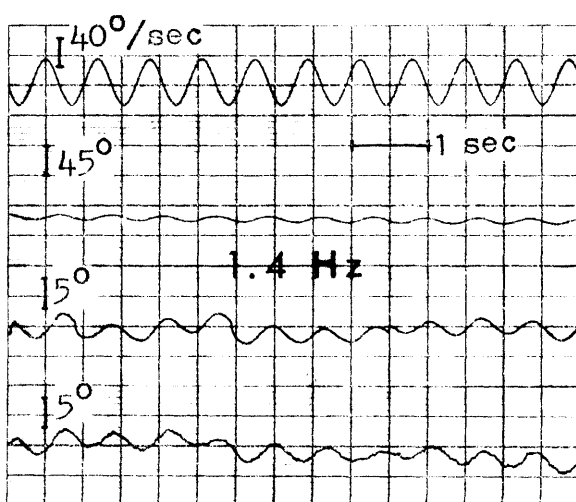
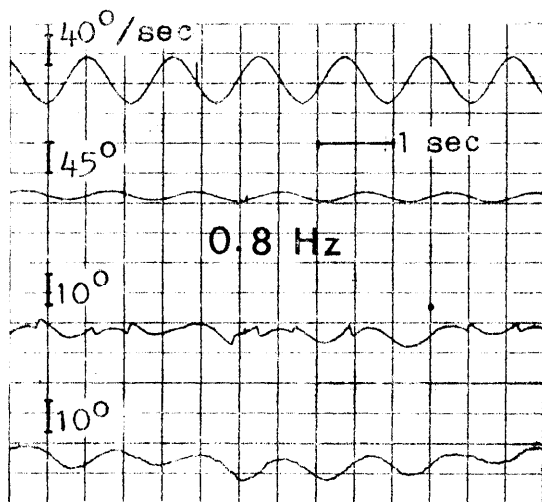
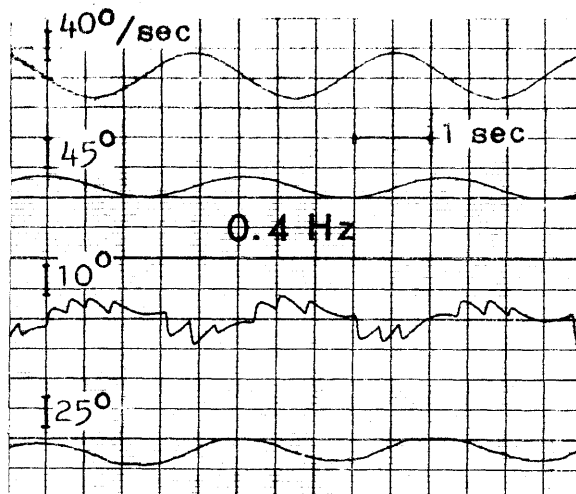
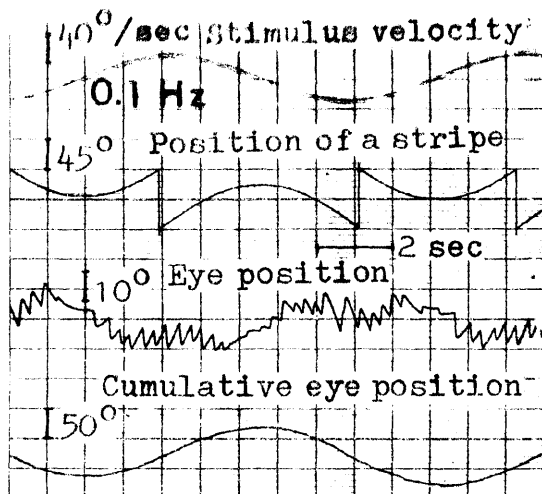


Fig. 6.7 Typical OKN records with sine wave stimuli of different frequencies

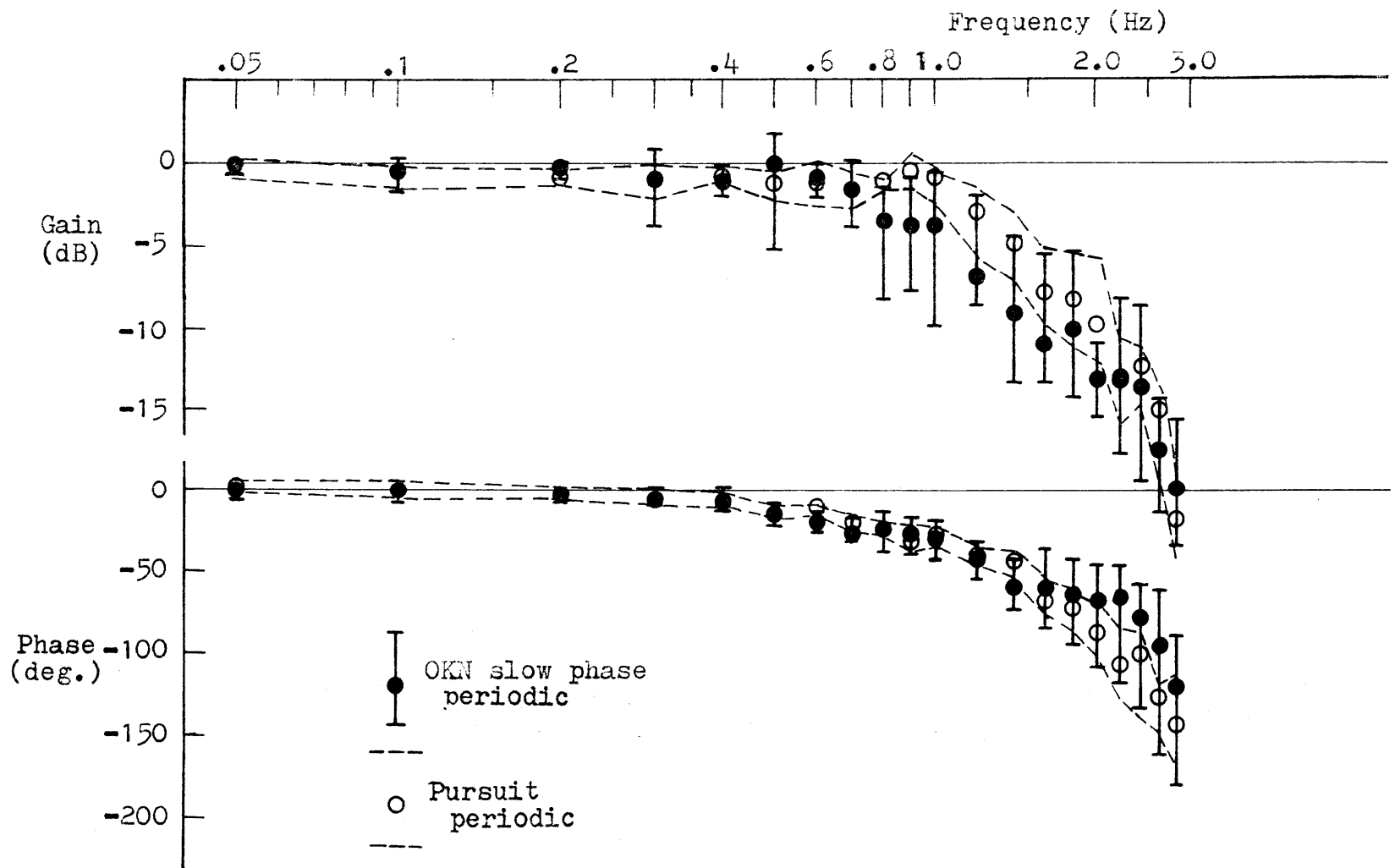


Fig. 6.8. OKN slow phase frequency response with periodic (sine wave) input (4 subjects) as compared with periodic pursuit result (4 subjects). Median data points and  $\pm$  one standard deviations are shown.



6.1-a at the end of this section\*.

However, the position amplitude of the stripe pattern's sinusoidal motion became progressively small as stimulus frequency increased, since the velocity amplitude was held constant in order to minimize the possibility of saturation in slow phase velocity. For example, already at 1 Hz the position amplitude was as small as about  $12^\circ$  (peak-to-peak), only twice as great as the horizontal separation between two adjacent stripes. Accordingly, one should suspect that the oculomotor response at a high OKN stimulus frequency may not have been actually OKN, but may have been the tracking eye movement that followed a particular stripe in oscillation. In fact, traces at 1.4 Hz and 2.2 Hz as given in Fig. 6.7 lack consistent generation of fast phase, making the response appear similar to the bottom trace of Fig. 4.5, which shows the eye movement during tracking of the single spot of target oscillating with a high-frequency and small-amplitude.

Although this apparent similarity could have been simply due to the much reduced number of both fast phase saccades (in the supposed OKN response) and fixation saccades (in the tracking movement) as presumably resulting from the underlying threshold effect being enhanced with small amplitude signals, the subsequent nonperiodic-input results further support the possibility that

---

\* However, when compared within individual subjects, some subjects show apparently consistent difference between periodic-input OKN slow phase (Fig. D.10) and periodic-input pursuit result (Fig. D.6), especially in gain in the intermediate frequency region. Although such an intra-subject observation should be equally important, only inter-subject statistical consideration is given here. (Both OKN and pursuit experiments used the same group of four individual subjects.)

"OKN slow phase" as induced here by a small-amplitude stimulus at a high frequency actually belongs to the same category as the smooth pursuit movement.

Even so, the present comparative examination may still allow one to conclude that the slow phase system of "stare type" OKN and the pursuit system behaves similarly during the predictive mode at least in the low frequency range below 1 Hz or so, where responses produced by the OKN stimulus are clearly OKN as indicated by traces at lower frequencies in Fig. 6.7.

### 6.3.3 Slow Phase Frequency Response : Nonperiodic-inputs

Hitherto, OKN slow phase and pursuit response characteristics have been very similar each other, tempting one to assume some common central mechanism. Frequency response results of the former with unpredictable stimuli are presented and discussed in the following.

Fig. 6.9 shows a representative trace with the pseudo-random stimulus, C. Note adequate performance of MITNYS in producing the cumulative eye position from the original OKN record. Nonperiodic-input OKN slow phase responses as determined by FFT are shown in Figs. 6.10, along with nonperiodic-input pursuit Bode plots obtained in Chapter IV with corresponding pseudo-random input signals (Figs. 4.15).

Figs. 6.10-a, b and c and the corresponding t-test results in Table 6.1-c show that, when the stimulus becomes unpredictable, a statistically significant difference emerges in the low-

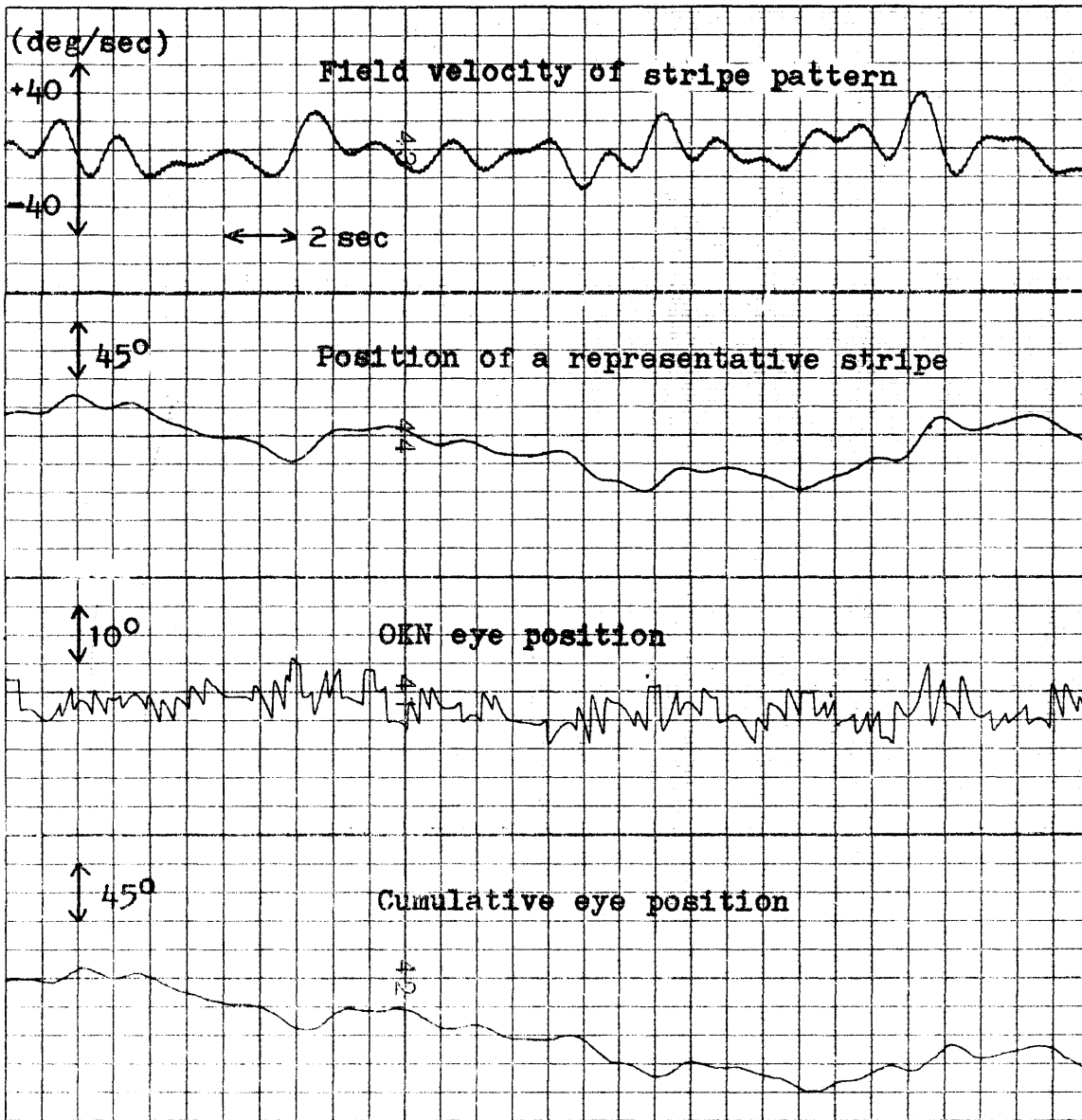
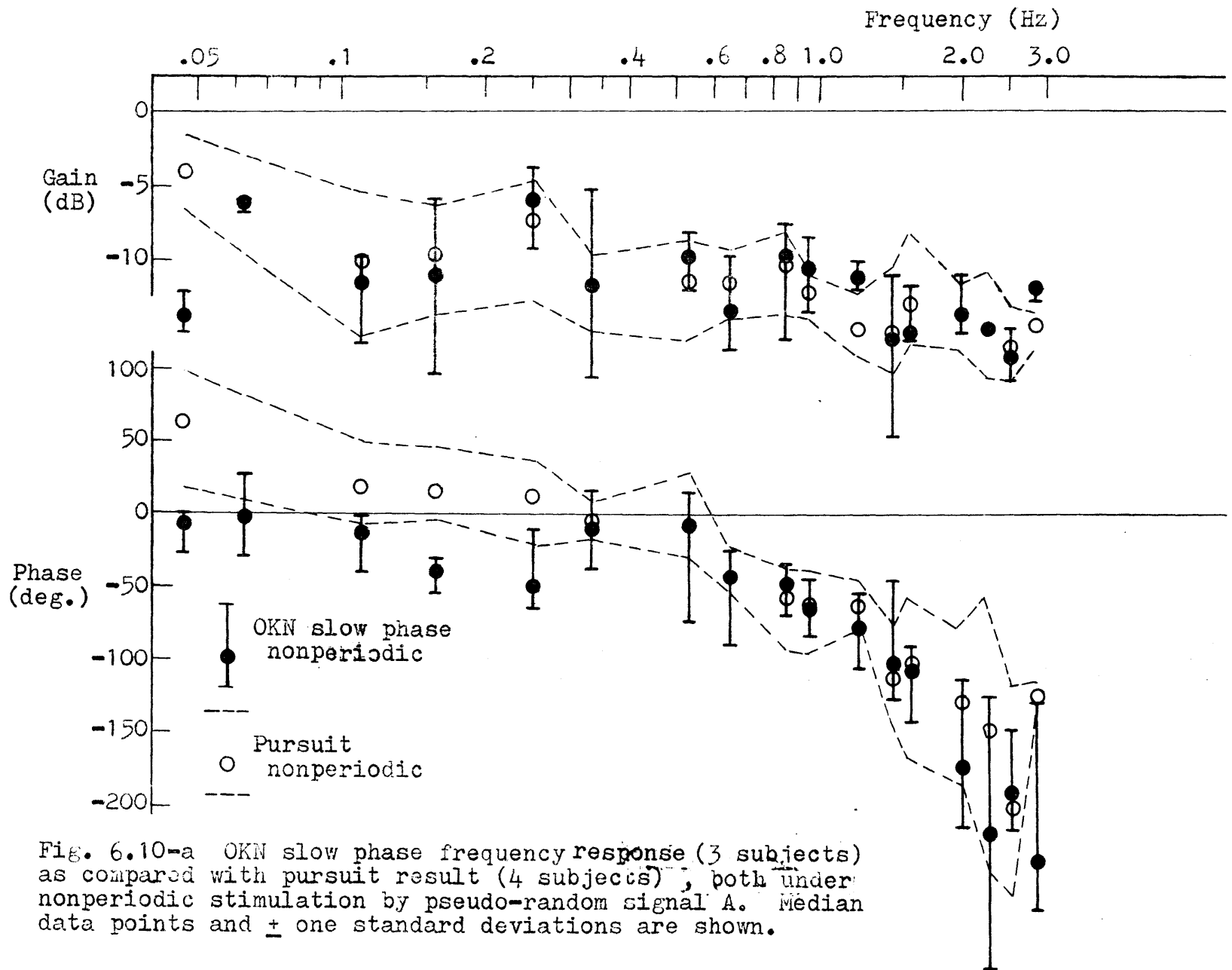


Fig. 6.9 A typical set of traces for OKN with pseudo-random stimulation (input C).



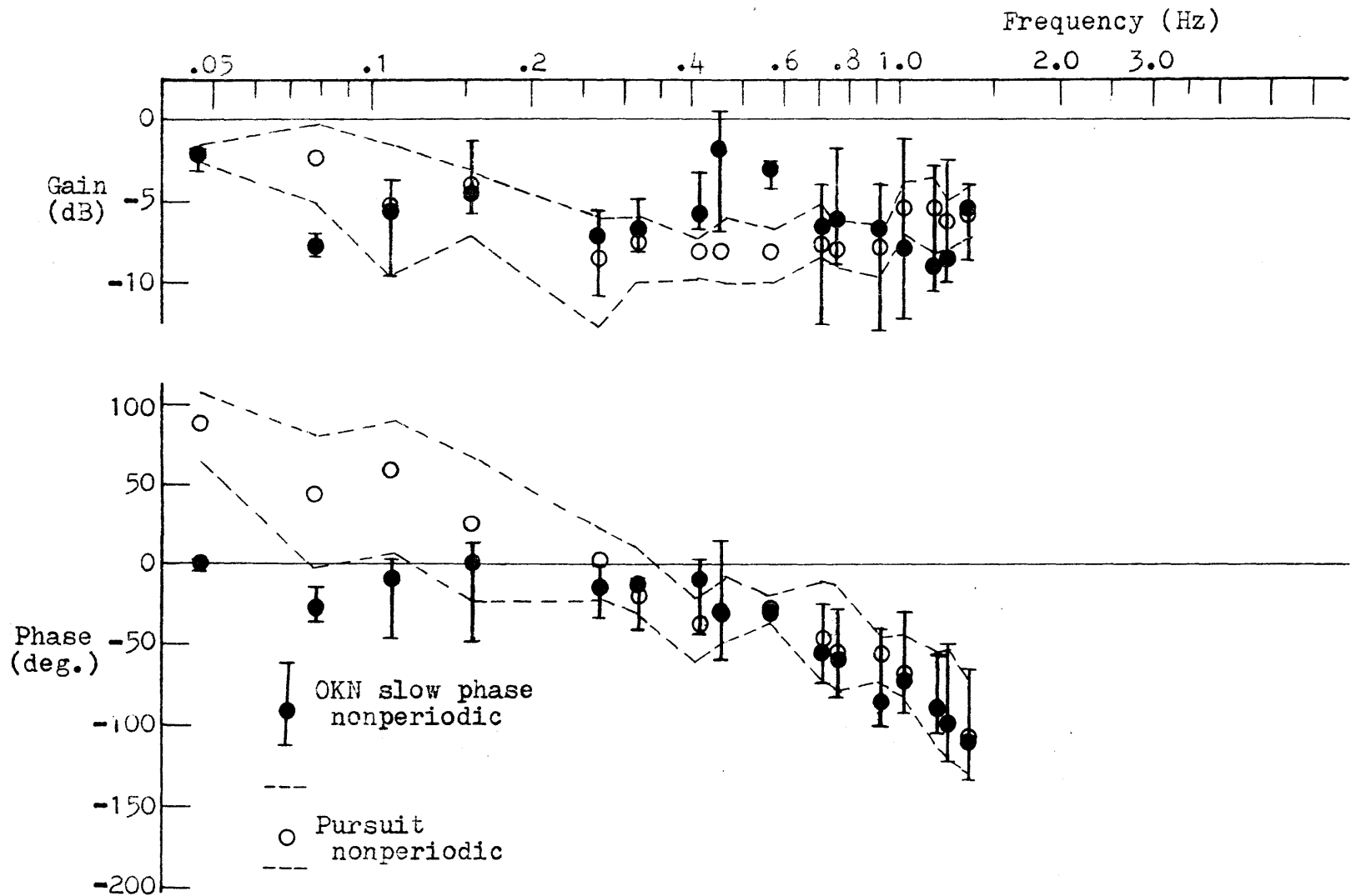


Fig. 6.10-b OKN slow phase frequency response (3 subjects) as compared with pursuit result (4 subjects), both under nonperiodic stimulation by pseudo-random signal B. Median data points and  $\pm$  one standard deviations are shown.

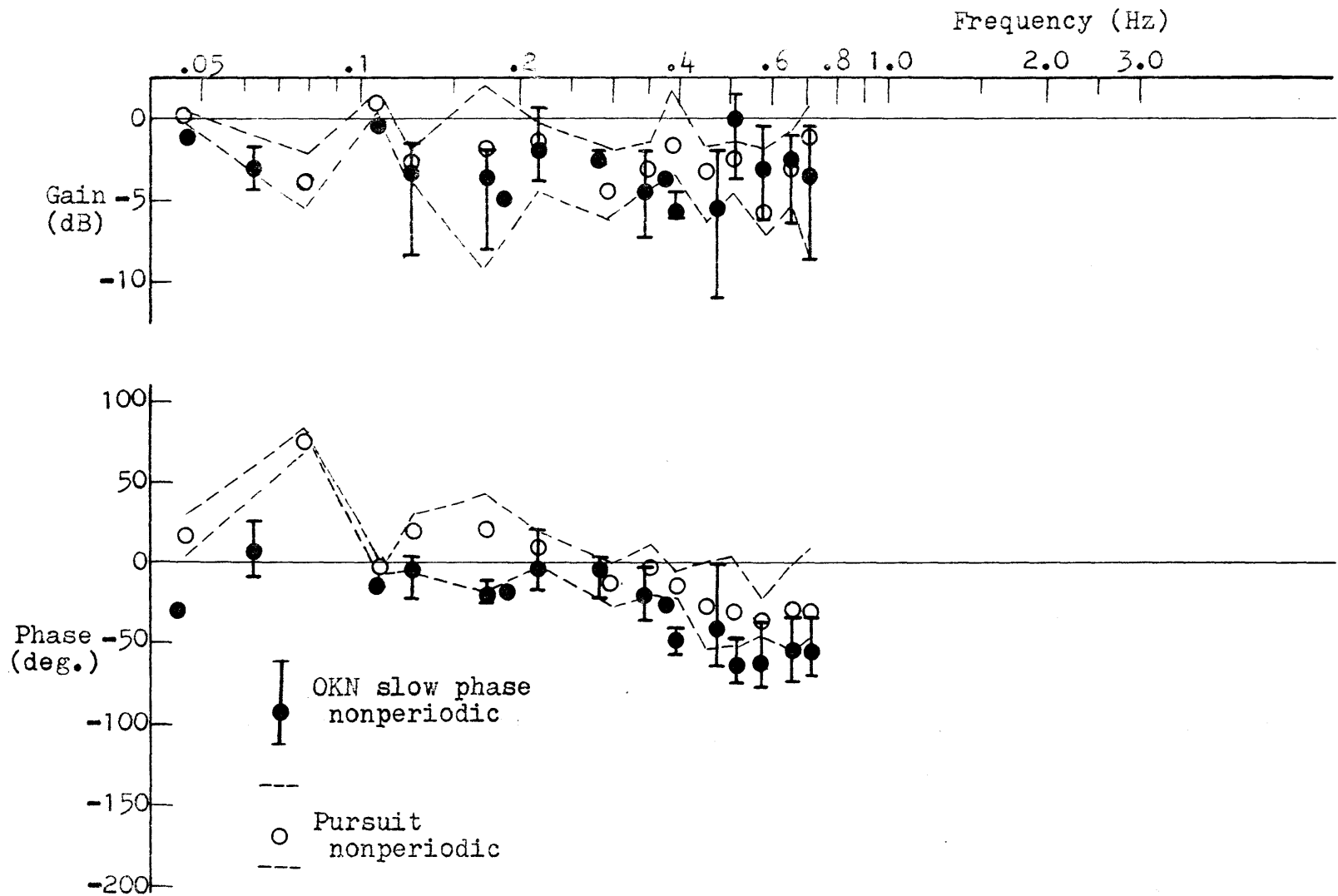


Fig. 6.10-c OKN slow phase frequency response (3 subjects) as compared with pursuit result (4 subjects), both under nonperiodic stimulation by pseudo-random signal C. Median data points and  $\pm$  one standard deviations are shown.

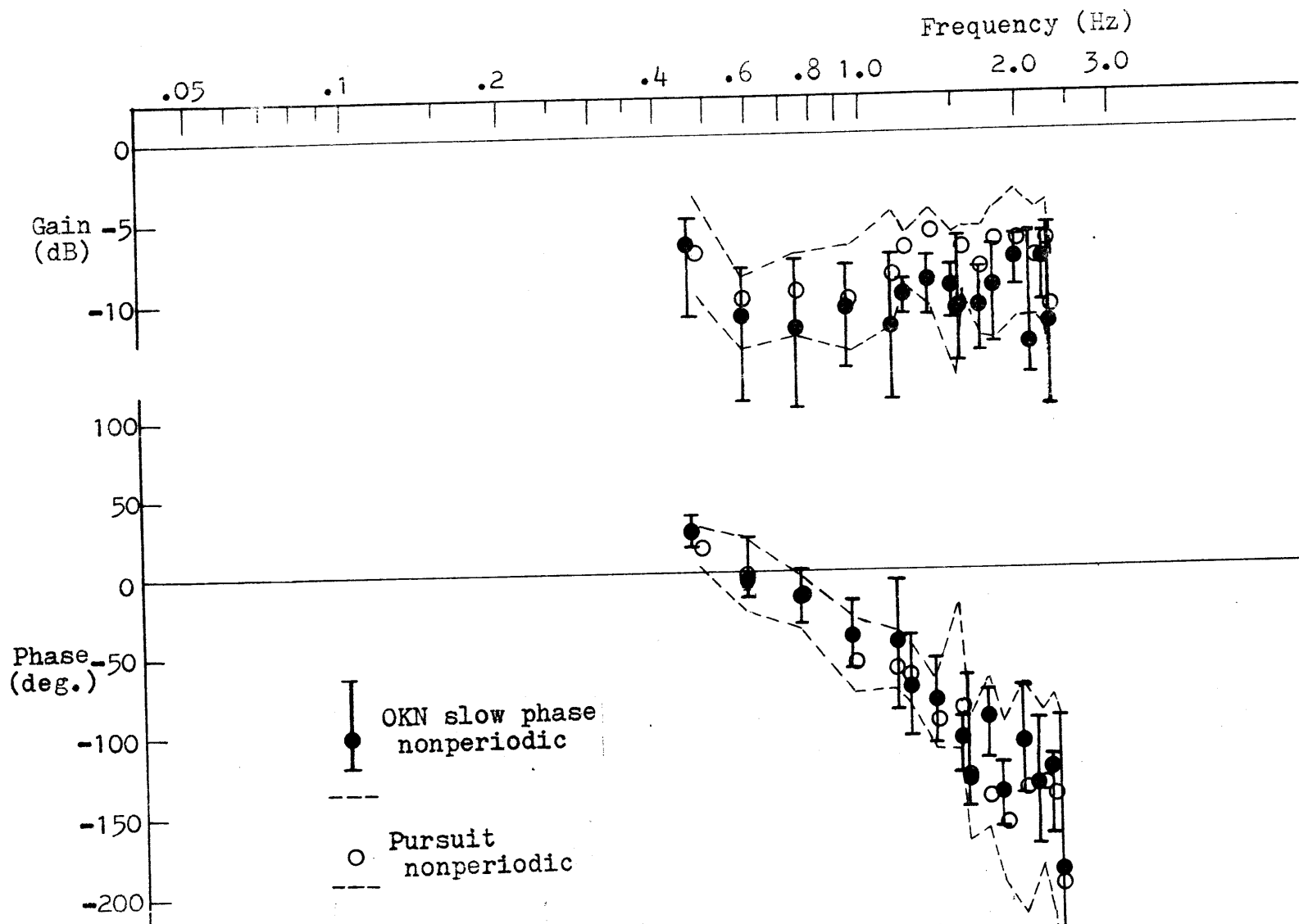


Fig. 6.10-d OKN slow phase frequency response (3 subjects) as compared with pursuit result (4 subjects) both under nonperiodic stimulation by pseudo-random signal D. Median data points and  $\pm$ one standard deviations are shown.

frequency phase behavior between OKN slow phase and pursuit frequency responses\*. In the low frequency region, the former produces little phase shift, failing to show such a large phase lead as conspicuously observed in the nonperiodic-input pursuit response.

While the above observation alone suggests some functional distinction between the OKN slow phase system and the pursuit system, there appears to be no other substantial difference in the rest of Bode plot features for a given input : Basically, both gain plots fall in the same range throughout the input frequency range, and both phase plots exhibit a similar trend of increasing phase lag with increasing frequency in the intermediate-high frequency range.

But, for a reason similar to one given in the previous periodic case, responses induced by high-frequency inputs may have been the pursuit movement, rather than OKN slow phase. This would account for the above failure to find any significant and consistent difference at high frequencies. Of particular relevance in this connection may be comparison between the OKN slow phase and pursuit result with input D (Fig. 6.10-d). This particular pseudo-random input signal is characterized by absence of low frequency components. As explored in Chapter IV, large phase lead in the lower-frequency region within a given stimulus bandwidth appears to be a general tendency of the pursuit system when exposed to a nonpredictable input. A similar large phase lead was found in the lower half of this stimulus band also for

---

\* Three subjects were used in the present OKN experiment. The same three subjects plus an additional subject participated in the pursuit tracking experiment.



OKN slow phase. In fact, OKN slow phase is quite similar to the pursuit result almost throughout the entire spectrum of stimulus D. This would reinforce the suggestion that what was intended to be OKN slow phase response in the present experiment was probably the smooth pursuit movement for high frequency components (which constitute input D in the highest proportion compared to the other random inputs used here).

Finally, each of the preceding nonperiodic-input OKN slow phase results is contrasted against the periodic-input counterpart as shown in Figs. 6.11. The corresponding t-test result is summarized in Table 6.1-b. However, for the aforementioned reason, results in the high frequency range as well as the whole result for input D should be discarded from comparison. The predictive response was clearly OKN at least up to 1 Hz as indicated by original traces in Fig. 6.7. Assuming that this is true also for the nonperiodic-input cases, periodic versus nonperiodic comparison is feasible for the right frequency range. Both subjective impression (Figs. 6.11-a, b and c) and the t-test (Table 6.1-b) indicate that the nonperiodic-input cases yield significant gain drop over the entire relevant frequency range and somewhat greater phase lag especially in the mid frequency region as compared to the the predictive results. Thus, one may conclude that difference exists in the frequency response of the "stare type" OKN slow phase depending upon the stimulus predictability\*.

\* This inter-subject conclusion is generally supported by intra-subject comparison (Fig. D.10 versus Figs. D.11 with exception of Fig. D.11-d), which is, however, applicable only for two subjects, TY and SY, who participated in both predictive and nonpredictive OKN experiments.

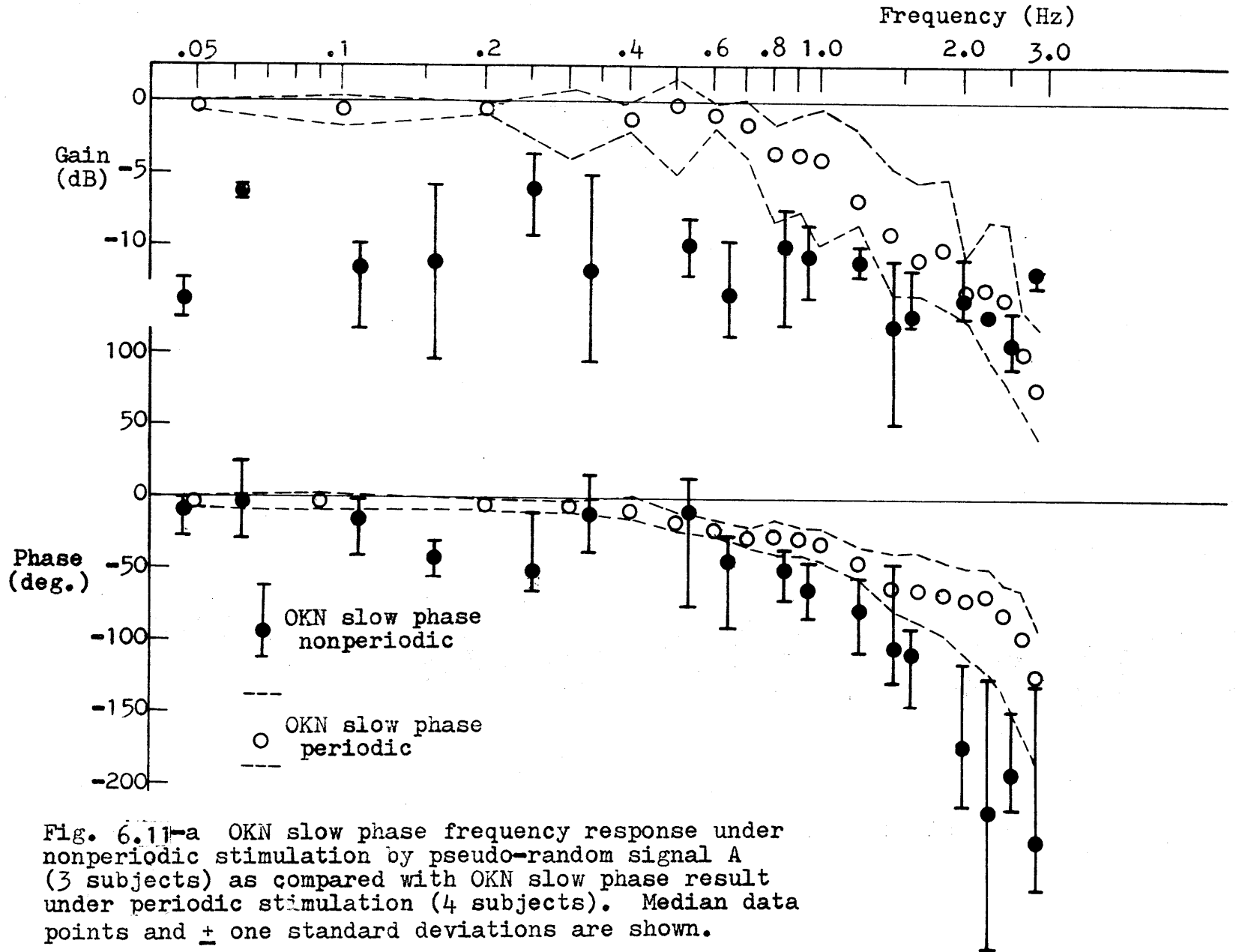


Fig. 6.11-a OKN slow phase frequency response under nonperiodic stimulation by pseudo-random signal A (3 subjects) as compared with OKN slow phase result under periodic stimulation (4 subjects). Median data points and  $\pm$  one standard deviations are shown.

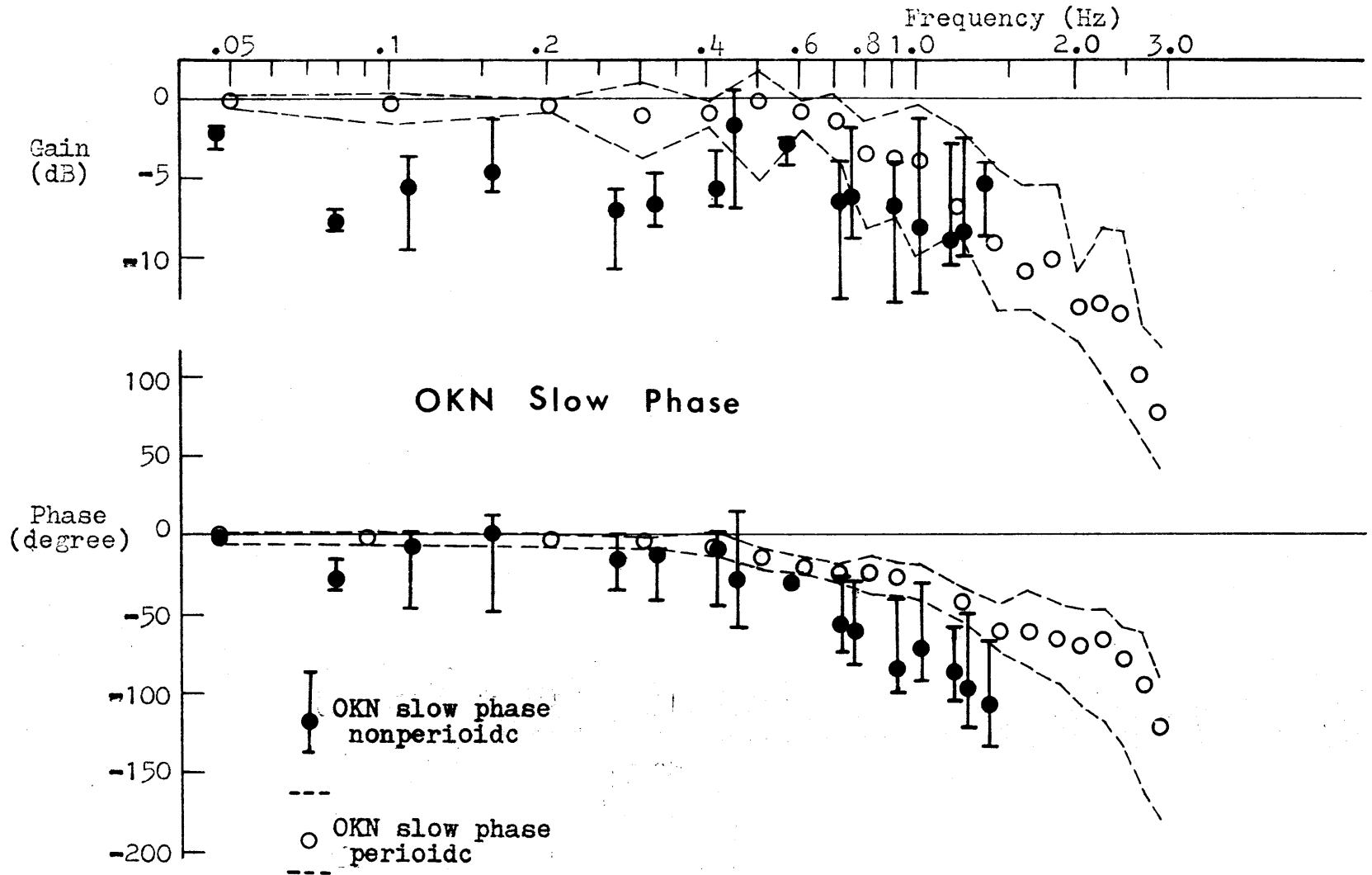


Fig. 6.11-b OKN slow phase frequency response under nonperiodic stimulation by pseudo-random signal B (3 subjects) as compared with OKN slow phase result under periodic stimulation (4 subjects). Median data points and  $\pm$  one standard deviations are shown.

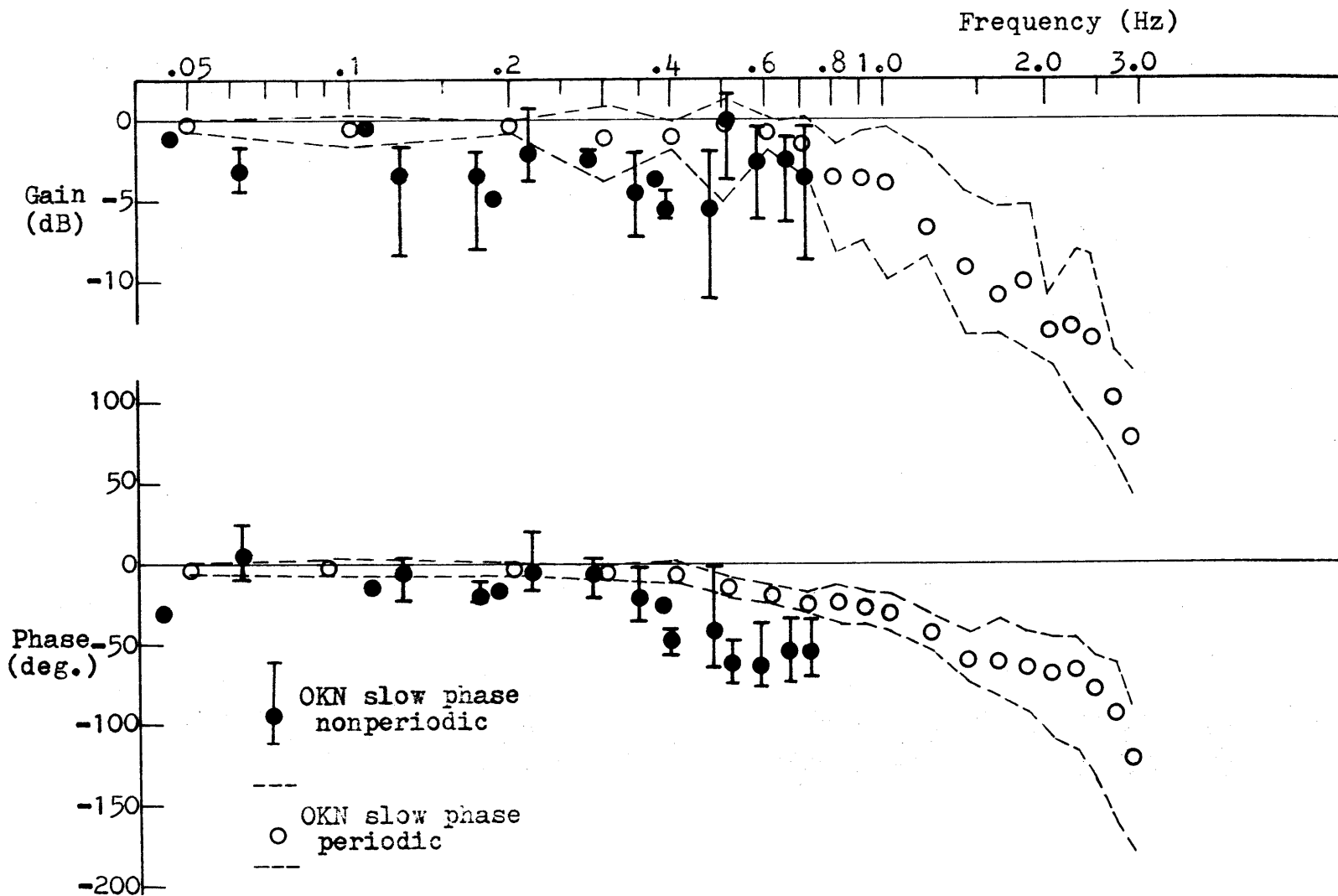


Fig. 6.11-c OKN slow phase frequency response under nonperiodic stimulation by pseudo-random signal C (3 subjects) as compared with OKN slow phase result under periodic stimulation (4 subjects). Median data points and  $\pm$  one standard deviations are shown.

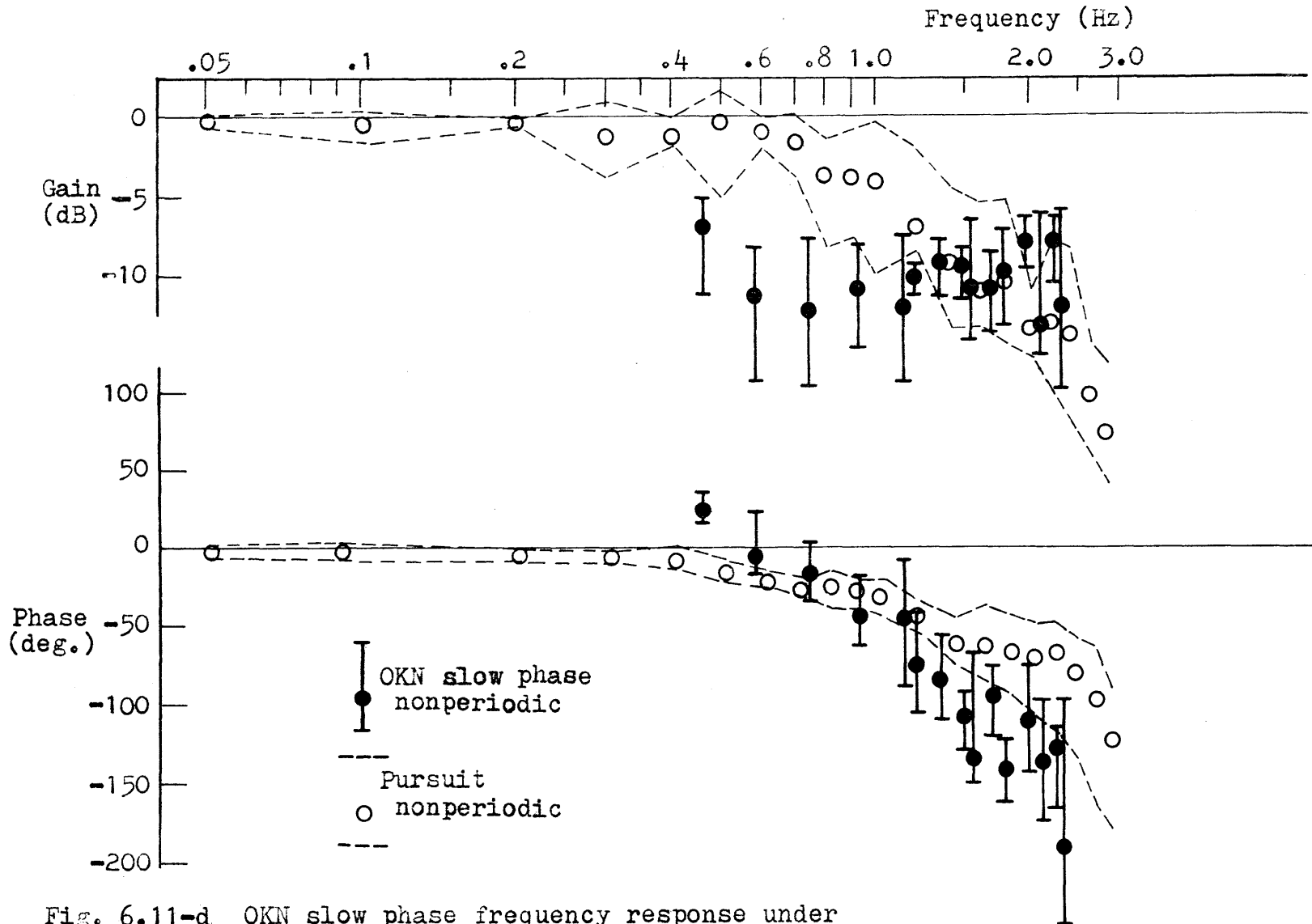


Fig. 6.11-d OKN slow phase frequency response under nonperiodic stimulation by pseudo-random signal D (3 subjects) as compared with OKN slow phase result under periodic stimulation (4 subjects). Median data points and  $\pm$  one standard deviations are shown.

However, when the stimulus becomes pseudo-random, this input-adaptive mechanism for OKN slow phase appears to act differently from the pursuit counterpart as suggested by phase comparison in the low frequency region (large pursuit phase lead versus little phase shift for OKN slow phase). This may be of interest especially considering that OKN slow phase and pursuit response characteristics otherwise appear quite similar to each other as shown by the preceding various observations.\* Also of interest may be the contrast with the functionally related vestibular nystagmus whose slow phase, according to the result given in Chapter III, failed to indicate presence of any form of predictive mechanism at least in the low to lower-intermediate frequency range examined.

---

\* Earlier, Merrill and Stark (1963a) also obtained evidence indicating that OKN slow phase is not the same in class as the smooth pursuit movement: They showed that, while the pursuit tracking summated linearly with the slow phase of OKN, two OKN slow phase responses (induced by two sets of stripes moving in opposite directions) did not summate but rather alternate periodically.

		Frequency (Hz)		.05	0.1	0.2	0.5	1.0	2.0	3.0
Period.	Fig. 6-8	Gain	OKN	0	0	0	0	0	0	0
			Pursuit	0	0	0	0	0	0	0
	Phase	OKN	-	0	0	0	0	0	0	0
		Pursuit	+	0	0	0	0	0	0	0

(a) OKN slow phase versus pursuit movement : periodic stimulation

				Frequency (Hz)							
				.05	0.1	0.2	0.5	1.0	2.0	3.0	
Fig. 6.11-a	Gain	OKN Random A	-	-	-	-	-	-	-	-	
		OKN Period.	+	+	+	+	+	+	+	+	
	Phase	OKN Random A	-	0	-	-	-	0	-	-	-
		OKN Period.	+	0	+	+	+	0	+	+	+
Fig. 6.11-b	Gain	OKN Random B	-	-	-	-	-	-	-	-	
		OKN Period.	+	+	+	+	+	+	+	+	
	Phase	OKN Random B	0	-	0	0	0	-	0	-	-
		OKN Period.	0	+	0	0	0	+	+	+	+
Fig. 6.11-c	Gain	OKN Random C	-	-	0	-	-	0	0	0	
		OKN Period.	+	+	0	+	+	0	+	+	
	Phase	OKN Random C	-	0	-	0	0	0	-	-	-
		OKN Period.	+	0	+	+	+	0	+	+	+
Fig. 6.11-d	Gain	OKN Random D	-	-	-	-	-	-	-	-	
		OKN Period.	+	+	+	+	+	+	+	+	
	Phase	OKN Random D	0	0	0	0	0	0	0	0	
		OKN Period.	0	+	+	+	+	+	+	+	

(b) Periodic versus nonperiodic stimulation for OKN slow phase

Tables 6.1 Summary of student's t-test results based on 5 % level of significance. In the illustrative example on right, mean value of a quantity at frequency of  $f_1$  is greater under condition X than Y with probability of at least 0.95. The converse statement is held at  $f_2$ . At  $f_3$ , no positive conclusion can be drawn with more than 95 % confidence as to dependence of the quantity upon the two different conditions X and Y.

	$f_1$	$f_2$	$f_3$
X	+	-	0
Y	-	+	0

(illustrative example)

			Frequency (Hz)															
			.05	0.1	0.2	0.5	1.0	2.0	3.0									
Random A	Fig. 6.10-a	Gain	OKN	-	-	0	0	0	0	0	0	0	0	0	0	0	0	0
			Pursuit	+	+	0	0	0	0	0	0	0	0	0	0	0	0	0
	Phase	OKN	-	-	-	-	0	0	0	0	0	0	0	0	0	0	0	0
		Pursuit	+	+	+	+	0	0	0	0	0	0	0	0	0	0	0	0
Random B	Fig. 6.10-b	Gain	OKN	0	-	0	0	0	0	+	+	+	0	0	0	0	0	0
			Pursuit	0	+	0	0	0	0	-	-	-	0	0	0	0	0	0
	Phase	OKN	-	-	-	-	0	0	+	0	0	0	0	0	0	0	0	0
		Pursuit	+	+	+	+	0	0	-	0	0	0	0	0	0	0	0	0
Random C	Fig. 6.10-c	Gain	OKN	-	0	-	0	0	0	-	-	0	0	0	0	0	0	0
			Pursuit	+	0	+	0	0	0	+	+	0	0	0	0	0	0	0
	Phase	OKN	0	-	-	0	0	0	0	-	0	-	-	-	0	0	0	0
		Pursuit	0	+	+	0	0	0	0	+	0	+	+	+	0	0	0	0
Random D	Fig. 6.10-d	Gain	OKN						0	0	0	0	0	0	0	0	0	0
			Pursuit						0	0	0	0	0	0	0	0	0	0
	Phase	OKN						+	0	0	0	0	0	0	0	0	0	0
		Pursuit						-	0	0	0	0	0	0	0	0	0	0

(c) OKN slow phase versus pursuit movement : nonperiodic stimulation

Tables 6.1 (continued)



#### 6.4 Summary and Conclusions

Optokinetic nystagmus (OKN) is investigated herein primarily in regard to behavior of its slow phase component. Interest is restricted to the "stare" type OKN in human subjects.

Presentation of the OKN stimulus pattern was accomplished based on a computer graphical display technique, which involved no mechanical component allowing an accurate and extremely fast control of the stimulus motion, a desirable stimulus feature especially for a close examination on transient response characteristics.

Despite differences in the type of visual stimulus, when compared in the time domain, OKN slow phase and the pursuit movement appear to share many common features with respect to : (1) selective sensitivity to velocity stimulus, (2) range of latency, (3) rapid development of response velocity in matching a velocity-step input, (4) linearity range in response to constant stimulus velocities. The present data are generally in agreement with these time-domain observations noted in the literature, supporting the popularly held notion that OKN slow phase component and the pursuit movement are governed by some common central mechanisms. The principal finding in the above time-domain assessment is that slow phase latency (100 msec - 200 msec) never exceeded fast phase latency (300 msec - 600 msec) in response to a sudden directional reversal of the stimulus motion. (Relative magnitude of these two OKN latencies has been in some dispute in the literature.)

Next, frequency-domain assessment of OKN slow phase was made. The maximum instantaneous stimulus speed was kept below the point of slow phase velocity saturation as determined by the preceding constant-velocity experiment. Nonperiodic-input nystagmus data underwent the two-step hybrid computer processing, MITNYS-FFT, for removing all fast phase saccades and then performing a Fourier analysis to ultimately obtain the desired frequency response, a procedure similarly taken in Chapters III and IV.

Similarity between OKN slow phase and the pursuit movement appears to still hold in the frequency domain if the stimulation is periodic.

However, when the stimulus became nonperiodic, discrepancy emerged particularly in low-frequency phase behavior between the pursuit response frequency response and OKN slow phase frequency response, both of which were obtained analogously by the MITNYS-FFT data reduction procedure : OKN slow phase failed to exhibit the large low-frequency phase lead as observed in Chapter IV with the pursuit system.

When examined within OKN, a nonperiodic input appears to yield somewhat greater phase lag in OKN slow phase than if the stimulation is periodic, suggesting existence of a predictive mechanism for OKN slow phase. This positive indication may be of interest when contrasted with the negative result obtained in Chapter III with the functionally related vestibular nystagmus slow phase, though both results were obtained from a relatively small population of subjects.

## Chapter VII

### Mechanism of Fast Phase Generation in Vestibular and Optokinetic Nystagmus

The nystagmus fast phase component manifests a characteristic feature within the over-all response pattern as noted by some previous authors. Preliminary observations show that this phenomenon is similar in both vestibular and optokinetic nystagmus, which is best demonstrated by its fairly stereotyped correlation with their slow phase components.

While this effect phenomenologically indicates another functional advantage of nystagmus, the observation suggests a common fast phase generating mechanism utilizing slow phase motor information irrespective of the stimulus modality. Relevant clinical and neuroanatomical evidence are cited and discussed to further support this viewpoint.

In an attempt to functionally substantiate such a common origin of fast phases, a series of controlled experiments are undertaken to assess the pertinent parameters underlying the observed fast phase behavior in question. A control engineering model is constructed based on these experimental results, and analyzed and simulated on a hybrid computer to demonstrate its essential feasibility for both types of nystagmus.

Finally, OKN stimulation is given selectively to the peripheral retina of a normal subject, which yields a preliminary result showing a similar OKN pattern change as reported in the

literature for a central scotomata patient.

## 7.1 Introduction

### 7.1.1 Preliminary Observations

### 7.1.2 Evidence for Common Central Control of Nystagmus Fast Phase

## 7.2 Experimental Results and Discussions

### 7.2.1 Response to Constant Velocity Stimuli: Linear Relations

### 7.2.2 Sinusoidal Response

## 7.3 A System Engineering Model

### 7.3.1 Functional Implication of Average Deviation

### 7.3.2 Conceptual Description of Models

### 7.3.3 Model Analysis

## 7.4 Simulation of Model

### 7.4.1 Simulation 1

### 7.4.2 Simulation 2

## 7.5 OKN Pattern Change by Selective Stimulation to Peripheral Retina

## 7.6 Summary and Conclusions

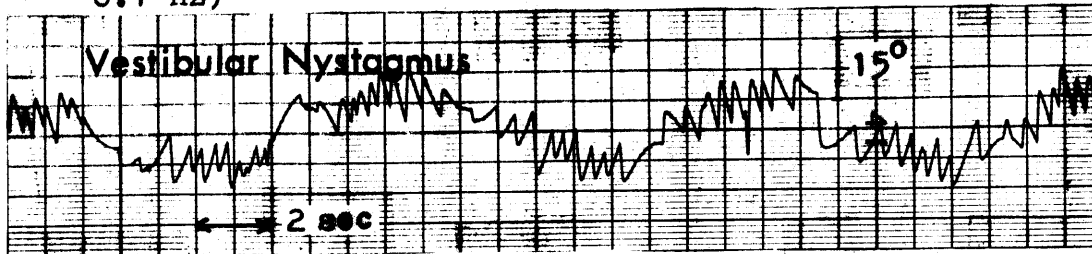
## 7.1 Introduction

### 7.1.1 Preliminary Observations

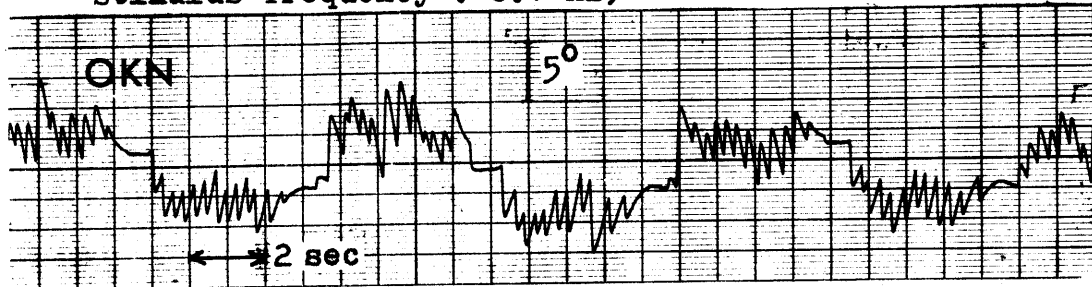
Fig. 7.1-a shows a typical vestibular nystagmus trace obtained by rotating a human sinusoidally about the earth-vertical axis. In otology, the significance of the slow phase component of vestibular nystagmus has been stressed because of its assumed relationship to semicircular canal cupula displacement (Steinhausen; 1931; Van Egmond et al, 1949). A number of subsequent single unit recordings of vestibular afferent fibres in various animals further support this assumption (Ross, 1936; Adrian, 1943; Gernandt, 1949; Groen, Lowenstein and Vendrik, 1952; Jones and Milsum, 1967, 1970; Goldberg and Fernandez, 1969).

However, it is apparent, according to this record, that not only slow phase but also the average over-all eye movement behaves in a nearly sinusoidal fashion related to the applied stimulus. Whereas both slow and fast phase components are examined in clinical nystagmography, this observation emphasizes the importance of studying both nystagmus components not separately but in terms of their topological relation that leads to the above particular feature of the over-all eye movement. Yet, in contrast to the substantial volume of research information as to slow phase characteristics, such an over-all behavior of vestibular nystagmus has not received much attention except from several investigators as referenced subsequently.

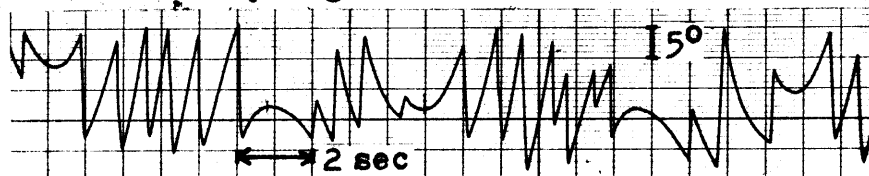
(a) Vestibular nystagmus in human (stimulus frequency : 0.1 Hz)



(b) Optokinetic nystagmus ("Stare" type) in human (stimulus frequency : 0.1 Hz)



(c) Vestibular nystagmus in rhesus monkey (Young, 1973)

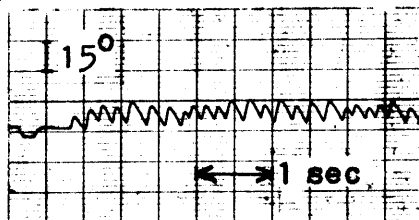


(d) OKN in rabbit (Collewijn et al, 1971)

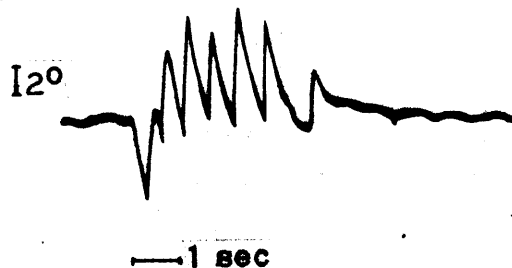


Figs. 7.1 Various nystagmus eye movement patterns. notice : (1) Fast phase shift is in direction away from center position, (2) Mean over-all eye position deviates in direction opposite to slow phase movement.

(a)



(b)



Figs. 7.2 Post-rotatory vestibular nystagmus : (a) in human and (b) in the pike, from ten Kate (1969).

As evident in Fig. 7.1-a, average eye position is about  $180^{\circ}$  out of phase relative to slow phase velocity. (Accordingly, Jones (1964) described this characteristic feature as "anti-compensatory" movement.)

A similar periodic pattern can be observed with optokinetic nystagmus of "stare" type induced by a sinusoidal motion of the stripe-pattern. Such OKN records have been described in the preceding chapter, and an example is reproduced here as shown in Fig. 7.1-b. The frequency of oscillation in this case was 0.1 Hz, the same as for the foregoing example of vestibular nystagmus. Despite the difference in stimulus modality, similarity between these two nystagmus patterns is so evident that it appears almost impossible to distinguish one from the other.

A visual inspection reveals the fact that fast phases are in direction away from primary position of gaze (center position) in both classes of nystagmus. This observation is quite contrary to the commonly held notion that fast phase is a centering reflex in order to reset eye position for negating accumulated drift resulting from preceding slow phase movement. Similar observations have been obtained and emphasized in the literature; for vestibular nystagmus by Jones (1964), Mishkin and Jones (1966), Schmid (1970) and Barnes (1973); for optokinetic nystagmus by Ohm (1938), Grüttner (1939) and more recently by Stark

(1969) and by Dix and Hood (1971).\*

It is this behavior of fast phase which ultimately causes the average over-all position to deflect from the neutral position toward the direction of fast phase, or in other words in the direction opposite to slow phase movement. This point is evident also in Fig. 7.2-a, which shows a typical post-rotatory nystagmus record.\*\* Consequently, in sinusoidal stimulation, mean eye position becomes about  $180^{\circ}$  out of phase with respect to slow phase velocity as observed in the both classes of nystagmus.

These relationships seem to hold in animals as well; for example, rhesus monkey's vestibular nystagmus (Fig. 7.1-c; Young, 1973), rabbit's OKN (Fig. 7.1-d; Collewijn et al, 1971) and the post-rotatory nystagmus in the pike (Fig. 7.2-b; ten Kate, 1969).

#### 7.1.2 Evidence for Common Central Control of Nystagmus Fast Phase

---

\* However, Jung (1973) cautions that the effect is variable and may even depend on alertness or instructions. Similarly, Weiss (1973) suggests dependence on volition presumably via the corticobulbar tract as based on his clinical data referenced later. In fact, apart from pathological cases discussed subsequently, some authors have described that fast phase direction is toward center position for vestibular nystagmus as opposed to the present observation, while it is away from center for OKN as confirmed here. It should be stressed then that nystagmus data dealt with in this chapter are based on the specific instruction described previously in the relevant experimental protocol (Subsection 3.4.3 for vestibular nystagmus and Subsection 6.2.2 for OKN (i.e., "stare" type OKN).

\*\* Nystagmus following a sudden stop of a constant-velocity head rotation.



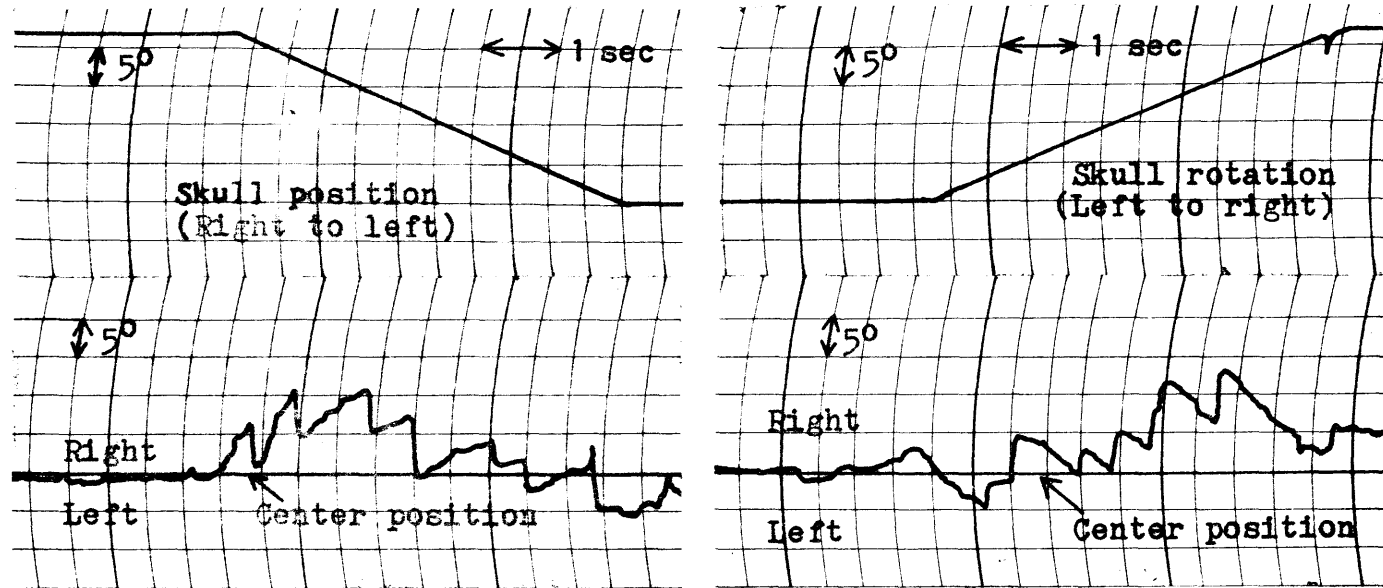
The foregoing preliminary observations suggest that this aspect of eye movement may be a characteristic of nystagmus in general, reflecting a certain common mechanism, not selective to stimulus origin but intrinsic to generation of fast phase. That is, such a mechanism would utilize probably slow phase motor information, rather than first-order afferent information that reports input stimulus of specific modality.

In support of this view, this subsection first cites a clinical case examined by Weiss (1973): The patient suffered from a large recurrent acoustic neuroma, and unilateral deterioration of the corticobulbar tract was diagnosed. Fig. 7.3 shows her vestibular and optokinetic nystagmus responses.

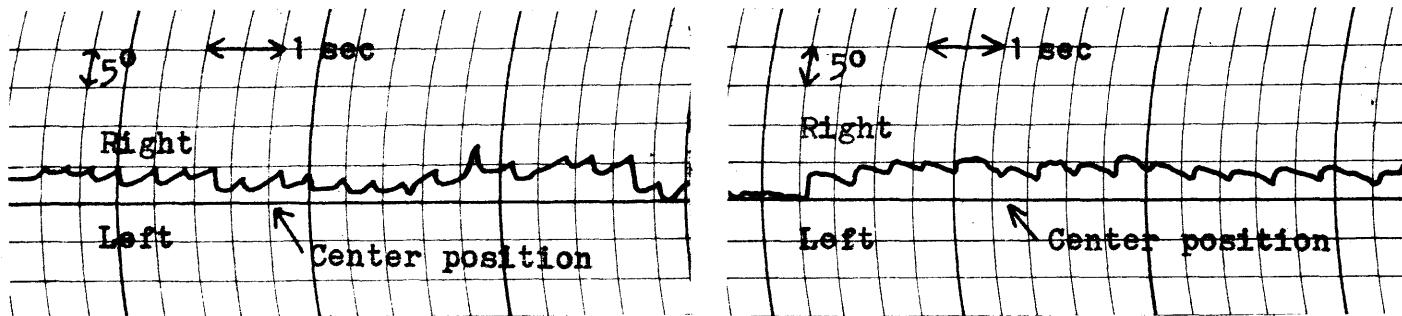
First, note that the direction of slow phase movement is normal in both nystagmus as expected from the relevant stimulus applied in either direction. However, it is apparent in both types of nystagmus that, when the slow phase is from left to right, fast phases are toward center and the mean eye position deviates to the direction of slow phase. This observation contradicts the situation in the normal case described previously. With the other direction of slow phase (right to left), however, the pertinent relationships apparently remain normal for both types of nystagmus in this particular clinical case.

In summary, the fast phase generation is unidirectionally disturbed in the same direction for vestibular and optokinetic nystagmus, apparently without affecting their slow phase response. Hence, this is good pathological evidence indicating

(a) Vestibular nystagmus



(b) OKN



Figs. 7.3 An acoustic neuroma case showing a unilateral disturbance selective to the fast phase behavior in both vestibular and optokinetic nystagmus: Fast phases are toward center with left-to-right slow phase movements, whereas the fast phase direction apparently remains normal (i.e., away from center) with right-to-left slow phase movements (Redrawn from data by Weiss; 1973).

that the two types of nystagmus, though mediated by different sensory modalities, share a common central mechanism for generating their slow phase component.\* Further, the unidirectional fast phase disturbance undoubtedly reflects the unilateral damage in the corticobulbar tract of this patient. And, as Weiss (1973) suggests, this may in turn imply that the corticobulbar tract has an important parametric influence upon the presumed fast phase generating mechanism, if not it is essential to the fast phase generation per se.\*\*

Another line of evidence for the common origin of nystagmus fast phase component comes from a number of neuroanatomical studies. The vestibular nuclei, for instance, must be precluded from the corresponding common anatomical site, for visual oculomotor pathways do not go through the vestibular nuclei and, in fact, neither fixation saccades nor OKN were much affected by vestibular nuclei lesions (Uemura and Cohen, 1972). Visual fixation saccades are phenomenologically similar to nystagmus fast phase in their quick response feature as well as periodic intermittence. Earlier, based on a multi-input behavioral evidence along with gross anatomical consideration of the oculomotor system, Stark et al (1965b) suggests that the location of the "intermittent operator" is, at least, below the level of the

---

\* Similar findings exist in patients with unilateral infarction of middle cerebral artery territory (Weiss, 1973).

\*\* The corticobulbar tract descends from area 8, the frontal eye fields in the cortex (Crosby et al, 1952; Levin, 1936; Brucher, 1966). The generally accepted belief based on indirect evidence (for example, Holms, 1938) is that the frontal eye fields are associated with voluntary saccadic eye movements.

accessory vestibular nuclei and above the oculomotor nuclei.\*

Recent studies show that neural events\*\* in the pontine reticular formation precedes each rapid eye movement (Cohen and Feldman, 1968; Henn and Cohen, 1971), and that lesions of this area cause profound changes in horizontal fixation saccades and fast phases of nystagmus to the ipsilateral side (Bender and Shanzer, 1964; Cohen et al, 1968; Coebel et al, 1971). Based on this information, Cohen (1969 and 1971) suggests that saccades and fast phases of optokinetic and vestibular nystagmus in the horizontal plane are probably generated primarily in the pontine reticular formation.\*\*\* Robinson (1969) maintains a similar view and has proposed some hypothetical neural organization for the vestibular nystagmus fast phase generation at this region of the brainstem.

In view of these evidence and discussions in this subsection, it appears that a neural mechanism common for vestibular and optokinetic nystagmus fast phases (probably including visual fixation saccades as well) exists in the pontine reticular formation, but that its operational settings are adjusted by auxiliary signals conveyed from the frontal eye fields via descending fibres of the corticobulbar tract.

---

\* Their consideration includes the compensatory oculomotor reflex originating in the neck stretch receptor. This eye movement generally lacks the fast phase component.

\*\* A rapid eye movement, either nystagmus fast phase or fixation saccade, is known to occur with a burst of neuron firing whose duration determines the eye movement's amplitude (Schaefer, 1965; Yamanaka and Bach-y-Rita, 1968; Horcholle and Tyc-Dumout, 1968; Robinson and Keller, 1971).

\*\*\* Classically, Lorente de N6 (1933) has shown that the vestibulo-ocular reflex incorporates polysynaptic pathways in the pontine reticular formation in addition to the three-neuron reflex arc described by Szent6gothai (1950).

## 7.2 Experimental Results and Discussions

On the basis of relevant vestibular and optokinetic nystagmus data accumulated earlier in this thesis, this section attempts to define more quantitatively the foregoing preliminary nystagmus observations by the author. It is hoped that such an assessment provides a further insight into the particular behavior of nystagmus fast phase in question as well as a clue to substantiate the fast phase generating mechanism common for both nystagmus as presumed in the preceding section.

### 7.2.1 Response to Constant Velocity Stimuli: Linear Relations

As noted previously, in addition to slow phase movements, average over-all response behaves essentially sinusoidally under sinusoidal stimulation. This suggests that the underlying system responsible for the average eye deviation is a linear process. In order to examine this possibility, it is desirable to obtain constant slow phase velocity persisting for a long interval. Slow phase velocity could then be treated as an independent variable. However, it is usually not practical for vestibular nystagmus to maintain a constant slow phase velocity, due to the semicircular canal's inherent response dynamics.

Instead, this demand was sufficed by OKN whose slow phase rose almost instantly to match input velocity with no apparent decay thereafter as noted in Chapter VI. Analysis was performed on OKN data obtained in Chapter VI for various levels of stimulus

speed with occasional directional reversals in the stimulus field motion. (OKN studied here thus corresponds to the "stare" type as defined in section 2.2.) Fig. 7.4 gives representative records with different magnitudes of stripe velocity. At first glance of these traces, the shift of mean over-all eye position increases with increasing slow phase velocity.

Crucial information for the present study was absolute eye position with respect to the center position. Using the photoelectric eye movement monitor, DC measurement over long periods was difficult. This was in part due to some DC drift inherent with the eye movement monitor employed and also because of possible small head movements. However, during the short time interval in which the OKN stimulus motion was reversed in direction, fairly reliable retrieval of absolute eye position was possible by considering position of both pre and post-reversal groups of nystagmus beats: The center position was assumed to lie at mid line between the two average positions of pre- and post-reversal nystagmus beats which deviated to opposite directions. Evaluation of relevant nystagmus parameters was based upon averaging a number of nystagmus beats collected only from such particular intervals that appeared several times in each run. Twenty to thirty successive beats, excluding the first few beats immediately following the reversal, were considered in each of these short intervals.

Fig. 7.5 schematically defines nystagmus parameters pertinent in the subsequent discussion: For the left-to-right

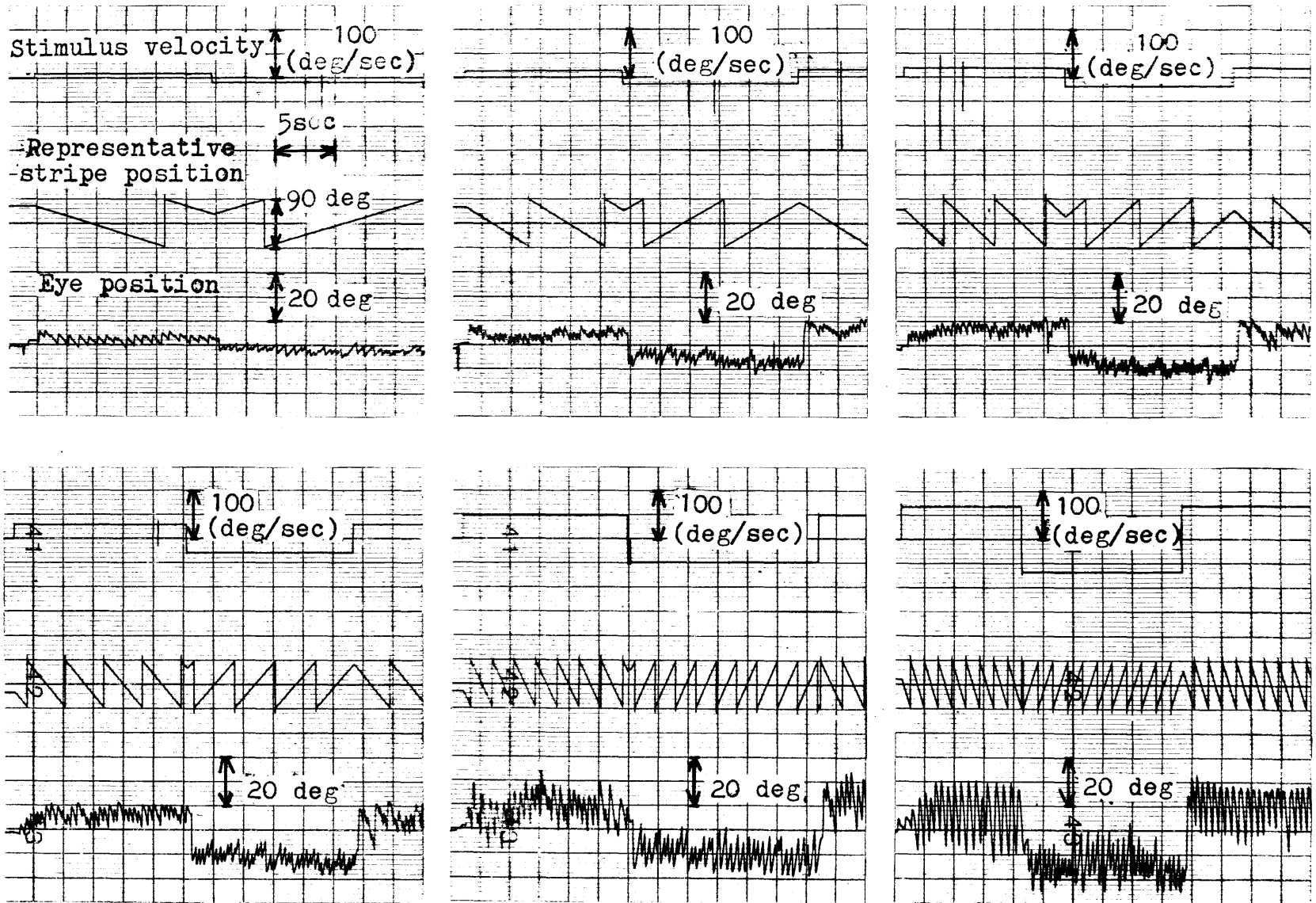


Fig. 7.4 OKN responding to various constant stimulus speeds with sudden reversals of stimulus field motion. Note that the shift of mean over-all eye position (or that of "fast phase reset position") increases with increasing slow phase velocity.

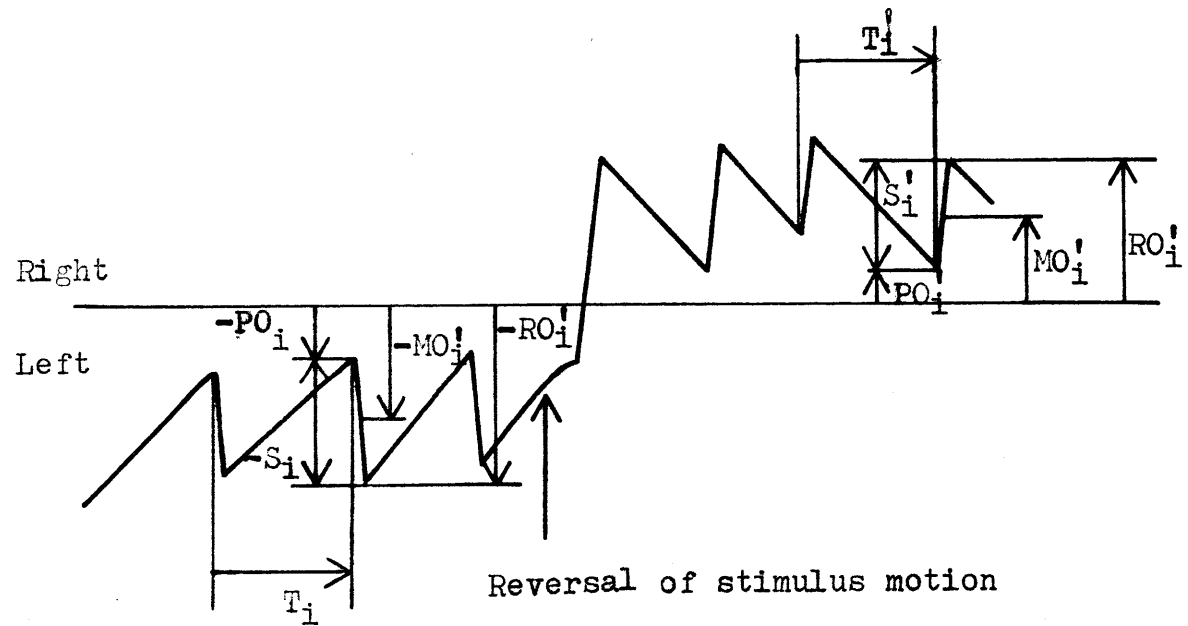


Fig. 7.5 Schematic illustration for nystagmus parameters



(temporal) i'th beat\*;

$V_i$  ; slow phase velocity(just prior to fast phase)

$S_i$  ; fast phase size (including polarity)

$T_i$  ; time interval to next fast phase

$MO_i$  ; eye position midway in fast phase jump (representing mean position for i'th beat)

$PO_i$  ; position just prior to fast phase

$RO_i$  ; position immediately after fast phase (reset position)

(Primed versions of these symbols indicate corresponding counterparts of right-to-left (nasal) nystagmus beats.) Statistical averages for  $S_i$ ,  $T_i$ ,  $MO_i$ ,  $PO_i$  and  $RO_i$  over many beats ( $i = 1, 2, \dots, n$ ) are designated by  $S$ ,  $T$ ,  $MO$ ,  $PO$  and  $RO$  respectively.

$v$  represents average slow phase velocity computed according to

$v = (S_1 + S_2 + \dots + S_n)/(T_1 + T_2 + \dots + T_n)$ . Total number

of OKN beats,  $n$ , considered in these statistical calculations

ranged from 50 to 100, depending on a particular run. Average

reset position,  $R$ , was determined finally by  $R = (RO - RO')/2$

for temporal and by  $R = -(RO - RO')/2$  for nasal nystagmus.\*\*

Average mean position,  $M$ , and average position preceding fast

phase,  $P$ , were calculated analogously.

First, average reset position,  $R$ , is plotted against average slow phase velocity  $v$  ( $v$  now stands for previous  $v$  and

---

\* Only the right eye's movement was measured and analyzed.  
\*\* When difference between pre- and post-reversal slow phase velocity magnitudes exceeded 15% level for any reason, the whole portion of such a record was not considered in analysis.

v' inclusively) for each subject, as presented in Fig. 7.6.\*

A relatively good linear relationship was found, as approximated by a straight line ;

$$R = -k_1 v \quad (7-1)$$

with best fit values (subjectively judged) for  $k_1$  as given for individual subjects in the numerical summary, Table 7.1, presented at the end of this subsection. Negativity of the proportionality constant, i.e.,  $-k_1$ , accounts for the fact that a fast phase movement resets the eye away from the center position in the direction opposite to slow phase movement, i.e., in the direction from which new stripes were coming.

Average size of fast phase saccade was also linearly related to average slow phase velocity as shown in Fig. 7.7:

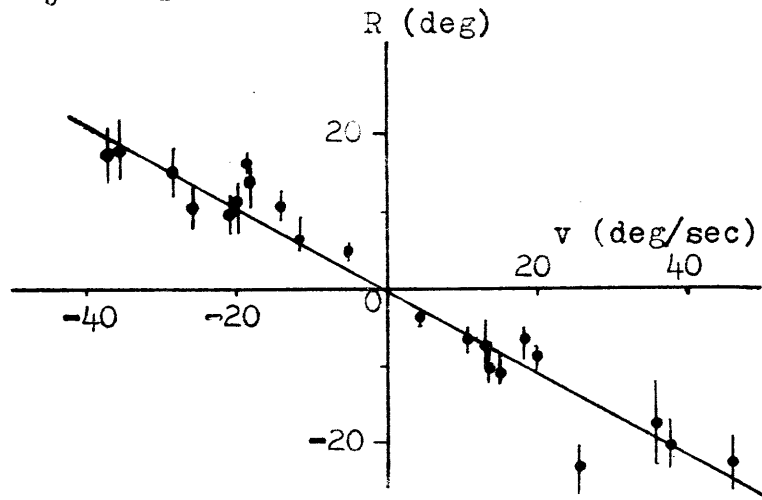
$$S = -k_2 v \quad (7-2)$$

Value for  $k_2$  is estimated and listed in Table 7.1 for each individual subject. However, this linear result is what may be expected from the steady-stage equilibrium condition of nystagmus: In order for OKN to maintain stable continuation, fast and slow phase components must balance each other during the average nystagmus beat, that is :

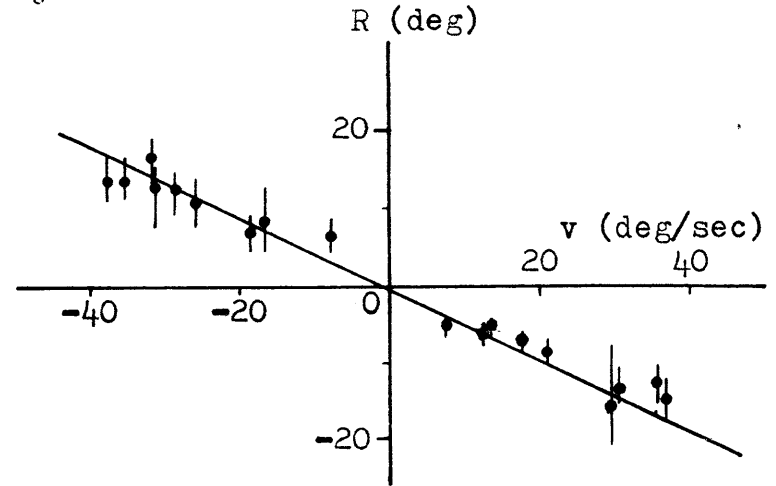
---

\* It is important to remember that abscissa in Fig. 7.6 does not indicate the stimulus velocity, nor does it represent maximum instantaneous slow phase velocity as evaluated in the previous chapter.

Subject TY



Subject SY



Subject JT

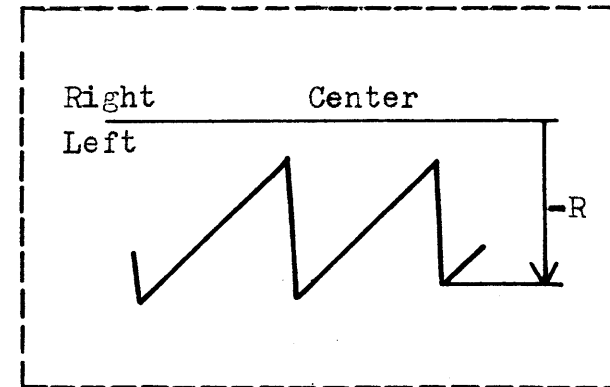
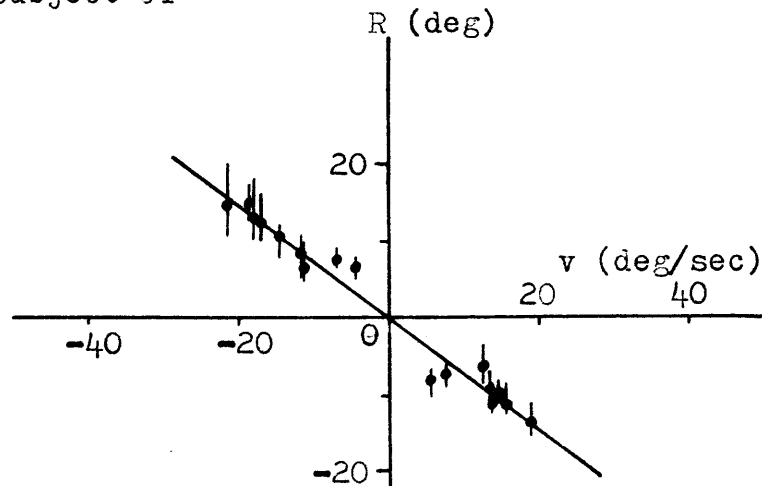


Fig. 7.6 OKN average reset position,  $R$ , versus average slow phase velocity,  $v$ . Each data point represents  $R$  in median value (with vertical bars indicating plus-minus one standard deviation), considering a number of successive nystagmus beats (50 to 100 beats) obtained with constant stimulus velocities. Straight line fit,  $R = -k_1 v$ , is given.

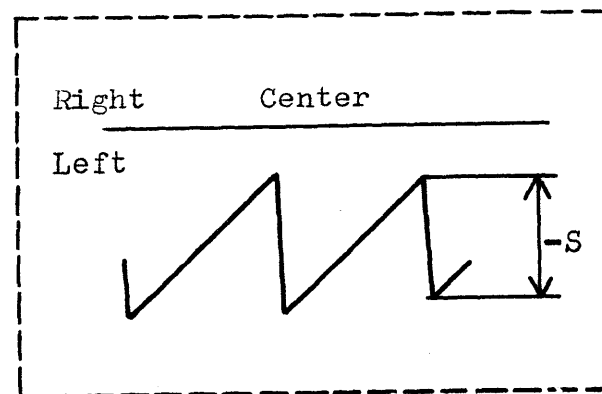
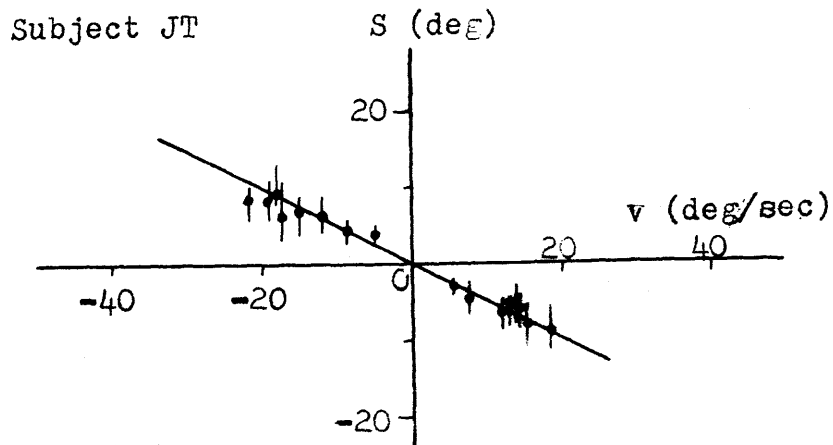
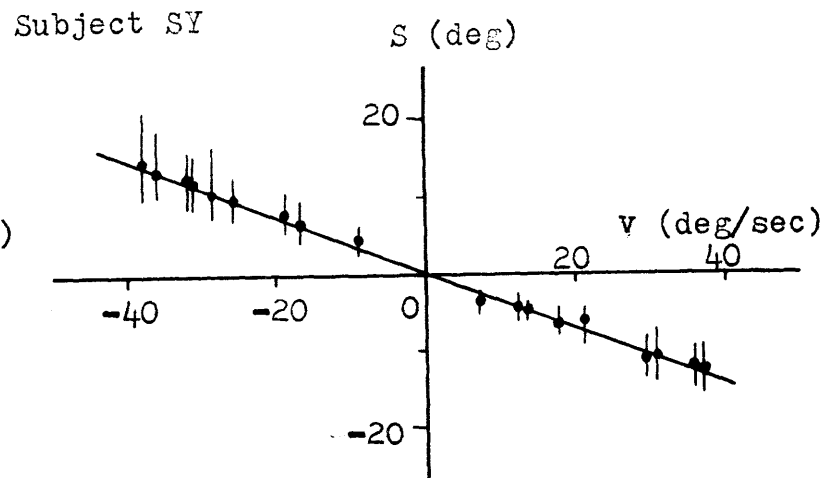
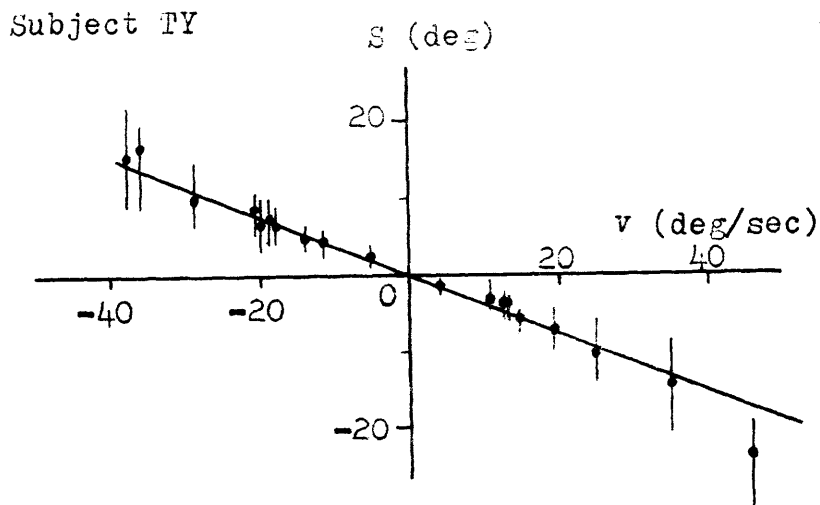


Fig. 7.7 OKN average fast phase size,  $S$ , versus average slow phase velocity,  $v$ . Each data point represents  $S$  in median value (with vertical bars indicating plus-minus one standard deviation), considering a number of successive nystagmus beats (50 to 100 beats) obtained with constant stimulus velocities. Straight line fit,  $S = -k_2 v$ , is given.

$$S = -Tv \quad (7-3)$$

where T represents average interval between two successive fast phase movements. As is apparent from Fig. 7.8, T was not strongly affected by v, but rather was approximately constant for a given subject.\* Accordingly, Eq. (7-3) basically describes a linear relation, and hence T identifies itself as  $k_2$  in Eq. (7-2). This point can be confirmed by observing the close relationship between T and  $k_2$  in their values obtained for each subject as given in Table 7.1.

Next, average mean over-all position, M, is plotted against average slow phase velocity in Fig. 7.9. Presence of all data points in second and fourth quadrants implies that deviation of mean over-all eye position was in the direction opposite to slow phase response. Further, despite considerable scattering of data points, there was some trend of linear relation between M and v within individual subjects. This can be accounted for as follows. By definition, M, is expressed as:

$$M \equiv R - \frac{1}{2}S \quad (7-4)$$

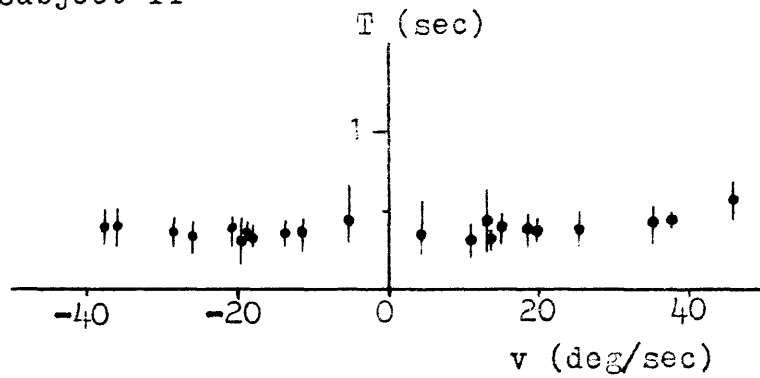
From Eq. (7-1) and (7-3), this becomes:

$$M = -k_3v \quad (7-5)$$

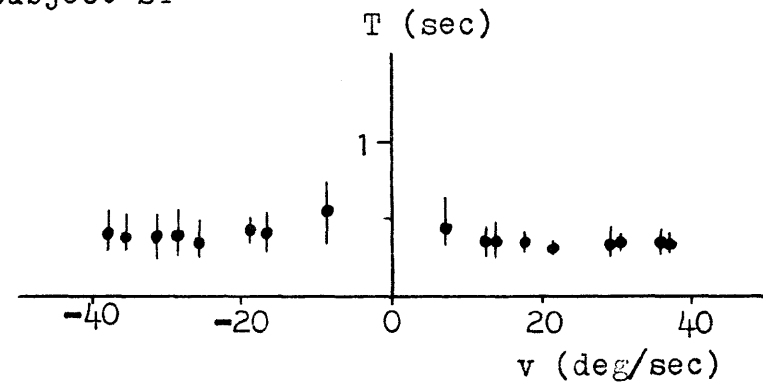
---

\* There was some increase at low stimulus speeds for subjects SY and JT, however.

Subject TY



Subject SY



Subject JT

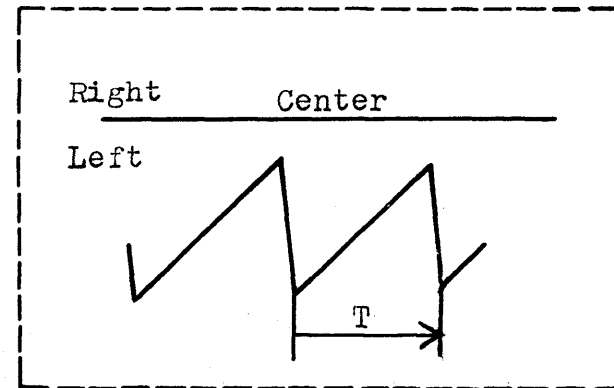
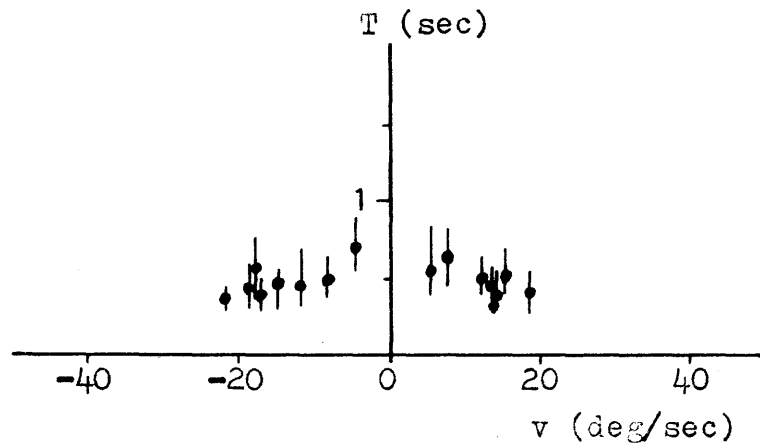


Fig. 7.8 OKN average fast phase interval,  $T$ , versus average slow phase velocity,  $v$ . Each data point represents  $T$  in median value (with vertical bars indicating plus-minus one standard deviation), considering a number of successive nystagmus beats (50 to 100 beats) obtained with constant stimulus velocities.

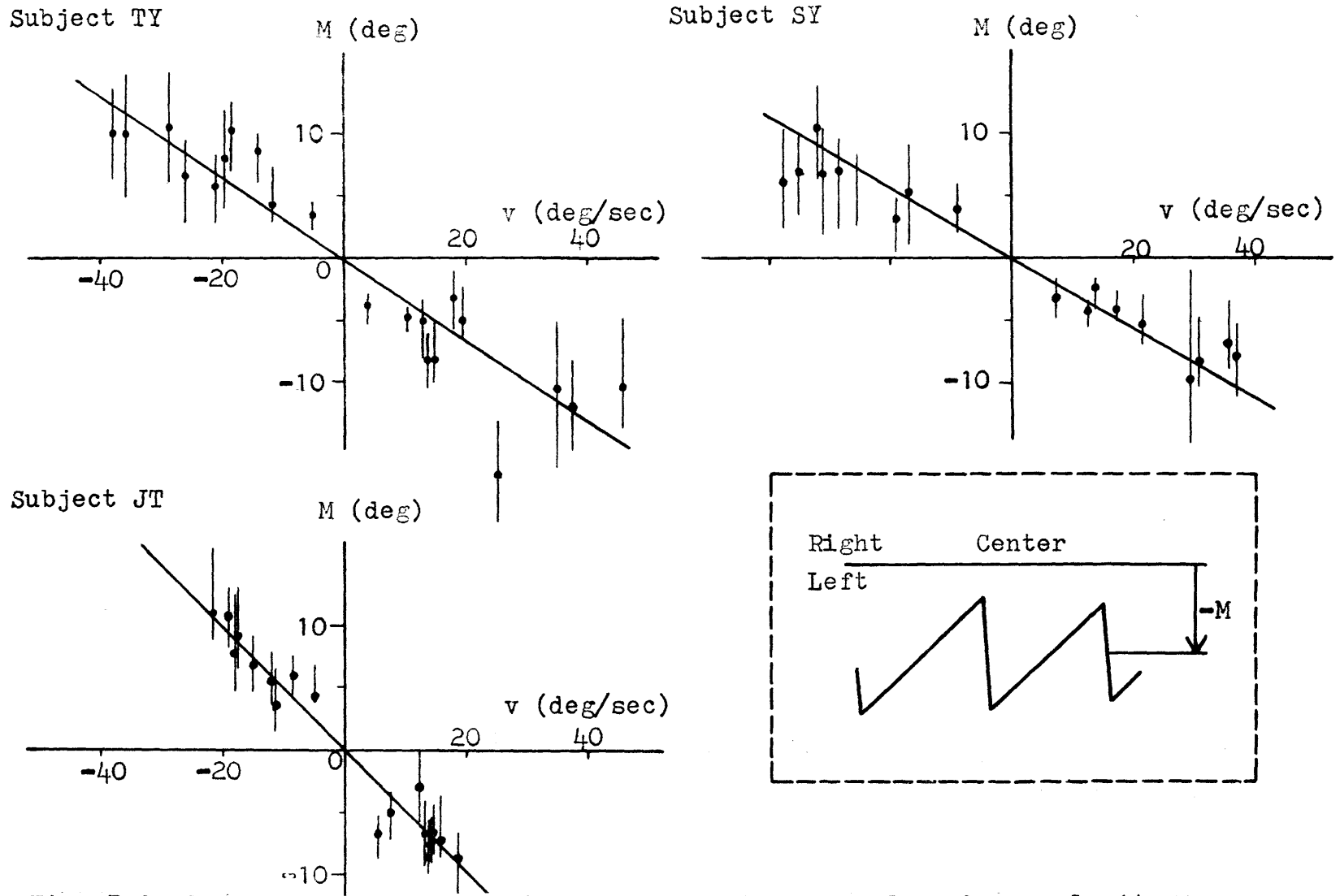


Fig. 7.9 OKN average mean position, M, versus average slow phase velocity, v. Each data point represents M in median value (with vertical bars indicating plus-minus one standard deviation), considering a number of successive nystagmus beats (50 to 100 beats) obtained with constant stimulus velocities. Straight line corresponds to prediction,  $M = -k_3 v$ , where  $k_3 = k_1 - T/2$ .

$$\text{where, } k_3 = k_1 - T/2 \quad (7-6)$$

$k_3$  was computed according to Eq. (7-6) using previous values for  $k_1$  and  $T$ , and the result is given in Table 7.1. The corresponding linear prediction by Eq. (7-5) is indicated in Fig. 7.9 showing a general agreement with the data as expected.

Finally, it is possible to account for not only deviation of mean and reset position as above, but also shift of the whole eye position to one particular side of the visual field (see traces as given in Fig. 7.4) depending on the direction of slow phase movement. Compare the average size of fast phase with average reset position (in absolute value) at a given slow phase velocity. The former (Fig. 7.7) was somewhat less than the latter (Fig. 7.6), implying the above point. Formally, position just prior to fast phase,  $P$ , is given by:

$$P = R - S \quad (7-7)$$

From Eq. (7-1) and (7-2), this can be rewritten as:

$$P = -k_4 v \quad (7-8)$$

$$\text{where, } k_4 = k_1 - k_2 \quad (7-9)$$

For each subject,  $k_1 > k_2$ , and hence  $k_4$  gives a positive value as shown in Table 7.1. As a result, execution of successive



nystagmus beats was confined within range between  $-k_4v$  and  $-k_1v$ , which occupied one side of the visual field opposite to the direction of slow phase movement.

	Subject		
	TY	SY	JT
T	0.35	0.37	0.50
$k_1$ ; R = $-k_1v$	0.50	0.45	0.75
$k_2$ ; S = $-k_2v$	0.40	0.38	0.50
$k_3$ ; M = $-k_3v$	0.33	0.28	0.50
$k_4$ ; P = $-k_4v$	0.10	0.07	0.25

Table 7.1 Numerical summary (all units in sec): Fast phase interval and various proportionality constants in relation to average OKN slow phase velocity. Note  $k_3 = k_1 - T/2$ .

### 7.2.2 Sinusoidal Response

Optokinetic and vestibular nystagmus have been recorded under sinusoidal stimulation as described in the previous chapters. Representative traces with various frequencies and for different subjects are presented here in Fig. 7.10 (OKN) and in Fig. 7.11 (vestibular nystagmus).

The nystagmus parameters (reset position R, mean position M, amount of fast phase jump S, and fast phase interval T) were

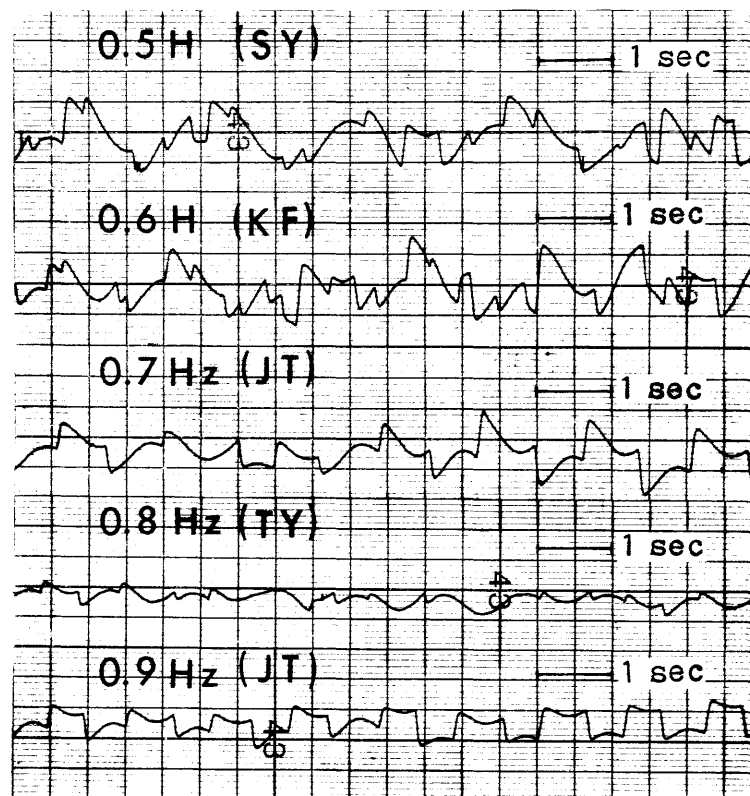
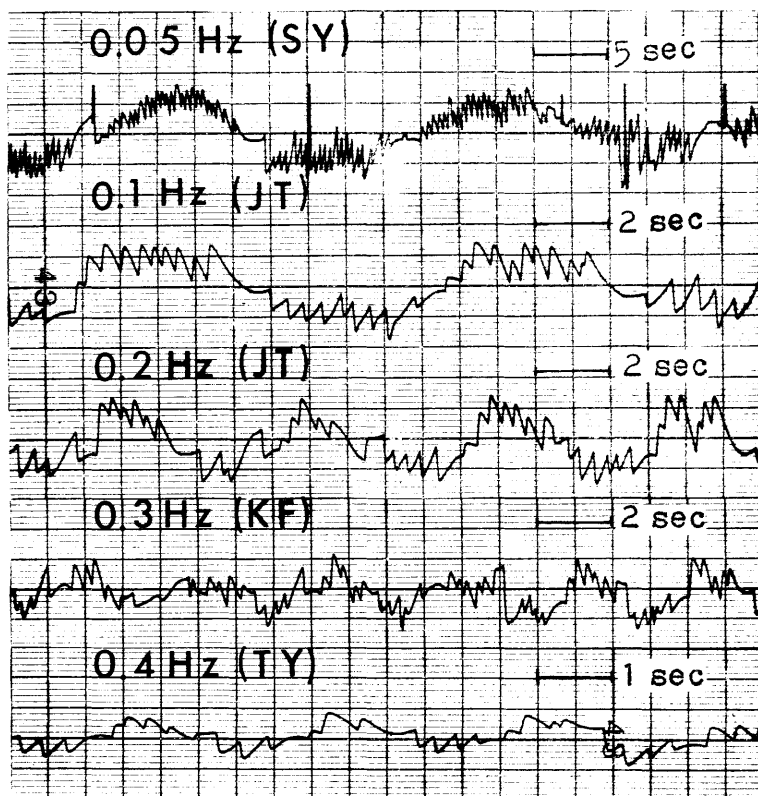


Fig. 7.10 Representative OKN patterns for various frequencies with different subjects. "Fast phase reset position" tends to be about 180° out of phase relative to slow phase velocity, as evident particularly at low frequencies.

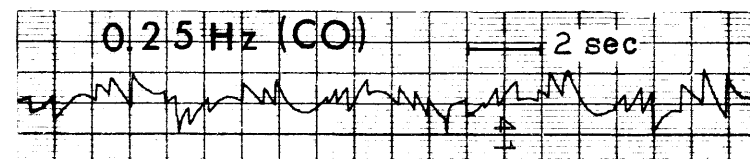
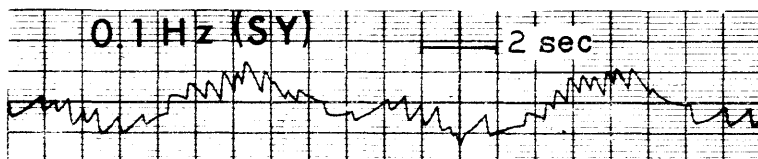


Fig. 7.11 Typical vestibular nystagmus patterns. Behavior of fast phase is similar to that of OKN.

measured for each nystagmus beat in terms of phase angle relative to slow phase velocity whose average profile maintained a sinusoidal shape. These data points were accumulated over several cycles for each trace in order to assess average trend. Examples of such results are depicted in Figs. 7.12 for OKN and vestibular nystagmus.

From the above original as well as cumulative data, nystagmus parameters, R, M, and S appear to exhibit some degree of phase lead from exact  $180^{\circ}$  phase shift relative to slow phase velocity. Further examination and discussion on the sinusoidal case will be given in the later part of the following section.

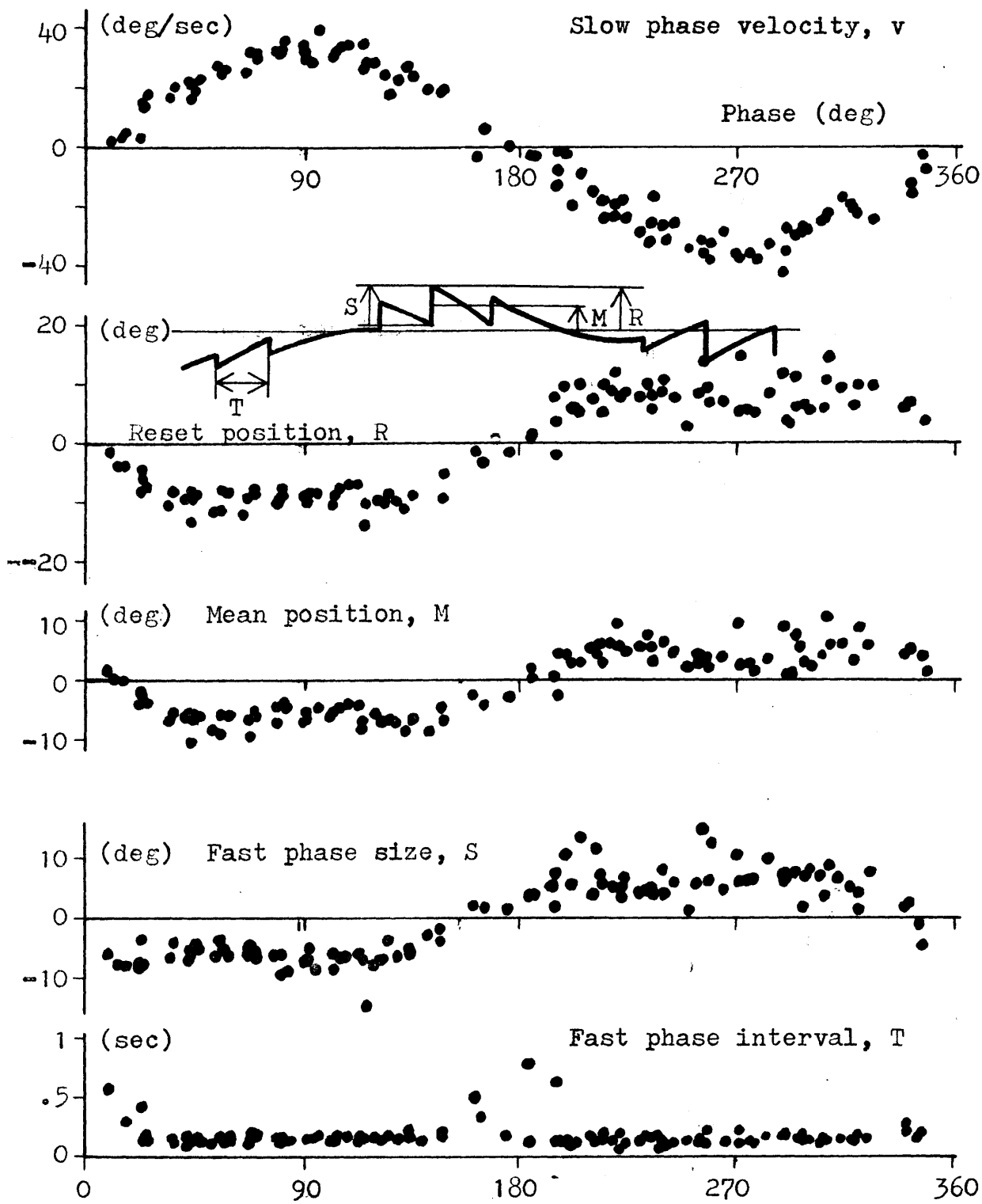


Fig. 7.12-a Typical behavior of OKN parameters with respect to slow phase velocity's phase angle under sinusoidal stimulation (0.1 Hz, Subject : TY). Data points were accumulated over 4 cycles.

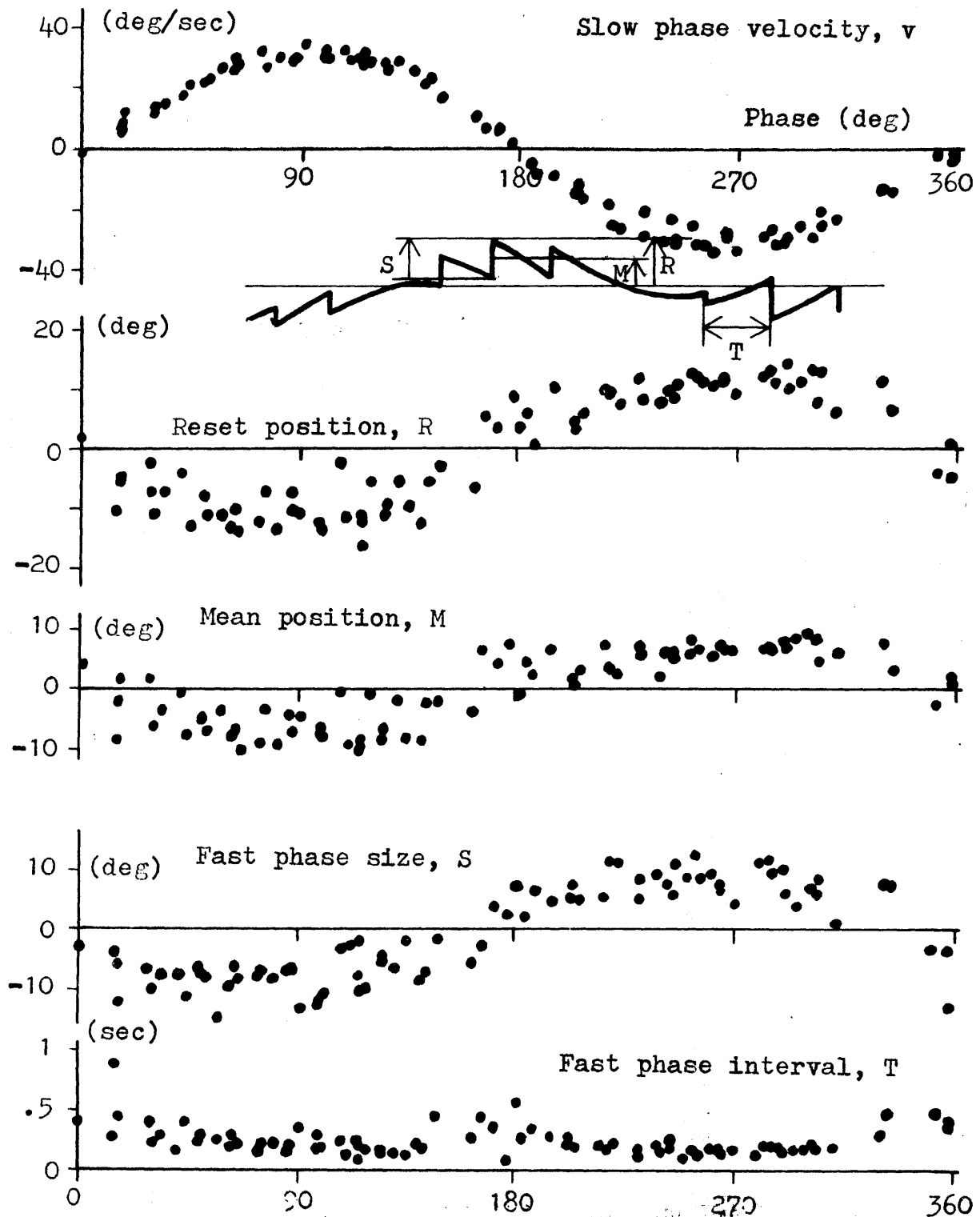


Fig. 7.12-b Typical behavior of vestibular nystagmus parameters with respect to slow phase velocity's phase angle under sinusoidal stimulation (0.1 Hz, Subject: SY). Data points were accumulated over 5 cycles.

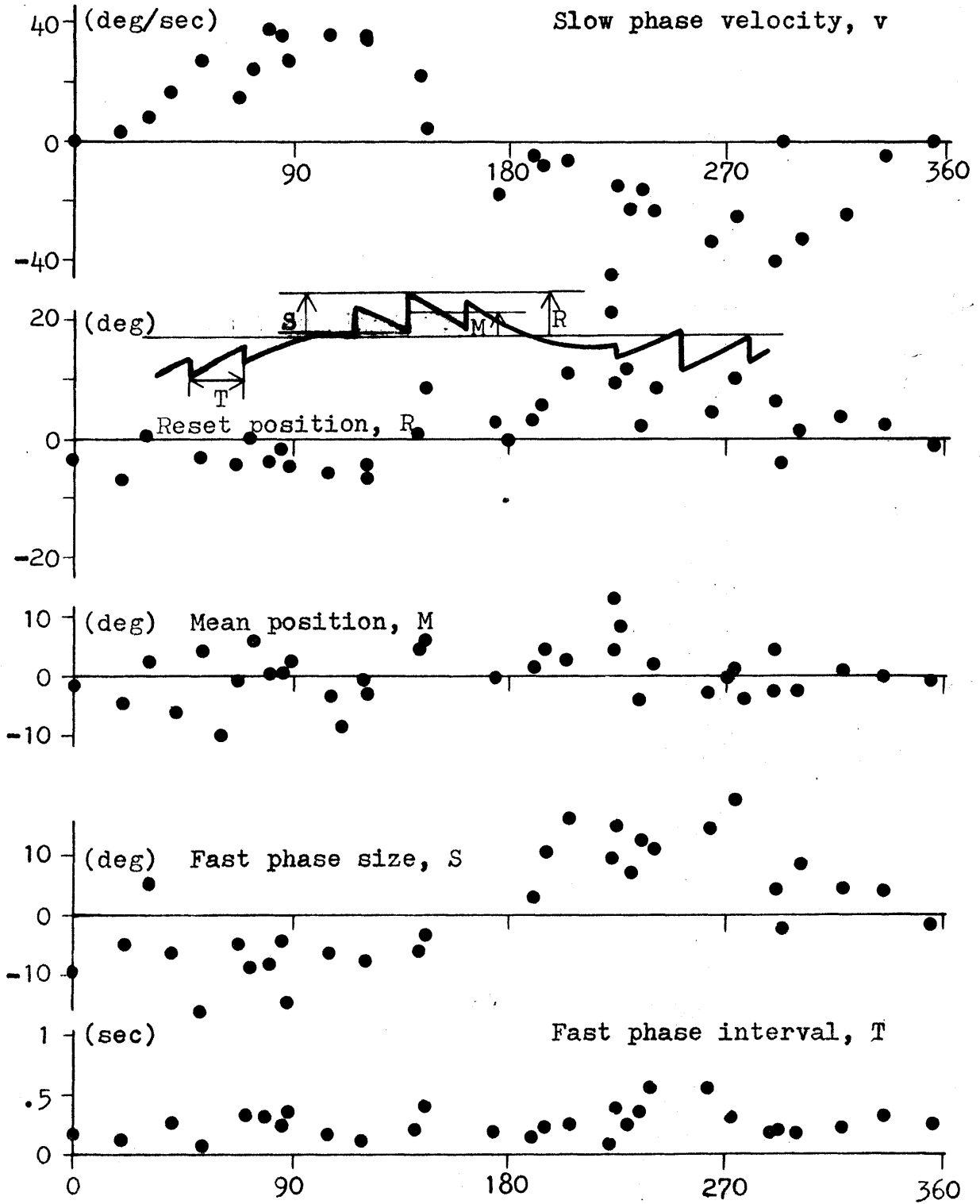


Fig. 7.12-c Typical behavior of OKN parameters with respect to slow phase velocity's phase angle under sinusoidal stimulation (0.5 Hz, Subject : SY). Data points were accumulated over 9 cycles.

### 7.3 A System Engineering Model

#### 7.3.1 Functional Implication

It is shown for both OKN and vestibular nystagmus that mean over-all eye position tends to shift in direction opposite to slow phase movement. This means that fast phase brings eye position toward where new visual objects are coming from (OKN) or to where new visual surroundings are expected to arise following a head movement (vestibular nystagmus). It appears that nystagmus eye movement may not only act to help stabilization of retinal images by means of compensatory slow phase movements, but also, at the same time, may assist in acquisition of new visual information by means of fast phase. A similar interpretation for the role of fast phase has been given by Stark (1969) for OKN, and by Barnes and Benson (1973) for vestibular nystagmus.

#### 7.3.2 Conceptual Description of Models

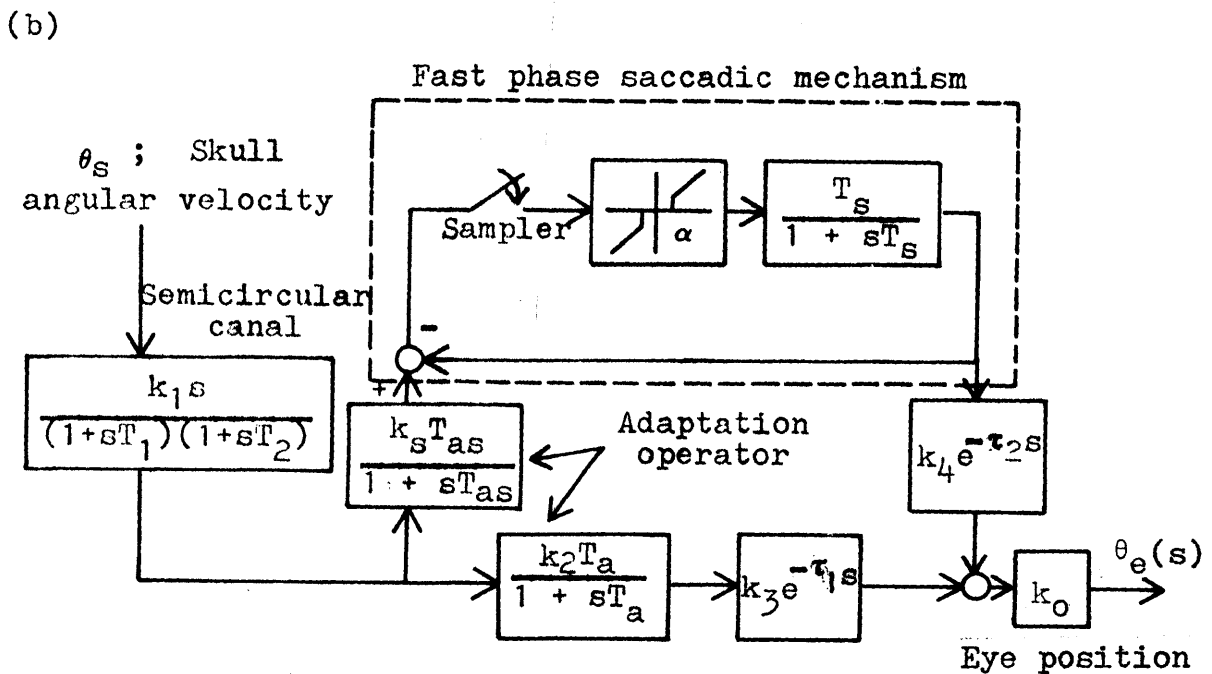
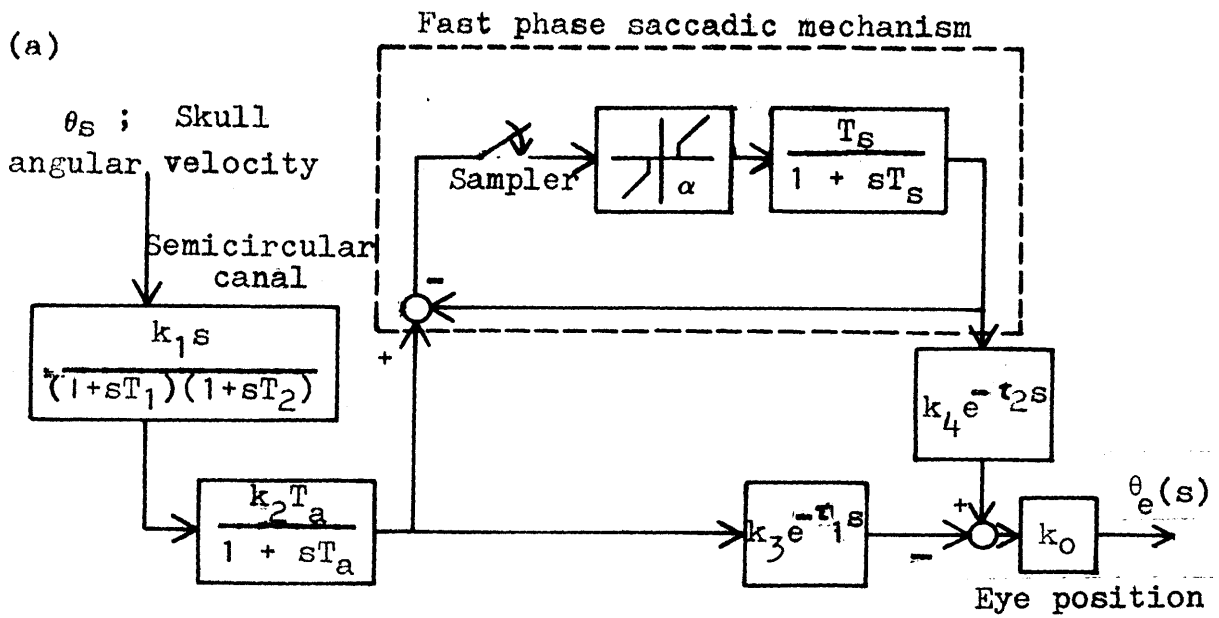
For vestibular nystagmus, Schmid has attempted to represent the present aspect of the oculomotor system in a mathematical models. His earlier models (Schmid, 1970; Schmid and Stefanelli, 1970) assumed proprioceptive feedback from the extraocular muscles. These models incorrectly predicted fast phase reset position to shift in the same direction as slow phase movement. But later he removed the proprioceptive feedback

path, and proposed a revised scheme, which operates on a slow phase efferent signal instead of feedback information. Figs. 7.13 reproduce two such alternatives of Schmid (1971), retaining his original notation. These versions effectively account for the adaptive behavior of the vestibular nystagmus slow phase as modelled by Young and Oman (1969; see Section 2.3), and include a low-pass filter placed after fast phase saccadic sampler as similar to the scheme proposed by Sugie and Jones (1965 and 1966; see Section 2.3) for vestibular nystagmus generation. Schmid has indicated that these models can predict the essential features of vestibular nystagmus pattern with the right direction of reset position, provided that  $\tau_1 > \tau_2$  in Fig. 7.13-a and  $T_a > T_{as}$  in Fig. 7.13-b if appropriate values are given for relevant parameters.

Stimulated by Schmid's early attempts and based upon the preliminary version of OKN data in this thesis, this author (1970) suggested in a thesis proposal a model with a feedforward structure similar to the above revised configuration of Schmid. However, unlike Schmid's revised scheme, this model does not assume a low-pass filter of Sugie-Jones type, nor does it relate itself specifically to the slow phase adaptation behavior.

Recently, Barnes and Benson have published another system engineering model for vestibular nystagmus generation, which also employs the efferent-feedforward concept, and can account for the observed behavior of the fast phase reset position and consequently the average eye deviation (Barnes, 1973; Barnes





Figs. 7.13 Recent versions of Schmid's model for vestibular nystagmus generation (parameters as defined in Schmid, 1971)

and Benson, 1973)\*.

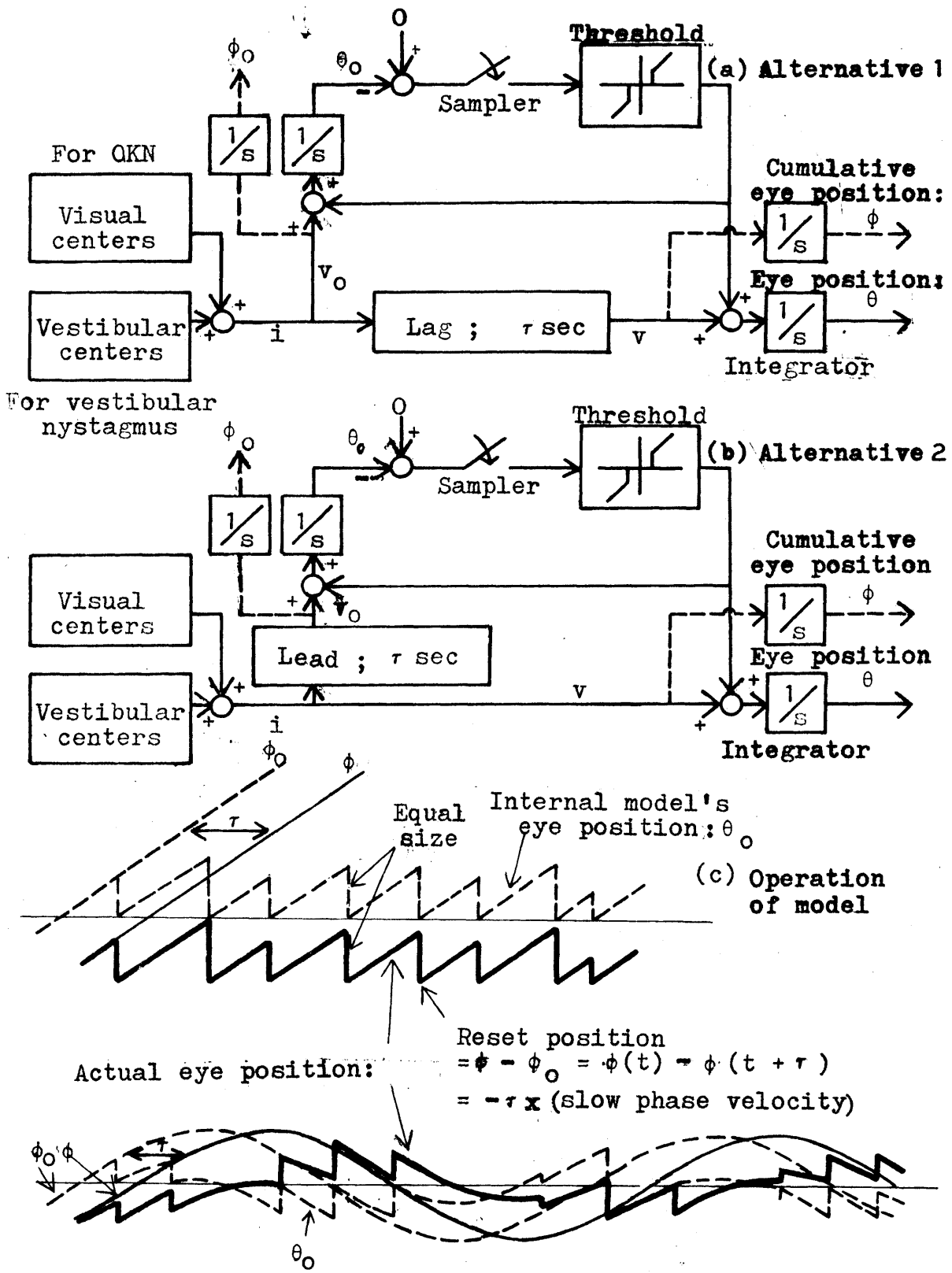
In contrast with these models by others, the model proposed herein appears somewhat simpler in its operational scheme. More importantly, in accordance with the preceding discussions from various viewpoints, the model focuses upon the fast phase generation of nystagmus irrespective of the stimulus origin, and thus it is intended to account for the characteristic over-all response pattern not only for vestibular nystagmus but also for OKN.

The underlying central concept is the assumption that the mechanism for fast phase generation utilizes slow phase efferent information slightly ahead of time relative to slow phase movement of the actual eye. In Figs. 7.14 are shown two such alternative configurations, both of which incorporate the same organization for generating fast phase. The difference between these two lies in the way of achieving the above relative transport time difference in the slow phase signal transmission: A lag element is cascaded in the primary slow phase path leading to the actual eye in Fig. 7.14-a, while a lead element operates upon the slow phase efferent copy message in Fig. 7.14-b.\*\* The relevant slow phase pathways convey slow phase velocity signal given by the model's input,  $i$ , which in turn originates either from vestibular centers (for vestibular nystagmus) or from

---

\* Instead of adopting the sampler-threshold unit for triggering fast phases as in other models including the author's, Barnes and Benson introduced the gate controlled by the feedforward signal. Similarly, Robinson (1969) proposed the principle of one-shot multivibrator for fast phase generation.

\*\* Question of appropriate type for lead (lag) element, i.e., for example, choice between pure lead (lag) and first-order lead (lag), will be discussed later.



Figs. 7.14 Model proposed to account for the observed nystagmus pattern, and illustration for its operation.

visual centers (for OKN)\*. As in the aforementioned models by others, the fast phase generator is essentially an internal model that "simulates" nystagmus eye movement based on the efferent motor information: The brain "computes" what the actual eye movement should be, instead of "measuring" it through the proprioceptive feedback. It is position error of the internally-simulated eye movement, which determines direction and magnitude of each fast phase movement, S. The functional structure of this internal fast phase generator is, in fact, analogous to that of Young's sampled-data saccadic model (1962), which deals with control of corrective saccades in the visual tracking situation. It is assumed in order to simplify the subsequent analysis that a fast phase is executed in both actual and internally-simulated eye at the same instance\*\*.

In the present model, the internally simulated eye position resets itself exactly at the center upon completion of a saccade. However, this is not true for the actual eye position due to the relative transmission time delay in producing actual slow phase component. The upper schematic trace in Fig. 7-14-c illustrates

---

\* Each integrator,  $1/s$ , in Figs. 7.14 must be placed after the corresponding summing junction of fast and slow phase components. Otherwise (i.e., separate integrators before mixing), the cumulative slow phase position would actually exist in the model, which would be physically impossible in reality: Consider, for example, OKN with a constant stimulus velocity, whose cumulative eye position would correspond to an ever increasing ramp signal with no limit.

\*\* A certain relative delay could be assumed similarly for execution of actual fast phase saccade without affecting essential points of the following analysis, provided that it is smaller than relative delay in actual slow phase movement as assumed here.

this point for the case of a constant slow phase velocity: From the actual eye's point of view, it appears as if fast phases were executed on the basis of "future" eye position. As a result, the actual eye position deviates from the center in direction of fast phase jump. The deviation is independent of frequency of fast phases. But, it is determined only by the relative slow phase time lag,  $\tau$ , so that the amount of deviation becomes proportional to slow phase velocity magnitude with  $\tau$  as proportionality constant.

Similarly, the lower drawing in Fig. 7.14-c depicts the model behavior corresponding to the case of a sinusoidal stimulus. Note the correct prediction with respect to direction of fast phases as well as phase relation between reset position and slow phase velocity.

According to the model, the system "attempts" to reset the eye exactly at the center position by each fast phase, in much the same way as Young's sampled-data describes the corrective saccadic movement for the visual fixation. But the inherent relative time lag as postulated here in the slow phase efferent interferes with such a goal. However, from the functional viewpoint as discussed in Subsection 7.3.1, this deviation actually can be interpreted as a useful feature in both vestibular and optokinetic nystagmus.

### 7.3.3 Model Analysis

The present model can be analyzed more rigorously as fol-

lows: In general, reset position of the actual eye,  $R(t_n) = \theta(t_n^+)$ , is given by:

$$R(t_n) = \theta(t_n^-) + S(t_n) \quad (7-10)$$

where  $t_n$  represents time of n'th occurrence of fast phase, and  $t_n^-$  and  $t_n^+$  indicate moments just before and after that fast phase, respectively. But the fast phase jump,  $S(t_n)$ , is given by:

$$S(t_n) = -\theta_o(t_n^-) \quad (7-11)$$

Furthermore, internally-simulated eye position immediately before n'th saccade,  $\theta_o(t_n^-)$ , is written as:

$$\theta_o(t_n^-) = \phi_o(t_n) - \sum_{i=1}^{n-1} S(t_i) \quad (7-12)$$

where  $\phi_o$  represents cumulative eye position which would be obtained with internally-simulated eye position,  $\theta_o$ . Similarly, for actual eye position, one obtains;

$$\theta(t_n^-) = \phi(t_n) - \sum_{i=1}^{n-1} S(t_i) \quad (7-13)$$

where  $\phi$  represents cumulative eye position which would be obtained from actual eye position,  $\theta$ .

From the above set of equations, reset position of the actual eye becomes:

$$R(t_n) = \phi(t_n) - \phi_o(t_n) \quad (7-14)$$

The slow phase velocity signal to the fast phase generating mechanism,  $v_o$ , is time-advanced with respect to slow phase velocity of the actual eye,  $v$ , by a factor of  $\tau$ . Meantime, a pure transport lead,  $e^{\tau s}$  (lag,  $e^{-\tau s}$ ) is assumed for the lead element in Fig. 7.14-a (for the lag element in Fig. 7.14-b), so that no difference exists in signal wave form between  $v_o$  and  $v$ . Thus:

$$v_o(t_n) = v(t_n + \tau) \quad \text{and} \quad \phi_o(t_n) = \phi(t_n + \tau) \quad (7-15)$$

Hence, Eq. (7-14) can be rewritten as:

$$R(t_n) = \phi(t_n) - \phi(t_n + \tau) \quad (7-16)$$

Thus:

$$R(t_n) = \tau \left[ \frac{\phi(t_n) - \phi(t_n + \tau)}{\tau} \right] \quad (7-17)$$

If slow phase velocity does not change much during time interval,  $\tau$ , the whole parenthesized expression in the right hand side of the above equation can be approximated by instantaneous slow phase rate,  $-d\phi/dt$  or  $-v$ . Then, reset position is given by:

$$R(t_n) \approx -\tau v(t_n) \quad (7-18)$$

In particular, if slow phase velocity is truly constant, exact equality holds for the above expression: This is in agreement with the proportional relation (Eq. 7.1) experimentally established in Subsection 7.2.1, and  $\tau$  can be identified as the previous proportionality constant,  $k_1$ .

General expressions for amount of fast phase saccade,  $S$ , and mean over-all eye position  $M$ , are;

$$S(t_n) = - \left\{ \phi_o(t_n) - \phi_o(t_{n-1}) \right\} \quad (7-19)$$

$$M(t_n) = R(t_n) - \frac{1}{2} S(t_n) \quad (7-20)$$

For a constant slow phase velocity, the above two equations reduce to what have been already given in Subsection 7.2.1:

$$S(t_n) = S(nT) = -Tv \quad (7-21)$$

$$\begin{aligned} M(t_n) &= M(nT) = R(nT) - \frac{1}{2} s(nT) \\ &= -(\tau - T/2)v \end{aligned} \quad (7-22)$$

where regular fast phase interval,  $T$ , is assumed.

A test for the present model would be to examine the case with fast-changing slow phase velocity signals, for which approximation by expression (7-18) may become less accurate. To this end, sinusoidal stimulation is considered and correspond-



ing equations are derived on an exact basis: Suppose that slow phase of the actual eye is given by:

$$\frac{d\phi(t)}{dt} = v(t) = \sin\omega t \quad (7-23)$$

where  $\omega$  stands for angular frequency. From Eq. (7-16), behavior of reset position is described as:

$$\begin{aligned} R(t_n) &= -\frac{\cos\omega t_n}{\omega} + \frac{\cos(\omega t_n + \omega \tau)}{\omega} \\ &= -\tau \frac{\sin(\omega T/2)}{\omega T/2} \sin(\omega t_n + \omega \tau/2) \end{aligned} \quad (7-24)$$

Similarly, fast phase saccade is expressed as:

$$S(t_n) = -T \frac{\sin(\omega T/2)}{\omega T/2} \sin(\omega t_n + \omega \tau - T/2) \quad (7-25)$$

where regular fast phase interval,  $T$ , is assumed, and the effect of threshold or dead zone for fast phase generation is ignored.

Value for  $\tau$  (note  $\tau = k_1$ ) is varied from 0.45 to 0.75 sec depending on a particular subject, as determined from the constant-velocity OKN experiment in Subsection 7.2.1.

Thus far, either  $e^{\tau s}$  or  $e^{-\tau s}$  has been assumed depending on a particular alternative chosen from Figs. 7.14 in accounting for the essential factor of the present model, i.e., the relative transport delay in the slow phase information. However, the characteristic OKN pattern can be observed almost immediately following an unexpected reversal of the stimulus motion, and

thus  $e^{\tau s}$  type of anticipation must be precluded from the model. Also, a pure delay,  $e^{-\tau s}$ , with the above range of  $\tau$  would be in direct conflict with much shorter latency actually observed for both vestibular and optokinetic nystagmus slow phase response.

An alternative scheme would be to replace  $e^{\tau s}$  or  $e^{-\tau s}$  by  $1+\tau s$  or  $1/(1+\tau s)$  respectively. In this case,

$$\phi_o(t_n) = \phi(t_n) + \tau \frac{d}{dt} \phi(t_n) \quad (7-26)$$

Hence, Eq. (7-14) gives:

$$R(t_n) = -\tau \frac{d}{dt} \phi(t_n) = -\tau v(t_n) \quad (7-27)$$

Accordingly, the linear relation of this type would exactly hold between reset position and instantaneous slow phase rate, not only for a constant slow phase velocity but also no matter how slow phase velocity may change from time to time. In particular, reset position would behave exactly  $180^\circ$  out of phase relative to sinusoidal slow phase velocity at any stimulus frequency. However, such an assumption fails to account for some trends noted previously (to be further examined) such as some phase lead of reset position from an exact  $180^\circ$  phase relation.

Second, given a unit sinusoidal slow phase velocity of the actual eye,  $v(t)=\sin\omega t$ , the fast phase displacement can be derived as:

$$S(t_n) = -T \frac{\sin(\omega T/2)}{\omega T/2} \sqrt{1 + \omega^2 \tau^2} \sin(\omega t_n + \tan^{-1} \omega \tau) \quad (7-28)$$

In the above expression,  $\sqrt{1 + \omega^2 \tau^2}$  in amplitude, and  $\tan^{-1} \omega \tau$  in phase, both come from the relative phase lead,  $1 + \tau s$ , currently imposed on the slow phase motor information to be used for generating fast phase. Despite  $\frac{\sin(\omega T/2)}{\omega T/2}$  being a decreasing function of frequency, the net amplitude increases with frequency due to  $\sqrt{1 + \omega^2 \tau^2}$ . For example, this would predict fast phase size of as large as  $29^\circ$  for OKN with subject SY at 0.5 Hz ( $\tau = 0.45$  sec average fast phase interval:  $T = 0.5$  sec), which was not the case as shown in Fig. 7.12-c. Furthermore, the algebraic fast phase size would lead slow phase velocity by  $55^\circ$  (from  $-180^\circ$ ), which is also too large as compared to the actual observation (about  $10^\circ - 15^\circ$  lead).

As an example to escape all the foregoing difficulties in finding an appropriate specific form for the lead (or lag) element in the model, a special arrangement has been made: the standard first-order lead network,  $1 + \tau_0 s$ , [or lag network,  $1/(1 + \tau_0 s)$ ] is gain-compensated by cascading  $1/\sqrt{1 + \omega^2 \tau_0^2}$  (or  $1 + \omega^2 \tau_0^2$ ), so that the net gain remains unity regardless of frequency as similar to behavior of  $e^{\tau s}$  (or  $e^{-\tau s}$ ) with respect to gain.

Physically, such an element is unusual. Its adoption might be too hypothetical, at least, in terms of the above exact form. Even so, this particular choice seems to suffice for purposes in the remainder of model discussion: In addition to retaining mathematical simplicity in the system analysis, the subsequent studies including computer simulation will show that the

resultant system's predictions are adequately consistent with experimental data in the pertinent aspects under investigation.

The model with this special component is analyzed and then compared with experiment as follows:

Slow phase movement of the actual eye delays (with no change in signal form or level) by a factor of  $\tan^{-1} \omega \tau_0$  in terms of phase angle relative to the efferent copy signal that enters to the fast phase generator. This delay corresponds to  $(\tan^{-1} \omega \tau_0) / \omega$  in terms of absolute time scale. Thus:

$$\tau = \frac{1}{\omega} \tan^{-1} \omega \tau_0 \quad (7-29)$$

Note that  $\tau$  becomes equal to  $\tau_0$  for the steady state case ( $\omega=0$ ). Consequently,  $\tau_0$  may assume the same value as determined for  $\tau$  by the previous constant-velocity OKN experiment.

For reset position and fast phase saccade, amplitude ratio and phase shift relative to slow phase velocity are computed according to Eqs. (7-24), (7-25) and (7-29), and plotted against frequency,  $\omega / 2\pi$  in Fig. 7.15.  $\tau_0$  is treated as a parameter, assuming values depending on individual subjects as determined previously. Fast phase interval,  $T$ , is assumed to be 0.3 sec in this particular plot. These results predict gradual amplitude decrease and some phase advancement (from  $-180^\circ$ ) with increasing frequency for both reset position and fast phase

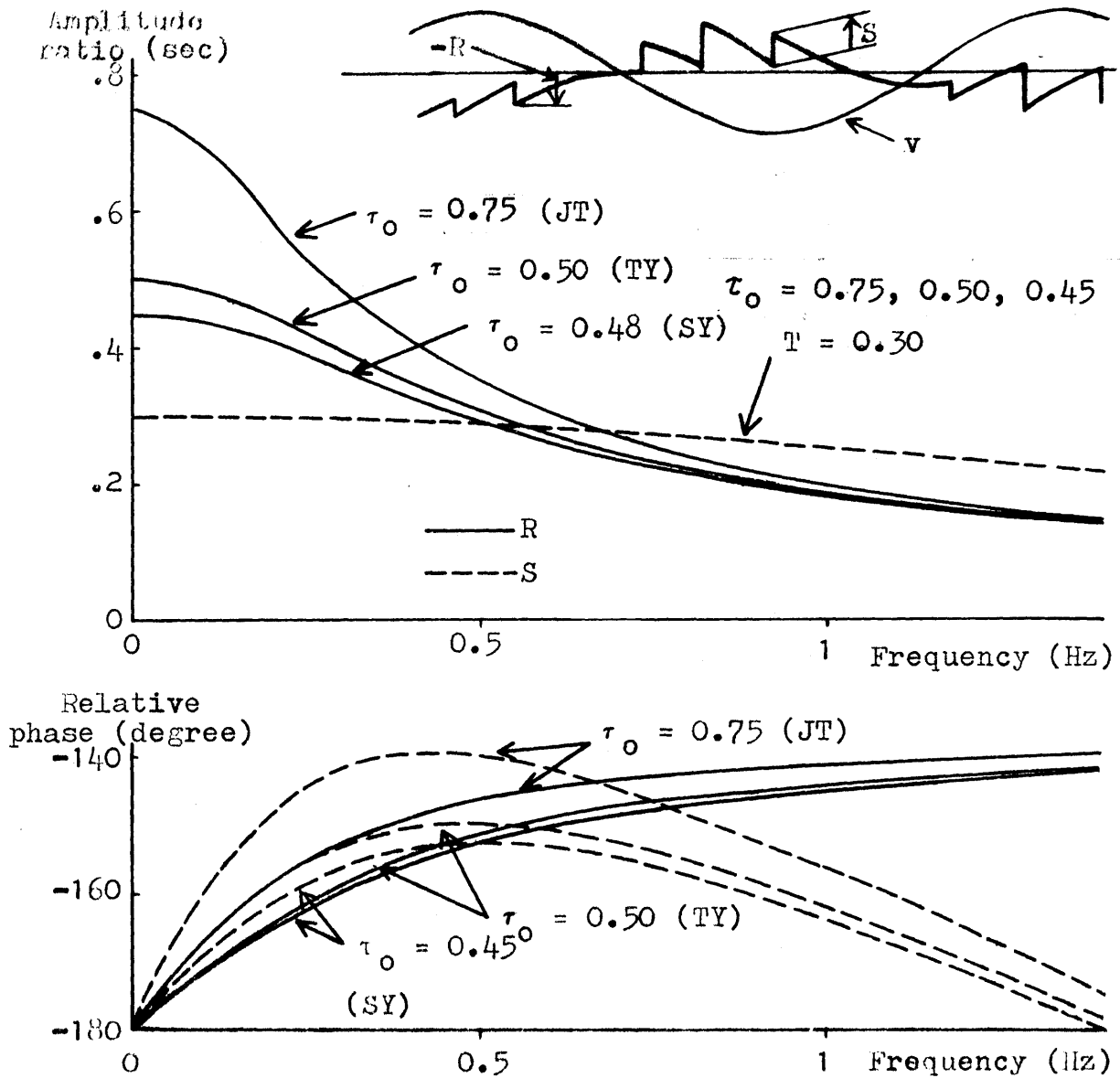


Fig. 7.15 Frequency-dependent behavior of reset position, R, and amount of fast phase saccade, S, relative to sinusoidal slow phase velocity, v, as predicted by the model:

$$v(t) = \sin \omega t ; \quad R(t_n) = -T \frac{\sin(\omega T/2)}{\omega T/2} \sin(\omega t_n + \omega \tau/2) ;$$

$$S(t_n) = -T \frac{\sin(\omega T/2)}{\omega T/2} \sin(\omega t_n + \omega \tau - T/2),$$

where  $\tau = -(\tan^{-1} \omega \tau_0) / \omega$ , and T is assumed to be 0.3 sec for this particular plot.

behavior relative to slow phase rate.\*

As shown in Figs. 7.16, this model prediction is compared with some experimental results obtained for OKN as well as vestibular nystagmus with various frequencies and different subjects. In each case, slow phase velocity, fast phase interval, reset position and fast phase size are measured for every nystagmus beat over several cycles. These accumulated data points are plotted against phase angle of a sinusoid that fits the average trace of slow phase velocity data points.

On the other hand, reset position and size of fast phase were computed theoretically in relation to the estimated average sinusoidal profile of slow phase. Equations (7-24), (7-25) and (7-29) were used in this calculation. Note that the average fast phase interval was estimated for each case presented in Figs. 7.16 and the resultant value was used for the parameter  $T$  in Eq. (7-25).

Figs. 7.16 include these model predictions as well. In each of the examples in Figs. 7.16, reset position deviated toward fast phase direction and its trace is approximately in  $180^\circ$  out of phase relative to the envelope of slow phase velocity data points. Due to considerable scattering of data points, some phase departure (from exact  $180^\circ$  out-of-phase

---

\* However, when  $T$  is great enough to satisfy  $\omega\tau < T/2$ , fast phase may lag appreciably from the  $180^\circ$  out-of-phase relation. But, such a theoretical prediction applies to only one case (Fig. 7.16-g) out of many test examples given in Figs. 7.16. On the other hand, this condition ( $\omega\tau < T/2$ ) can be always met at low enough frequencies, but the resultant phase lag itself would be too small to be significant in terms of phase angle at such low frequencies.

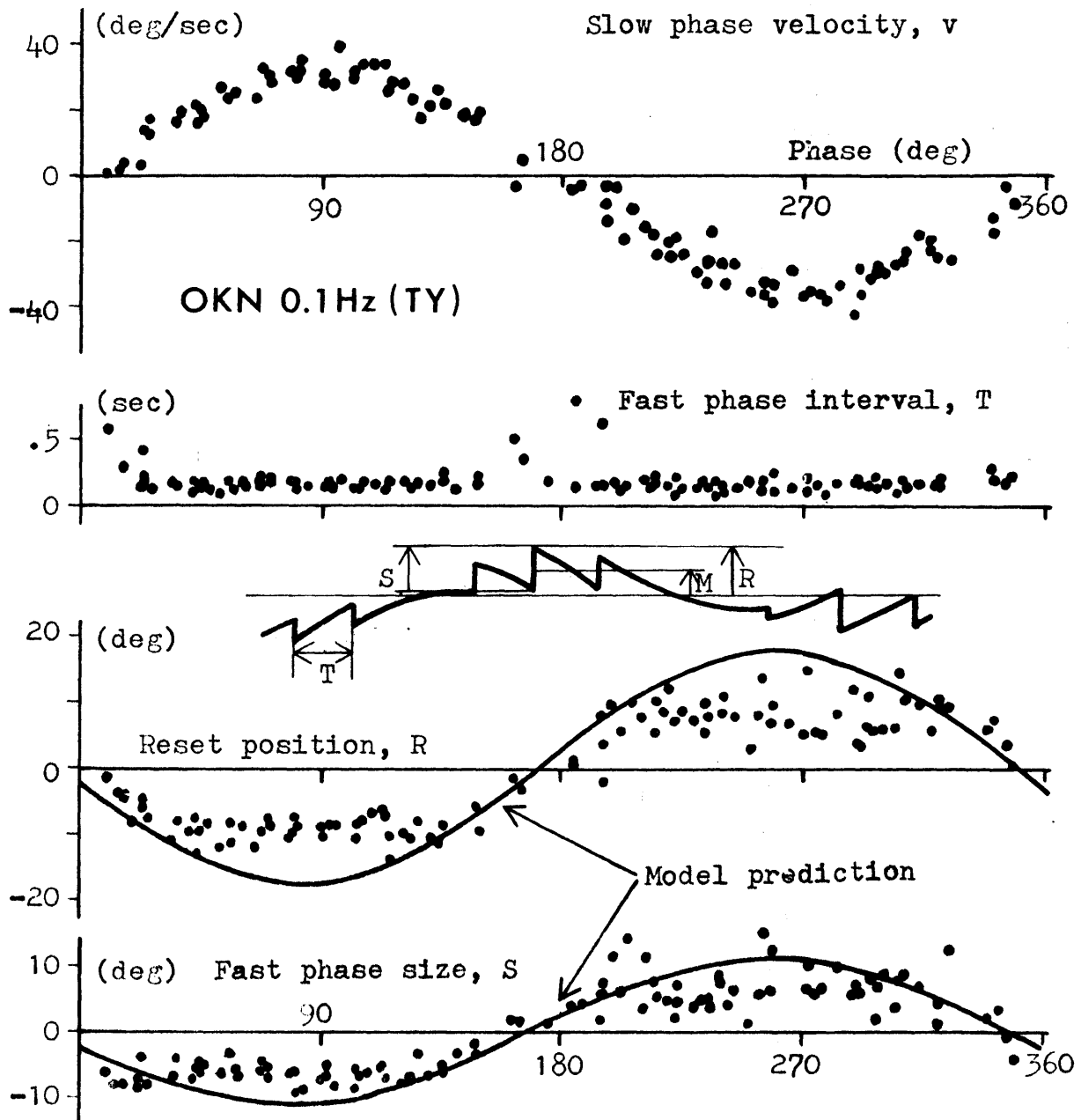


Fig. 7.16-a Behavior of OKN parameters with respect to slow phase velocity's phase angle under sinusoidal stimulation (0.1 Hz, Subject : TY). Experimental data points were accumulated over 4 cycles. Reset position and fast phase size are compared with model prediction which indicates some phase lead (from  $180^\circ$  position) relative to slow phase velocity.

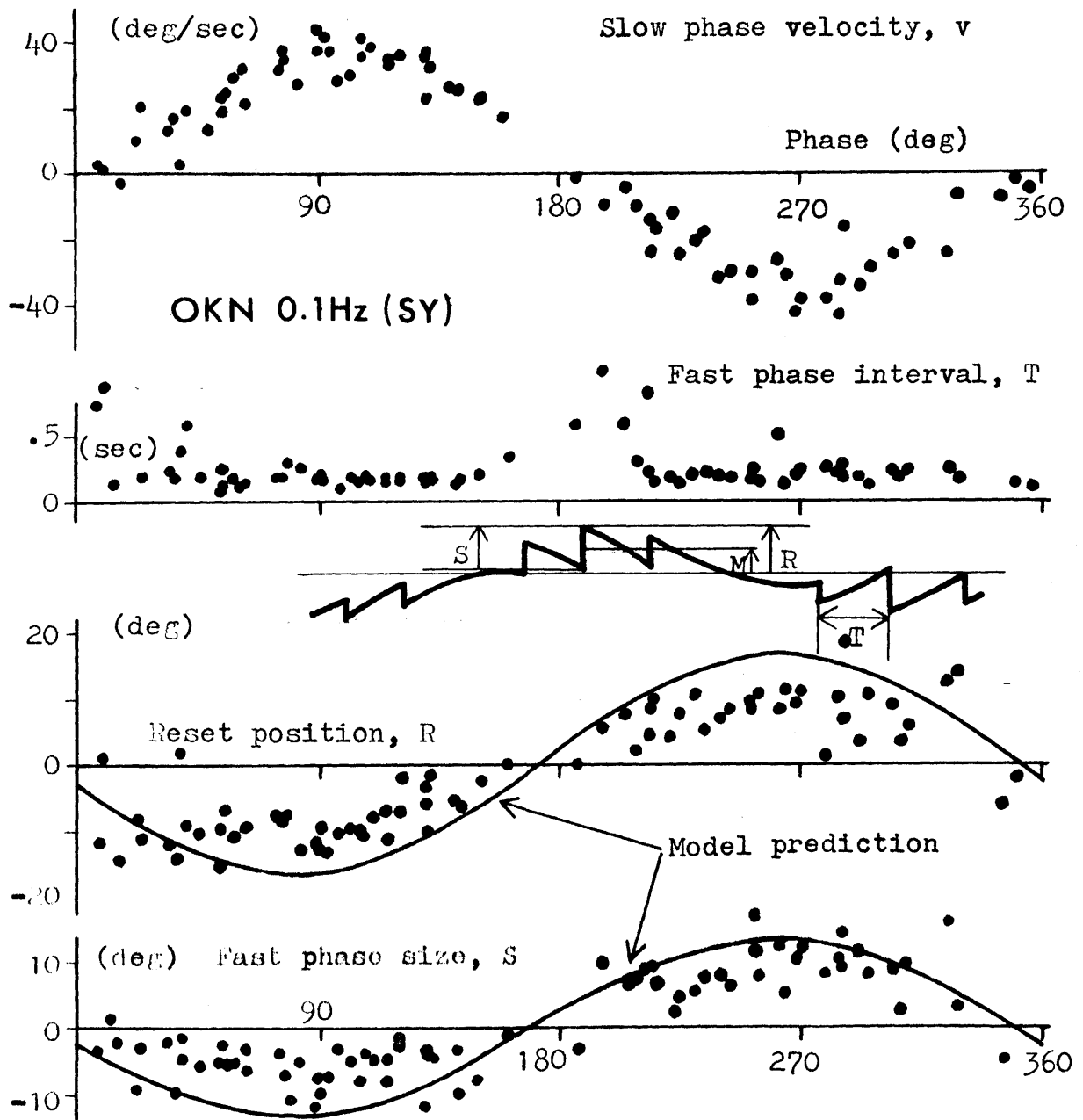


Fig. 7.16-b Behavior of OKN parameters with respect to slow phase velocity's phase angle under sinusoidal stimulation (0.1 Hz, Subject : SY). Experimental data points were accumulated over 4 cycles. Reset position and fast phase size are compared with model prediction which indicates some phase lead (from  $180^\circ$  position) relative to slow phase velocity.



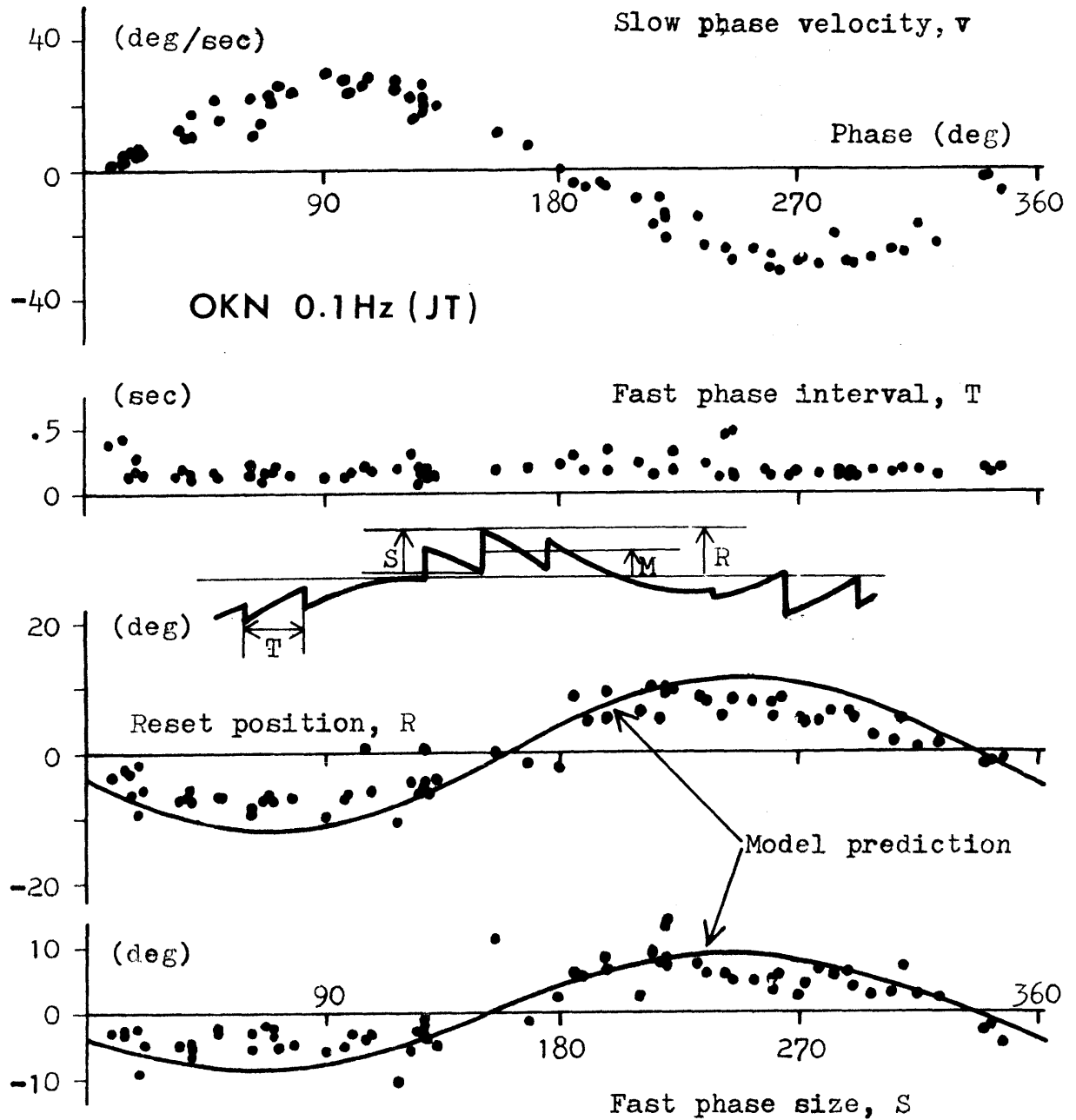


Fig. 7.16-c Behavior of OKN parameters with respect to slow phase velocity's phase angle under sinusoidal stimulation (0.1 Hz, Subject : JT). Experimental data points were accumulated over 4 cycles. Reset position and fast phase size are compared with model prediction which indicates some phase lead (from 180° position) relative to slow phase velocity.

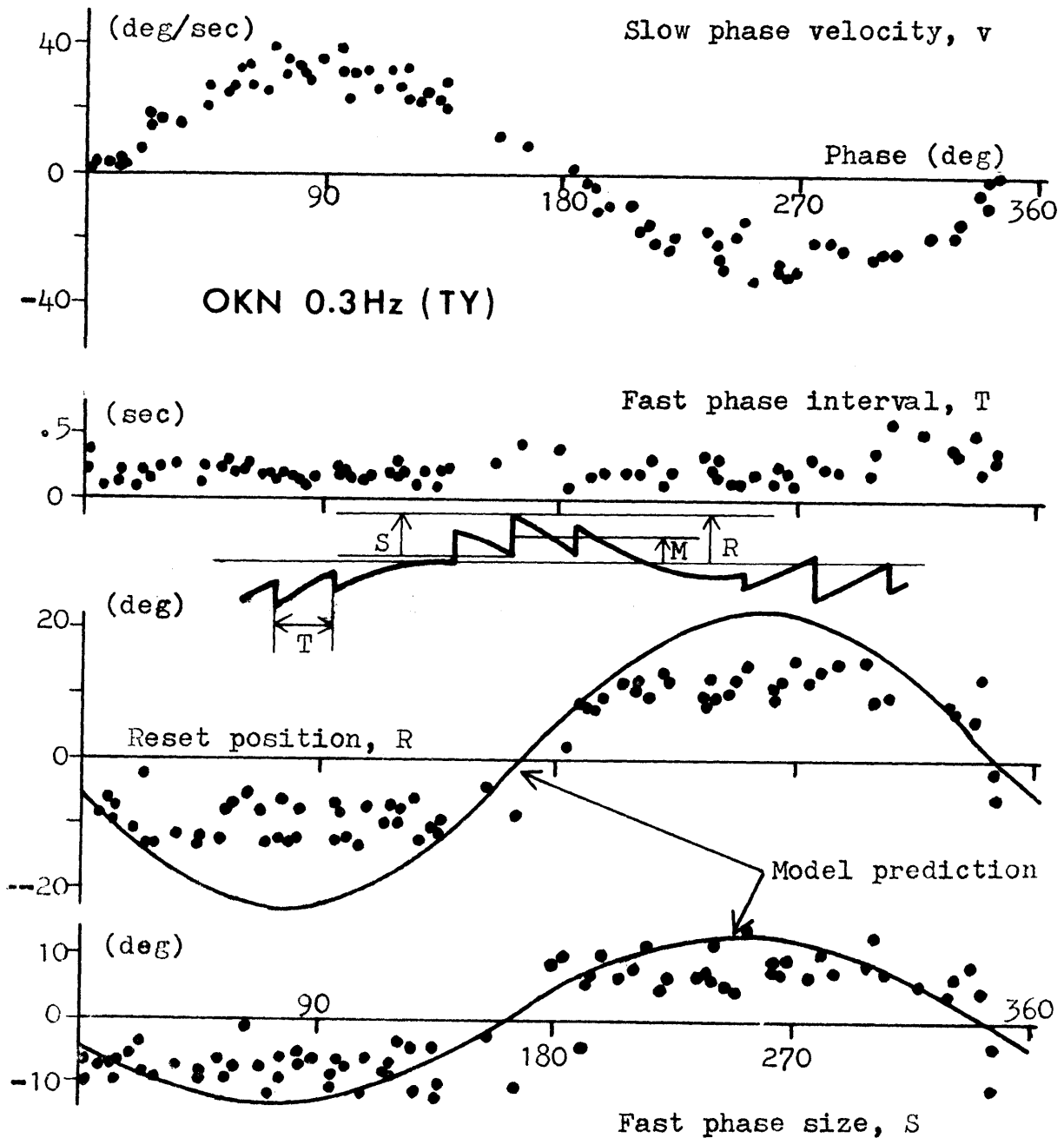


Fig. 7.16-d Behavior of OKN parameters with respect to slow phase velocity's phase angle under sinusoidal stimulation (0.3 Hz, Subject : TY). Experimental data points were accumulated over 6 cycles. Reset position and fast phase size are compared with model prediction which indicates some phase lead (from 180° position) relative to slow phase velocity.

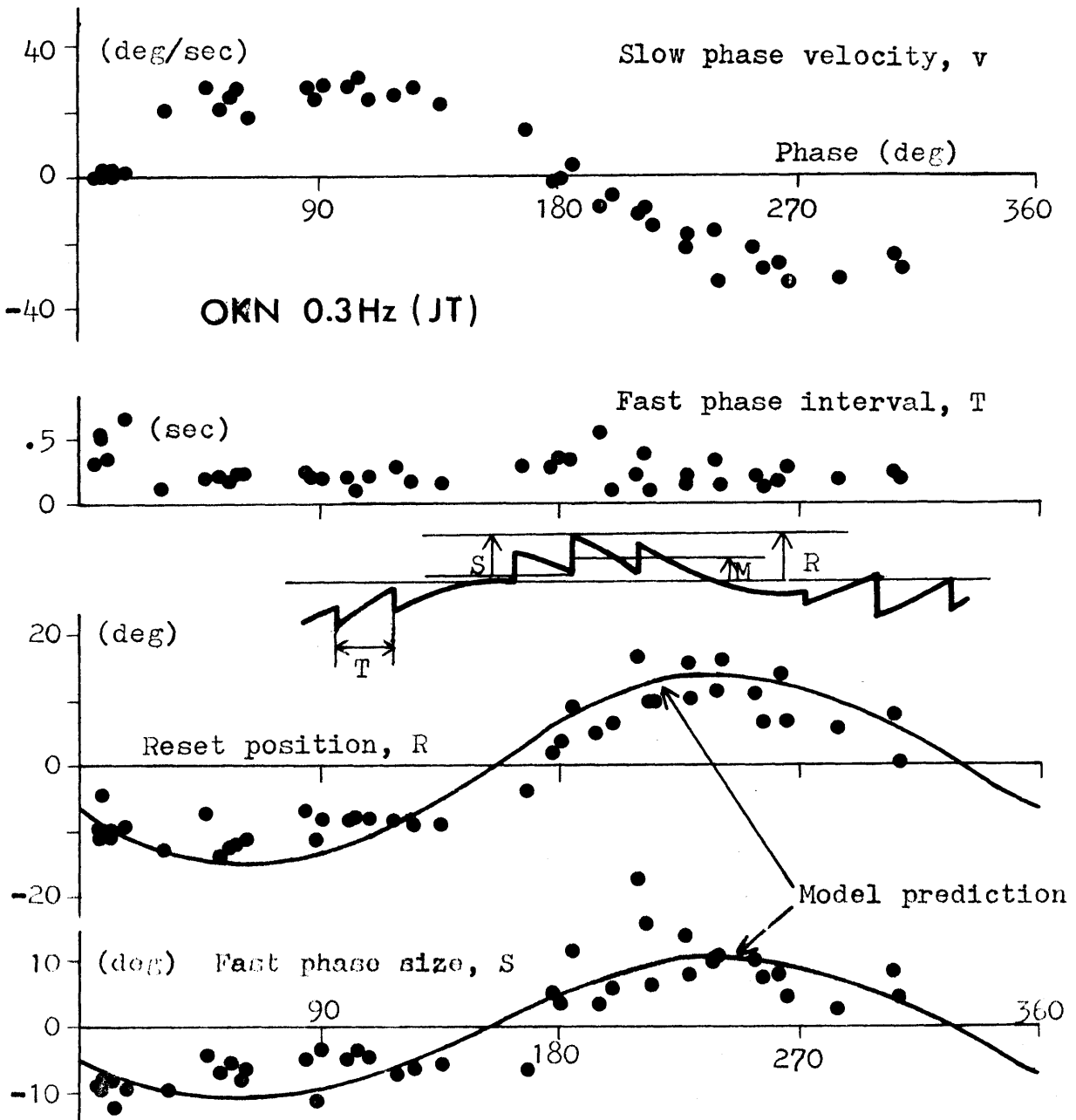


Fig. 7.16-e Behavior of OKN parameters with respect to slow phase velocity's phase angle under sinusoidal stimulation (0.3 Hz, Subject : JT). Experimental data points were accumulated over 6 cycles. Reset position and fast phase size are compared with model prediction which indicates some phase lead (from 180° position) relative to slow phase velocity.

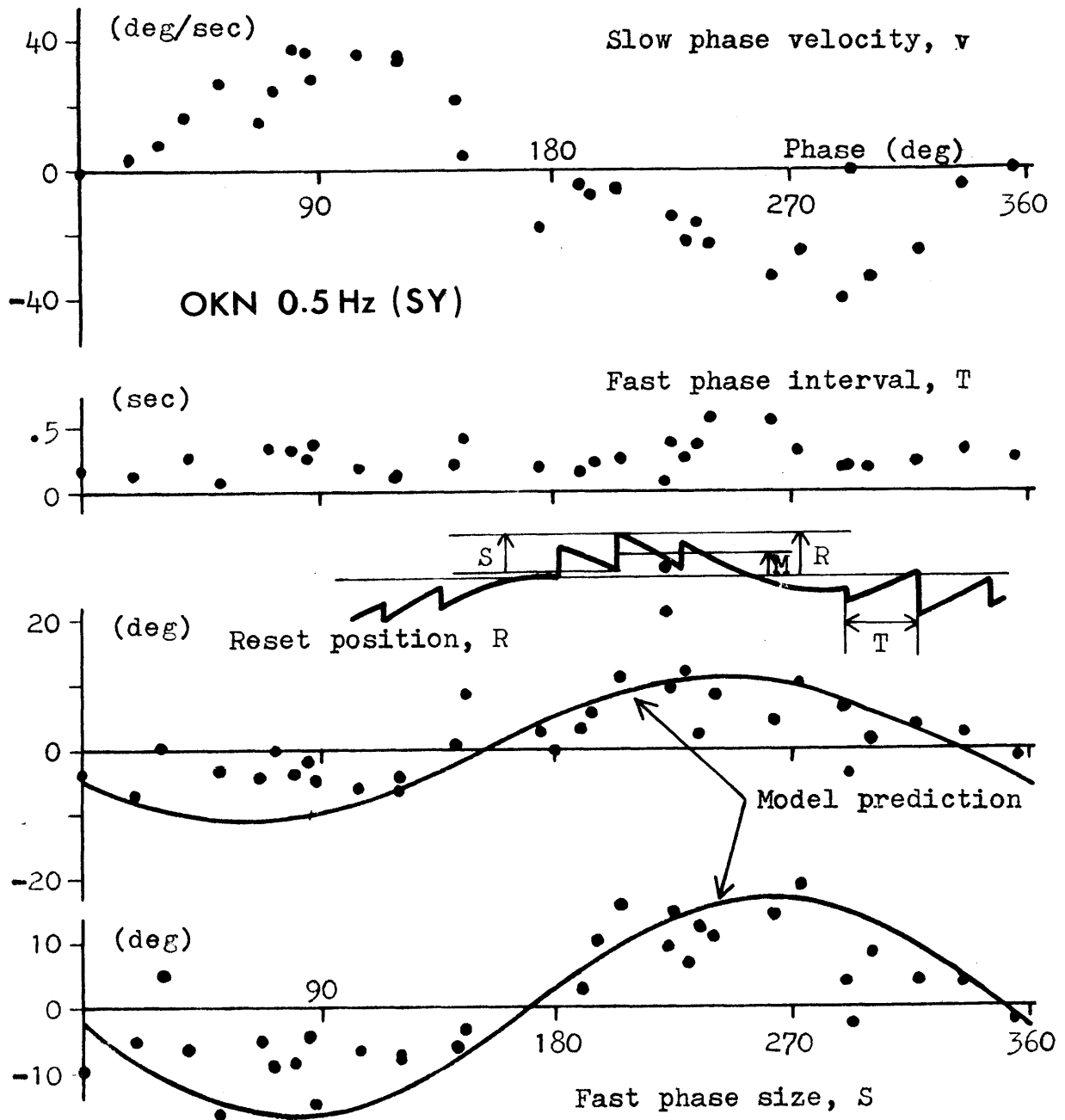


Fig. 7.16-f Behavior of OCN parameters with respect to slow phase velocity's phase angle under sinusoidal stimulation (0.5 Hz, Subject : SY), Experimental data points were accumulated over 9 cycles. Reset position and fast phase size are compared with model prediction which indicates some phase lead (from 180° position) relative to slow phase velocity.

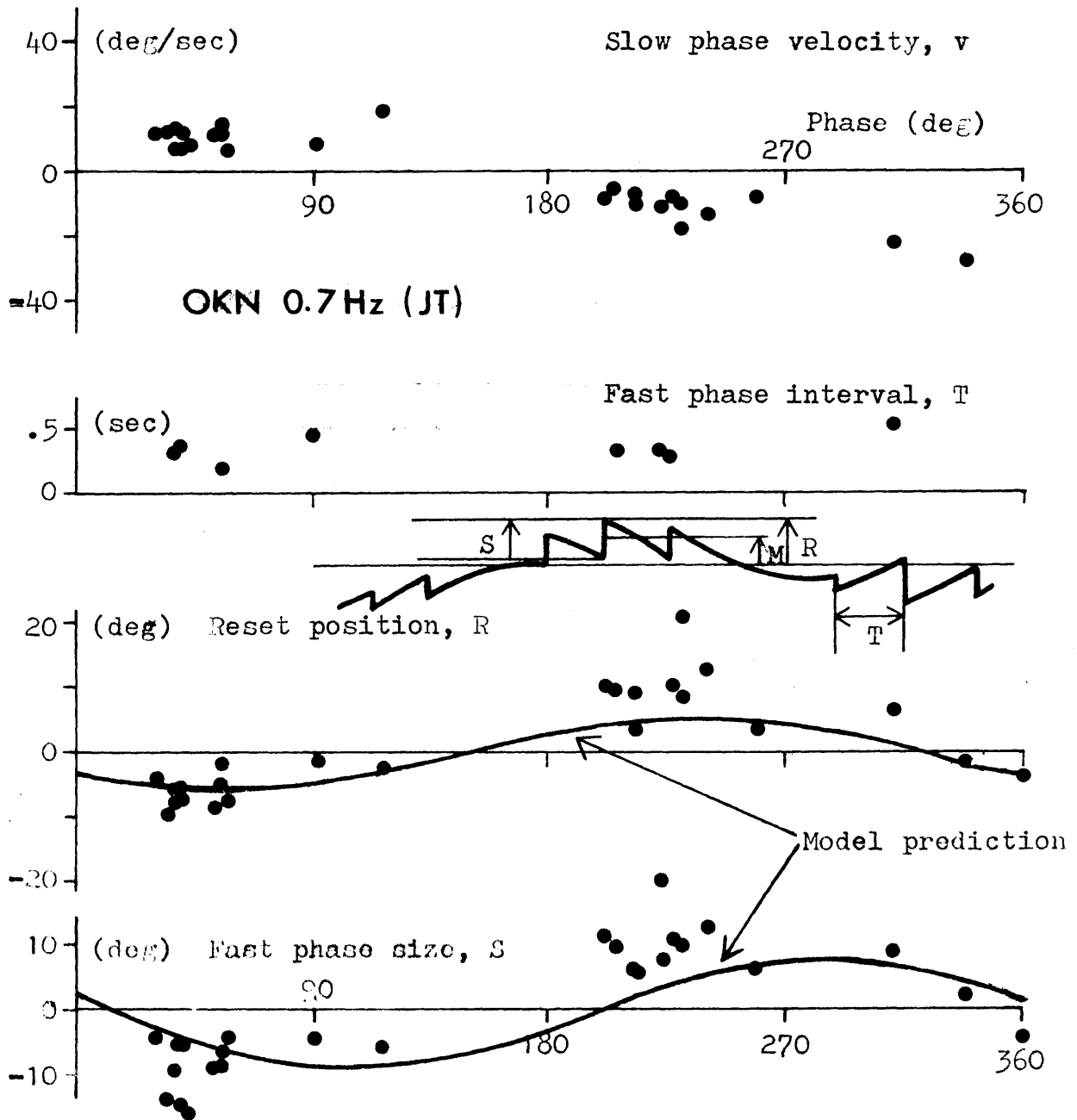


Fig. 7.16-g Behavior of OKN parameters with respect to slow phase velocity's phase angle under sinusoidal stimulation (0.7 Hz, Subject : JT). Experimental data points were accumulated over 13 cycles. In this particular high frequency example, model predicts some phase lead for reset position but some phase lag for fast phase size (from 180° position) relative to slow phase velocity (assuming  $T=0.7$  sec and  $\tau_0=0.75$  sec).

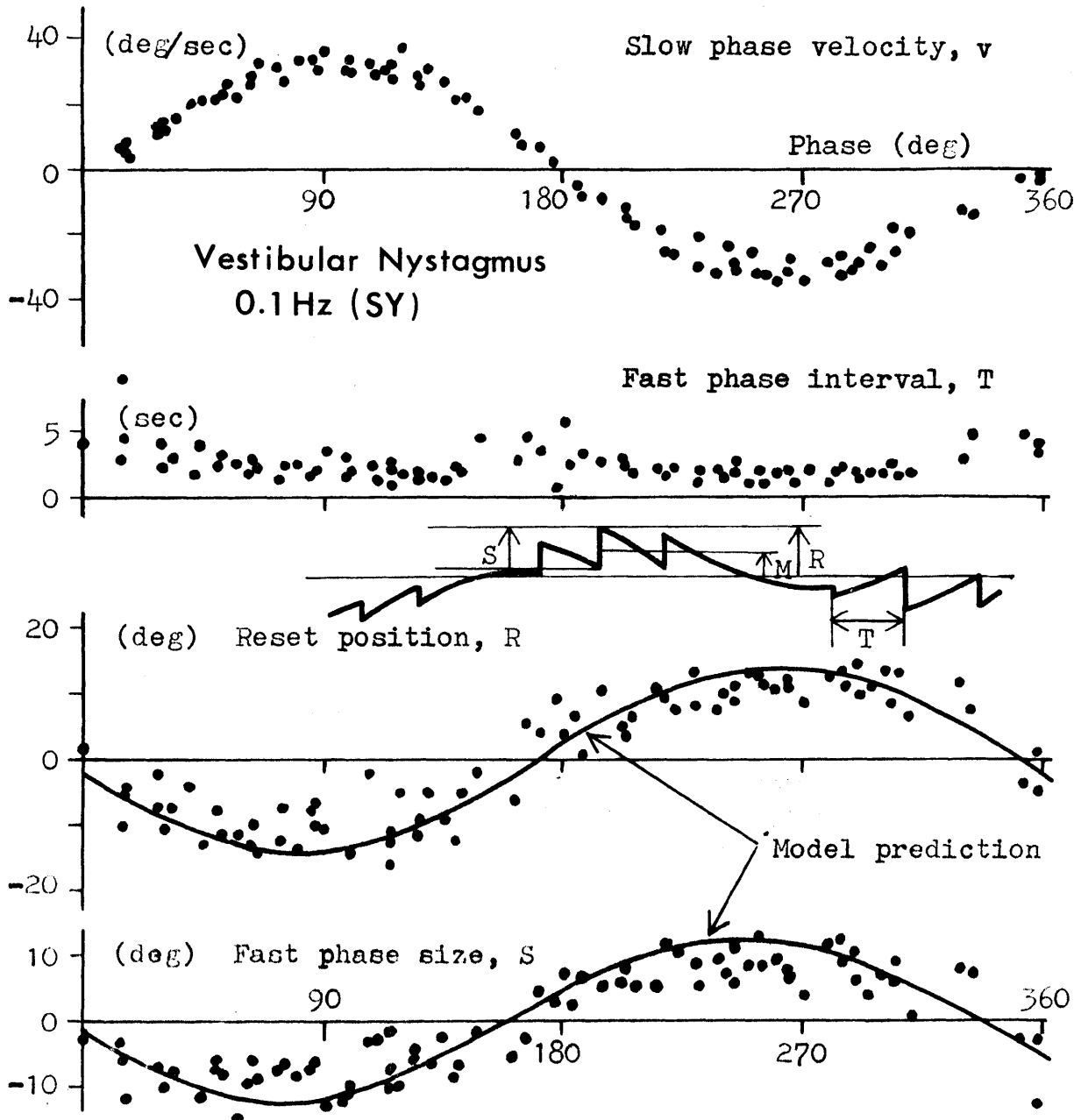


Fig. 7.16-h Behavior of vestibular nystagmus parameters with respect to slow phase velocity's phase angle under sinusoidal stimulation (0.1 Hz, Subject SY). Experimental data points were accumulated over 5 cycles. Reset position and fast phase size are compared with model prediction which indicates some phase lead (from 180° position) relative to slow phase velocity.

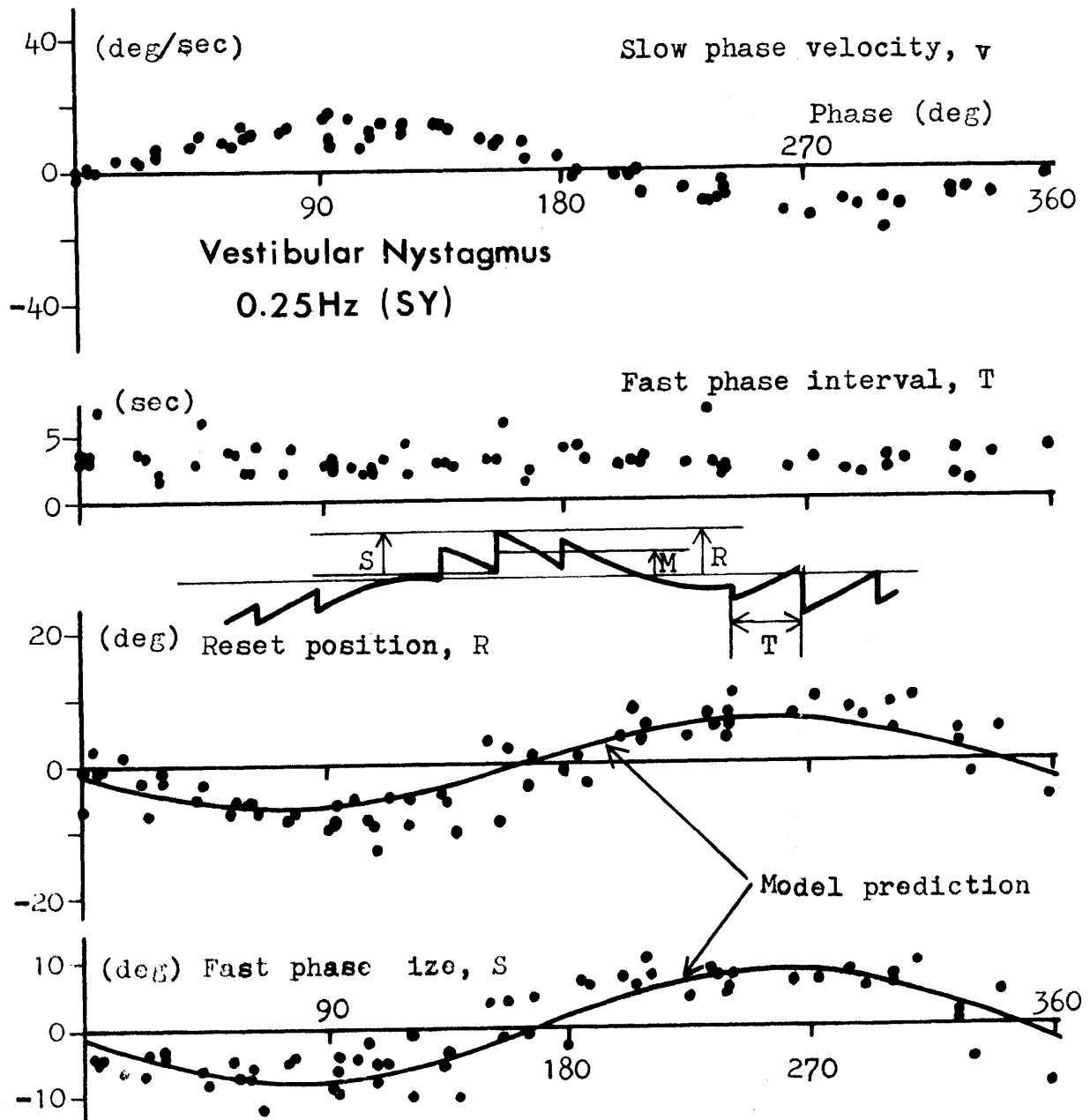


Fig. 7.16-1 Behavior of vestibular nystagmus parameters with respect to slow phase velocity's phase angle under sinusoidal stimulation (0.25 Hz, Subject SY). Experimental data points were accumulated over 10 cycles. Reset position and fast phase size are compared with model prediction which indicates some phase lead (from  $180^\circ$  position) relative to slow phase velocity.

relation) predicted by the model is not so evident in these experimental results for either reset position or fast phase size. Even so, there are some cases (Figs. 7.16-c, d, e and h), where the trend of data appears to indicate, qualitatively, some presence of the predicted phase lead.

Average amplitude for reset position as well as that of fast phase jumps was somewhat smaller than the corresponding prediction in most cases. Actually, fast phase's reset position and size behaved more or less as a square-wave rather than sine wave in some cases studied here (Fig. 7.16-d, for example). This feature due to flattening of sinusoidal peaks resulted, at least in part, from the inherent limitation of the present eye movement monitor's linearity range.\*

Assessment for high frequency cases is somewhat difficult with data of this type for both vestibular or optokinetic nystagmus, due to limited number of available data points (resulting from reduced number of nystagmus beats per cycle) that tend to concentrate in some particular phase regions, for example, as shown in Fig. 7.16-g for OKN with 0.7 Hz. Instead, higher frequency model behavior was tested on the basis of comparison between the subsequent computer simulation of the model and the actual original nystagmus records.

---

\* Sinusoidal nystagmus data discussed here were borrowed from earlier chapters (III and VI) of the thesis, where the major objective was evaluation of frequency response of slow phase movement. The wide linearity range (potentially up to  $\pm 20^\circ$ ), though desirable here, was actually sacrificed in most occasions in favor of a better resolution that was more important in those chapters (see Appendix A).



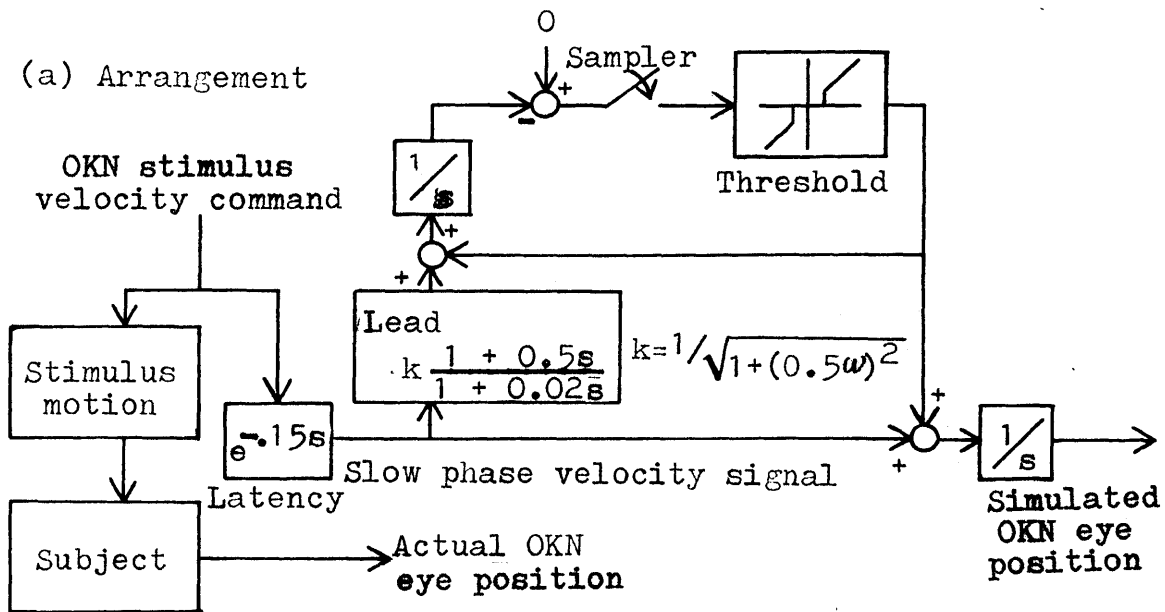
## 7.4 Simulation of Model

The proposed model for nystagmus generation was tested for optokinetic and vestibular nystagmus by simulation on a hybrid computer. Constant and sinusoidal velocity inputs were considered in both classes of nystagmus. Two different approaches were employed in this simulation. The following subsection describes the first one.

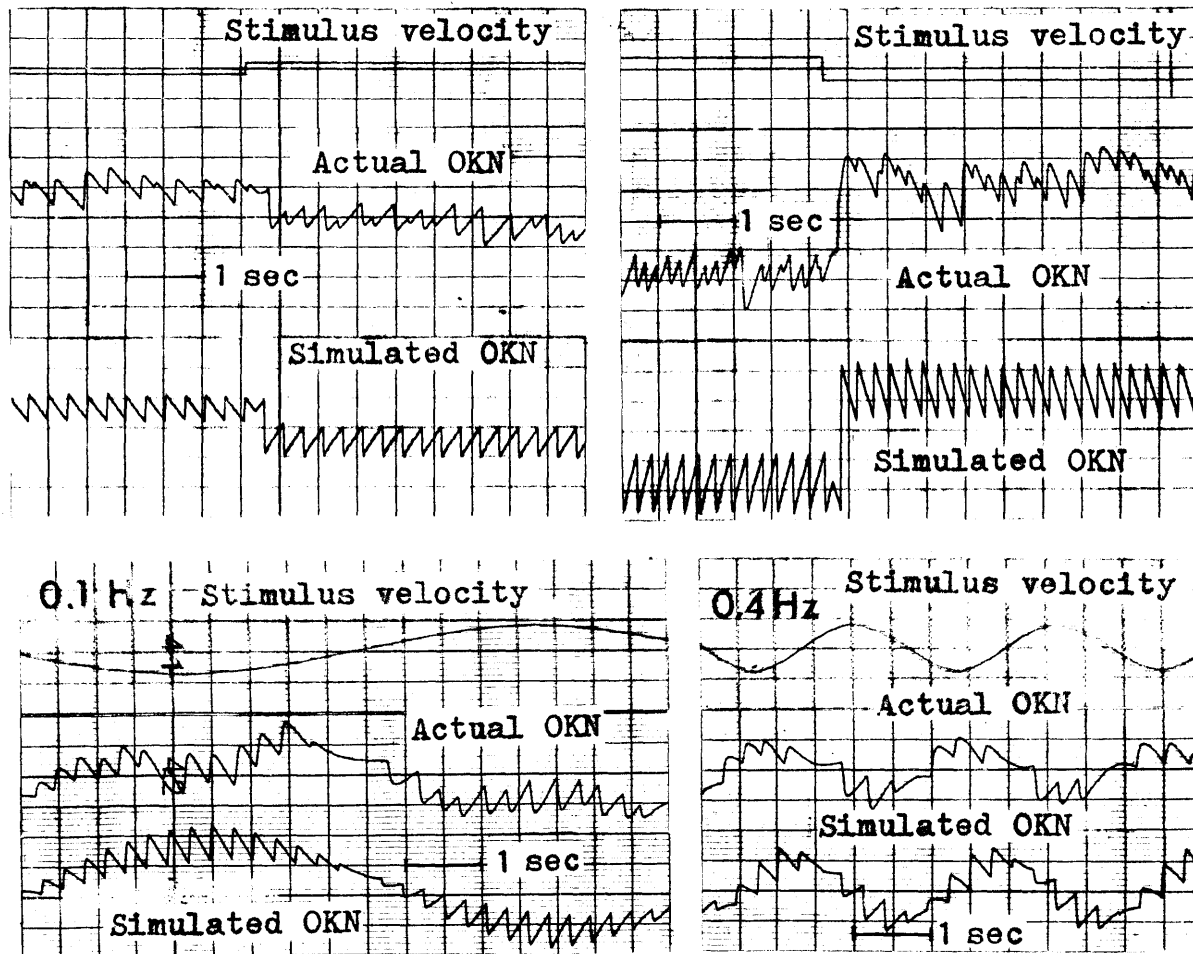
### 7.4.1 Simulation 1

Fig. 7.17-a shows a diagram of the simulated system for OKN, which implements the scheme envisioned in Fig. 7.14. The key concept of the proposed scheme was that slow phase information used by the fast phase generator leads slow phase response of the actual eye. According to discussions in the previous section, this lead element has been assumed to take the special form,  $(1 + \tau_0 s) / \sqrt{1 + \omega^2 \tau_0^2}$ . Actually, this was approximated here by an analog network of  $(1 + \tau_0 s) / (1 + 0.02s) \sqrt{1 + \omega^2 \tau_0^2}$ . The preceding model analysis has shown that  $\tau_0$  corresponds to the proportionality constant,  $k_1$  associated with the linear relation as obtained in Subsection 7.2.1 between average OKN reset position and average constant slow phase velocity. As an example to demonstrate model's feasibility for OKN, model response was compared with actual response of OKN with subject TY. Value of  $\tau_0$  was chosen at 0.5 sec, the number obtained previously for this particular

(a) Arrangement



(b) Results



Figs. 7.17 Simulation of the model for OCN

subject. Pure time delay of 150 msec was introduced additionally as indicated in Fig. 7.17-a, in order to reflect the OKN slow phase latency which was discussed in the previous chapter. This time delay was realized easily by a hybrid routine.

The simulated system was run in parallel with the subject : That is, velocity command signal for moving the OKN pattern in the actual experiment was simultaneously fed to the simulated system. (For simplicity, some dynamics associated with OKN slow phase response was not considered in this simulation.) Fig. 7.17-b gives typical simulation results as compared to actual responses, for constant and sinusoidal slow phase velocities. The model's sampling period and threshold level were adjusted appropriately by comparison to the actual response. Although the simulated response pattern was bound to be too stereotyped compared to the actual counterpart, both responses agreed each other with respect to the basic features of over-all oculomotor response discussed thus far, in particular, regarding behavior of fast phase reset position in relation to slow phase movement.

The model was tested also in regard to vestibular nystagmus with a similar arrangement as shown in Fig. 7.13-a. Meiry's description of semicircular canal's dynamics (Meiry, 1965) was implemented on the analog computer to produce slow phase velocity signal in accordance with a given time course of head angular rotation. The model's outputs were in essential agreement with actual vestibulo-oculomotor response patterns (Subject: SY,  $\tau_0 = 0.45$  sec), as shown in Fig. 7.18-b.

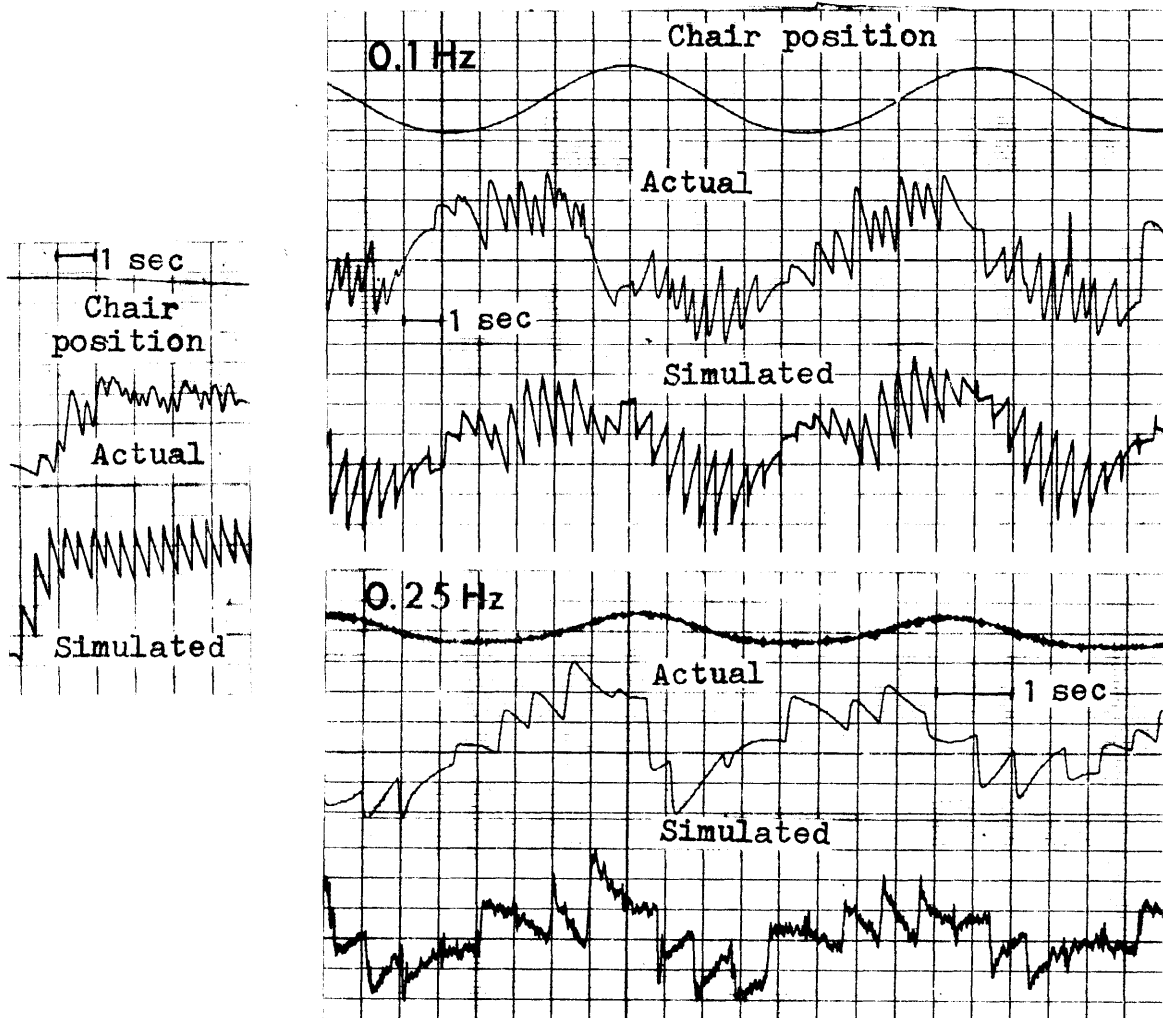
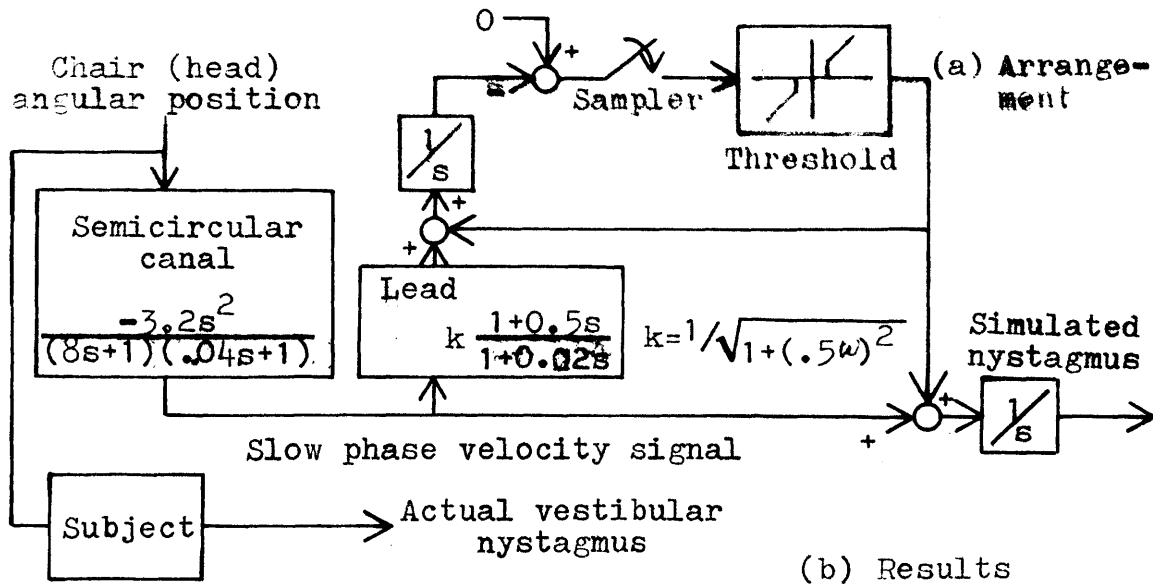


Fig. 7.18 Simulation of the model for vestibular nystagmus (noises in simulated eye movements are due to the double differentiation involved in simulating the semicircular canal as indicated in the diagram.)

#### 7.4.2 Simulation 2

The present model is ~~intended~~ to describe behavior of fast phase in relation to a given slow phase movement signal. In the preceding simulation, besides generation of fast phase, slow phase signal was also simulated appropriately for a given stimulus input. Such a slow phase simulation was, in fact, not essential to testing the model. Furthermore, the previous simulation employed a regular sampler in the fast phase generating mechanism, whereas actual fast phase saccades are not necessarily spaced evenly.. These features might well interfere with the intrinsic feasibility of the model in predicting the over-all nystagmus response pattern in question.

The following second version of simulation was designed to improve the above aspects : First, the slow phase information used in the model is obtained on the basis of the actual oculomotor response. Second, model's generation of fast phase is made synchronized with actual fast phase occurrence.

These revisions were accomplished by the hybrid routine, MITNYS (see Subsection 3.4.4), as illustrated in Fig. 7.19-a. Assuming validity of the proposed model (the preceding model structure becomes operationally equivalent to one enclosed by broken line in Fig. 7.19-a), MITNYS recovers (by producing the cumulative eye position) what would be the slow phase information given to the model's fast phase generator. In addition, MITNYS indicates occurrence of each fast phase by a pulse. This pulse

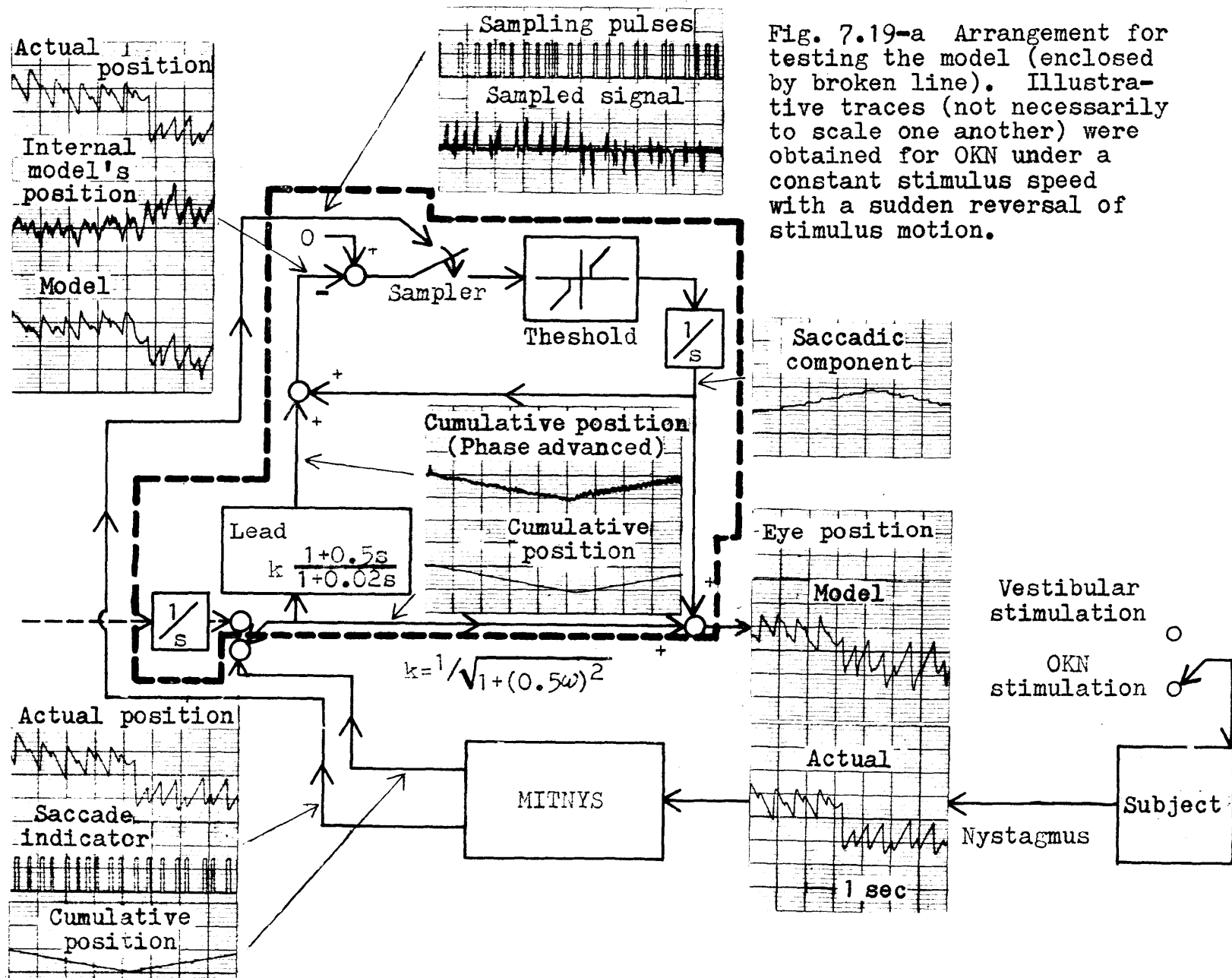


Fig. 7.19-a Arrangement for testing the model (enclosed by broken line). Illustrative traces (not necessarily to scale one another) were obtained for OKN under a constant stimulus speed with a sudden reversal of stimulus motion.

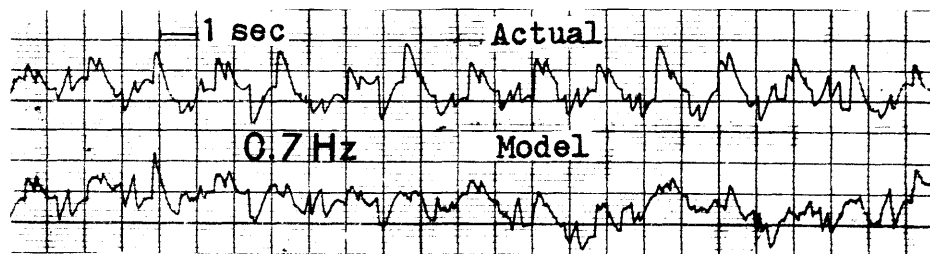
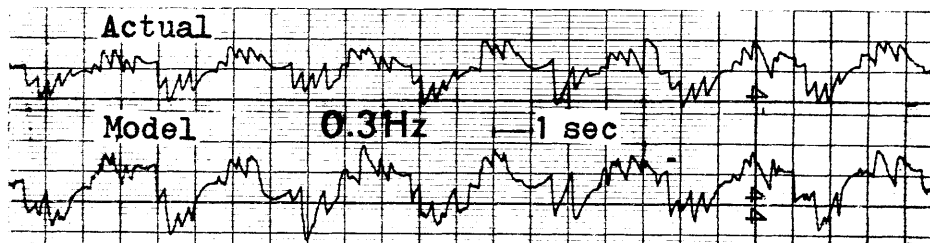
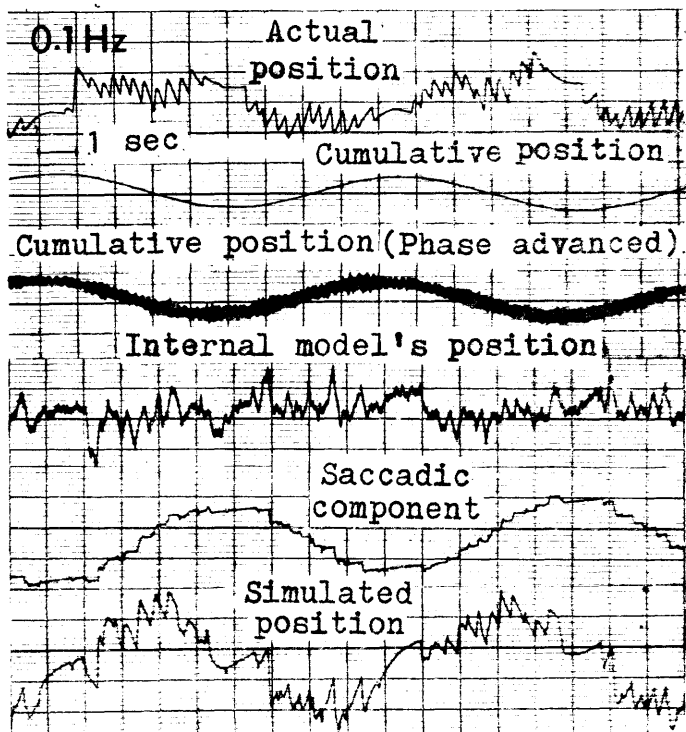
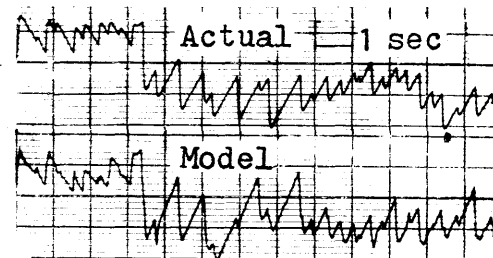
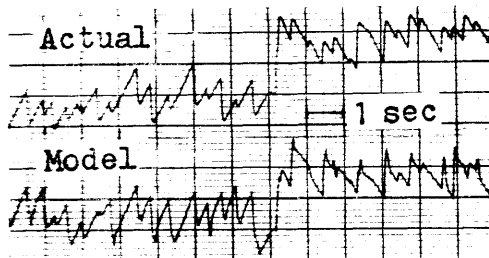
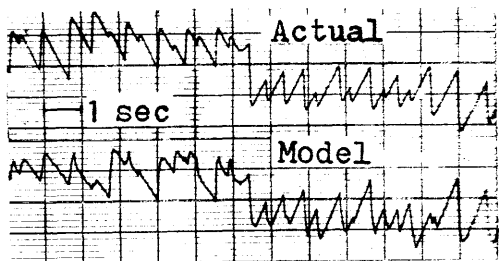


Fig. 7.19-b Actual OKN as compared with model prediction obtained by the arrangement given in Fig. 7.19-a

(The above traces are not necessarily to scale one another.)

was used to close an electronic switch employed as model's sampler. As a result, model's fast phase jumps become synchronized in time with actual ones.

Simulation by this arrangement was expected to allow a more direct and realistic comparison between the model prediction and actual oculomotor behavior. Representative results for OKN, as presented in Fig. 7.19-b, show marked similarity between model and actual responses (not only from over-all point of view but also often in detailed response features as well) even for some portions obtained with a high stimulus frequency at 0.7 Hz.

Fig. 7.20-a shows a typical result for vestibular nystagmus (stimulus frequency : 0.25 Hz), where model prediction also reflects many of detailed features in the actual eye movement.

Finally, as noted previously, the structure of the model's fast phase generator is analogous to that of the sampled-data model of Young (1962 ; and discussed in Chapter V), which deals with the saccadic response to visual inputs. A visual tracking model such as Young's may be combined with a model for nystagmus generation, in study of the oculomotor behavior in presence of visual and vestibular inputs both acting at the same time. While such a two-input case has been discussed in the context of the oculomotor control system by Meiry (1965) and Sugie (1968), and by this author in connection with the experiment reported in Chapter III, consider the particular situation, in which the subject is provided with a visual target at his straight ahead position during sinusoidal head rotation in otherwise total



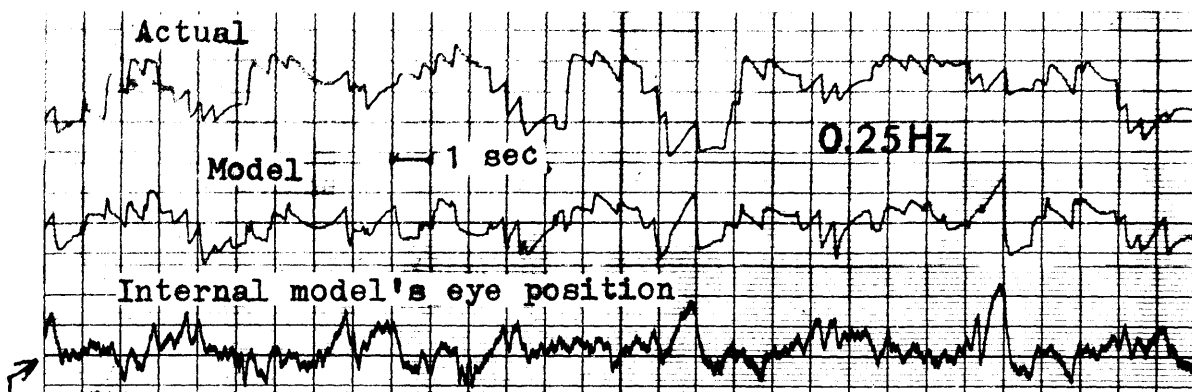


Fig. 7.20-a Actual vestibular nystagmus in the dark as compared with model prediction obtained by the arrangement given in Fig. 7.19-a.

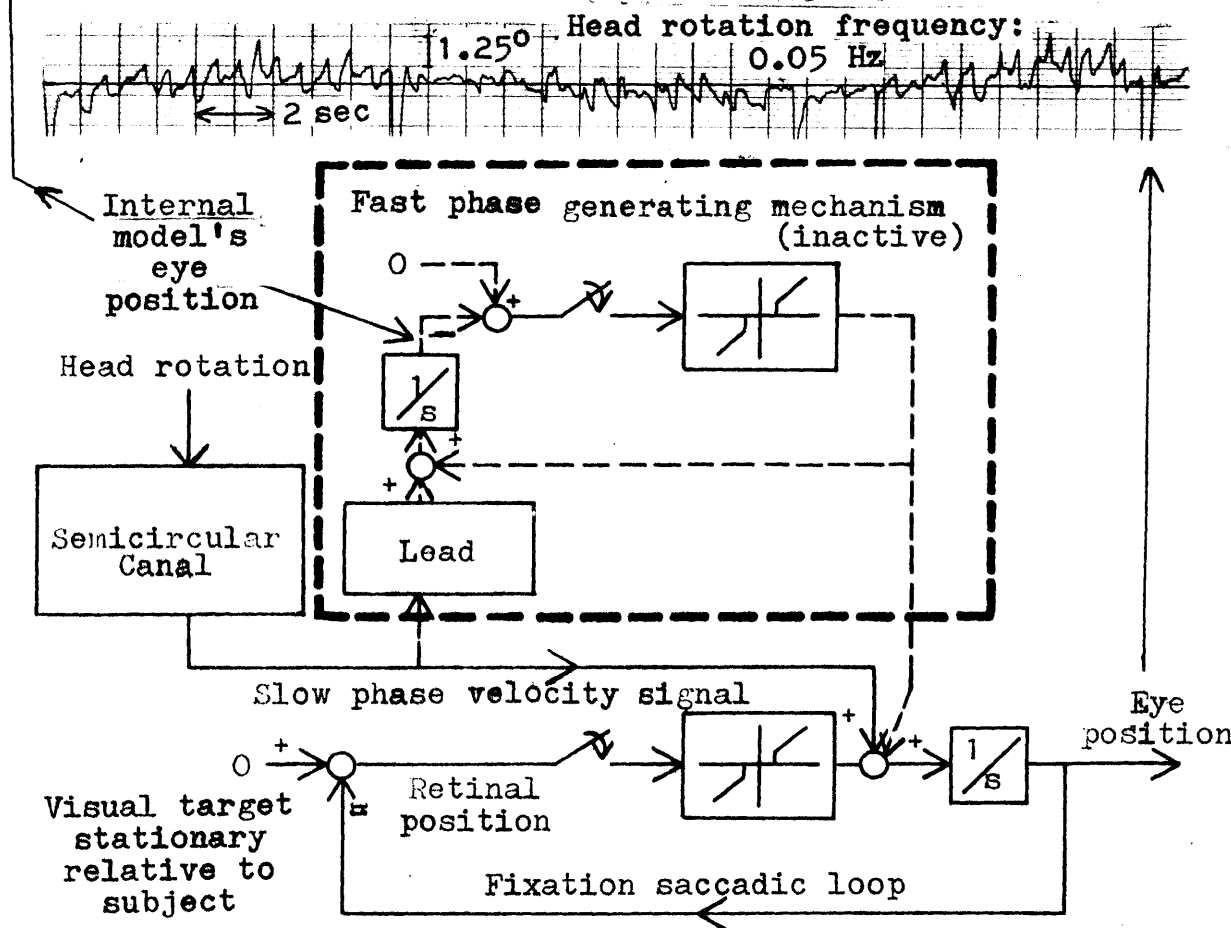


Fig. 7.20-b Trace shows vestibular nystagmus in presence of a visual fixation target. Diagram shows a simple eye movement model for this condition, which is obtained by introducing the saccadic visual tracking loop (Young's sampled-data saccadic model, 1962) in place of the fast phase generating mechanism. But the resultant system still retains a structure analogous to the fast phase generating mechanism, which may account for similarity (fast phase toward center) between the trace here and the bottom trace in Fig. 7.20-a, i.e., internal model's eye movement pattern during vestibular nystagmus in the dark.

darkness. A typical eye movement trace in this condition is presented in Fig. 7.20-b\*. Direction of saccades tends to be toward center, as opposed to the normal vestibular nystagmus with no vision. Presumably, these saccades are of the fixation type, which override fast phases of vestibular nystagmus in correcting fixation errors due to slip of the retinal image resulting from slow phase movements.

As shown in Fig. 7.20-b, this process may be modelled, for example, by Young's saccadic model in place of the fast phase generating mechanism considered thus far for vestibular nystagmus in the dark\*\*. But, the latter is actually analogous to the former from an operational point of view. Accordingly, as apparent from the diagram in Fig. 7.20-b, the resultant system nevertheless retains the functional organization analogous to the fast phase generating mechanism that has been removed. The vestibular nystagmus eye movement with visual fixation target would thus become phenomenologically similar to the internal model's eye position in the above analogy (ignoring the lead element in the model). To examine this point, the bottom trace in Fig. 7.20-a presents the internal model's eye position obtained in the present simulation study, which in fact, similar to the actual eye movement trace in the vestibular/visual two input case, direction of saccades\*\*\*

\* Fig. 3.17 has shown a similar eye movement record in conjunction with discussion on the oculogyral illusion.

\*\* A potential pursuit feedback is not considered here.

\*\*\* Had there not been the noise problem inherently associated with practical realization of the lead network involved in the simulated model, the internal model's eye position would have reset itself exactly at center by each fast phase saccade.

## 7.5 OKN by Selective Stimulation to Peripheral Retina

Hood (1967) reports that a subject with a central scotomata (lacking foveal vision) produces OKN fast phase saccades in direction toward center position as contrasted to the normal subject. Fig. 7.21 schematically illustrates this point. This finding by Hood relates itself to one of most controversial issues in OKN study; dependence of OKN response upon central versus peripheral vision.

For a normal subject, presentation of the OKN stimulus pattern in a restricted area of central or peripheral visual field (relative to observer's head) may not properly suffice to investigate the relevant problems underlying in this direction of research: Stimulation of this type may not be accurately selective in terms of retinal area because of the very eye movement induced by such a stimulation itself. For example, the OKN pattern presented peripherally in the external visual field does not necessarily mean stimulation to the peripheral retina, if the eye is to respond to that stimulus pattern.

A proper method would be to blank a desired portion of the OKN pattern in accordance with information as to where changing direction of gaze is currently pointed. This was easily accomplished with the present computer-graphical approach to generation of the OKN pattern. The basic hybrid software as outlined in the previous chapter and detailed in Appendix E was modified to allow elimination of a specified number of successive vertical stripes whenever falling in an area determined by

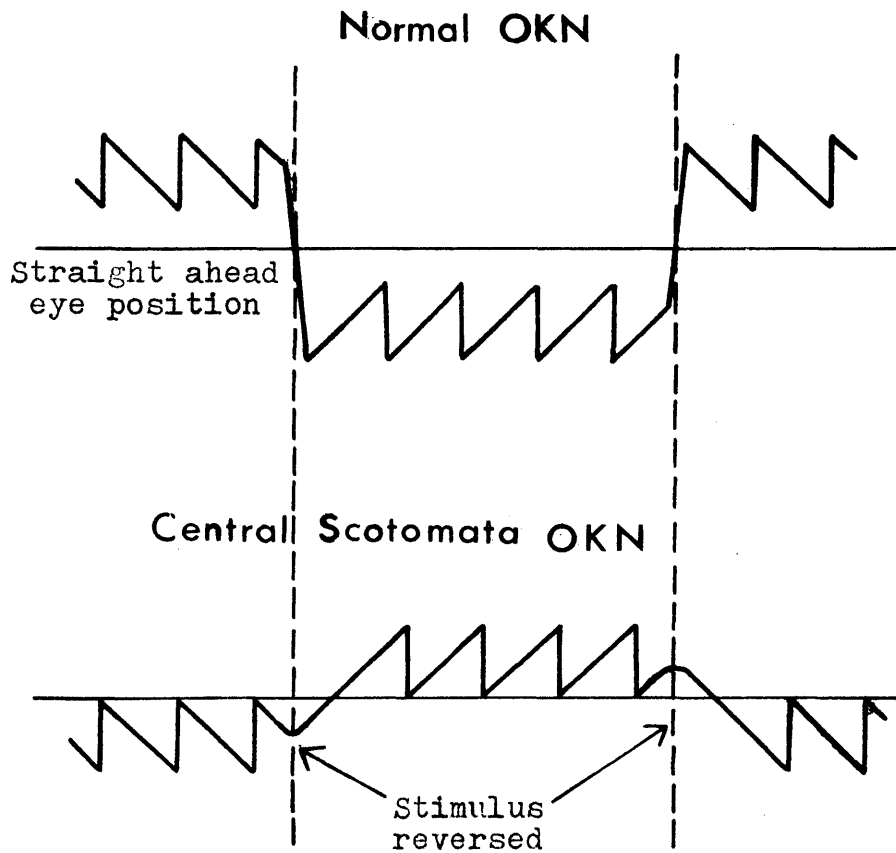


Fig. 7.21 Schematic presentation of two distinct OKN patterns (from Hood, 1967). Upper trace corresponds to OKN in the normal subject, where fast phase is direction opposite to slow phase movement and mean eye position shifts in that direction. This normal pattern, as confirmed also in this chapter, is contrasted by lower trace showing OKN in a subject with a central scotomata where the above normal eye movement direction is reversed.

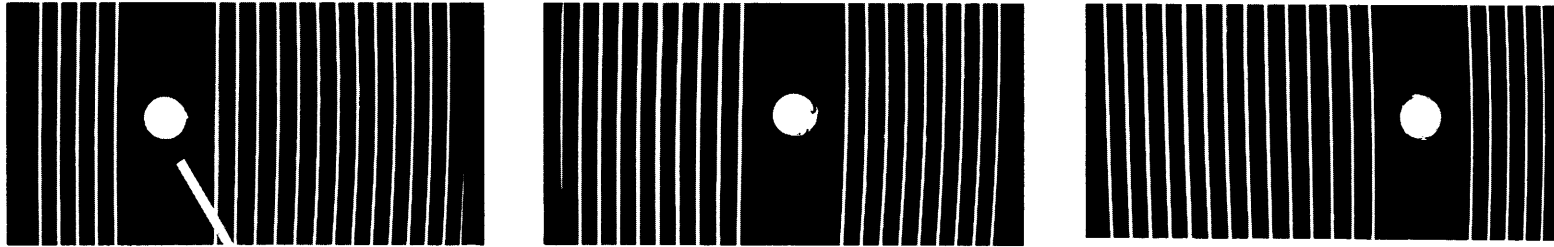
feedback signal from the eye movement monitor. In order to stimulate the peripheral retina only, a moving vertical stripe disappears and reappears when it hits and passes the blanked area respectively. At the same time, this blanked area itself moves with instantaneous eye position in order not to stimulate the fovea. That is, there was always no stripe present in the vicinity of where the subject was looking. Fig. 7.22-a presents a series of photographs of such an OKN pattern with different eye positions. Selective stimulation to the central retina, though not actually investigated in this thesis, could be attained in a manner converse to the above, as illustrated in Fig. 7.22-b. Appendix E includes computer algorithm for these modified versions of the OKN stimulus pattern.

The selective peripheral stimulation by the above arrangement was expected to mimic the condition of central scotomata in the normal subject. In the hope to observe a similar OKN pattern as found in a real central scotomata patient by Hood, a preliminary experiment was conducted with a normal subject (TY).

The crucial point in this experiment was not to stimulate the foveal region by stripes. In order to take a conservative measure to this end, the blanked area was made large,  $20^{\circ}$  wide (eliminating four vertical stripes) as compared to the total stimulus field of  $\pm 45^{\circ}$  in horizontal direction. This presumably tolerated errors in eye movement measurement as well as in pertinent instrumental calibrations that might affect accuracy of the feedback-blanking.

Due to the nature of the experiment, there was a consider-

(a) Peripheral stimulation



Current eye position as known from eye movement monitor

(b) Central stimulation

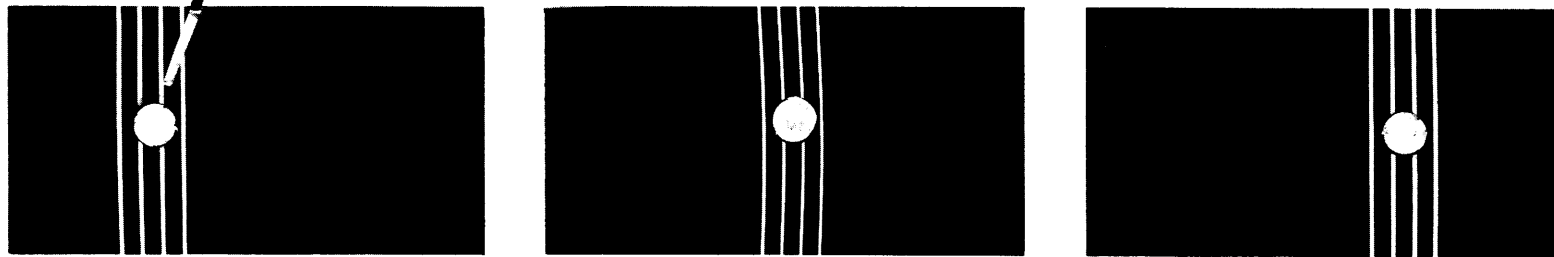


Fig. 7.22 Computer-generated stripe-pattern for OKN stimulation to selective retinal area based on feedback-blanking: Appropriate portion of stimulus field is blanked through updated eye position information, while group velocity of stripes can be controlled independently. See also Fig. E.1 in Appendix E.

able difficulty in finding a proper instruction to the subject: The instruction, "stare straight ahead", as used in the previous chapter under the normal condition was not appropriate (evoking little response), since no visual object existed here in the straight-ahead area due to the blanking. So, the subject was asked additionally to maintain her attention to the peripheral vision while she attempted to keep staring straight ahead. Because of the understandable difficulty in following such an instruction, the resultant OKN response was often erratic, with average over-all movement wandering to one direction or the other.

Even so, there were periods of stable response, which appeared to indicate the expected pattern with fast phase direction toward center as found in the scotomata patient by Hood. Some of such records are shown in Fig. 7.23, along with normal response (with fast phase away from center) obtained from the same subject without blanking.

This positive result may imply that the anomaly of OKN pattern seemingly characterizing the central scotomata case is really a normal physiological reaction resulting from deprivation of the foveal vision.

However, this is only a tentative conclusion: The subject soon learned that the blanked area moved with her eye position, although she was instructed not to pay attention to movement of the blanked area. Therefore, the subject could know that her gaze had deviated from center (which meant violation of the instruction), and accordingly she would likely reset her eye

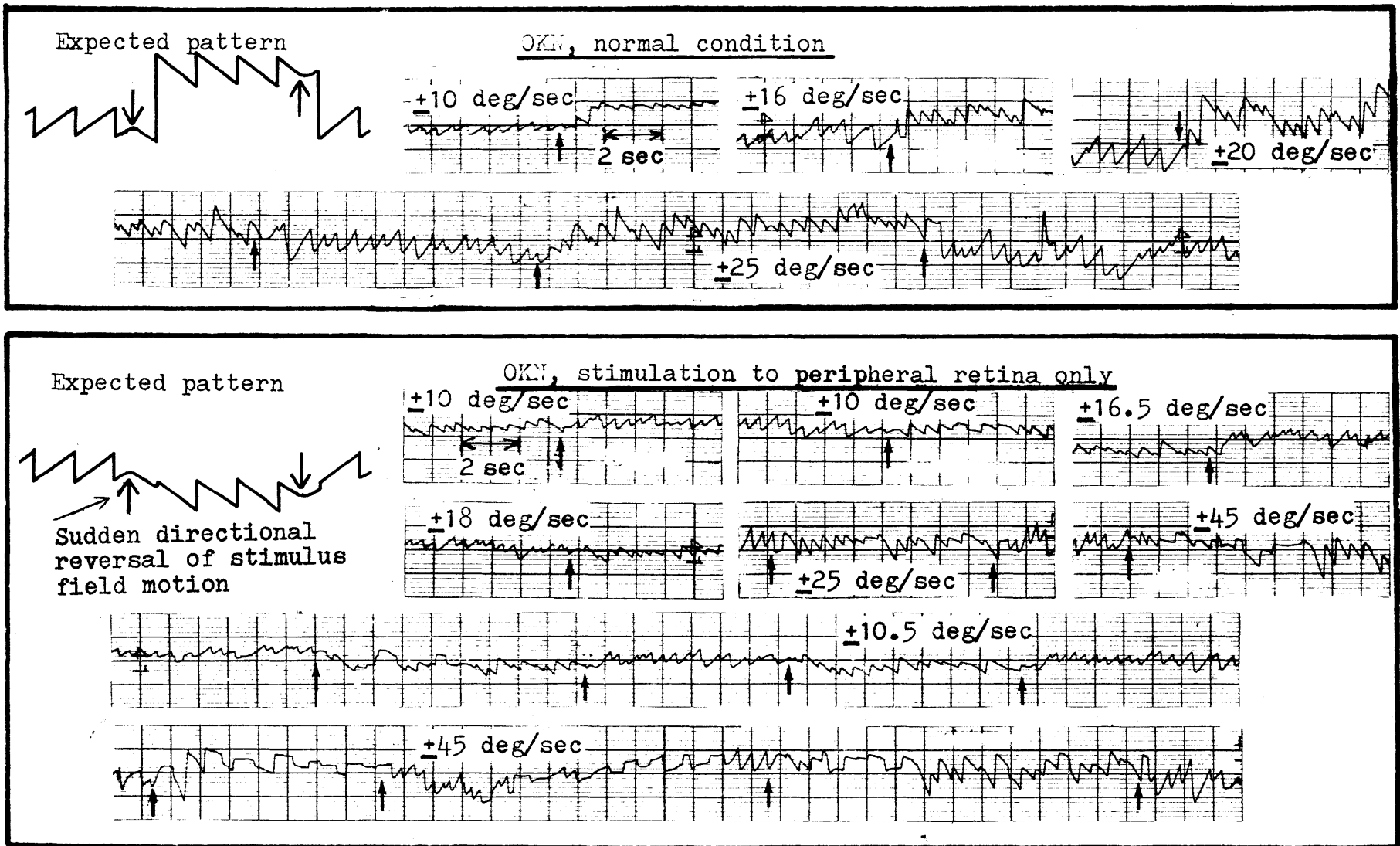


Fig. 7.23 OKN patterns by selective stimulation to peripheral retina, in contrast with normal patterns. Direction of stimulus motion (with a constant speed as indicated in each trace) was suddenly reversed as marked by arrow.



position to center by a voluntary saccade. This might result in the observed pattern as shown above. The subject did not particularly agree with this possibility herself, but she admitted that she felt as if she were tracking movement of the blanked area (rather than responding to the moving stripes).

Thus, before drawing the final conclusion, further investigation would be necessary to work out these problems associated with the experimental instruction and corresponding subject's mental attitude.

## 7.6 Summary and Conclusions

The particular nystagmus phenomena dealt with in this chapter have attracted attention from some previous investigators. However, there are some conflicting opinions in the literature, presumably due to differences in experimental instructions and subject's mental attitudes. Even so, the series of controlled experiments have confirmed the following phenomenological features in both vestibular and optokinetic nystagmus ("stare" type of OKN).

Mean over-all eye position tends to deviate from center in the direction opposite to slow phase movement. Actually, this is a secondary observation stemming from the fact that fast phase brings the eye ball away from center in the above described direction, which in turn indicates that fast phase is not a simple centering reflex. Thus, for instance, not only slow phase, but also over-all eye movement tends to behave sinusoidally with sine wave inputs, maintaining its pattern about 180° out of phase with respect to the slow phase velocity profile.

Preliminary observation with sinusoidal stimulation shows an almost indistinguishable over-all response pattern in vestibular and optokinetic nystagmus at a given stimulus frequency, suggesting some common fast phase generating mechanism which utilizes slow phase oculomotor information regardless of stimulus modality. While this view is generally supported by various neuroanatomical evidence in the literature, clinical data by Weiss (1973) are particularly specific to the present point.

This is an acoustic neuroma case showing unilateral reversal of the fast phase direction (i.e., toward center as opposed to the normal case) in both types of nystagmus without apparent disturbance to their slow phase component.

As a clue to assess the function of such a common fast phase generator, various nystagmus parameters were investigated in their average relation to slow phase velocity by examining a number of successive nystagmus beats obtained for vestibular and optokinetic nystagmus under DC as well as sinusoidal stimulations. In particular, behavior of "reset position" (eye position immediately after fast phase) was emphasized throughout this study. For instance, OKN response records with different constant input velocities show that the average shift of reset position is approximately proportional to average slow phase velocity magnitude with proportionality constant ranging from 0.45 sec to 0.70 sec depending on the individual subject.

Based on these experimental results, a simple conceptual model is developed, which incorporates the sampled-data saccadic model of Young's type (Young, 1962, which originally deals with corrective saccades in visual fixation) as an internal model that determines fast phases by utilizing slow phase motor outflow. While similar models employing such an efferent feed-forward structure have been recently proposed by others for vestibular nystagmus (Schmid, 1971; Barnes, 1973), the present model is intended to include OKN as well. In addition, central to the model is that slow phase information is time-advanced in comparison to slow phase response of the actual eye, by a factor

corresponding to the foregoing proportionality constant determined in the constant stimulus velocity OKN experiment.

According to the model, the system "attempts" to reset the eye exactly at the center. But, the above relative time lag in the slow phase signal transmission interferes with such a goal, resulting in errors in the reset position. Considering the observed direction of this shift, however, this nystagmus feature should be functionally advantageous, since it facilitates quick acquisition of new visual information through successive fast phases in both types of nystagmus.

The model was analyzed mathematically. Theoretical predictions were compared back with preceding experimental counterparts. While the model is in general agreement with experiment in basic aspects, it predicts a certain degree of frequency dependence as characterized, for instance, by some phase lead of reset position from the exact  $180^\circ$  out-of-phase relation with slow phase velocity. Such detailed aspects were apparent in some of vestibular and optokinetic nystagmus data with sinusoidal stimuli.

Further confirmation of the feasibility of the proposed scheme was obtained by two versions of specially arranged hybrid computer simulation.

Finally, the OKN stimulus was applied selectively to the peripheral retina by blanking the part of the stimulus field which covered the central retina. This was accomplished on the basis of feeding up-dated eye position signal from the photo-electric eye movement monitor back to the computer that

generated the OKN pattern. The aim was to effectively eliminate the foveal stimulus to a normal subject in the hope of observing a similar OKN pattern as reported by Hood (1967) in a central scotomata patient (person suffering from no foveal vision); namely, eye movements with reversed fast phase direction as in the aforementioned acoustic neuroma case. A preliminary experiment with the above feedback blanking method has yielded some positive evidence of the expected change in the OKN pattern. This result may, in turn, suggest that what appears to be an abnormal OKN pattern in the central scotomata case is actually a normal physiological reaction resulting from the loss of foveal stimulus.

## Chapter VIII

### Principal Results, Conclusions and Recommendations

This chapter presents conclusions along with major findings and results obtained in this dissertation directed toward a bio-cybernetic study on the human oculomotor system. The description is a self-contained summary of the thesis when combined with Section 1.1, which states the rationales and objectives of the research. Recommendations for possible improvement, extension and modification of the present experiments and concepts are also included herein,\* while their potential applications are suggested in a more general context in Section 2.2.

- 8.1 On a Perceptual Feedback Model for the Pursuit Oculomotor System
- 8.2 On Optokinetic Nystagmus Slow Phase versus Pursuit Movement
- 8.3 Quest of Predictive Behavior in the Oculomotor System
- 8.4 On Saccadic Frequency Response with Nonperiodic Inputs
- 8.5 Fast Phase Behavior in Relation to Slow Phase Movement in Vestibular and Optokinetic Nystagmus

---

\* Increase of the number of subjects would be an obvious improvement common to all formal experiments in this thesis, which have employed only three or four subjects.

## 8.1 On a Perceptual Feedback Model for the Pursuit Oculomotor System

This part of the research has considered, elaborated and experimentally supported the hypothesis that smooth pursuit eye movements might be produced based on what the observer subjectively perceives as target velocity, not necessarily on the actual target velocity nor on the retinal velocity per se.

Given that the intimate participation of the oculomotor information in the mechanism of visual motion perception is well known in psychophysics and, in fact, has been conceptually modeled by the cancellation theory or corollary discharge theory, it might be also possible that the perceived information in turn influences the system that controls the eye movement. This concept of perceptual feedback has led to a new closed-loop version of the classical theory, which in turn forms a skeleton model of the pursuit oculomotor control system examined herein. The whole structure now describes the two systems, perceptual and oculomotor, at the same time, and is characterized by an internal regenerative feedback as emerged from looping the corollary discharge outflow and the postulated perceptual feedback pathway.

The experiment was designed to aim at differentiating this characteristic feature of the regenerative loop by the forced visual tracking of a small foveal after-image which appeared to move with the sinusoidal head rotation about the earth-vertical

axis. While such a vestibularly-induced after-image motion has been reported in the literature, the present emphasis lies in the controlled eye movement measurement and analysis as well as the subsequent interpretation given to the result.

The resultant eye movement was characterized by the tendency toward disappearance of the vestibular nystagmus fast phase component. A transient period was observed as the after-image was about to fade. Close examination of data during this stage indicates that disappearance and reappearance of fast phases are correlated respectively with subjective (rather than physical) maintenance and loss of the after-image target.

The smooth eye movement lacking fast phases during the maintained after-image tracking has yielded the frequency response at a statistically significant variance with that obtained for the normal vestibular nystagmus slow phase in complete darkness without after-image: In relation to the same sinusoidal skull rotation with the Bárány type chair, the after-image tracking eye movement amplitude tended to be greater than the vestibular nystagmus slow phase with no vision (for example, the amplitude difference was approximately two-fold at 0.7 Hz) whereas the opposite trend was observed for the relative phase lag. This difference is pronounced especially for higher-frequency amplitude and for lower-frequency phase shift, although the lower-frequency data are probably less accurate, quantitatively, due to a technical problem that inherently arose at that frequency region.



In any event, the presence of the conspicuous eye movement difference, aside from its detailed frequency-dependent features at present, appears to form sufficient evidence for the perceptual feedback hypothesis for the following reasons: An after-image is impossible to move relative to the retina, so that its apparent motion must be due purely to the corollary discharge which initially represents the vestibular nystagmus slow phase outflow in the present experimental arrangement. The subject's effort to visually follow that apparent after-image motion selectively activates the internal regenerative loop (the corresponding instruction to the subject was, therefore, particularly important here), which additively creates a certain pursuit oculomotor efferent as a secondary product of the original vestibular nystagmus slow phase efferent, and thereby some eye movement difference must result when compared with the vestibular nystagmus slow phase in the total darkness without after-image.

Further, the perceived trajectory of the after-image motion must describe the tracking eye movement itself according to the corollary discharge theory. This supplementary point was also supported by comparison between the eye movement trace and the report from the subject through the 3-position switch indicating the updated direction of the apparent after-image motion.

It is thus concluded that the perceived velocity of a visual target, obtained through the mechanism by the corollary discharge theory or the cancellation theory, is in turn, sent back to the oculomotor centers responsible for generating and commanding the pursuit tracking movement.

The experiment repeated with a pseudo-random chair motion also yielded a statistically significant difference in the eye movement between the condition of after-image tracking and that without after-image. The after-image's apparent motion was presumably unpredictable, whereas it was essentially sinusoidal and therefore predictable in the preceding case. Hence, it appears that periodicity or predictability of the perceived visual information is not an essential factor for operation of the perceptual feedback.

A possible refinement of the present oculomotor model is discussed on a preliminary basis from a servomechanical viewpoint coupled with certain subjective visual phenomena including the oculo-ocular illusion, as reviewed here in one of the subsequent recommendations.

In addition to the objective information regarding external physical input/output quantities whose measurement has been the base of most of the published engineering models for the oculomotor system, subjective perceptual information can be recognized as another useful system variable that reflects, to some degree, the underlying mechanism internal to the over-all biological control system in question.

### Recommendations

[1] Apparatus improvement and frequency sensitivity analysis

The principal goal at the present stage of the investigation

had been to determine whether or not the eye movement difference would actually be obtained as expected from the hypothesized perceptual feedback pursuit tracking model. Having obtained the affirmative result, the next step would be to closely examine the frequency dependence of the eye movement differences. This would shed further light on the internal organization of the model, especially as to the dynamical aspect of the characteristic regenerative feedback loop to which the eye movement difference has been attributed.

To this end, it is strongly suggested that the after-image tracking experiment be repeated with the following hardware improvements in order to increase the accuracy of the data particularly in the low frequency region: (1) an eye movement monitor with a much wider linear range, (2) a rotating chair allowing smaller amplitude oscillation at low driving frequencies.

Due to the loss of almost all fast phase saccades that would reset the eye position in the normal vestibular nystagmus in the dark, the range of the after-image tracking eye movement became too great at low frequencies to remain in the present eye movement monitor's linearity range. In addition, the eye movement itself probably suffered from saturation upon reaching an extreme position in the orbit as is apparent from the perceived trajectory of the after-image motion. For these reasons, the low-frequency portion of the current Bode plot stemmed from the eye velocity estimated at a presupposed center position in the eye movement trace.

But, it would be undoubtedly preferable to work with the eye position without saturation (which was the case for the current high-frequency result) for more reliable quantitative assessment of the frequency response.

It may be added that ultimate refinement of the perceptual feedback pursuit model should consider also results of the experiment on the pursuit system approached from a different point of view as given in the next section.

[2] Transient observation

The after-image tracking experiment with a velocity-step chair motion might be of interest, although the expected loss of fast phase would cause a too quick saturation of the eye movement in the direction of the applied stimulus.

[3] Possible interference by the Sugie-Jones theory

On the face of the observed tendency toward disappearance of the nystagmus fast phase component during the after-image tracking, there is a chance that the present interpretation in favor of the perceptual feedback hypothesis could be interfered with, if not entirely jeopardized, by the idea of Sugie and Jones (1965 and 1966), which stresses a functional importance of the fast phase component in integrating the vestibular afferent so as to properly produce the subsequent compensatory slow phase. Though

some evidence is cited here against this theory, further clarification is recommended in this connection: For example, more accurate frequency response measurement as well as transient observation as recommended previously, coupled with relevant mathematical analysis of the Sugie-Jones Model, might lead to the final resolution of the issue.

[4] Questions from the servomechanical viewpoint

The present perceptual-oculomotor model reduces to the appearance of an open-loop feedback configuration, resulting from the cancellation between the actual eye movement and the corollary discharge, or in other words between the innate negative visual feedback and the internal positive feedback emerged from the perceptual feedback hypothesis. This is, in fact, why the open-loop pursuit model by Young et al (1968) has been interpreted by Robinson (1969) and Rashbass (1969) as a similar type of model as is considered here. Yet, an open-loop (nonfeedback) system may be hard to conceive, especially for a biological system. It would be even more strange, if the oculomotor system were to avoid taking advantage of the visual feedback that already exists. As discussed in Chapter III on a preliminary basis, a solution to this problem could be that the cancellation is accomplished only partially for the pursuit movement. The system as a whole would then remain under negative feedback control, without losing the

beneficial feature of corollary discharge scheme for perceptual purposes. In fact, this possibility appears to be consistent with the phenomenon of the oculogyral illusion as well as the psychophysical evidence by Dichgans et al (1969) which shows that the afferent visual information evokes about 1.7 times greater visual velocity sensation than the efferent motor information.

It is recommended that the above points be considered in the course of further refinement of the suggested perceptual feedback pursuit tracking model.

[5] Real-image alternative

The real reason for using the visual after-image in the current experiment was because it was a simple and exact means of establishing the desired stimulus condition, namely no retinal image motion.

Actually, the experiment might be duplicated by replacing the after-image by a real visual target, provided that the target could be stabilized at the foveal region. This requirement could be met by driving an otherwise motionless real target in accordance with the feedback signal from the eye movement monitor (This might call for a CRT being available inside the rotating chair cab). The original signal for the retinally-stabilized target motion would be supplied by the chair motion via vestibular

nystagmus. This indirect feature might be contrasted with previous stabilized-image experiments (also based on eye movement feedback) aiming at investigating the open-loop visual tracking characteristics (Fender and Nys, 1961; Young 1962, and others).

Although the retinal image stabilization would no longer be as accurate as with the after-image, the real target would not fade out, permitting a longer observation time. Everything else including the experimental procedure, instructions and rationale would remain unchanged.

The intriguing question special to this real-image version would be whether the nystagmus fast phase component would tend to disappear similarly as observed in the case of the after-image tracking. The affirmative answer would imply that the disappearance should be due to the stabilization of retinal image at the fovea not due to the foveal after-image per se.

[6] Oculogyral illusion and the perceptual feedback hypothesis

If the foregoing real target is left stationary with respect to the observer without introducing the external eye movement feedback, it would set up a typical environment to induce the oculogyral illusion. Once persistence of the oculo-gyral illusion is assured by applying an intense angular acceleration to the head, the time course of the illusion could be recorded quantitatively by some psychophysical method.

The remnant of smooth eye movement component interrupted by visual fixation saccades might be analyzed closely in relation to the applied chair motion. (Such eye movement records have been obtained and discussed in Chapters III and VII.) The resultant slow phase profile behavior might be then compared with the slow phase profile obtained in complete darkness under the same vestibular stimulation. The difference, if it exists, could be discussed with respect to the previously recorded time history of the illusions. Similarly, as in the after-image tracking experiment, the question underlying the above procedure aims at further testing the perceptual feedback hypothesis for the pursuit tracking; namely whether the pursuit system might respond to the illusory velocity of the target that actually has no physical motion relative to the observer.

[7] Extension to OKN slow phase

An analogous perceptual-oculomotor model might be tried for optokinetic nystagmus slow phase. The experiment could be arranged in the same way except for the required visual image: It is a reasonably wide stripe pattern instead of the small spot which is to be stabilized relative to the retina. The after-image impression does not appear technically sound enough in this case. Instead, the computer-graphically generated OKN stimulus pattern developed in this thesis would suffice for the desired retinal stabilization using the eye movement feedback



signal to command the stripe motion.

This particular experiment would be assessed also from a different point of view: the problem of influence of OKN stimulus upon the subjective sensation of self-rotation, which has received increasing attention lately. In this context, the above experiment would provide a special case, where the OKN pattern moves relative to the observer but is maintained stationary with respect to his retina.

## 8.2 On Optokinetic Nystagmus Slow Phase versus Pursuit Movement

Despite the difference in the type of visual stimulus, when compared in the time domain, OKN slow phase ("stare" type OKN) and the pursuit movement appear to share many common phenomenological features, suggesting that the two systems might be under control of common central mechanisms. By using a fast-reacting OKN stimulus pattern specially built, based on a computer-graphic technique, a close examination was undertaken with respect to certain specific aspects including latency, transient appearance and steady-state linearity range. The result generally appears to confirm the above popularly held notion:

In response to sudden and instant reversals of the stimulus motion, OKN slow phase latency was found to fall between 100 msec and 200 msec as consistent with the pursuit latency range. Furthermore, it was found that the slow phase latency never exceeded the fast phase latency (300 msec - 600 msec), clarifying some previous dispute regarding relative magnitude of the two latency times of OKN. Also as in the pursuit system, the eye velocity overshoot was occasionally observed in the velocity-step response. The steady-state velocity matching between stimulus and eye was maintained up to about  $\pm 40$  deg/sec, also in substantial agreement with the performance by the pursuit tracking.

In spite of these observations, however, the similarity between OKN slow phase and pursuit response broke in the frequency domain as revealed in the next section.

### Recommendation

#### Open-loop experiment and the extraocular muscle proprioception

Open-loop experiment would be possible with respect to the slow phase component of OKN in the human subject, not by immobilizing one eye and observing the other eye's response as described in the literature (Ter Braak, 1936; Collewijn, 1969; Collewijn et al, 1971; Körner, 1971), but by the external feedback arranged on the basis of including the on-line hybrid nystagmus processor MITNYS in the present computer graphic algorithm generating the OKN stimulus pattern: The updated OKN slow phase velocity computed by the former program is added to the original command signal that determines the OKN stimulus field velocity. (With collaboration of the author's colleague, Mr. John Tole, such a combined hybrid software has been prepared.) This approach is methodologically analogous to the open-loop experiment devised and performed by Robinson (1965) with respect to the pursuit tracking system through eliminating the effect of saccades.

If the extraocular muscle proprioceptive feedback were involved in the control of OKN slow phase, the open-loop condition formed this way would operationally differ from that

achieved in the literature with the immobilized eye in animals. Comparative eye movement investigation between the above two alternative open-loop preparations might enlighten, from behavioral standpoints, the controversial issue on the functional role of muscle spindles present in the human extraocular muscles.

### 8.3 Quest of Predictive Behavior in the Oculomotor System

One of the most interesting oculomotor characteristics is its input-adaptive capacity. This is known as a predictive or learning behavior, in which the stimulus periodicity is detected and utilized to improve the accuracy of visual tracking.

Table 8.1 summarizes pertinent information regarding the question of predictive behavior in the various oculomotor systems along with the specially cited manual control system. Enclosed by heavier lines are those eye movements dealt with in this thesis, which include the composite dual-mode tracking movement (saccade and pursuit), saccadic movement, pursuit movement, optokinetic nystagmus slow phase and vestibular nystagmus slow phase.

Frequency response of the composite system has been re-evaluated, confirming the input-adaptive predictive behavior as being in general agreement with results in the literature regarding relevant features except for the following point: Analysis of the gain-phase relation in the present periodic-input data failed to show a clear feature of the less-than-minimum phase behavior contrary to the widely held opinion, rather it appears to support the minimum-phase behavior or even some degree of the greater-than-minimum phase behavior. Hence, the result indicates a nearly effective compensation of the innate oculomotor reaction time by prediction, rather than an overcompensation implied by the less-than-minimum phase

Eye Movement Type	Stimulus modality	Voluntary or not	Predictive behavior?	Information Source
Dual-mode Composite (saccade & pursuit)	Visual	Voluntary	Yes	Chapter IV; Sündlerhauf (1960); Fender & Nye (1961); Stark <u>et al</u> (1962); Dallos & Jones (1963); Michael & Jones (1966); Werner <u>et al</u>
Saccade	Visual	Voluntary	Yes	Chapter V*; Stark <u>et al</u> (1962); Dallos & Jones (1963)
Pursuit	Visual	Semi-voluntary**	Yes	Chapter IV; Vossius (1965)
OKN slow phase	Vestibular	Involuntary	Yes	Chapter VI
Vestibular nystagmus slow phase	Visual	Involuntary	No	Chapter III
Vergence	Visual	Semi-voluntary	Yes	Zuber (1965)
Accommodation	Visual	Semi-voluntary	Yes	Stark <u>et al</u> (1965a)
Pupillary	Light intensity	Involuntary	No	Stark (1968)
Visual tracking in rhesus monkey	Visual		No	Fuchs (1967)
Manual Control	Visual	Voluntary	Yes	Elkind & Forgie (1958); McRuer & Krendel (1959); Stark <u>et al</u> (1961)

Table 8.1 Summary of oculomotor predictive results

\* Nonperiodic-input study only.

\*\*Turned on and off on voluntary basis, but under involuntary control once engaged in action.

behavior. This discrepancy from the literature likely stemmed from the relatively low level of stimulus velocity intentionally adopted in this thesis. The maximum target speed was carefully adjusted in the present series of frequency response measurements in order to prevent the pursuit system from possible velocity saturation, whereas it appears in most previous works that such a precaution has been overlooked leading to what appears to be the less-than-minimum phase behavior. An effect of non-linear oculomotor characteristics such as this should not be confused with the intrinsic nature of the predictive behavior, which, incidentally, is also a nonlinear property.

Continuous traces of the pure smooth pursuit movement were extracted from the same original composite data by removing all saccades through the special hybrid processor MITNYS developed by Allum et al (1973), allowing the separate investigation which focussed on the pursuit system alone. These data have also provided a basis of further substantiating the input-adaptive characteristics of the other distinct constituent subsystem, the saccadic system. While assessment of the saccadic system will be reviewed separately in the next section, the major finding for the pursuit system is as follows:

The nonperiodic-input frequency response exhibits a conspicuous tendency toward large phase lead (up to about  $90^\circ$ ) in the low frequency region within a given input frequency band. Zero-phase shift occurs at some mid frequency (0.3 - 0.5 Hz

depending on the particular nonperiodic input used), above which phase lag develops. This result may be contrasted with nonperiodic-input results for the composite response, which have shown no such phase lead as above, but rather produce some phase lag as is consistent with relevant results in the literature.

An interpretation of this nonperiodic-input pursuit phase behavior is suggested, in part, on the basis of the theory of Michael and Jones (1966), which regards stimulus predictability (as represented by bandwidth) as a continuous parameter affecting the system response. Based upon a comparative close examination on pursuit phase data with various input bandwidths including zero bandwidth (corresponding to the periodic-input case), an inherent phase lag associated with the pursuit system is hypothesized and calculated to yield an increasing function of frequency. Subtraction of this phase lag from the phase plot for the periodic-input tracking (which is also a phase lag increasing with increasing frequency, showing no phase lead) has led to a positive-valued and frequency-dependent phase lead. This phase result is interpreted as a potential source of the additive phase lead for compensating the aforementioned inherent phase lag. It is further assumed that the phase compensation strategy during the nonperiodic-input tracking considers only the mean value of the corrective phase lead function averaged over the given input bandwidth. By advancing the postulated inherent phase lag uniformly over the input spectrum by a



factor corresponding to the average phase lead determined above, only a region around the mid frequency would receive any real benefit in reducing the phase error, at the cost of excess phase lead at lower frequencies and insufficient compensatory phase lead at higher frequencies. This accounts for the observed tendencies of the nonperiodic-input pursuit phase data. It is also important to stress that this conceptual scheme can treat the periodic-input phase behavior as a special case of its general content. Thus according to the present interpretation, the rather unexpected pursuit phase behavior as found here (showing that the system is at least input-adaptive) can still be regarded as a manifestation of a predictive mechanism, which operates, in principle per se, even with an "unpredictable" target motion.\*

The phenomenological similarity, as observed in the time domain comparison, between OKN slow phase and pursuit movement has been described in the previous section. This similarity appears to hold also in the frequency domain with periodic stimuli. However, when the stimulus became nonperiodic, a discrepancy in the phase behavior emerged: OKN slow phase failed to exhibit the large low-frequency phase lead that was obtained with the pursuit system, suggesting some functional difference in the two systems in question. When compared within OKN,

---

\* Time domain evidence for predictive capacity of the pursuit tracking system has been demonstrated by Vossius (1965), as cited in Chapter III.

nonperiodic-input OKN slow phase has yielded somewhat greater phase lag as compared with its periodic-input counterpart, thus indicating the existence of a predictive mechanism which probably employs a strategy somewhat different from that suggested for the pursuit system.

Finally, vestibular nystagmus slow phase failed to show any predictive behavior, at least in the frequency range examined here. This statistically negative result is of interest when contrasted with the positive result obtained with the functionally related OKN slow phase.

In conclusion, the positive evidence for OKN slow phase disproves the suggestion that the predictive oculomotor behavior might belong to eye movements that are more or less under voluntary control. The negative evidence for vestibular nystagmus slow phase, on the other hand, might suggest that underlying predictive mechanisms depend upon the visual source of information. Even more strongly stated, all classes of visually-induced human eye movements exclusively incorporate the predictive capacity or input-adaptive characteristics of one form or another. Reviewing relevant results in this thesis along with those found elsewhere, no counter-example seems to be available at this moment against such an assertion. In any event, it has become more apparent here that the mode of predictive or input-adaptive behavior differs from one type of eye movement to another, indicating separate predictive schemes or mechanisms being adopted by different oculomotor systems.

## Recommendations

### [1] Open-loop assessment

The suggested pursuit phase control model, which has stemmed from the closed-loop input-output observation, suffers from difficulty in its visualization in terms of a functional block diagram. This shortcoming is in part due to its special strategy for phase compensation, and in part due to its failure to include any gain consideration, although the latter fact might be defended by the possibility that gain and phase could be controlled separately, not necessarily obeying the engineering textbook standard. Anyhow, the input-adaptive behavior of the pursuit system deserves further investigation, which might confirm, improve or extend the present result as well as its suggested interpretation. The following recommendations outline specific examples to this end, which could be readily worked out.

The next step would be frequency response measurement with periodic and nonperiodic inputs under the open-loop condition arranged with respect to the pursuit system. Similar to Robinson's variable feedback method selective to the pursuit system (Robinson, 1965), the external pursuit velocity feedback required in such experiments could be made feasible by the on-line operation of MITNYS. Alternatively, on the basis of pure calculation, the desired open-loop information could be inferred indirectly

from the closed-loop experimental data already available here. In either case, the object is analogous to that pursued by Dallos and Jones (1963) for the composite eye movement of the dual-mode visual tracking; assessment of the predictor's own transfer function as a cascaded element in the forward path of the oculomotor tracking control loop. A variable feedback experiment would be a more general extension to follow the above open-loop experiment.

These types of experiments could be performed similarly with respect to OKN slow phase.

## [2] Useful information for predictor

One of the motivations behind the open-loop experiment recommended above is the expectation that the underlying predictor would be reflected explicitly in the response output, whereas it is hidden inside the closed-loop structure under normal conditions. Actually, however, this would be the case only if the predictive mechanism operates essentially upon the retinal image motion that represents the system error. But, this error-based prediction appears somewhat difficult to accept for the reason that the retinal error information should be "less predictable" as argued by Young (1973).

On the other hand, the original predictability of the stimulus motion could be fully recovered by the cancellation theory, which would imply that the predictive part of the

tracking eye movement is synthesized based on the visually perceived information, that is, the predictive response results, because the observer sees the target as predictable. Still another possible information source for prediction would be the corollary discharge that essentially represents the eye movement itself.

The after-image tracking experiment, which was previously described in support of the perceptual feedback pursuit model, could give some clue also to this question of what signal the predictive mechanism might utilize. Periodic and nonperiodic vestibular stimulation should lead respectively to predictable and unpredictable after-image apparent motion, while the after-image can produce no retinal motion in either case. Given, in addition the finding that the vestibular nystagmus slow phase without after-image is not affected by the periodicity of head rotation, the following proposition may be asserted:

Both the perceptual-based and corollary-discharge-based schemes of prediction should give rise to some significant difference in the eye movement between the two different stimulus conditions (predictable and unpredictable) in the after-image tracking, whereas the error-based alternative should produce no substantial difference.

These periodic and nonperiodic versions of the after-image tracking experiment were both actually conducted in this thesis. Unfortunately, however, the comparative result between these two turned out statistically equivocal, and therefore recommended

that the experiment be repeated with the improved equipment as suggested before.

#### 8.4 On Saccadic Frequency Response with Nonperiodic Inputs

Nonperiodic (unpredictable) input frequency response characteristics of the saccadic system were evaluated on the basis of an indirect method utilizing the nonperiodic-input frequency response results experimentally obtained earlier for the composite and pursuit system.

Analytical study incorporated in this approach has illuminated some conceptually important points associated with the operation of the dual-mode visual tracking: though the composite eye movement, by definition, is a sum of saccadic and pursuit movement, the straight-forward vectorial subtraction of the pursuit Bode plot from the composite counterpart gives only an apparent saccadic frequency response. This is due to the inherent interference effect of pursuit movements upon the saccadic system. Real input to the saccadic system is not the original target motion, but the tracking error resulting from any inadequate performance of the pursuit system. This pursuit dependent "effective saccadic input" was computed with further use of the pursuit data, and used to correct the apparent saccadic frequency response for the pursuit interference. The result is the intrinsic saccadic frequency response, which would be obtained if the saccadic system were acting alone under a random pattern of discrete stimulus movements.

The predictive capacity of the saccadic tracking system was confirmed on the basis of phase comparison between this nonperiodic-input result and the periodic-input phase plot

inferred from the saccadic latency data obtained by Dallos and Jones (1963) with periodic square-wave inputs.\*

The present intrinsic frequency response data were examined closely in the theoretical framework of Young's sampled-data saccadic model. This model is intended to describe nonperiodic-input response and adequately predicts many aspects of the saccadic response in various conditions (Young, 1962; Young and Stark, 1963), but has not been tested previously in the frequency domain in terms of the intrinsic saccadic characteristics as implied here. Young assumed 200 msec for both sampling period and saccadic delay in his original model. However, for the particular eye movement data obtained here with two different sets of input frequency spectrum, the mean effective sampling period (inter-saccadic interval averaged over four subjects) was 510 msec and 800 msec, both considerably larger than 200 msec. Nevertheless, a good agreement was achieved between experiment and model in both gain and phase, provided that the saccadic delay is reduced drastically from the presumed innate value of 200 msec to 45 msec and -100 msec in accordance with the forced change of sampling period from 200 msec to 510 msec and 800 msec respectively.

Thus, it appears as though the system attempts to maintain the effective delay (i.e., based on sampled-data analysis, pure time delay plus one half of the sampling interval) at constant

---

\* A similar saccadic latency result has been reported by Stark et al (1962).



value of 300 msec, that is  $45 + 510/2 = -100 + 800/2 = 300$  msec.

In any event, the foregoing significantly reduced saccadic latencies, especially the negative latency of -100 msec, indicate a powerful compensatory effect by the oculomotor prediction mechanism, even under random stimulation.

On the other hand, with periodic square-wave inputs, Dallos and Jones, (1963) as well as Stark et al (1962), have obtained similar respective values at the stimulus repetition interval of  $2 \times 510$  msec and  $2 \times 800$  msec for the observed decrease of saccadic latency.

This coincidence might suggest that the saccadic system's predictive mechanism is capable of reducing the innate system delay, presumably based upon a certain statistical average of the sampling behavior, which in turn reflects some average frequency band characteristics of the given input. Such an interpretation is consistent with the notion of Michael and Jones (1966), which also has based the pursuit phase control scheme suggested previously in this thesis.

Finally, the reconciliation made between experiment and model does not support the prevailing concept of the saccadic system's velocity sensitivity, for the model does not consider differentiation of the position error signal.

## Recommendation

### Direct evaluation by discrete random inputs

The intrinsic saccadic frequency response could be obtained directly by presenting a target undergoing a random series of step displacements. This arrangement would lead to virtual absence of the pursuit response, and thereby no pursuit interference could act upon the saccadic system. The effective saccadic input would be the target motion itself. The object might be to compare the result with that obtained with the present indirect method and also with prediction by Young's model. Some hypothetical suggestions made regarding the saccadic reaction delay might also be assessed from this approach.

## 8.5 Fast Phase Behavior in Relation to Slow Phase Movement in Vestibular and Optokinetic Nystagmus

This particular aspect of nystagmus has been described by several authors. Various factors such as experimental instructions to the subject might affect the relevant response features in question. Nevertheless, the present series of controlled experiments have provided an adequate basis to confirm the following trends in both vestibular nystagmus and optokinetic nystagmus of the "stare" type.

Nystagmus fast phase resets the eye ball away from the center in the direction of fast phase, suggesting that fast phase is not a simple centering reflex. As a result, mean over-all eye position normally tends to deviate in the direction of fast phase.

These nystagmus phenomena, when assessed in relation to the slow phase component, were found not only qualitatively but also quantitatively similar between the two types of nystagmus in question. Thus, they are interpreted as a manifestation reflecting some common fast phase generating mechanism, which utilizes slow phase information regardless of its stimulus origin. Strong evidence for this view comes from clinical data by Weiss (1973) in an acoustic neuroma patient, which show a unilateral disturbance selective to the fast phase behavior affecting both vestibular and optokinetic nystagmus; fast phase direction toward center as opposed to the

normal case, while the slow phase response remains apparently normal.

As a clue to substantiate the function of the presumed common fast phase generator, OKN response records with different constant input velocities were examined to evaluate average behavior of various pertinent nystagmus parameters as a function of average slow phase velocity. For instance the average shift of "reset position" was found approximately proportional to average slow phase velocity magnitude with proportionality constant ranging from 0.45 sec to 0.70 sec depending on the individual subject. Considering the direction of fast phase as well, it appears as though fast phases were executed based on "future" eye position at 0.45 - 0.70 sec later.

Principally based on these observations a simple conceptual model is developed, which incorporates Young's sampled-data saccadic model (1962, which originally deals with fixation saccades during visual oculomotor tracking) as an internal model that determines fast phase by utilizing the slow phase motor outflow. While similar feedforward type models have been proposed in the literature recently for vestibular nystagmus generation (Schmid, 1971; Barnes, 1973), the present model aims at describing the aforementioned characteristic fast phase behavior as well as over-all response pattern for either vestibular or optokinetic nystagmus depending upon the relevancy of the given slow phase information. The key point in this model operation is that the slow phase motor signal to the fast phase

generator is slightly time-advanced in comparison to slow phase response of the eye, by a factor corresponding to the foregoing proportionality constant determined in the constant stimulus velocity experiment for OKN.

Similarly evaluated were vestibular and optokinetic nystagmus with sinusoidal stimuli of various frequencies, and these experimental results were compared with corresponding analytical predictions by the model. The data exhibited a certain degree of frequency dependence, in some agreement with the model. Also, the model's essential feasibility in accounting for the present aspect of nystagmus was demonstrated by a series of specially arranged hybrid computer simulations.

According to the model, the fast phase generator "attempts" to reset eye position exactly at center, based upon the internally computed eye position rather than the proprioceptive feedback signal from the eye. But, the attempted goal is interfered with by the postulated inherent time lag of the actual slow phase movement with respect to the upstream slow motor information, upon which the fast phase generating process depends. This results in errors in the eye's reset position with the observed relations with the instantaneous slow phase velocity. Actually, however, this deviation by fast phase can be regarded as another functionally advantageous feature of nystagmus, in addition to the compensatory aspect of the slow phase component that helps to stabilize retinal images: successive fast phase flicks bring the eye position away from center in the direction where new

new visual objects are coming from (OKN), or expected to come from following a head movement (vestibular nystagmus), thereby in both cases assisting in quick acquisition of new visual information.

Finally, the feedback-blanking method specially devised here in order to realize a selective OKN stimulation to the peripheral retina has yielded some positive evidence in the normal subject for the OKN pattern change that has been observed by Hood (1967) in a subject with no foveal vision, i.e., central scotomata patient; similar to the acoustic neuroma case, eye movements with fast phase toward center position opposed to the normal case were observed. This result might, in turn, indicate that the seemingly pathological OKN pattern, which appears to characterize the central scotomata case, is actually a normal physiological reaction resulting from the loss of foveal stimulus.

#### Recommendations

[1] Other kinematic stimulus relations and inter-species study

Besides horizontal OKN and vestibular nystagmus by horizontal head rotation as dealt with here in the human subject sitting upright, the present line of investigation might be worked out similarly with respect to nystagmus eye movements with some other variation of stimulus directions and body posture. Vestibular nystagmus induced by translational

head motion might be included as well. Also of interest might be a comparative inter-species study on the fast phase behavior.

[2] Pathological cross-examination and animal lesion study

While nystagmus data in the two pathological cases, acoustic neuroma and central scotomata, are discussed in the thesis, a more extensive clinical case study would be undoubtedly of value in order to shed further light on the nature of nystagmus fast phase generation. Based on examination of various diseases affecting vestibular and/or optokinetic nystagmus, the proposed control theory model, for example, might find some neuro-anatomical correspondance for its conceptual pathways and elements. Animal lesion studies may be another recommendation for similar prospects.

[3] Relation to the differential delay effect at the retina

The suggested model attributes the particular aspect of the over-all nystagmus pattern essentially to the transmission lag of the actual slow phase response relative to the slow phase efferent information used by the suggested fast phase generator. The OKN pattern change apparently resulting from the loss of foveal vision suggests that the model should properly include a distinction in optomotor pathways, i.e., between the slow phase signal originating in the peripheral retina and

that in the central retina. This suggestion, on the one hand, might interfere with the model's underlying theme; treatment of both vestibular and optokinetic nystagmus fast phase within a simple and common conceptual framework. But, on the other hand, as suggested by Richards (1973), this raises the possibility that the differential transmission time, assumed as a key factor of the model, might be understood in relation to the known latency difference phenomenon (manifested as the Pulfrich illusion (Pulfrich, 1922) in processing visual signals from the peripheral retina as compared to that from the central retina. Further research along this line may be recommended.



## Appendix A

### Eye Movement Monitor: Sample Calibration Records

Throughout the thesis, eye movements were measured using a Biometrics pulsed infrared photoelectric eye movement monitor, Model SG HV-2. The instrument was mounted on a spectacle frame worn by the subject as viewed in Fig. 4.1-a.

The maximum linearity range and the maximum resolution are  $\pm 150^\circ$  and  $\pm 1/4^\circ$  respectively according to the specification. Actually, however, one of these numbers can be somewhat further improved at a cost of the other, depending on adjustable distance between the eye and the infrared generator/detector unit of the eye movement monitor: Within a certain adjustable limit, the linearity range can become wider with increasing distance, whereas the resolution is improved with decreasing distance. Fig. A.1 presents some representative calibration records under different controls of this effect. Appropriate compromise was made between linearity range and resolution, depending upon the main purpose of a particular experiment in this thesis.

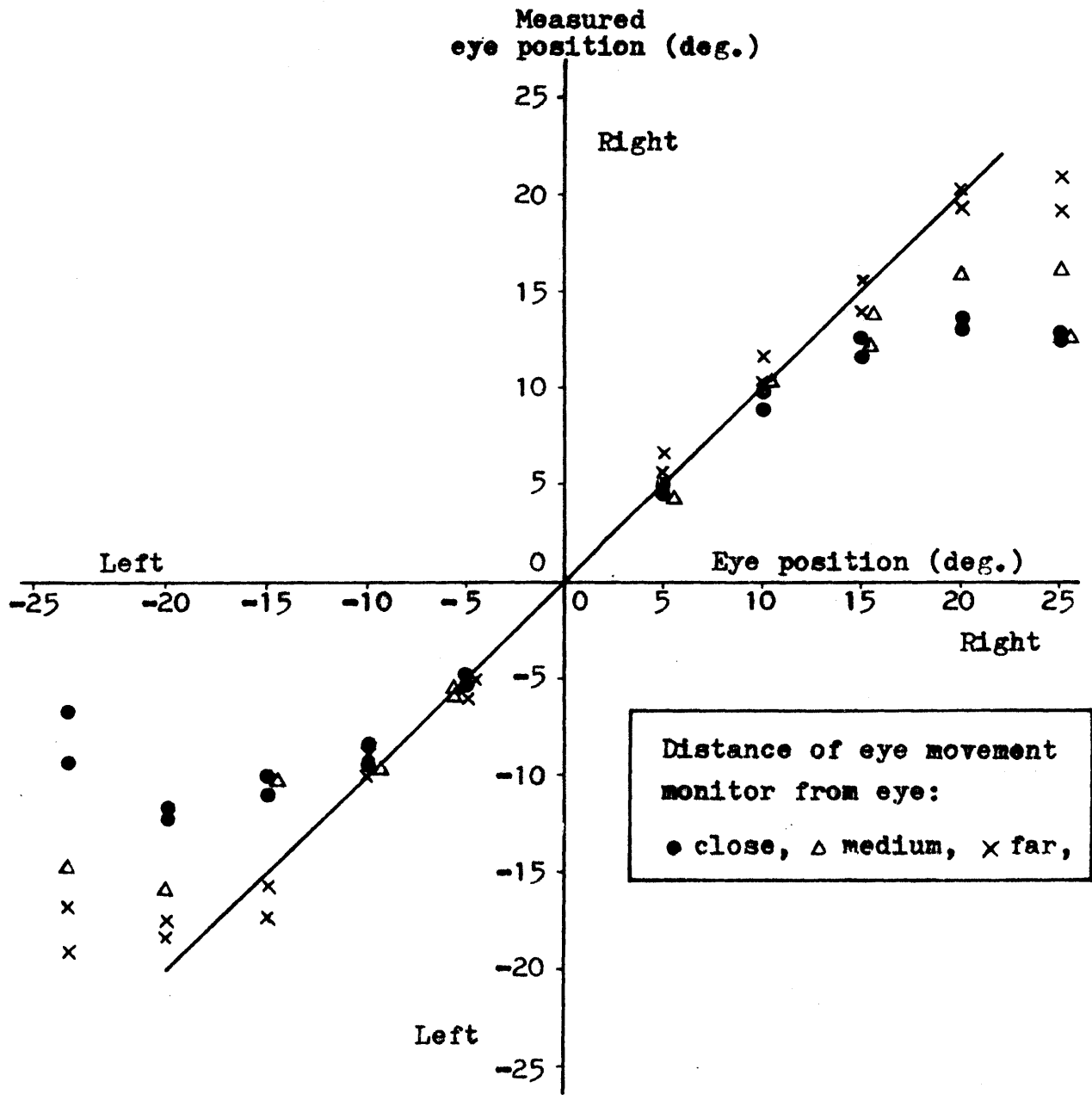


Fig. A.1 Sample calibration records of eye movement monitor.

## Appendix B

### MITNYS-FFT, Two-step Data Reduction Procedure

This special computerized process was undertaken in obtaining nonperiodic-input Bode plot data for three different types of smooth eye movement; pursuit movements during the dual-mode visual tracking (Chapter IV), vestibular nystagmus slow phase (Chapter III) and optokinetic nystagmus (Chapter VI).

While each of these chapters has separately described application of this procedure to the particular eye movement dealt with therein, operational features involved are analogous one another as summarized in Fig. B.1:

A continuous trace of the desired pure smooth eye movement was extracted from the relevant original data by removing all fast phases or saccades through the hybrid computer routine MITNYS originally developed by Tole and Young (1971) and later improved by Allum et al (1973).<sup>\*</sup> The resultant record (which has been called cumulative eye position) was then Fourier-analyzed in relation to the applied stimulus input by means of another hybrid program, FFT, given in the next appendix.

---

\* For detailed technical information of MITNYS including the computer program listing, consult Allum and Tole (1972).

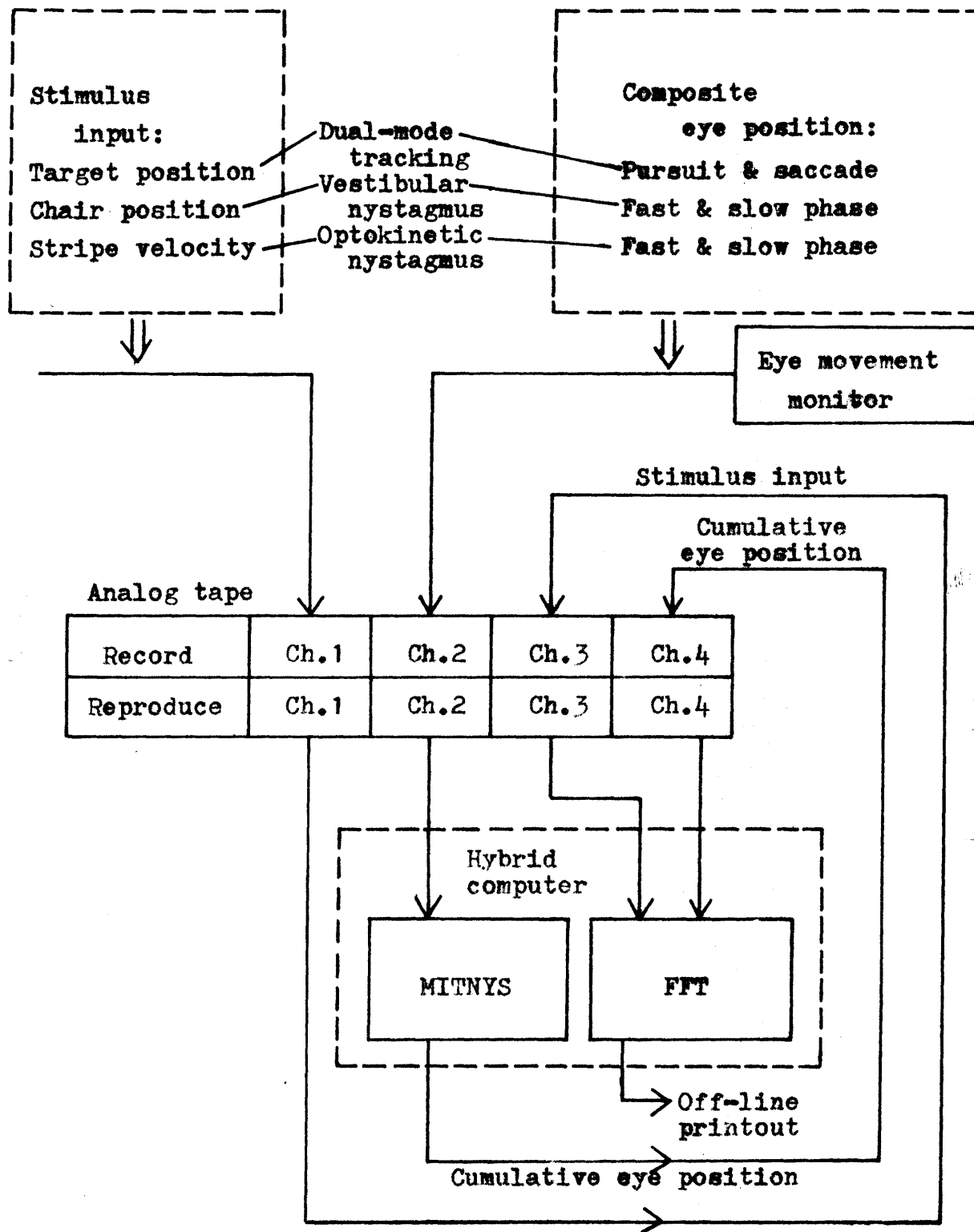


Fig. B.1 Generalized operational diagram for MITNYS-FFT data reduction procedure.

## Appendix C

### FFT, Program Outline

FFT is a hybrid computer routine used to obtain non-periodic-input eye movement frequency response data in the thesis. The program was written in PAL III program assembly language for a PDP-8 computer, based on the fast Fourier transform algorithmism by Cooley and Tukey (1965).\*

Table C.1 lists the complete program of FFT. A/D conversion of the two data signals was performed through A/D channel 1 for stimulus input and channel 2 for eye movement output. The sampling rate (which must be a power of 2) was chosen at 8 Hz, permitting Fourier analysis up to  $8/2=4$  Hz (Nyquist frequency). Buffer memory for each data signal consisted of 512 locations, so that interval of sampling epoch (total sampling time) was  $512/8=64$  sec and frequency resolution was  $1/64=0.0156$  Hz.\*\* The result was printed out in the format as appeared in Table D.1 of Appendix D.

The present program incorporated triple precision routines

---

\* A similar PAL III program for the fast Fourier transform has been previously developed by Van Houtte, N.A.J. ("Display Instrumentation for V/STOL Aircraft in Landing", Sc.D. Thesis, M.I.T., 1970).

\*\* Some runs for the after-image tracking experiment with pseudo-random vestibular stimulation employed the sampling rate of 16 Hz instead of 8 Hz. At expense of the increased frequency resolution limit (0.0312 Hz), this cut the sampling epoch in half (32 sec) so as to roughly match the average lasting time of visual after-image. (Sampling rate of 16 Hz was used also in obtaining some of nonperiodic-input OKN slow phase Bode plots.)

for crucial computations, and includes tables for logarithmic and trigonometric functions supplemented by their linear interpolation routine. But, it is subject to theoretical pitfalls inherent to a discrete Fourier transform with finite sampling epoch as discussed, for example, by Berglad (1969).<sup>\*</sup> Nevertheless, test runs (with sampling frequency at 8 Hz) on several first and second-order model plants with known frequency response characteristics yielded less than 10% gain error (in terms of dB) and no greater than 5° phase error both of which indicate adequate accuracy of FFT for the purposes of this thesis.

---

\* Among these problems is a constant drift of data signal, as often obtained in the cumulative eye position trace in relevant chapters. Fourier transform of a drift with unit rate (i.e., unit ramp signal,  $t$ ) is given by:

$$\int_{-T}^T t e^{-j\omega t} dt = 2T^2 (\sin\omega T) / \omega T$$

, where  $T$ : sampling epoch interval,  $\omega$ : angular frequency,  $t$ : time, and  $j = \sqrt{-1}$ .

This is an increasing function with decreasing frequency, thus suggesting a potential source of errors in FFT result at low frequencies. It was for this reason that any conspicuous drift associated with the cumulative eye position was removed by applying an appropriate artificial counter-drift.

Table C.1 "FFT" program listing

```

*200/FAST FOURIER TRANSFORM: MAIN PROGRAM S.YASUI
0200 7300 START,CLA CLL/PHASE 1 START
0201 1375 TAD 375/TAD LOC1
0202 3023 DCA BUFR1
0203 1376 TAD 376/TAD LOC2
0204 3024 DCA BUFR2
0205 1001 TAD 1/TAD M1000
0206 3021 DCA COUNT
0207 4541 JMS I PSAMP/GET DATA
0210 7300 CLA CLL/PHASE 2 STARTS
0211 7402 HLT
0212 7604 LAS/SET NUMBER OF SAMPLES PER SECOND
0213 3022 DCA NSAMP
0214 1377 TAD 377/TAD M400
0215 3371 DCA COUNT1
0216 7402 HLT
0217 7604 LAS/SCALE BY FACTOR OF POWER OF TWO
0220 3026 DCA SCALE/POSITIVE;AMPLIFY,NEGATIVE;ATTENUATE
0221 3025 DCA J
0222 4774 JMS I 374
0223 7402 HLT
0224 7604 DO1,LAS
0225 7450 SNA/MANUAL OR AUTOMATIC?
0226 4544 JMS I PMANUL
0227 7041 CIA
0230 3373 DCA N/AUTOMATIC PRINTOUT EVERY N'TH FREQUENCY
0231 1375 TAD 375/TAD LOC1
0232 3023 DCA BUFR1
0233 1376 TAD 376/TAD LOC2
0234 3024 DCA BUFR2
0235 1001 TAD 1/TAD M1000
0236 3372 DCA COUNT2
0237 1004 TAD 4/TAD M4
0240 3021 DCA COUNT
0241 1175 TAD TTAB15
0242 3015 DCA 15
0243 1176 TAD TTAB16
0244 3016 DCA 16
0245 1177 TAD TTAB17
0246 3017 DCA 17
0247 3415 DCA I 15
0250 3416 DCA I 16
0251 3417 DCA I 17
0252 2021 ISZ COUNT
0253 5247 JMP .-4
0254 7300 DO2,CLA CLL
0255 1175 TAD TTAB15
0256 3015 DCA 15
0257 1176 TAD TTAB16
0260 3016 DCA 16
0261 1177 TAD TTAB17
0262 3017 DCA 17
0263 4542 JMS I PGETM

```

0264	4543	JMS I PSNCS
0265	1423	TAD I BUFFR1
0266	7421	MQL
0267	1042	TAD COS
0270	4545	JMS I PMUL
0271	3030	DCA R2
0272	7501	MQA
0273	3031	DCA R3
0274	4546	JMS I PADJST/SCALING
0275	4547	JMS I PSUMTN
0276	7000	NOP
0277	1423	TAD I BUFFR1
0300	7421	MQL
0301	1043	TAD SIN
0302	4545	JMS I PMUL
0303	3030	DCA R2
0304	7501	MQA
0305	3031	DCA R3
0306	4546	JMS I PADJST
0307	4547	JMS I PSUMTN
0310	7000	NOP
0311	1424	TAD I BUFFR2
0312	7421	MQL
0313	1042	TAD COS
0314	4545	JMS I PMUL
0315	3030	DCA R2
0316	7501	MQA
0317	3031	DCA R3
0320	4546	JMS I PADJST
0321	4547	JMS I PSUMTN
0322	7000	NOP
0323	1424	TAD I BUFFR2
0324	7421	MQL
0325	1043	TAD SIN
0326	4545	JMS I PMUL
0327	3030	DCA R2
0330	7501	MQA
0331	3031	DCA R3
0332	4546	JMS I PADJST
0333	4547	JMS I PSUMTN
0334	7000	NOP
0335	2372	ISZ COUNT2
0336	5340	JMP .+2
0337	5344	JMP .+5
0340	2023	ISZ BUFFR1
0341	2024	ISZ BUFFR2
0342	7000	NOP
0343	5254	JMP D02
0344	4556	JMS I PFREQ
0345	4550	JMS I PXYUV
0346	4551	JMS I PMGNTD
0347	4552	JMS I PLOGMG
0350	4553	JMS I PDB
0351	4554	JMS I PPHASE



0352	4555	JMS I PWRITE	0046	0000	DS3,0
0353	7604	LAS	0047	0000	XH,0
0354	7041	CIA	0050	0000	YH,0
0355	3373	DCA N	0051	0000	UH,0
0356	1373	TAD N	0052	0000	VH,0
0357	7450	SNA	0053	0000	XL,0
0360	5224	JMP DO1/FOR MANUAL	0054	0000	YL,0
0361	7300	CLA CLL	0055	0000	UL,0
0362	2371	ISZ COUNT1	0056	0000	VL,0
0363	5365	JMP .+2	0057	0000	HIGH1,0
0364	7402	HLT/ALL DONE	0060	0000	LOW1,0
0365	2025	ISZ J	0061	0000	AH,0
0366	2373	ISZ N	0062	0000	AL,0
0367	5362	JMP .-5	0063	0000	HIGH2,0
0370	5224	JMP DO1	0064	0000	LOW2,0
0371	0000	COUNT1,0	0065	0000	HIGH3,0
0372	0000	COUNT2,0	0066	0000	LOW3,0
0373	0000	N,0	0067	0000	XXYYH,0
		*374	0070	0000	UUUVH,0
0374	1400	1400	0071	0000	XXYYL,0
0375	2000	2000/LOC1	0072	0000	UUUVL,0
0376	3000	3000/LOC2	0073	0000	LGARGI,0
0377	7400	7400/M400	0074	0000	LGARGF,0
		*1	0075	0000	LOG8I,0
0001	7000	7000/M1000	0076	0000	LOG8F,0
0002	7777	7777/M1	0077	0000	LG8I,0
0003	7775	7775/M3	0100	0000	LG8F,0
0004	7774	7774/M4	0101	0000	DBI,0
0005	7766	7766/M12	0102	0000	DBF,0
0006	0012	0012/C12	0103	0000	ARPH,0
0007	4000	4000/C4000	0104	0000	ABQH,0
		*20	0105	0000	ABPL,0
0020	0777	0777/C777	0106	0000	AEQL,0
0021	0000	COUNT,0	0107	0000	ANGLEH,0
0022	0000	NSAMP,0	0110	0000	ANGLEL,0
0023	0000	BUFFR1,0	0111	0000	PH,0
0024	0000	BUFFR2,0	0112	0000	QH,0
0025	0000	J,0	0113	0000	PL,0
0026	0000	SCALE,0	0114	0000	QL,0
0027	0000	R1,0	0115	0000	AXH,0
0030	0000	R2,0	0116	0000	AYH,0
0031	0000	R3,0	0117	0000	AUH,0
0032	0000	FINTGR,0	0120	0000	AVH,0
0033	0000	FFRCTN,0	0121	0000	AXL,0
0034	0000	INTGR,0	0122	0000	AYL,0
0035	0000	FRCTN,0	0123	0000	AUL,0
0036	0000	COUNT3,0	0124	0000	AVL,0
0037	0000	SIGN,0	0125	0000	PHASEH,0
0040	0000	LINK,0	0126	0000	PHASEL,0
0041	0000	M,0	0127	0000	CHECK,0
0042	0000	COS,0	0130	0306	K306,0306
0043	0000	SIN,0	0131	0275	K275,0275
0044	0000	DS1,0	0132	0240	K240,0240
0045	0000	DS2,0	0133	0330	K330,0330

0134	0312	K312,0312
0135	0274	K274,0274
0136	0262	K262,0262
0137	0265	K265,0265
0140	0266	K266,0266
0141	0600	PSAMP,SAMP
0142	0400	PGETM,GETM
0143	1200	PSNCS,SNCS
0144	4600	PMANUL,MANUL
0145	0670	PMUL,MUL
0146	0460	PADJST,ADJST
0147	1023	PSUMTN,SUMTN
0150	0635	PXYUV,XYUV
0151	5000	PMGNTD,MGNTD
0152	5314	PLOGMG,LOGMG
0153	5200	PDB,DB
0154	5600	PPHASE,PHASE
0155	4200	PWRITE,WRITE
0156	1000	PFREQ,FREQ
0157	4000	PBDCNV,BDCNV
0160	4110	PTDGT,TDGT
0161	4400	PASKJ,ASKJ
0162	4470	PRFADJ,READJ
0163	4640	PCRLF,CRLF
0164	4620	PTYPE,TYPE
0165	4630	PLISN,LISN
0166	1125	PABSLT,ABSLT
0167	1600	PSQURE,SQURE
0170	5400	PLOG8,LOG8
0171	6000	PATAN,ATAN
0172	4677	TTAB11,TAB11-1
0173	4707	TTAB12,TAB12-1
0174	4717	TTAB13,TAB13-1
0175	1347	TTAB15,TAB15-1
0176	1353	TTAB16,TAB16-1
0177	1357	TTAB17,TAB17-1
		*400
0400	0000	GETM,0
0401	7300	CLA CLL
0402	1257	TAD 457/TAD M11
0403	3036	DCA COUNT3
0404	7001	IAC
0405	3254	DCA MASK
0406	1256	TAD TTAB14
0407	3014	DCA 14
0410	1023	TAD BUFFR1
0411	3255	DCA NNN
0412	7100	CLL
0413	1025	TAD J/REPEAT
0414	0254	AND MASK
0415	7650	SNA CLA
0416	5222	JMP .+4
0417	1255	TAD NNN
0420	0020	AND 20/AND C777

0421	7410	SKP
0422	7300	CLA CLL
0423	3414	DCA I 14
0424	2036	ISZ COUNT3
0425	7410	SKP
0426	5242	JMP .+14
0427	7421	MQL
0430	1255	TAD NNN
0431	7413	SHL
0432	0000	0000
0433	3255	DCA NNN
0434	7100	CLL
0435	1254	TAD MASK
0436	7004	RAL
0437	3254	DCA MASK
0440	7100	CLL
0441	5213	JMP GETM+13/JMP REPEAT
0442	1256	TAD TTAB14
0443	3014	DCA 14
0444	1257	TAD 457/TAD M11
0445	3036	DCA COUNT3
0446	1414	TAD I 14
0447	2036	ISZ COUNT3
0450	5246	JMP .-2
0451	3041	DCA M
0452	7100	CLL
0453	5600	JMP I GETM
0454	0000	MASK,0
0455	0000	NNN,0
0456	1157	TTAB14,TAB14-1
		*457
0457	7767	7767/M11

```

*460
0460 0000 ADJST,0
0461 7300 CLA CLL
0462 1030 TAD R2
0463 7510 SGEZ
0464 5270 JMP .+4
0465 7200 CLA
0466 3027 DCA R1
0467 5273 JMP .+4
0470 7300 CLA CLL
0471 1002 TAD 2/TAD M1
0472 3027 DCA R1
0473 1026 TAD SCALE
0474 7440 SZA
0475 5300 JMP .+3
0476 4776 JMS I 576
0477 5660 JMP I ADJST
0500 0377 AND 577/AND C3777
0501 1002 TAD 2/TAD M1
0502 3373 DCA FACTOR
0503 1373 TAD FACTOR
0504 3323 DCA .+17/DCA SIFTL1
0505 1373 TAD FACTOR
0506 3333 DCA .+25/DCA SIFTL2
0507 1373 TAD FACTOR
0510 3357 DCA .+47/DCA SIFTR1
0511 1373 TAD FACTOR
0512 3367 DCA .+55/DCA SIFTR2
0513 1026 TAD SCALE
0514 7510 SGEZ
0515 5351 JMP REDUCE
0516 7300 CLA CLL
0517 1030 TAD R2
0520 7421 MQL
0521 1027 TAD R1
0522 7413 SHL
0523 0000 0000/SIFTL1
0524 3044 DCA DS1
0525 7501 MOA
0526 3374 DCA DS2H
0527 7100 CLL
0530 1031 TAD R3
0531 7421 MQL
0532 7413 SHL
0533 0000 0000/SIFTL2
0534 3375 DCA DS2L
0535 7501 MOA
0536 3046 DCA DS3
0537 1375 TAD DS2L
0540 1374 TAD DS2H
0541 3045 DCA DS2
0542 1027 TAD R1
0543 0007 AND 7/AND C4000

```

0544	1044	TAD DS1
0545	7004	RAL
0546	7630	SZL CLA
0547	7402	HLT/OVER FLOW
0550	5660	JMP I ADJUST
0551	7300	REDUCE,CLA CLL
0552	1030	TAD R2
0553	7421	MQL
0554	1027	TAD R1
0555	7415	ASR
0556	0000	0000/SIFTR1
0557	3044	DCA DS1
0560	7501	MOA
0561	3045	DCA DS2
0562	1031	TAD R3
0563	7421	MQL
0564	1030	TAD R2
0565	7415	ASR
0566	0000	0000/SIFTR2
0567	7300	CLA CLL
0570	7501	MOA
0571	3046	DCA DS3
0572	5660	JMP I ADJUST
0573	0000	FACTOR,0
0574	0000	DS2H,0
0575	0000	DS2L,0
		*576
0576	1760	1760/SUBROUTINA TO NO SCALING
0577	3777	3777/C3777
		*600
0600	0000	SAMP,0
0601	7300	CLA CLL
0602	6541	ADCC
0603	6544	ADIC
0604	6532	ADCV
0605	6531	ADSF
0606	5205	JMP .-1
0607	6534	ADRB
0610	3423	DCA I BUFFER1
0611	6544	ADIC
0612	6532	ADCV
0613	6531	ADSF
0614	5213	JMP .-1
0615	6534	ADRB
0616	3424	DCA I BUFFER2
0617	6454	CLAF
0620	6461	SNAF
0621	7610	SKP CLA
0622	5220	JMP .-2
0623	2021	ISZ COUNT
0624	5226	JMP .+2
0625	5600	JMP I SAMP
0626	2023	ISZ BUFFER1
0627	2024	ISZ BUFFER2

0630	5201	JMP SAMP+1	0721	5670	JMP I MUL
0631	7300	CLA CLL			HIGHER=MLTPLR
0632	5600	JMP I SAMP			*1600
		*635	1600	0000	SQURF,0
0635	0000	XYUV,0	1601	7300	CLA CLL
0636	7300	CLA CLL	1602	1063	TAD HIGH2
0637	1175	TAD TTAB15	1603	7421	MQL
0640	3015	DCA 15	1604	1063	TAD HIGH2
0641	1176	TAD TTAB16	1605	3207	DCA .+2
0642	3016	DCA 16	1606	7405	MUY
0643	1415	TAD I 15	1607	0000	0000
0644	3047	DCA XH	1610	7440	SZA
0645	1415	TAD I 15	1611	7410	SKP
0646	3050	DCA YH	1612	7430	SZL
0647	1415	TAD I 15	1613	7402	HLI/OVER FLOW
0650	3051	DCA UH	1614	7501	MQA
0651	1415	TAD I 15	1615	7510	SGEZ
0652	3052	DCA VH	1616	5213	JMP .-3
0653	1416	TAD I 16	1617	3273	DCA HIH1H
0654	3053	DCA XL	1620	1063	TAD HIGH2
0655	1416	TAD I 16	1621	7421	MQL
0656	3054	DCA YL	1622	1064	TAD LOW2
0657	1416	TAD I 16	1623	3225	DCA .+2
0660	3055	DCA UL	1624	7405	MUY
0661	1416	TAD I 16	1625	0000	0000
0662	3056	DCA VL	1626	3274	DCA HILOWH
0663	7100	CLL	1627	7501	MQA
0664	5635	JMP I XYUV	1630	3275	DCA HILOWL
		*670	1631	1064	TAD LOW2
0670	0000	MUL,0	1632	7421	MQL
0671	7100	CLL	1633	1064	TAD LOW2
0672	7510	SPA	1634	3236	DCA .+2
0673	7061	CIA CML	1635	7405	MUY
0674	3305	DCA MLTPLR	1636	0000	0000
0675	7501	MQA	1637	3276	DCA LWLWH
0676	7510	SPA	1640	7100	CLL
0677	7061	CIA CML	1641	1276	TAD LWLWH
0700	7421	MQL	1642	1275	TAD HILOWL
0701	7430	SZL	1643	1275	TAD HILOWL
0702	7040	CMA	1644	3066	DCA LOW3
0703	3037	DCA SIGN	1645	7100	CLL
0704	7405	MUY	1646	1274	TAD HILOWH
0705	0000	MLTPLR,0	1647	1274	TAD HILOWH
0706	2037	ISZ SIGN	1650	1273	TAD HIH1H
0707	5670	JMP I MUL	1651	3065	DCA HIGH3
0710	3305	DCA HIGHER	1652	7100	CLL
0711	7501	MQA	1653	1276	TAD LWLWH
0712	7141	CLL CIA	1654	1275	TAD HILOWL
0713	7421	MQL	1655	7420	SNL
0714	1305	TAD HIGHER	1656	5261	JMP .+3
0715	7040	CMA	1657	2065	ISZ HIGH3
0716	7430	SZL	1660	7100	CLL
0717	7001	IAC	1661	1275	TAD HILOWL
0720	7100	CLL	1662	7420	SNL

1663	7410	SKP
1664	2065	ISZ HIGH3
1665	7300	CLA CLL
1666	1065	TAD HIGH3
1667	7510	SGEZ
1670	5213	JMP SQUIRE+13
1671	7300	CLA CLL
1672	5600	JMP I SQUIRE
1673	0000	HIHIH,0
1674	0000	HILOWH,0
1675	0000	HILOWL,0
1676	0000	LWLWH,0
		*1000
1000	0000	FREQ,0
1001	7300	CLA CLL
1002	7421	MQL
1003	1022	TAD NSAMP
1004	7041	CIA
1005	1220	TAD 1020/TAD C10
1006	3212	DCA .+4
1007	7100	CLL
1010	1025	TAD J
1011	7417	LSR
1012	0000	0000
1013	3032	DCA FINTER
1014	7501	MOA
1015	3033	DCA FFRCTN
1016	7100	CLL
1017	5600	JMP I FREQ
		*1020
1020	0010	0010
		*1023
1023	0000	SUMIN,0
1024	7300	CLA CLL
1025	1417	TAD I 17
1026	1046	TAD DS3
1027	3315	DCA S3
1030	7204	GLK
1031	1416	TAD I 16
1032	1045	TAD DS2
1033	3314	DCA S2
1034	7204	GLK
1035	1415	TAD I 15
1036	3312	DCA A
1037	7100	CLL
1040	1312	TAD A
1041	0007	AND 7/AND C4000
1042	1044	TAD DS1
1043	7430	SZL
1044	5255	JMP .+11/BOTH NEGATIVE
1045	7004	RAL
1046	7630	SZL CLA
1047	5251	JMP .+2/OPPOSITE SIGN
1050	5264	JMP .+14/BOTH POSITIVE

1051	1312	TAD A/OPPOSITE SIGN
1052	1044	TAD DS1
1053	3313	DCA S1
1054	5271	JMP .+15/JMP GO
1055	7300	CLA CLL/BOTH NEGATIVE
1056	1312	TAD A
1057	1044	TAD DS1
1060	7500	SMA
1061	7402	HLT/OVER FLOW
1062	3313	DCA S1
1063	5271	JMP .+6/JMP GO
1064	1312	TAD A/BOTH POSITIVE
1065	1044	TAD DS1
1066	7510	SPA
1067	7402	HLT/OVER FLOW
1070	3313	DCA S1
1071	1015	TAD 15/GO
1072	1002	TAD 2/TAD M1
1073	3015	DCA 15
1074	1016	TAD 16
1075	1002	TAD 2/TAD M1
1076	3016	DCA 16
1077	1017	TAD 17
1100	1002	TAD 2/TAD M1
1101	3017	DCA 17
1102	1313	TAD S1
1103	3415	DCA I 15
1104	1314	TAD S2
1105	3416	DCA I 16
1106	1315	TAD S3
1107	3417	DCA I 17
1110	7100	CLL
1111	5623	JMP I SUMTN
1112	0000	A,0
1113	0000	S1,0
1114	0000	S2,0
1115	0000	S3,0
		*1125
1125	0000	ABSLT,0
1126	7300	CLA CLL
1127	1057	TAD HIGH1
1130	7510	SGEZ
1131	5336	JMP .+5
1132	3061	DCA AH
1133	1060	TAD LOW1
1134	3062	DCA AL
1135	5725	JMP I ABSLT
1136	7300	CLA CLL
1137	1060	TAD LOW1
1140	7041	CIA
1141	3062	DCA AL
1142	7204	GLK
1143	3040	DCA LINK
1144	1057	TAD HIGH1



1145	7040	CMA
1146	1040	TAD LINK
1147	3061	DCA AH
1150	7100	CLL
1151	5725	JMP I ABSLT
		*1160
1160	0000	TAB14,0

\*1200

1200	0000	SNCS,0
1201	7300	CLA CLL
1202	1041	TAD M
1203	0020	AND 20/AND C777
1204	3336	DCA MM
1205	1336	TAD MM
1206	0345	AND 1345/AND C600
1207	7450	SNA
1210	5222	JMP IQD
1211	0344	AND 1344/AND C400
1212	7450	SNA
1213	5241	JMP IIQD
1214	7200	CLA
1215	1336	TAD MM
1216	0343	AND 1343/AND C200
1217	7450	SNA
1220	5265	JMP IIIQD
1221	5312	JMP IVQD
1222	7300	IQD,CLA CLL
1223	1346	TAD 1346/TAD C6600
1224	1336	TAD MM
1225	3337	DCA PSINTB
1226	1737	TAD I PSINTB
1227	3043	DCA SIN
1230	1336	TAD MM
1231	7041	CIA
1232	1343	TAD 1343/TAD C200
1233	1346	TAD 1346/TAD C6600
1234	1002	TAD 2/TAD M1
1235	3337	DCA PSINTB
1236	1737	TAD I PSINTB
1237	3042	DCA COS
1240	5600	JMP I SNCS
1241	7300	IIQD,CLA CLL
1242	1343	TAD 1343/TAD C200
1243	7041	CIA
1244	1336	TAD MM
1245	3336	DCA MM
1246	1336	TAD MM
1247	7041	CIA
1250	1343	TAD 1343/TAD C200
1251	1346	TAD 1346/TAD C6600
1252	1002	TAD 2/TAD M1
1253	3337	DCA PSINTB
1254	1737	TAD I PSINTB
1255	3043	DCA SIN
1256	1346	TAD 1346/TAD C6600
1257	1336	TAD MM
1260	3337	DCA PSINTB
1261	1737	TAD I PSINTB
1262	7041	CIA
1263	3042	DCA COS

1264	5600	JMP I SNCS
1265	7300	IIIQD,CLA CLL
1266	1344	TAD 1344/TAD C400
1267	7041	CIA
1270	1336	TAD MM
1271	3336	DCA MM
1272	1346	TAD 1346/TAD C6600
1273	1336	TAD MM
1274	3337	DCA PSINTB
1275	1737	TAD I PSINTB
1276	7041	CIA
1277	3043	DCA SIN
1300	1336	TAD MM
1301	7041	CIA
1302	1343	TAD 1343/TAD C200
1303	1346	TAD 1346/TAD C6600
1304	1002	TAD 2/TAD M1
1305	3337	DCA PSINTB
1306	1737	TAD I PSINTB
1307	7041	CIA
1310	3042	DCA COS
1311	5600	JMP I SNCS
1312	7300	IVQD,CLA CLL
1313	1345	TAD 1345/TAD C600
1314	7041	CIA
1315	1336	TAD MM
1316	3336	DCA MM
1317	1336	TAD MM
1320	7041	CIA
1321	1343	TAD 1343/TAD C200
1322	1346	TAD 1346/TAD C6600
1323	1002	TAD 2/TAD M1
1324	3337	DCA PSINTB
1325	1737	TAD I PSINTB
1326	7041	CIA
1327	3043	DCA SIN
1330	1346	TAD 1346/TAD C6600
1331	1336	TAD MM
1332	3337	DCA PSINTB
1333	1737	TAD I PSINTB
1334	3042	DCA COS
1335	5600	JMP I SNCS
1336	0000	MM,0
1337	0000	PSINTB,0
		*1343
1343	0200	0200/C200
1344	0400	0400/C400
1345	0600	0600/C600
1346	6600	6600/C6600
		*1350
1350	0000	TAB15,0
		*1354
1354	0000	TAB16,0
		*1360

1360		TAB17,
		*4000
4000	0000	BDCNV,0
4001	7300	CLA CLL
4002	3037	DCA SIGN
4003	1004	TAD 4/TAD M4
4004	3036	DCA COUNT3
4005	1172	TAD TTAB11
4006	3011	DCA 11
4007	1300	TAD TTAB10
4010	3010	DCA 10
4011	3411	DCA I 11
4012	2036	ISZ COUNT3
4013	5211	JMP .-2
4014	1172	TAD TTAB11
4015	3011	DCA 11
4016	1034	TAD INTGR
4017	7450	SNA
4020	5255	JMP FRCT
4021	7500	SMA
4022	5236	JMP .+14
4023	7201	CLA IAC
4024	3037	DCA SIGN
4025	7100	CLL
4026	1035	TAD FRCTN
4027	7041	CIA
4030	3035	DCA FRCTN
4031	7204	GLK
4032	3040	DCA LINK
4033	1034	TAD INTGR
4034	7040	CMA
4035	1040	TAD LINK
4036	3276	NEXTIR,DCA AINTGR
4037	1410	TAD I 10
4040	3244	DCA .+4
4041	1276	TAD AINTGR
4042	7421	MQL
4043	7407	DVI
4044	0000	0000
4045	3277	DCA REMAIN
4046	7501	MOA
4047	3411	DCA I 11
4050	1277	TAD REMAIN
4051	7450	SNA
4052	5255	JMP FRCT
4053	2036	ISZ COUNT3
4054	5236	JMP NEXTIR
4055	7300	FRCT,CLA CLL
4056	1004	TAD 4/TAD M4
4057	3036	DCA COUNT3
4060	1173	TAD TTAB12
4061	3012	DCA 12
4062	7100	NEXTR,CLL
4063	1035	TAD FRCTN

4064	7421	MQL
4065	7405	MUY
4066	0012	0012
4067	3412	DCA I 12
4070	7501	MOA
4071	3035	DCA FRCTN
4072	2036	ISZ COUNT3
4073	5262	JMP NEXTFR
4074	7300	CLA CLL
4075	5600	JMP I BDCNV
4076	0000	AINTGR,0
4077	0000	REMAIN,0
4100	4100	TTAB10,TAB10-1
4101	1750	TAB10,1750
4102	0144	0144
4103	0012	0012
4104	0001	0001
		*4110
4110	0000	TDGT,0
4111	7300	CLA CLL
4112	6046	TLS
4113	1004	TAD 4/TAD M4
4114	3036	DCA COUNT3
4115	1037	TAD SIGN
4116	7450	SNA
4117	7410	SKP
4120	5324	JMP .+4
4121	7200	CLA
4122	1132	TAD K240
4123	5326	JMP .+3
4124	7200	CLA
4125	1376	TAD 4176/TAD K255,-
4126	4564	JMS I PTYPE
4127	1172	TAD TTAB11
4130	3011	DCA 11
4131	3367	DCA ACCUM
4132	1411	NEXTI,TAD I 11/TYPE INTEGER PART
4133	3370	DCA DIGIT
4134	1370	TAD DIGIT
4135	1367	TAD ACCUM
4136	3367	DCA ACCUM
4137	1367	TAD ACCUM
4140	7440	SZA
4141	5344	JMP .+3
4142	1132	TAD K240
4143	5347	JMP .+4
4144	7200	CLA
4145	1370	TAD DIGIT
4146	1375	TAD 4175/TAD C260
4147	4564	JMS I PTYPE
4150	2036	ISZ COUNT3
4151	5332	JMP NEXTI
4152	1377	TAD 4177/TAD K256,.
4153	4564	JMS I PTYPE

4154	1004	TAD 4/TAD M4
4155	3036	DCA COUNT3
4156	1173	TAD TTAB12
4157	3012	DCA 12
4160	1412	NEXTF,TAD I 12/TYPE FRACTION PART
4161	1375	TAD 4175/TAD C260
4162	4564	JMS I PTYPE
4163	2036	ISZ COUNT3
4164	5360	JMP NEXTF
4165	7300	CLA CLL
4166	5710	JMP I TDGT
4167	0000	ACCUM,0
4170	0000	DIGIT,0
		*4175
4175	0260	0260/C260
4176	0255	0255/K255
4177	0256	0256/K256

		*5000			
5000	0000	MGNTD,0		5064	1065 TAD HIGH3
5001	7300	CLA CLL		5065	3335 DCA YYH
5002	1047	TAD XH		5066	1066 TAD LOW3
5003	3057	DCA HIGH1		5067	3341 DCA YYL
5004	1053	TAD XL		5070	1117 TAD AUH
5005	3060	DCA LOW1		5071	3063 DCA HIGH2
5006	4566	JMS I PABSLT		5072	1123 TAD AUL
5007	1061	TAD AH		5073	3064 DCA LOW2
5010	3115	DCA AXH		5074	4567 JMS I PSQURE
5011	1062	TAD AL		5075	1065 TAD HIGH3
5012	3121	DCA AXL		5076	3336 DCA UUH
5013	1050	TAD YH		5077	1066 TAD LOW3
5014	3057	DCA HIGH1		5100	3342 DCA UUL
5015	1054	TAD YL		5101	1120 TAD AVH
5016	3060	DCA LOW1		5102	3063 DCA HIGH2
5017	4566	JMS I PABSLT		5103	1124 TAD AVL
5020	1061	TAD AH		5104	3064 DCA LOW2
5021	3116	DCA AYH		5105	4567 JMS I PSQURE
5022	1062	TAD AL		5106	1065 TAD HIGH3
5023	3122	DCA AYL		5107	3337 DCA VVH
5024	1051	TAD UH		5110	1066 TAD LOW3
5025	3057	DCA HIGH1		5111	3343 DCA VVL
5026	1055	TAD UL		5112	7100 CLL
5027	3060	DCA LOW1		5113	1340 TAD XXL
5030	4566	JMS I PABSLT		5114	1341 TAD YYL
5031	1061	TAD AH		5115	3071 DCA XXYL
5032	3117	DCA AUH		5116	7204 GLK
5033	1062	TAD AL		5117	1334 TAD XXH
5034	3123	DCA AUL		5120	1335 TAD YYH
5035	1052	TAD VH		5121	3067 DCA XYYH
5036	3057	DCA HIGH1		5122	7100 CLL
5037	1056	TAD VL		5123	1342 TAD UUL
5040	3060	DCA LOW1		5124	1343 TAD VVL
5041	4566	JMS I PABSLT		5125	3072 DCA UUVVL
5042	1061	TAD AH		5126	7204 GLK
5043	3120	DCA AVH		5127	1336 TAD UUH
5044	1062	TAD AL		5130	1337 TAD VVH
5045	3124	DCA AVL		5131	3070 DCA UUVVH
5046	1115	TAD AXH		5132	7100 CLL
5047	3063	DCA HIGH2		5133	5600 JMP I MGNTD
5050	1121	TAD AXL		5134	0000 XXH,0
5051	3064	DCA LOW2		5135	0000 YYH,0
5052	4567	JMS I PSQURE		5136	0000 UUH,0
5053	1065	TAD HIGH3		5137	0000 VVH,0
5054	3334	DCA XXH		5140	0000 XXL,0
5055	1066	TAD LOW3		5141	0000 YYL,0
5056	3340	DCA XXL		5142	0000 UUL,0
5057	1116	TAD AYH		5143	0000 VVL,0
5060	3063	DCA HIGH2			*5200
5061	1122	TAD AYL		5200	0000 DB,0
5062	3064	DCA LOW2		5201	7300 CLA CLL
5063	4567	JMS I PSQURE		5202	3037 DCA SIGN
				5203	1077 TAD LG8I
				5204	7510 SGEZ

5205	2037	ISZ	SIGN	5273	1304	IAI	SUMH
5206	7300	CLA	CLL	5274	7040	CMA	
5207	1077	TAD	LG8I	5275	1040	TAD	LINK
5210	3057	DCA	HIGH1	5276	3101	DCA	DBI
5211	1100	TAD	LG8F	5277	7100	CLL	
5212	3060	DCA	LOW1	5300	5600	JMP	I DB
5213	4566	JMS	I PABSLT	5301	0000	SAVEH	,0
5214	1061	TAD	AH	5302	0000	SAVEL	,0
5215	7421	MQL		5303	0000	SUML	,0
5216	7405	MUY		5304	0000	SUMH	,0
5217	7163	7163	/LOG(10)8			*5314	
5220	3301	DCA	SAVEH	5314	0000	LOGMG	,0
5221	7501	MOA		5315	7300	CLA	CLL
5222	3302	DCA	SAVEL	5316	1067	TAD	XXYYH
5223	7100	CLL		5317	3073	DCA	LGARGI
5224	1062	TAD	AL	5320	1071	TAD	XXYYL
5225	7421	MQL		5321	3074	DCA	LGARGF
5226	7405	MUY		5322	4570	JMS	I PLOG8
5227	7163	7163		5323	1075	TAD	LOG8I
5230	1302	TAD	SAVEL	5324	3366	DCA	XYLOGI
5231	3302	DCA	SAVEL	5325	1076	TAD	LOG8F
5232	7204	GLK		5326	3367	DCA	XYLOGF
5233	1301	TAD	SAVEH	5327	7100	CLL	
5234	3301	DCA	SAVEH	5330	1070	TAD	UUVVH
5235	1005	TAD	5/TAD M12	5331	3073	DCA	LGARGI
5236	3036	DCA	COUNT3	5332	1072	TAD	UUVVL
5237	3303	DCA	SUML	5333	3074	DCA	LGARGF
5240	3304	DCA	SUMH	5334	4570	JMS	I PLOG8
5241	7100	CLL		5335	1075	TAD	LOG8I
5242	1302	TAD	SAVEL	5336	3370	DCA	UVLOGI
5243	1303	TAD	SUML	5337	1076	TAD	LOG8F
5244	3303	DCA	SUML	5340	3371	DCA	UVLOGF
5245	7204	GLK		5341	7100	CLL	
5246	1301	TAD	SAVEH	5342	1367	TAD	XYLOGF
5247	1304	TAD	SUMH	5343	7041	CIA	
5250	3304	DCA	SUMH	5344	3373	DCA	MXYLGF
5251	7100	CLL		5345	7204	GLK	
5252	2036	ISZ	COUNT3	5346	3040	DCA	LINK
5253	5241	JMP	.-12	5347	7100	CLL	
5254	1037	TAD	SIGN	5350	1366	TAD	XYLOGI
5255	7440	SZA		5351	7040	CMA	
5256	5265	JMP	.+7	5352	1040	TAD	LINK
5257	7300	CLA	CLL	5353	3372	DCA	MXYLGI
5260	1304	TAD	SUMH	5354	7100	CLL	
5261	3101	DCA	DBI	5355	1371	TAD	UVLOGF
5262	1303	TAD	SUML	5356	1373	TAD	MXYLGF
5263	3102	DCA	DBF	5357	3100	DCA	LG8F
5264	5600	JMP	I DB	5360	7204	GLK	
5265	7300	CLA	CLL	5361	1370	TAD	UVLOGI
5266	1303	TAD	SUML	5362	1372	TAD	MXYLGI
5267	7041	CIA		5363	3077	DCA	LG8I
5270	3102	DCA	DBF	5364	7100	CLL	
5271	7204	GLK		5365	5714	JMP	I LOGMG
5272	3040	DCA	LINK	5366	0000	XYLOGI	,0



5367	0000	XYLOGF,0
5370	0000	UVLOGI,0
5371	0000	UVLOGF,0
5372	0000	MXYLGI,0
5373	0000	MXYLGF,0
		*5400
5400	0000	LOG8,0
5401	7300	CLA CLL
5402	1074	TAD LGARGF
5403	7421	MQL
5404	1073	TAD LGARGI
5405	7413	SHL
5406	0000	0000
5407	3341	DCA ARG I
5410	7501	MOA
5411	3342	DCA ARGF
5412	1341	TAD ARG I
5413	7650	SNA CLA
5414	7410	SKP
5415	5226	JMP .+11
5416	1342	TAD ARGF
5417	7450	SNA
5420	7410	SKP
5421	5247	JMP NEGODR
5422	3076	DCA LOG8F
5423	1377	TAD 5577/TAD M5
5424	3075	DCA LOG8I
5425	5600	JMP I LOG8
5426	1002	TAD 2/TAD M1
5427	3075	DCA LOG8I
5430	1342	TAD ARGF
5431	7421	MQL
5432	1341	TAD ARG I
5433	7417	LSR
5434	0002	0002
5435	3343	DCA SAVE
5436	2075	ISZ LOG8I
5437	7000	NOF
5440	1343	TAD SAVE
5441	7440	SZA
5442	5233	JMP .-7
5443	7300	CLA CLL
5444	7501	MOA
5445	3345	DCA ARG
5446	5275	JMP LOGTAB
5447	7300	NEGODR,CLA CLL
5450	3344	DCA COUNT4
5451	1342	TAD ARGF
5452	7421	MQL
5453	7413	SHL
5454	0002	0002
5455	3343	DCA SAVE
5456	2344	ISZ COUNT4
5457	7000	NOF

5460	1343	TAD SAVE	5546	0000	ARGINT,0
5461	7450	SNA	5547	0000	TABLCL,0
5462	5253	JMP .-7	5550	0000	VALUE1,0
5463	7417	LSR	5551	0000	VALUE2,0
5464	0002	0002	5552	0000	INT,0
5465	7440	SZA			*5577
5466	7402	HLT/CONTRADICTION	5577	7773	7773/M5
5467	7300	CLA CLL			
5470	7501	MQA			
5471	3345	DCA ARG			
5472	1344	TAD COUNT4			
5473	7041	CIA			
5474	3075	DCA LOG8I			
5475	7300	LOGTAB,CLA CLL			
5476	1345	TAD ARG			
5477	7421	SQL			
5500	7407	DVI			
5501	0040	0040			
5502	3346	DCA ARGINT			
5503	7501	MQA			
5504	1001	TAD 1/TAD C7000			
5505	3347	DCA TABLCL			
5506	7100	CLL			
5507	1747	TAD I TABLCL			
5510	3350	DCA VALUE1			
5511	2347	ISZ TABLCL			
5512	1747	TAD I TABLCL			
5513	3351	DCA VALUE2			
5514	1350	TAD VALUE1			
5515	7041	CIA			
5516	1351	TAD VALUE2			
5517	3331	DCA INCR			
5520	7100	CLL			
5521	7421	SQL			
5522	1346	TAD ARGINT			
5523	7407	DVI			
5524	0040	0040			
5525	7300	CLA CLL			
5526	7501	MQA/ARGINT/40			
5527	7421	SQL			
5530	7405	MUY			
5531	0000	INCR,0			
5532	3352	DCA INT			
5533	7100	CLL			
5534	1350	TAD VALUE1			
5535	1352	TAD INT			
5536	3076	DCA LOG8F			
5537	7100	CLL			
5540	5600	JMP I LOG8			
5541	0000	ARGI,0			
5542	0000	ARGF,0			
5543	0000	SAVE,0			
5544	0000	COUNT4,0			
5545	0000	ARG,0			

		*5600			
5600	0000	PHASE,0		5664	7300
5601	7300	CLA CLL		5665	5600
5602	1047	TAD XH		5666	4571
5603	3111	DCA PH		5667	1107
5604	1053	TAD XL		5670	3322
5605	3113	DCA PL		5671	1110
5606	1050	TAD YH		5672	3323
5607	3112	DCA QH		5673	7100
5610	1054	TAD YL		5674	1323
5611	3114	DCA QL		5675	7041
5612	1115	TAD AXH		5676	3325
5613	3103	DCA ABPH		5677	7204
5614	1121	TAD AXL		5700	3040
5615	3105	DCA ABPL		5701	7100
5616	1116	TAD AYH		5702	1322
5617	3104	DCA ABQH		5703	7040
5620	1122	TAD AYL		5704	1040
5621	3106	DCA ABQL		5705	3324
5622	3127	DCA CHECK		5706	7100
5623	4340	JMS TEST		5707	1321
5624	7300	CLA CLL		5710	1325
5625	1127	TAD CHECK		5711	3126
5626	7450	SNA		5712	7204
5627	5232	JMP .+3		5713	1320
5630	7300	CLA CLL		5714	1324
5631	5600	JMP I PHASE		5715	3125
5632	4571	JMS I PATAN		5716	7100
5633	1107	TAD ANGLEH		5717	5600
5634	3320	DCA TETAH		5720	0000
5635	1110	TAD ANGLEL		5721	0000
5636	3321	DCA TETAL		5722	0000
5637	1051	TAD UH		5723	0000
5640	3111	DCA PH		5724	0000
5641	1055	TAD UL		5725	0000
5642	3113	DCA PL			
5643	1052	TAD VH		5740	0000
5644	3112	DCA QH		5741	7300
5645	1056	TAD VL		5742	1103
5646	3114	DCA QL		5743	7440
5647	1117	TAD AUH		5744	5740
5650	3103	DCA ABPH		5745	1105
5651	1123	TAD AUL		5746	7440
5652	3105	DCA ABPL		5747	5740
5653	1120	TAD AVH		5750	1104
5654	3104	DCA ABQH		5751	7440
5655	1124	TAD AVL		5752	5740
5656	3106	DCA ABQL		5753	1106
5657	4340	JMS TEST		5754	7440
5660	7300	CLA CLL		5755	5740
5661	1127	TAD CHECK		5756	2127
5662	7450	SNA		5757	5740
5663	5266	JMP .+3			
					*6000
				6000	0000
				6001	7300
					ATAN,0
					CLA CLL

6002	1200	TAD ATAN
6003	3741	DCA I PRTRN1
6004	7100	CLL
6005	3743	DCA I PINVRT
6006	1106	TAD ABQL
6007	7041	CIA
6010	1105	TAD ABPL
6011	3376	DCA 6176
6012	7204	GLK
6013	3040	DCA LINK
6014	1104	TAD ABQH
6015	7040	CMA
6016	1103	TAD ABPH
6017	1040	TAD LINK
6020	3377	DCA 6177
6021	1377	TAD 6177
6022	7450	SNA
6023	7410	SKP
6024	5230	JMP .+4
6025	1376	TAD 6176
6026	7450	SNA
6027	5744	JMP I PSPECL
6030	7300	CLA CLL
6031	1377	TAD 6177
6032	7500	SMA
6033	5237	JMP .+4
6034	7300	CLA CLL
6035	2743	ISZ I PINVRT
6036	4770	JMS I 6170
6037	7300	CLA CLL
6040	1103	TAD ABPH
6041	0371	AND 6171/AND C2000
6042	7450	SNA
6043	7410	SKP
6044	5276	JMP .+32
6045	7300	CLA CLL
6046	3272	DCA CNT
6047	1105	TAD ABPL
6050	7421	MQL
6051	1103	TAD ABPH
6052	7413	SHL
6053	0000	0000
6054	3103	DCA ABPH
6055	1103	TAD ABPH
6056	0371	AND 6171/AND C2000
6057	7440	SZA
6060	5263	JMP .+3
6061	2272	ISZ CNT
6062	5251	JMP .-11
6063	7300	CLA CLL
6064	7501	MQA
6065	3105	DCA ABPL
6066	1106	TAD ABQL
6067	7421	MQL

6070	1104	TAD ABQH
6071	7413	SHL
6072	0000	CNT,0
6073	3104	DCA ABQH
6074	7501	MOA
6075	3106	DCA ABQL
6076	7300	CLA CLL
6077	1104	TAD ABQH
6100	7041	CIA
6101	1103	TAD ABPH
6102	7450	SNA
6103	5744	JMP I PSPECL
6104	7500	SMA
6105	7410	SKP
6106	7402	HLT/CONTRADICTION
6107	7300	CLA CLL
6110	1103	TAD ABPH
6111	3316	DCA .+5
6112	1106	TAD ABQL
6113	7421	MQL
6114	1104	TAD ABQH
6115	7407	DVI
6116	0000	0000
6117	7300	CLA CLL
6120	7501	MOA
6121	3372	DCA 6172/DCA TAN
6122	1372	TAD 6172/TAD TAN
6123	7421	MQL
6124	7407	DVI
6125	0040	0040
6126	3745	DCA I PDARG
6127	7501	MOA
6130	3373	DCA 6173/DCA LOC
6131	1374	TAD 6174/TAD C7200
6132	1373	TAD 6173/TAD LOC
6133	3746	DCA I PTBLCH
6134	7100	CLL
6135	1375	TAD 6175/TAD C7400
6136	1373	TAD 6173/TAD LOC
6137	3747	DCA I PTBLCL
6140	5742	JMP I PCNTN1/CONTINUED TO NEXT PAGE
6141	6345	PRTRN1,RTRN1
6142	6200	PCNTN1,6200
6143	6354	PINVRT,INVERT
6144	6244	PSPECL,SPECIL
6145	6346	PDARG,DARG
6146	6347	PTBLCH,TELOCH
6147	6350	PTBLCL,TBLOCL
		*6170
6170	1700	1700/INVERTION
6171	2000	2000/C2000,2000
6172	0000	0/TAN,0
6173	0000	0/LOC,0
6174	7200	7200/C7200,7200

6175	7400	7400/C7400,7400
6176	0000	0000/DIFFERENCE,HIGHER
6177	0000	0000/DIFFERENCE,LOWER
		*6200/ATAN CONTINUES
6200	1750	TAD I TBLOCL
6201	3351	DCA LANGL1
6202	2350	ISZ TBLOCL
6203	1350	TAD TBLOCL
6204	7041	CIA
6205	1366	TAD 6366/TAD C7400
6206	7440	SZA
6207	5213	JMP .+4
6210	1367	TAD 6367/TAD C1631
6211	5220	JMP .+7
6212	7300	CLA CLL
6213	1750	TAD I TBLOCL
6214	3352	DCA LANGL2
6215	1351	TAD LANGL1
6216	7041	CIA
6217	1352	TAD LANGL2
6220	3232	DCA DANGLE
6221	7100	CLL
6222	7421	MQL
6223	1346	TAD DARG
6224	7407	DVI
6225	0040	0040
6226	7300	CLA CLL
6227	7501	MQA
6230	7421	MQL
6231	7405	MUY
6232	0000	DANGLE,0
6233	3353	DCA INCANG
6234	7100	CLL
6235	1351	TAD LANGL1
6236	1353	TAD INCANG
6237	3110	DCA ANGLEL
6240	7204	GLK
6241	1747	TAD I TBLOCH
6242	3107	DCA ANGLEH
6243	5250	JMP .+5
6244	7300	SPECIL,CLA CLL
6245	1370	TAD 6370/TAD C55
6246	3107	DCA ANGLEH
6247	3110	DCA ANGLEL
6250	1354	TAD INVERT
6251	7450	SNA
6252	5266	JMP .+14
6253	7300	CLA CLL
6254	1110	TAD ANGLEL/BACK TO ORIGINAL ANGLE
6255	7041	CIA
6256	3110	DCA ANGLEL
6257	7204	GLK
6260	3040	DCA LINK
6261	1107	TAD ANGLEH

6262	7040	CMA	6350	0000	TBLOCL,0
6263	1040	TAD LINK	6351	0000	LANGL1,0
6264	1371	TAD 6371/TAD C132	6352	0000	LANGL2,0
6265	3107	DCA ANGLEH	6353	0000	INCANG,0
6266	7300	CLA CLL	6354	0000	INVERT,0
6267	1111	TAD PH			*6366
6270	0007	AND 7/AND C4000	6366	7400	7400
6271	1112	TAD QH	6367	1631	1631
6272	7430	SZL	6370	0055	0055/C55,0055
6273	5322	JMP .+27/JMP IIIQ	6371	0132	0132/C132,0132
6274	7004	RAL	6372	0264	0264/C264,0264
6275	7630	SZL CLA	6373	0550	0550/C550,0550
6276	5300	JMP .+2			
6277	5745	JMP I RTRN1			
6300	7300	CLA CLL			
6301	1111	TAD PH			
6302	7510	SGEZ			
6303	5305	JMP .+2/JMP IIQ			
6304	5330	JMP .+24/JMP IVQ			
6305	7300	CLA CLL/IIQ			
6306	1110	TAD ANGLEL			
6307	7041	CIA			
6310	3110	DCA ANGLEL			
6311	7204	GLK			
6312	3040	DCA LINK			
6313	1107	TAD ANGLEH			
6314	7040	CMA			
6315	1040	TAD LINK			
6316	1372	TAD 6372/TAD C264			
6317	3107	DCA ANGLEH			
6320	7100	CLL			
6321	5745	JMP I RTRN1			
6322	7300	CLA CLL/IIIQ			
6323	1107	TAD ANGLEH			
6324	1372	TAD 6372/TAD C264			
6325	3107	DCA ANGLEH			
6326	7100	CLL			
6327	5745	JMP I RTRN1			
6330	7300	CLA CLL/IVQ			
6331	1110	TAD ANGLEL			
6332	7041	CIA			
6333	3110	DCA ANGLEL			
6334	7204	GLK			
6335	3040	DCA LINK			
6336	1107	TAD ANGLEH			
6337	7040	CMA			
6340	1040	TAD LINK			
6341	1373	TAD 6373/TAD C550			
6342	3107	DCA ANGLEH			
6343	7100	CLL			
6344	5745	JMP I RTRN1			
6345	0000	RTRN1,0			
6346	0000	DARG,0			
6347	0000	TBLOCH,0			

6600	0000	6664	2303
6601	0031	6665	2323
6602	0062	6666	2353
6603	0113	6667	2377
6604	0144	6670	2423
6605	0176	6671	2423
6606	0227	6672	2446
6607	0258	6673	2471
6610	0311	6674	2514
6611	0342	6675	2537
6612	0373	6676	2561
6613	0423	6677	2603
6614	0454	6678	2626
6615	0505	6679	2647
6616	0536	6700	2671
6617	0567	6701	2713
6620	0617	6702	2734
6621	0648	6703	2755
6622	0700	6704	2775
6623	0731	6705	3016
6624	0761	6706	3036
6625	1012	6707	3056
6630	1122	6710	3076
6631	1152	6711	3116
6632	1202	6712	3135
6633	1232	6713	3154
6634	1262	6714	3173
6635	1311	6715	3212
6636	1341	6716	3230
6637	1370	6717	3246
6640	1417	6722	3317
6641	1447	6723	3334
6642	1476	6724	3351
6643	1524	6725	3365
6644	1553	6726	3401
6645	1602	6727	3415
6646	1630	6728	3431
6647	1657	6729	3444
6650	1705	6732	3460
6651	1733	6733	3472
6652	1761	6734	3505
6653	2007	6735	3517
6654	2034	6736	3531
6655	2062	6737	3543
6656	2107	6740	3555
6657	2134	6741	3566
6660	2161	6742	3577
6661	2206	6743	3607
6662	2233	6744	3617
6663	2257	6745	3630
		6746	3637
		6747	3647
		6750	3656

\*6600/SIN TABLE



6752	3665	3665
6753	3673	3673
6754	3702	3702
6755	3710	3710
6756	3715	3715
6757	3723	3723
6760	3730	3730
6761	3734	3734
6762	3741	3741
6763	3745	3745
6764	3751	3751
6765	3754	3754
6766	3760	3760
6767	3763	3763
6770	3765	3765
6771	3767	3767
6772	3771	3771
6773	3773	3773
6774	3775	3775
6775	3776	3776
6776	3776	3776
6777	3777	3777

\*7020/LOG TABLE

7020	0000	0000
7021	0167	0167
7022	0350	0350
7023	0522	0522
7024	0667	0667
7025	1027	1027
7026	1163	1163
7027	1312	1312
7030	1436	1436
7031	1557	1557
7032	1674	1674
7033	2006	2006
7034	2116	2116
7035	2223	2223
7036	2326	2326
7037	2426	2426
7040	2525	2525
7041	2621	2621
7042	2714	2714
7043	3005	3005
7044	3075	3075
7045	3163	3163
7046	3247	3247
7047	3333	3333
7050	3414	3414
7051	3475	3475
7052	3554	3554
7053	3633	3633
7054	3710	3710
7055	3764	3764
7056	4040	4040

7057	4112	4112
7060	4164	4164
7061	4234	4234
7062	4304	4304
7063	4353	4353
7064	4421	4421
7065	4467	4467
7066	4534	4534
7067	4600	4600
7070	4643	4643
7071	4706	4706
7072	4750	4750
7073	5012	5012
7074	5053	5053
7075	5114	5114
7076	5154	5154
7077	5213	5213
7100	5252	5252
7101	5311	5311
7102	5347	5347
7103	5404	5404
7104	5442	5442
7105	5476	5476
7106	5533	5533
7107	5567	5567
7110	5622	5622
7111	5655	5655
7112	5710	5710
7113	5743	5743
7114	5775	5775
7115	6026	6026
7116	6060	6060
7117	6111	6111
7120	6142	6142
7121	6172	6172
7122	6222	6222
7123	6252	6252
7124	6302	6302
7125	6331	6331
7126	6360	6360
7127	6407	6407
7130	6435	6435
7131	6464	6464
7132	6512	6512
7133	6537	6537
7134	6565	6565
7135	6612	6612
7136	6637	6637
7137	6664	6664
7140	6711	6711
7141	6735	6735
7142	6761	6761
7143	7005	7005
7144	7031	7031

7145	7055	7055
7146	7100	7100
7147	7123	7123
7150	7147	7147
7151	7171	7171
7152	7214	7214
7153	7237	7237
7154	7261	7261
7155	7303	7303
7156	7325	7325
7157	7347	7347
7160	7370	7370
7161	7412	7412
7162	7433	7433
7163	7455	7455
7164	7476	7476
7165	7517	7517
7166	7537	7537
7167	7560	7560
7170	7600	7600
7171	7621	7621
7172	7641	7641
7173	7661	7661
7174	7701	7701
7175	7721	7721
7176	7740	7740
7177	7760	7760

\*7200/ARCTANGENT TABLE---INTEGER PART

7200	0000	0000
7201	0000	0000
7202	0000	0000
7203	0001	0001
7204	0001	0001
7205	0002	0002
7206	0002	0002
7207	0003	0003
7210	0003	0003
7211	0004	0004
7212	0004	0004
7213	0004	0004
7214	0005	0005
7215	0005	0005
7216	0006	0006
7217	0006	0006
7220	0007	0007
7221	0007	0007
7222	0010	0010
7223	0010	0010
7224	0010	0010
7225	0011	0011
7226	0011	0011
7227	0012	0012
7230	0012	0012
7231	0013	0013
7232	0013	0013
7233	0013	0013
7234	0014	0014
7235	0014	0014
7236	0015	0015
7237	0015	0015
7240	0016	0016
7241	0016	0016
7242	0016	0016
7243	0017	0017
7244	0017	0017
7245	0020	0020
7246	0020	0020
7247	0020	0020
7250	0021	0021
7251	0021	0021
7252	0022	0022
7253	0022	0022
7254	0022	0022
7255	0023	0023
7256	0023	0023
7257	0024	0024
7260	0024	0024
7261	0024	0024
7262	0025	0025
7263	0025	0025

7264	0026	0026
7265	0026	0026
7266	0026	0026
7267	0027	0027
7270	0027	0027
7271	0030	0030
7272	0030	0030
7273	0030	0030
7274	0031	0031
7275	0031	0031
7276	0031	0031
7277	0032	0032
7300	0032	0032
7301	0032	0032
7302	0033	0033
7303	0033	0033
7304	0033	0033
7305	0034	0034
7306	0034	0034
7307	0035	0035
7310	0035	0035
7311	0035	0035
7312	0036	0036
7313	0036	0036
7314	0036	0036
7315	0037	0037
7316	0037	0037
7317	0037	0037
7320	0040	0040
7321	0040	0040
7322	0040	0040
7323	0040	0040
7324	0041	0041
7325	0041	0041
7326	0041	0041
7327	0042	0042
7330	0042	0042
7331	0042	0042
7332	0043	0043
7333	0043	0043
7334	0043	0043
7335	0044	0044
7336	0044	0044
7337	0044	0044
7340	0044	0044
7341	0045	0045
7342	0045	0045
7343	0045	0045
7344	0045	0045
7345	0046	0046
7346	0046	0046
7347	0046	0046
7350	0047	0047
7351	0047	0047

7352	0047	0047
7353	0047	0047
7354	0050	0050
7355	0050	0050
7356	0050	0050
7357	0050	0050
7360	0051	0051
7361	0051	0051
7362	0051	0051
7363	0051	0051
7364	0052	0052
7365	0052	0052
7366	0052	0052
7367	0052	0052
7370	0053	0053
7371	0053	0053
7372	0053	0053
7373	0053	0053
7374	0054	0054
7375	0054	0054
7376	0054	0054
7377	0054	0054

\*7400/ARCTANGENT TABLE -- FRACTION PART

7400	0000	0000
7401	3451	3451
7402	7122	7122
7403	2573	2573
7404	6243	6243
7405	1712	1712
7406	5360	5360
7407	1025	1025
7410	4470	4470
7411	0132	0132
7412	3571	3571
7413	7226	7226
7414	2661	2661
7415	6311	6311
7416	1736	1736
7417	5361	5361
7420	1000	1000
7421	4413	4413
7422	0023	0023
7423	3427	3427
7424	7027	7027
7425	2422	2422
7426	6011	6011
7427	1374	1374
7430	4752	4752
7431	0322	0322
7432	3666	3666
7433	7224	7224
7434	2554	2554
7435	6077	6077
7436	1414	1414

7437	4723	4723	7525	4542	4542
7440	0224	0224	7526	7126	7126
7441	3516	3516	7527	1501	1501
7442	7002	7002	7530	4042	4042
7443	2260	2260	7531	6373	6373
7444	5526	5526	7532	0712	0712
7445	0766	0766	7533	3221	3221
7446	4216	4216	7534	5516	5516
7447	7440	7440	7535	0003	0003
7450	2652	2652	7536	2256	2256
7451	6054	6054	7537	4521	4521
7452	1247	1247	7540	6753	6753
7453	4433	4433	7541	1174	1174
7454	7606	7606	7542	3404	3404
7455	2752	2752	7543	5604	5604
7456	6106	6106	7544	7772	7772
7457	1232	1232	7545	2151	2151
7460	4345	4345	7546	4316	4316
7461	7450	7450	7547	6453	6453
7462	2543	2543	7550	0600	0600
7463	5626	5626	7551	2714	2714
7464	0700	0700	7552	5020	5020
7465	3741	3741	7553	7113	7113
7466	6772	6772	7554	1177	1177
7467	2012	2012	7555	3251	3251
7470	5021	5021	7556	5314	5314
7471	0020	0020	7557	7347	7347
7472	3006	3006	7560	1371	1371
7473	5762	5762	7561	3403	3403
7474	0726	0726	7562	5406	5406
7475	3660	3660	7563	7400	7400
7476	6602	6602	7564	1363	1363
7477	1513	1513	7565	3336	3336
7500	4412	4412	7566	5301	5301
7501	7300	7300	7567	7234	7234
7502	2155	2155	7570	1160	1160
7503	5021	5021	7571	3074	3074
7504	7653	7653	7572	5000	5000
7505	2475	2475	7573	6675	6675
7506	5305	5305	7574	0563	0563
7507	0103	0103	7575	2441	2441
7510	2671	2671	7576	4310	4310
7511	5445	5445	7577	6147	6147
7512	0210	0210			
7513	2741	2741			
7514	5462	5462			
7515	0170	0170			
7516	2666	2666			
7517	5352	5352			
7520	0025	0025			
7521	2467	2467			
7522	5120	5120			
7523	7537	7537			
7524	2145	2145			

```

*4200
4200 0000 WRITE,0
4201 7300 CLA CLL
4202 1200 TAD WRITE
4203 3756 DCA I PRTRN2
4204 6046 TLS
4205 4563 JMS I PCRLF
4206 1130 TAD K306
4207 4564 JMS I PTYPE
4210 1131 TAD K275
4211 4564 JMS I PTYPE
4212 1032 TAD FINTGR
4213 3034 DCA INTGR
4214 1033 TAD FFRCTN
4215 3035 DCA FRCTN
4216 4557 JMS I PBDCNV
4217 4560 JMS I PTDGT
4220 1004 TAD 4/TAD M4
4221 3036 DCA COUNT3
4222 1132 TAD K240
4223 4564 JMS I PTYPE
4224 2036 ISZ COUNT3
4225 5222 JMP .-3
4226 1366 TAD 4366/TAD K304,D
4227 4564 JMS I PTYPE
4230 1367 TAD 4367/TAD K302,B
4231 4564 JMS I PTYPE
4232 1131 TAD K275
4233 4564 JMS I PTYPE
4234 1127 TAD CHECK
4235 7450 SNA
4236 5242 JMP .+4
4237 7300 CLA CLL
4240 4776 JMS I 4376/DB UNDEFINED
4241 5250 JMP .+7
4242 1101 TAD DPI
4243 3034 DCA INTGR
4244 1102 TAD DBF
4245 3035 DCA FRCTN
4246 4557 JMS I PBDCNV
4247 4560 JMS I PTDGT
4250 1003 TAD 3/TAD M3
4251 3036 DCA COUNT3
4252 1132 TAD K240
4253 4564 JMS I PTYPE
4254 2036 ISZ COUNT3
4255 5252 JMP .-3
4256 1370 TAD 4370/TAD K320,P
4257 4564 JMS I PTYPE
4260 1371 TAD 4371/TAD K310,H
4261 4564 JMS I PTYPE
4262 1372 TAD 4372/TAD K301,A
4263 4564 JMS I PTYPE

```

4264	1373	TAD	4373/TAD K323,S
4265	4564	JMS	I PTYPE
4266	1374	TAD	4374/TAD K305,E
4267	4564	JMS	I PTYPE
4270	1131	TAD	K275
4271	4564	JMS	I PTYPE
4272	1127	TAD	CHECK
4273	7450	SNA	
4274	5300	JMP	+.4
4275	7300	CLA	CLL
4276	4776	JMS	I 4376/PHASE UNDEFINED
4277	5306	JMP	+.7
4300	1125	TAD	PHASEH
4301	3034	DCA	INTGR
4302	1126	TAD	PHASEL
4303	3035	DCA	FRCTN
4304	4557	JMS	I PRDCNV
4305	4560	JMS	I PTDGT
4306	4563	JMS	I PCRLF
4307	1004	TAD	4/TAD M4
4310	3036	DCA	COUNT3
4311	1132	TAD	K240
4312	4564	JMS	I PTYPE
4313	2036	ISZ	COUNT3
4314	5311	JMP	.-3
4315	1133	TAD	K330
4316	4564	JMS	I PTYPE
4317	1131	TAD	K275
4320	4564	JMS	I PTYPE
4321	1047	TAD	XH
4322	3034	DCA	INTGR
4323	1053	TAD	XL
4324	3035	DCA	FRCTN
4325	4557	JMS	I PRDCNV
4326	4560	JMS	I PTDGT
4327	1003	TAD	3/TAD M3
4330	3036	DCA	COUNT3
4331	1132	TAD	K240
4332	4564	JMS	I PTYPE
4333	2036	ISZ	COUNT3
4334	5331	JMP	.-3
4335	1375	TAD	4375/TAD K331,Y
4336	4564	JMS	I PTYPE
4337	1131	TAD	K275
4340	4564	JMS	I PTYPE
4341	1050	TAD	YH
4342	3034	DCA	INTGR
4343	1054	TAD	YL
4344	3035	DCA	FRCTN
4345	4557	JMS	I PRDCNV
4346	4560	JMS	I PTDGT
4347	1003	TAD	3/TAD M3
4350	3036	DCA	COUNT3
4351	1132	TAD	K240



4352	4564	JMS I PTYPE
4353	2036	ISZ COUNT3
4354	5351	JMP .-3
4355	5757	JMP I PCNTN2/CONTINUE TO *6400
4356	6522	PRTRN2,RTRN2
4357	6400	PCNTN2,6400
		*4366
4366	0304	0304/K304,D
4367	0302	0302/K302,B
4370	0320	0320/K320,P
4371	0310	0310/K310,H
4372	0301	0301/K301,A
4373	0323	0323/K323,S
4374	0305	0305/K305,E
4375	0331	0331/K331,Y
4376	4750	4750/SUBROUTINE FOR UNDEFINED
		*4400
4400	0000	ASKJ,0
4401	7300	CLA CLL
4402	6046	TLS
4403	1003	TAD 3/TAD M3
4404	3036	DCA COUNT3
4405	4563	JMS I PCRLF
4406	2036	ISZ COUNT3
4407	4563	JMS I PCRLF
4410	2036	ISZ COUNT3
4411	5207	JMP .-2
4412	1130	TAD K306
4413	4564	JMS I PTYPE
4414	1131	TAD K275
4415	4564	JMS I PTYPE
4416	1132	TAD K240
4417	4564	JMS I PTYPE
4420	4560	JMS I PTDGT
4421	1132	TAD K240
4422	4564	JMS I PTYPE
4423	1133	TAD K330
4424	4564	JMS I PTYPE
4425	1132	TAD K240
4426	4564	JMS I PTYPE
4427	1134	TAD K312
4430	4564	JMS I PTYPE
4431	1004	TAD 4/TAD M4
4432	3036	DCA COUNT3
4433	1132	TAD K240
4434	4564	JMS I PTYPE
4435	2036	ISZ COUNT3
4436	5233	JMP .-3
4437	1134	TAD K312
4440	4564	JMS I PTYPE
4441	1264	TAD 4464/TAD K274,<
4442	4564	JMS I PTYPE
4443	1265	TAD 4465/TAD K262,2
4444	4564	JMS I PTYPE

4445 1266 TAD 4466/TAD K265,5  
4446 4564 JMS I PTYPE  
4447 1267 TAD 4467/TAD K266,6  
4450 4564 JMS I PTYPE  
4451 4563 JMS I PCRLF  
4452 1134 TAD K312  
4453 4564 JMS I PTYPE  
4454 1131 TAD K275  
4455 4564 JMS I PTYPE  
4456 1132 TAD K240  
4457 4564 JMS I PTYPE  
4460 5600 JMP I ASKJ  
\*4464  
4464 0274 0274/K274,<  
4465 0262 0262/K262,2  
4466 0265 0265/K265,5  
4467 0266 0266/K266,6  
\*4470  
4470 0000 READJ,0  
4471 7300 CLA CLL  
4472 1003 TAD 3/TAD M3  
4473 3036 DCA COUNT3  
4474 1174 TAD TTAB13  
4475 3013 DCA 13  
4476 6032 KCC  
4477 4565 JMS I PLISN  
4500 1376 TAD 4576/TAD M260  
4501 3362 DCA JOCTDT  
4502 1362 TAD JOCTDT  
4503 7510 SGFZ  
4504 5354 JMP QUESTN  
4505 1005 TAD 5/TAD M12  
4506 7510 SGFZ  
4507 7610 SKP CLA  
4510 5354 JMP QUESTN  
4511 1362 TAD JOCTDT  
4512 3413 DCA I 13  
4513 2036 ISZ COUNT3  
4514 5277 JMP READJ+7/READ ANOTHER LETTER  
4515 1003 TAD 3/TAD M3  
4516 3036 DCA COUNT3  
4517 1174 TAD TTAB13  
4520 3013 DCA 13  
4521 1413 TAD I 13  
4522 7421 MQL  
4523 1375 TAD 4575/TAD C144  
4524 4545 JMS I PMUL  
4525 7300 CLA CLL  
4526 7501 MQA  
4527 3363 DCA JOCT1  
4530 1413 TAD I 13  
4531 7421 MQL  
4532 1006 TAD 6/TAD C12  
4533 4545 JMS I PMUL

4534	7300	CLA CLL
4535	7501	MOA
4536	3364	DCA JOCT2
4537	1413	TAD I 13
4540	3365	DCA JOCT3
4541	1363	TAD JOCT1
4542	1364	TAD JOCT2
4543	1365	TAD JOCT3
4544	3025	DCA J
4545	1025	TAD J
4546	7041	CIA
4547	1374	TAD 4574/TAD M400
4550	7510	SGEZ
4551	7610	SKP CLA
4552	5354	JMP QUESTN
4553	5360	JMP .+5
4554	7300	QUESTN,CLA CLL
4555	1377	TAD 4577/TAD K277,?
4556	4564	JMS I PTYPE
4557	6046	TLS
4560	4563	JMS I PCRLF
4561	5670	JMP I READJ
4562	0000	JOCTDT,0
4563	0000	JOCT1,0
4564	0000	JOCT2,0
4565	0000	JOCT3,0
		*4574
4574	7400	7400/M400
4575	0144	0144/C144
4576	7520	7520/M260
4577	0277	0277/K277,?
		*4600
4600	0000	MANUL,0
4601	7201	CLA IAC
4602	3025	DCA J
4603	4556	JMS I PFRFQ
4604	1032	TAD FINTGR
4605	3034	DCA INTGR
4606	1033	TAD FFRCTN
4607	3035	DCA FRCTN
4610	4557	JMS I PBDCNV
4611	4561	JMS I PASKJ
4612	4562	JMS I PREADJ
4613	7300	CLA CLL
4614	5600	JMP I MANUL
		*4620
4620	0000	TYPE,0
4621	6041	TSF
4622	5221	JMP .-1
4623	6046	TLS
4624	7300	CLA CLL
4625	5620	JMP I TYPE
		*4630
4630	0000	LISN,0

4631	6031	KSF
4632	5231	JMP .-1
4633	6036	KRB
4634	6046	TLS
4635	5630	JMP I LISN
		*4640
4640	0000	CRLF,0
4641	1250	TAD 4650/TAD K215
4642	4564	JMS I PTYPE
4643	1251	TAD 4651/TAD K212
4644	4564	JMS I PTYPE
4645	7300	CLA CLL
4646	5640	JMP I CRLF
		*4650
4650	0215	0215/K215
4651	0212	0212/K212
		*4700
4700	0000	TAB11,0
		*4710
4710	0000	TAB12,0
		*4720
4720	0000	TAB13,0
		*4750/PRINT OUT ----
4750	0000	0
4751	1004	TAD 4/TAD M4
4752	3036	DCA COUNT3
4753	1365	TAD 4765/TAD K255,-
4754	4564	JMS I PTYPE
4755	2036	ISZ COUNT3
4756	5353	JMP .-3
4757	7300	CLA CLL
4760	5750	JMP I 4750
		*4765
4765	0255	0255/K255,-

		*6400	6464	4557	JMS I PBDCNV
6400	1376	TAD 6576	6465	4560	JMS I PTDGT
6401	4564	JMS I PTYPE	6466	1004	TAD 4/TAD M4
6402	1131	TAD K275	6467	3036	DCA COUNT3
6403	4564	JMS I PTYPE	6470	1132	TAD K240
6404	1051	TAD UH	6471	4564	JMS I PTYPE
6405	3034	DCA INTGR	6472	2036	ISZ COUNT3
6406	1055	TAD UL	6473	5270	JMP .-3
6407	3035	DCA FRCTN	6474	1376	TAD 6576
6410	4557	JMS I PBDCNV	6475	4564	JMS I PTYPE
6411	4560	JMS I PTDGT	6476	1376	TAD 6576
6412	1003	TAD 3/TAD M3	6477	4564	JMS I PTYPE
6413	3036	DCA COUNT3	6500	1373	TAD 6573
6414	1132	TAD K240	6501	4564	JMS I PTYPE
6415	4564	JMS I PTYPE	6502	1377	TAD 6577
6416	2036	ISZ COUNT3	6503	4564	JMS I PTYPE
6417	5214	JMP .-3	6504	1377	TAD 6577
6420	1377	TAD 6577	6505	4564	JMS I PTYPE
6421	4564	JMS I PTYPE	6506	1131	TAD K275
6422	1131	TAD K275	6507	4564	JMS I PTYPE
6423	4564	JMS I PTYPE	6510	1070	TAD UUVVH
6424	1052	TAD UH	6511	3034	DCA INIGR
6425	3034	DCA INTGR	6512	1072	TAD UUVVL
6426	1056	TAD VL	6513	3035	DCA FRCTN
6427	3035	DCA FRCTN	6514	4557	JMS I PBDCNV
6430	4557	JMS I PBDCNV	6515	4560	JMS I PTDGT
6431	4560	JMS I PTDGT	6516	1371	TAD 6571
6432	4563	JMS I PCRLF	6517	4564	JMS I PTYPE
6433	7300	CLA CLL	6520	4563	JMS I PCRLF
6434	1005	TAD 5/TAD M12	6521	5722	JMP I RTRN2
6435	3036	DCA COUNT3	6522	0000	RTRN2,0
6436	1132	TAD K240			*6571
6437	4564	JMS I PTYPE	6571	0251	0251/)
6440	2036	ISZ COUNT3	6572	0250	0250/(
6441	5236	JMP .-3	6573	0253	0253/+
6442	1372	TAD 6572	6574	0330	0330/X
6443	4564	JMS I PTYPE	6575	0331	0331/Y
6444	1374	TAD 6574	6576	0325	0325/U
6445	4564	JMS I PTYPE	6577	0326	0326/V
6446	1374	TAD 6574			*1400
6447	4564	JMS I PTYPE	1400	0000	0
6450	1373	TAD 6573	1401	7300	CLA CLL
6451	4564	JMS I PTYPE	1402	1022	TAD NSAMP
6452	1375	TAD 6575	1403	3207	DCA .+4
6453	4564	JMS I PTYPE	1404	1363	TAD 1563/TAD C2000
6454	1375	TAD 6575	1405	7421	MQL
6455	4564	JMS I PTYPE	1406	7413	SHL
6456	1131	TAD K275	1407	0000	0000
6457	4564	JMS I PTYPE	1410	3034	DCA INTGR
6460	1067	TAD XYYH	1411	7501	MOA
6461	3034	DCA INTGR	1412	3035	DCA FRCTN
6462	1071	TAD XYYL	1413	6046	TLS
6463	3035	DCA FRCTN	1414	4563	JMS I PCRLF
			1415	1350	TAD 1550

1416	4564	JMS I PTYPE
1417	1351	TAD 1551
1420	4564	JMS I PTYPE
1421	1352	TAD 1552
1422	4564	JMS I PTYPE
1423	1353	TAD 1553
1424	4564	JMS I PTYPE
1425	1132	TAD K240
1426	4564	JMS I PTYPE
1427	1354	TAD 1554
1430	4564	JMS I PTYPE
1431	1355	TAD 1555
1432	4564	JMS I PTYPE
1433	1356	TAD 1556
1434	4564	JMS I PTYPE
1435	1357	TAD 1557
1436	4564	JMS I PTYPE
1437	1353	TAD 1553
1440	4564	JMS I PTYPE
1441	1132	TAD K240
1442	4564	JMS I PTYPE
1443	1131	TAD K275
1444	4564	JMS I PTYPE
1445	4557	JMS I PRDCNV
1446	4560	JMS I PTDGT
1447	1004	TAD 4/TAD M4
1450	3036	DCA COUNT3
1451	1132	TAD K240
1452	4564	JMS I PTYPE
1453	2036	ISZ COUNT3
1454	5251	JMP .-3
1455	7300	CLA CLL
1456	7421	MQL
1457	1022	TAD NSAMP
1460	7041	CIA
1461	1360	TAD 1560
1462	3266	DCA .+4
1463	7100	CLL
1464	7001	IAC
1465	7417	LSR
1466	0000	0000
1467	3034	DCA INTGR
1470	7501	MOA
1471	3035	DCA FRCTN
1472	1350	TAD 1550
1473	4564	JMS I PTYPE
1474	1361	TAD 1561
1475	4564	JMS I PTYPE
1476	1362	TAD 1562
1477	4564	JMS I PTYPE
1500	1353	TAD 1553
1501	4564	JMS I PTYPE
1502	1132	TAD K240
1503	4564	JMS I PTYPE

1504	1354	TAD 1554	1742	0000	0/ABQHO
1505	4564	JMS I PTYPE	1743	0000	0/ABQLO
1506	1355	TAD 1555			*1760
1507	4564	JMS I PTYPE	1760	0000	0
1510	1356	TAD 1556	1761	7300	CLA CLL/NO SCALING
1511	4564	JMS I PTYPE	1762	1027	TAD R1
1512	1357	TAD 1557	1763	3044	DCA DS1
1513	4564	JMS I PTYPE	1764	1030	TAD R2
1514	1353	TAD 1553	1765	3045	DCA DS2
1515	4564	JMS I PTYPE	1766	1031	TAD R3
1516	1132	TAD K240	1767	3046	DCA DS3
1517	4564	JMS I PTYPE	1770	7100	CLL
1520	1131	TAD K275	1771	5760	JMP I 1760
1521	4564	JMS I PTYPE			
1522	4557	JMS I PBDCNV			
1523	4560	JMS I PTDGT			
1524	4563	JMS I PCRLF			
1525	5600	JMP I 1400			
		*1550			
1550	0315	0315/M			
1551	0301	0301/A			
1552	0330	0330/X			
1553	0256	0256/.			
1554	0306	0306/F			
1555	0322	0322/R			
1556	0305	0305/E			
1557	0321	0321/Q			
1560	0010	0010			
1561	0311	0311/I			
1562	0316	0316/N			
1563	2000	2000			
		*1700			
1700	0000	0/INVERTION			
1701	7300	CLA CLL			
1702	1103	TAD ABPH			
1703	3340	DCA 1740/DCA ABPHO			
1704	1105	TAD ABPL			
1705	3341	DCA 1741/DCA ABPLO			
1706	1104	TAD ABQH			
1707	3342	DCA 1742/DCA ABQHO			
1710	1106	TAD ABQL			
1711	3343	DCA 1743/DCA ABQLO			
1712	1340	TAD 1740/TAD ABPHO			
1713	3104	DCA ABQH			
1714	1341	TAD 1741/TAD ABPLO			
1715	3106	DCA ABQL			
1716	1342	TAD 1742/TAD ABQHO			
1717	3103	DCA ABPH			
1720	1343	TAD 1743/TAD ABPLO			
1721	3105	DCA ABPL			
1722	5700	JMP I 1700			
		*1740			
1740	0000	0/ABPHO			
1741	0000	0/ABPLO			

A	1112	FFRCTN	0033	MANUL	4600
ABPH	0103	FINTGR	0032	MASK	0454
ABPL	0105	FRCT	4055	MGNTD	5000
ABQH	0104	FRCTN	0035	MLTPLR	0705
ABQL	0106	FREQ	1000	MM	1336
ABSLT	1125	GETM	0400	MPHAIH	5724
ACCUM	4167	HIGHER	0705	MPHAIL	5725
ADJST	0460	HIGH1	0057	MUL	0670
AH	0061	HIGH2	0063	MXYLGF	5373
AINTGR	4076	HIGH3	0065	MXYLGI	5372
AL	0062	HIHIH	1673	N	0373
ANGLEH	0107	HILOWH	1674	NEGODR	5447
ANGLEL	0110	HILOWL	1675	NEXTF	4160
ARG	5545	IIIOD	1265	NEXTFR	4062
ARGF	5542	IIOD	1241	NEXTI	4132
ARGI	5541	INCANG	6353	NEXTIR	4036
ARGINI	5546	INCR	5531	NNN	0455
ASKJ	4400	INT	5552	NSAMP	0022
ATAN	6000	INTGR	0034	PABSLT	0166
AUH	0117	INVERT	6354	PADJST	0146
AUL	0123	IOD	1222	PASKJ	0161
AVH	0120	IVQD	1312	PATAN	0171
AVL	0124	J	0025	PBDCNV	0157
AXH	0115	JOCTDT	4562	PCNTN1	6142
AXL	0121	JOCT1	4563	PCNTN2	4357
AYH	0116	JOCT2	4564	PCRLF	0163
AYL	0122	JOCT3	4565	PDARG	6145
BDCNV	4000	K240	0132	PDB	0153
BUFFR1	0023	K262	0136	PFREQ	0156
BUFFR2	0024	K265	0137	PGETM	0142
CHECK	0127	K266	0140	PH	0111
CNT	6072	K274	0135	PHAIH	5722
COS	0042	K275	0131	PHAIL	5723
COUNT	0021	K306	0130	PHASE	5600
COUNT1	0371	K312	0134	PHASEH	0125
COUNT2	0372	K330	0133	PHASEL	0126
COUNT3	0036	LANGL1	6351	PINVRT	6143
COUNT4	5544	LANGL2	6352	PL	0113
CRLF	4640	LGARGF	0074	PLISN	0165
DANGLE	6232	LGARGI	0073	PLOGMG	0152
DARG	6346	LG8F	0100	PLOG8	0170
DB	5200	LG8I	0077	PMANUL	0144
DBF	0102	LINK	0040	PMGNTD	0151
DBI	0101	LISN	4630	PMUL	0145
DIGIT	4170	LOGMG	5314	PPHASE	0154
DO1	0224	LOGTAB	5475	PREADJ	0162
DO2	0254	LOG8	5400	PRTRN1	6141
DS1	0044	LOG8F	0076	PRTRN2	4356
DS2	0045	LOG8I	0075	PSAMP	0141
DS2H	0574	LOW1	0060	PSINTB	1337
DS2L	0575	LOW2	0064	PSNCS	0143
DS3	0046	LOW3	0066	PSPECL	6144
FACTOR	0573	LWLWH	1676	PSQUIRE	0167
		M	0041	PSUMTN	0147



FIBLCH	6146
PTBLCL	6147
PTDGT	0160
PTYPE	0164
PWRITE	0155
PXYUV	0150
QH	0112
QL	0114
QUESTN	4554
READJ	4470
REDUCE	0551
REMAIN	4077
RTRN1	6345
RTRN2	6522
R1	0027
R2	0030
R3	0031
SAMP	0600
SAVE	5543
SAVEH	5301
SAVEL	5302
SCALE	0026
SIGN	0037
SIN	0043
SNCS	1200
SPECIL	6244
SQURE	1600
START	0200
SUMH	5304
SUML	5303
SUMTN	1023
S1	1113
S2	1114
S3	1115
TABLCL	5547
TAB10	4101
TAB11	4700
TAB12	4710
TAB13	4720
TAB14	1160
TAB15	1350
TAB16	1354
TAB17	1360
TBLOCH	6347
TBLOCL	6350
TDGT	4110
TEST	5740
TETAH	5720
TETAL	5721
TTAB10	4100
TTAB11	0172
TTAB12	0173
TTAB13	0174
TTAB14	0456

TTAB15	0175
TTAB16	0176
TTAB17	0177
TYPE	4620
UH	0051
UL	0055
UUH	5136
UUL	5142
UUVVH	0070
UUVVL	0072
UVLOGF	5371
UVLOGI	5370
VALUE1	5550
VALUE2	5551
VH	0052
VL	0056
VVH	5137
VVL	5143
WRITE	4200
XH	0047
XL	0053
XXH	5134
XXL	5140
XXYH	0067
XXYL	0071
XYLOGF	5367
XYLOGI	5366
XYUV	0635
YH	0050
YL	0054
YYH	5135
YYL	5141

## Appendix D

### Individual Subjects' Frequency Response Data

Subsequent figures in this appendix present original Bode plot results that show individual subjects' data points for each set of frequency response experiments conducted in the thesis, i.e., vestibular nystagmus slow phase (with and without visual after-image; Chapter III), dual-mode visual tracking (composite, and pursuit only; Chapter IV) and optokinetic nystagmus slow phase (Chapter VI). Each of these classes of eye movement was investigated under two stimulus conditions, periodic and nonperiodic.

Nonperiodic-input cases involved a Fourier analysis by the hybrid computer program FFT outlined in the preceding appendix. Table D.1 gives a sample printout of FFT result. As in this illustrative example, peaks of input power (square of Fourier amplitude) and those of output do not necessarily occur at the same frequencies, for the system is not perfectly linear. Gain and phase shift at a given frequency were read and retrieved, only if both input and output exhibit their peaks at that frequency. Total number of such common peak frequencies in a complete FFT run is designated as  $m_0$ , whereas total number of input peaks and that of output peaks are represented by  $n$  and  $m$  respectively. If the system were perfectly linear, one would obtain  $n=m=m_0$ . (The sample result in Table D.1 gives  $n=4$   $m=3$   $m_0=2$ .) The degree of overlapping between input and output peaks

```

.....
F=      .1406      DB=-      2.0043      PHASE=-      80.8945
X=-      .6850      Y=      .1115      U=      .1735      V=      .5229
      (XX+YY=      .4814      UU+VV=      .3034)

F=      .1562      DB=-      .8544      PHASE=-      112.8491
X=-      2.3479      Y=-      .0080      U=-      .8330      V=      1.9572
      (XX+YY=      5.5124      UU+VV=      4.5246)

F=      .1718      DB=-      13.7597      PHASE=      221.2128
X=-      .4675      Y=-      .4658      U=-      .1359      V=-      .0087
      (XX+YY=      .4353      UU+VV=      .0183)

F=      .1875      DB=-      19.6777      PHASE=      191.4860
X=      .8305      Y=-      1.7145      U=      .0493      V=-      .1923
      (XX+YY=      3.6293      UU+VV=      .0390)

F=      .2500      DB=-      10.2954      PHASE=-      88.7277
X=-      .3842      Y=-      .5886      U=-      .1777      V=      .1218
      (XX+YY=      .4938      UU+VV=      .0461)

F=      .2656      DB=-      1.6625      PHASE=      266.0166
X=-      .0964      Y=-      2.9074      U=-      2.4001      V=-      .0878
      (XX+YY=      8.4626      UU+VV=      5.7680)

F=      .2812      DB=-      7.2656      PHASE=      9.5515
X=      .3615      Y=      .1645      U=-      .1667      V=-      .0444
      (XX+YY=      .1574      UU+VV=      .0295)

F=      .2968      DB=      19.2968      PHASE=-      38.1904
X=      .0534      Y=      .0603      U=-      .0422      V=-      .7197
      (XX+YY=      .0061      UU+VV=      .5192)

F=      .3125      DB=-      12.7392      PHASE=      216.2128
X=-      .8830      Y=-      1.9375      U=-      .4282      V=-      .2404
      (XX+YY=      4.5336      UU+VV=      .2409)

F=      .3281      DB=      4.7436      PHASE=-      101.3469
X=-      .2460      Y=-      .0676      U=-      .1979      V=      .3933
      (XX+YY=      .0649      UU+VV=      .1936)
.....

```

<NOTE> F: FREQUENCY IN HZ, X & Y: REAL AND IMAGINARY INPUT FOURIER COEFFICIENTS, U & V: REAL AND IMAGINARY OUTPUT FOURIER COEFFICIENTS, XX+YY: INPUT POWER, UU+VV: OUTPUT POWER

Table D.1 Illustrative sample of FFT printout (frequency resolution, 0.0156 Hz): Input peaks at 0.1562, 0.1875, 0.2656 and 0.3125 Hz, while output peaks at 0.1562, 0.2656 and 0.2968 Hz.

may be recognized as a measure of system linearity. For this reason, values of  $n$ ,  $m$  and  $m_0$  are tabulated below for each non-periodic-input experiment and each individual subject.

Tables summarizing total numbers of Fourier amplitude peaks for frequency response experiments involving pseudo-random stimulation. Number of peaks; stimulus input (n), eye movement output (m) and common (m<sub>o</sub>).\*

Table D.2-a Vestibular nystagmus slow phase with no vision

Subject	n	m	m <sub>o</sub>
BC	37	44	21
CO	27	20	18
JT	24	21	15
SY	40	26	24

Table D.2-b Smooth eye movement during after-image tracking under vestibular stimulation

Subject	n	m	m <sub>o</sub>
BC	49	55	41
JT	30	29	21
SY	41	40	29

Table D.3-a Dual-mode visual tracking eye movement: Composite (pursuit and saccade)

Subject	Input A			Input B			Input C			Input D		
	n	m	m <sub>o</sub>	n	m	m <sub>o</sub>	n	m	m <sub>o</sub>	n	m	m <sub>o</sub>
BC	51	89	40	50	60	47	37	38	32	45	84	31
CO	50	64	48	51	49	46	37	39	32	45	60	40
TY	51	95	45	51	76	46	38	79	36	45	69	36
SY	51	63	48	51	65	41	39	41	34	45	74	41

Table D.3-b Dual-mode visual tracking eye movement: Pursuit only

Subject	Input A			Input B			Input C			Input D		
	n	m	m <sub>o</sub>	n	m	m <sub>o</sub>	n	m	m <sub>o</sub>	n	m	m <sub>o</sub>
BC	50	66	25	51	48	33	37	37	23	45	49	32
CO	51	70	32	51	54	40	39	38	26	45	61	42
TY	51	69	38	51	59	38	38	36	27	45	57	23
SY	51	78	30	49	70	37	39	39	26	45	70	34

---

\* Each number in tables was cumulated over 2 to 4 FFT runs with sampling epoch occupying different portions of the same data trace.

Table D.4 OKN slow phase

Subject	Input A			Input B			Input C			Input D		
	n	m	m <sub>0</sub>	n	m	m <sub>0</sub>	n	m	m <sub>0</sub>	n	m	m <sub>0</sub>
CO	51	53	26	51	58	40	26	27	13	45	54	33
TY	35	38	17	50	49	34	25	21	10	45	48	36
SY	51	60	28	51	55	28	39	36	29	45	42	28

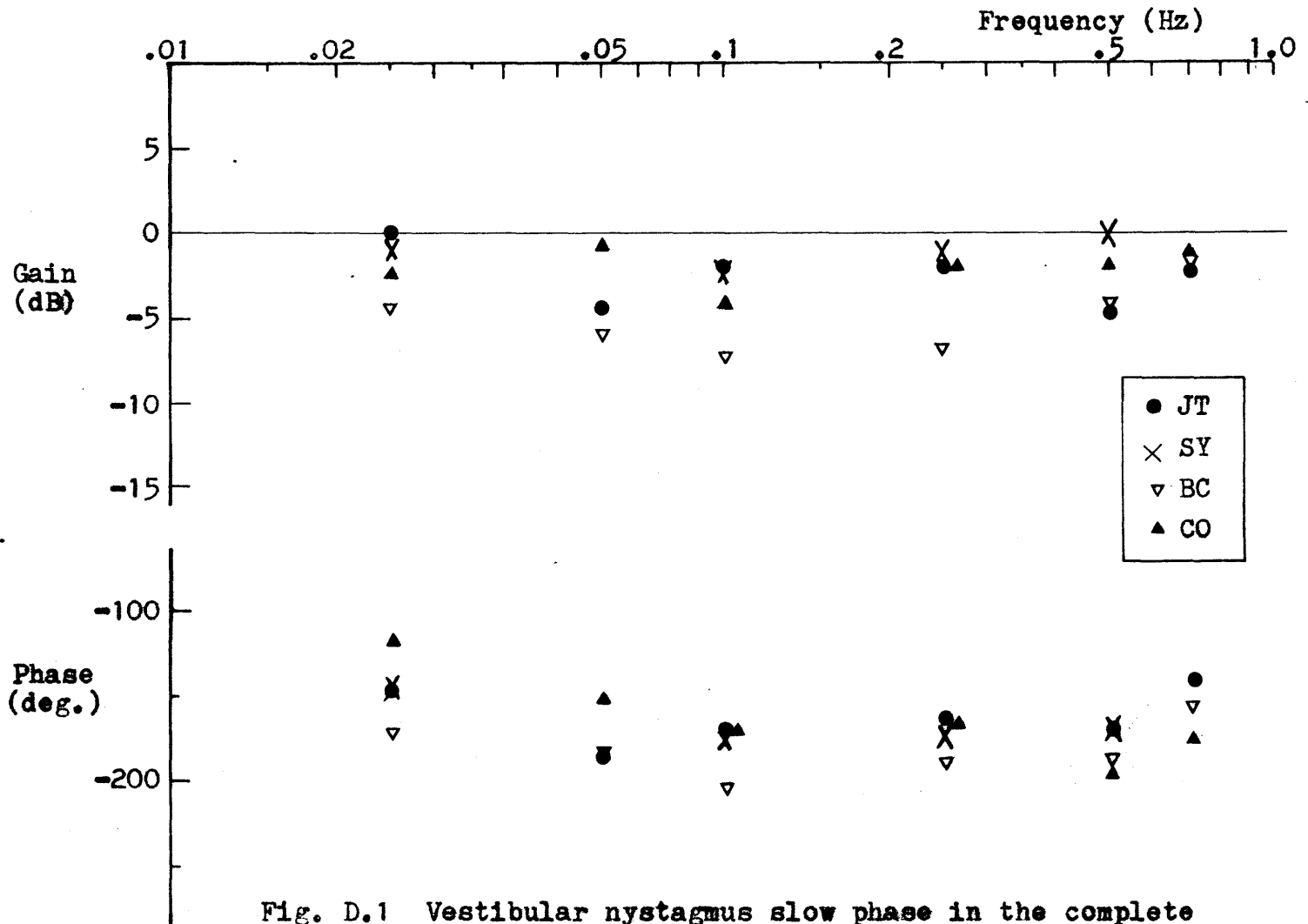


Fig. D.1 Vestibular nystagmus slow phase in the complete darkness: Frequency response to sinusoidal head rotation leading to the statistical reduced version shown in Fig. 3.11.

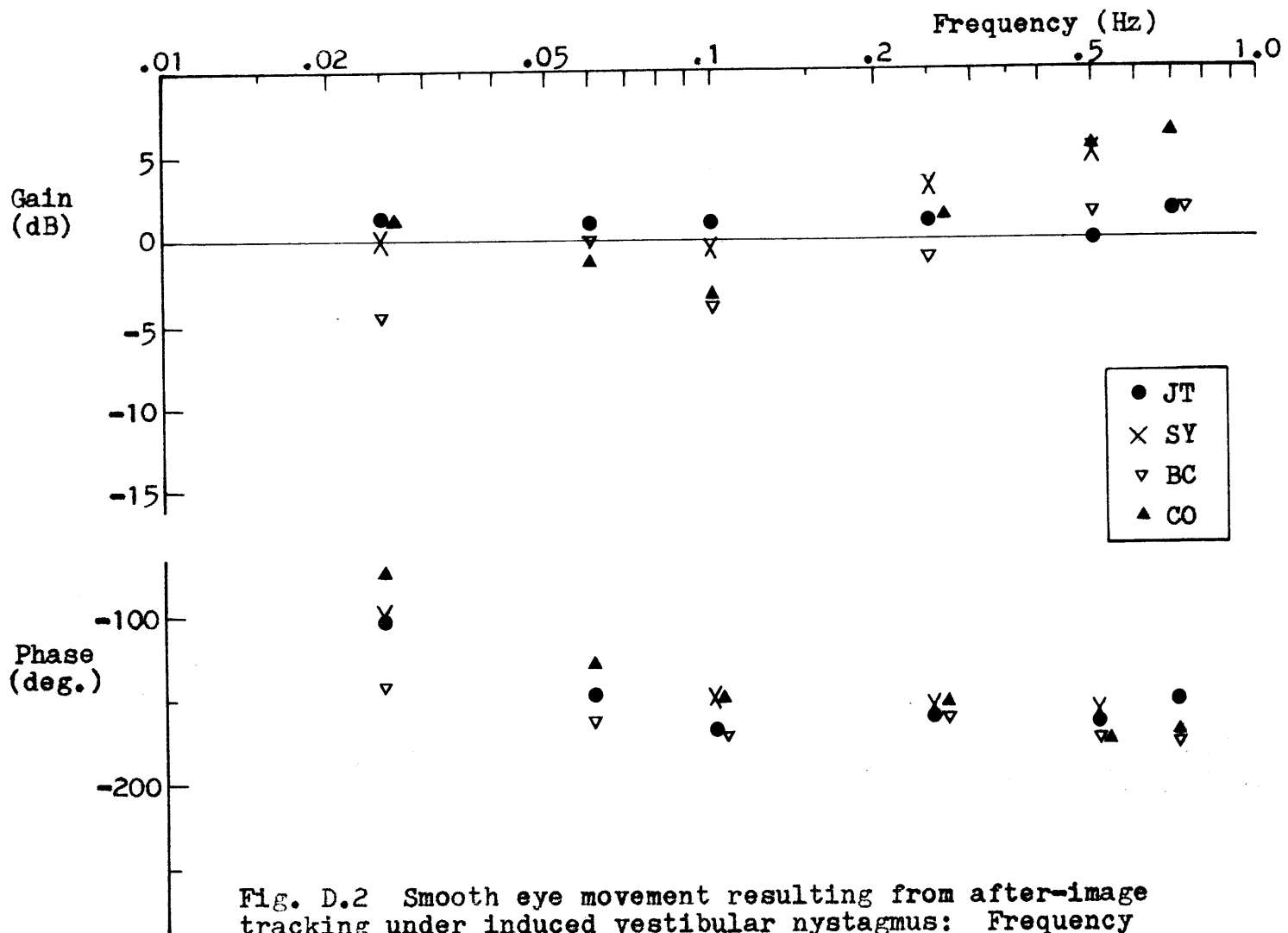


Fig. D.2 Smooth eye movement resulting from after-image tracking under induced vestibular nystagmus: Frequency response to sinusoidal head rotation leading to the statistically reduced version shown in Fig. 3.12.



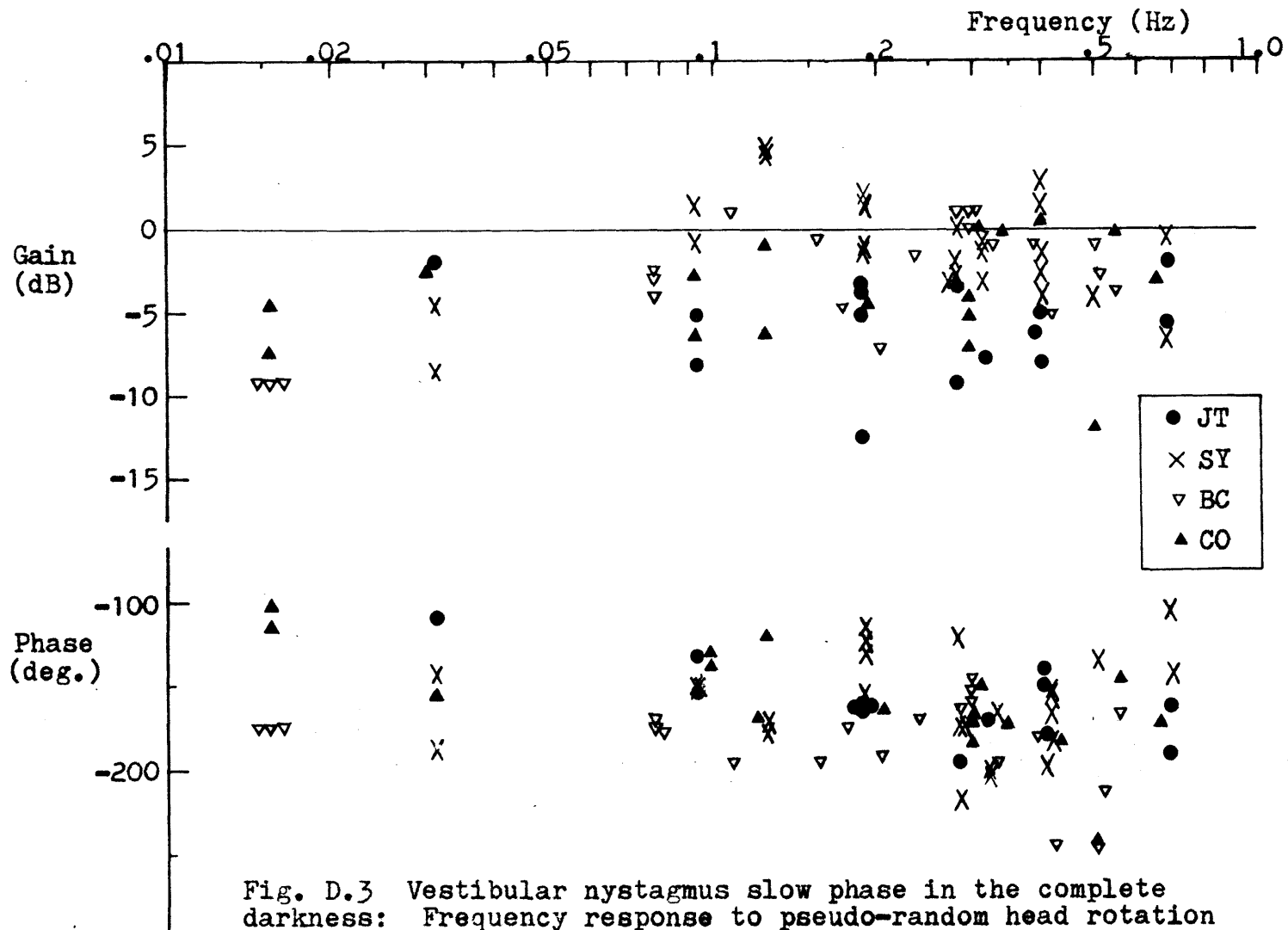


Fig. D.3 Vestibular nystagmus slow phase in the complete darkness: Frequency response to pseudo-random head rotation leading to the statistically reduced version shown in Fig. 3.14.

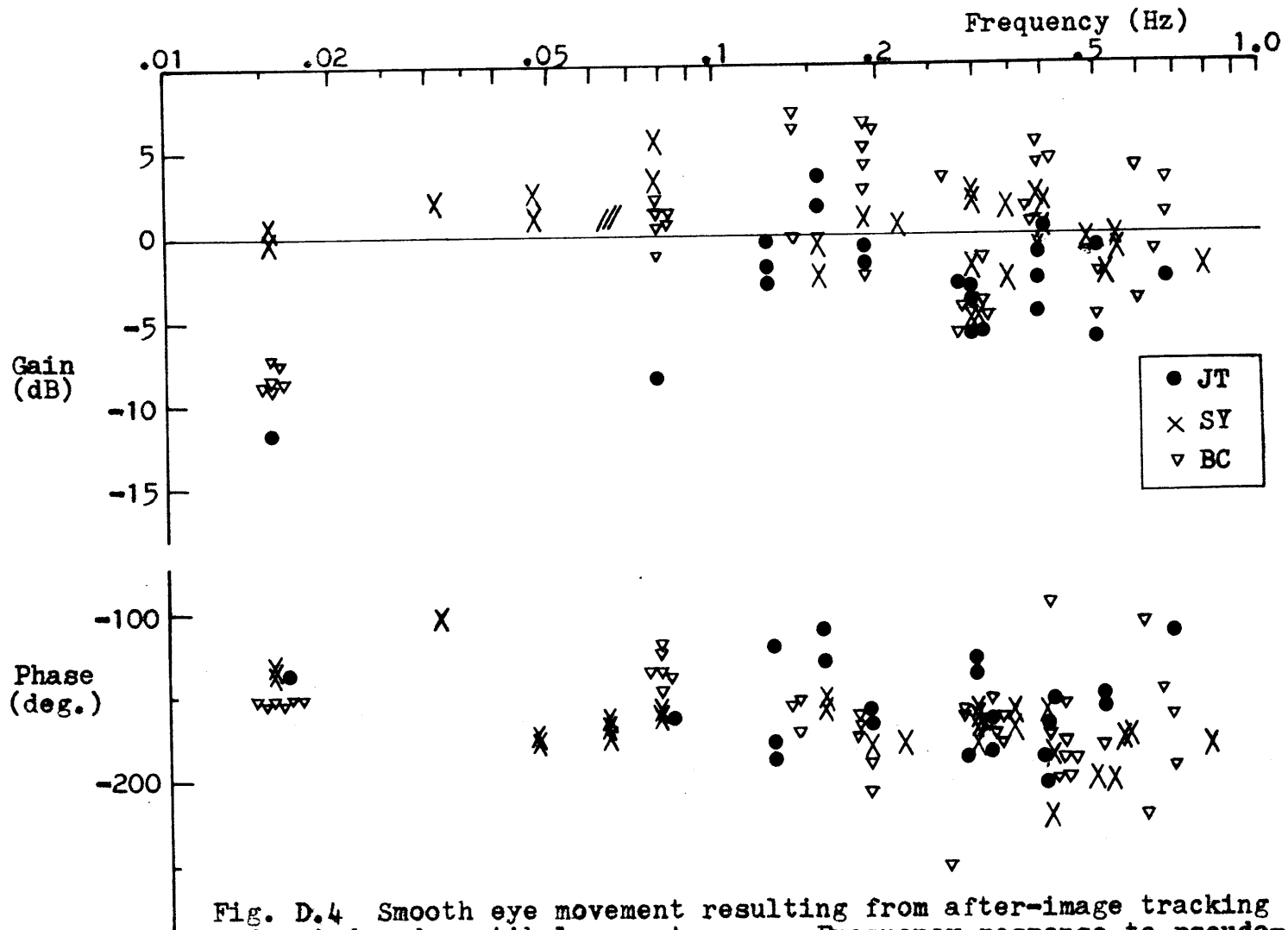


Fig. D.4 Smooth eye movement resulting from after-image tracking under induced vestibular nystagmus: Frequency response to pseudo-random head rotation leading to the statistically reduced version shown in Fig. 3.15.

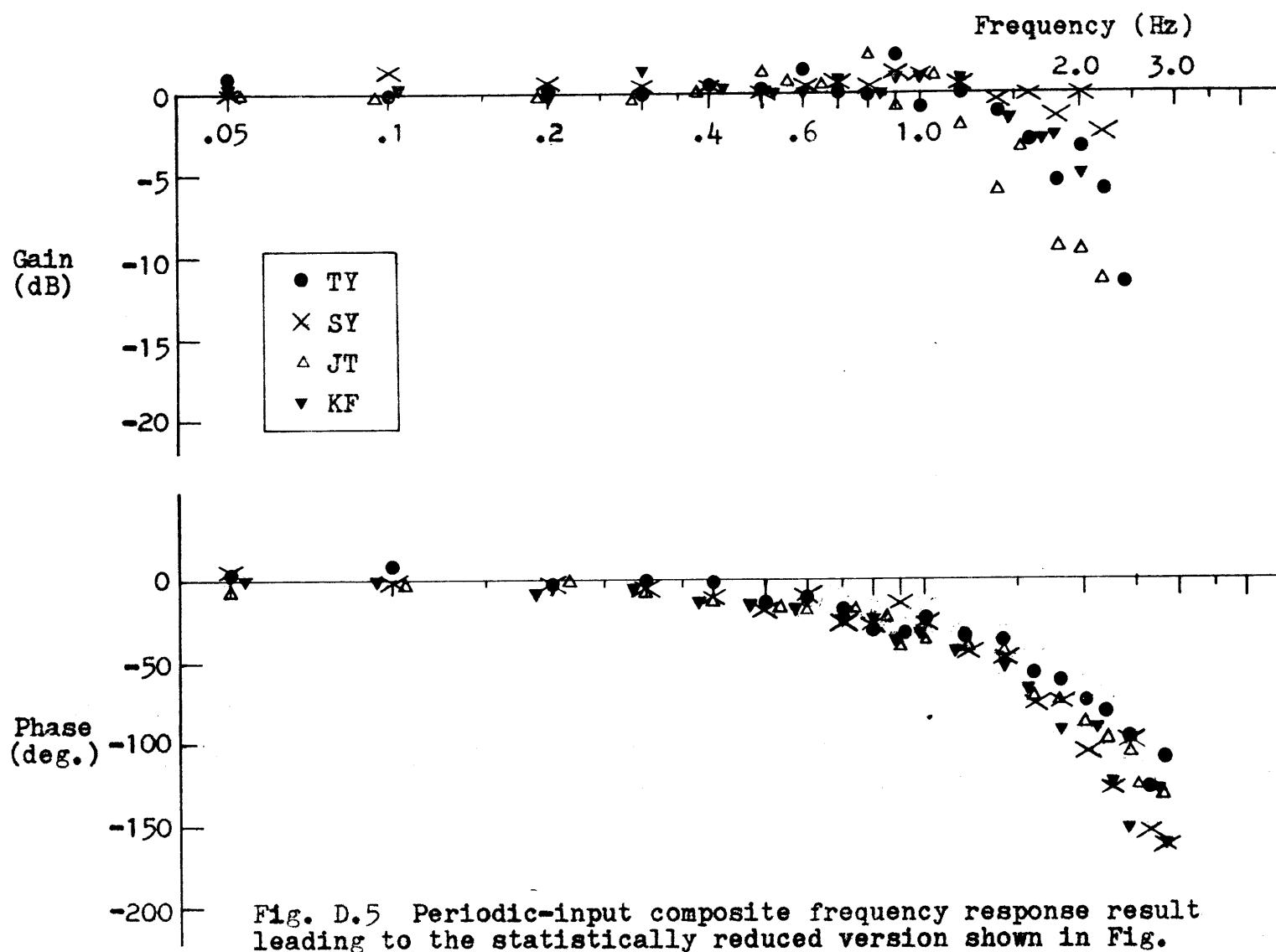


Fig. D.5 Periodic-input composite frequency response result leading to the statistically reduced version shown in Fig. 4.7.

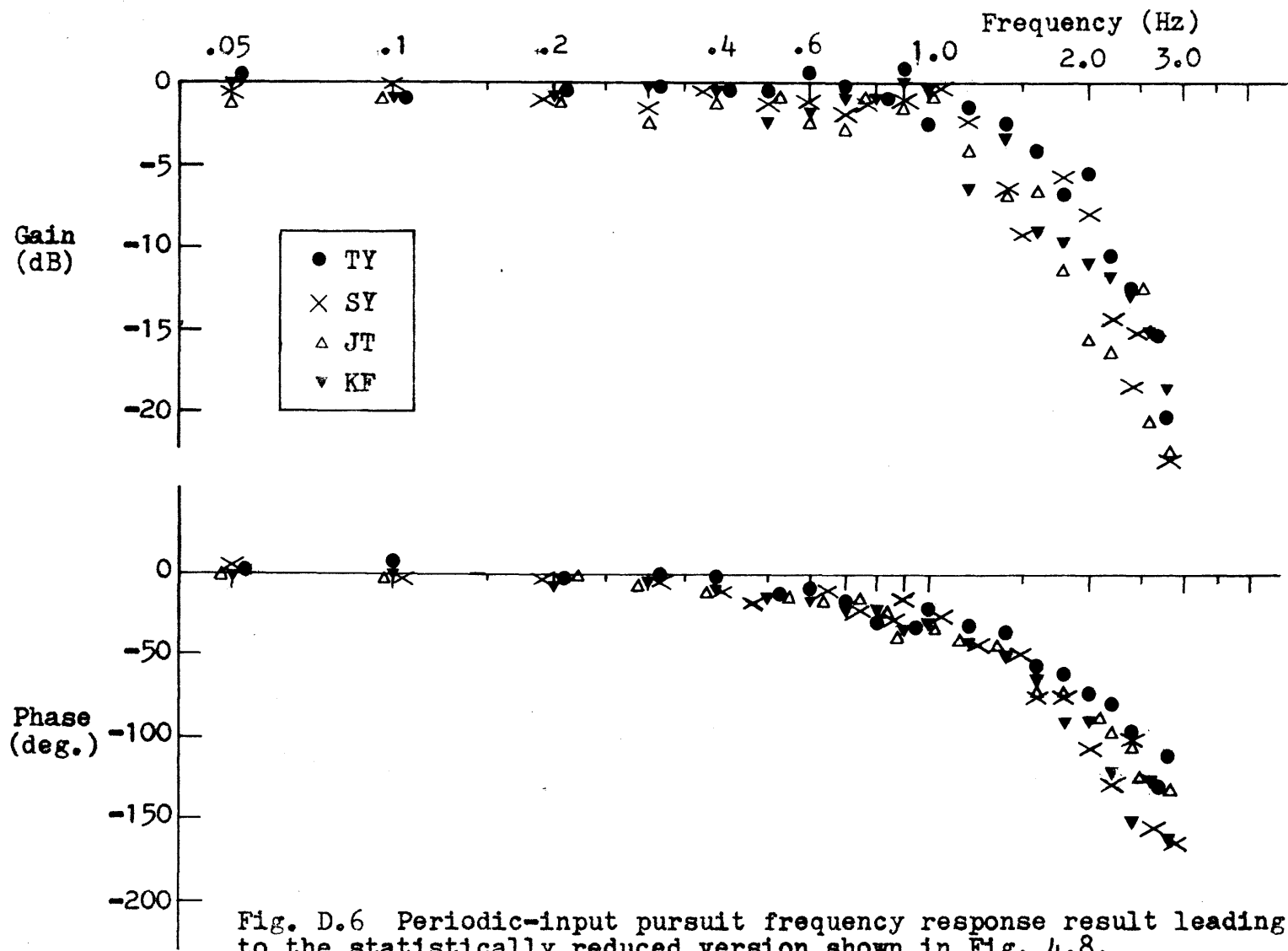


Fig. D.6 Periodic-input pursuit frequency response result leading to the statistically reduced version shown in Fig. 4.8.

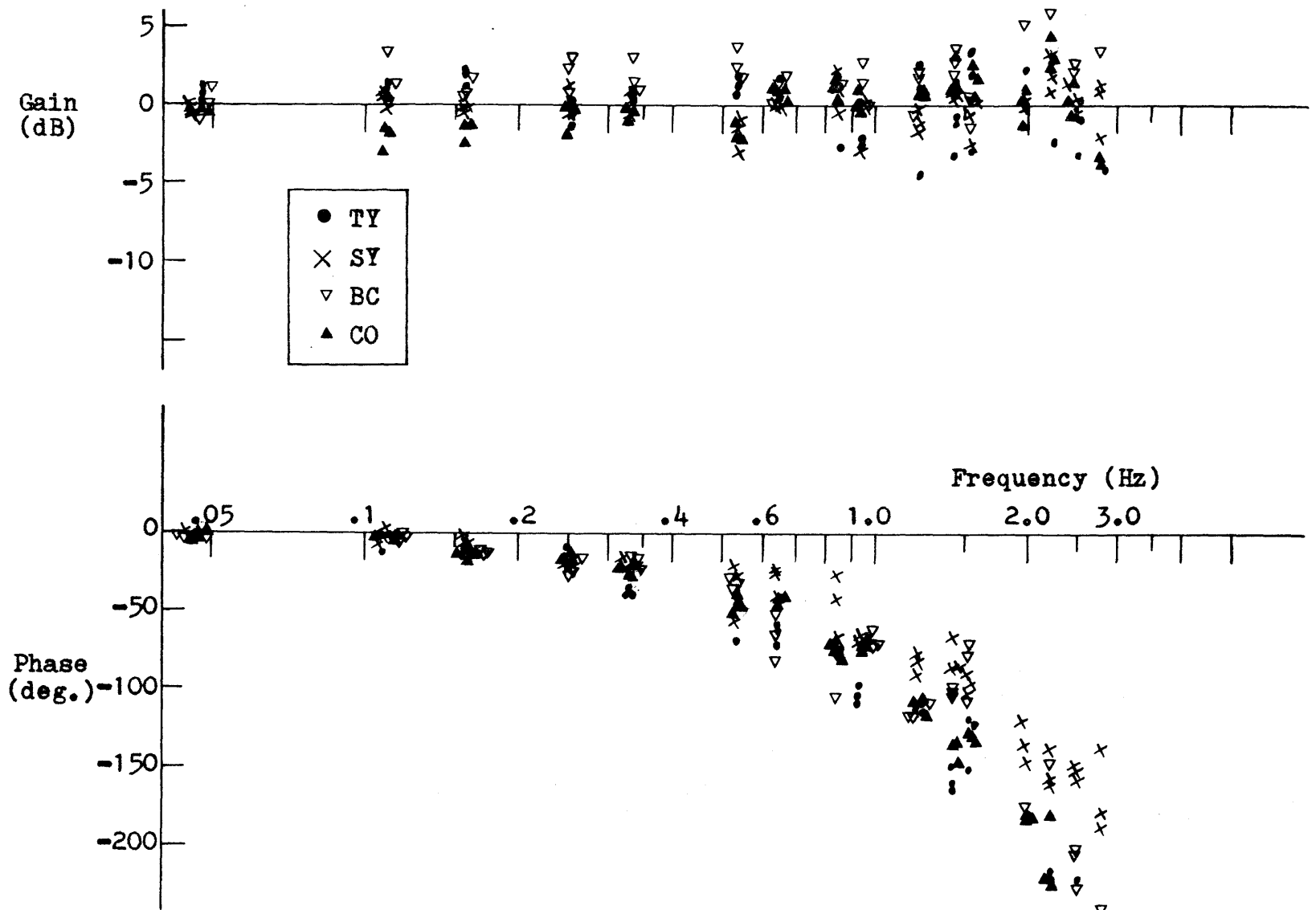


Fig. D.7-a Nonperiodic-input composite frequency response result leading to the statistically reduced version shown in Fig. 4.13-a: Pseudo-random input A.

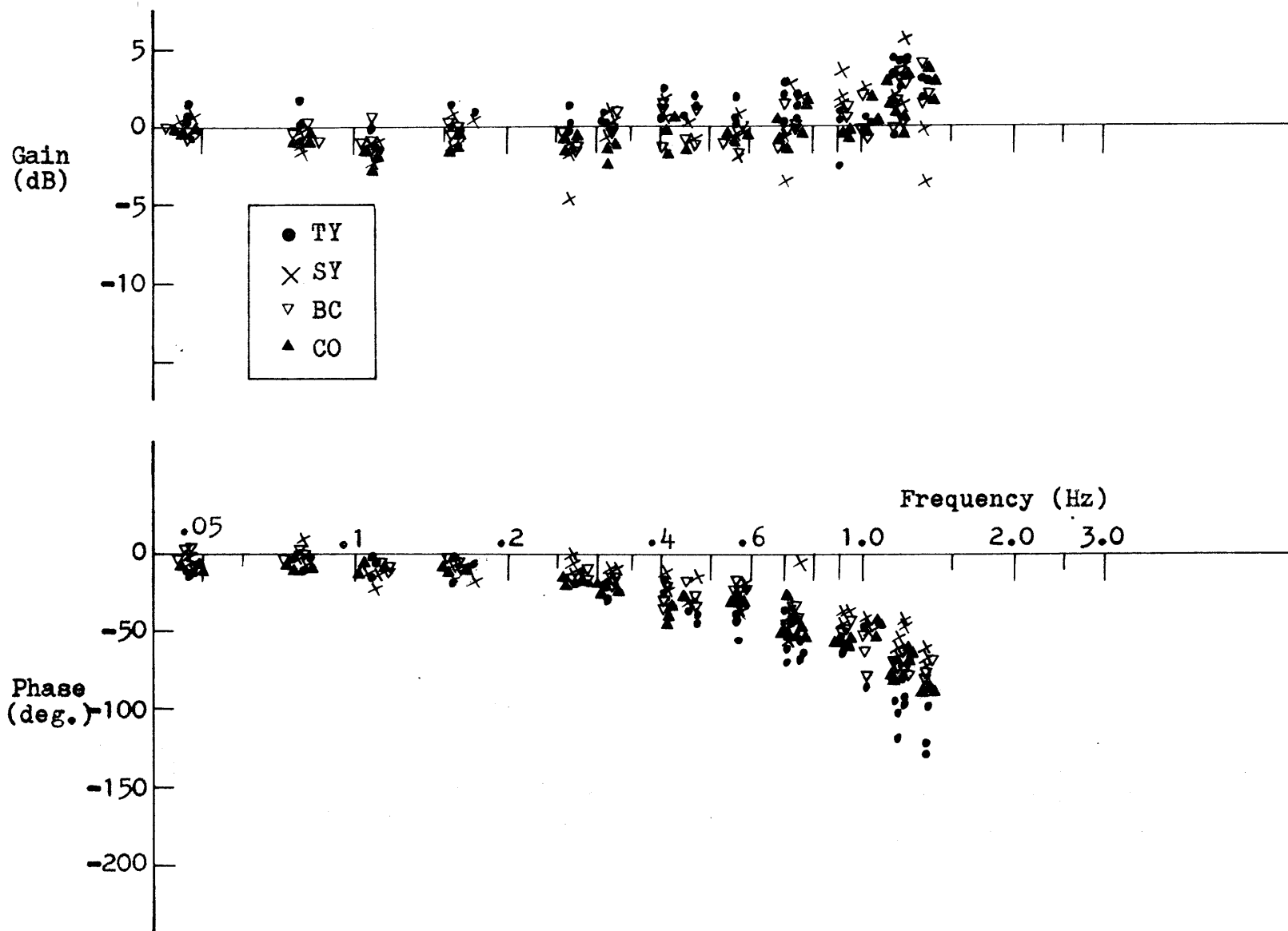


Fig. D.7-b Nonperiodic-input composite frequency response result leading to the statistically reduced version shown in Fig. 4.13-b: Pseudo-random input B.

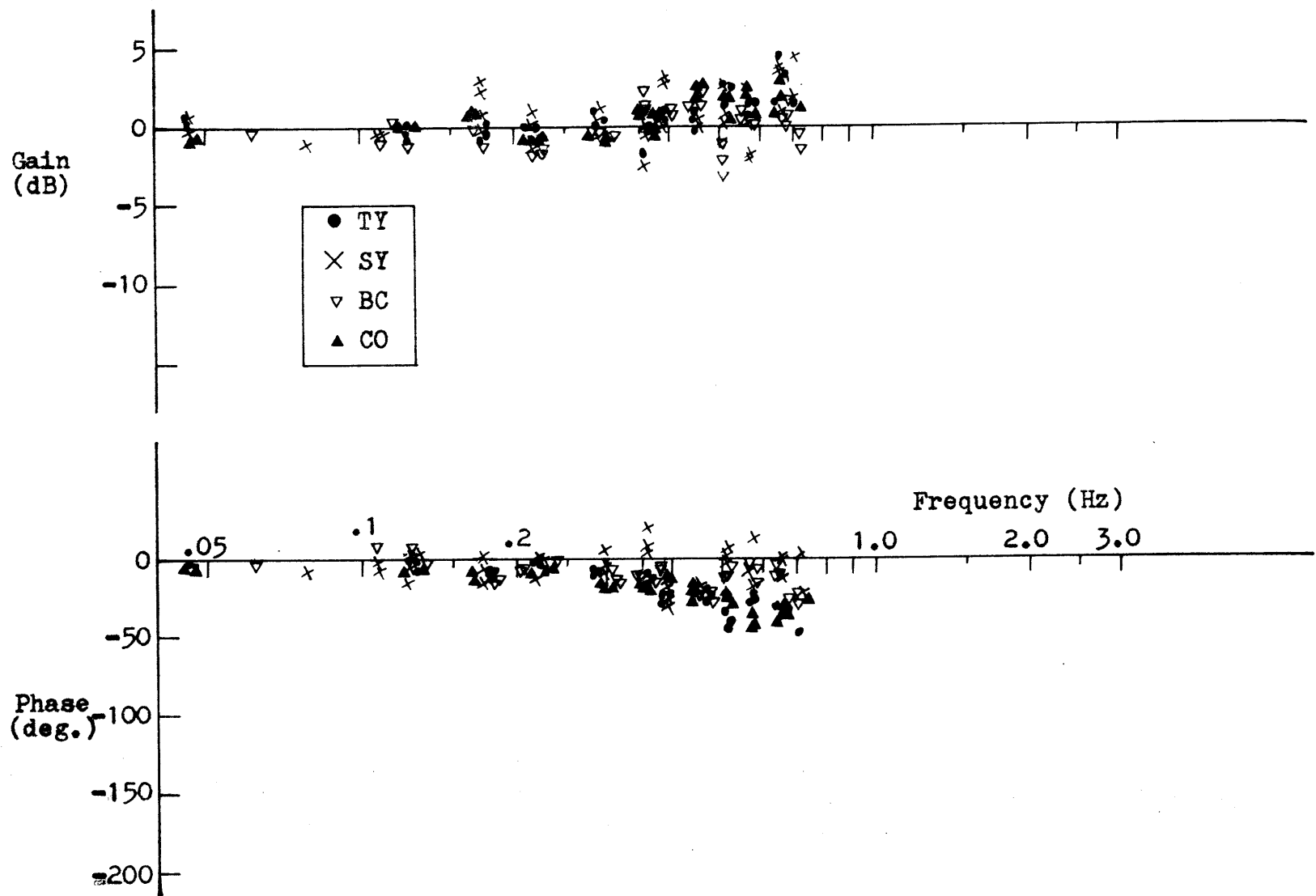


Fig. D.7-c Nonperiodic-input composite frequency response result leading to the statistically reduced version shown in Fig. 4.13-c: Pseudo-random input C.

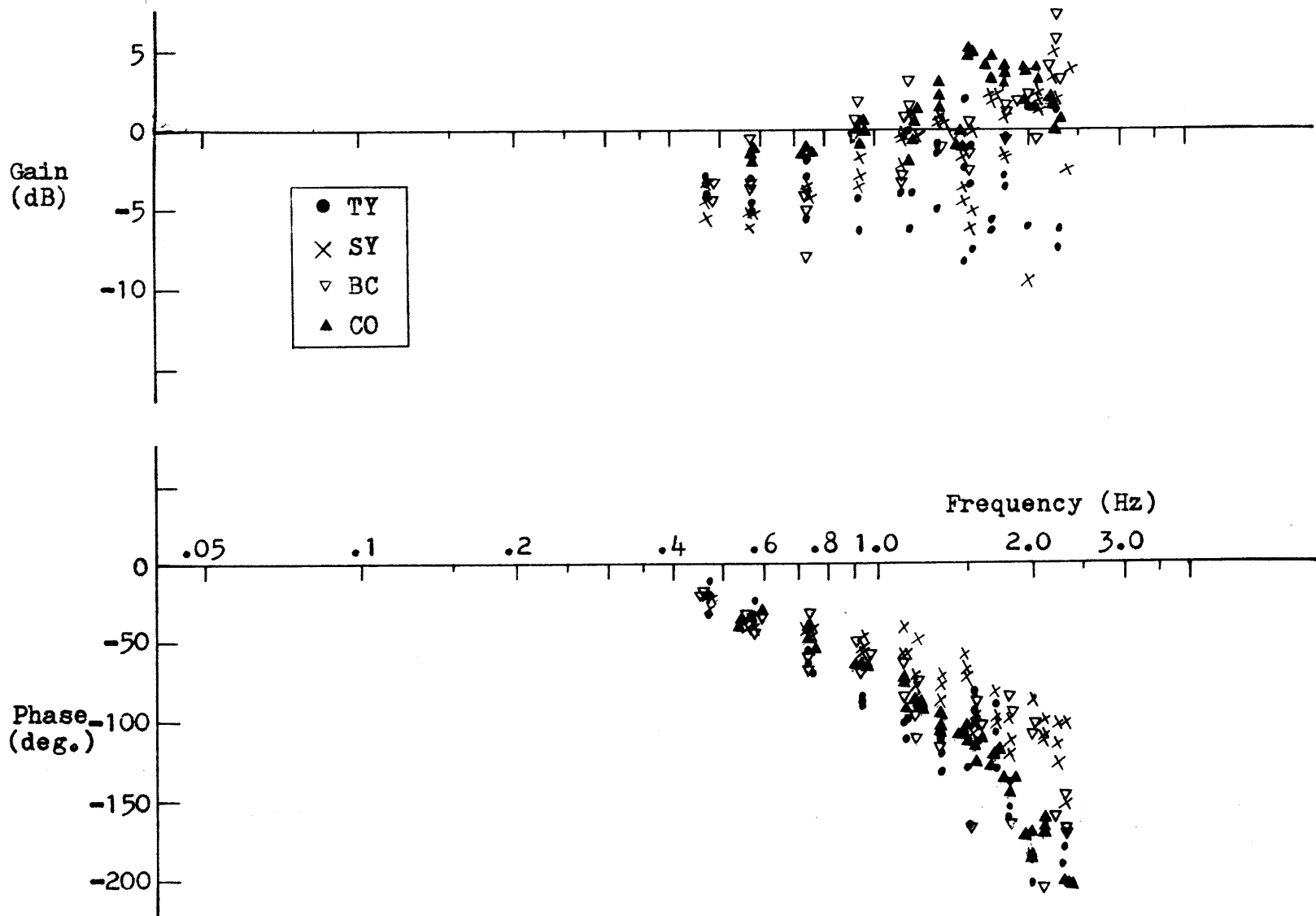
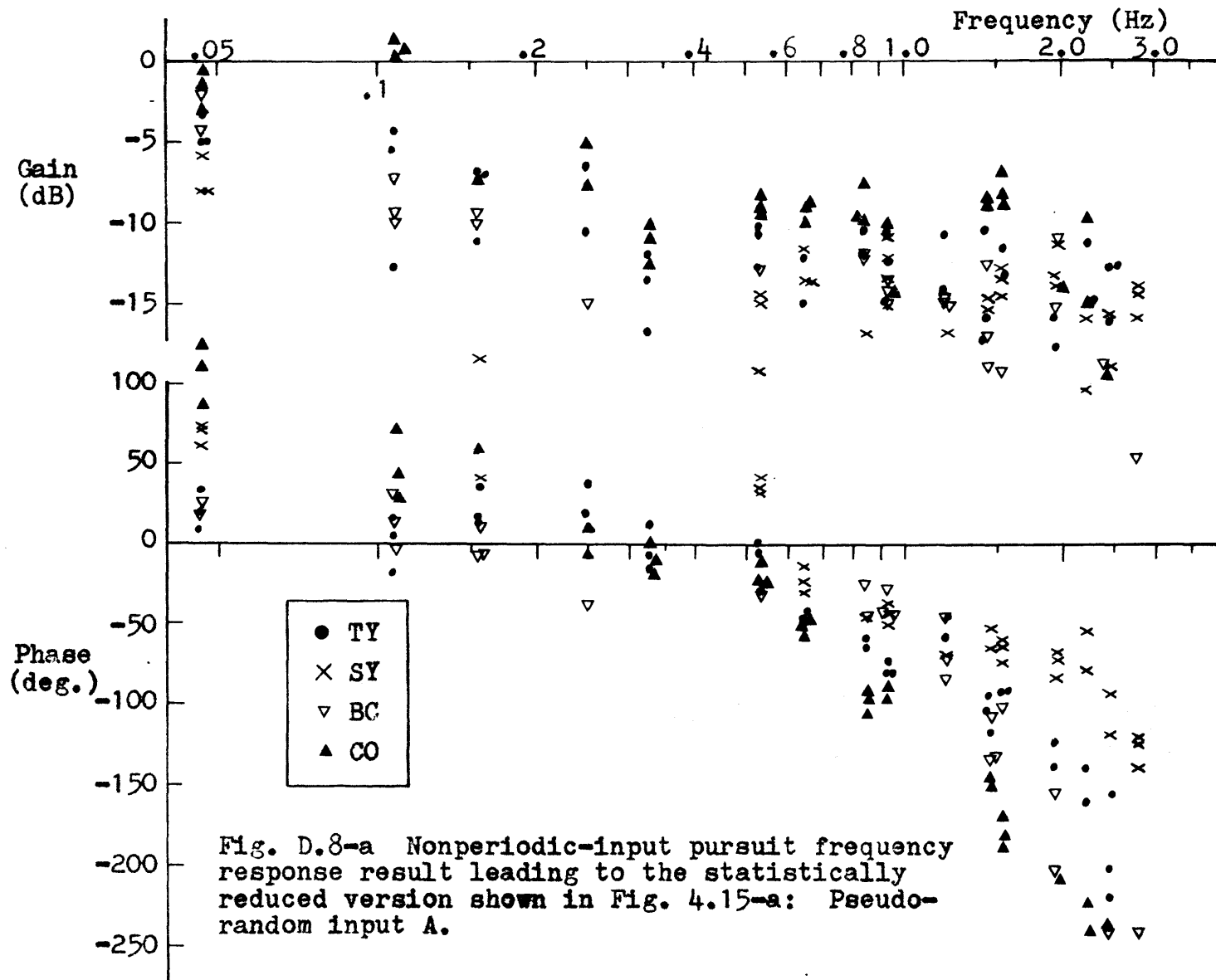


Fig. D.7-d Nonperiodic-input composite frequency response result leading to the statistically reduced version shown in Fig. 4.13-d: Pseudo-random input D.





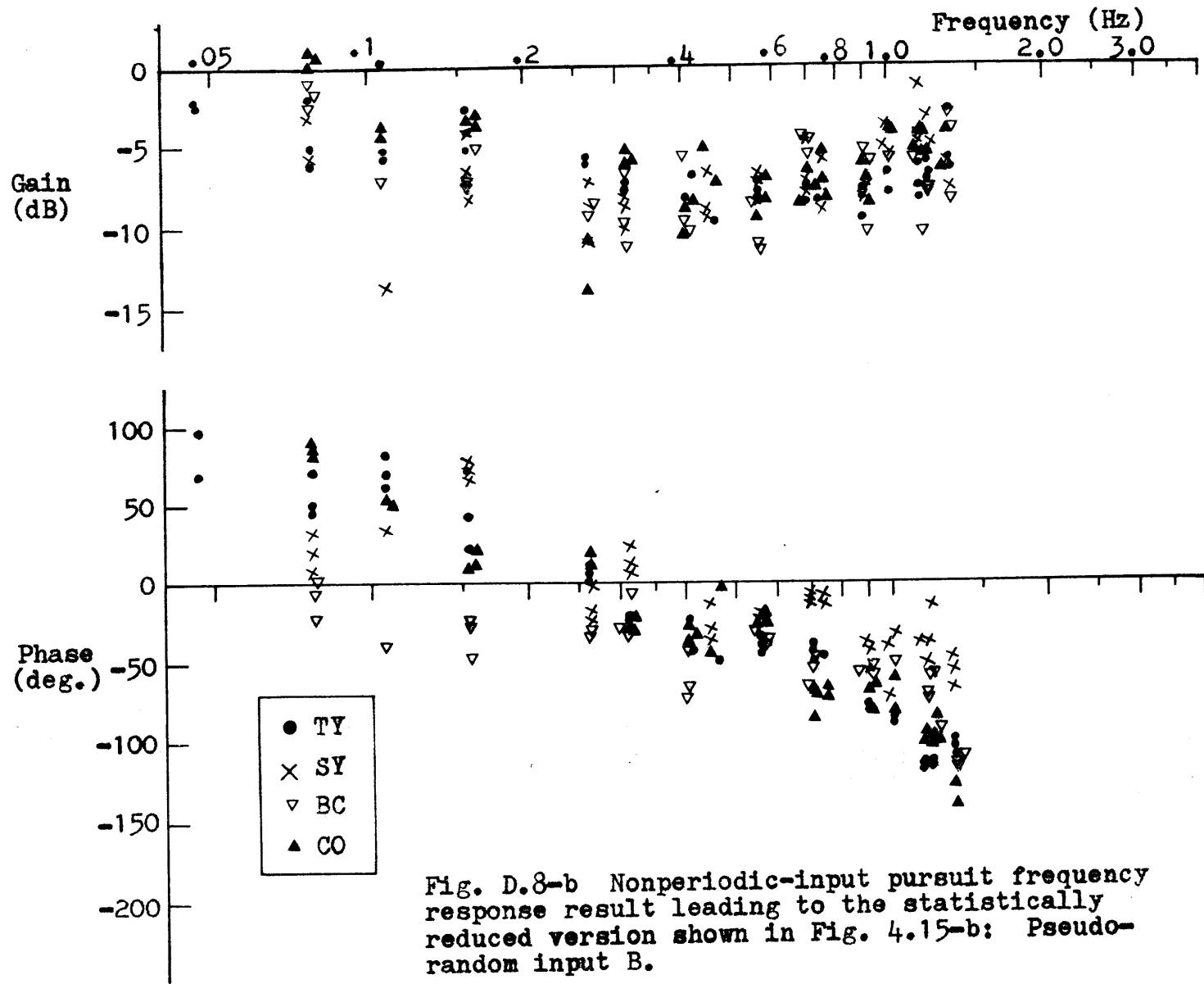
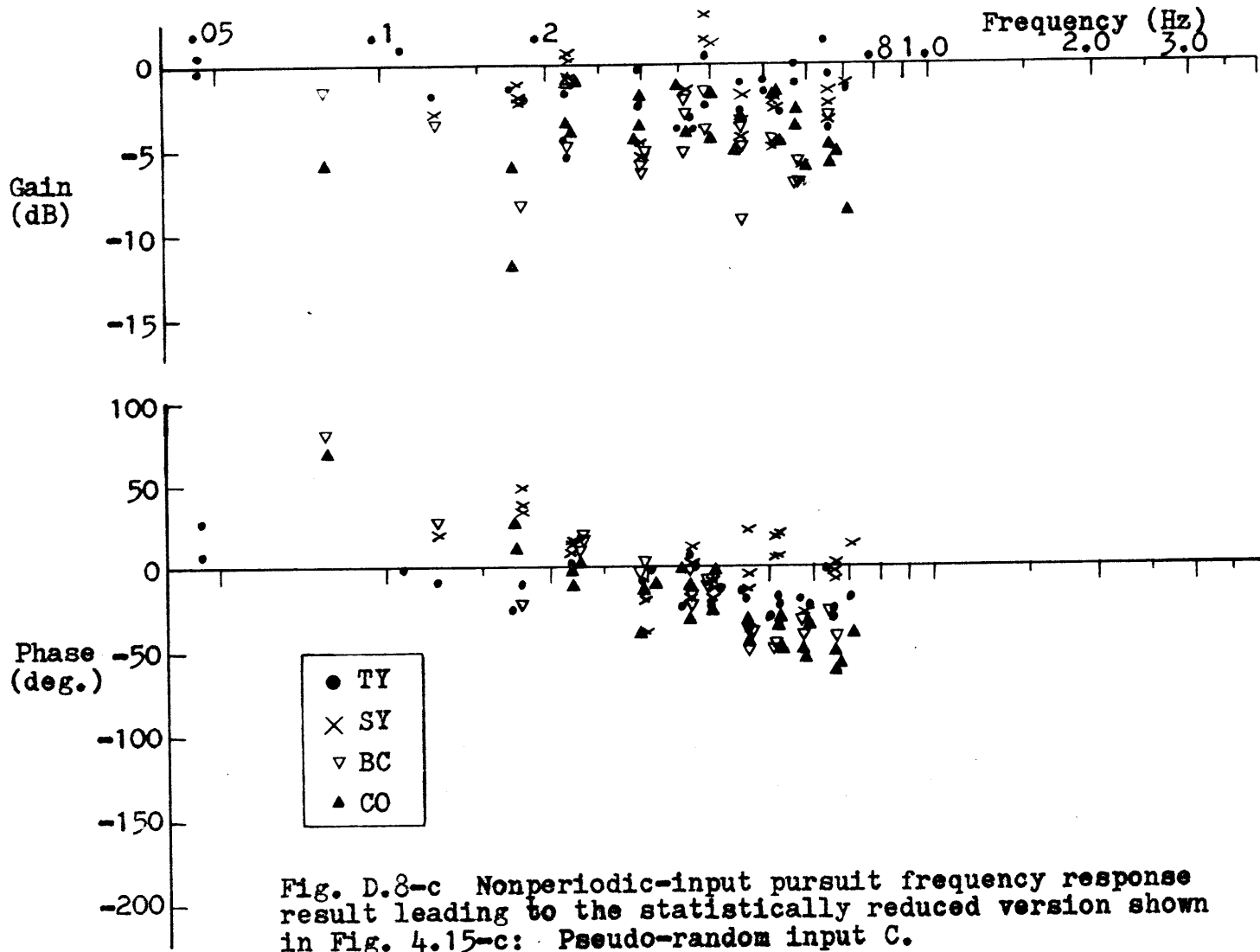
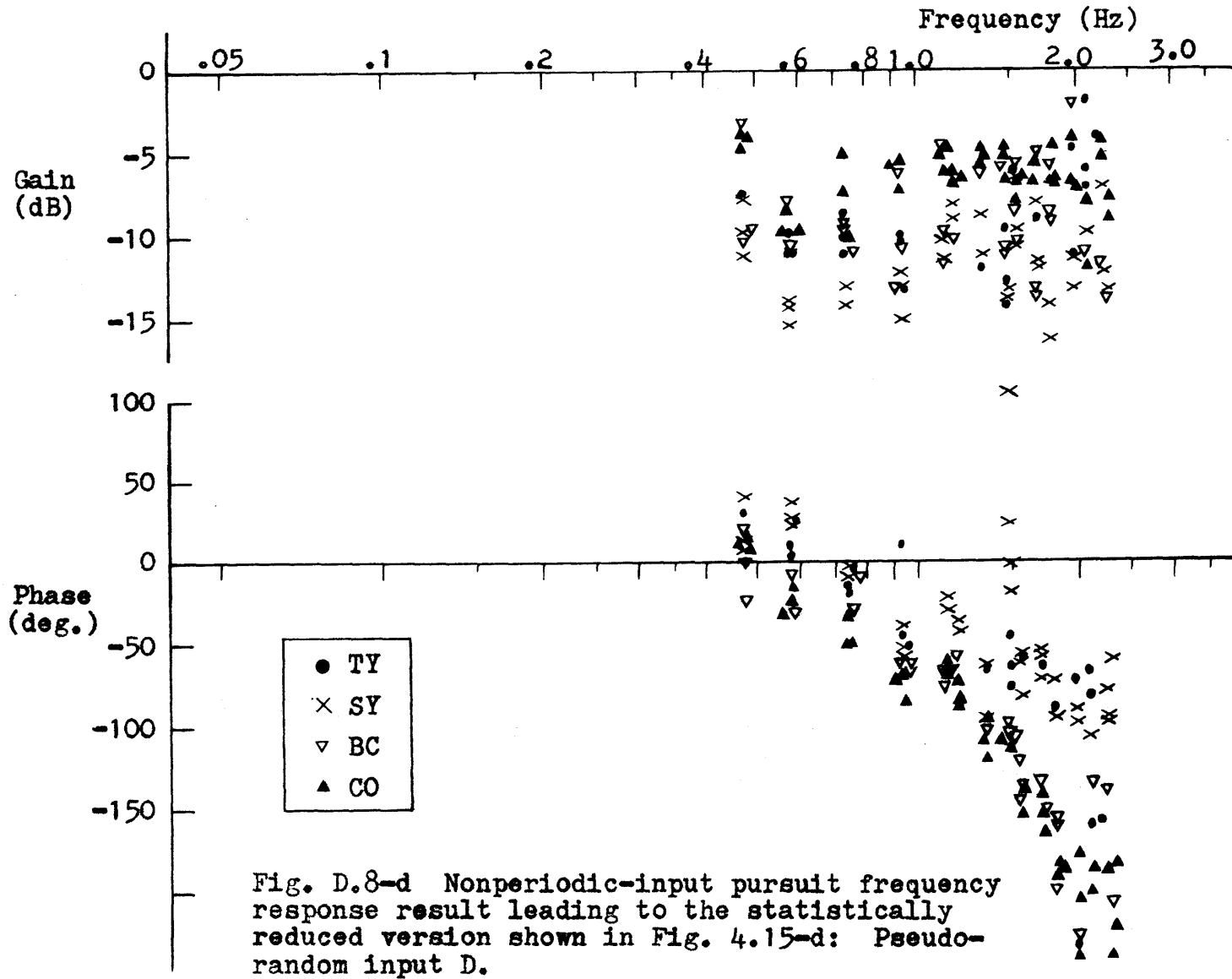


Fig. D.8-b Nonperiodic-input pursuit frequency response result leading to the statistically reduced version shown in Fig. 4.15-b: Pseudo-random input B.





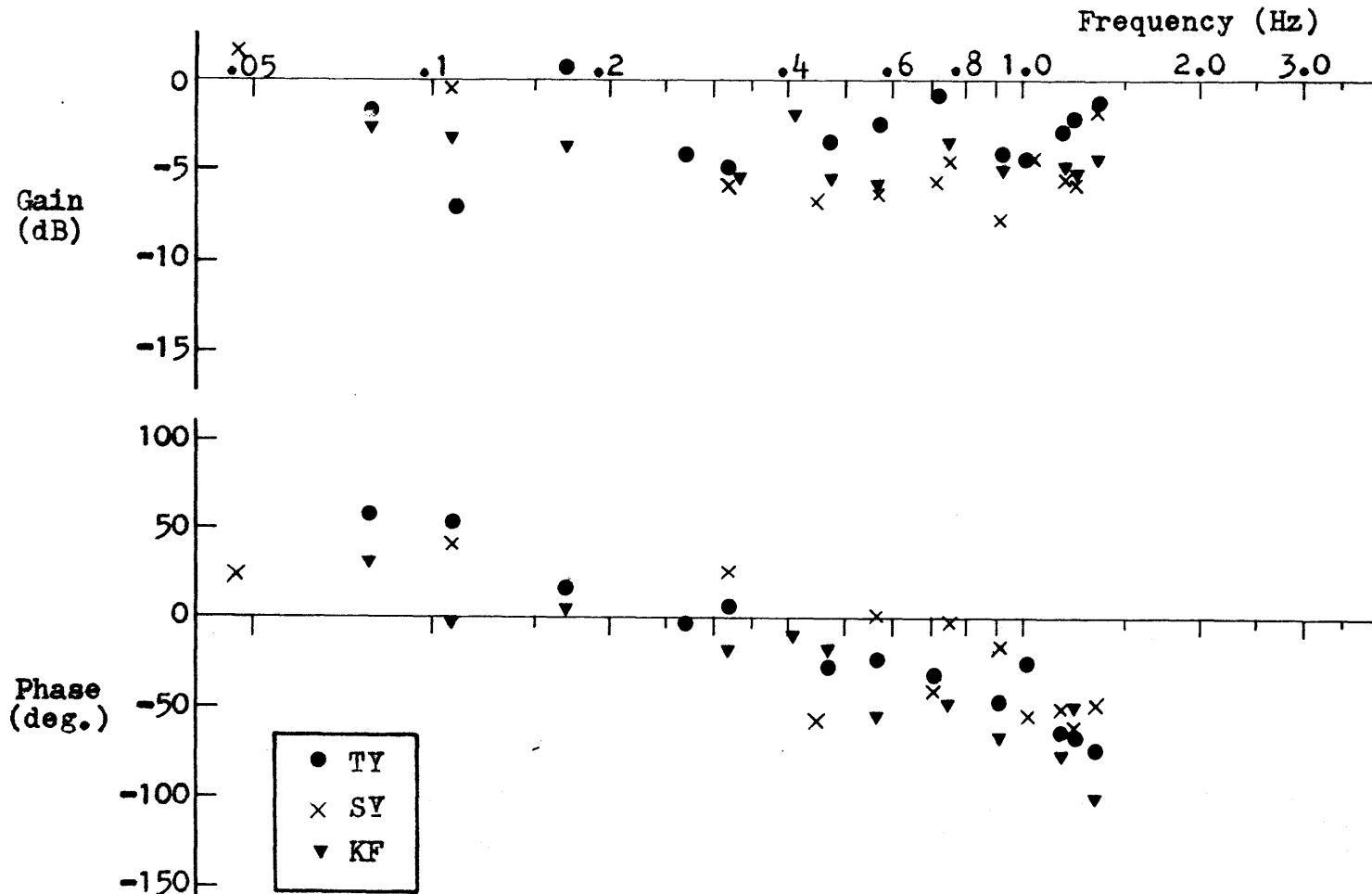


Fig. D.9 Nonperiodic-input pursuit frequency response:  
Test run data with direct target presentation on CRT  
(see Subsection 4.4.1).

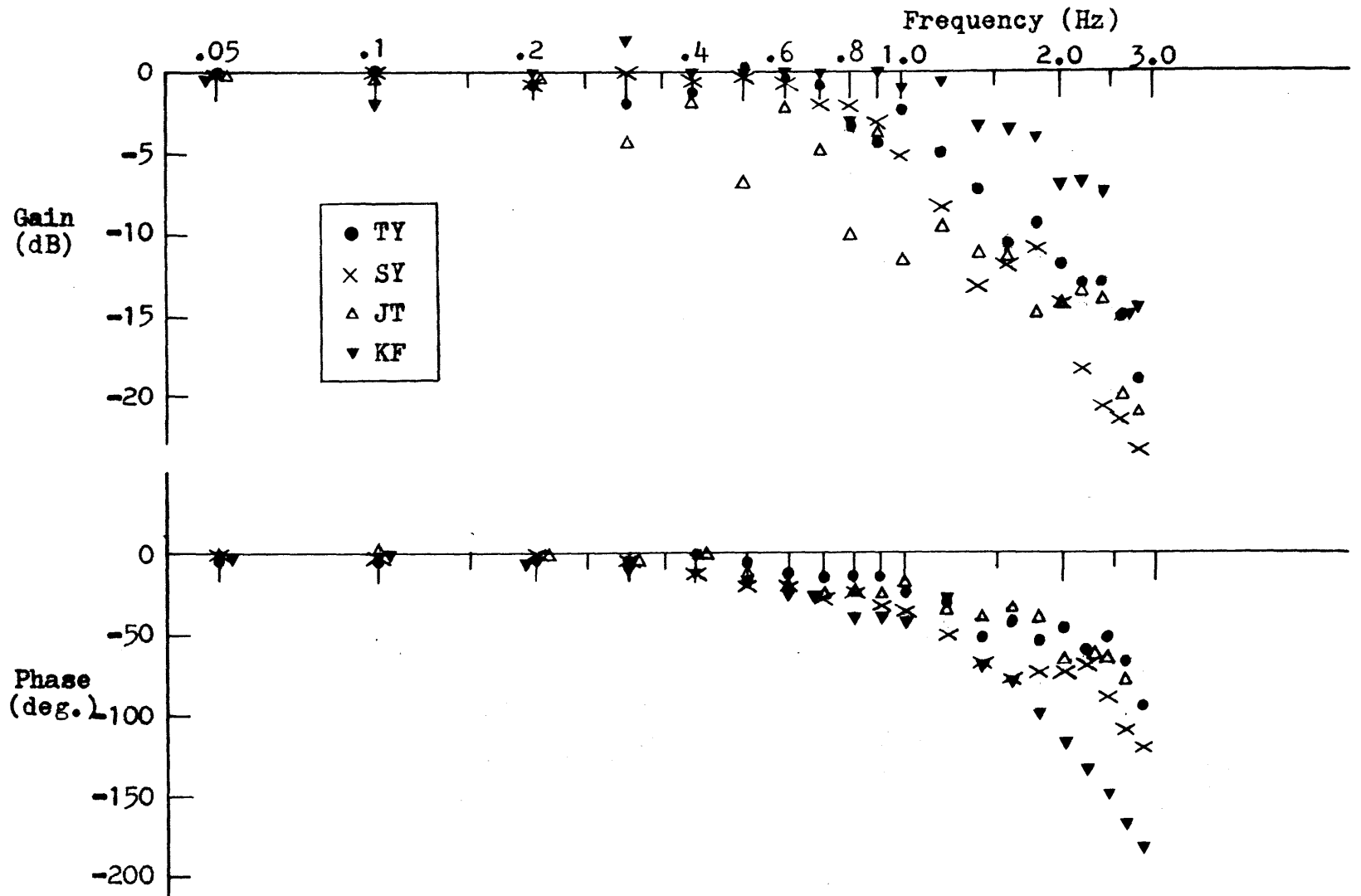
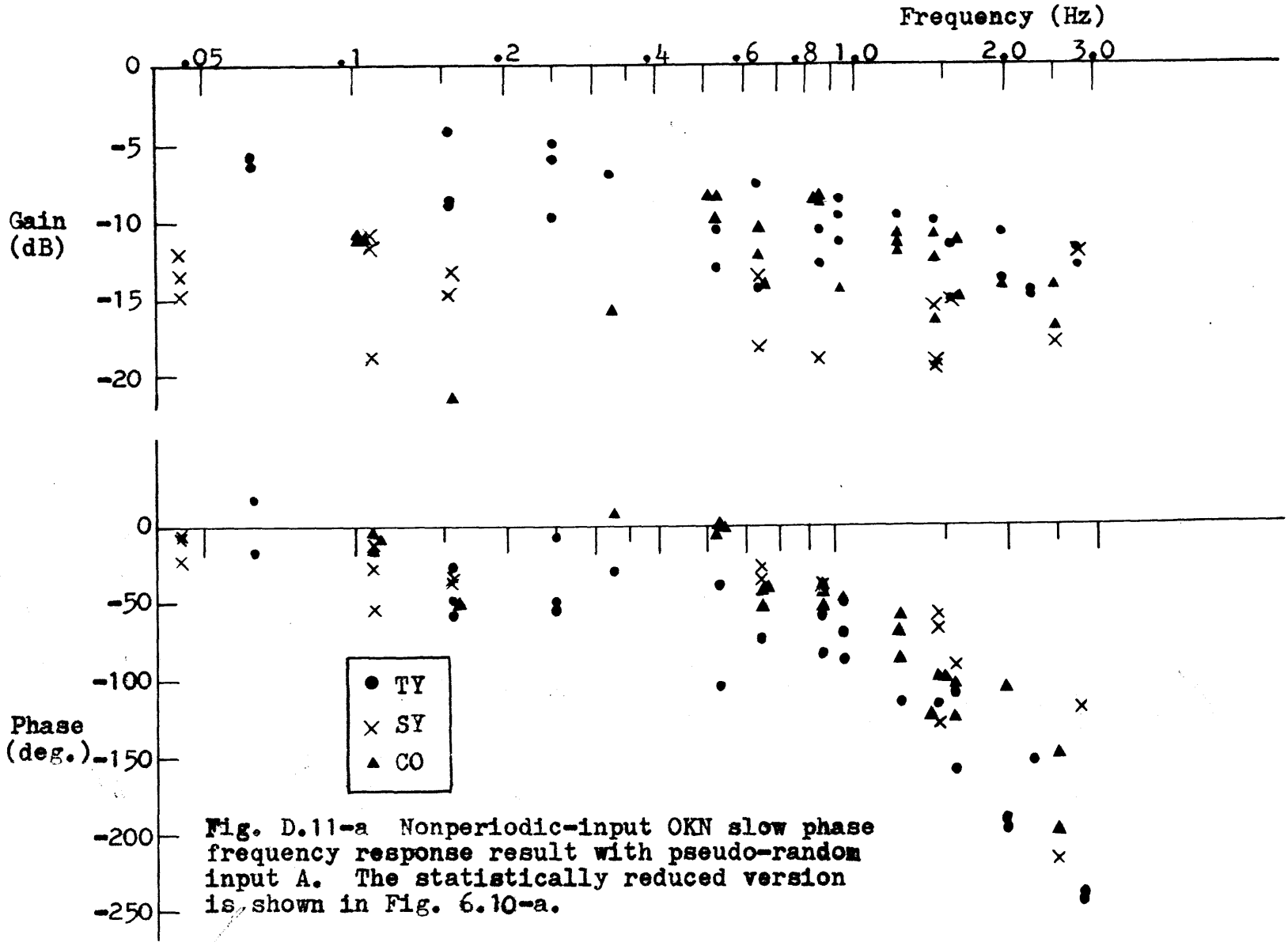
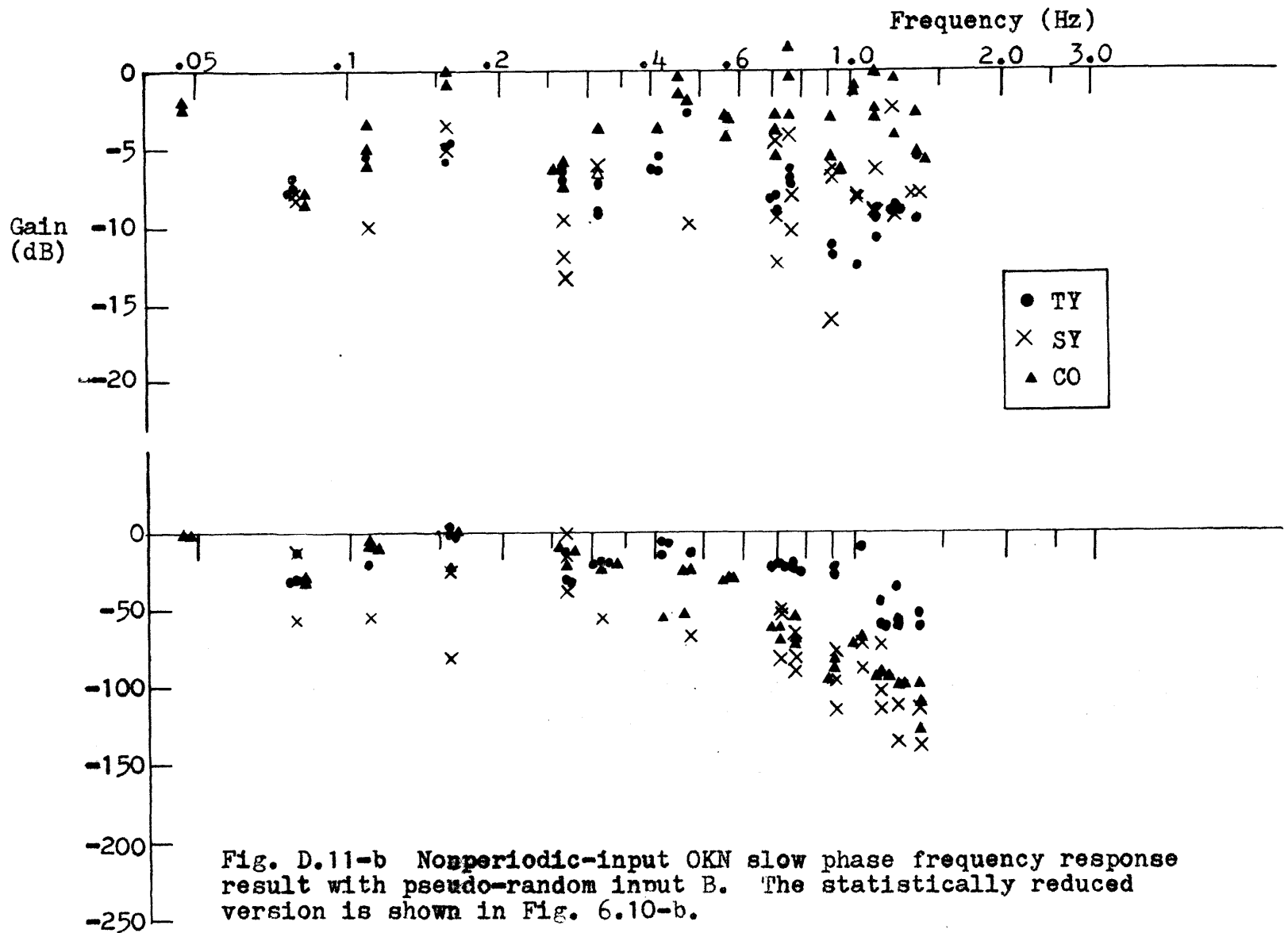
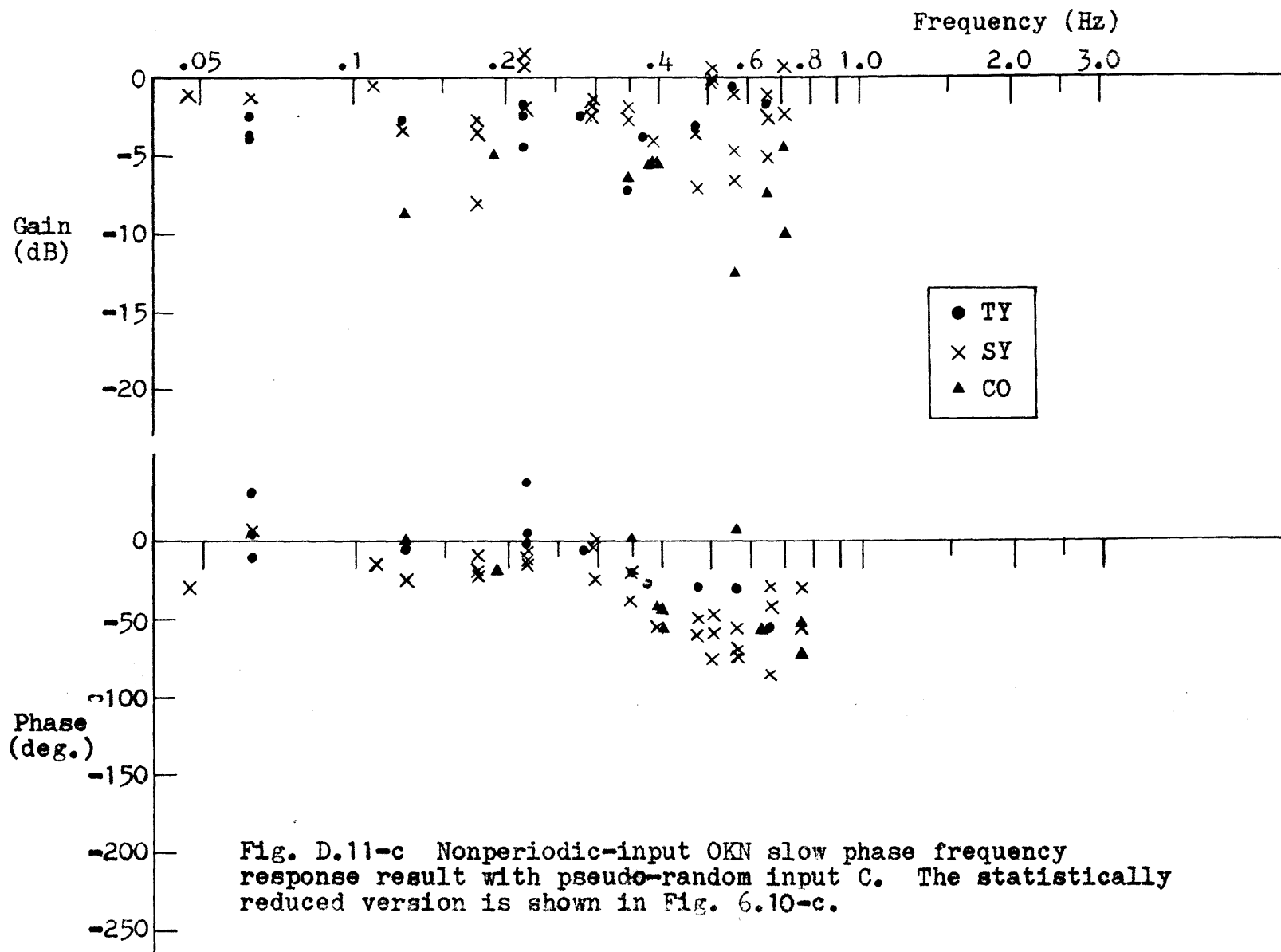


Fig. D.10 Periodic-input OKN slow phase frequency response result. The statistically reduced version is shown in Fig. 6.8.









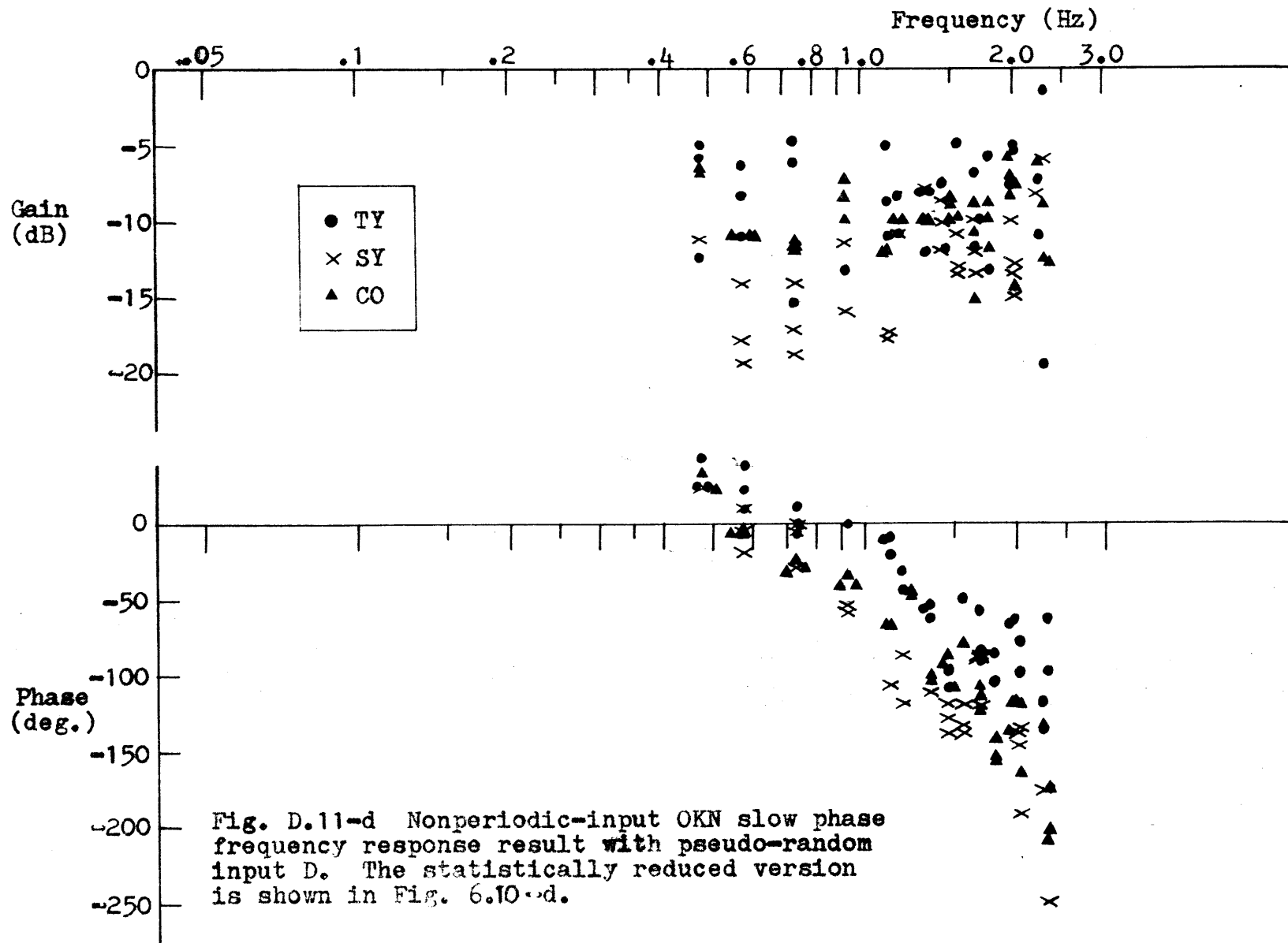


Fig. D.11-d Nonperiodic-input OKN slow phase frequency response result with pseudo-random input D. The statistically reduced version is shown in Fig. 6.10-d.

## Appendix E

### OKN Stimulus Display by Computer Graphics

OKN experiments in the thesis (Chapters VI and VII) employed a computer graphical method for generating and controlling the stripe pattern stimulus. Advantage of this approach has been discussed in Chapter VI. Table E.1 gives listing of the corresponding computer program "OKN" written in PAL III assembly language. Hybrid connections are shown in Fig. E.1. Optional features include selective OKN stimulation to central or peripheral part of the retina through elimination of appropriate stripes based on eye movement feedback information as described in Section 7.5. Vertical stripes were generated in the following manner:

Successive additions of a constant octal number DLINE, say  $400_8$ , in the PDP-8 digital computer cause an over-flow in the D/A buffer, which in turn automatically resets itself to the initial state ("reference buffer content, HLINE0 + LLINE0).<sup>\*</sup> A high speed cyclic operation of this process results in sixteen ( $=8000_8/400_8=20_8$ ) evenly-spaced dots visible on X-axis of the X-Y display console.<sup>\*\*</sup> Additional Y-axis sweep with a sine wave of still much higher frequency (say, 100k Hz) makes each dot

---

\* Provided that some octal integer  $\times$  DLINE gives  $8000_8=0$ .

\*\* Negative of expected number of lines, NMB, must be loaded in advance by switch register along with the specified separation of adjacent two lines, i.e.,  $-20_8=7760_8$  at location  $21_8$ , and  $400_8$  at location  $20_8$ .

appear as a continuous vertical line as viewed in Fig. 6.1. All such lines are made capable of moving smoothly in a desired speed, by incrementing the reference buffer content by a factor determined in accordance with the A/D - converted stimulus velocity command, VEL. The sixteenth line may disappear from the field of visual pattern, but it will instantly reappear as the first line in the other edge. The higher part of the double-precision reference buffer content, which represents a particular vertical line's position, is D/A - converted in order to retrieve up-dated information as to the group motion of the stripe pattern. This signal was useful in the velocity calibration, which resulted in a good linear relation in the relevant range between analog velocity command input and actual group velocity of the stripes as shown in Fig. E.2.

Table E.1 "OKN" program listing

```

/OKN DISPLAY-----SELECTIVE STIMULATIONS WITH
/OPTIONAL EYE POSITION FEEDBACK BLANKING
/ SYOZO YASUI      JUNE 27,1972
*200
0200  7300  START,CLA CLL
0201  3030  DCA LLINE0
0202  3031  DCA HLINE0
0203  7402  HLT
0204  7300  CASES,CLA CLL
0205  7604  LAS
0206  7440  SZA
0207  5224  JMP .+15
0210  4445  JMS I PEYE/CASE 0: EYE POSITION FEEDBACK CALIBRATION
0211  1026  TAD EYEPOS
0212  6552  DAL1
0213  7300  CLA CLL
0214  1026  TAD EYEPOS
0215  6554  DAL2
0216  7300  CLA CLL
0217  6564  DAL4
0220  7300  CLA CLL
0221  6551  DACX
0222  6561  DACY
0223  5204  JMP CASES
0224  7300  CLA CLL
0225  7604  LAS
0226  1040  TAD M1
0227  7440  SZA
0230  5240  JMP .+10
0231  3023  DCA BLANK/CASE 1: NO BLANKING
0232  3025  DCA FEED
0233  1053  TAD C1000
0234  3052  DCA CASE
0235  7001  IAC
0236  3024  DCA WHICH
0237  5310  JMP FRAME
0240  7300  CLA CLL
0241  7604  LAS
0242  1041  TAD M2
0243  7440  SZA
0244  5256  JMP .+12
0245  1022  TAD BLANK0/CASE 2: PERIPHERAL STIMULATION WITH
0246  3023  DCA BLANK /FEEDBACK BLANKING ON CENTRAL RETINA
0247  1026  TAD EYEPOS
0250  3025  DCA FEED
0251  1054  TAD C2000
0252  3052  DCA CASE
0253  7001  IAC
0254  3024  DCA WHICH
0255  5310  JMP FRAME
0256  7300  CLA CLL
0257  7604  LAS
0260  1042  TAD M3

```

0261	7440	SZA
0262	5273	JMP .+11
0263	1022	TAD BLANK0/CASE 3: CENTRAL STIMULATION WITH
0264	3023	DCA BLANK /FEEDBACK BLANKING ON PERIPHERAL RETINA
0265	1026	TAD EYEPOS
0266	3025	DCA FEED
0267	1055	TAD C3000
0270	3052	DCA CASE
0271	3024	DCA WHICH
0272	5310	JMP FRAME
0273	7300	CLA CLL
0274	7604	LAS
0275	1043	TAD M4
0276	7440	SZA
0277	5307	JMP .+10
0300	1022	TAD BLANK0/CASE 4: CENTRAL STIMULATION WITH NO
0301	3023	DCA BLANK /FEEDBACK
0302	3025	DCA FEED
0303	1044	TAD C3777
0304	3052	DCA CASE
0305	3024	DCA WHICH
0306	7410	SKP
0307	5204	JMP CASES
0310	7300	FRAME,CLA CLL
0311	1021	TAD NMB
0312	3032	DCA COUNT
0313	4445	JMS I PEYF.
0314	6544	ADIC
0315	6532	ADCV
0316	6531	ADSF
0317	5316	JMP .-1
0320	6534	ADRB
0321	1050	TAD BIAS1
0322	7100	CLL
0323	3033	DCA VEL
0324	1026	TAD EYEPOS
0325	6554	DAL2
0326	7300	CLA CLL
0327	1052	TAD CASE
0330	6564	DAL4
0331	7300	CLA CLL
0332	1025	TAD FEED
0333	1023	TAD BLANK
0334	3034	DCA UPPER
0335	1023	TAD BLANK
0336	7041	CIA
0337	1025	TAD FEED
0340	3035	DCA LOWER
0341	7100	CLL
0342	7421	MQL
0343	1033	TAD VEL
0344	7415	ASR
0345	0000	SCALE,0
0346	3036	DCA HVFL

0347	7501	MQA	0445	7300	CLA CLL
0350	3037	DCA LVEL	0446	1044	TAD C3777
0351	7100	CLL	0447	6552	DAL1
0352	1030	TAD LLINE0	0450	7300	CLA CLL
0353	1037	TAD LVEL	0451	6454	CLAF
0354	3030	DCA LLINE0	0452	6461	SNAF
0355	7204	GLK	0453	7610	SKP CLA
0356	1031	TAD HLINE0	0454	5252	JMP .-2
0357	1036	TAD HVEL	0455	6551	DACX
0360	3031	DCA HLINE0	0456	6561	DACY
0361	1031	TAD HLINE0	0457	7300	CLA CLL
0362	6562	DAL3	0460	2032	ISZ COUNT
0363	7300	CLA CLL	0461	7410	SKP
0364	1031	TAD HLINE0	0462	5447	JMP I PCASES
0365	3027	DCA HLINE	0463	1027	TAD HLINE
0366	5446	JMP I PDISP	0464	1020	TAD DLINE
		*400	0465	3027	DCA HLINE
0400	1034	DISPLY,TAD UPPER	0466	5200	JMP DISPLY
0401	7041	CIA			*500
0402	1027	TAD HLINE	0500	0000	EYE,0
0403	7510	SGEZ	0501	7300	CLA CLL
0404	5212	JMP .+6	0502	6541	ADCC
0405	7300	CLA CLL	0503	6544	ADIC
0406	1024	TAD WHICH	0504	7000	NOP
0407	7450	SNA	0505	7000	NOP
0410	5245	JMP DRAW+13	0506	6532	ADCV
0411	5232	JMP DRAW	0507	6531	ADSF
0412	7300	CLA CLL	0510	5307	JMP .-1
0413	1035	TAD LOWER	0511	6534	ADRB
0414	7041	CIA	0512	7100	CLL
0415	1027	TAD HLINE	0513	1051	TAD BIAS2
0416	7510	SGEZ	0514	3026	DCA EYEPOS
0417	5225	JMP .+6	0515	5700	JMP I EYE
0420	7300	CLA CLL			*20
0421	1024	TAD WHICH	0020	0200	DLINE,0200
0422	7450	SNA	0021	7740	NMB,7740
0423	5232	JMP DRAW	0022	0000	BLANK0,0
0424	5245	JMP DRAW+13	0023	0000	BLANK,0
0425	7300	CLA CLL	0024	0000	WHICH,0
0426	1024	TAD WHICH	0025	0000	FEED,0
0427	7450	SNA	0026	0000	EYEPOS,0
0430	5245	JMP DRAW+13	0027	0000	HLINE,0
0431	5232	JMP DRAW	0030	0000	LLINE0,0
0432	7300	DRAW,CLA CLL	0031	0000	HLINE0,0
0433	1027	TAD HLINE	0032	0000	COUNT,0
0434	6552	DAL1	0033	0000	VEL,0
0435	7300	CLA CLL	0034	0000	UPPER,0
0436	6454	CLAF	0035	0000	LOWER,0
0437	6461	SNAF	0036	0000	HVEL,0
0440	7610	SKP CLA	0037	0000	LVEL,0
0441	5237	JMP .-2	0040	7777	M1,7777
0442	6551	DACX	0041	7776	M2,7776
0443	6561	DACY	0042	7775	M3,7775
0444	5257	JMP .+13	0043	7774	M4,7774

0044	3777	C3777,3777
0045	0500	PEYE,EYE
0046	0400	PDISP,DISPLY
0047	0204	PCASES,CASES
0050	0000	BIAS1,0
0051	0000	BIAS2,0
0052	0000	CASE,0
0053	1000	C1000,1000
0054	2000	C2000,2000
0055	3000	C3000,3000

BIAS1	0050
BIAS2	0051
BLANK	0023
BLANK0	0022
CASE	0052
CASES	0204
COUNT	0032
C1000	0053
C2000	0054
C3000	0055
C3777	0044
DISPLY	0400
DLINE	0020
DRAW	0432
EYE	0500
EYEPOS	0026
FEED	0025
FRAME	0310
HLINE	0027
HLINE0	0031
HVEL	0036
LLINE0	0030
LOWER	0035
LVEL	0037
M1	0040
M2	0041
M3	0042
M4	0043
NMB	0021
PCASES	0047
PDISP	0046
PEYE	0045
SCALE	0345
START	0200
UPPER	0034
VEL	0033
WHICH	0024



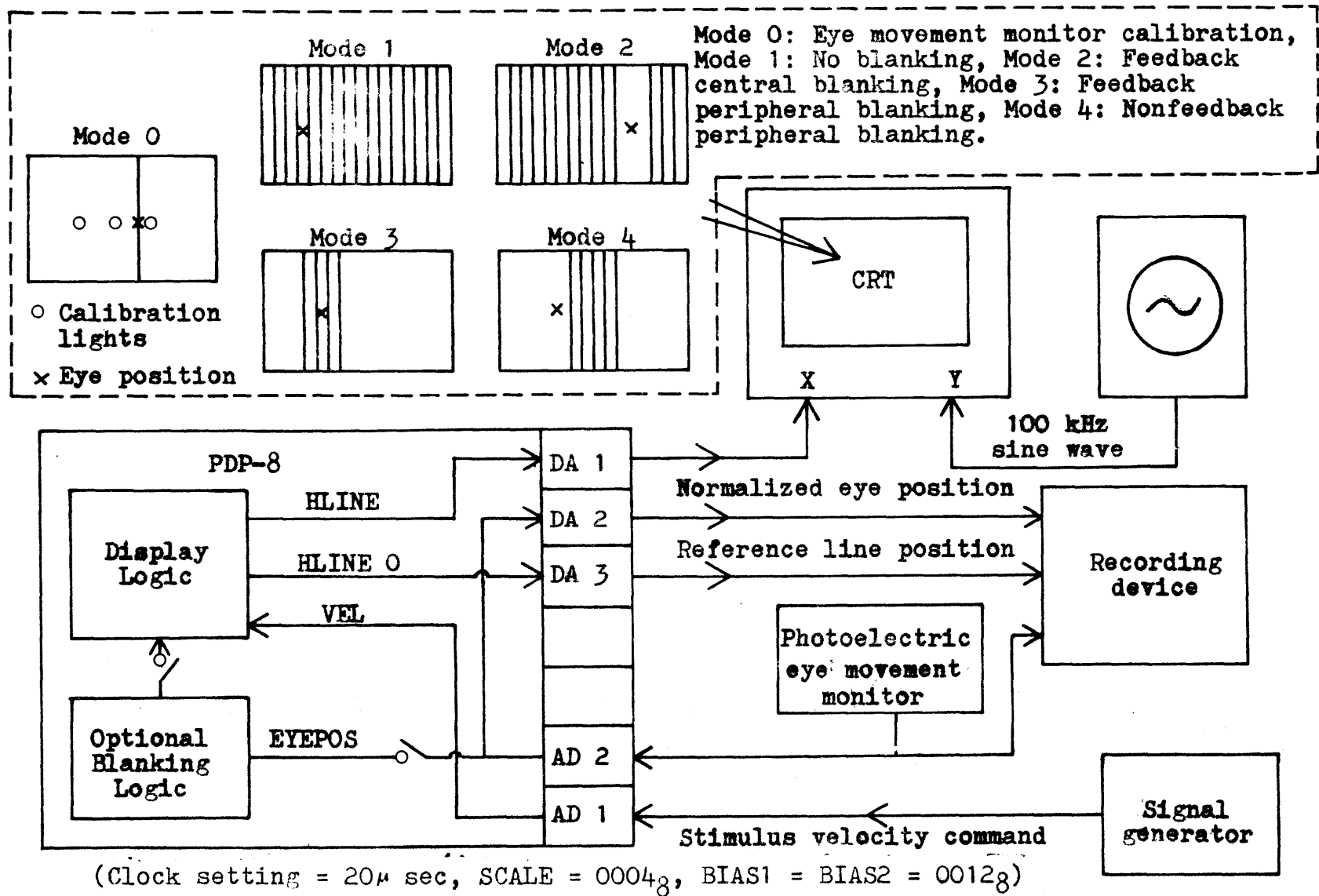


Fig. E.1 OKN stimulus display system and schematic illustration for optional visual patterns including selective stimulation to peripheral and central retina.

Speed of stripes

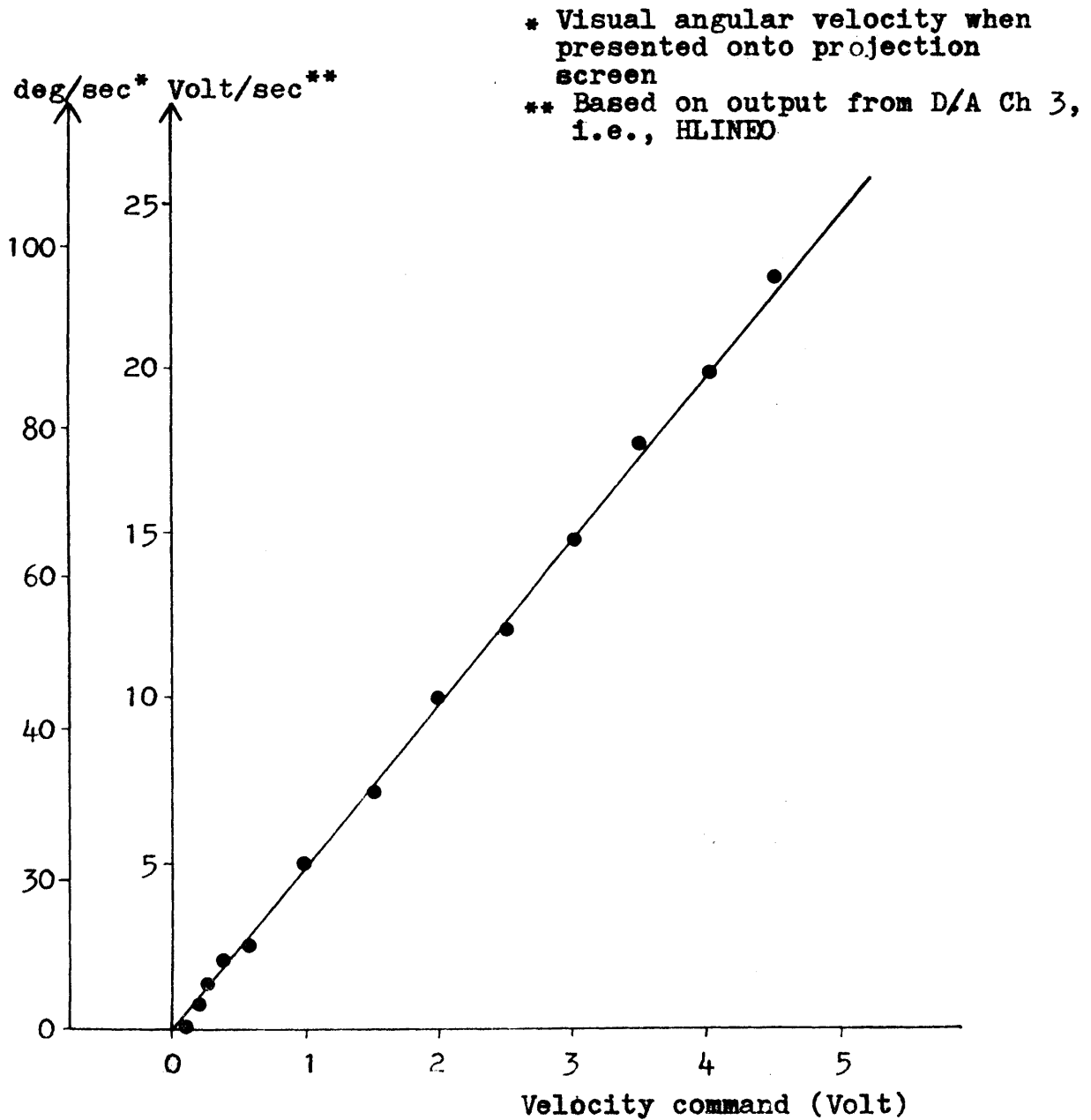


Fig. E.2 OKN stimulus velocity calibration record

## Appendix F

### Bode's Phase-attenuation Theorems and an Approximated Formula for the First Theorem

Since the phase shift and gain attenuation characteristics of servomechanisms and regulators determine their performance as well as their stability, it is important to understand the relationship between these characteristics. Theorems of Bode (1945) clarify this point in a rigorous mathematical framework. They show that, if the attenuation characteristics of a class of linear and lumped-parameter system is given arbitrarily, the phase shift characteristics of the system is defined and vice versa.

Linear systems that obey Bode's theorems are known as the "minimum phase" type. A minimum phase system is one that has the minimum phase shift possible for the number of energy storage elements in the network.

Contrasted with the minimum phase system is the "non-minimum phase" system. Such non-minimum phase system can be further divided into two subtypes, greater-than-minimum phase and less-than-minimum phase systems, producing the phase shift respectively greater and less than that would be expected from Bode's first theorem described subsequently.\* A minimum phase

---

\* Within the framework of Bode's theorems, the phase shift usually refers to the phase lag resulting from the gain attenuation. In this context, "greater" and "less" are implied in terms of absolute value of the phase shift.

system could become either a greater-than-minimum system or a less-than-minimum system by adding a transport delay or a negative delay (predictor) respectively.

The first theorem of Bode is particularly relevant to the thesis as applied in conjunction with discussion of results in Chapter IV. In essence, the theorem states:

The phase shift of a minimum phase system or network at any desired frequency can be determined from the slope of its attenuation-versus-frequency characteristic over the range of frequencies from  $-\infty$  to  $+\infty$ . The slope of the attenuation-frequency characteristic at the desired frequency is weighed most heavily, and the attenuation-frequency slope at frequencies further away from the desired frequency has a lesser importance.

This is formulated mathematically as follows:

$$B(\omega) = \frac{\pi}{2} \left. \frac{dA}{du} \right|_{u=0} + \frac{1}{\pi} \int_{-\infty}^{+\infty} \left[ \left. \frac{dA}{du} \right| - \left. \frac{dA}{du} \right|_{u=0} \right] \ln \left( \coth \left| \frac{u}{2} \right| \right) du \quad (F-1)$$

where  $B(\omega)$  is the phase shift of the system in radians at the desired frequency  $\omega$ ,  $A=A(u)$  is the gain attenuation in nepers<sup>\*</sup>, and  $u$  is a variable that is the logarithm of the ratio of the dummy frequency variable  $\xi$  to the frequency  $\omega$  at which the phase shift is sought. Thus

$$u = \ln \frac{\xi}{\omega}$$

---

\* 1 neper =  $\ln |e|$

$(dA/du)$  is the slope of the attenuation logarithm-frequency curve in nepers per unit change in  $u$ , that is, a change in frequency of the ratio of 2.718 : 1.\*  $(dA/du)_{u=0}$  is the attenuation-frequency slope at the reference point  $\xi=\omega$ , such that  $u=0$ .

In Chapter IV, phase-attenuation relations of the visual oculomotor tracking system were discussed on the basis of the following approximated version of Bode's original formula given by (F-1): As shown in Fig. F.1, gain data are fitted piecewise linearly in logarithmic scales, so that the slope,  $S=dA/du$  remains constant within a straight line segment.

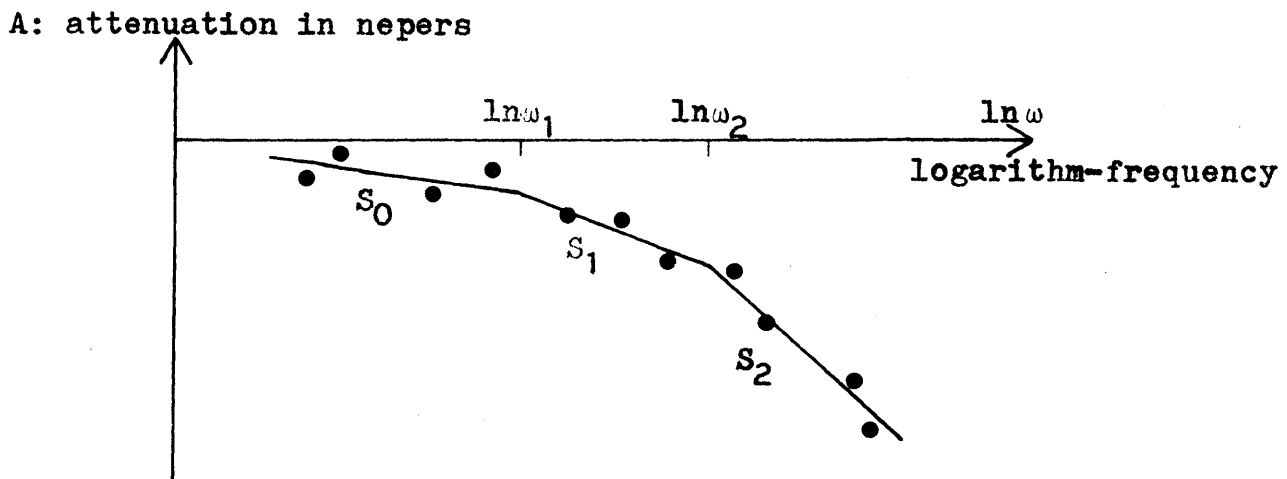


Fig. F.1 Illustrative sketch showing piece-wise linear approximation for gain data used to compute corresponding phase shift characteristics based on Bode's first theorem. Gain slope,  $S=dA/du$  (see text for definition of  $u$ ).

By performing the integration associated with (F-1) employing

---

\* The slope in decibels per decade corresponds to the rate of change of  $u$  being equal to 20 dB per decade or approximately 6 dB per octave.

double transformation of variables,\* the following analytical approximation can be obtained for the phase shift corresponding to the illustrative gain profile sketched in Fig. F.1:

$$0 \leq \omega \leq \omega_1$$

$$B(\omega) \approx \frac{\pi}{2}S_0 - \frac{2}{\pi}(S_1-S_0) \left[ \frac{\omega+1}{\xi} \left( \frac{\omega}{\xi} \right)^3 \right]_{\omega_1}^{\omega_2} - \frac{2}{\pi}(S_2-S_0) \left[ \frac{\omega+1}{\xi} \left( \frac{\omega}{\xi} \right)^3 \right]_{\omega_2}^{\infty}$$

$$\omega_1 \leq \omega \leq \omega_2$$

$$B(\omega) \approx \frac{\pi}{2}S_1 - \frac{2}{\pi}(S_1-S_0) \left[ \frac{\xi}{\omega+1} \left( \frac{\xi}{\omega} \right)^3 \right]_0^{\omega_1} - \frac{2}{\pi}(S_2-S_1) \left[ \frac{\omega+1}{\xi} \left( \frac{\omega}{\xi} \right)^3 \right]_{\omega_2}^{\infty}$$

$$\omega_2 \leq \omega \leq \infty$$

$$B(\omega) \approx \frac{\pi}{2}S_2 - \frac{2}{\pi}(S_2-S_0) \left[ \frac{\xi}{\omega+1} \left( \frac{\xi}{\omega} \right)^3 \right]_0^{\omega_1} - \frac{2}{\pi}(S_2-S_1) \left[ \frac{\xi}{\omega+1} \left( \frac{\xi}{\omega} \right)^3 \right]_{\omega_1}^{\omega_2}$$

(F-2)

---

\*  $p = \ln \coth \frac{u}{2}$  and  $q = \tanh \frac{p}{2}$ . The process involves a further approximation,  $\tanh^{-1} q = q + q^3/3$ , where  $q$  proves to be always less than 1.

## REFERENCES

- Adrian, E.D., "Discharges from Vestibular Receptors in the Cat," J. Physiol. (London), 101:389-407, 1943.
- Allum, J.H.J., and Tole, J.R., "Operational Details of MITNYS-II: A Digital Program for On-line Analysis of Nystagmus," Man-Vehicle Laboratory Report, M.I.T., 1972.
- Allum, J.H.J., Tole, J.R., and Weiss, A.D., "MITNYS-II. A Digital Program for On-line Analysis of Nystagmus," Acta Otolaryng. (Stockh.), 1973 (in press).
- Alpern, M., "Movements of the Eyes," in the Eye, ed., H. Davson, Volume 3, Muscular Mechanics, Part I, Academic Press, New York and London, 1962.
- Bach-y-Rita, P., "Neurophysiology of Eye Movements," Symp. on the Control of Eye Movements, San Fransisco, Calif., 1969; also in The Control of Eye Movements, ed., P. Bach-y-Rita, and C.C. Collins, Academic Press, New York and London, 1971.
- Bach-y-Rita, P., "Extraocular Proprioception and Muscle Function," Symp. on Cerebral Control of Eye Movements and Motion Perception, Freiburg i.Br., 1971; also in Bibl. Ophthal., 82: 56-60, 1972.
- Barlow, H.B., Hill, R.M., and Levick, W.R., "Retinal Ganglion Cells Responding Selectively to Direction and Speed of Image Motion in the Rabbit," J. Physiol., 173:377-407, 1964.
- Barnes, G.R., "The Generation of Saccadic Eye Movements in Vestibular Nystagmus," IAM Rept. No. 529, Royal Air Force Insti. of Aviation Med., 1973.
- Barnes, C.R., and Benson, A.J., "A Model for the Prediction of the Nystagmus Response to Angular and Linear Acceleration Stimuli," AGARD Conference, Pre-print No. 128, 1973.
- Becker, W., "The Control of Eye Movements in the Saccadic System," Symp. on Cerebral Control of Eye Movements and Motion Perception, Freiburg i.Br., 1971; also in Bibl. Ophthal., 82:233-243, 1972.
- Bender, M.B., and Shanzer, S., "Oculomotor Pathways defined by Electric Stimulation and Lesion of the brain Stem of Monkey," in The Oculomotor System, ed., M.B. Bender, Harper and Row, new York, 1964.

- Benson, A.J., and Bodin, M.A., "The Effects of the Direction of a Linear Acceleration Vector on Post-Rotational Vestibular Responses in Man," AGARD Conference Proceedings series No. 2:9-22, 1965.
- Benson, A.J., "Interaction between Semicircular Canals and Gravireceptors," Proceedings XVIII International Congress of Aviation and Space Medicine, Amsterdam, 1969; also in Recent Advances in Aerospace Medicine, ed., D.E. Busby, D. Reidel Publishing Co., Dordrecht, Holland, 1969.
- Bergland, G.D., "A Guided Tour of the Fast Fourier Transform," IEEE Spectrum, July 1969.
- Bode, H.W., Network Analysis and Feedback Amplifier Design, D. Van Nostrand Co., New York, 1945.
- Bowen, R.W., "Control of Voluntary Conjugate Eye Movements," Dept. of Psychology, Columbia University, 1971.
- Brindley, G.S., and Merton, P.A., "The Absence of Position Sense in the Human Eye," J. Physiol. (London), 153:127-130, 1960.
- Brucher, J.M., "The Frontal Eye Fields of the Monkey," Internat'l J. Neurol., 5:262-281, 1966.
- Bruell, J.H., and Albee, G.W., "Notes toward a Motor Theory of Visual Egocentric Localization," Psychol. Rev., 62(5): 391-400, 1955.
- Byford, G.H., "Eye Movements and the Optogyral Illusion," FPRC/1174, Air Ministry Flying Personnel Research Committee, April 1961.
- Childress, D.S., "A Study of the Mechanism of Horizontal Movement of the Human Eye," Ph.D. Thesis, Northwestern University, 1967.
- Childress, D.S., and Jones, R.W., "Mechanics of Horizontal Movement of the Human Eye," J. Physiol. (London), 188:273-284, 1967.
- Clark, B., Graybiel, A., and MacCorquodale, K., "The Illusory Perception of Movement Caused by Angular Acceleration and Centrifugal Force during Flight:II. Visually Perceived Motion and Displacement of a Fixed Target during Turns," J. Exp. Psychol., 39:219-227, 1949.
- Clark, B., "Visual Space Perception as Influenced by Unusual Vestibular Stimulation," Human Factors, 5(3):265-274, 1963.



- Coebel, H., Komatsuzaki, A., Bender, M.B., and Cohen, B., "Lesions of the Pontine Tegmentum and Conjugate Gaze Paralysis," *Arch. Neurol.*, 24:431-440, 1971.
- Cohen, B., and Feldman, M., "Relationship of Electrical Activity in the Pontine Reticular Formation and Lateral Geniculate Body to Rapid Eye Movements," *J. Neurophysiol.*, 31:806-817, 1968.
- Cohen, B., Komatsuzaki, A., and Bender, M.B., "Electrooculographic Syndrome after Pontine Reticular Formation Lesions," *Arch. Neurol.*, 18:78-92., 1968.
- Cohen, B., "Vestibulo-ocular Relations," Symp. on the Control of Eye Movements, San Fransisco, Calif., 1969; also in the Control of Eye Movements, ed., P.Bach-y-Rita, and C.C.Collins, Academic Press, New York and London, 1971.
- Cohen, B., "Origin of Quick Phases of Nystagmus," XXV International Congress of Physiological Sciences, Pisa, Italy, 1971; also in Progress in Brain Research, Vol. 37, ed., A.Brodal, and O.Pompeiano, Elsevier Publishing Co., Amsterdam/London/New York, 1972.
- Collewijn, H., "Optokinetic Eye Movements in the Rabbit. Input-output Relations," *Vision Res.* 9:117-132, 1969.
- Collewijn, H., Oyster, C.W., and Takahashi, E., "Rabbit Optokinetic Reactions and Retinal Direction-Selective Cells," Symp. on Cerebral. Control of Eye Movements and Motion Perception," Freiburg i.Br., 1971; also in *Bibl. Ophthal.*, 82: 280-287, 1972.
- Collewijn, H., "Latency and Gain of the Rabbit's Optokinetic Reactions to Small Movements, *Brain Res.* 36:59-70, 1972.
- Collins, W.E., "Further Studies of the Effect of Mental Set upon Vestibular Nystagmus," US Army Med. Res. Lab., Fort Knox, Ky., Rept. No. 443, 1960.
- Collins, W.E., Crampton, C.H., and Posner, J.B., "The Effect of Mental Set upon Vestibular Nystagmus and the Electroencephalogram," US Army Med. Res Lab., Fort Knox, Ky., Rept. No. 439, 1960.
- Cook, G., and Stark, L., "Derivation of a Model for the Human Eye Positioning Mechanism," *Bull. Math. Biophys.*, 29:153-174, 1967.
- Cooley, J.W., and Tukey, J.W., "An Alogorithm for the Machine Calculation of Complex Fourier series," *Math. Comput.*, 19: 297-301, 1965.

- Cooper, S., and Daniel, P.M., "Muscle Spindles in Human Extrinsic Eye Muscles," *Brain*, 72:1-24, 1949.
- Cooper, S., Daniel, P.M., and Whitteridge, D., "Nerve Impulses in the Brainstem of the Goat: Short Latency Response obtained by Stretching the Extrinsic Eye Muscles and the Jaw Muscles," *J. Physiol. (London)*, 120:471-490, 1953.
- Cooper, S., Daniel, P.M., and Whitteridge, D., "Nerve Impulses in the Brainstem of Goat: Responses with Long Latencies obtained by Stretching the Extrinsic Eye Muscles," *J. Physiol. (London)*, 120:491-513, 1953.
- Cooper, S., Daniel, P.M., and Whitteridge, D., "Muscle-spindles and other Sensory Endings in the Extrinsic Eye Muscles; the Physiology and Anatomy of these Receptors and of their Connections with the Brain-stem," *Brain*, 78:564-583, 1955.
- Crosby, E.C., Yoss, R.E., and Henderson, J.W., "The Mammalian Midbrain and Isthmus Regions. Part II. The Fiber Connections. D. The Pattern for Eye Movements on the Frontal Eye Field and the Discharge of Specific Portions of this Field to and through Midbrain Levels," *J. Comp. Neurol.* 97:357-383, 1952.
- Dallos, P.J., and Jones, R.W., "Learning Behavior of the Eye Fixation Control System," *IEEE Trans. Automatic Control*, Ac-8:218-227, July 1963.
- Dement, W., "Eye Movements during Sleep," in The Oculomotor System, ed., M. Bender, Harper and Row, New York, 1964.
- Dichgans, J., Körner, F., and Voigt, K., "Vergleichende Skalierung des afferenten und efferenten Bewegungssehens beim Menschen: Lineare Funktionen mit verschiedener Aufstiegssteilheit," *Psychol. Forsch.* 32:277-295, 1969.
- Dix, M.R., and Hood, J.D., "Further Observations upon the Neurological Mechanism of Optokinetic Nystagmus," *Acta Otolaryng. (Stockh.)*, 71:217-226, 1971.
- Dodge, R., Travis, R.C. and Fox, J.C., "Optic Nystagmus III. Characteristics of the Slow Phase," *Arch. Neurol. and Psychia.*, 24:21-34, 1930.
- Drewell, N.H., "The Effect of Preview on Pilot Describing Functions in a Simple Tracking Task," UTIAS Technical Rept. No. 176, Institute for Aerospace Studies, University of Toronto, 1972.
- Elkind, J.I., and Forgie, C.D., "Characteristics of the Human Operator in Simple Manual Control Systems," *IRE Trans. Automatic Control*, AC-4:45-55, 1959.

- Fender, D.H., and Nye, P.W., "An Investigation of the Mechanisms of Eye Movement Control," *Kybernetik*, 1:81-88, 1961.
- Fender, D.H., "The Eye-movement Control System: Evolution of a Model," in Neural Theory and Modeling, ed., R.F.Reiss, Stanford University Press, 1962.
- Fender, D.H., "Control Mechanisms of the Eye," *Sci. Am.*, 24-33, July 1964.
- Fuchs, A.F., "Periodic Eye Tracking in the Monkey," *J. Physiol. (London)*, 193:161-171, 1967.
- Fuchs, A.F., and Kornhuber, H.H., "Extraocular Muscle Afferents to the Cerebellum of the Cat," *J. Physiol. (London)*, 200:711-722, 1969.
- Fuchs, A.F., and Luschei, E.S., "Firing Patterns of Abducens Neurons of Alert Monkeys in Relationship to Horizontal Eye Movement," *J. Neurophysiol.*, 33:382-392, 1970.
- Gernandt, B., "Response of Mammalian Vestibular Neurones to Horizontal Rotation and Caloric Stimulation," *J. Neurophysiol.*, 12:173-184, 1949.
- Goldberg, J.M., and Fernández, C., "Response of First-order Vestibular Afferents to Controlled Angular Accelerations," *J. Acoust. Soc. Am.*, 46:105, 1969.
- Goldberg, J.M., and Fernández, C., "Physiology of Peripheral Neurons Innervating Semicircular Canals of the Squirrel Monkey," *J. Neurophysiol.*, 34:635-683, 1971.
- Graybiel, A., and Hupp, D.I., "The Oculogyral Illusion," *J. aviat. med.*, 17:3-27, 1946.
- Greene, T., and Jampel, R., "Muscle Spindles in the Extraocular Muscles of the Macaque," *J. Comp. Neurol.*, 126:547-550, 1966.
- Gregory, R.L., "Eye Movements and the Stability of the Visual World," *Nature (London)*, 182:1214-1216, 1958.
- Groen, J.J., Lowenstein, O., and Vendrik, A.J.M., "The Mechanical Analysis of the Responses from the End Organs of the Horizontal Semicircular Canal in the Isolateral Elasmobranch Labyrinth," *J. Physiol. (London)*, 117:329-346, 1952.
- Groen, J.J., "Problems of the Semicircular Canal from a Mechanico-Physiological point of View," *Acta Otolaryng. (Stockh.)*, Suppl. 163:59-67, 1960.

- Grüttner, R., "Experimental Studies of Optokinetic Nystagmus," *Zeitschrift für Sinnesphysiologie*, 68(1):1-48, 1939.
- Grüsser, O.J. and Grüsser-Cornehls, U., "Interaction of Vestibular and Visual Inputs in the Visual System." XXV International Congress of Physiological Sciences, Pisa, Italy, 1971; also in Progress in Brain Research, Vol. 37, ed., A. Brodal, and O. Pompeiano, Elsevier Publishing Co., Amsterdam/London/New York, 1972.
- Helmholtz, H. von, Handbuch der physiologischen Optik, (Voss, Leipzig), 1866.
- Henn, V., and Cohen, B., "Pontine Neural Activity Preceding Saccades, Quick Phases of Nystagmus and Blinks in Alert Monkeys," *Fed. Proc.*, 30:666, 1971.
- Hering, E., "Der Raumsinn und die Bewegungen der Augen" in Hermann Handbuch der Physiologie, Vol. 3, 1879.
- Holmes, G., "The Cerebral Integration of the Ocular Movements," *Brit. Med. J.*, 107-112, July 16, 1938.
- Holst, E. von, and Mittelstaedt, H., "Das Reafferenzprinzip (Wechselwirkungen zwischen Zentralnervensystem und Peripherie). *Naturwissenschaften*, 10:464-476, 1950.
- Holst, E. von, "Relations between the Central Nervous System and the Peripheral Organs," *Brit. J. anim. Behav.*, 2:89-94, 1954.
- Holst, E. von, "Aktive Leitungen der menschlichen Gesichtswahrnehmung," *Studium gen.*, 10:234, 1957.
- Honrubia, V., Downey, D.P., Mitchell, B.A., and Ward, P.H., "Experimental Studies on Optokinetic Nystagmus: II Normal Humans," *Acta Otolaryng.(Stockh.)*. 65:441-448, 1968.
- Hood, J.D., "Observations upon the Neurological Mechanism of Optokinetic Nystagmus with Special Reference to the Contribution of Peripheral Vision," *Acta Otolaryng.(Stockh.)*, 63: 208, 1967.
- Hood, J.D., Discussion in Myotatic, Kinesthetic and Vestibular Mechanism, ed., Aus de Rulk and Knight. Little, Brown and Co., Boston, 1967.
- Horcholle, G., and Tyč-Dumont, S., "Activités Unitaires des Neurones Vestibulaires et Oculomoteurs au Cours du Nystagmus," *Exp. Brain Res.*, 5:16-31, 1968.

- Howard, I.P., and Templeton, W.B., Human Spatial Orientation, John Wiley & Sons, New York, 1966.
- Hubel, D.H., and Wiesel, T.N., "Receptive Fields, Binocular Interaction and Functional Architecture in the Cat's Visual Cortex," *J. Physiol. (London)*, 160:106-154, 1962.
- Ito, F., Bach-y-Rita, P., and Yamanaka, Y., "Extraocular Muscle Intracellular and Motor Nerve Responses to Semicircular Canal Stimulation," *Exp. Neuro.*, 24:438-449, 1969.
- Johnson, L.E., "Human Eye Tracking of Aperiodic Target Functions," Systems Research Center, 37-B-63-8, Case Inst. of Tech., 1963.
- Jones, G.M., Barry, W., and Kowalsky, N., "Dynamics of the Semicircular Canals Compared in Yaw, Pitch and Roll," *Aerospace Med.*, 35(10):984-989, 1964.
- Jones, G.M., "Predominance of Anti-compensatory Oculomotor Response during Rapid Head Rotation," *Aerospace Med.*, 35:965-968, 1964.
- Jones, G.M., and Milsum, J.H., "Spatial and Dynamic Aspects of Visual Fixation," *IEEE Trans. Bio-Medical Engineering*, BME-12:54-62, 1965.
- Jones, G.M., and Milsum, J.H., "Relations between Neural and Mechanical Responses of the Semicircular Canal," Pro. 38th Ann. Sci. Meeting, Aerospace Med. Assoc., 252-253, 1967.
- Jones, G.M., and Milsum, J.H., "Characteristics of Neural Transmission from the Semicircular Canal to the Vestibular Nuclei of Cats," *J. Physiol. (London)*, 209:295-316, 1970.
- Jung, R., "Eine elektrische Methode zur mehrfachen Registrierung von Augenbewegungen und Nystagmus," *Klin. Wchnschr*, 18:21, 1939.
- Jung, R., and Mittermier, R., *Arch. Ohr. Nas. und Kehlk-Heilk*, 146:410-439, 1939.
- Jung, R., "How do we see with Moving Eyes," Symp. on Cerebral Control of Eye Movements and Motion Perception," *Freiburg i.Br.*, 1971; also in *Bibl. Ophthal.*, 82:377-395, 1972.
- Jung, R., Personal Communication with L.R. Young, 1973.
- Katz, G.B., "Perception of Rotation-Nystagmus and Subjective Response at Low Frequency Stimulation," S.M. Thesis, M.I.T., September 1967.

- Kommerell, G., and Täumer, R., "Investigations of the Eye Tracking System through Stabilized Retinal Images," Symp. on Cerebral Control of Eye Movements and Motion Perception," Freiburg i. Br., 1971; also in *Bibl. Ophthalmol.*, 82:280-287, 1972.
- Körner, F., "Optokinetic Stimulation of an Immobilized Eye in the Monkey," Symp. on Cerebral Control of Eye Movements and Motion Perception," Freiburg i.Br., 1971; also in *Bibl. Ophthalmol.*, 82:298-307, 1972.
- Kornmuller, A.E., "Ein experimentelle Anästhesie der äusseren Augenmuskeln am Menschen und ihre Auswirkungen," *J. Psychol. Neurol., Lpz.*, 41:354-336, 1930.
- Lässig, P., "Critical Observations on the Study of the Eye-following System with Unpredictable Movements of the Aiming Object," *Acta Biol. Med. Ger.*, 14:618-629, 1965.
- Levin, P.M., "The Efferent Fibres of the Frontal Lobe of the Monkey, macaca mulatta," *J. Comp. Neurol.*, 63:369-419, 1936.
- Lorente de N6, R., "Vestibulo-ocular Reflex Arc," *Arch. Neurol. and Psychiat.*, 30:245-291, 1933.
- Mach, E., "Beiträge zur Analyse der Empfindungen," 1st ed., Fischer, Jena., 1886.
- Mackay, D.M., "Perceptual Stability of a Stroboscopically lit Visual Field containing self-luminous Objects," *Nature (London)*, 181:507-508, 1958.
- Mayne, R., "The Constants of the Semicircular Canal Differential Equation," Good Year Aerospace Corp., Rept. No. GERA-1083, 1965.
- Meiry, J.L., "The Vestibular System and Human Dynamic Space Orientation, Sc. D. Thesis, M.I.T., 1965.
- Merrill, E.G., and Stark, L., "Optokinetic Nystagmus: Double Stripe Experiment," *Quart. Prog. Rept., Res. Lab. Electr., M.I.T.*, 70:357-359, 1963a.
- Merrill, E.G., and Stark, L., "Smooth Phase of Optokinetic Nystagmus in Man," *Quart. Prog. Rept., Res. Lab. Electr. M.I.T.*, 71:286-291, 1963b.
- Merton, J.L., "Absence of Conscious Position Sense in the Human Eyes," in the Oculomotor System, ed., M.B.Bender, Harper and Row, New York, 1964.

- Michael, J.A., and Jones, G., "Dependence of Visual Tracking Capability upon Stimulus Predictability," *Vis. Res.* 6:707-716, 1966.
- Mishkin, S., and Jones, G.M., "Predominant Direction of Gaze During Slow Head Rotation," *Aerospace Med.* 37(9):897-900, 1966.
- Money, K.E., Bonen, L., Beatly, J., Kuehn, L., Sokoloff, M., and Weaver, R., "The Physical Properties of Fluids and Structures of the Vestibular Apparatus of the Pigeon," *Amer. J. Physiol.* 220:140-147, 1971.
- McRuer, D.T., and Krendel, E.S., "The Human Operator as a Servo System Element," *J. Franklin Inst.*, 267:1, 1959.
- Nelson, D., and Stark, L., "Optokinetic Nystagmus in Man," *Quart. Prog. Rept., Res Lab. Electr., M.I.T.*, 66:366-369, 1962.
- Niven, J.I., and Hixon, W.C., "Frequency Response of the Human Semicircular Canals: I. Steady State Ocular Nystagmus Response to High Level Sinusoidal Angular Rotations," *BuMed. Proj. MR 005. 13-6001, Subtask 1, Rept 58, NASA Order No. 1*, 1961.
- Ohm, J., "Über die Beziehungen zwischen der Halbblindheit und dem Optokinetischen Nystagmus," *Graefes Arch. Ophth.*, 136:341, 1937.
- Oman, C.M., "Dynamic Response of the Semicircular Canal and Lateral Line Organs," *Ph.D. Thesis, M.I.T.*, 1972.
- Outerbridge, J.S., "Experimental and Theoretical Investigation of Vestibularly-Driven Head and Eye Movement," *Ph.D. Thesis, McGill University*, 1969.
- Peters, R.A., "Dynamics of the Vestibular System and their Relation to Motion Perception, Spatial Disorientation, and Illusions," *NASA CR-1309*, 1969.
- Pulfrich, C., *Naturwissenschaften*, 10:553, 569, 596, 714, 735, 751, 1922.
- Rademaker, G.G.J., and Ter Braak, J.W.G., "On the Central Mechanism of Some Optic Reactions," *Brain*, 71:48-76, 1948.
- Rashbass, C., "The Relationship between Saccadic and Smooth Tracking Eye Movements," *J. Physiol. (London)*, 159:326-338, 1961.

- Rashbass, C., "Second Thoughts on Smooth Pursuit," Symp. on the Control of Eye Movements, San Fransisco, Calif. 1969; also in the Control of Eye Movements, ed., P.Bach-y-Rita, and C.C.Collins, Academic Press, New York and London, 1971.
- Richards, W., Personal Communication, 1973.
- Riggs, L.A., and Tuluney, S.U., "Visual Effects of Varying the Extent of Compensation for Eye Movements," J. Opt. Soc. AM., 49:741-745., 1959.
- Robinson, D.A., "The Mechanics of Human Saccadic Eye Movement," J. Physiol.(London), 174:245-264, 1964.
- Robinson, D.A., "The Mechanics of Human Smooth Pursuit Eye Movement," J. Physiol.(London), 180:569-591, 1965.
- Robinson, D.A., "The Oculomotor Control System: A Review," IEEE Proceedings, 56(6):1032-1049, June 1968.
- Robinson, D.A., "Models of Oculomotor Neural Organization," Symp. on the Control of Eye Movements, San Fransisco, Calif., 1969; also in the Control of Eye Movements, ed., P.Bach-y-Rita, and C.C.Collins, Academic Press, New Yowk and London, 1971.
- Robinson, D.A., and Keller, E.L., "The Behavior of Eye Movement Motoneurons in the Alert Monkey," Symp. on Cerebral Control of Eye Movements and Motion Perception," Freiburg i.Br., 1971; also in Bibl. Ophthal., 82:7-16, 1972.
- Ross, D.A., "Electrical Studies on the Frog's Labyrinth," J. Physiol.(London), 86:117-146, 1936.
- Schaefer, K.P., "Die Erregungsmuster einzelner Neurone des Abducens-Kernes beim Kaninchen," Pflüg. Arch. Ges. Physiol., 284:31-51, 1965.
- Schmid, R., and Stefanelli, M., "A Mathematical Model for the Vestibulo-ocular Reflex," Laboratorio di Controlli Automatici Relazione Interna 70-13, Istituto di Electrotecnica ed Electronica del Politecnico di Milano, 1970.
- Schmid, R., "System Analysis of the Vestibulo-ocular System," Laboratorio di Controlli Automatici Relazione Interna 70-14, Istituto di Electrotecnica ed Electronica del Politecnico di Milano, 1970.
- Schmid, R., Personal Communication with L.R.Young, 1971.



- Sherrington, C.S., "Observations on the Sensual Role of the Proprioceptive Nerve Supply of the Extrinsic Ocular Muscles," *Brain*, 41:332-343, 1918.
- Smith R.H., "On the Limits of Manual Control," *IEEE Trans. Human Factors in Electronics*, HFE-4(1):56-59, 1963.
- Stark, L., Iida, M., and Willis, P.A., "Dynamic Characteristics of the Motor Coordination System in Man," *Biophys. J.*, 1:279-300, 1961.
- Stark, L., Vossius, G., and Young, L.R., "Predictive Control of Eye Tracking Movements," *IRE Trans. Human Factors in Electronics*, HFE-3:52-56, 1962.
- Stark, L., Takahashi, Y., and Zames, G., "Nonlinear Servoanalysis of Human Lens Accommodation," *IEEE Trans. System Science and Cybernetics*, SSC-1:75-83, 1965a.
- Stark, L., Kupfer, C., and Young, L.R., "Physiology of the Visual Control System," *NASA CR-238*, June 1965b.
- Stark, L., Neurological Control Systems: Studies in Bioengineering, Plenum Press, New York, 1968.
- Stark, L., "The Control System for Versional Eye Movements," *Symp. on the Control of Eye Movements, San Fransisco, Calif., 1969*; also in The Control of Eye Movements, ed., P. Bach-y-Rita, and C.C. Collins, Academic Press, New York and London, 1971.
- St-Cyr, G.J., and Fender, D.H., "Nonlinearity of the Human Oculomotor System: Time Delays," *Vis. Res.* 9:1491-1503, 1969.
- Steer, R.W., "The Influence of Angular and Linear Acceleration and Thermal Stimulation on the Human Semicircular Canal," *Sc.D. Thesis, M.I.T.*, 1967.
- Steinbach, M.J., and Held, R., "Eye Tracking of Observer-generated Target Movements," *Science*, 161:187-188, 1968.
- Steinhausen, W., "Uber den Nachweis der Bewegung der Cupula in der intaken Bogengang-ampulle des Labyrinthes bei der natuerlichen rotatorischen und calorischen Reizung," *Pflug. Arch. ges. Physiol.*, 228:322, 1931.
- Sterling, P., and Wichelgren, B.G., "Visual Receptive Fields in the Superior Colliculus in the Cat," *J. Neurophysiol.*, 32: 1-15, 1969.

- Sugie, N., and Jones, G.M., "A Mathematical Model of the Vestibulo-ocular System," Digest 6th Int. Conf. Med. Electr. Biol. Eng., Tokyo, 1965.
- Sugie, N., and Jones, G.M., "The Mechanism of Eye Movements II. Eye Movements Elicited by Head Rotation." Bull. Electro-technical Lab. (Tokyo) 30:574-586, 1966.
- Sugie, N., "Analysis of the Eye Movement System," Electro-technical Laboratory Rept. 693 (Tokyo). 1968.
- Sünderhauf, A., "Untersuchungen über die Regelung der Augenbewegungen," Klinische Monatsblätter für Augenheilkunde, 136:837-852, 1960.
- Szentagothai, J., "The Elementary Vestibulo-ocular Reflex Arc," J. Neurophysiol., 13:395-407, 1950.
- Ten Kate, J. "The Oculo-vestibular Reflex of the Growing Pike," Ph.D. Thesis, Rijksuniversiteit te Groningen, 1969.
- Ter Braak, J.W.G., "Untersuchungen über optokinetischen Nystagmus," Arch. néerl. Physiol. 21:309-376, 1936.
- Thomas, J.G., "The Torque-angle Transfer Function of the Human Eye," Kybernetik, 3:254-263, 1967.
- Thomas, J.G., "The Dynamics of Small Saccadic Eye Movements," J. Physiol. (London), 200:109-127, 1969.
- Tole, J.R., and Young, L.R., "MITNYS. A Hybrid Program for On-line Analysis of Nystagmys," Aerospace Med., 42:508-511, 1971.
- Uemura, T., and Cohen, B., "Vestibulo-ocular Reflexes: Effects of Vestibular Nuclear Lesions," XXV International Congress of Physiological Sciences, Pisa, Italy, 1971; also in progress in Brain Research, Volume 37, ed., A. Brodal, and O. Pompeino, Elsevier Publishing Co., Amsterdam/London/New York, 1972.
- Van Egmond, A.J., Groen, J.J., and Jongkees, L.B.W., "The Mechanics of the Semicircular Canal," J. Physiol. (London), 110:1-17, 1949.
- Vossius, G., "Der Kybernetische Aspekt der Willkürbewegung," in Progress in Cybernetics, Elsevier Publishing Co., New York, 1965.
- Watanabe, A., and Yoshida, T., "Control Mechanisms of the Smooth Pursuit Eye Movement," Inst. Electronics Comm. Engrs. Japan, MBE 68-13, 1968.

- Weiss, A.D., Unpublished Data and Personal Communication, 1973.
- Werner, J., Wunder, R., and Jahns, R., "Untersuchungen zur Linearität des okulomotorischen Systems," *Kybernetik* 11:112-117, 1972.
- Westheimer, G., "Mechanism of Saccadic Eye Movements," *AMA Arch. Ophthalmol.*, 52:710-724, 1954a.
- Westheimer, G., "Eye Movement Responses to a Horizontally Moving Visual Stimulus," *AMA Arch. Ophthalmol.* 52:932-941, 1954b.
- Wheeless, L.L., Boynton, R.M., and Cohen, G.H., "Eye Movement Responses to Step and Pulse-step Stimuli," *J. Opt. Soc. Am.*, 56:956-960, 1966.
- Wheeless, L.L., Cohen, G.H., and Boynton, R.M., "Luminance as a Parameter of the Eye Movement Control System," *J. Opt. Soc. Am.*, 57:394-400, 1967.
- Whiteside, T.C.D., Graybiel, A., and Niven, J.I., "Visual Illusions of Movement," Rept. No. 90, Naval School of Aviation Medicine, June 1963.
- Wurtz, R.H., and Goldberg, M.E., "Superior Colliculus Cell Responses Related to Eye Movements in Awake Monkeys," *Science*, 171:82-84 (in a footnote), 1971.
- Yamanaka, Y., and Bach-y-Rita, P., "Conduction Velocities in the Abducens Nerve Correlated with Vestibular Nystagmus in Cats," *Exp. Neurol.* 20:143-155, 1968.
- Yarbus, A.L., Eye Movements and Vision, Plenum Press, New York, 1967.
- Yasui, S., Thesis Proposal Submitted to Doctoral Committee, 1970.
- Young, L.R., "A Sampled Data Model for Eye Tracking Movements," Sc.D. Thesis, M.I.T., 1962.
- Young, L.R., and Stark, L., "Variable Feedback Experiments Testing a Sampled Data Model for Eye Tracking Movement," *IEEE Trans. Human Factors in Electronics*, HFE-4(1):38-51, 1963.
- Young, L.R., "The Dead Zone to Saccadic Eye Movements," Symp. on Biomedical Engineering, Marquette University, 1966.
- Young, L.R., Forster, J.D., and Van Houtte N., "A Revised Stochastic Sampled Data Model for Eye Tracking Movements," Fourth Annual NASA-University Conference on Manual Control, University of Michigan, Ann Arbor, Mich., March 1968.

Young, L. R. , and Oman, C.M. , "A Model for Vestibular Adaptation to Horizontal Rotation," Aerospace Med., 40:1076-1080, 1969.

Young, L. R. , "Pursuit Eye Tracking Movements," Symp. on the Control of Eye Movements, San Fransisco, Calif., 1969; also in the Control of Eye Movements, ed., P.Bach-y-Rita, and C.C.Collins, Academic Press, New York and London, 1971.

Young, L.R. , Personal Communication, 1971.

Young, L.R. , Unpublished Data and Personal Communication, 1973.

Zuber, B.L. , "Physiological Control of Eye Movements in Humans," Ph.D. Thesis, M.I.T. , 1965.

### Biographical Sketch

Syozo Yasui was born on September 11, 1940 in Kamakura, an old capital of Japan, where he spent childhood days. He entered the University of Tokyo in 1959 and graduated with the degree of Kogakushi from the Department of Aeronautics in 1963. From 1963 to 1968, he was an employee of Tokyo Shibaura Electric Company in a group assigned to aerospace systems design and development.

He came to M.I.T. in 1965 as a graduate student in the Department of Aeronautics and Astronautics. Since then (interrupted by one year leave), he has been a research assistant in the Man-Vehicle Control Laboratory, where he carried out the work leading to this dissertation as well as that for M.S. thesis on adaptive control completed in 1968.